SESSION 4
STUDIES IN GROUNDWATER

Keynote Addresses

Groundwater for sustainable development opportunities and constraints
F.A.R. Attia

How can isotope research contribute to understanding and managing water quality issues?
N.E. Peters

ORIGIN, DYNAMICS, DATING, INTERRELATIONS

Development of accelerator mass spectrometry (AMS) for the detection of ^{81}Kr and first application to groundwater dating
P. Collon, W. Kutschera, B.E. Lehmann, H.H. Loosli, R. Purtschert, A. Love, L. Sampson, B. Davids, M. Fauerbach, R. Harkewicz, D.J. Morrissey, B.M. Sherrill, M. Steiner, R.C. Pardo, M. Paul

Environmental tracers as indicators of groundwater flow and evolution in a fractured rock aquifer, Clare Valley, South Australia
A.J. Love, P.G. Cook, A.L. Herczeg, C.T. Simmons

Estimation of recharge from Nile Aquifer to the desert fringes at Qena area, Egypt
M.S. Hamza, A.I.M. Aly, M.A. Awad, A.A. Nada, S.G. Abdel-Samie, M.A. Sadek, W.M. Salem, F.A. Attia, T.M. Hassan, N.E. El-Arabi, K. Froehlich, M.A. Geyh

Current and future impact of an uranium mine waste disposal site on groundwater
P. Schneider, K. Osenbrück, K. Nindel, S. Voerkelius, M. Forster, J. Schreyer

Isotopically highly enriched shallow groundwater below overlying dry sediments
M.A. Geyh, Gu Weizu

Isotopic studies of natural waters in the Skagafjördur region, N-Iceland. Deuterium excess and ^{14}C age of groundwater
A.E. Sveinbjörnsdóttir, S. Arnórsson, J. Heinemeier, E. Boaretto

A multi-isotope (B, Sr, O, H) and age dating (^{3}H-^{3}He, ^{14}C) study of groundwater from Salinas Valley, California
A. Vengosh, J. Gill, M.L. Davisson, G.B. Hudson

Recharge quantification with radiocarbon: Independent corroboration in three Karoo aquifer studies in Botswana
B.Th. Verhagen, D.B. Bredenkamp, H.J. Van Rensburg, J.L. Farr

Noble gas data from the Great Artesian Basin provide a temperature record of Australia on time scales of 10^5 years
U. Beyerle, W. Aeschbach-Hertig, F. Peeters, R. Kipfer, R. Purtschert, B. Lehmann, H.H. Loosli, A. Love

Importance of isotope hydrology techniques in water resources management: A case study of the Makutupora basin in Tanzania
F.H. Senguji

Groundwater origin investigation with isotopic compositions for evaluation of high productive deep aquifers in Khon Kaen area, northwest Thailand
C. Buaphan, W. Yangme, L. Wannakao, V. Sriboonlue, A. Tassanasorn, S. Buapeng

An isotopic approach to the functioning of multilayered aquifer systems in central Tunisia: The cases of the North Gafsa and Hajeb el Aioun-Djelma basins
K. Zouari, B. Ouda, M. Yermani, A. Mamou, J.L. Michelot, E. Gibert-Massault

Validity of Chlorofluorocarbons (CFCs) as an age-dating tool in karstic aquifers, Taurids – Southern Turkey
N.N. Özyurt, C.S. Bayari

Palaeo-ages of groundwaters in a fissured chalk aquifer, UK
T. Elliot

POLLUTION, SOURCE/TRANSPORT OF CONTAMINANTS, SALINIZATION, WATER–ROCK INTERACTIONS, GEOTHERMAL SYSTEMS

Applications of compound-specific carbon isotope ratios in organic contaminant studies
R. Aravena, D. Hunkeler, Y. Bloom, B. Butler, E. Edwards, S.K. Frape, E. Cox

Major ions, $\delta^{18}O$, ^{2}H, and $^{87}Sr/^{86}Sr$ as tracers of the origin and evolution of dissolved salts in groundwaters of the Murray basin, Australia
S.S. Dogramaci, A.L. Herczeg

Isotopic evidence for geochemical provinces in the Astian sandy aquifers (Mediterranean coast, southern France)
F. Barbecot, L. Dever, C. Hillaire-Marcel, E. Gilbert, Y. Travi, C. Marlin

Isotopic and chemical composition of groundwater in the Bolivian Altiplano: Present space evolution records hydrologic conditions since 11 000 years
A. Coudrain, A. Talbi, M. Loubet, R. Gallaire, C. Jusserand, E. Ramirez, E. Ledoux

^{18}O isotopic characterisation of non-point source contributed heavy metals (Zn and Cu) contamination of groundwater
P.S. Datta, K.M. Manjaiah, S.K. Tyagi

Tracing and age-dating recycled waste water recharged for potable reuse in a seawater injection barrier, southern California, USA
M.L. Davisson, G.B. Hudson, B.K. Esser, B. Ekwurzel, R.L. Herndon

Isotope and hydrogeochemical studies of Southern Jiangxi geothermal systems, China
Wenbin Zhou, Xueli Li, Weijun Shi, Zhanxue Sun

A combined tool for water-rock interactions studies: B, Sr, O, H isotopes in groundwater
W. Klopmann, Ph. Negrel, J. Casanova

Isotopic and geochemical assessment of the geothermal field of Limnos Island, Greece
E. Dotsika, D. Poutoukis,E. Lagios, J.L. Michelot

Geochemistry of CO_2-rich water in the Jungwon area, Korea
Y.K. Koh, C.S. Kim, D.S. Bae, K.S. Kim, H.S. Choi

Monitoring the movement of the cooler fluids in the deep geothermal reservoirs of greater Tongonan geothermal field, Philippines
J.S. Seastres, Jr., N.D. Salonga, F.L. Siega

Keynote Address

GROUNDWATER FOR SUSTAINABLE DEVELOPMENT OPPORTUNITIES AND CONSTRAINTS

Fatma Abdel Rahman Attia
Director of the Research Institute for Groundwater
Cairo, Egypt

Water is the most spread natural resource on earth. It plays a vital role in both the environment and human life. Among all fresh water resources, groundwater is the most widely distributed one on earth. The rise and decline of civilizations have been linked to climatic changes which, in turn, controlled the natural recharge of aquifers and regulated the pollution of groundwater and soils.

> Aquifers have specific characteristics that distinguish them from other water bodies: (i) they can help in removing suspended solids and disease-causing organisms; (ii) they can store water in quantities exceeding those which are or conceivably could be stored in all natural and artificial surface-water bodies; (iii) they can regulate the water temperature and its chemical quality; (iv) they transport water from areas of recharge to areas of need; and (v) they slow-down the natural discharge of water to the surface. As such, aquifers can be utilized as strategic storage reservoirs for water to make up the bulk of the dry-weather flow of streams.

In addition to secular changes in groundwater caused by climatic variations, there are now serious threats to both quantity and quality of groundwater resources caused by the accelerating human intervention.

The main challenge facing the present and future availability of groundwater is “How to sustain this precious natural resource and protect it from degradation? ". Groundwater protection is thus a major challenge.

The groundwater protection framework constitutes of a series of actions. Some are preventive while others are corrective. These should be directed to the software (mostly socio-economy and legislation) as well as the hardware (technical). Main causes of software problems and conflicts include: (i) short-versus-long-term considerations; (ii) externalities, which occur when private costs or benefits do not equal social costs or benefits; and (iii) risks and uncertainties, including conflicts among water user sectors. This dictates a change from individual development and management to integrated development and management that is accompanied by close monitoring and evaluation of actions. Technical actions include among others: (i) proper assessment of the resource; (ii) appropriate dynamic planning; and (iii) proper development and management.

The problems related to groundwater protection are more serious in arid zones due to the hydrogeologic complexity of water systems in such zones. For this reason, UNESCO identified as a priority theme in the Fifth Hydrologic Program (IHPV) “Groundwater at risk”. Under this theme, among others, two networks have been initiated, one on wadi hydrology and the other on groundwater protection in the Arab region (being one of the most arid regions in the world). Various types of activities have already been identified and are under implementation, including: (i) initiation of a “Data Base” for groundwater protection; (ii) development of “Manuals” in various areas related to groundwater protection (various users categories); (iii) regular training programs for various categories; (iv) development of “Systematic approaches to research and implementation” for priority aquifers in the region; (v) development of suitable “Dissemination means”; and (vi) development of awareness means

WATER RESOURCES AVAILABILITY-AN OVERVIEW

Water Resources

> Water is the most widely spread natural resource on earth. It plays a vital role in both the environment and human life.

The current estimate of water storage on earth (in the hydrosphere) is about 1386 million cubic kilometers. However, 97.5 % of this amount is saline water, and only 2.5 % is fresh water. The major portion of available fresh water (68.7 %) is in the form of ice and permanent snow cover in the Antarctic, the Arctic, and in the mountainous regions; 29.9% exists as fresh groundwater; and only 0.26% is surface waters (lakes, rivers, reservoirs, etc.).

Source: Igor A. Shiklomanov (1998)

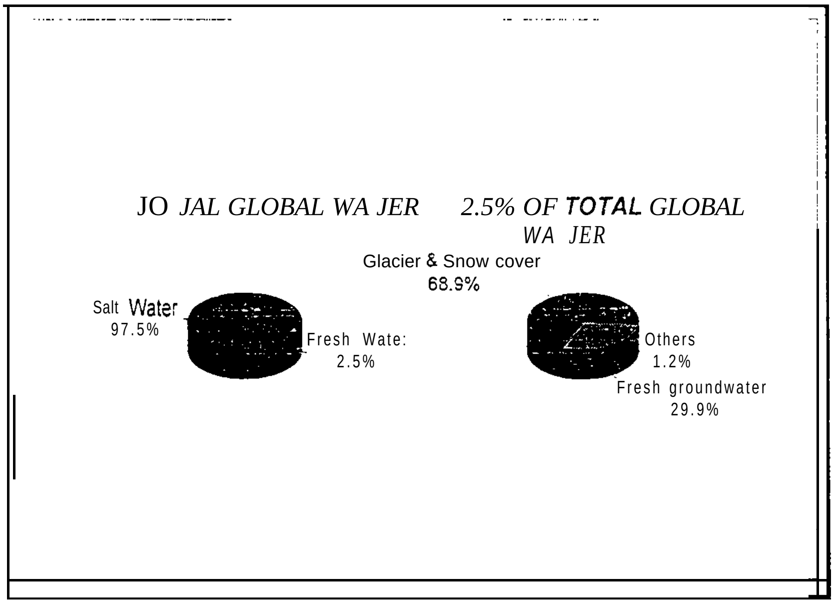

Fresh water is characterized by its spatial and temporal variation. Temporal variations can be quite significant, especially in arid regions where actual values are small.

Water Demand

Water demand is generally a function of various factors, among which, physiographic (including climate) features, area served, population, and socio-economic status.

Source: Igor A. Shiklomanov (1998)

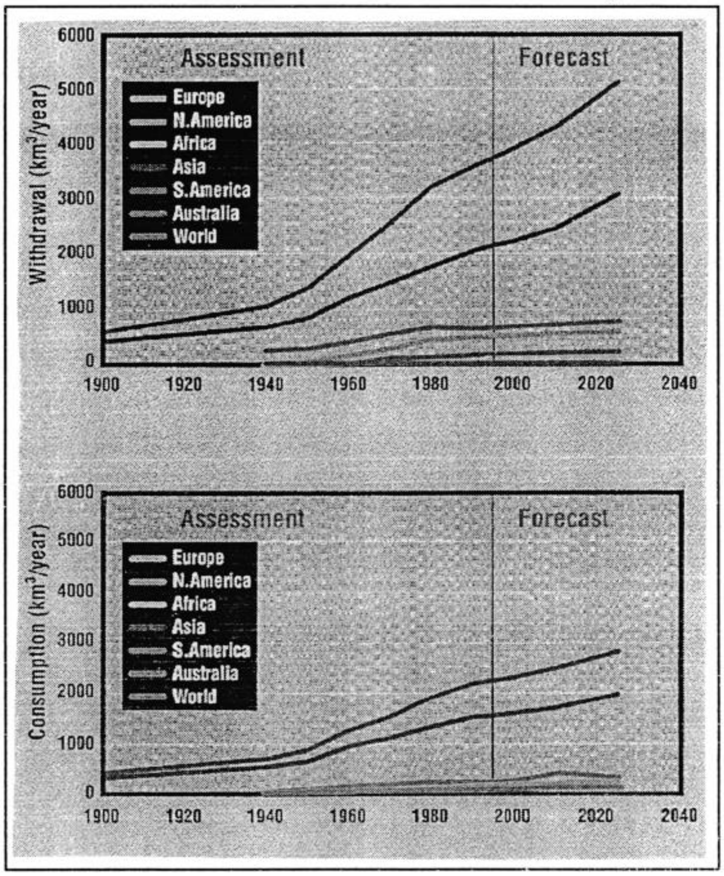

The major water user sectors differ from one country to another based on the above mentioned factors. For example, the major water consumer sector in North America is industry; being irrigated agriculture in Asia, Africa, and South America. In general, the irrigation sector is generally the sector which experiences the highest water withdrawal and the highest consumption due to the involved high losses.

Source: Igor A. Shiklomanov (1998)

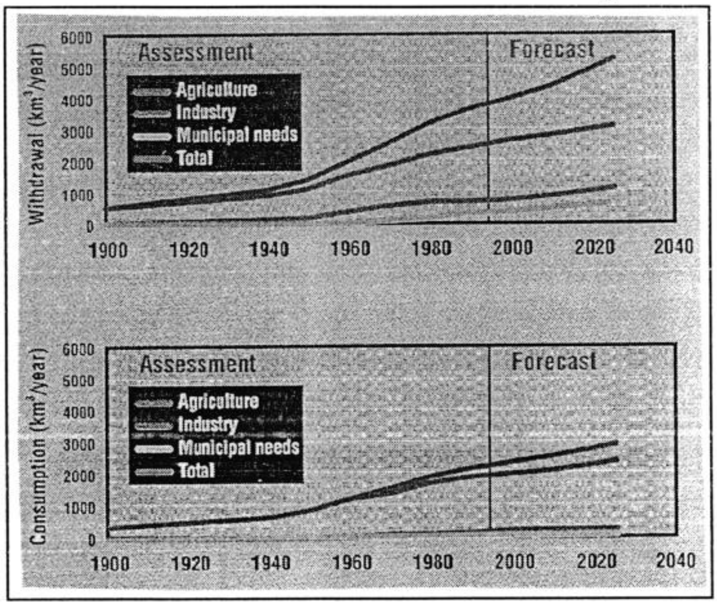

Water Availability and Deficits

The availability of water is not solely a function of volumes, but also of human factors. Human factors affect water availability in various forms. They can either reduce available water (e.g. deforestation increased evaporation, etc.) or promote it (e.g. decreased evaporation by changing water storage modes). This is in addition to the impacts of global warming which are still not clearly defined in many regions of the world.

Sorce: Igor A. Shiklomanov (1998)

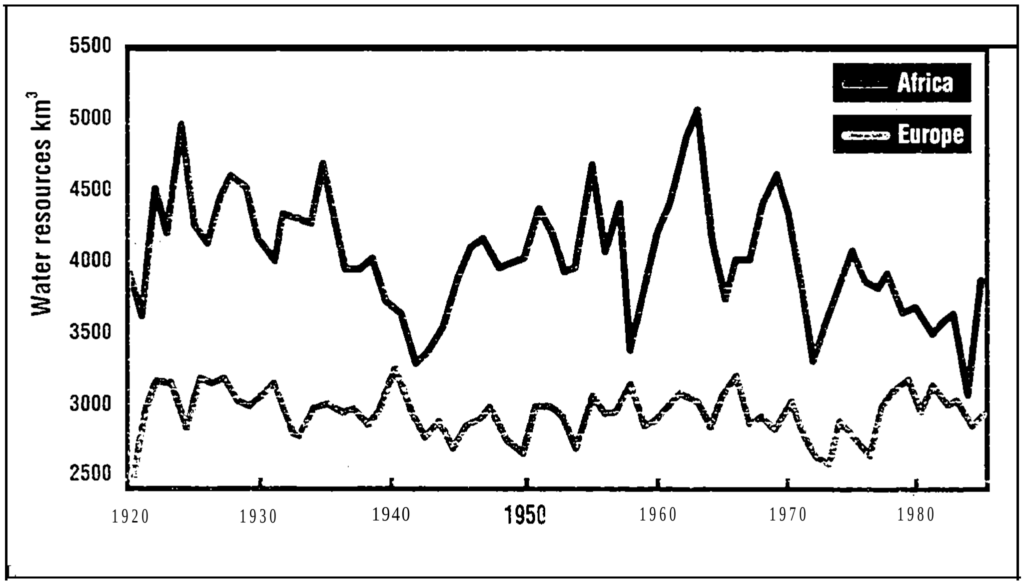

Of Importance here is the type of distribution. of fresh water resources on earth which does not follow the population growth. If only renewable water is considered as available, statistics indicate that 75% of the world population has a specific water availability around 5,000 m^3 per year per capita, with 35% having less than 1,000 m^3 per year per capita. This situation will deteriorate further in the beginning of the next century, especially in arid regions.

SUSTAINABLE DEVELOPMENT-CONCEPT AND CONSTRAINTS

The Concept

Interest in sustainable development has arisen as a consequence of national, regional and, subsequently, global concerns about the environment and in particular its natural heritage. It began to articulate in Europe and North America in the 1960s and 1970s. In 1983, the U.N. General Assembly established the World Commission on Environment and Development and received the report on the so-called "Our Common Future" (Brundtland Commission, 1987). Good Development will protect and enhance the environment; attention paid to environmental concerns will strengthen developmental progress and projects.

The FAO definition adopted by its council in 1988, in the context of agriculture, forestry and fisheries is: "Sustainable development is the management and conservation of natural resource base and the orientation of technological and institutional change in such a manner as to ensure the attainment and continued satisfaction of human needs for present and future generations. Such sustainable development (in agriculture, forestry, and fishery sectors) which conserves land, water, plant and animal genetic resources, is environmentally non-degrading, technically appropriate,economically viable and socially acceptable".

In the run-up of the UNCED "The Earth Summit 92", the International Conference on Water and the Environment (ICWE), concluded with the Dublin statement on Water and Sustainable Development: "Scarcity and misuse of fresh water pose a serious and growing threat to sustainable development and protection of the environment; human health and welfare, food security, industrial development and the ecosystems on which they depend, are all at risk unless water and land resources are managed more effectively in the present decade and beyond they have been in the past".

Some Issues of Sustainable Development

Identification of development aspects that make development unsustainable has been more successful than the development of remedial measures that reduce or eliminate those undesirable effects. For example, if sustainable groundwater resources development is considered, it is known that pumpage in excess of long-term recharge will result (in the long or short term) in uneconomic (or even in stopping the) development. Similarly, if excessive use of fertilizer and pesticide in agriculture is experienced by farmers, the use of groundwater for drinking will be impaired.

Reasons behind the failure of developments include, among others:

1) Short-versus Long-term Considerations: Any plan that does not consider the conflict of short-versus long-term sustainable development and attempt to identify realistic alternatives to overcome the problem, is expected to fail.

2) Externalities: Externalities occur when private costs or benefits do not equal social costs or benefits. Individuals operate primarily on the basis of their own private costs (e.g. cost of sewage/waste disposal, cost of water, etc.) and benefits. If they perceive opportunities which could reduce their costs and/or increase potential benefits, they often take actions which could be beneficial to them but are unlikely to serve the common good. A proper solution would be the internalization of external cost by various means (e.g. taxes, subsidies, regulations, etc .) .

3) Risks and Uncertainties: For example, the increase in population dictate intensive agricultural production, which is generally accompanied by intensive water development. This may create conflicts among the various uses either due to other economic types of demands and/or due to the reuse of low quality water. This issue will become more important in the future and needs a change from individual development and management to integrated development and management that is accompanied by close monitoring and evaluation of actions.

GROUNDWATER PROTECTION FOR SUSTAINABLE DEVELOPMENT

The Framework

A unique framework for groundwater protection is generally not possible as the forms of groundwater deterioration are diversified. However, there is one agreed upon issue regarding groundwater protection which implies preventing or at least minimizing groundwater deterioration. This issue is based on the fact that prevention is always simple and less expensive than restoration.

In general terms, the framework for groundwater protection constitutes of a series of actions. Some are preventive while others are corrective. These should be directed to both the software as well as the hardware.

Preventive measures

Preventive measures include, among others: (i) groundwater assessment; (ii) groundwater resources planning; (iii) groundwater resources management; and (iv) monitoring. Table 1 gives a summary of the main elements constituting groundwater protection prevention measures.

Groundwater assessment is the base for any sustainable development. A proper assessment of the resource dictates a proper understanding of the groundwater system (configuration), the conceptual frame (present state) and system response to future stresses. The key of such a proper assessment is the availability of data and information, and well trained professionals who can apply all types of technologies in determining the state of the system (static and dynamic). Various tools can be applied, including surface and sub-surface investigations, hydrogeological maps, potential maps, vulnerability maps, models, etc.

Planning of groundwater development undertakings, on the other hand, needs a clear identification of water needs. Planning should be based on the interaction between the planners, managers, policy makers, and the public. Involvement of the public at the various stages of the planning is a key issue in ensuring the sustainability of the undertakings. Long- as well as short-term plans should be clear and well oriented to the needs. It should be stressed here that the plans should be dynamic, i.e., plans should be revised at proper time spans.

Groundwater management should always be carried out in the framework of integrated management to ensure the sustainability of the resource. Technical tools, including models, should be considered only as support tools. Pilot schemes are good means in the testing of new management policies/strategies, and dessimination of results to decision makers and the public.

Finally, monitoring represents the end of the chain. Monitoring should not be considered a nuisance, but a support for early corrections of management and planning activities. Monitoring does not only consider the system response, but also the users response. As such, monitoring should be included in the planning and carried out at all stages.

Monitoring can be implemented at various levels and scales, including regional, project, or problem specific; each of which has its objectives and design. Feed back from the monitoring activities should be disseminated to the users, polluters, and decision makers. Results are also used to enforce the groundwater protection laws and to decide upon appropriate corrective measures.

Table 1. A Possible Classification of The Groundwater Preventive

Measure/Issue	Hardware	Software
1. Groundwater Assessment	1.1 Proper identification of the static properties of the system, including its boundaries, geology, groundwater vulnerability to pollution, etc. 1.2 Proper identification of dynamic conditions, including interaction with other water bodies, water fluctuation, quality, recharge-discharge, land use, groundwater use, etc.	1.1 Human resource through systematic t
2. Groundwater Resources Planning	2.1 Proper assessment of water needs. 2.2 Application of conservation means, including conjunctive use of water resources. 2.3 Application of land and water planning. 2.4 Application of new technologies and instruments, including GIS, models, etc. 2.5 Long-term as well as short-term planning is a must.	2.1 Involvement of through proper and t users/stakeholder pa the planning phases. 2.2 Human resource
3. Groundwater Resources Management	3.1 Application of proper tools, including management models. 3.2 Application of integrated water resources management means. 3.3 Implementation of pilot projects and dissemination of findings.	3.1 Raising Public a management issues. 3.2 Human resource
4. Monitoring Groundwater Performance	4.1 At the land surface, including land use, emissions, etc. 4.2 In the unsaturated zone. 4.3 In the saturated zone. 4.4 On regional (reference) as well as for problem-specific.	4.1 Raising public a impacts based on fin 4.2 Involvement of t monitoring.

Corrective Measures

In the case of groundwater degradation, which could be a result of the feed back from the monitoring system, corrective measures should be implemented before the problem becomes more severe. Corrective measures, include among others: (i) artificial recharge, which is directed to correct depletion of groundwater, sea water intrusion, deterioration of groundwater quality? etc.; (ii) restrictions on land use, aiming at minimizing the long-term effect; (iii) treatment of effluent at the source or its direction to other sites of less importance with respect to groundwater; or (iv) other remedial measures, including removal of soil, etc.

SPECIFIC WATER ISSUES IN ARID ZONES

Definition of Arid Zones

A precise definition of arid zones is not straightforward, as each discipline can have its own view point. However: for hydrologists, arid zones are those regions characterized by low average rainfall and the absence of perennial rivers. Generally, these basic criteria are correlated with high mean annual temperatures and low atmospheric humidities giving rise to a high rate of potential evapotranspiration. Water resources are mainly limited to groundwater, which may be derived from annual, ephemeral or fossil replenishment, by a variety of possible recharge mechanisms.

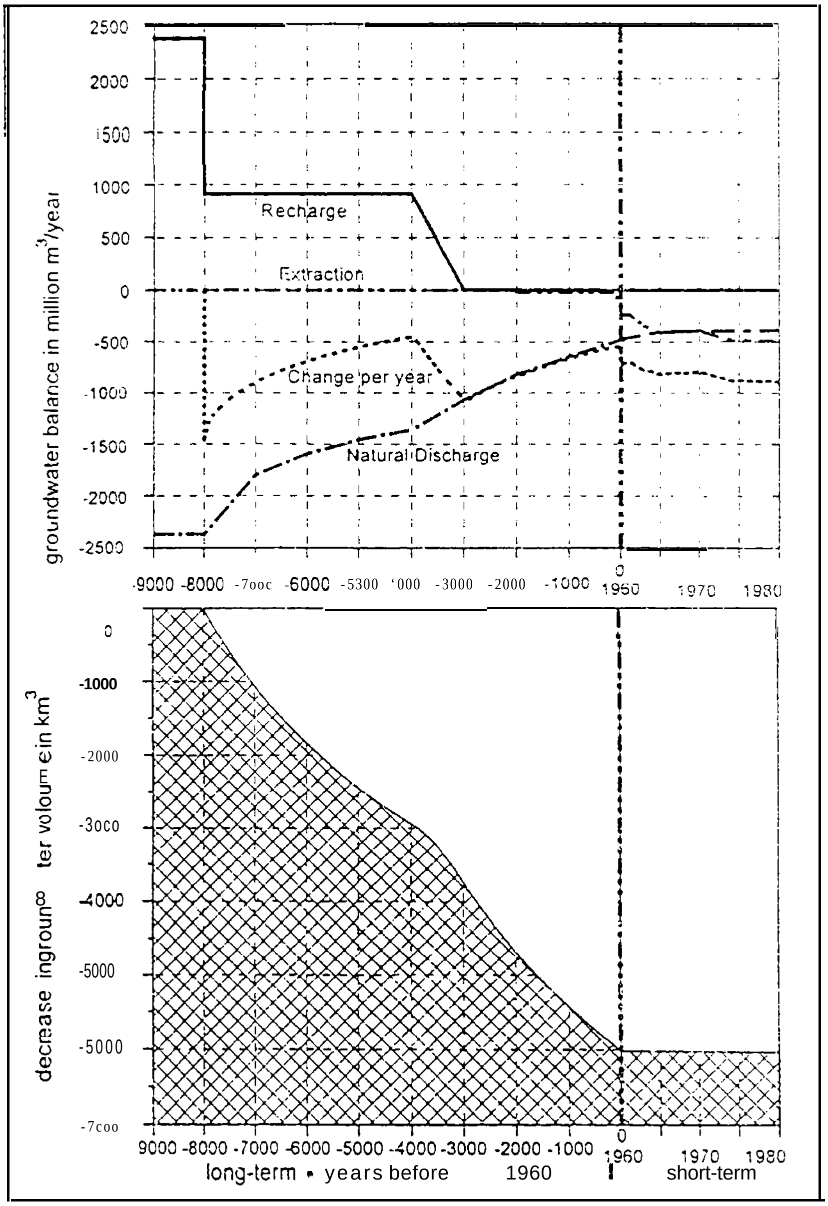

The variability of groundwater recharge in such zones is very large. Replenishable groundwater resources may be available in regions where present day recharge is potentially very low or nil (e.g. Nubian Sandstone in North Africa). Similarly, it may not be possible to correlate directly the presence of higher rainfall belts in certain areas in recent years with the size of the local groundwater storage.

Issues of Groundwater Development and Management in Arid Zones

The main aim of groundwater development and management is to ensure the sustainability of the resource and developments based on it. This requires, as mentioned previously, a good knowledge of the system configuration, present state, and response to future stresses.

System Configuration: Geophysical investigations (especially geoelectrical profiling), which are generally considered cheap tools in defining the configuration of aquifer systems, meet several limitations in arid zones. Main reasons are: (i) the relatively dry medium in the shallow horizons which make them very resistant resulting in false resistivity; and (ii) deep horizons may contain saline water obeying the density gradient, making the penetration of the signal difficult and its discrimination is low.

Present State: A good understanding of the present state of the system is generally based on clear identification of boundaries, flow rates, and hydraulic characteristics. The main problems in arid zones is the proper determination of the water balance components and the hydraulic continuity.

> The water balance reads, in its simplest form:
>
> *RECHARGE = DISCHARGE + CHANGE IN STORAGE*
>
> Recharge can be natural (rainfall) or artificial. Discharge can also be natural (visible as sinks or seeps, or invisible as evaporation or uptake by plants) or artificial (e.g. wells, surface and subsurface drains). Change in storage is a function of the change in groundwater heads and the aquifer storativity .

The question of recharge is one of the most critical factors for groundwater management in dry areas. If recharge is occurring, further important problems arise dealing with possible mechanisms of recharge, e.g. : (i) vertical direct infiltration of rains; (ii) lateral seepage of river flood water and groundwater from adjacent aquifers; and (iii) upward leakage from deep aquifers.

Whatever the depth of the water table, evaporative discharge is expected through the soil zone or through sabkas. The phenomenon of aquifer discharge is relatively simple to evaluate when it gives rise to permanent surface runoff. This is not the case in arid zones where perennial surface flow does not exist. In coastal regions, however, discharge may occur directly to the sea. In internal drainage basins which occur widely in arid and semi-arid zones, discharge occurs either through springs (oases) or though diffuse evaporation across the unsaturated zone. The latter process is the most frequent, although very difficult to quantify, it is very important for the groundwater balance.

The need for an accurate assessment of whether a small rate of recharge is occurring appears rather trivial when the withdrawal from an aquifer clearly surpasses the present day maximum possibilities of infiltration through the catchment area. This problem, however, is not specific to arid zones since most of the largest, confined aquifers are overexploited as evidenced by pressure decreases which sometimes may have important consequences on soil stability.

Estimation of groundwater flow depends to a large extent on groundwater heads and hydraulic characteristics. In the majority of the sediment basins in arid regions, estimation of hydraulic characteristics through aquifer tests is very difficult due to the associated long recovery time. In the case of fractured formations, it becomes even more difficult to investigate the hydraulic continuity.

In arid regions, where deep aquifers provide sometimes the only source of water supply, the question is of major importance for groundwater management. The major problem of groundwater mining in arid regions is mainly related to the main unconfined aquifers. At A first glance, groundwater mining can also be deduced from hydraulic balances and decreases in the depth of the water table. However, for both confined and unconfined aquifers the answer to this important question appears rather complex and strongly dependent on the time scales of replenishment and of development.

Groundwater Quality: Groundwater salinization may occur according to several processes, including: (i) concentration through evaporation of surface water before or during infiltration of flood episodes; (ii) diffuse discharge through unsaturated soils between two episodes of sporadic recharge; (iii) leaching by surface waters of salt beds within the aquifer; (iv) chemical weathering of silicates which leads to the formation of clay minerals and oxides with subsequent increase in ions (particularly Ca^{2+} and Na^{+}); (v) irrigation return flow; and (vi) fertilizer application.

A special case of salinization exists in coastal aquifers. Here, the heavier sea water tends to flow inland below the fresh groundwater, even if the net inflow is toward the sea. Thus, even under natural conditions, it is common that in coastal aquifers, fresh water - flowing seaward - overlies stagnant sea water in deeper parts of the aquifer. Pumping from such aquifers would attract the deep salt water until the well is affected. This process is complicated and needs integration of various tools to identify the source of saline water.

NETWORK ON GROUNDWATER PROTECTION IN THE ARAB REGION

Specifics of the Arab Region

The Arab region is suffering at present from water scarcity, which will become more severe in the next century. The prevailing arid to semi-arid climate is generally a common feature. Most rivers originate outside the borders of the region and their water is almost fully utilized. Although extensive aquifer systems are encountered, groundwater contained in such systems is deep and almost non-renewable (at present). Renewable groundwater, on the other hand, is limited to specific regions where aquifers of limited extent are prevailing. The percapita fresh water in some countries is as low as 100 m^3/year, or even less. This has already resulted in or will soon dictate recycling of used water (multiple use); thus approaching closed water systems.

The present problems related to groundwater management in the Arab region can be summarized as follows: (i) extensive drawdowns that are affecting sustainability of the resource, especially the socio-economy; (ii) saline water intrusion and upconing in coastal aquifers; (iii) pollution from various sources; (iv) lack of proper management tools and related knowledge; (v) poor enforcement of legislation; and (vi) lack of public participation and public awareness.

Groundwater protection is thus a major challenge for the sustainable development of the region. It dictates the initiation and implementation of several actions, including: (i) the implementation of monitoring system(s); (ii) development of proper tools to support groundwater protection, e. g . hydrogeological maps, groundwater potential maps, groundwater vulnerability maps, etc. ; (iii) enforcement of legislation, including well licensing, types of agro-chemicals, proper disposal of effluents, etc. ; (iv) special attention to environmental concerns and caution with the use of sewage water in irrigation, which should be limited to regions of low vulnerability; (v) raising public awareness in relation to the protection of the resource; (vi) development of simple technologies to protect groundwater, which should be based on multi-criteria analysis of their appropriateness, capability to improve, and adoption by the users; (vii) preparation for significant changes which may present opportunities, but with potential adverse impacts.

Objectives of the Network

The main objectives of the network are to promote information exchange among researchers and decision makers within the Arab region and other regions; and to demonstrate the technical, economical, institutional, and environmental feasibility and constraints of groundwater protection means and technologies.

The program is thus expected to contribute to rational development and appropriate management of groundwater resources leading ultimately to sustainable socio-economic development through: (i) assisting in strengthening and coordinating research concerning groundwater assessment, planning, and management; (ii) assisting in the transfer of adequate technology from other countries to the Arab region and among the Arab countries; and(iii) assisting in disseminating and exchanging information on the state-of-the-art of groundwater protection though meetings, workshops, etc.

Selection of Priority Areas for Cooperation/Coordination

The main priority areas for cooperation and coordination are as follows:

- Initiation of a “Data Base” for Groundwater protection.

- Development of “Manuals” in various areas related to groundwater protection (various users categories). The first manual will be targeted to technicians and young hydrogeologists responsible for the collection of hydrogeological data.

- Two on-going training programs in the region will be considered as the main official programs, the “groundwater protection” given by the Research Institute for

Groundwater, and "groundwater hydrology" given by Bahrain University. Other ad-hoc training courses covering specific topics are also encouraged (sea water intrusion, artificial recharge, etc.).

- Development of "Systematic approaches to research and implementation" for the priority aquifers.

Type of aquifer and threat(s)	Examples	Countries
1. Regional non-renewable aquifers with deep groundwater, subjected to overexploitation.	Nubian sandstone, Continental Intercalaire	Egypt, Libya, Sudan, Tunisia, Algeria
2. Coastal aquifers, subjected to saline water intrusion (sea or formation)	Mediterranean, Others	Egypt, Syria, Morocco
3. Aquifers underlying wadis, essentially for integrated research to enhance water conservation	Various	Many countries
4. Local aquifers subjected to recharge with non-conventional water (e.g. sewage), subjected to high pollution risks	Various	Many

- Selection of suitable "Dissemination means" and their preliminary outlines (web site, newsletter, etc.).

- Development of appropriate awareness means.

CONCLUSIONS AND RECOMMENDATIONS

Conclusions

Water is the most spread natural resource on earth. It plays a vital role in both the environment and human life. Groundwater is the most widely distributed fresh water resource on earth. The rise and decline of civilizations have been linked to climatic changes which, in mm, controlled the natural recharge of aquifers and regulated the pollution of groundwater and soils.

In addition to secular changes in groundwater caused by climatic variations, there are now serious threats to both quantity and quality of groundwater resources caused by the accelerating human intervention.

The main challenge facing the present and future availability of groundwater is "How to sustain this precious natural resource and protect it from degradation?". Groundwater protection is thus a major challenge.

The problems related to groundwater protection are more serious in arid zones due to the hydrogeologic complexity of water systems. For this reason, UNESCO identified as a priority theme "Groundwater at risk". Under this theme, among others, two networks have been initiated, one on wadi hydrology and the other on groundwater protection in the Arab region (being one of the most arid regions in the world). Various types of activities have already been identified and are under implementation, including: (i) initiation of a "Data Base" for groundwater protection; (ii) development of "Manuals" in various areas related to groundwater protection (various users categories); (iii) regular training programs for various categories; (iv) development of "Systematic approaches to research and implementation" for the priority aquifers; (v) development of suitable "Dissemination means"; and (vi) development of awareness means.

Recommendations

Groundwater protection is a major challenge in arid region. It requires several actions:

1) Clear and systematic approach to protection.

2) Systematic training of professionals and technicians.

3) Development of proper tools for groundwater protection, e.g. hydrogeological maps, groundwater potential maps, groundwater vulnerability maps, monitoring systems, etc.

4) Development of appropriate tools for groundwater assessment and protection (e.g. isotope).

5) Enforcement of legislation, including licensing, types of agro-chemicals, and proper disposal of effluent, etc.

6) Increasing public awareness on water protection.

7) Selection of water conservation technologies based on multi-criteria analysis of their appropriateness, capability to improve, and adoption by the users.

8) Preparation of decision makers and the public for significant changes in water management styles which may present opportunities, but with potential adverse impacts, on disadvantaged groups.

REFERENCES

ACSAD (1997). Wadi resources in the Arab region. The seventh regional UNESCO meeting, Rabat, Morocco.

ATTIA, F.A.R. (1996). Community participation-a mean for water conservation in Greater Cairo. Proceeding of the preparatory meeting of Habitat II, Beijing, China.

ATTIA, F. A.R. (1997). The vulnerability of groundwater to pollution and strategies for its protection under the farming conditions in the Mediterranean countries. Proceedings of the international conference on " Water management, salinity and pollution control towards sustainable irrigation in the Mediterranean region", Bari, Italy, pp 23-44.

EDMUNDS, W .M. (1996). Indicators in the groundwater environment of rapid environmental change. Geoindicators, ed. Antony R. Berger and William J. Aims. Rotterdam, Balkema. : 135-153.

Igor A. Shilomanov (1998). World water resources-A new appraisal and assessment for the 21st century, A UNESCO technical document.

JEAN MARGAT (1996). Les eaux souterraines dans le bassin mediterraneen. (PNUE).98p.

Ulf Thorweihe and Manfred Heinl (1998). Aquifers of the major basins non renewable water resource, Groundwater resources of the Nubian sandstone aquifer system-Synthesis; OSS.

Keynote Address

HOW CAN ISOTOPE RESEARCH CONTRIBUTE TO UNDERSTANDING AND MANAGING WATER QUALITY ISSUES?

N.E. Peters
US Geological Survey,
Atlanta, Georgia, United States of America

Advances in the understanding of hydrological processes, particularly water quality, have increased rapidly over the last few decades. One major, recent factor leading to improved knowledge in the field has been the use of isotopes in conjunction with hydrometric and biogeochemical information. The choice of isotopes is presently constrained as some elements are easier to study than others due to different levels of progress in experimental technology and sample processing techniques. This presentation will explore schemes for the successful use of isotopes in water-quality issues by discussing several recent advances in the comprehension of hydrological processes, and will suggest some fertile areas for research. The use of $^{87}Sr/^{86}Sr$ has improved the understanding of the relative contributions of weathering, general patterns of long-term mineral transformations, water-quality evolution within catchment pathways, and the biological cycling of base cations, particularly Ca^{2+}. The simultaneous analyses of $\delta\ ^{14}N$ and $\delta^{18}O$ of NO_3^- have helped to determine the role of sources such as atmospheric deposition and fertilizer or manure application and oxidation state in N cycling and nutrient transport. These isotopes have also been used to assess the efficiency and mechanisms for N removal related to implementation of best management practices for specific ecosystem types such as wetlands. A multi-component approach using elemental concentrations and ^{11}B, ^{87}Sr, and ^{18}O has been used to study the origin of salinity and formation of saline plumes in groundwater. In all hydrological studies, it is important to determine water pathways, fluxes and residence times in order to understand water-quality evolution or genesis. Consequently, isotopes have been very useful to date young groundwater using ^{3}H, ‘He, ^{85}Kr, and ^{35}S and to date ice cores and sediments using

^{14}C and ^{36}Cl. The ice cores and sediments can then be studied to determine long-term **changes** in climate with the use of ^{18}O and ^{13}C. Isotopes are useful in studying other paleo-environmental indices such as groundwater (D, ^{18}O, ^{13}C, ^{36}Cl), clay minerals (^{13}C, D, ^{18}O), pedogenic carbonates (^{13}C, ^{18}O), tree rings (D, ^{18}O, ^{14}C), and plant fossils (D, ^{18}O, ^{13}C). Relative enrichments of other elements with respect to the isotopic content suggest patterns of chemical evolution. Patterns, processes and rates of sediment erosion and deposition and associated transport and transformation of pesticides and herbicides have been discovered using ^{10}Be, ^{7}Be, ^{137}Cs, and ^{210}Pb. The importance of biological activity in cycling S and N has been quantified under controlled conditions and from experimental field investigations of pathways and transport rates, using ^{34}S ^{35}S, and ^{14}N. The importance of atmospheric S sources in headwater watersheds and the subsequent transformation and transport of the element have been elucidated using ^{35}S and ^{34}S. In most of these research areas the greatest advances were made by establishing comprehensive data collections and data analysis schema, which included hydrometric and ancillary biogeochemical information. For example, an evaluation of only the ^{87}Sr/^{86}Sr ratio of groundwaters does not show the entire process of water-quality evolution. Additional solid phase data, hydrometric information and a broader spectrum of hydrochemistry provides complementary information on the direction and potential magnitude of transport and processes controlling temporal variations, solid phase adsorption characteristics and potential end-member contributions to ^{87}Sr/^{86}Sr, solid and liquid Sr concentrations, and relative compositions of associated elements. Finally, a discussion will be given on the use of isotopes to ascertain the biological processes in - and energy flow through ñ aquatic food webs, which are central to most of the critical water-quality health-related issues.

Development of Accelerator Mass Spectrometry (AMS) for the Detection of ^{81}Kr and first application to groundwater dating

P. Collon, W. Kutschera
Institut für Radiumforschung und Kemphysik der Universität Wien, Boltzmanngasse 3, A-1090 Wien, Austria

B.E. Lehmarm, H.H. Loosli, R. Purtschert
Universität Bern, Physikalisches Institut, Sidlerstrasse 5, CH-3012 Bern

A. Love, L.Sampson
Primary Industries and Resources of South Australia, 101 Grenfell St. Adelaide, Australia

B. Davids, M. Fauerbach, R. Harkewicz, D.J. Morrissey, B.M. Sherrill, M. Steiner
National Superconducting Cyclotron Laboratory, Michigan State University, East Lansing, MI 48824, USA

R.C. Pardo
Physics Division, Argonne National Laboratory, Argonne, IL 60439, USA

M. Paul
Racah Institute for Physics, Hebrew University of Jerusalem, Israel 91904

Abstract: Isotopic ratios of ^{81}Kr/Kr were measured with accelerator mass spectrometry in pre-nuclear atmospheric krypton and in modem krypton. Within the experimental uncertainty (±30%) the ^{81}Kr/Kr ratios were found to be the same. This establishes ^{81}Kr ($t_{1/2}$ = 230,000 years) as a long-lived cosmogenic radionuclide essentially unaffected by anthropogenic contributions. First applications of ^{81}Kr to groundwater dating in the Great Artesian Basin of Australia enabled to obtain mean residence times of 225,000 to 400,00 years.

1 Introduction

The main interest of ^{81}Kr lies in the possibility it provides for dating deep ice from the polar ice caps, and old groundwater. Due to its favourable geochemical properties it is possibly the only cosmogenic radionuclide that has the potential to become a reliable absolute chronometer for these applications. However the extremely low concentration of ^{81}Kr in these reservoirs (≈1000 atoms per kg ice or water) demands a very high overall detection efficiency.

The development of an AMS technique for the detection of ^{81}Kr as well as the first application of this method to date groundwater samples from the Great Artesian Basin of Australia has been an ongoing program at our Institute. The first measurement of the ^{81}Kr concentration in atmospheric krypton using AMS in 1994 [1] and the first experimental comparison of the ^{81}Kr concentration in pre-nuclear and modem atmospheric krypton samples in 1996 [2] laid down the base for this first dating application.

2. Comparison of pre-nuclear and modern atmospheric krypton

Our initial result obtained in 1994, ^{81}Kr/Kr = $(5.3\pm1.2)\times10^{-13}$, agrees well with previously known values from low-level counting of pre-nuclear krypton [3, 4]. This experiment encouraged us to pursue this measuring technique as part of a program to develop AMS for long-lived noble gas radionuclides [5] using the Superconducting Cyclotron facility of Michigan State University. The main technical problem for the detection of ^{81}Kr with AMS resides in the separation of the ^{81}Kr from the isobaric ^{81}Br background and as there is still very little understanding of the source of bromine we concentrated our efforts on the separation of ^{81}Kr from ^{81}Br using full stripping at high energies (see Fig. 1).

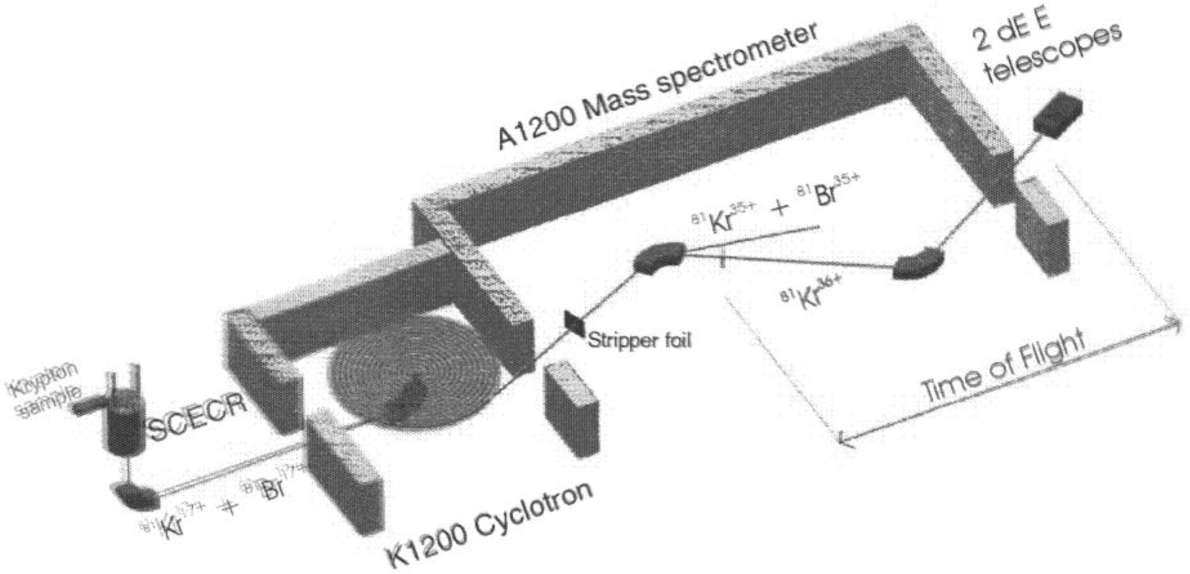

Fig. 1. Schematic view of the experimental set-up at Michigan State University. The superconducting ECR (SCECR) ion source coupled to the K1200 cyclotron and the A1200 mass spectrometer is used to separate the ^{81}Kr-^{81}Br isobars using full stripping at high energies. The ions emerging from the foil were analysed in the A1200 mass spectrometer.

Due to the very small mass difference between the isobars ($\Delta M/M = 3.7\times10^{-6}$) a ^{81}Kr-^{81}Br mass separation in the cyclotron is not possible and as a result, it was necessary to develop the following detection set-up: after the initial acceleration of the $^{81}Kr^{17+}$ ions to 45 MeV/A in the cyclotron, the ions pass through a Be stripper foil (18.8 mg/cm^2). The fully-stripped $^{81}Kr^{36+}$ ($\approx$70%) are then separated from the $^{81}Br^{35+}$ using the A1200 mass spectrometer. Various experimental configurations as well as support gasses for the ion source and stripper foils have been tested in an attempt to optimise this method.

In order to handle the injection of small krypton gas samples ($\approx$0.5 cm^3 gas STP) to the ECR ion source it was also necessary to develop a portable computer controlled gas handling system [1, 2].

In 1996, a subsequent AMS experiment [2] enabled us to determine isotopic ratios of ^{81}Kr/Kr in the range of 10^{-13} in pre-nuclear atmospheric krypton and in modern krypton. Within our experimental uncertainty (see Fig. 2) the ^{81}Kr/Kr ratios were found to be the same. This established ^{81}Kr as a long-lived cosmogenic radionuclide essentially unaffected by anthropogenic contributions, and therefore well suited for dating applications. The anthropogenic "cleanliness" of ^{81}Kr is in accord with estimates for contributions from various human activities.

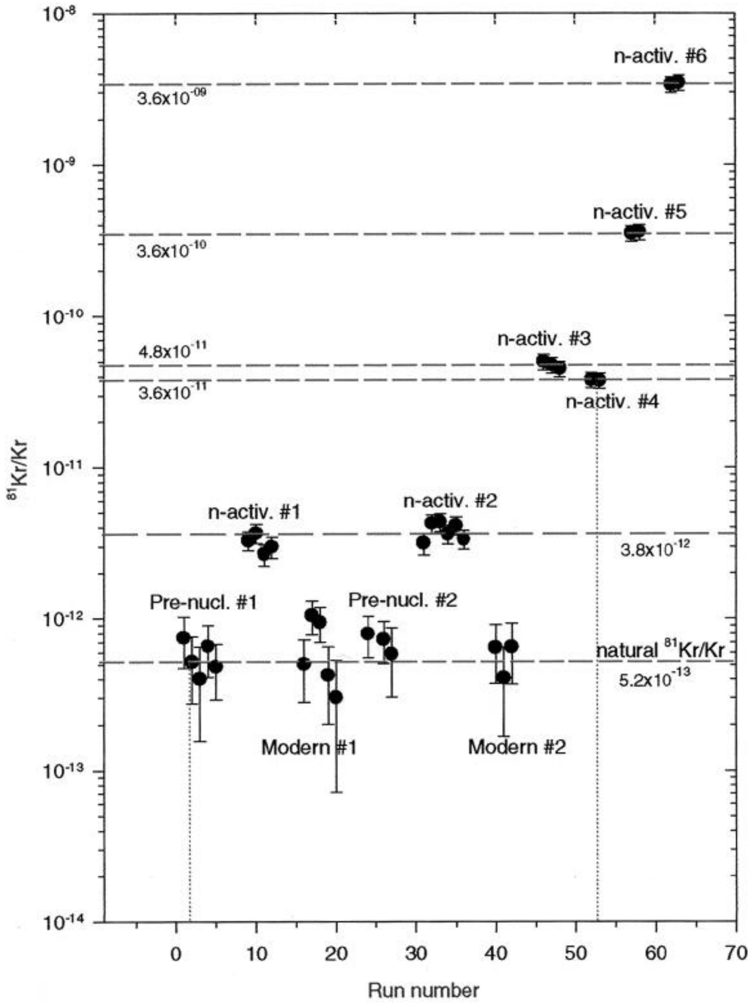

Fig. 2. Summary of all ^{81}Kr/Kr ratio measurements [2]. Each point in this figure represents an individual run of 60 minutes. The runs are grouped together by samples in a chronological order. The various samples were as follows: 1) Pre-nucl. #1 and #2 correspond to the 2 pre-nuclear krypton samples obtained from the University of Bern, 2) Modern #1 and #2 correspond to samples obtained from a present-day krypton gas bottle, 3) The n-activated samples correspond to natural krypton samples that were neutron activated at the TRIGA research reactor in Vienna. We produced 5 batches with ^{81}Kr/Kr ratios ranging from 10^{-12} to 10^{-9}. The dashed horizontal lines correspond to nominal ^{81}Kr/Kr ratios. The individual ^{81}Kr/Kr ratios measured with AMS were determined relative to those of runs #2 and #53 (dotted lines) which were normalised to $5.2x10^{-13}$ and $3.6x10^{-11}$.

These results encouraged us to undertake the next step in this program: The ^{81}Kr dating of groundwater samples.

3. First applications to groundwater dating

In a first project to date groundwater from the Great Artesian Basin of Australia, four wells where sampled during a field trip in January 1998. The sampling sites are in the south-west segment of the GAB, approximately 1000 km north to north-west of Adelaide, South Australia (see Fig. 3). At each sampling site 16,000 litres of water where degassed on-site using a fully automatic water degassing system, developed at the University of Bern. The resulting 320 litres of gas per well where stored in standard gas bottles and then shipped to Bern where the krypton gas was separated in an elaborate procedure from the extracted gasses.

The resulting pure Krypton samples with a volume of ~0.5cm^3 gas STP where then sealed in quartz ampoules and shipped to Michigan State University.

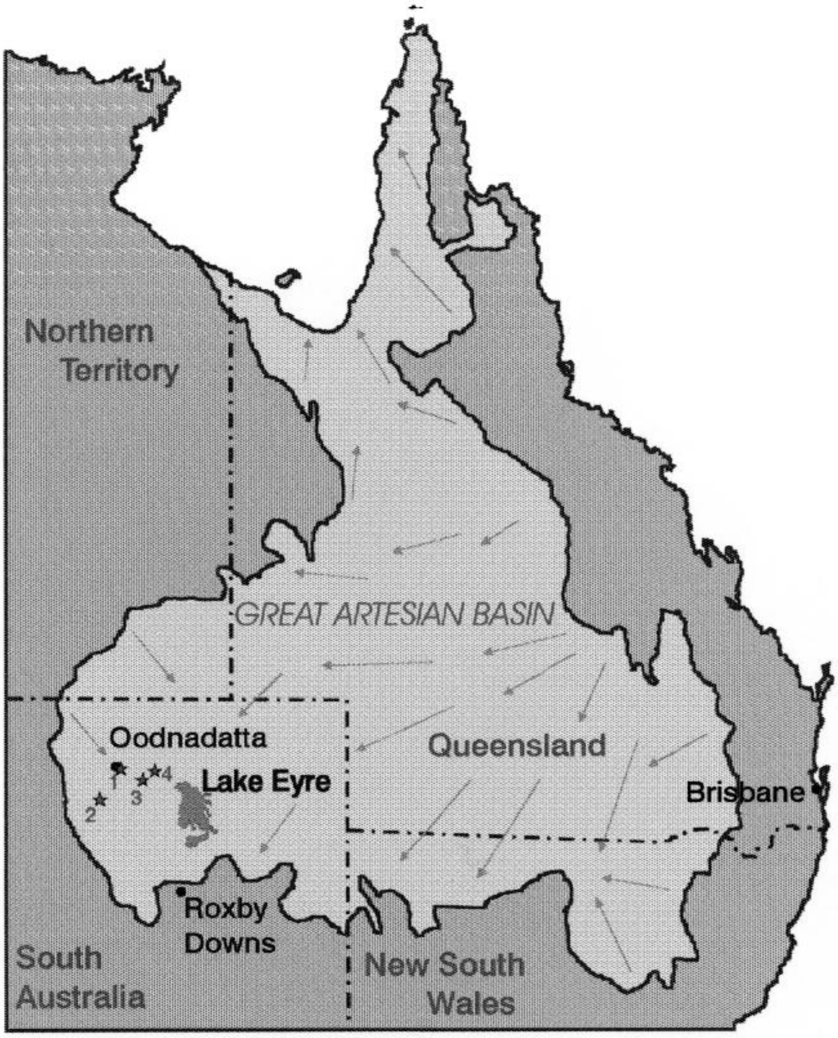

Fig. 3. Map of the Great Artesian Basin in Australia. The four sampling sites are represented by the four red stars and referred to by their well name: 1) Oodnadatta, 2) Raspberry Creek, 3) Watson Creek, 4) Duck Hole. The arrows represent the general flow direction of the groundwater in the basin.

The AMS measurement of the krypton samples at MSU resulted in clearly depleted ^{81}Kr/Kr ratios for the groundwater samples with respect to the atmospheric value. This enabled us to determine following ages for the groundwater samples (see Fig. 4):

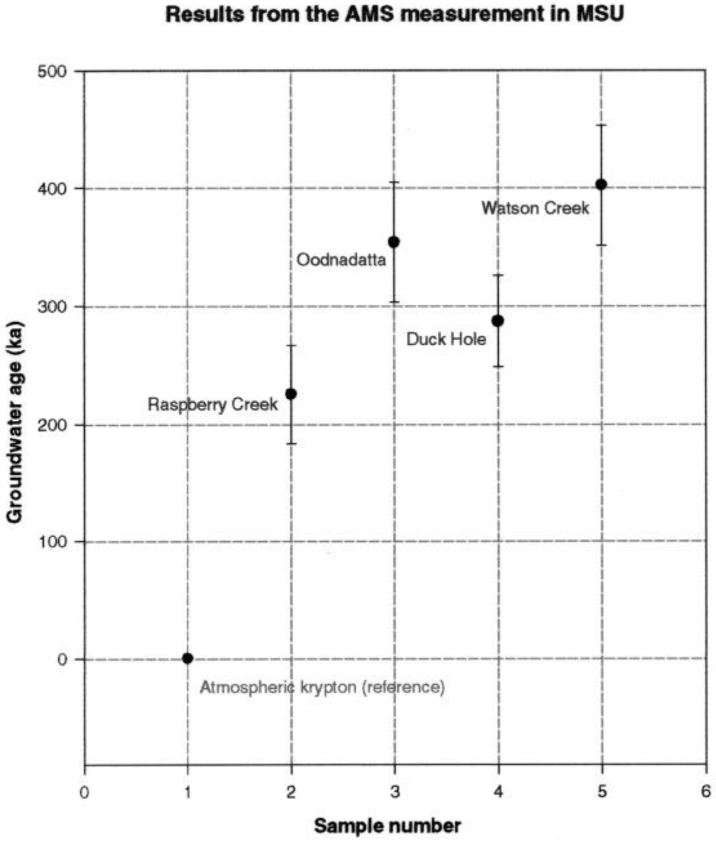

Fig. 4. Ages for the groundwater samples as determined using the AMS counting method. The sample names are derived from the geographic location where they where taken. The ratios where obtained relative to the one of an atmospheric Kr sample measured during the same experiment. Uncertainties in the groundwater samples are mainly due to counting statistics. For the calculation of the mean residence time, the uncertainty of the ^{81}Kr half-life (4.8%) must also be considered. All uncertainties are standard deviations (1 σ)

The interpretation of these results as well as comparisons with ^{36}Cl data are still being worked on. However, our results confirm ^{81}Kr as a reliable tool to date old groundwater and opens up the possibility for an investigation on a much larger scale.

For this project we thankfully acknowledge the support of the *Hydrology Section of the IAEA*.

REFERENCES

[1] P. Collon, T.A. Antaya, B. Davids, M. Fauerbach, R. Harkewicz, M. Hellstrom, W. Kutschera, D.J. Morrissey, R.C. Pardo, M Paul, B.M. Sherrill, M. Steiner., *Measurement of ^{81}Kr in the atmosphere*, Nucl. Instr. Meth. B123 (1987) 122.

[2] P. Collon, D. Cole, B. Davids, M. Fauerbach, R. Harkewicz, W. Kutschera, D.J. Monissey, RC. Pardo, M Paul, B.M. Shenill, M. Steiner., ***Measurement of the long-lived radionuclide ^{81}Kr in pre-nuclear and present-day atmospheric krypton,*** Accepted for publication in Radiochimica Acta (In press).

[3] H. Oeschger, ***AMS and Ice Core Research,*** Nucl. Instr. Meth. B29 (1987) 196202

[4] Kuzminov, V.V., Pomanski, A A, ***^{81}Kr Production Rate in the Atmosphere.*** Proc. 18th Int. Cosmic Ray Conf., Bangalore, India, Vol 2, 357 (Int. Union Pure and Applied Physics, 1983).

[5] W. Kutschera, M Paul, I. Ahmad, T.A. Antaya, P.J. Bilquist, B.G. Glagola, R. Harkewicz, M. Hellstrom, D.J. Morrissey, R.C. Pardo, K.E. Rehm, B.M. Sherrill, M. Steiner, ***Long-lived noble gas radionuclides***, Nucl. Instr. Meth. B 92 (1994) 241-248

ENVIRONMENTAL TRACERS AS INDICATORS OF GROUNDWATER FLOW AND EVOLUTION IN A FRACTURED ROCK AQUIFER, CLARE VALLEY, SOUTH AUSTRALIA

A.J. LOVE
Primary Industries and Resources South Australia and CGS, Adelaide, South Australia

P.G. COOK, A.L. HERCZEG
CSIRO Land and Water and CGS, Glen Osmond, South Australia

C.T. SIMMONS
Flinders University of South Australia and CGS, Adelaide, South Australia

Australia

Abstract

Environmental tracers, chemistry and hydraulic data have been used to develop a conceptual model for groundwater flow in a fractured rock aquifer, at Clare, South Australia. In the upper 36 m there is relatively high horizontal flow, closely spaced fractures and large apertures. Below 36 m, horizontal flow rates are less and apertures become smaller. A sub horizontal fracture at 36 m separates the upper system from flow systems below. There is minimum vertical connection of groundwater above and below 36 m as indicated by low hydraulic conductivity and a steep ^{14}C concentration gradient. The observed linear trends in chemistry and isotope data are a result of mixing between old saline water and relatively younger fresh water. Greater mixing has occurred in the upper 36 m, with the amount of mixing diminishing with depth. We propose that this mixing is a recent process that has been triggered as a result of increased recharge to the system since the clearing of native vegetation approximately 100 years ago. Increased recharge of lower salinity water has resulted in the establishment of concentration gradients between the matrix and the fractures. This has resulted in diffusion of relatively immobile water in the matrix into relatively fast moving water in the fractures. Greater flushing has occurred in the upper 36 m due greater fracture density and larger apertures and higher horizontal flow rates.

1. INTRODUCTION

Fractured rock aquifer research to date has largely focused on the development of a number of complex hydraulic and solute transport models [1, 2, 3]. Applied tracer tests have often been used to characterise fractured flow at small scale field sites [4, 5]. However, little effort has been placed on the use of environmental tracer data to characterise fracture flow, or the coupling of environmental tracer data with numerical models. Environmental tracer techniques have advantages over hydraulic methods, as they can integrate over temporal and spatial scales. Hydraulic methods provide only a ‘snap shot’ of the present day flow regime. Where possible both environmental tracers and hydraulic data should be used together to help develop or constrain conceptual and numerical models.

A distinctive feature of the Clare Valley fractured rock aquifers is that the groundwater is stratified with respect to salinity. In a number of bores in the district, salinity can increase by a factor of four over a vertical distance of only 100 meters. The unique feature of this stratification is that salinity changes abruptly, with rapid changes (up to 3000 $\mu S cm^{-1}$) occurring in a step-like fashion over vertical distances of only 1-5 m. In this paper we examine chemical, isotopic and hydraulic data from the Wendouree field site in the Clare Valley, in an attempt to elucidate the major flow processes and aquifer characteristics occurring, including water velocities, fracture spacings, apertures and connectivity.

2. FIELD SITE

The Clare Valley is located 100 km north of Adelaide, South Australia and forms part of the Adelaide Geosyncline which is an ancient failed rift margin. Proterozoic rocks (600 -800 million years old) are exposed as indurated and fractured quartzites, shales and dolomites with low porosity that have been subjected to low grade regional metamorphism.

The climate is Mediterranean with hot dry summers and cold winters. Precipitation varies from 590 to 650 mm yr^{-} 1, throughout the region and is winter dominated from June to August. Average annual evaporation is 1975 mm yr-1 at Clare. Today the dominant land use is vineyards and pasture with only a minor amount of native vegetation remaining. Large scale clearing of native vegetation occurred approximately 100 years ago as a result of the introduction of European style agriculture. In other parts of Australia land clearing has resulted in an order of magnitude increase in groundwater recharge [6]. The impact that land clearing has had on increased groundwater recharge in Clare has not yet been assessed.

Groundwater of variable quality (500 – 7000 mg L-l) and low yield (0.5 to 20 L s-l) is stored in these low porosity rocks. The major use of this groundwater is for domestic and irrigation supplies of grape vines. Over the past few decades the demand for increased grape yield and volume from the district has led to increased irrigation from groundwater. This has raised concerns in the community about the long term sustainability of the groundwater resource.

The data reported here is from a carbonaceous dolomite aquifer at the Wendouree field site. The first well drilled is 200 mm in diameter to a depth of 117.5 m, and completed as an uncased open hole. Vertical profiles of electrical conductivity (EC) and temperature were taken using a down hole logging probe. 222Rn and major ion data were collected in situ in the unpurged open bore hole by means of a bailer. This well, and another well drilled to a depth of 55 meters, 2 meters to the north, were later converted to a series of nested piezometers. The nested site has ten different well completions intervals located between 2 and 100 m below the water table. The piezometers are open to the aquifer by slotted casing at their base. The slotted intervals varies from 2 to 6 meters. Individual piezometers are gravel packed around the slots and are separated by cement and bentonite seals. Piezometers were sampled for environmental tracers ^{14}C, ^{13}C, ^{2}H, ^{18}O, ^{3}H and CFCs. Hydraulic conductivity was determined on the piezometers by standard pumping tests. Porosity of a rock core from at 8.2 m was measured to be 4.7 % using helium porosimetry. The vertical hydraulic gradient at the site is less than 5 $x10^{-3}$.

3. GROUNDWATER FLOW AND FRACTURES

3.1 EC, temperature and ^{222}Rn

Electrical conductivity (EC), temperature and radon profiles have been used to infer the location of fracture flow into the open borehole (Figure 1). Step-like changes in EC of between 300 to 1500 µS/cm occur over vertical distances of only 1-3 metres. At the same depths a small temperature spike of 0.08 to 0.12 ^{o}C is observed. These changes in EC and temperature occur at depths of 36, 52, 77 and 82 meters below the water table. We believe these represent locations of major groundwater inflow to the bore via fractures.

Cook et al [7] have shown that 222Rn concentrations in unpurged bores can be used as a qualitative indicator of groundwater flow rate. Radon is produced from decay of uranium and thorium minerals in the aquifer and has a half life of 3.8 days. High concentrations of radon in streams have been used as a quantitative indicator of groundwater discharge [8]. In a similar way, high concentrations of radon in the borehole should indicate active groundwater inflow. If there was zero flow from the aquifer to the borehole we would expect radon concentrations in the borehole to be zero due to radiogenic decay. However if flow through the well is faster than radon can decay then we would expect significant concentrations of radon in the well. If we assume that the concentrations of 222Rn are uniform in the aquifer over the length of the borehole, then radon concentrations can be related to groundwater flow rate.

We observe high 222Rn concentrations in the upper 36 metres of the bore indicating relatively rapid horizontal flow. Because radon concentrations are relatively high and uniform in the upper flow system we suggest that there is relatively high fracture density in this region as well as high horizontal flow throughout this zone. A small peak of 222Rn at a depth of 52 metres correspond to a step change in EC and a small temperature spike. Another small peak of radon occurs at about 75 m. We believe these represent the location of active fractures intersecting the borehole. As the 222Rn peak at 52 m is larger than the one at 75 m we infer that groundwater inflow at the fracture at 52 m is greater than that at 75 m.

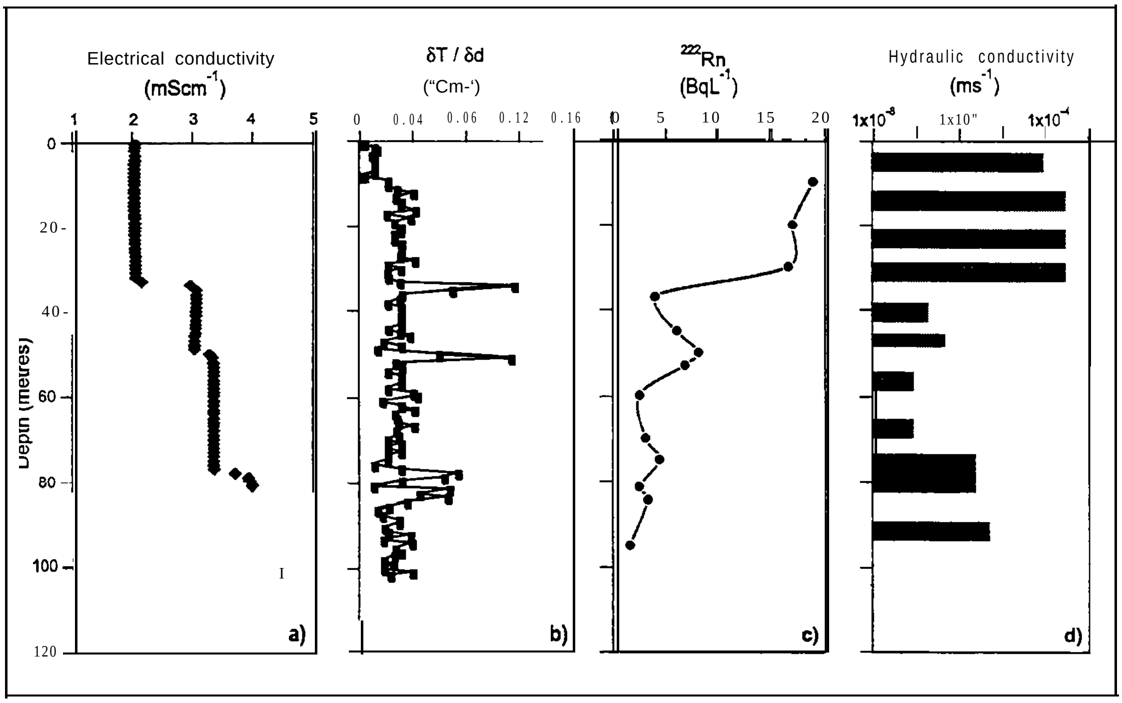

Figure 1 Electrical conductivity, temperature, radon and hydraulic conductivity data at Wendouree a) EC profile data from open hole b) Temperature gradient open hole, c) Radon concentrations unpurged open hole, d) Horizontal hydraulic conductivity obtained from pumping tests in the piezometers. The depths are shown below standing water level. The horizontal hatched bar in d represents the length of the piezometer interval.

3.2 Hydraulic data

Hydraulic conductivity varies by four orders of magnitude with values decreasing with depth (Figure 2d). High values of hydraulic conductivity in the top four piezometers correspond to high unpurged ^{222}Rn concentrations in the open borehole indicating rapid throughflow in the top 36 m. Below the fracture at 36 m, hydraulic conductivity and 222Rn concentrations are much lower than in the upper section of the borehole, indicating reduced horizontal flow. The radon peak at 52 m corresponds to relatively low hydraulic conductivity while the smaller radon peak at 75 m corresponds to higher hydraulic conductivity. However we would not necessarily expect hydraulic conductivity and radon to have a direct correlation. Rather, the data may indicate a decrease in the horizontal hydraulic gradient with depth.

The dolomite aquifer has been mapped in an exposure approximately 2 kms north of the field site. The outcrop data shows fracture spacing of 0.1 to 0.5 m, which is probably representative of the upper 36 m at the Wendouree site. Open fractures at outcrop have apertures ranging from 2 to 0.01 mm, with a mean of approximately 0.6 mm. Fracture planes are parrel to bedding, both at outcrop and at Wendouree. Evidence for this is the presence of mineral striations on the bedding surfaces. A number of sub-horizontal fracture planes are also evident at outcrop.

Flow through individual fractures can be represented by analogy to laminar flow between two smooth parallel plates according to the cubic law [9]. In the analysis below we have assumed that each piezometer interval tested has only one single fracture. By rearranging the cubic law, fracture apertures can be estimated from values of hydraulic conductivity in the piezometers by:

$$b_f = \left(\frac{12 \mu K_f L}{\rho g N} \right)^{1/3} \tag{1}$$

where bf is the aperture, μ is the viscosity of the fluid, Kf is the hydraulic conductivity of the interval tested, L is the length of the aquifer test , ρ is the fluid density, g is the acceleration of gravity and N is the number of open fractures intersected in the test interval.

We compute horizontal apertures ranging between 1540 μm for the upper section of the bore and 72 μm for the lower section of the bore. If we assumed a more realistic fracture spacing ranging between 0.5 to 0.1 m (based on outcrop data) for the upper 36 m, then apertures reduce to between 850 and 500 μm respectively. For an aperture of 500 μm and a vertical hydraulic gradient of less than 5 x 1 O-3 this would correspond to vertical flow through a single fracture of less than 9 mday- 1. Similar way if we assume an aperture of 72 μm below 36 m deep this would permit a vertical velocity in the fracture of up to 0.18 m day-l.

As discussed previously we believe that the variation in EC down the borehole indicates the location of different water bodies entering the well. For the upper 36 m of the bore, there is high fracture density, high horizontal flow and relatively large apertures. We assume that most of the water entering the well moves horizontally through the well. At 36 m, the bore intersects a new fracture containing water with a higher EC. We believe that the constant EC between 36 and 52 m is due to some of the water from this fracture moving down through the bore. As EC is constant and there is no radon peak or temperature spike we believe that no major fracture intersects the well from 36 to 52 m. At 52 m another step change in EC occurs, representing a new fracture intersecting the bore containing water of a higher EC. We assume that this fracture has a smaller aperture (based on aperture estimated from hydraulic conductivity) and a reduced flow rate (from radon data) from the fracture above. This new fractured water can move either horizontally through the well into the aquifer or vertically in the bore. Again as the EC in the bore does not change between 52 and

77 m we assume that no major new fracture has intersected the well until 77 m where there is another step change in EC.

We propose that the step changes in salinity are a result of mixing between immobile water in the matrix and mobile water in the fractures. We believe this mixing is a result of increased recharge to the system due to land clearing approximately 100 years ago. Under this scenario, greater flushing of the system has occurred in the upper 36 m due to higher horizontal hydraulic conductivity, closer fracture spacings and larger apertures. Groundwater in this section of the bore move horizontally. Decreased flushing occurs for the lower flow systems due to decreased flow rates.

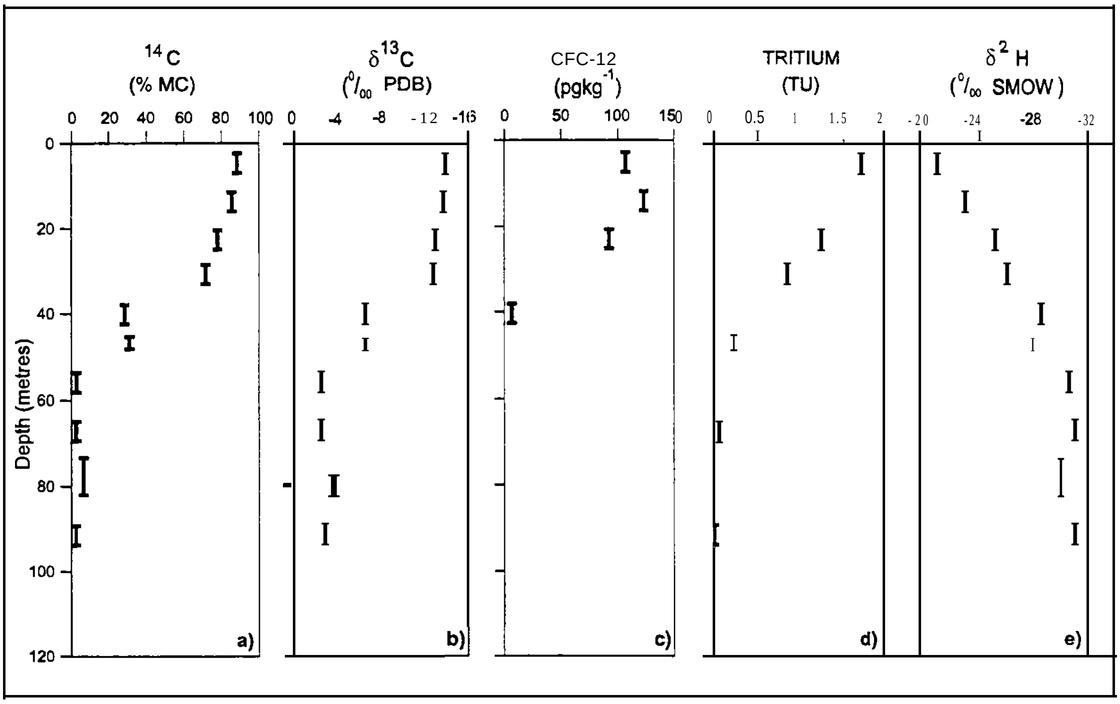

Figure 2. Environmental tracer data in the piezometer nest, a) ^{14}C, b) ^{13}C, c) CFC-12, d) Tritium, e) Deuterium. The depths are shown below standing water level. The vertical bar represents the length of the piezometer interval.

3.3 3H and CFC-12

3H and CFC- 12 depth profiles can provide information on the vertical hydraulic connection at the site. The presence of CFC-12 to a depth of 25 meters and thermonuclear tritium at 36 meters below the water table indicates that a proportion of relative modern water has reached these depths (Figure 2 c & d). Solutes transport in a fractured rock aquifer is characterised by rapid advection in the fractures with a diffusive exchange between water in the fracture and relatively immobile water in the matrix. This diffusion process is driven by a concentration gradient between the matrix and the fractures. The gradient can be either from the fracture to the matrix or visa versa depending on the characteristic of the solute. In the case of CFC-12 and ^{14}C diffusion occurs from the fracture to the matrix which can result in significant retardation of the solute [10]. For tritium diffusion will be from the fracture to the matrix, until the bomb peak has passed and then tritium will back diffuse from the matrix to the fracture.

The measured concentrations of 3H and CFC- 12 can provide information on minimum vertical velocities in the fractures. The CFC-12 concentration of 92 pgkg-1 at 25 m below the water table corresponds to a groundwater age of 23 years (sampling occurred in 1998). This can be converted to a minimum velocity Vf $\geq$ 1.1 myr^{-1} (25m /23 yrs). In a similar way the presence of post 1963 3H at 36 m below the water table converts to Vf $\geq$ 1.0 myr 1 (36 m/ 35 years). However the actual groundwater velocities may be orders of magnitude greater than this depending on the extent of matrix diffusion which is difficult to quantify.

3.4 Major ions, δ^2H and $\delta^{18}O$ data

The major ion data plotted against chloride (Figure 3 a and b) all display positive linear correlations, with the concentrations of all dissolved ions increasing with depth (correlation coefficients (r^2) = 0.86 - 0.97).

For the total range in Cl concentrations the K/Cl marine ratio is preserved. The Cl/Br mole ratios range from 500 to 700 indicating preservation of the marine aerosol ratio (632) with no dissolution of evaporites in the groundwater system (Br data not presented). For Cl concentrations < 13 mmol L-l, the Na/Cl and SO_4/Cl marine ratio is preserved which indicates that at low chloride concentrations (ie, in the top 36 m) that Br, K, Na and SO4 behave conservatively and the ions are concentrated by evapotranspiration prior to recharge. For Cl > 13 mmol L-l (ie, > 36 m) both Na and SO4 are above the ion/Cl marine ratio suggesting that addition of these ions to the groundwater above the seawater dilution line is by water/rock interactions.

Ca/Cl and Mg/Cl ratios are well above their marine ion/Cl ratios for the entire range of concentrations. As the groundwaters are saturated with respect to calcite and dolomite any addition of Ca and Mg from carbonate dissolution in the groundwater system is unlikely and therefore the enhanced concentration of these ions must have must have occurred via dissolution of Mg -carbonates in the unsaturated zone prior to groundwater recharge.

The linear correlations for all ions versus Cl may be the result of a number of possible processes; 1) variable evapotranspiration of a single input water during recharge, 2) progressive addition of ions via water/rock interactions, 3) mixing of two different water bodies with different end member compositions. In this case the mixing process would be by diffusion, where older more saline stagnant water in the matrix would mix by diffusion into the relatively younger fresher more mobile water in the fractures.

The stable isotopes of the water molecule plot on or near the meteoric water line (Figure 3c). δ^2H and $\delta^{18}O$ compositions are relatively enriched in 2H and ^{18}O just below the water table and progressively become more depleted with depth (Figure 2e). This increasingly negative signature with depth (i.e, a • 10 per mil shift in δ^2H in 100 m) corresponds to increased chloride and EC. This is the opposite to what is normally observed throughout the world where more negative δ^2H and $\delta^{18}O$ values are often associated with lower chloride concentrations due to colder climatic conditions at the time of recharge. There are many examples of this in the literature from the last glacial period [11, 12].

The chemical and isotope data suggests two end members with a continuum of concentrations between these two end members, 1) low salinity groundwater controlled by evapotranspiration in the top 36 m and 2) higher salinity groundwater with an increased contribution from water/ rock interactions at depth. We suggest that the observed linear correlations in chemical and isotopic data between these two end members is a result of mixing between old more saline water in the matrix and fresher younger water in the fractures, particularly in the top 36 m. Addition of solutes via mineral weathering is

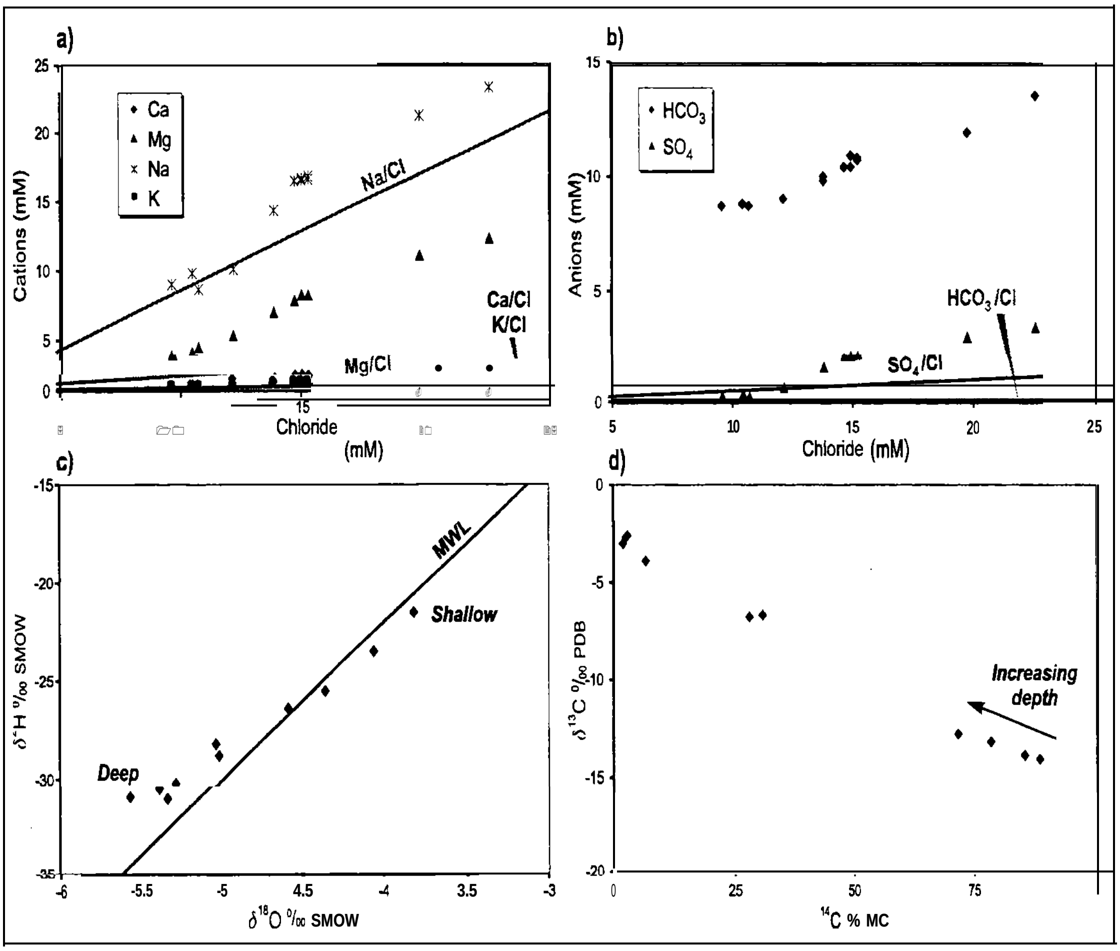

Figure 3. Compostional diagrams a) Ca, Mg, Na, K versus Cl, the ion/Cl lines represents the seawater dilution line b) HC03, SO4 versus chloride, the ion/Cl lines represents the seawater dilution line c) δ^2H versus $\delta^{18}O$, MWL = World Meteoric Water Line d) ^{14}C versus ^{13}C

relatively unimportant because Cl bearing minerals are absent and all other ions are correlated with Cl. Increasing evaporation of a single recharge source would tend to enrich ^2H and ^{18}O with increasing Cl, which is the opposite of that observed. The exact origin of the relatively depleted saline end member is unknown, we assume that the water is older than the last glacial, possibly recharged in a more arid environment with episodic recharge events.

The major source of dissolved salts in the system is from concentration of rainfall cyclic salts due to evapotranspiration in the upper 36 m with a greater contribution from water/rock interactions with depth. As discussed previously the step-like changes in salinity are most likely a result of increased recharge to the system since the clearing of native vegetation -100 years ago. Pre clearing recharge to the system was low (estimated to be < 5 mmyrl) and the dissolved ion concentrations were in equilibrium between matrix and the fractures. Since clearing, recharge has increased by an order of magnitude, which has resulted the introduction of lower salinity groundwater which is currently flushing the fracture systems and has established a concentration gradient between matrix and fracture components. Dissolved ions now back diffuse from the matrix into the fractures.

3.5 ^{14}C and ^{13}C data

Uncorrected ^{14}C concentration above 36 m are all > 70 %MC, the decrease of ^{14}C concentration with depth reflects an increases in age (Figure 2a). The steep ^{14}C “age” gradient below the fracture at 36 m (ie between piezometer 4 and 5) indicates minimum connection between groundwaters in the upper 36 m and those below. As the sub horizontal fracture at 36 m has a large hydraulic conductivity we would expect a decrease in groundwater “age” below this depth as a large proportion of groundwater would discharges horizontally at 36 m. Another steep ^{14}C age gradient occurs below the fracture at 52 m (ie between piezometers 6 and 7) again indicating reduced vertical connection with increasing depth.. As piezometer 6 has a higher hydraulic conductivity than piezometer 7 we would expect a large proportion of groundwater moving vertically in the bore to be discharge into the aquifer via the sub horizontal fracture at 52 m..

The 14C versus ^{13}C data (Figure 3d) also shows a remarkable linear correlation with ^{14}C concentrations at 90 %MC at 2 meters below the water table to background (<2 %MC) at 100 meters below the water table (Figure 2a and b). 13C becomes progressively enriched relative to ^{12}C, increasing from • 14.1 per mil at 2 meters below the water table to – 3 per mil at 100 meters. As with the chemical data we need to determine whether this linear correlation is a result of mixing from two end members or is caused by geochemical evolution which results in more enriched ^{13}C and lower ^{14}C than the initial recharge value.

Geochemical processes that may produce this trend of increasing $^{13}C/^{12}C$ values include i) incongruent dissolution of dolomite, and ii) methanogenisis (where ^{13}C enriched CO2 is produced as a by product). Incongruent dissolution of dolomite involves dissolution of a MgC03 initially with increased concentrations of Ca and Mg followed by re-precipitation of a lower MgC03 which will result in increased concentrations of the dissolved Mg/Ca ratio. As the Mg/Ca mole ratio remains relatively constant (between 3-4) throughout the profile we can discount incongruent dissolution. Methanogenesis appears to be not important because the alkalinity/ DIC ratio is near unity and $CO_2(aq)$ concentrations are relatively constant with increasing depth, if methane production were important, the alkalinity/DIC ratio would be much less than unity as well the $CO_2(aq)$ concentrations would increase [13, 14].

The carbon isotopic dam supports the geochemical and stable isotopic evidence for mixing between two end members. The shallow near surface end member has modem ^{14}C with a $\delta^{13}C$ composition consistent with equilibrium with the soil CO2 reservoir; the deep end member has background ^{14}C with an enriched ^{13}C of -3 per mil, which is consistent with equilibrium with the dolomite. We assume that the near surface end member represents the influx of new recharge water into the fractures and that the older end member at depth represents water sourced from the matrix. In this case ^{14}C would diffuse from the fracture to the matrix, while ^{13}C would back diffuse from the matrix to the fracture. With increasing depth down the profile there tends to be a greater contribution from the older water component.

4. CONCLUSIONS

Interpretation of chemical, isotopic, temperature and hydraulic data have provided information on the internal structure and groundwater flow in a fractured rock aquifer. Groundwater fractures can be identified by step-like changes in EC, temperature spikes and radon peaks. Groundwater flow through these fractures decreases with depth as supported by smaller radon peaks and smaller apertures determined from hydraulic conductivity. In the upper 36 m there is high fracture density, relatively large apertures and high horizontal groundwater flow. Groundwater has been dominated by cyclic salts that have been concentrated by evapotranspiration prior to recharge. Connection of groundwater in the upper 36 m with that below is minimal. Below 36 m, apertures are smaller and horizontal flow is less than above 36 m. In the lower flow systems there is a greater contribution of salt from water/rock interactions, due to the longer contact times.

The observed isotopic and chemical profiles are a result of mixing of older more saline water with fresher younger water. This mixing was most likely triggered by land clearing approximately 100 years ago which has resulted increased recharge to the groundwater. Concentration gradients for salt between the matrix and the fractures have been established which is resulting in the system being flushed by back diffusion.

REFERENCES

[1] MOENCH, A.F. 1984. Double-porosity models for a fissured groundwater reservoir with fractured skin, Water Resources Research, 20: 831-846.

[2] LONG, J.C.S and BILLAUX, D.M. 1987. From field data to fracture network modeiling: An example incorporating spatial structure, Water Resources Research, 23 : 1201- 1216.

[3] THERRIEN, R., AND STUDICKY, E.A., 1996. Three-dimensional analysis of variably-saturated flow and solute in discretely-fractured porous media. Journal of Contaminant Hydrology. 23 : 1-44.

[4] McKAY, L. D., CHERRY, J.A., AND GILLHAM, R.W., 1993. Field experiments in a fractured clay till, 2, Solute and colloid transport, Water Resources Research., 29:3879-3890.

[5] NOVAKOWSKI, KS., LAPCEVIC, P.A., VORALEK, J. AND BICKERTON, G., 1995. Preliminary interpretation of tracer experiments conducted in a discrete rock fracture under conditions of natural flow. Geophysical Research Letters., 22 (11) 1417- 1420.

[6] ALLISON, G.B. COOK, P.G., BARNETT, S.R., WALKER G.R., JOLLY, I.D AND HUGHES, M.W. 1990. Land clearance and river salinisation in the Western Murray Basin, Australia. Journal of Hydrology. 119: 1-20.

[7] COOK, P.G., LOVE, A.J AND DIGHTON, J.C., 1999. Inferring groundwater flow in fractured rock from dissolved radon. Ground Water, accepted

[8] ELLINS, K.K., ROMAN-MAS AND LEE, R. 1990 Using 222Rn to examine groundwater/surface discharge interactions in the Rio Grande de Manatai, Puerto Rico. Journal of Hydrology, 115:319-341.

[9] SNOW, D.T., 1968. Rock fracture spacings, openings and porosities. Journal Soil Mech. Found. Div. Amer. Soc. Civil Eng., 94(SM1) 73.

[10] MALOSZEWSKI, P., AND ZUBER, A., 1991. Influence of matrix diffusion and exchange reactions on radiocarbon ages in fissured carbonate aquifers. Water Resources Research, 27(8): 1937-1945.

[11] DEAK, J., 1979. Environmental isotopes and water chemical studies for groundwater research in Hungary. Isotope Hydrology 1978. IAEA, Vienna

[12] RULDOLPH, J., RATH, H.K. AND SONNTAG, C., 1984. Noble gases and stable isotopes in 14C dated palaeowaters from central Europe and the Sahara. Isotope Hydrology, 1983, IAEA, Vienna, 467-477.

[13] HERCZEG, A.L., RICHARDSON, S.B. AND DILLON, P.J. 1991. Importance of methanogenesis for organic carbon mineralisation in groundwater contaminated by liquid effluent, South Australia. Applied Geochemistry, 6: 533-542.

[14] DEFFEYES, K.S. 1965 Carbonate equilbria: a graphic and algebraic approach. Limmonology. Oeanography. 10: 412-426.

Estimation of Recharge from Nile Aquifer to the desert fringes at Qena Area, Egypt

M.S. Hamza, A.I.M. Aly, M.A. Awad, A.A. Nada, S.G. Abdel-Samie, M.A. Sadek and W.M. Salem
National Center for Nuclear Safety and Radiation Control, Atomic Energy Authority, Nasr City 11762, P.O. Box 7551, Cairo Egypt
F.A. Attia, T.M. Hassan and N.E. El-Arabi
Research Institute for Groundwater, National Water Research Center, El-Kanater El-Khayria, Egypt.
K. Froehlich
Isotope Hydrology Section, Division of Physical and Chemical Sciences, IAEA.
Wagramerstrasse 5, P.O. Box 100, A-1400, Vienna, Austria
M.A. Geyh
Joint Geoscientific Research Institute of the German State Geological Surveys, Stilleweg 2, D-30655, Hanover, Germany

Abstract

In Qena area, fresh groundwater is present in the Quaternary aquifer (5-50m depth), fresh to brackish groundwater is pumped from the aquifer of the Plio-Pleistocene and of Wadi deposits (60-100m) both on elevated structural plateau. Below 150m locally semi-confined or confined Nubian Sandstone aquifer is situated and contains fresh water under artesian conditions. It may have hydraulic contacts to the shallow Quaternary aquifer by structural zones and fractures. One of the objectives of the isotope hydrological study was to estimate the contribution of different groundwater to the water budget. The dominate process is mixing, there are six possible end member components with different isotope signature as follows:

1- River Nile water before construction of Aswan High Dam (NRo).
2- River Nile water after construction of Aswan High Dam (NR).
3- Canal water which transports River Nile water with different isotopic compositions (CW).
4- Irrigation water return which is isotopically enriched water (Ir).
5- Flood waters (FW), frequently occuring every year since 1993 may contribute to the groundwater recharge. This water is about 3 to 4‰ isotopically less enriched in ^{18}O than the Nile water.
6- Nubian Sandstone water (NS): This water is isotopically most depleted and was recharged in cool and humid periods {Pleistocene time}.

Applying different mixing models using several end members resulted in the following contributions from palaeo water for the different aquifers: Quaternary aquifer, (1 to 5%), Plio-Pleistocene aquifer, (9 to 16%) and in Wadi deposits and Basement aquifers, (25 to 35%).

INTRODUCTION

The increasing population in Egypt are putting a great pressure on the existing water supplies of the Nile system which is the main resource of water. Therefore groundwater resources seem to be one of the most promising solution to the drinking water shortage. However there are serious limitations about the intensive use of groundwater resources as some of these resources are non-renewable. For this reason, it is of utmost importance to identify the possibility of recent recharge of the groundwater aquifers on the fringes of the Nile Valley. The Egyptian Authorities selected a series of land reclamation projects. In order to put a sensible water management plan, it is important to investigate the relation between the River Nile system and the existing groundwater aquifers. Fig. (1 ,2) show the location map of the studied area and the land use. The selected area where land reclamation projects started represents an ideal site for the use of the isotope hydrology techniques to answer some of the questions about the water availability and its recharge.

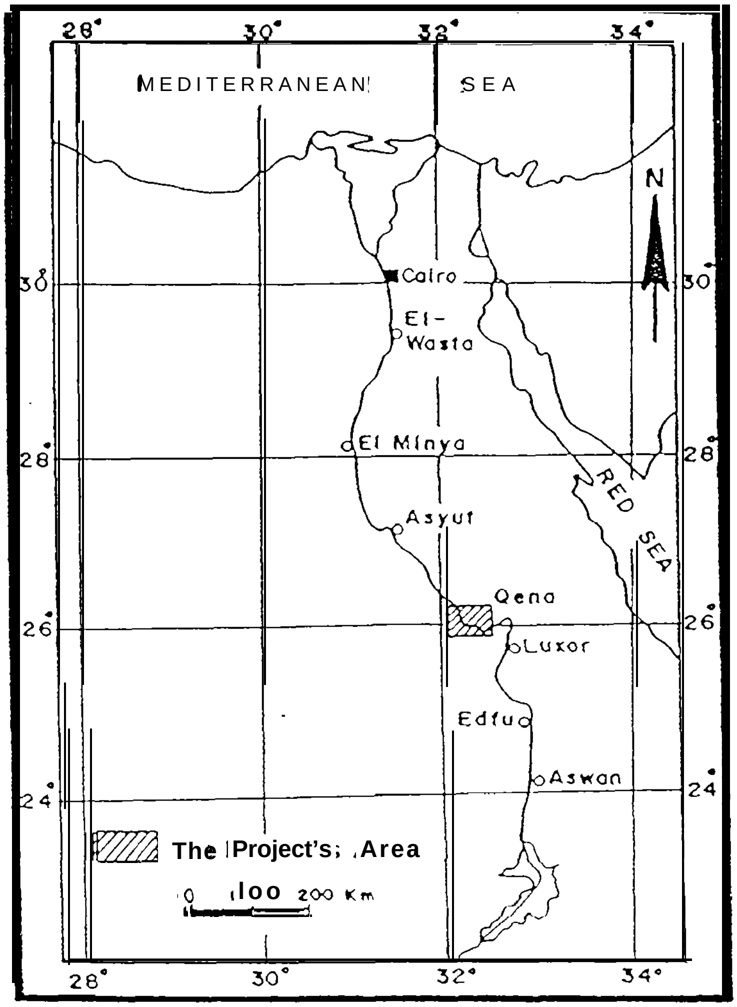

Fig. (1) Location map

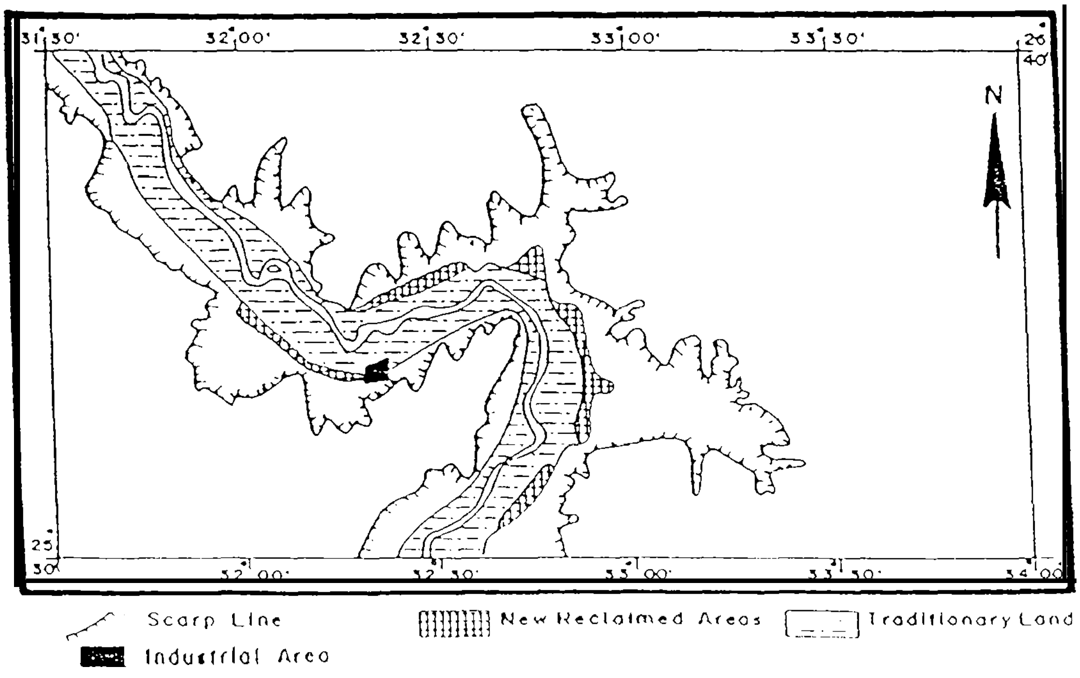

Fig .(2) Land use in the Qena area

GEOMORPHOLOGY

In Qena area, two geomorphic units exist. They include the alluvial plains and the structural plateau (Pig. 3). The alluvial plains are differentiated into the young plain, which is intensively cultivated, and the old plains, which are developed into terraces. Parts of which are under reclamation. The young alluvial plain occupies the central portion of the Nile Valley and is underlain by a thin silty clay layer that was developed as result of the successive floods of the Nile.

The course of the River Nile cuts the plain close to the eastern side and flows in S-N direction. The old alluvial plains occupy the outer portions of the valley. They are underlain by mixed sand and gravel and are developed into successive terraces rising up to 100m above the present level of the flood plain. These terraces are dissected by complex drainage lines (Wadis) directed towards the low portions of the valley. The structural plateaux determine the edges of the Nile trough. The surface of these plateaux is rough and is underlain by weathered resistant limestone. The plateaux terminate with faults - controlled escarpments, which rise abruptly from the alluvial plains.

REGIONAL GEOLOGICAL SETTING

Qena area, located in the central portion of the Nile Valley, occupies a portion of a sub-regional sedimentary basin (Assiut Basin) having a depth exceeding 3000m. This basin is located in the foreland side of the Arabian - Nubian Massif, where the dip is regionally in the westward direction. In this basin the top portion of the sedimentary section is dominated by carbonate rocks belonging to the Eocene and the Upper Cretaceous, and the lower portion is mainly clastics belonging to the Paleozoic and the Mesozoic (Nubian Sandstone Complex). The sedimentary section is locally overlain in the Nile Valley itself by late Tertiary clays and Quaternary fluviatile silty clay, sand and gravel. The basin was affected by tensile stresses which are responsible for the formation of a complex fault system running in NW-SE direction. Basaltic extrusions are generally associated with

Table 1: Characteristics of the hydrogeological units

Units	**Description**	**Saturated thickness (m)**	**Depth to groundwater level (m)**	**Transmissivity (cm2/day)**
Unit (1)	Highly productive unit, consisting of quatemary graded sand and gravel with clay lenses. Continuous recharge from irrigation.	10 - 140	< 5	5.000 - 20.000
Unit (2)	Moderately productive unit consisting of graded sand and gravel with clay lenses, occasional recharge from irrigation, surface runoff and local rainfall.	20 - 100	5 - 10	5.000 - 10.000
Unit (3)	Low productive unit consisting of Plio-Pleistocene sand and gravel and clay, continuous recharge from irrigation and occasionally from surface runoff and local rain.	20 - 80	5 - 15	3.000 - 10.000
Unit (4)	Low to moderately productive unit consisting of: ▪ Eocene Limestone with paleokarst feature; ▪ Upper Cretaceous shale, Paleocene shale;and Pliocene clay (non aquifer); ▪ Upper Cretaceous Paleozoic Nubian Sandstone complex.		Unexplored	

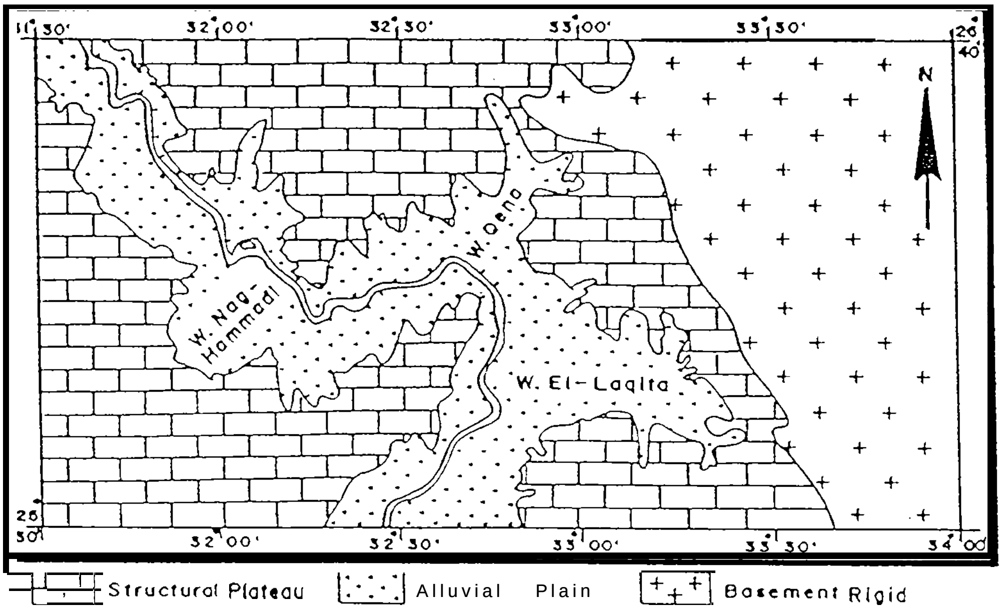

Fig.(3) Geomorphic units in the Qena area

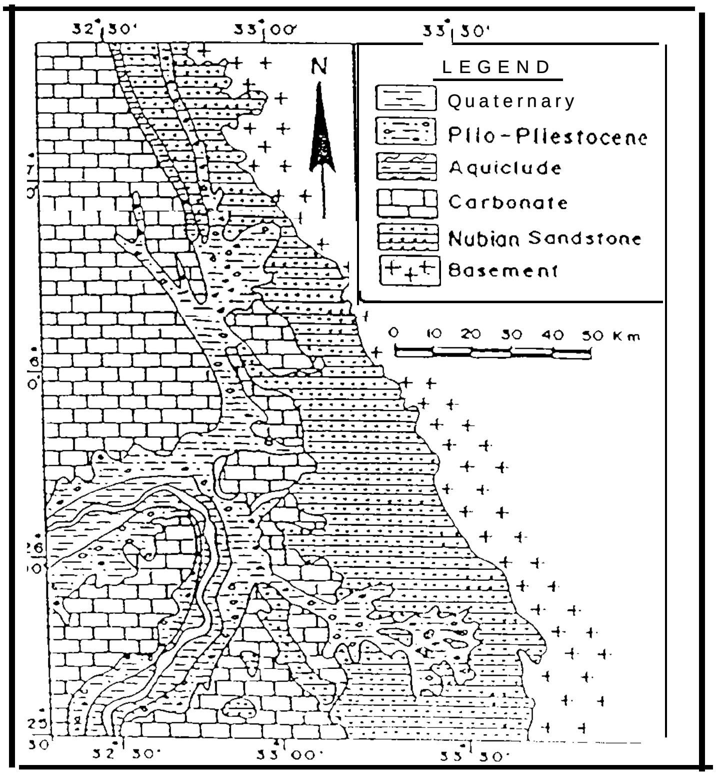

Fig.(4) Hydrogeological units

such faults, but these are not recorded a the Qena area. In Qena area, the stratigraphy of the surface and the near surface sedimentary succession as outlined by [I] is as follows from top to base;

1- Holocene: silty clay (Neonile and young wadi deposits).
2- Late Pleistocene: graded sand and gravel (Prenile deposits).
3- Plio-Pleistocene: clay sand and conglomerate (Protonile deposits).
4- Pliocene: clay (Paleonile deposits) and,
5- Eocene: limestone (shallow marine deposits).

HYDROGEOLOGY

In the discussion of the hydrogeology of Qena area emphasis is given to the Quaternary fluviatile and the Plio-Pleistocene fluviomarine aquifer systems. The main sources of information are the observation wells drilled by the Research Institute for Groundwater (RIGW) and the private wells. This information includes the lithology, groundwater levels, groundwater extraction and quality. The other aquifer systems, particularly the carbonates and the Nubian sandstone, are not explored in this area. The main aquifers are of granular type. Based on their area extent and productivity, these aquifers are classified into four hydrogeological units (Table 1) and (Fig. 4), [2].

The Quaternary aquifer is continuously recharged from vertical percolation of irrigation water (from canals and irrigation return flow). On the other hand, the Plio-Pleistocene aquifer is either recharged from irrigation return flow, runoff, or vertically from deeper aquifers (Nubian Sandstone complex). Groundwater discharge from the Quatemary aquifer is either through transversal flow to the River or to the adjacent aquifers, or vertically through pumping. The Plio-Pleistocene aquifer is discharged mainly through horizontal flow to the Quaternary; or vertically by groundwater pumping. The Eocene carbonate aquifer system is recharged from local rainfall or from other aquifers in direct contact. Groundwater discharge is generally through groundwater flow to the adjacent aquifers depending on groundwater heads.

CONDITIONS OF THE STUDY AREA

Fresh groundwater is present in the Quaternary aquifer (S-50111 depth), fresh to brackish groundwater is pumped from the Plio-Pleistocene aquifer and of the Wadi deposits (60-I 00m depth) both located on the elevated structural plateaux. Hydrograph records from 1982-1992 show a fast and a delayed hydraulic response of the groundwater level of the Quaternary aquifer and the Plio-Pleistocene aquifer, respectively, to level changes of the River Nile. Hence, these aquifers form joint hydraulic systems. The groundwater tables of the Quaternary aquifer and the Plio-Pleistocene aquifer range from a few meters to 15m and from 20 to 40m below the ground respectively. Below 150m, the locally semi-confined or confined Nubian Sandstone aquifer is situated and contains artesian fresh water. It may have hydraulic contacts to the shallow Quaternary aquifer by structural zones and fractures [3]. The Nile River crosses the study area. Its water is artificially distributed via channels for irrigation agriculture into the inland. Irrigation return flow and leakage from the drainage systems pollute the groundwater in the Quaternary aquifer and in the aquifer of Wadi deposits. These fluxes explain why the groundwater in the upper aquifer consists mainly of Nile Water. In addition, episodically occurring floods may contribute to the groundwater recharge.

EXPERIMENTAL WORK

Water samples for hydrochemical and isotope hydrological analyses were collected four times: before a flood in April 1995, just after this event in October/November 1995, in August 1996 and in October 1996. Fig. 5 shows the sampling sites for the study area. The isotope analyses (^{14}C, ^{3}H, ^{18}O, 2H and ^{13}C) were done in three laboratories: BARC, Bombay, India; IAEA, Vienna, Austria and GSF, Neuherberg, Germany. The major ion species (Na, K, Ca, Mg, Cl, SO4 and HCO_3) were determined in Cairo. The electrical conductivity, pH, temperature and depth to water table were measured in the field. The corresponding isotope and chemical data are compiled.[4]

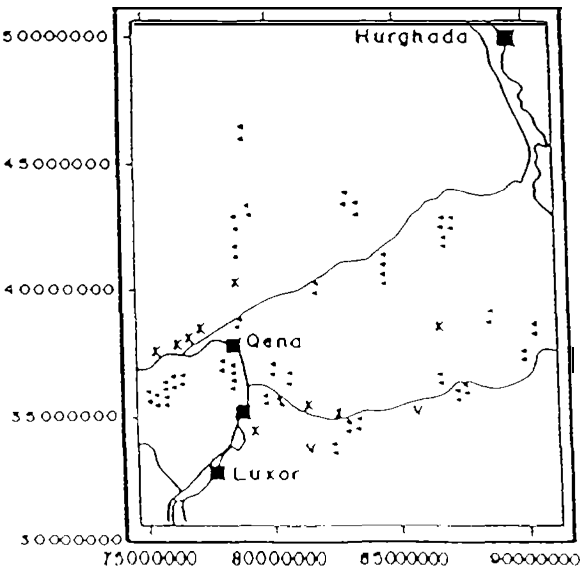

Fig.(5) Sampling sites

HYDROCHEMICAL RESULTS

The salinity of the groundwater in the Quaternary aquifer varies from 478 to 2205 mg/l with an average of 888 mg/l, while in the Plio-Pleistocene aquifer, the salinity found is in the range of 388 - 7819 with an average of 2020 mg/l. The salinity of the groundwater of the Nubian Sandstone aquifer varies from 14.53 to 6480 with an average of 2325 mg/l. In the wadi deposits and Basement aquifer,. the salinity ranges from 518 to 10545 mg/l with an average of 2990 mg/l for groundwater The groundwater of the Quaternary aquifer belongs to the Ca-HC03 or NaCl type. It is fresh and does not undergo any hydrochemical reaction with the rocks in the aquifers. The groundwater of the Plio-Pleistocene aquifer is fresh to brackish and of CaC12 or NaCl type. The sulfate concentration (up to 245 mg/l) of the water in the Quaternary aquifer is attributed to anthropogenic sources (e.g. fertilizers). Higher sulfate concentrations between 200-2200 mg/l in the groundwater of the Plio-Pleistocene aquifer could be due to the dissolution of naturally occurring gypsum. The nitrate concentrations are below the permissible limits. By using the geochemical trilinear diagram [5] two main groups are differentiated as follows (Fig. 6). The first group occupies the lower side of the diamond shape. The water in this group is dominated by secondary alkalinity, where Ca + Mg > S04 + Cl and calcium & magnesium bicarbonate salts prevail. The second group occupies the upper side of the diamond shape. The water in this group is characterized by secondary salinity where SO_4+Cl> Na+K and calcium & magnesium sulpahte and chloride salts dominate. The presence of Na_2SO_4, MgS04 reflects the mixed water type in the Plio-Pleistocene aquifer. The existence of MgCl2 in small amounts reflects the up-coning of saline water due to over pumping from both Quaternary and Basement aquifers.

ISOTOPE HYDROLOGICAL RESULTS

I- Groundwater wells in the Nubian Sandstone Aquifer

The water samples from wells in the Nubian Sandstone aquifer yielded $\delta^{18}O$ and δ^2H values ranging from –5.39‰ to –7.66‰ and from –38.5‰ to – 60.9‰, respectively. The mean values for all data is -6.8±0.9‰ and -51.5±7.8‰ for $\delta^{18}O$ and δ^2H, respectively. The $\delta^{18}O$/ δ^2H diagram is shown in Fig.(7). A few data fit the Global Meteoric Water Line with d=10‰ and the others belong to a local palaeowater line with d=4‰. A similar low d value was found by [6,7]. Studied groundwater from the Nubian Sandstone aquifer in the Sahara desert obtained $\delta^{18}O$ and δ 2H values between -10 to - 11‰ and -78 to –90‰, respectively. The deuterium excess amounts to +5‰. Sonntag et al., [7] explained this low d value as result of a lower moisture deficit over the source area of the water in the

Quaternary aquifer **Plio-Pleistocene aquifer**

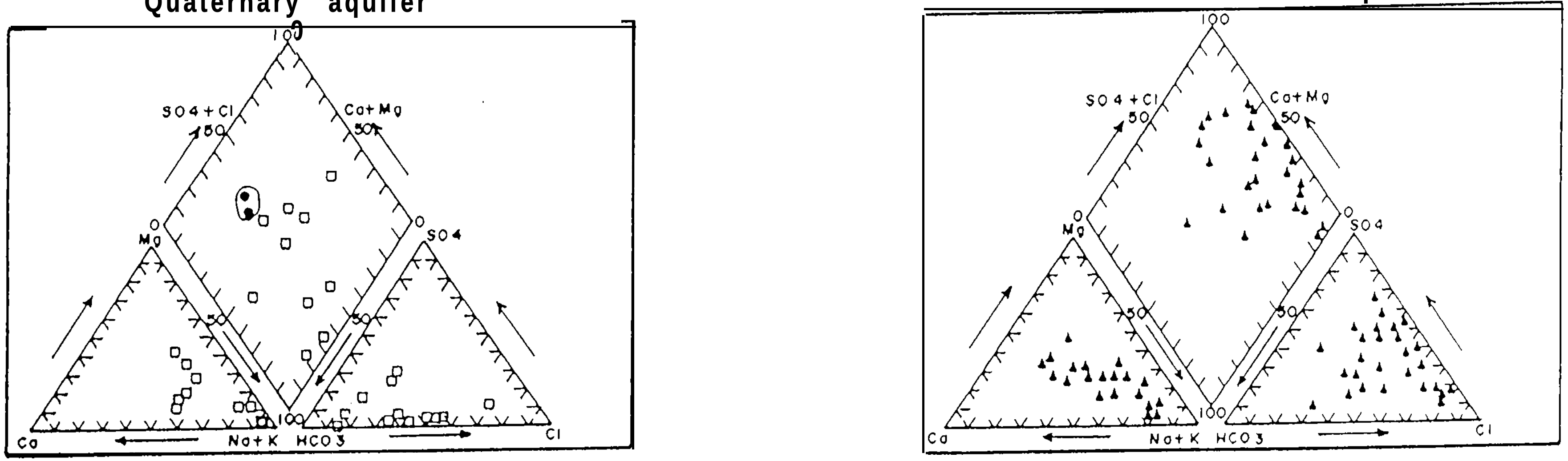

Basement & Wadi deposits aquifers Nubian **Sandstone oquifer**

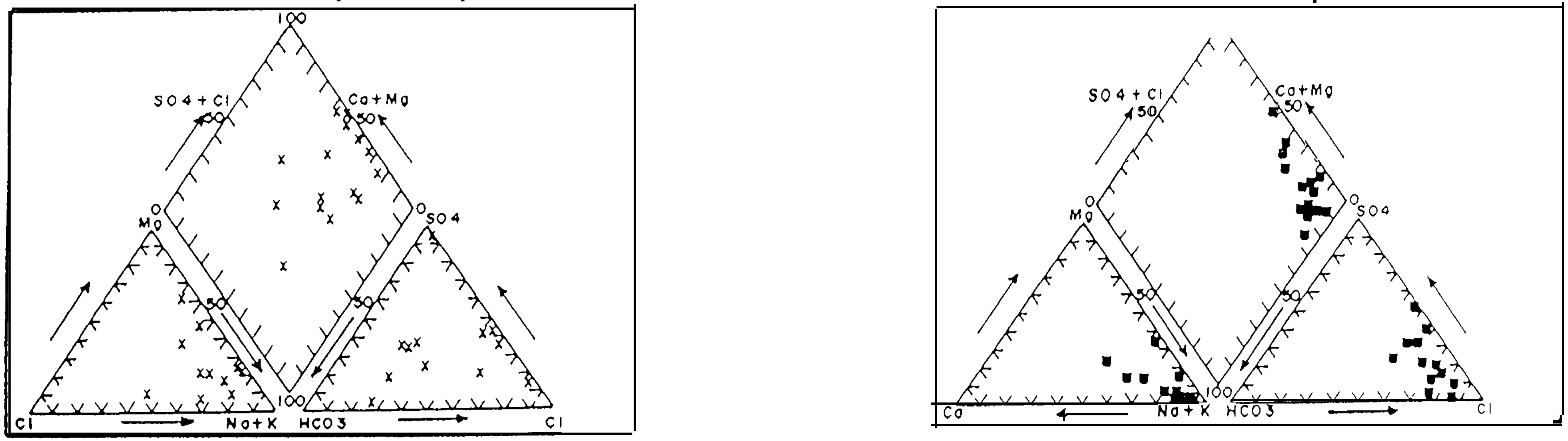

Fig.(6) **Piper diagram for the different aquifers at Qena area** past compared to the present. Hamza et al., [8] published a $\delta^{18}O$ value of −10.7‰ for the Nubian Sandstone water. The higher O-18 and H-2 values found in this study in water of wells in the Nubian sandstone aquifer at Wadi Qena (Eastern Desert) suggest an admixture of flood water. In recent years, floods have been ovserved in this area every year and the isotopic composition of the flood water has been found to be -1.0‰ for O-18 and -5.0‰ for H-2.

II- Nile River and Canal Waters

During the sampling campaigns in the Qena area, water was collected from the River Nile along its course between the High Dam and Cairo, as well as from canals in the region. It was found that the $\delta^{18}O$ values of the Nile water samples occupy a rather narrow range characterized by the analytical accuracy with a mean value of +2.3‰. (Other authors found values up to +3.2‰ for O-18 and +28.3‰ for H-2) The canal samples are slightly depleted with respect to Nile water; the mean values are +2.0 ± 0.5‰ for $\delta^{18}O$ and +19.5 + 1.8‰ for δ 2. The results suggest that the canal water contains portions of Nile water from periods before the construction of the High Dan [9], [10]. In order to distinguish River Nile Water from the groundwater of other origin in the study area, the mean isotope compositions and their temporal variability should be precisely known. When the High Dam in Aswan came into operation (constructed between 1964 and 1970) in 1967, the isotope compositions of the Nile Water changed.

The situation before 1967 in Upper Egypt was reconstructed from the present inflow of native Nile River water into the dam. It has average $\delta^{18}O$ and δ 2H values of -1.24 ± 0.08‰ and 0.8 ± 0.6‰, respectively, in December 1988 [6]. Hence, the present Nile water is by 3.5‰ higher in $\delta^{18}O$. There are other indications that there are long-term variations of the isotope compositions of the Nile water. Hamza et al. [8] found an enrichment of 6‰ in δ IH-2 between Beba and Cairo. The mean value of the $\delta^{2}H$ was +21.15‰ compared to +28.3‰ given by Simpson et al. [11]. Near the High Dam area the scatter of the data is smaller and range from +19.7 to 23.5‰ (Table 2). In summary, the $\delta^{18}O$ value of the Nile water changed from −1.2+0.1‰ before 1967 to about +2.3 to +3.3‰ afterwards. Correspondingly, the δ 2H value increased by 7 to 8‰. This result suggests long-term variations of the isotopic compositions of the Nile water.

III- Quaternary Aquifer

The $\delta^{18}O$/ δ 2H plot of the water samples of the quaternary aquifer is **shown** in Fig. (7). The points in this figure are situated below the MWL. The $\delta^{18}O$ heavy values range from +1.64 to +3.87‰. There is a trend of increasing salinity with enrichment of the stable isotopes which is the result of evaporation and the admixture of irrigation return flows.

IV- Basement Rock and Wadi Deposits Aquifer

The $\delta^{18}O$/ δ 2H plot of the water samples of the wadi deposits and the Basement rocks are shown in Fig. (7). The $\delta^{18}O$ values range widely from +6.5‰ to −7.1‰. A large number of delta values form a distinct evaporation line with a slope of 5.8. This side range of scattered points depend on its location near different adjacent aquifers and depth of sampling.

V- Plio-Pleistocene Aquifer

The delta values of the groundwater from the Plio-Pleistocene aquifer fit the MWL or are located just below (Fig. 7). The bulk of the data are concentrated around the old River Nile Water before the construction of the High Dam. There is a possibility of leakage from the depleted water of the Nubian Sandstone aquifer as indicated by several points. The distribution of the delta values show the effect of mixing and evaporation processes.

AGE ESTIMATION

Several tritium and carbon-14 measurements on groundwater samples were carried out in the Qena region. Applying the exponential model [12] to 3H values, the mean residence time (MRT) for the groundwater of the Plio-Pleistocene aquifer ranges from decades and several centuries. The conventional carbon-14 age for the Plio-Pleistocene aquifer amounts to a few thousand years. The reason for deviating 3H MRT and carbon-14 water ages may be a choice of the erratic initial carbon-14 value. If it would amount to 55 pMC instead of the applied 85 pMC the reservoir correction

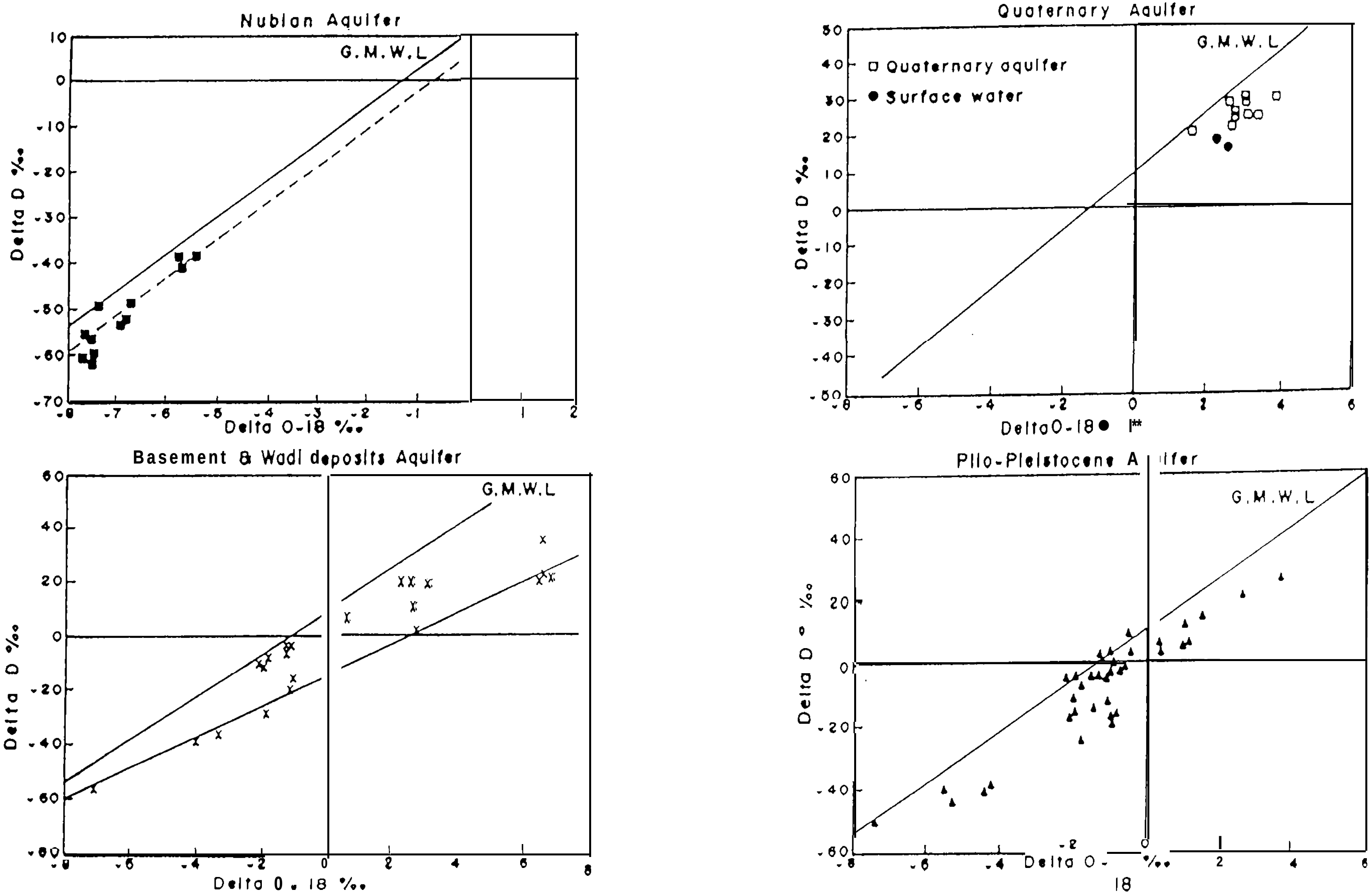

Fig.(7) **Delta oxygen-18 Vs. Delta deuterium diagram for the different aquifers**

Table (2) Values applied for mixing calculation for the possible end members

Component	$\delta^{18}O$	δD
River Nile water before High Dam (RNo) [6,13]	-1.2 .-0.6	0.8, 4.3
River Nile water after High Dam (RN)	2.30, 3.20	19.7, 28.3
Canal water (CW)	2.70	17.1
Irrigation Return (Ir)[9]	4.20	26.3
Nubian Sandstone water Eastern Desert (NS)	-6.60	-50.2
Nubian Sandstone water (average) (NS) [14]	-7.50	-58
Flood Water (FW) [15]	-1.00	-5

decreases from-1300 yr to -5000 yr. Another reason for such deviation can be a hydrochemically induced decrease of the ^{14}C value and the corresponding apparent increase of the ^{14}C water age [3]. Last but not least, mixture of young and old groundwater has to be taken into account.

DISCUSSION OF THE ISOTOPE HYDROLOGICAL RESULTS

The goal of the isotope hydrological study has been to estimate the contribution of different groundwater to the water budget. The dominant process is mixing. The isotopic data of the distinguished components are listed in Table 2.

THREE – COMPONENT MIXING MODEL (MX3)

The most simple interpretation of the isotope results can be based on mixing considerations of three major components RNo, RN and NS. The four other components are considered as absent and isotopic enrichment after mixing is neglected. It is assumed that the delta values of the end members do not vary temporally. The used end member values are compiled in Table 3.

Table 3: End member values applied for the MX3 model [3]

Component	$\delta^{18}O$	$\delta^{2}H$	d-excess
River Nile water before 1967	-1.2±0.‰	+0.8+1.0‰	+10.4‰
River Nile water after 1967	+2.8±0.5‰	+21.6+1.5‰	-0.8‰
Nubian sandstone water	-7.5±0.6‰	-58.0+4.0‰	+1.0‰

The effect of a wrong choice of the end member values is shown in Table 4, we applied the end member values of Table 3 and considered different mixtures of these three components. The sample water had a $\delta^{18}O$ value of -3‰.

Table 4: Two – component mixing calculations for a sample with a $\delta^{18}O$ value of –3‰ [3]

End members River Nile water		Proportion of River Nile water	Proportion of Nubian sandstone water
Before 1967	After 1967		
100%	0 %	71%	29%
50%	50%	46	54%
0%	100%	56%	44%

The results confirm that the modeled mixing proportions are very sensitive to the choice of the end member value.

MIXING MODEL WITH CORRECTION FOR EVAPORATIVE ISOTOPE ENRICHMENT (MX2)

There are two major mixing components with known isotopic compositions: NS and RNo. The third is flood water. The other four components consists of the three major components although their isotope compositions might had been modified by enrichment due to evaporation. Hence, we can reduce the number of mixing components to two (or maximum three) by correction of the $\delta^{18}O$ and $\delta^{2}H$ values for evaporative isotope enrichment. By this, the problem of different isotopic compositions of the River Nile water before and after 1967 would also be solved. The isotope data of the native River Nile water fit the MWL while those from the High Dam outflow reflect isotope enrichment due to a partial loss of water by evaporation [6]. The slope of the evaporation lines was determined to be 5.68. We found 5.8 for the Qena region. A slope of 5.95 was calculated for the Qusier-Safaga area, Eastern Desert in Upper Egypt [IS]. Although a slope of 6 is unusually high compared to 4.5, this value seems to be representative for Upper Egypt. We adopt the mean value of 5.8. The correction for evaporative isotope enrichment is done with equations using the raw $\delta^{18}O$ and δ^2H and the corrected $\delta^{18}O_e$ and δ *He values, respectively:

$$\delta^{18}O_C = (\delta^2H - S \times \delta^{18}O - 10) \;/\; (8 - S) \quad \text{and} \quad \delta^2H_C = 8 \times \delta^{18}O_C + 10$$

By this, the $\delta\ ^{18}O$ and δ 2H values of the end members were corrected for evaporative isotope enrichment. We used the calculated mean values of the data by Aly et al., [6] instead of the end member values given in Table 3. The uncorrected and corrected the $\delta\ ^{18}O$ and $\delta\ ^2H$ values of both Nile waters are shown in Table (5).

Table 5: End member the $\delta\ ^{18}O$ values for Nile water and Nubian Sandstone water

	$\delta^{18}O$ [‰]	δ^2H [‰]	$\delta^{18}O$ [‰]	6 % [‰]
	uncorrected		Corrected (S = 5.8)	
Nile water before 1967	-1.20 ± 0.23	+0.8 ± 1.0	-1.02 ± 0.7	+1.8 ± 5.6
Nile water after 1967	+2.30 ± 0.5	+19.7 ± 1.0	-1.65 ± 1.4	-3.2 ± 11.2
Mean			-1.32 ± 1.1	+0.2 ± 5.0
Nubian Sandstone water	-7.40 ± 0.6	-55.2 ± 0.4	-10.4 ± 0.5	-73 ± 12.8

The procedure of the $\delta^{18}O$ correction for evaporative isotope enrichment before the application of the MX2 model is demonstrated in Fig. 8. It is of minor importance if isotope enrichment occurs before or after the mixing.

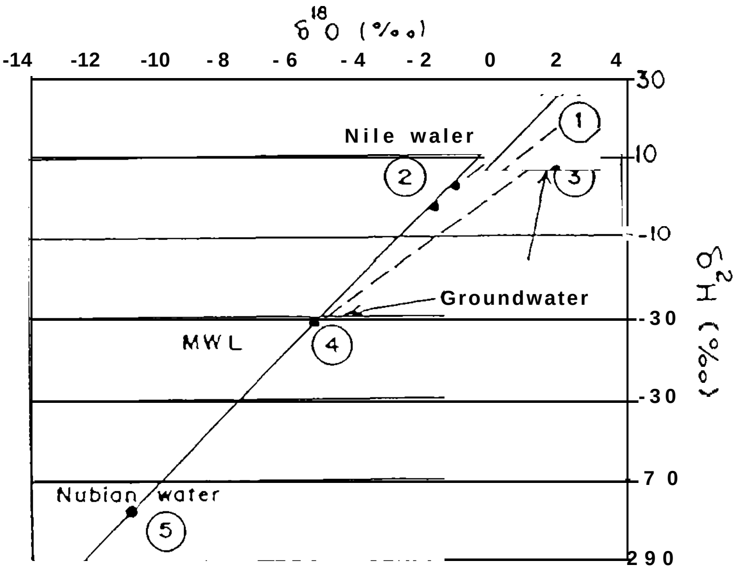

Fig.(8) Scheme of the application Of the two-component mixing model with the correction of the 6 180 values for evaporative isotope enrichment.The raw and corrected6 180 values of the Nile water are represented by the points 1 and 2 ,respectively The determined 6 180 value of the sample and the corrected ones using a slope of 5·8 are represented by the points 3 and 4. The end member value of the Nubian sandstone water is found at point 5

The MX2 model give more reliable results than MX3 model. The reliability check is based on the proportions of the River Nile water calculated for the samples of surface water and of the Quaternary aquifer. Both kinds of water should contain 100% River Nile water.

Applying third mixing model using several end members resulted in the following contributions from palaeo water in the different aquifers. For the Quaternary aquifer, the contribution of Palaeo water is 1 to 5%, Plio-Pleistocene aquifer, (9 to 16%) to in Wadi deposits & Basement aquifer, (25 to 35%).

The main results of the chemical and the isotope hydrological evaluation are:

1- The mean residence time of the groundwater in the Quaternary aquifer ranges from a few decades to centuries, while in the Plio-Pleistocene aquifer it ranges from 3 few centuries to millennia as indicated from tritium and carbon-14 measurements.
2- The majority of the groundwater samples was affected by partial evaporation as shown by the slopes of their regression lines.
3- The recharge contribution of the palaeo water of the Nubian sandstone aquifer is estimated to be up to 35% of the total input sources.

ACKNOWLEDGEMENT

The authors gratefully acknowledge the International Atomic Energy Agency (IAEA) Vienna, Austria, for supporting this work under a regional technical cooperation project.

REFERENCES

[1] SAID, R, “Geology of Egypt” Elsevier Publishing Company, Amsterdam, The Netherlands (1962).

[2] Research Institute for Groundwater (RIGW) “Development and Management of Groundwater Resources in the Nile Valley and Delta”, RIGW/IWACO, Technical note 70, 120-88-06 project (1988).

[3] GEYH, M.A., “Interpretation of isotope - hydrological results” “IAEA report of an expert mission, RAF/8/022, 43 pp. Cairo - Egypt (1996).

[4] National Center for Nuclear Safety and Research Institute for Groundwater, “Model Project On the Estimation of Recharge from Nile Aquifer to the Desert Fringes at West Esna & Wadi Qena in Upper Egypt” RAF/8/022, Final Report, 105 pp Cairo, Egypt (1998).

[5] PIPER, A.M., “A graphic procedure in geochemical interpretation of water analysis” Am. Geophys. Union Trans., 6914 (1945).

[6] ALY, A.I.M., FROEHLICH, K., NADA, A., AWAD, M., HAMZA, M., SALEM, W.M., “Study of environmental isotope distribution in the Aswan High Dam lake (Egypt) for estimation of evaporation of lake water and its recharge to adjacent groundwater”. Environmental Geochemistry & Health 15 (11: 37-39 (1993).

[7] SONNTAG, C., KLITZ, E., LOEHNERT, E.P., EL-SHAZLY E.M., MUENNICH, K.O., JUNGHANS, CH., THORWEIHE, U., WEISTROFFEROFER, K., SWAILEM F.M., “Palaeoclimatic information from deuterium and oxygen-18 and carbon-14 dated north Saharan groundwater - In: Isotope Hydrology 1978: 569-581; IAEA, Vienna.

[8] HAMZA, M.S., SWAILEM, F., ABDEL-MONEM, A., “Groundwater hydrology of Wadi El-Natrun III. Distribution of radium and deuterium contents”. Isotope & Rad. Res. 12(1): 17-23 (1980).

[9] EL-BAKRI, A., TANTAWI, M.A., HAMZA, M.S., AWAD, M.A. “Estimation of groundwater inflow to irrigation drains in Minia, Upper Egypt, based on a deuterium and oxygen-18 evaporation pan technique”. Hydrological Science Journal Vol. 41 No. 1 pp. 41-48 (1996).

[10] SHIVANNA, K., “Isotopes in Groundwater Resources Development. Technical Backstopping to Field Activities - Report on Expert Mission: RAF/8/022, 23 pp., : Cairo, (1996).

[11] SIMPSON, H.J. HAMZA, M.S. WHITE, T.W.J. NADA, A., AWAD, M.A., “Evaporation enrichment of deuterium and ^{18}O in arid irrigation - In : Isotope Techniques in Water Resources Development. 241-256; IAEA, Vienna (1987).

[12] ALY, A.I.M., FROEHLICH, K., AWAD, M., MOUSTAFA, W.M., NADA, A., "A model of hydrologic interpretation of tritium content of groundwater in Egypt". Mutah Journal, Res. Studies, 9(2): pp 263-279 (1994).

[13] AWAD, M.A., FARID, M.S., HAMZA, M.S., "Studies on the recharge of the aquifer system in the southern portion of the Nile Delta by use of radioisotopes and hydrochemistry" Isotope & Rad. Res. Vol. 26, No. 2, pp 21-25 (1994).

[14] GEYH, M.A. "The ^{14}C time scale of groundwater Correction and linearity In : Isotope Techniques in Water Resources Development 1991 : 167-177 Proc., IAEA - SM- 319/17 IAEA, Vienna (1992).

[15] AWAD, M.A., HAMZA, M.S., ATWA, S.M., SALLOUMA, M.K., "Isotopic and hydrochemical evaporation of groundwater at Qusier - Safaga area, eastern desert, Egypt". Environmental Geochemistry and health vol. 18: pp. 47-54 (1996).

CURRENT AND FUTURE IMPACT OF AN URANIUM MINE WASTE DISPOSAL SITE ON GROUNDWATER

P. SCHNEIDER’, K. OSENBRUCK[3], K. NINDEL’, S. VOERKELIUS”,
M. FORSTER[3], J. SCHREYER’

Hydroisotop-Piewak GmbH, Oberfrohnaer Strasse 84, 09 117 Chemnitz
[2] Wismut GmbH, Jagdschänkenstrasse 29, 09117 Chemnitz
[3] Hydroisotop GmbH, Woelkestrasse 9, 85301 Schweitenkirchen

Abstract

At Schtisselgrund valley, East Germany an uranium mine dump of about 4 Mil m^3 had been built due to an intensive exploitation of uranium ore deposit near Dresden. In order to evaluate and to specify the current and future environmental impact of the disposal site, investigations of environmental and radioactive isotopes have been performed as part of a hydrogeological and hydrochemical study at the Schtisselgrund Mine Dump. Beneath the dump we find significantly contaminated water in the first and second aquifer in a narrow strip of faulted rock. The main contaminants comprise of uranium and radium as well as of zinc, nickel and sulphate. The mean residence time of those waters percolating the dump is about 1 to 5 years with contributions of an older component. The ^3H and ^{85}Kr contents in the groundwater of the first aquifer yield a mean residence time of about 20 years, which obviously is less than the life time of the dump (built in 1967). The second aquifer shows a groundwater mixing system. Within this study, the groundwater of the third aquifer with ^3H contents close to or below detection limit did not show any detectable influence of the dump waters. This is supported by high groundwater ages of several thousand years according to the ^{14}C values. Close to the former mine system, there are local groundwater samples from the third aquifer showing ^3H contents of up to 8 TU, which may be caused by groundwater flowing on fractures and on pathways within the former mine system. Part of the dump waters drain into the nearby rivers by interflow processes as indicated by stable isotopes.

1. INTRODUCTION

The Königstein Uranium Mine in East Germany has been closed in 1990 due to the end of uranium production in the former GDR. In consequence of the intensive exploitation of the uranium ore deposit, a mine dump of about 4 Mil m^3 has been built at Schtisselgrund valley near Königstein [1]. After remediation of the dump, the groundwater will become the most important pathway for the migration of radioactive and toxic contaminants, which are released from the dump into the environment. Due to adjacent groundwater resources, efficient and sustainable remediation concepts are needed.

In order to comply with the requirements of radiological protection [2], long time scenarios for the current and future environmental impact of the dump and its effluent waters have to be derived. The aim of this study was to investigate the geochemical characteristics of the surface and groundwater near the dump, the migration processes and the time scales of the release and subsequent transport of contaminants within the groundwater. This can only be fulfilled by a combination of hydrogeological, isotope, specific radiological and hydrochemical investigations. The paper presented here, will focus on the characteristics and time scales of the aqueous contaminant transport derived from isotope geochemical investigations.

The results provide a basis for an integrated risk assessment [3] of man's radiological and toxicological exposure due to possible water usage in the surrounding areas. Moreover, the results allow to derive an optimised concept for remediation of the Schüsselgrund Mine Dump.

2. DESCRIPTION OF THE SCHÜSSELGRUND MINE DUMP

The Schüsselgrund mine dump is situated in the south east of Saxonia, Germany, next to the National park „Sächsische Schweiz". It was filled from 1967 to 1990, when the uranium mining in the former GDR took place. Due to the intensive exploitation of uranium from ore deposits in Saxonia, a dump of 24 hectares in extension and $4 \cdot 10^6$ m^3 in volume has been built up at the Schüsselgrund valley. The dump has a thickness of 10 to 30 m. The study site (Fig. 1) receives an average annual precipitation of 800 mm with maxima in march, april and august.

The material deposited on the Schüsselgrund mine dump is of different composition and heterogeneously distributed. We find mining residues of the host rock (sandstone), iron, building material and bricks from the abandoned mine and residues of the percolation water treatment (mud and pressed mud). The majority of the sandstone material is of block size (> 6.3 cm). Due to acid in-situ leaching of uranium, the dump waters are characterized by low pH-values of about 3. Only the residues of the water treatment show a buffering capacity due to their carbonate content. The sandstone is nearly free of carbonates (< 1 weight-%) and therefore has no buffering and sorption capacity for heavy metals and radionuclides [4].

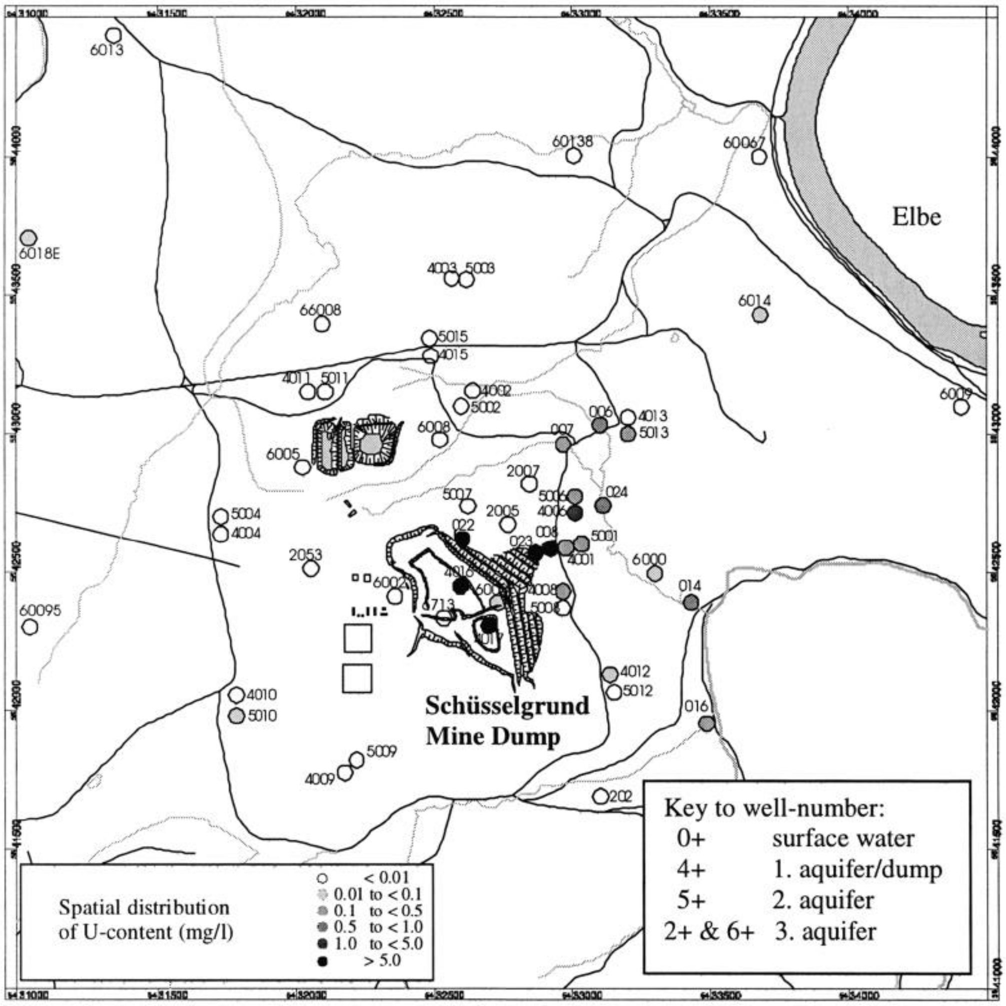

FIG. 1. Map showing the location of the Schüsselgrund Mine Dump and of the observation wells. The contamination plume in the groundwater downstream the dump is indicated by high uranium contents.

3. GEOLOGICAL AND HYDROGEOLOGICAL SETTING

The underground of the study area is formed by Upper Cretaceous sandstones. The Schüsselgrund Mine Dump is covering the former Schüsselgrund valley, which was formed by weathering of the outcropping sandstone formations. Due to fractures and tectonic structures the sandstone is classified as a combined pore and fracture aquifer [5]. There are four different aquifers in the investigation area (Fig. 2). These aquifers are separated by partly confining silt- and claystone layers. In pre-mining times the groundwater of the third level had been confined, but due to the mining activities the water tables of the different aquifers declined locally, which in the case of the fourth aquifer resulted in a nearly complete removal of water.

The main groundwater flow direction is from south to north in the third and from southwest to northeast in the upper two aquifers, governed by drainage to the Elbe river and its local tributaries. Referring to pumping tests, the mean hydraulic conductivities of these aquifers range from 10^{-5} to 10^{-7} m/s, with elevated values of 10^{-4} m/s in tectonic structures. Recharge into the unconfined aquifers takes place throughout the study area by infiltration of precipitation and vertical leakage. The main recharge area of the third groundwater level is considered to be the outcrops of the Lower Turonian about 6 km to the south of the dump.

Water saturation within the dump is maintained only at the bottom with an extension of about 2 m. In most parts of the dump, an impermeable basement is missing. Consequently, percolating dump waters can directly enter the first groundwater level. The amount of infiltrating dump waters range from about 50 to $100 \cdot 10^3$ m³/year as shown by calculations of the dump water balance [6].

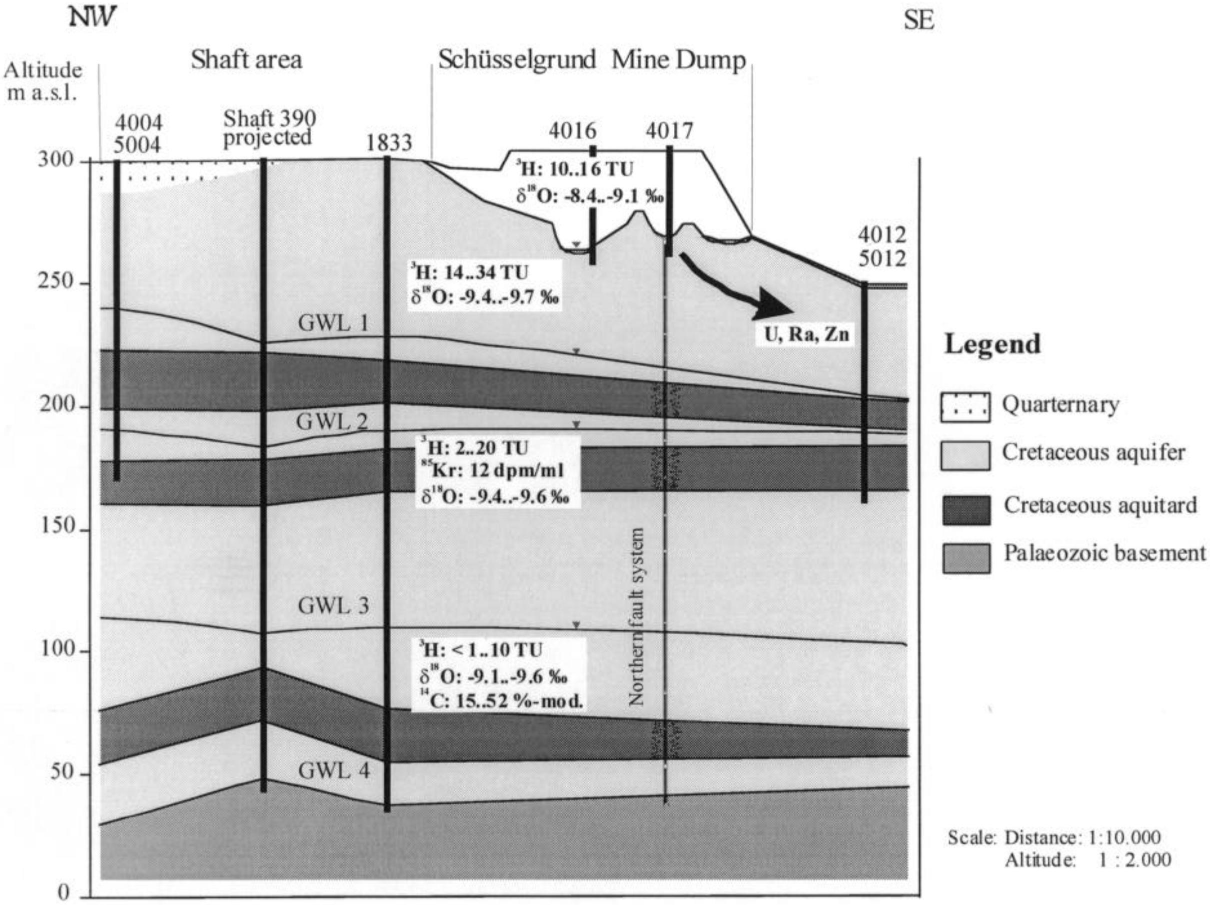

FIG. 2. Schematic cross section of the Schüsselgrund site along the groundwater flow direction.

4. RESULTS OF ENVIRONMENTAL ISOTOPES AND HYDROCHEMISTRY

4.1. Hydrochemistry of the surface and groundwater

Groundwater and surface water samples were taken at selected monitoring wells upstream and downstream from the Schiisselgrund Mine Dump (Fig. 1). The hydrochemical results clearly indicate the release of contaminated dump water into the surface- and groundwater. High oxygen contents and low pH inside the dump result in a prevailing mobilising milieu for radionuclides and heavy metals. Thus. the porewater from two observation wells inside the dump (nos. 4016 and 4017) as well as from basins collecting the percolating water (nos. 022 and 023) show high contents of uranium (20 to 30 mg/l), thorium 230 (150 to 250 Bq/l), radium 226 (about 1 Bq/l) and actinium 227 (2 to 10 Bq/l). In addition high contents of the heavy metals zinc (50 to 150 mg/l) and nickel (2 to 4 mg/l) also high sulphate contents of 2 to 4 g/l are present in the dump water. The low pH of about 3 is due to residues of leaching acid in the pore water of the dump material and only secondarily due to pyrite oxidation.

The influence of the dump on the surface waters of the study area can be seen from elevated contents of the main contaminants U, Ra, Zn and Ni at the sampling sites in the small Eselsbach creek (nos. 014 and 024). According to the difference of more than 10 m between the position of the Eselsbach and the water level of the first aquifer, the contaminants are assumed to migrate to the river by interflow of dump water in the sandstone formations.

The groundwaters of the first and second aquifer are dominated by SO_4 and HCO_3-SO_4 types. Underneath the dump we find significantly contaminated water with uranium contents up to 2 mg/l in a narrow strip of fractured rock less than 1 km downstream the dump (Fig. 1). The water of the second aquifer is characterized by lower concentrations of the contaminants, but still higher concentrations than the geological background. A value of about 25 % of contaminated dump water in the first aquifer can be derived by a mixing estimation based on chloride and sulphate (no. 4006). Within this study, the groundwater of the third aquifer did not show any detectable influence of the dump waters.

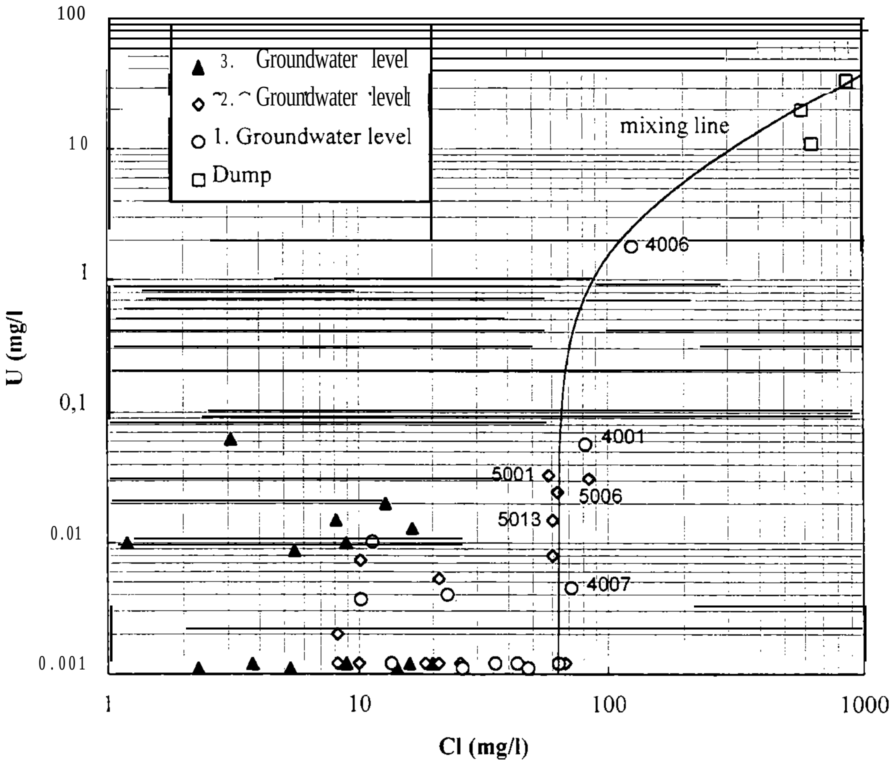

FIG. 3. Plot of U against Cl content. The numbers indicate samples from the contamination plume. The curved shape of the mixing line is due to the double logarithmic scale of the diagram.

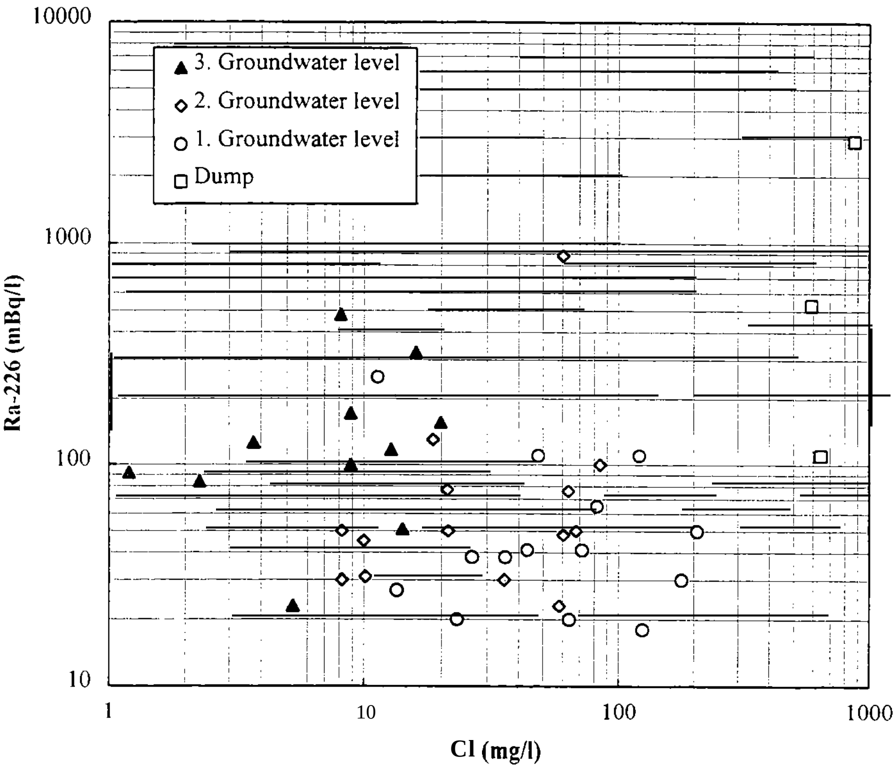

FIG. 4. Plot of ^{226}Ra against Cl content. ^{226}Ra background values range from 40 to about 200 mBq/l.

The mobility of the dissolved contaminants in the groundwater can be verified by comparison with a conservative tracer like chloride. In case of uranium (Fig. 3) the groundwater samples from the contamination plume downstream the dump plot along a mixing line with porewater from the dump. This suggests that only a minor part of uranium is removed from solution by sorption effects. In contrast to uranium the radium contents do not exhibit a distinct correlation with chloride (Fig. 4). Most likely radium 226 and other radionuclides are precipitated by changes of the geochemical conditions when released from the dump.

4.2. Stable Isotopes ^{18}O and ^{2}H in surface and groundwater

The dump waters are characterized by mean $\delta^{18}O$ and $\delta^{2}H$ values of -8.8 ‰ and -61 .O ‰, respectively and agree reasonably well with the isotope signature of the surface waters (e.g. nos. 0 14 and 024 in the Eselsbach creek). In contrast to this the groundwaters below the dump show significantly different $\delta^{18}O$ and $\delta^{2}H$ values ranging from -9.3 to -9.8 ‰ and -65 to -69 ‰ (Fig. 5). An influence of evaporation effects cannot be identified in neither the groundwater samples nor the dump and surface waters.

The identical range of $\delta^{18}O$ values in the third (almost tritium free) and the uppermost two aquifers (high tritium contents) indicates, that the groundwaters found in the study area are of Holocene origin. There is no evidence for a contribution of groundwaters significantly depleted in the stable isotopes ^{18}O and ^{2}H, due to recharge under cooler climatic conditions in the Late Pleistocene.

From the contaminant content in the surface water of the Eselsbach creek an admixture of dump water has been concluded. The $\delta^{18}O$ value of the surface sampling sites along the river are in good agreement with the isotopic composition of the dump waters and do not show an admixture of waters with more negative $\delta^{18}O$ values, which are typical for the first groundwater level. This confirms, that the migration of contaminants is due to an interflow of dump water into the Eselsbach creek.

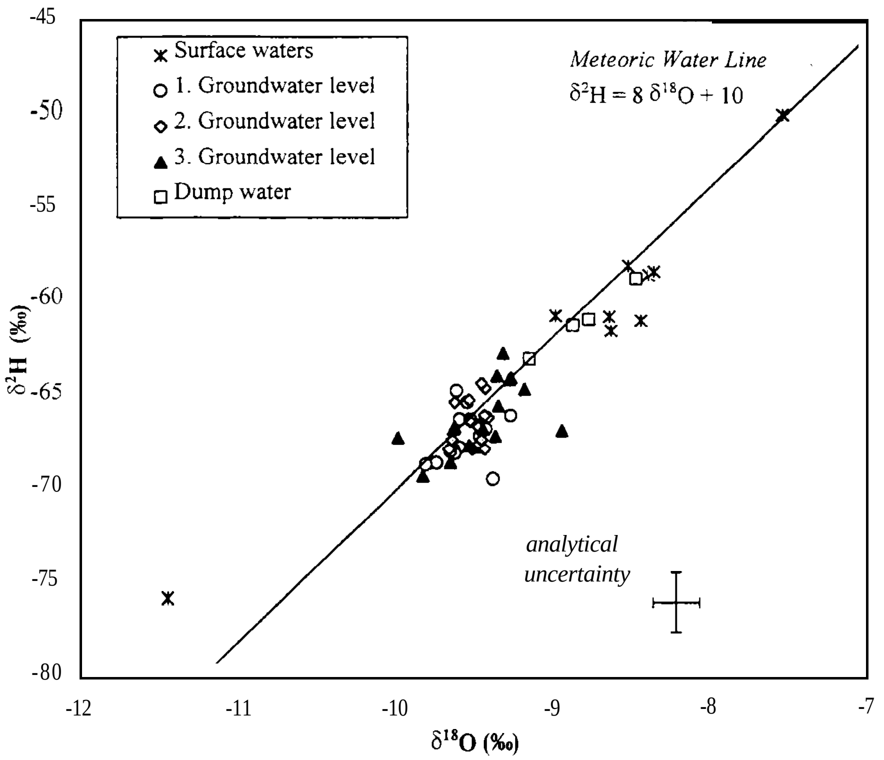

FIG. 5. Plot of $\delta^{18}O$ ugainst δ^2H to characterize the investigated surface, dump and groundwater.

The time scale of these interflow processes is derived by comparison of the time series of the $\delta^{18}O$ values with the annual variation of ^{18}O in precipitation. The surface near dump waters take about one month to drain into the nearby rivers, A similar annual variation of the $\delta^{18}O$ values has been found in the dump water (no. 4016), which suggests the contribution of a fast infiltrating water component with residence times of less than 1 year to the water percolating the dump.

4.3. Tritium (^3H) and ^{85}Kr content of surface- and groundwater

The tritium content of the dump waters is in good agreement with the tritium range of the actual precipitation (Fig. 6). This supports the dominance of a young water component with residence times of less than 5 years. Two samples show lower tritium contents of about 10 TU, which is confirmed by a low ^{85}Kr content of 28 dpm/ml_{Kr}, as against the current specific activity of the atmosphere of about 70 dpm/ml_{Kr} [7]. A consistent age estimation of about 10 years for ^3H and ^{85}Kr is derived if the piston flow model is applied to the dump waters. An alternative explanation of the low tritium and krypton-85 content is the admixture of an old ^3H and ^{85}Kr free water. On a first view this contradicts the time-span of about 30 years of the dump existing at the study site. This discrepancy is solved, if the block size of the dump material is taken into account. In addition to residues of the leaching acid, blocks with grain sizes above 10 cm are likely to contain residues of the original, tritium free pore water from the fourth groundwater level of the pre-mining era.

The groundwaters of the first and second aquifer are characterized by tritium contents ranging from 2 to 34 TU. Values of more than 20 TU are exclusively found within the first groundwater level, but still the groundwaters here show large variations from 14 to 35 TU. Tritium contents of 14 to 18 TU in some samples from the first aquifer, which agrees with the tritium activity of recent precipitation, indicate the presence of recent infiltration (< 5 years) in areas of high permeability along the fault system. In contrast to this, tritium values above 25 TU suggest residence times of about 20 years according to the exponential model. In correspondence with the hydrogeology of the study area, the range of tritium contents can be explained by exchange and/or mixing processes between fast flowing water on fractures and groundwater in the pore spaces of the sandstones with higher residence times.

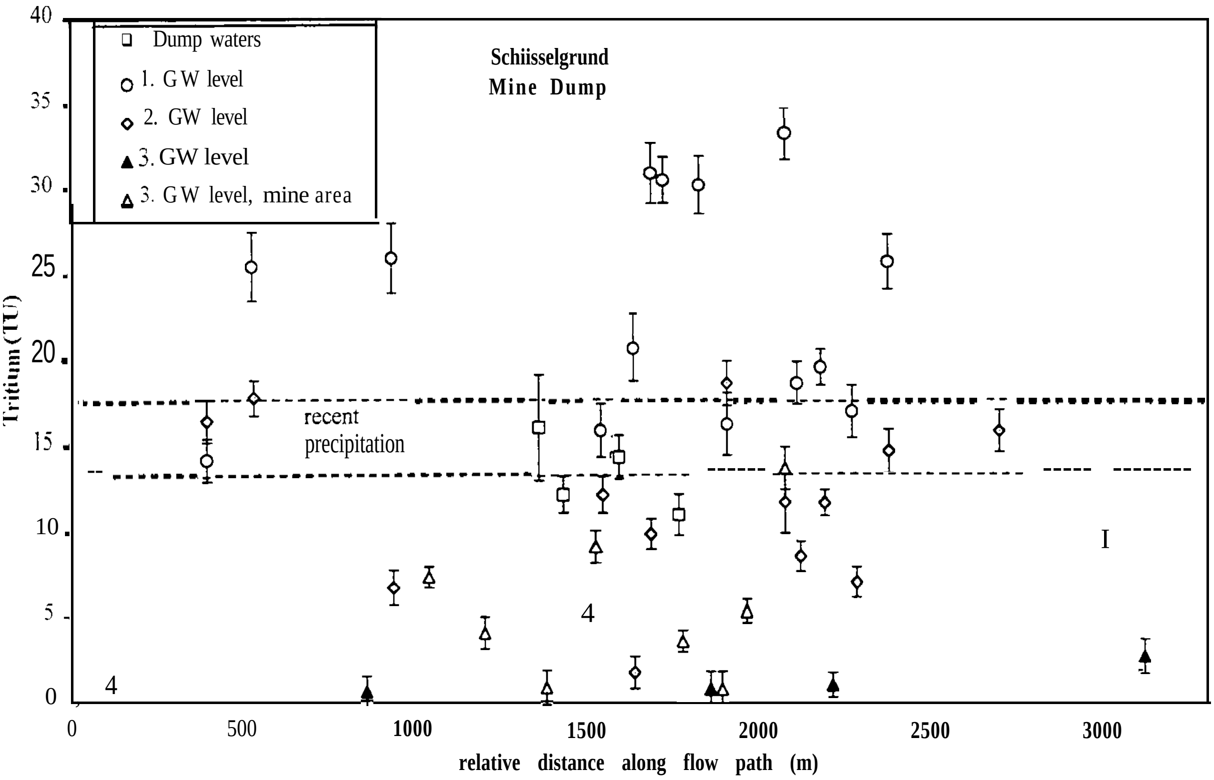

FIG. 6. Variation of the tritium content in flow direction. The locations of the observation wells are projected onto a cross section through the dump inji'ow direction.

The tritium contents of 2 to 19 TU in the second aquifer are most likely due to a mixing system consisting of ^{3}H containing groundwater from the first level and 'H-free groundwater from a distant recharge to the second aquifer. The mixing process is confirmed by ^{85}Kr contents of about 12 dpm/ml$_{Kr}$, which suggests an addition of about 50 to 60% of an old (> 40 years) ^{3}H and ^{85}Kr free component [7]. Due to several shafts and exploration boreholes as well as natural hydraulic windows between the surface near aquifers, connections between the different groundwater levels exist and obviously result in the observed mixing. Thus, it can be concluded, that the low contaminant concentrations in the second aquifer are due to dilution by uncontaminated water.

Outside the mining area, the third aquifer shows ^{3}H contents close to or below detection limit. The absence of a polluted groundwater component in this part of the third aquifer is supported by high groundwater ages according to the ^{14}C values. Local groundwater samples, which are expected to be influenced by the uranium mine (most of these samples were taken from exploration boreholes in mine galleries) show ^{3}H contents of up to 14 TU, which may be caused by the leakage of groundwater from the first and second level flowing on fractures and artificial pathways of the former mine system.

4.3. Carbon isotopic composition of the third groundwater level

The ^{14}C contents in the deep groundwater of the third groundwater level range from 15 to 53 %-modern. Due to the very low carbonate contents of the Cretaceous sandstones the dissolved inorganic carbon (DIC) contents of the groundwater are also low (HCO_3 contents of less than 1.5 mmol/l, see Fig. 7). The δ^{13}C of the DIC shows values of -20 to -15 ‰, which suggests dominating carbonate dissolution under closed conditions within the aquifer.

Only one sample (no. 6013) from the undisturbed part of the third aquifer shows a high DIC content of 3.5 mmol/l. The δ^{13}C value of -9.9 ‰ indicates the influence of additional isotope exchange processes, which may have led to a further dilution of the ^{14}C content towards the measured value of 15 %-modern.

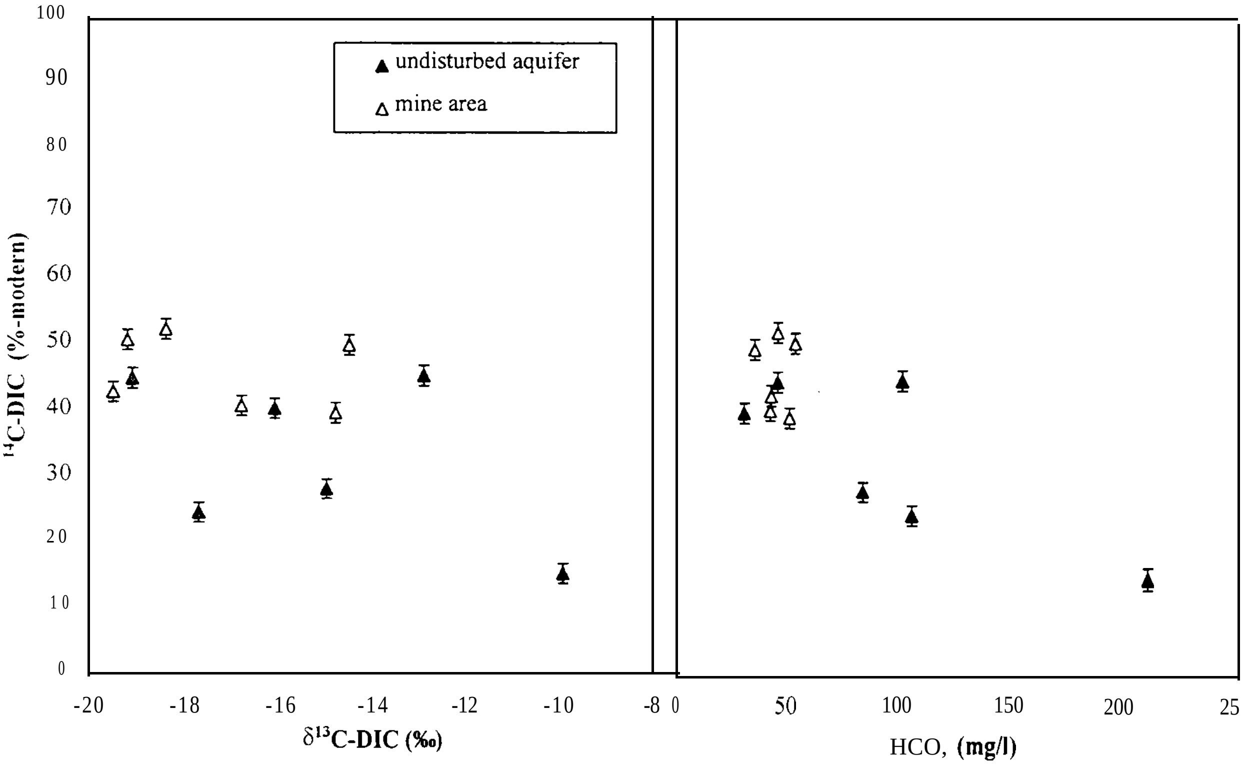

FIG. 7. Plot of δ^{13}C-DIC content (left) and HCO_3 content (right) against the ^{14}C-DIC content of samples from the third groundwater level.

The groundwater samples in close relation to the former mine system have been shown to contain tritium, which is due to local mixing with groundwater from the surface near aquifers. Therefore, the decrease of the ^{14}C contents as a function of δ^{13}C and HCO_3 values in Fig. 7 is supposed to be only partly due to carbonate evolution but also due to mixing with a young groundwater component.

The observation of tritium in samples of low ^{14}C content can be explained in two ways. Due to exploration shafts and boreholes in connexion with the uranium mining and the local decrease in water levels around the mine, young tritium bearing surface near groundwater entered the third groundwater level by hydraulic connections. Such a mixing system is indicated in Fig. 8 as hydraulic mixing. The "old endmember" is best represented by the tritium free groundwater sample of observation well no. 60 13 with a ^{14}C content of 15 %-modern. Assuming a reasonable initial ^{14}C content of about 50 to 80 %-modern a residence time of about 10000 years can be estimated from the ^{14}C content. This is in agreement with the stable isotopes, which suggested Holocene recharge of the groundwater.

An additional mixing process is expected to originate from the hydrogeological conditions of the investigated aquifers, which are characterized by a combination of groundwater flow in the pore space and preferential flow on fractures and fissures of the fault system, In this case mixing is also due to an exchange of solutes and isotopes between the mobile groundwater on fractures and relatively slow moving pore water within the sandstone matrix by molecular diffusion [8]. Using a mean hydraulic conductivity of about $5\cdot10^{-6}$ m/s, a total porosity of about 0.15 and a hydraulic gradient of about 0.02 known from pumping tests in the third aquifer, a theoretical distribution of ^{3}H and ^{14}C contents along a mixing line from matrix diffusion has been calculated in Fig. 8.

The distribution of the data points suggests the ^{3}H and ^{14}C values to be the result of a combination of the discussed processes. Their specific relevance depends on the complex hydrogeological conditions of the considered sampling site.

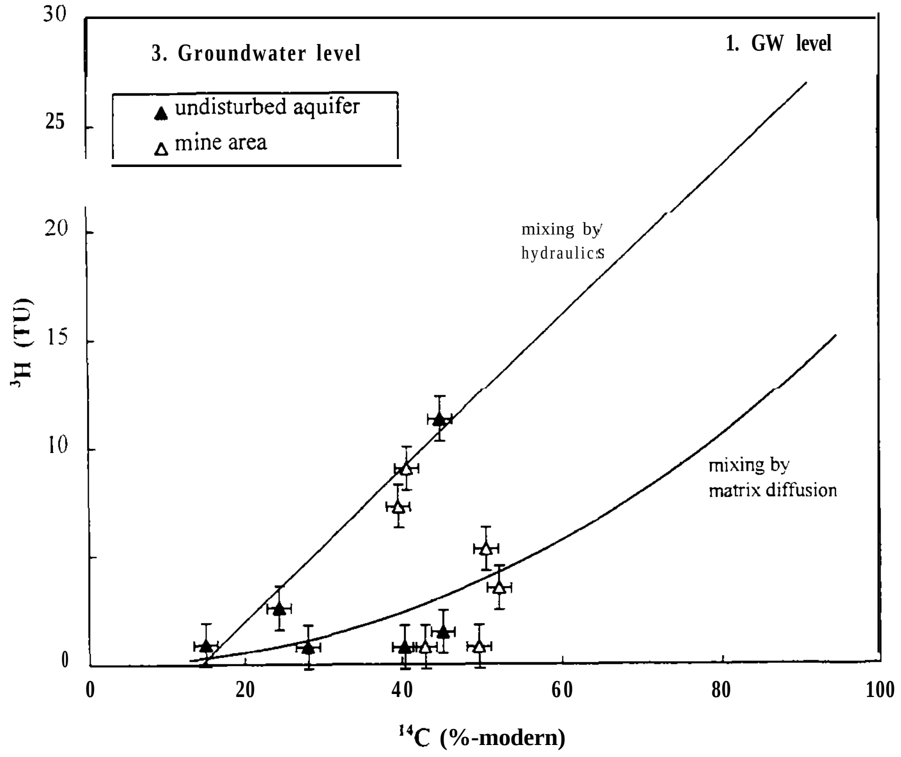

FIG. 8. Plot of tritium against ^{14}C-DIC content of the third groundwater level.

5. CONCLUSIONS

The impact of the Schüsselgrund Mine Dump on the aquatic environment is determined by the evolution of the contaminants dissolved in the dump water and the amount of water released from the dump per year. Precipitation will infiltrate into the mostly uncovered dump body and eluate contaminants. Due to the heterogeneous structure of the dump, preferential flow paths for percolating waters are assumed to be responsible for the dominating water with low residence times, indicated by variations in $\delta^{18}O$ and recent ^{3}H values. This is also confirmed by first geochemical modelling of the dump water, which suggests non equilibrium conditions of the dissolved uranium with uranium minerals present in the dump material. In addition, minor contributions of water with residence times of about 10 years or even above (according to ^{3}H and ^{85}Kr) are due to a porous flow in less permeable parts of the dump or to small admixtures of pore waters from the sandstone blocks.

Because of the continuous addition of acid to the percolating dump water the delivery of heavy metals and radionuclides cannot be stopped but minimized. Therefore an in-situ-remediation with covering the dump with compacted soil in order to reduce the infiltration rate was proposed. The reduced input of infiltrating water will result in an increased residence time of the dump water approaching the values deduced from ^{3}H and ^{85}Kr due to the disappearance of the fast flowing component, which was supplied by single rain events. Longer residence times will presumably also increase the uranium content of the dump water due to solution kinetics. Changes in the geochemical conditions for example by a distinct decrease in redox-conditions by a geochemical barrier may help to prevent uranium from being mobilised.

Besides the behaviour of the dump itself, the future impact of the Schiisselgrund Mine Dump is also affected by the time scales of groundwater flow and contaminant transport deduced from the isotope investigations. The contaminant content present in the first aquifer represents the utmost contamination at the prevailing geochemical conditions, which is feasible within the aqueous environment of the dump. This can be concluded from groundwater residence times of up to 20 years in the groundwater of the first aquifer, which obviously is less than the life time of the dump (build in 1967).

Although retardation effects by sorption cannot be ruled out, the results of the hydrochemical investigations show, that in case of the dissolved uranium, sorption effects during groundwater flow are only of minor importance. The influence of uranium retardation by diffusive exchange with pore water is already taken into account by the groundwater residence time derived by isotope measurements. A retardation factor of about 5 is revealed for the first aquifer by comparing the groundwater flow velocity of about 1.5 m/d (hydraulic conductivity of $5 \cdot 10^{-5}$ m/s; hydraulic gradient of 0.05; porosity of 0.15) with the tracer velocity of 0.3 m/d (residence time 20 years; flow distance 2500 m). Due to strong dilution by uncontaminated groundwater, no contaminant contents can be found in the third groundwater level. There is no evidence of a present or future influence of the Schüsselgrund mine dump on the groundwater wells situated in the third aquifer downstream of the mine.

ACKNOWLEDGEMENTS

We thank W. Knabe and P. Slesacek of the Sanierungsbetrieb Kbnigstein for helpful discussions and assistance in the field. We are grateful to H.H. Loosli, Universitat Bern, for the ^{85}Kr measurements.

REFERENCES

[1] FORSTER, M., NINDEL, K., PIEWAK, M., SCHNEIDER, P., SCHREYER, J., "Gestaltungskonzept der Schüsselgrundhalde unter Beachtung der Einordnung in das angrenzende Landschaftsschutzgebiet", Revitalisierung/Wiedernutzbarmachung der Bergbaufolgelandschaft des Uranerzbergbaues in Sachsen und Thüringen (Proc. Symp. Chemnitz, 1996). Wismut GmbH (1996).

[2] International Commission on Radiological Protection: Recommendations of the International Commission on Radiological Protection, ICRP Publication 26, Pergamon Press Ltd., Oxford (1977).

[3] Bundesamt fur Strahlenschutz (BfS), Sachsisches Staatsministerium für Umwelt und Landesentwicklung (SMU), Integrierte Bewertung radiologischer und chemisch toxischer Kontaminanten, (Proc. Workshop, Dresden, 1997), SMU, Dresden (1997).

[4] SCHNEIDER, P., NINDEL, K., SCHREYER, J., FORSTER, M., PIEWAK, M., "Complex Hydrochemical and Isotopic Investigation to Specify the Environmental Impacts of an Uranium Ore Disposal Site - Practical Approach, Investigation Methods and Results-".Mining and the Enviroment II (Proc. Symp. Sudbury, 1999), Centre In Mining and Mining Environment Research (1999).

[5] PIETZSCH, K., Geologie von Sachsen, Deutscher Verlag der Wissenschaften, Berlin (1963).

[6] SCHNEIDER, P., NINDEL, K., ZADDACH, V., FORSTER, M., PIEWAK, M., "Wasserhaushalt der Schüsselgrundhalde des Sanierungsbetriebes Königstein - Lösungsansatz, meßtechnische Untersuchung zur Kalibrierung des Modells und computergesttitzte Modellierung mit dem Programm HELP", Old Crust - New Problems, Geodynamics and Utilisation, Terra Nostra 99/1, Schriften der Alfred-Wegener-Stiftung e.V., (1999) 1 SO- 189.

[7] BERTLEFF, B., WATZEL, R., EICHINGER, L., HEIDINGER, M., SCHNEIDER, K., LOOSLI H.H., STICHLER, W., "The use of isotope based modelling techniques for groundwater management in a Quaternary aquifer system", Isotope Techniques in the Study of Environmental Change (Proc. Symp. Vienna, 1997), IAEA, Vienna (1997).

[8] MALOSZEWSKI, P., ZUBER, A., On the theory of tracer experiments in fissured rocks with a porous matrix, J. Hydrol. 79 (1985) 333-358.

ISOTOPICALLY HIGHLY ENRICHED SHALLOW GROUNDWATER BELOW OVERLYING DRY SEDIMENTS

M.A. GEYH
Joint Geoscientific Research Institute,
Hannover, Germany

GU WEIZU
Bureau of Water Conservancy of Chuzhou,
Chuzhou, China

Abstract

The isotopic compositions of oxygen and hydrogen of the shallow groundwater in the Gurinai Grasslands west of the Badajilin Desert in China are unusual: Both the $\delta^{18}O$ and δ^2H values fit an apparent local meteoric water line with an unusually low deuterium excess of <-20 ‰. Four possible causes have been considered: (a) an admixture of fossil lake water, (b) an admixture of water from the Black River, (c) unusual isotopic compositions of the regional precipitation, and (d) processes which secondarily modify the isotope signature. Cases (a) and (b) have been excluded on the basis of our former isotope results.

In two other case studies in Chile and Canada similar unusual isotope compositions were found for shallow groundwater in the Valle del Rio Copiapó in the arid part of central Chile and for water in lakes located along the northern tree line of Canada, respectively.

The extremely low deuterium excess can be explained with the physical processes occurring in the unsaturated zone which modify the isotopic compositions of the pore water in arid regions. The slope of the evaporation lines in the $\delta^{18}O/\delta^2H$ plot decrease from 4 to 5 for open water systems down to about 2.0 in the unsaturated zone with increasing thickness of the dry cover sediment.

In the Gurinai Grasslands and at the foot of the megadunes in the Badajilin Desert the dry cover sediments are 0.5 to 3.5 m thick, both the water level and the isotope enrichment due to evaporation are constant over the year. There is a linear interrelationship between $\delta^{18}O$ values and the depth of the water table, Assuming varying slopes of the evaporation lines, a similar grain size composition of the cover sediments throughout the study area, steady-state conditions of the isotope profiles in the unsaturated zone before succeeding recharge events and groundwater recharge lower than the amount of pore water in the unsaturated zone the described phenomenon is explainable. It is also reflected from the observed isotopic results of the described case studies in Chile and Canada. It may be applicable to estimate regional evaporation rates and recharge rates for groundwater balance studies.

1. INTRODUCTION

A long-term isotope hydrological study on the shallow groundwater in the Gurinai Grasslands western Inner Mongolia, China, revealed unusual properties [1, 2]: The stable isotope compositions of hydrogen and oxygen fit an apparent local meteoric water line (MWL) with an extremely low deuterium excess of d < -20%. Four explanations have been considered: 1) Admixture of ancient lake water. A lake might had existed until 1920 AD and disappeared due to an increasing aridity parallel to the steep global warming since that time accompanied with an ecohydrological degeneration of the vegetation in the study area. In contrast to this assumption, a Swedish expedition in 1929 a described the “Gurinai depression” as densely forested. Mongolian nomads produced charcoal and mined soda from former lake sediments for sale. The groundwater level was high. 2) Decreasing recharge of water from the Black River into the Gurinai aquifer due to an increased use of river water for irrigation. In contrary, a geological fault seems to separate geohydraulically the river from the Gurinai depression and does not allow a direct groundwater inflow. Moreover, small mean residence times of most of the shallow groundwater exclude a travel over distances of more than 80 km. 3) Unusual isotope compositions of the regional precipitation can be excluded. The $\delta^{18}O$ and $\delta^{2}H$ values of the precipitation are as usual and fit a MWL with $d \approx +10‰$. 4). There remain processes which secondarily modify the isotope signature of the groundwater.

This paper discusses preferentially the topics 2) to 4).

2. SITE SITUATION

A substantial portion (ca. 33 %) of China is arid and belongs to the worldwide arid belt stretching SW-NE from South America via Africa to Asia. The Gurinai Grasslands are an oasis within the largest arid area of China. It stretches over an area of about 3000 km^2, extending from 100°45' E to 101°30'E and from 40°30' N to 41°20' N. It is surrounded by the Badajilin Desert in the east and south and bordered by the Gobi Desert and the Black River in the west. The Helishan, Beidashan and Yabraishan mountains are located in the south and a wide depression with the terminal lakes Sogo Nur and Gaxun Nor are located in the north.

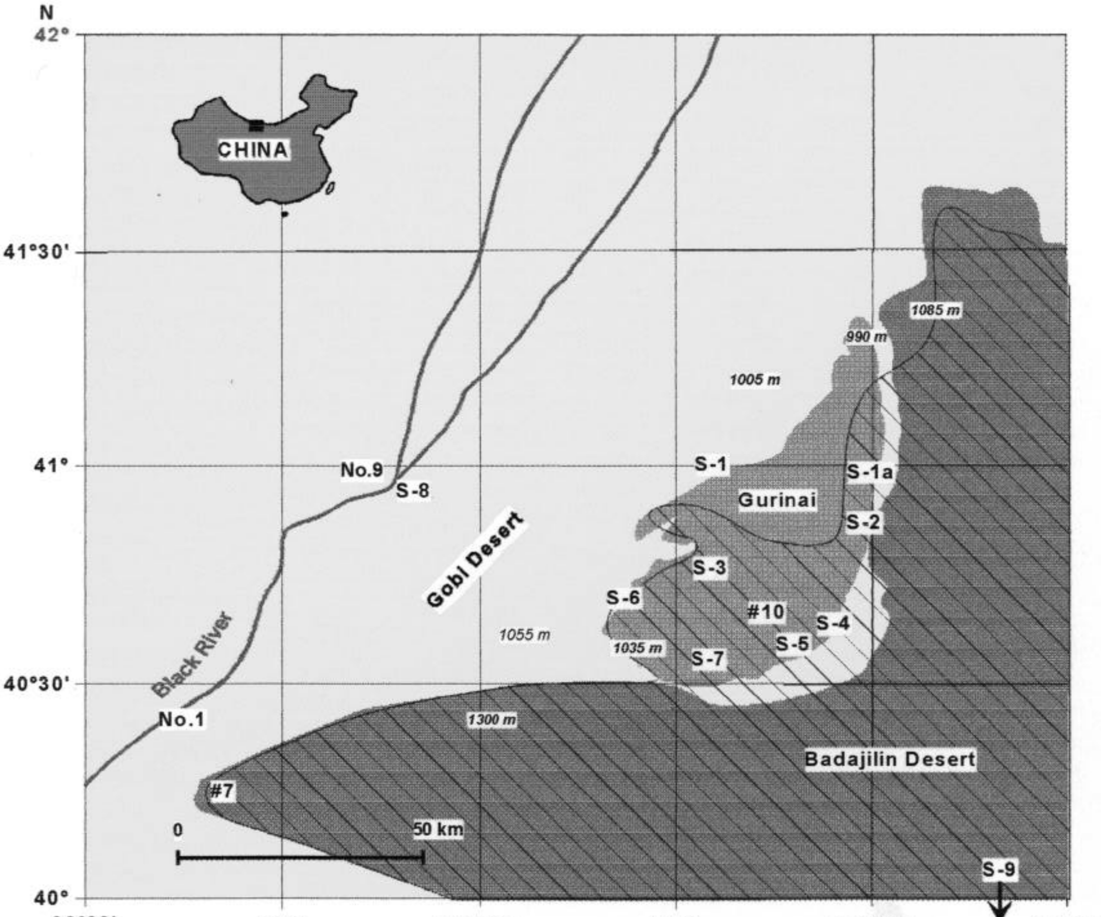

Fig. 1. The Gurinai-Grasslands study area with the Gobi Desert and the Black River in the west and the Badajilin Desert in the east. Sampling sites were shallow dug wells and springs. In the hatched area the corresponding deuterium excess of the shallow groundwater is lower than -20‰. In the other area the groundwater and the precipitation has a deuterium excess ≈ +10‰.

2.1. GEOLOGICAL, GEOGRAPHICAL AND ECOLOGICAL SITUATION

The Gurinai Basin was tectonically formed during the Mesozoic and Cenozoic periods and is divided by the ephemeral Black River: which discharges into two terminal lakes (Gaxun Nur and Sogo Nur) to the north. Satellite images show that erosion has formed the Gurinai depression for a long time and the material was transported to the east and southeast forming the megadune field of the Badajilin Desert. The Gurinai Grasslands are minimum 80 km away from the Black River. There was a very large lake in this area as early as the Pliocene period (Ju-Yan lake). The last lake period started in the Pleistocene. The Gurinai Grasslands consist of low rolling hills between 990 and 1050 m above m.s.l.

Today, about 1000 nomads with their camels and sheep inhabit this area. Anthropogenic causes are supposed to be responsible for increasing desertification. Dense herbage and sacsaoul cover have been displaced by bushes. The water quality is steadily declining. Only a few wells contain water suitable for drinking. The nomads and their livestock suffer from endemic diseases which is attributed to the high fluorine content of up to 4 mg/l.

2.2. HYDROGEOLOGICAL AND GEOHYDRAULIC ASPECTS

The not well-known piezometric surface of the study area does not support a hydraulic connection between the Black River and the shallow groundwater in the Gurinai Grasslands. The high tritium values indicate low mean residence times of the shallow groundwater in the Gurinai Grasslands which excludes an 80-km movement from far away. Minimum transit times of at least 4000 to 8000 years were estimated for the possible gradient of 40 m/80 km, a reasonable hydraulic conductivity between 5 and 15 m/day, and a porosity of 10%. The $\delta^{13}C$ values of the dissolved inorganic carbon compounds of the shallow groundwater reflecting the C_4 assimilating vegetation in the Gurinai Grasslands are well distinct from those reflecting of C_3 vegetation of the groundwater in the alluvions of the Black River. Last but not least, a buried anticline seems to exist serving as a groundwater divide between the Black River and the Gurinai Grasslands. As consequence, local direct recharge is most likely though soil temperatures rise as high as 69°C in summer. Rare and irregular rain storms of very high intensity (up to 100 mm per hour), but of very limited area1 extension of only a few km’ are assumed as main source of direct groundwater recharge. A secondary source may be groundwater entering the Gurinai Grasslands from the Badajilin Desert in the east.

There are many dug wells and one spring with rather fresh water in the Gurinai Grasslands (Table 1). Brackish water and brine are also found in the near-surface unconfined aquifer, whose water table is only 0.5 to 3.5 m below ground. The groundwater flows to the northeast.

Annual precipitation varies considerably, from 10 to 88 mm, with a mean of 40 - 50 mm. The estimated annual groundwater recharge based on the diurnal temperature changes in the soil is 6 mm/yr. Dew may contribute a maximum of 20 mm/yr maintaining the vegetation. The humidity is low year-around. The potential evaporation rate exceeds 2580 mm/yr and may approach 3700 mm/yr.

2.3. ISOTOPE HYDROLOGICAL SITUATION OF THE SHALLOW GROUNDWATER

The isotopic compositions of oxygen and hydrogen of the shallow groundwater in the Gurinai Grasslands are unusual: The $\delta^{18}O$ /$\delta^{2}H$ values fit an apparent local meteoric water line with an extremely low deuterium excess of <-20 ‰ (Fig. 2; [1, 2]).

The results of conventional isotope hydrological analyses - ^{14}C, ^{3}H, $\delta^{13}C$, $\delta^{18}O$, $\delta^{2}H$ - carried out on water samples from September 1989 and December 1990 yield a differentiated picture of the sources of groundwater. The samples for stable isotope analyses were collected monthly in 1987/88 from a meteorological station at the Black River, from the river itself, as well as from a spring, various dug wells in and around the Gurinai Grasslands and a drilled well.

One group of data fit the global meteoric water line (MWL) with d ≈ +10‰, the other group fits an apparent local water line with d < -20% (Fig. 2).

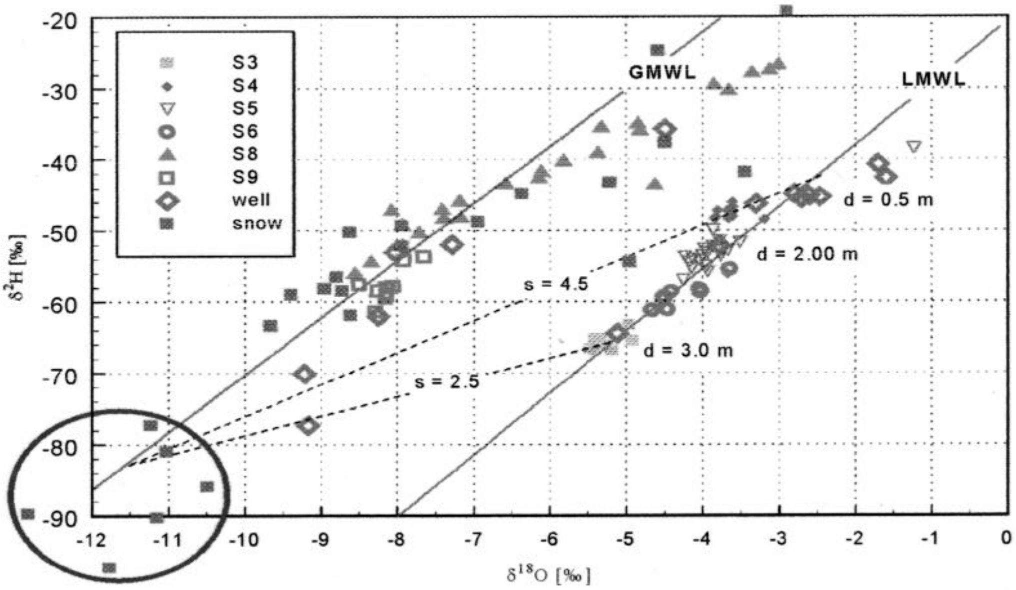

Fig. 2. Apparent "Local Meteoric Water Line" (LMWL) with a deuterium excess of −25‰ from the Gurinai Grasslands in the arid central China [1]. The encircled blue dotes belong to precipitation from the Gurinai Grasslands and the others from the Badajilin Desert in the east. The green dotes representing the water from the Black River which is isotopically enriched during the hot summer time. There is a linear interrelationship between the $\delta^{18}O$ and the depth of the water table (Fig. 4). The $\delta^{18}O$ and $\delta^{2}H$ values may be explained by assuming the slope of the evaporation line decreases from 4.5 to 2.5 with increasing thickness of the top sediment.

Table 1. Results of isotope hydrological analysis of groundwater samples from dug wells in the Gurinai Grasslands area and surroundings (Fig. 1). All sites were sampled in September 1989 and many from it again in December 1990.

No.	Site	$\delta^{13}C$ ‰	^{14}C value pMC	^{3}H TU	$\delta^{18}O$ ‰	$\delta^{2}H$ ‰	d_{exc} ‰	salt g/l
Black-River area west of Gurinai Grasslands								
No. 1	drilled well	-11.2	102.5±0.9	82.9	-6.11	-41.7	+7.2	0.7
S-8	river water	-5.2	88.9±0.9	80.0	-8.34	-54.4	+12.3	fresh
Footland of southern mountains south of Gurinai Grasslands								
No.9	drilled well	-5.8	52.1±1.1	4.2	-8.02	-53.0	+11.2	fresh
S-9	dug well	-11.7	112.7±0.8	34.4	-7.65	-53.6	+7.6	0.7
Gurinai Grasslands, Badajilin Desert and Gobi Desert								
S-1	dug well	-6.2	38.7±0.7	<2.4	-9.21	-70.0	+3.7	44.9
S-2	dug well	-5.2	95.3±1.0	5.3	-1.70	-40.6	-27.0	0.9
		-5.6	100.3±0.9	8.1	-1.50	-43.5	-30.5	
S-3	dug well	-7.2	51.9±0.6	3.2	-5.27	-66.2	-24.0	52.5
		-6.6	76.1±1.2	1.6	-5.40	-66.7	-23.5	
S-4	dug well	-5.7	77.8±0.8	5.0	-2.59	-45.9	-24.3	3.4
		-0.6	101.0±1.0	6.6	-2.27	-43.3	-25.1	
S-5	dug well	-6.5	101.5±0.7	5.5	-3.67	-52.7	-23.3	0.6
		-8.1	97.8±0.9	1.4	-3.77	-54.5	-24.3	
S-6	dug well	-6.1	107.0±0.8	<2.3	-4.80	-60.2	-23.6	3.3
		-5.6	99.5±0.8	<2.6	-3.64	-55.4	-26.5	
S-7	dug well	-8.8	88.2±1.3	4.7	-2.79	-44.8	-22.5	0.8-1.3
		-1.8	60.8±0.5	<1.6	-2.79	-46.0	-23.7	
# 7	spring	-5.1	82.4±1.7	<1.6	-2.61	-45.0	-24.1	fresh
#10	spring	-5.2	30.4±0.6	-	-4.02	-52.0	-19.8	brackish
		-2.8	24.6±0.5	<1.2	-4.52	-57.9	-21.7	

The samples of the first group stem from precipitation at the meteorologic station at the Black River and at different places within the Gurinai Grasslands. River water and groundwater from wells in the alluvium as well as at the foot of the mountains in the south also belong to this group. Most of these samples contained tritium and therefore were young. A few isotope data reflect partial evaporative isotope enrichment. They belong to samples from the river collected during summer when its water level and its width approached the maximum (about 50 cm and a few kilometers, respectively) at a temperature as high as 42°C. Other samples came from the most shallow dug well S-1 which is possibly located already outside of the Gurinai Grasslands (Fig. 1) or a depression where indirect groundwater recharge may occur.

The samples of the other group are isotopically well distinct from the first group. They were collected from dug wells in the Gurinai Grasslands. The isotope compositions (just as the water level) have not been varied seasonally (Fig. 3) but are well distinct from one well to another one. Surprisingly, most of these samples were fresh groundwater, contained tritium and had ^{14}C values even exceeding 100 pMC. Hence, the groundwater is recent. Only two groundwater samples had ^{14}C values down to 25 pMC though one contained tritium (Table 1). Both samples were highly mineralized (up to 53 g/l salt).

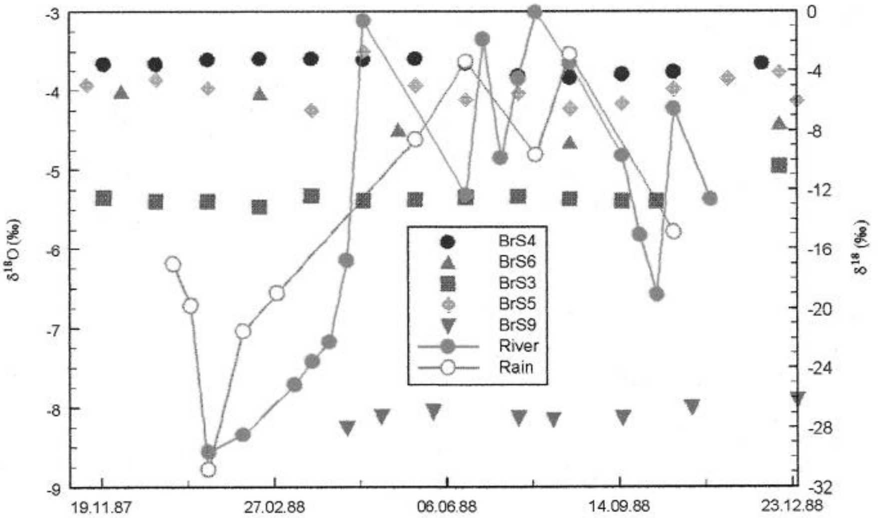

Fig. 3. Missing seasonal variation of the $\delta^{18}O$ values of the shallow groundwater. The $\delta^{18}O$ values of the precipitation and the Black river vary similarly.

In the Gurinai Grasslands the dry top sediments are 0.5 to 3.5 m thick. Fig. 4 shows a linear relationship between the $\delta^{18}O$ values and the depth of the water table for most of the samples from the dug wells. The well S-6 is an exception. It is located at the southwestern margin of the Gurinai Grasslands where the morphological situation already changes.

2.4 CASE STUDIES IN CHILE AND CANADA

Another isotope hydrological study on the groundwater in the 115 km long, hyper-arid valley of the Río Copiapó in central Chile was carried out [3]. The valley stretches over an altitude range of 1000 m. There are four limited swampy regions (vegas) where the groundwater table decreases from more than 20 m down to a few meters below ground. The isotope signature of the groundwater in these swampy regions of the lower part of the river channel fits an apparent local meteoric water line with $d \approx -4‰$ (Fig. 5). In this region precipitation is rare but still exists. The isotope compositions of the groundwater in the vegas of the upper part of the valley fit an evaporation line with a slope of 4.5.

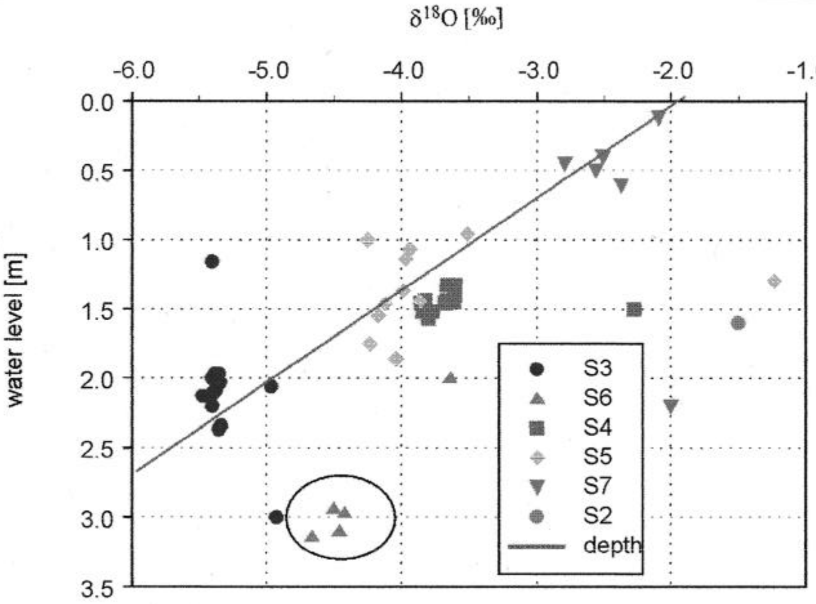

Fig. 4. Linear relationship between the $\delta^{18}O$ values of the shallow groundwater and the depth of its water table in the Gurinai Grasslands. The outlyer belong to the well S-6 at the southwestern margin of this oasis where the morphologic situation may already be different.

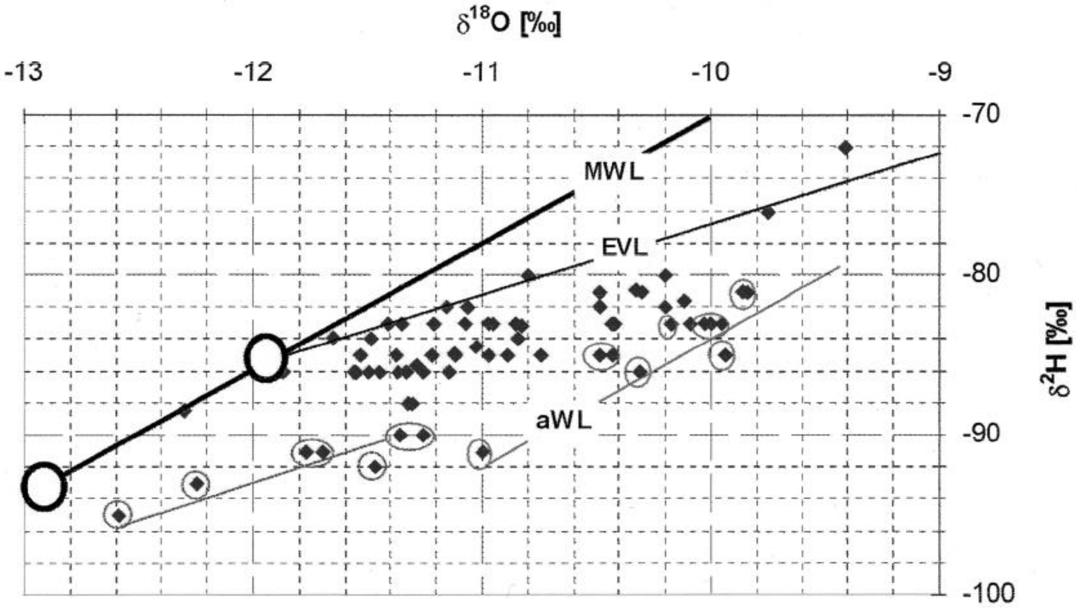

Fig. 5. The isotope compositions of the shallow groundwater in the lower part of the Valle del Río Copiapó [3] fit an apparent local MWL (aWL) with d ≈ -4‰ (points and line in red). There, low precipitation occurs. The blue dots and line belong to isotope data from groundwater in the vegas of the hyper-arid upper part of the valley. They reflect evaporative isotope enrichment.

Along the northern tree line of Canada lake water was isotopically analyzed. The isotope compositions of the water collected at the end of a very dry summer are unusual and fit a line in the $\delta^{18}O/\delta^{2}H$ plot with a slope ≈ 4.5. In the uppermost part the slope increases to about 8. This attached line meets the Y-axis at about −20‰ (Fig. 6; [4]).

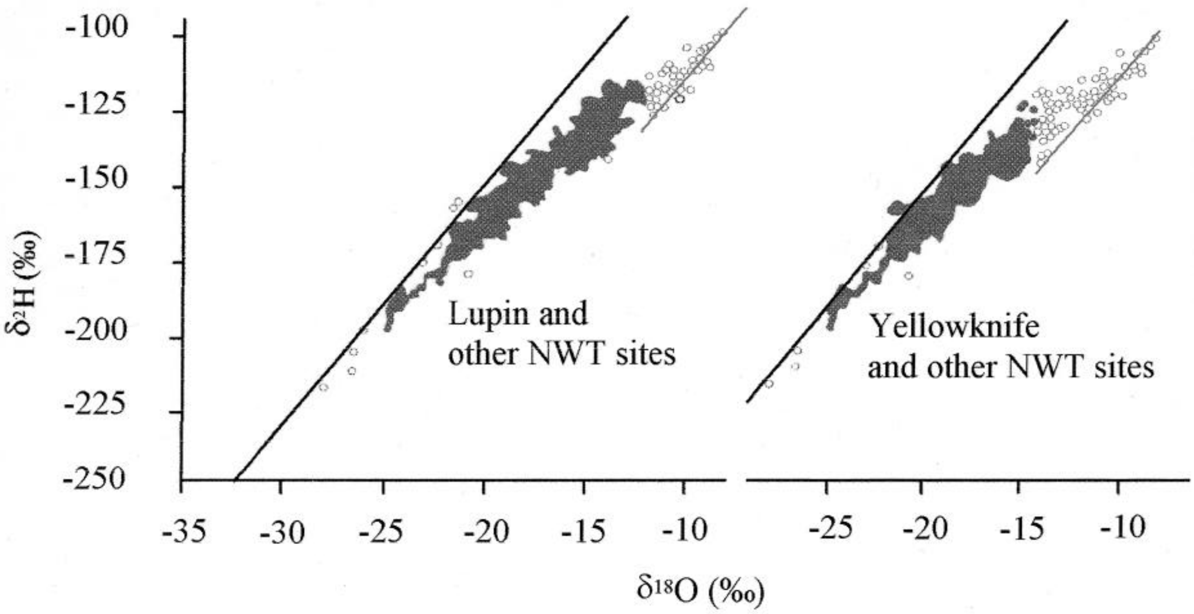

Fig. 6. $\delta^{18}O/\delta^2H$ plot of water of different lakes located along the northern tree line in Canada [4] The red dots belong to samples collected after a long dry summer. The attached red line met the Y-axis at −20‰.

3. DISCUSSION

After exclusion of an admixture of ancient lake water, a flow of water from the Black River towards the Gurinai Grasslands and of unusual isotopic compositions of the regional precipitation, only processes are left which secondarily modify the isotope signature.

3.1. ISOTOPE HYDROLOGICAL FUNDAMENTALS

The extremely low apparent deuterium excess of the groundwater in the Gurinai Grasslands is explainable based on the isotopic compositions of the pore water in the unsaturated zone under dry cover sediments. Evaporation of the soil moisture in the unsaturated soil causes enrichment of ^2H and ^{18}O with respect to the corresponding lighter isotopes. The enrichment peaks at the evaporation front from where vapor diffuses though the rather dry top soil into the air. Due to backwards diffusion of isotopically depleted atmospheric moisture the $\delta^{18}O$/depth profile is peak shaped under steady-state conditions ([5, 6, 7]; Fig. 7).

As the evaporating front moves further into the soil profile by evaporation the relative importance of the isotopic kinetic effect increases. This is due to the development of a superficial dry layer where diffusive transport of water vapor dominates. The effect is explained in terms of increased thickness of the laminar layer through which evaporating water molecules escape. As a result, the slope of the evaporation line decreases from 4 to 5 for open water systems to as low as 2 with increasing thickness of the cover sediment [5]. Soil water evaporation during long dry periods in arid regions produces isotopically enriched water below the evaporation front. There is a linear relationship between the evaporation rate and the slope of the evaporation line in the $\delta^{18}O/\delta^2H$ plot [6].

Laboratory experiments [6, 7] on sand columns confirmed these results. The slope of the $\delta^{18}O/\delta^2H$ evaporation lines of the soil moisture in sand columns with different grain size increases a) with increasing humidity and b) with increasing grain size (Fig. 8). The slope for a grain sizes > 1 mm corresponds to that for open water. Seasonal or other changes of delta values of precipitation are preserved in the isotopically enriched soil moisture. The corresponding delta values form a line shifted parallel to the right from the MWL similar to that shown in Fig. 2.

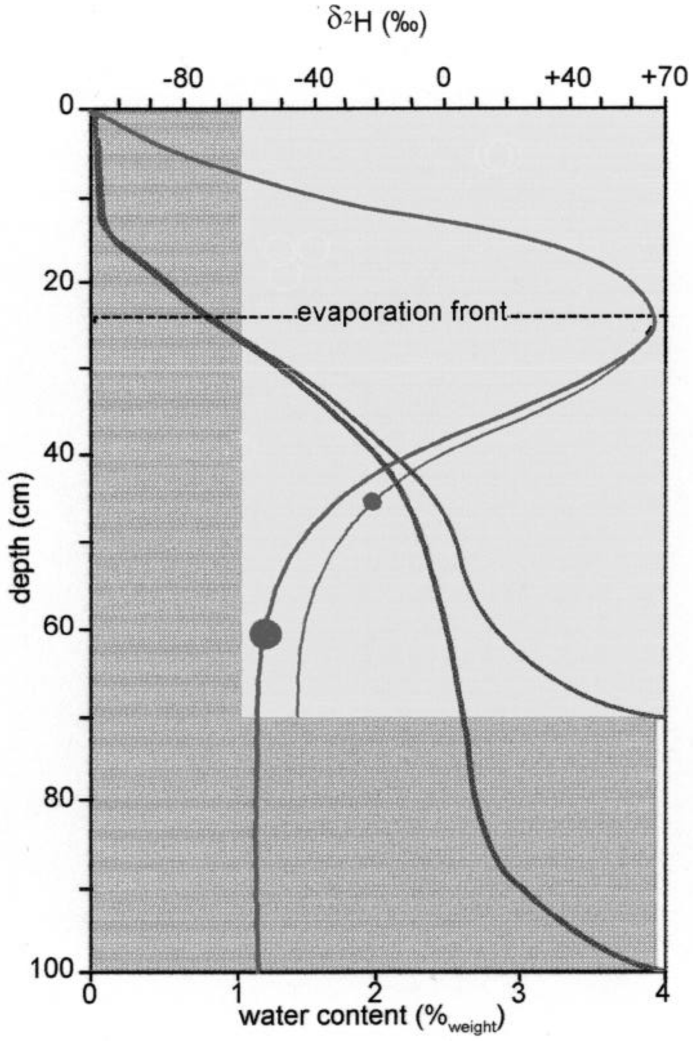

Fig. 7. Schematic δ^2H profiles (red) and soil moisture distributions (blue) in the unsaturated zones under steady-state conditions in 100 cm (bold) and 70 cm (thin) columns. The red dots are the mean delta value of the pore water recharged from the thick (orange) and thin (yellow) sediment profiles (after SONNTAG et al. [6, 7]).

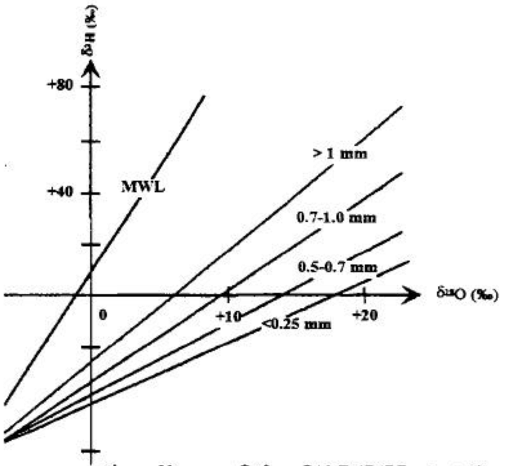

Fig. 8: Differing slopes of the evaporation lines of the $\delta^{18}O/\delta^2H$ plot for sand of different grain sizes evaporating into dry air [6].

3.2. DISCUSSION OF THE RESULTS FROM THE GURINAI GRASSLANDS

According to Fig. 3 the monthly scatter of the $\delta^{18}O$ and $\delta^{2}H$ values of the shallow groundwater over one year is low. Fig. 4 shows a linear relationship between the $\delta^{18}O$ values and the depth of the water table for most of the samples from the dug wells. The most simple explanation for these phenomena and of the unusual isotope compositions would be a widely varying initial isotope composition of the precipitation, groundwater recharge and finally isotope enrichment due to partial evaporative isotope enrichment according to SONNTAG et al. [6]. This interpretation can, however, not be valid as the groundwater of each well site has distinct, individual isotope compositions. One cannot assume that the isotope compositions of the precipitation has such well defined spatial distribution within the restricted area of the Gurinai Grasslands. Hence, another explanation must be found.

According to our concept the shallow groundwater in the Gurinai Grasslands has only one origin (even it may be a mixture of different resources) with similar initial isotope compositions. The cover sediments have similar grain size compositions and are dry most of the year. As the water table differs the evaporations lines of the soil moisture have a wide range of slopes in the $\delta^{18}O/\delta^{2}H$ plot. The deeper the groundwater table the lower is the slope of the corresponding evaporation line. During the long dry season the isotope profile of the soil moisture approaches steady-state conditions. The shape of the $\delta^{18}O$ profile of different thick unsaturated zones may correspond to those shown in Fig. 7.

In case of rainfall and small groundwater recharge the lower part of the soil moisture profile enters the saturated zone without loosing its isotope signature. For the same rate of recharge the mean $\delta^{18}O$ value is the higher the lower the sediment thickness. That means that the delta values will move on the evaporation line to the right in the $\delta^{18}O/\delta^{2}H$ plot. The distance from the MWL will be the larger the steeper the slope of the evaporation line or the thinner the dry cover sediment. The result is a more or less linear distribution of the isotope points as shown in Fig. 2. It may be an artifact that this shifted line is fairly parallel to the MWL.

Groundwater recharge may occur by the statistically well distributed, occasionally occurring rainfall events of high intensity. It cannot exceed, however, the amount of pore water in the unsaturated zone. Otherwise, the groundwater looses the isotope signature of the soil moisture in the unsaturated zone and approaches that of the precipitation. The maximum recharge is determined by the water content in the sediment column: 30 mm at 3% moisture in of 1 m.

The water of the well S-6 is an exception. The isotope compositions deviate from the common $\delta^{18}O$/depth relationship (Fig. 4); but they fit into that of the $\delta^{2}H/\delta^{18}O$ plot (Fig. 2). This may be due to different sediment compositions at the margin of the Gurinai Grasslands (Fig. 1) or to not yet approached steady-state conditions of the isotope profile in the unsaturated zone.

Unfortunately, there are no sediment profiles and analysis of the isotope compositions of the soil moisture from the unsaturated zone have not yet been done. There is no meteorological station in the desert and the counterparts does not have pH or EC meters. Hydrochemical analyses have also not yet been carried out. Even the mailing of the isotope samples has often been a problem.

The weakest point in our concept to explain the unusual isotope phenomenon is the initial isotope composition of the freshly recharged groundwater. According to Fig. 2 one should expect $\delta^{18}O$ and $\delta^{2}H$ values of −11.5‰ and −85‰ for young groundwater, respectively. The isotope compositions of the precipitation along the Black River and its water scatter widely around these values but do not form a narrow cluster. The few samples of rain and snow collected within the Gurinai Grasslands have $\delta^{18}O$ and $\delta^{2}H$ values which scatter around this point. We hope to get more samples of precipitation in order to prove empirically the extrapolated point.

In spite of this reservation our concept is also applicable to interpret the isotope compositions of the shallow groundwater in the vegas of the Valle del Río Copiapó [3]. The $\delta^{18}O$ and $\delta^{2}H$ values of the shallow groundwater in the lower part cluster around an apparent MWL with $d \approx -4‰$. There, groundwater recharge occasionally may occur. In the upper region of the Valle del Río Copiapó rainfall is missing and the $\delta^{18}O$ values are arranged around an evaporation line with a slope of 4.5.

According to the hydraulic situation around the lakes in northern Canada shallow groundwater enters the lakes through peat layers [4]. At the end of the summer the pore water in the peat layers may be isotopically enriched and the isotope compositions may be similar to the the soil moisture in the unsaturated zone. The first autumn rainfall will mobilize this isotopically enriched pore water which flows into the shallow lakes.

4. SUMMARY

The isotopic compositions of shallow groundwater in arid regions with low recharge rates may reflect an isotope enrichment similar to that in the pore water of the unsaturated zone below dry cover sediments. This concept, if valid, may allow to estimate regional evaporation rates and maximum recharge rates for groundwater balance studies.

Our future tasks are the measurement of the isotope compositions of the pore water in the unsaturated zone at sites with different deep groundwater table (e.g. at the dug wells S-3 and S-7). Further isotope analyses of precipitation samples has to be done. In addition, isotope analyses of the deep groundwater has to be carried out. According to our concept usual isotope compositions are expected supported by the results of the spring water (Table 1). Last but not least, we will dry to explain theoretically our empirical results.

ACKNOWLEDGEMENT

We acknowledge the continuos help and support of Mr. Dong, Ejina, during our project. The staff of the Section 3 – Dating and Isotope Hydrology – at the Joint Geoscientific Research Institute in Hannover run the isotope analyses. The stable isotope analyses of the water samples from the Valle del Río Copiapó were done by the Chemical Laboratory at the Chilean Atomic Energy Commission, Santiago de Chile, under the leadership of Dr. A. Pollastri.

REFERENCES

[1] Geyh, M.A., Weizu, Gu (1992). Preliminary isotope hydrological study in the arid Gurinai Grassland area, Inner Mongolia.- Isotope Techniques in Water Resources Development 1991: 661 – 662; Proc., IAEA-SM-319/23P; IAEA, Vienna.

[2] Geyh, M.A., Gu Weizu, Jäkel, D. (1996). Groundwater recharge study in the Gobi Desert, China.– Geowissenschaften, 14: 7 – 8.

[3] Geyh, M.A. (1998). Isotope hydrological study in the Valle del Río Copiapó.- BGR-Report, File-No. 6354/98: 18 pp.; 2 Table.

[4] Gibson, J.J., Prowse, T.D. (1998). Water balance trends across the northern treeline inferred from isotopic enrichment in lakes.- Isotope Techniques in the Study of Environmental Change: 207 – 224; Proc. IAEA, Vienna.

[5] BARNES, C.J., ALLISON, G.S. (1983). The distribution of deuterium and oxygen-18 in dry soils: I Theory.– J. Hydrol, 60: 141 – 156.

[6] Sonntag, C., Christmann, D., MüNNICH, K.O. (1985): Laboratory and field experiments on infiltration and evaporation of soil water by means of deuterium and oxygen-18.- In: Stable and Radioactive Isotopes in the Study of Unsaturated Soil Zone. IAEA-TECDOC-357: 145 – 159, IAEA (Vienna).

[7] Christmann, D. Sonntag, C. (1987): Groundwater from East Saharian depressions by means of deuterium and oxygen-18 in soil moisture.- In: Isotope Techniques in Water Resources Development: 189 – 204, IAEA (Vienna).

[8] Allison, G.B., Barnes, C.J., Hughes, M.W. (1983): The distribution of deuterium and oxygen-18 in dry soils: II Experimental.– J. Hydrol., 64: 377 – 397.

ISOTOPIC STUDIES OF NATURAL WATERS IN THE SKAGAFJÖRDUR REGION, N-ICELAND. DEUTERIUM EXCESS AND ^{14}C AGE OF GROUNDWATER

Á. E. SVEINBJÖRNSDÓTTIR, S. ARNÓRSSON
Science Institute, University of Iceland, IS-107 Reykjavík, Iceland
J. HEINEMEIER, E. BOARETTO[1]
Institute of Physics and Astronomy, University of Aarhus, DK-8000 Aarhus, Denmark

Abstract

Interpretation of the stable isotopic and chemical composition of the natural waters from the Skagafjördur region, N-Iceland, suggests that some of the geothermal waters originate, at least partly, from the last glaciation i.e. >10.000 years ago. This is further supported by ^{14}C analyses, which after boron based ^{14}C dilution calculations, indicate that the oldest water is ca. 10.500 years old BP. A negative correlation is observed between deuterium excess and ^{14}C apparent age of the groundwater. The water samples with the lowest d-values are the oldest but not necesserely the hottest samples, as they range in temperature from 30 to 70 °C. Two possible explanations are offered for the low d-values of these old samples. Firstly, they originate as precipitation from different climate regime when precipitation had different d-values from those of today and secondly, in this low temperature range the age of the water is the dominant factor that controls the water-rock interaction and hence the amount of oxygen shift.

1. INTRODUCTION

The Skagafjördur region in N-Iceland is geothermally active on both sites of the valley, where the water temperatures range from the annual mean temperature (~ 5°C) up to 90 °C and 43 °C on the western and eastern site of the valley, respectively. There is a continuum from non-termal groundwaters to thermal waters permitting evaluation of how early water-rock interaction changes the chemistry of surface waters as they seep into the ground and gain heat.

The bedrock in the area is mainly a monotonous pile of Miocene flood basalts. It has very low permeability except where it has been fractured by recent earth movements and the geothermal activity is mostly connected to young, open fissures. 253 water samples have been collected for chemical analyses of major and trace elements and selected isotopes both from the Skagafjördur valley and the highlands south of the valley (Fig.1). The main objectives of the project are to study; 1) changes in water chemistry caused by water-rock interaction, 2) origin and age of the groundwater by stable isotopes and other natural chemical tracers, 3) the origin of carbon in the water and 4) processes that control concentration of some trace elements in the water.

In this contribution emphasis is put on the origin and age of the groundwater.

---

[1] Present adress: Kimmel Center for Archaeological Science ESER dept. The Weizmann Institute of Science 76100 Rehovot (Israel)

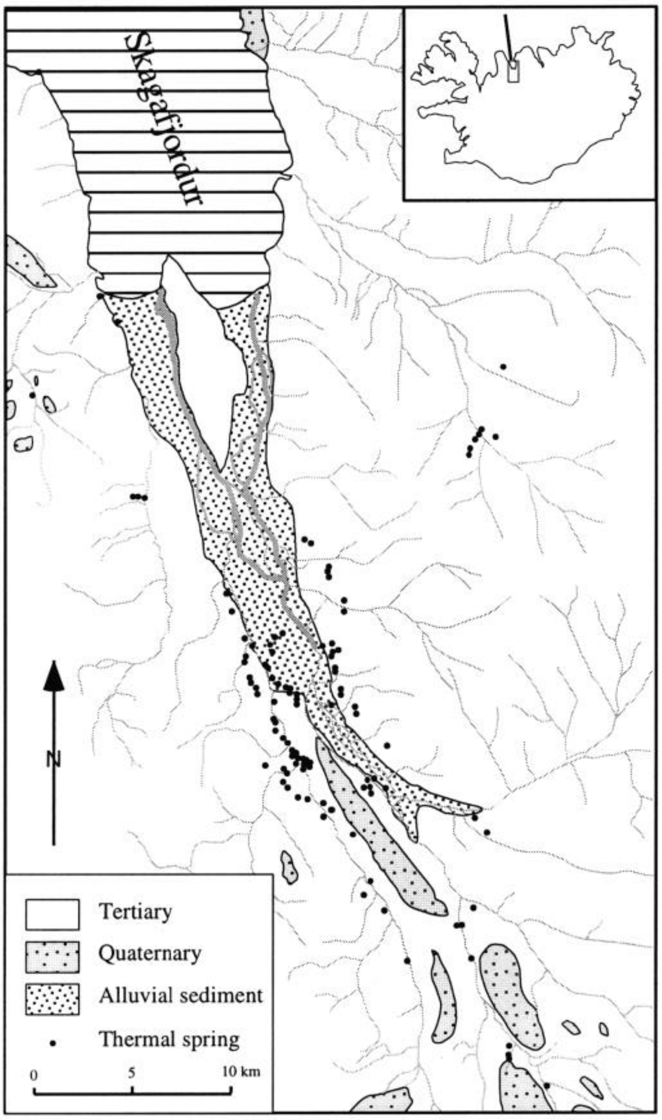

Fig. 1. The Skagafjördur valley showing distribution of thermal springs (dots).

2. CHEMICAL CHARACTERISTICS OF THE SKAGAFJÖRDUR WATER

Water-samples are devided into the following five groups on basis of their chemical composition and geological occurance:

(1) ground water, ranging from non-thermal to thermal
(2) surface water (rivers)
(3) soil water
(4) spring water in the highlands
(5) lakes in the highlands

Most of the surface waters contain 40-80 mg/l dissolved solids, the soil waters range between 30-260 mg/l, largly due to higher Ca, Mg and HCO_3 contents and the thermal groundwaters from 60-310 mg/l, rising smoothly with increasing temperature [1]. Springs in the highlands are considered as a separate group as they possess some chemical and isotopic difference from those in the lowlands, mainly due to higher permeability in the highlands causing a short resedence time of the water and thus less rock dissolution.

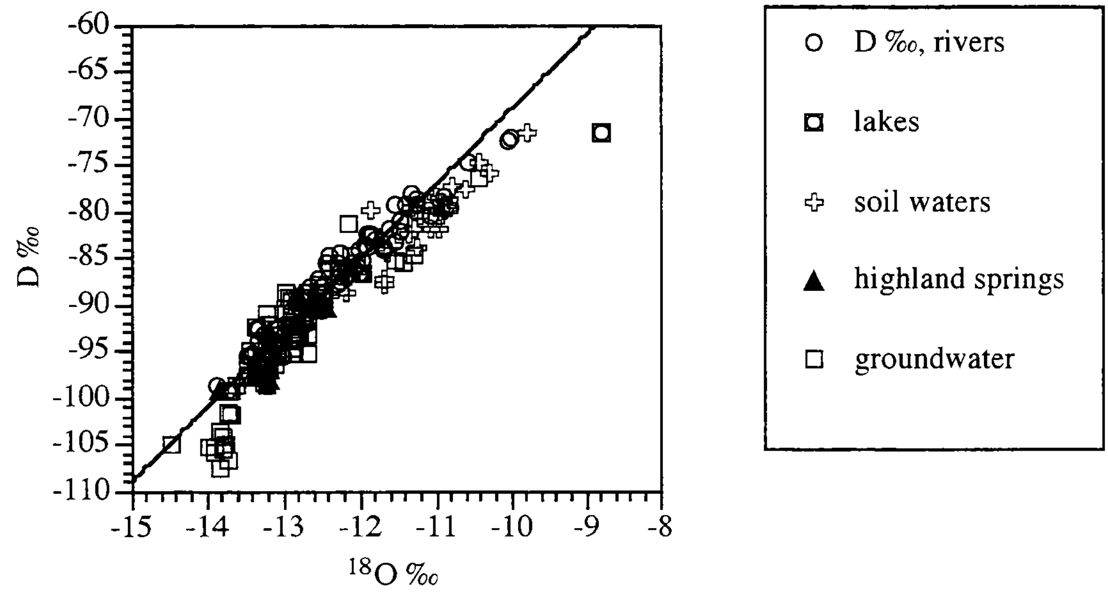

Fig. 2. $\delta^{18}O$ - δD relation of natural water from the Skagafjörður region N. Iceland.

The pH of the surface waters is most often in the range 7-8, whereas the soil waters tend to have lower pH. Groundwater both thermal and non-thermal have considerably higher pH. It reaches maximum (ca. 10) around 10-25°C but decreases with increasing temperature [1].

3. ISOTOPIC COMPOSITION OF THE SKAGAFJÖRDUR WATER

The deuterium content of the mean annual precipitation in Iceland has been mapped [2] allowing deuterium to be used extensively to trace the origin of groundwater. In almost all of the Icelandic geothermall systems, the isotopic content of the geothermal waters is somewhat lower (more negative) than that of the local precipitation. However, the $\delta^{18}O$ - δD relationship of these waters indicate that they are of meteoric origin. The difference between the isotopic values of the geothermal waters and those of the local precipitation has been considered to indicate that the recharge areas to the geothermal systems lie farther inland at a higher elevation [3].

Figure 2 shows that $\delta^{18}O$ and δD of the waters follow the meteoric line that has been defined for Iceland [4], apart from the isotopically lightest samples, which show a slight oxygen shift (< 1‰) and the soil waters that plot just below the line. In addition some of the lakes show substantial evaporation.

The relationship between $\delta^{18}O$ and rock-derived Cl in the water as evaluated after the method described in Ref. [5] is shown on Fig. 3a. The figure suggests that with increasing water-rock interaction the waters become isotopically lighter. The conventional interpretation of these results suggests that the isotopically lightest waters, originate from the highlands, farthest away from the sampling point, and have therefore been interacting with the rock longer than waters with less depleted waters. This interpretation is, however, not valid for all geothermal waters in Skagafjördur as can be seen from Fig. 3b where the relation between the $\delta^{18}O$ and the Cl of marine origin in the water, as estimated after the method discussed in Ref. [5] is shown.

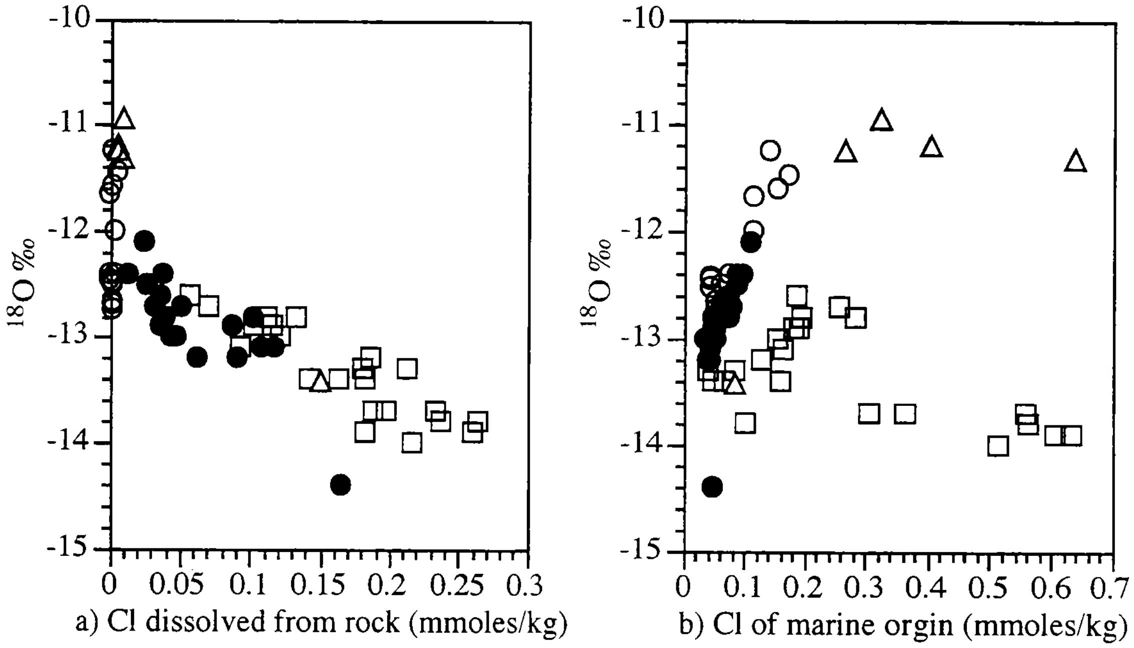

Fig. 3. The relationship between $\delta^{18}O$ and a) rock-derived Cl in the water and b) the Cl of marine origin in the water. Legends: Geothermal water:western (squeres) and eastern (dots) site of the valley. Rivers: open circles and soil water: triangles.

It can be seen from the figure that the data points fall into two populations. One shows decreasing Cl with decreasing $\delta^{18}O$ (more negative values) and can be accounted for by altitude effect. The other populations shows a negative correlation between these two parameters. That can be explained by assuming the geothermal water to consist of two components, one corresponding with today's local precipitation and the other with water relatively high in Cl of marine origin but depleted in $\delta^{18}O$. It is suggested that this latter component represents a mixture of at least three components: (1) seawater that has infiltrated the Skagafjördur region at the end of the last glaciation, some 10.000 years ago, when the hydrolgical conditions of the area allowed infiltration of seawater (which is not possible today) (2) precipitation also from that time, which is isotopically light due to the cold climate at that time and (3) precipitation from the present climate regime.

4. AGE OF THE WATER

The interpretation of the $\delta^{18}O$ - Cl relationship discussed above suggests that some of the geothermal water in the Skagafjördur valley is more than 10.000 years old. Tritium and the ^{14}C radioisotope were used to further estimate the age of the natural waters.

The tritium results for surface and soil waters range from 8 to 12 TU, whereas tritium is not detected in waters with temperatures >40°C. Thus the warm waters are at least older than the beginning of the atmospheric nuclear bomb testing in the late 1950's. In some instances tritium is detected in warm waters with temperature <40°C, possibly because of mixing with younger surface waters. The largest glacier rivers contain less tritium than normal surface waters, due to their component of tritium-poor icemelt of old glaciers.

Carbon in groundwater may be derived from several sources with different ^{14}C concentration and $\delta^{13}C$. In Iceland at least three different sources of carbon supply to the water are expected: atmospheric CO_2, soil CO_2 of organic origin and CO_2 leached from the rock through which the water seeps. Addition of carbon from the rock dilutes the ^{14}C concentration of the water and in this way yields a high apparent ^{14}C age. Because of the multiple character of the carbon supply to the water, a simple two-component isotopic dilution model [6] is inadequate to correct ^{14}C measurements for the Icelandic samples. In Ref. [7] it is shown that by assuming that the ratio of boron to CO_2 is the same in rock and groundwater, it is possible to correct for the contribution of rock-derived carbon to the groundwater. The corrected values for most of the Skagafjördur samples lie in the range 10.500 BP to modern.

Figure 4 shows the relationship between tritium and ^{14}C apparent age. The figure demonstrates a good correlation between low tritium values and low apparent ^{14}C age. As stated above no tritium was detected in water samples > 40°C and radiocarbon measurements suggest that most of these waters range in age from 10.500 BP to 500 BP, after applying the boron correction procedure.

4.1. $\delta^{13}C$ results

The $\delta^{13}C$ in cold surface waters ranges from -1 to -7 ‰ whereas in soil waters the $\delta^{13}C$ much lighter and ranges from -16 to -22 ‰. In the geothermal waters the $\delta^{13}C$ lies most commonly in the range -6 to -13 ‰. A linear relationship is observed for the $\delta^{13}C$ of geothermal water and the calulated ^{14}C dilution based on the Boron concentration of the water discussed in Ref. [7], except where the thermal waters emerge in thick peat soil explaining their low $\delta^{13}C$ values.

5. DEUTERIUM EXCESS

It has been shown that the deuterium excess, defined as d= δD-8* $\delta^{18}O$, in precipitation is mostly governed by temperature at the source region [8]. Accordingly the difference in d-values observed in Greenland ice from the last glacial period is explained in Ref [8] by different source regions for the precipitation during interstadials and the coldest glacial periods.

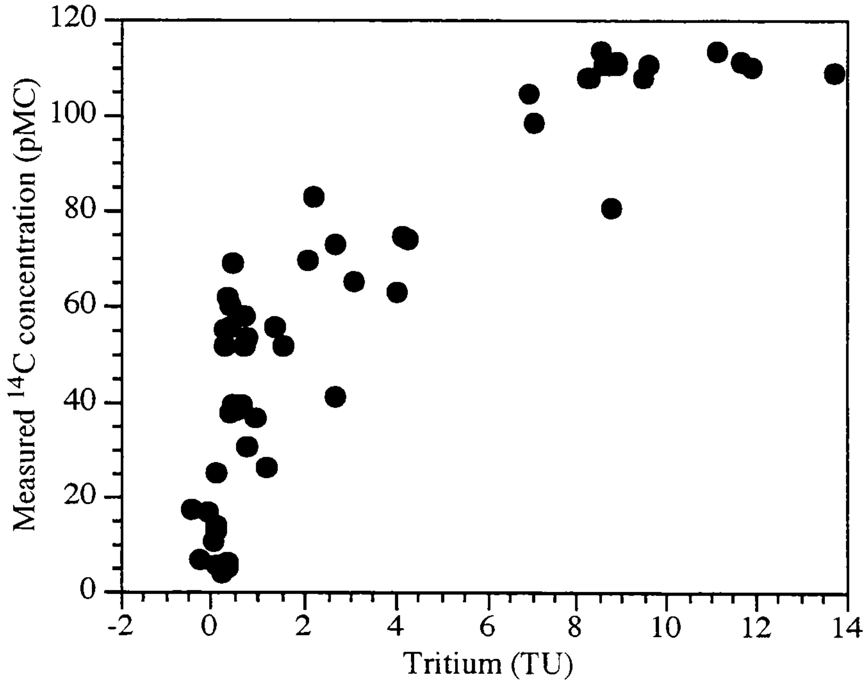

Fig. 4. The relationship between tritium concentration and the ^{14}C apparent age of the groundwater.

In Ref. [9] the deuterium excess values in cold groundwater and low temperature thermal water was used to recognize old groundwater originating from precipitation when the climate was different from today. In order to do that it is essential however, to know the deuterium excess values of natural waters of our climate regime. The Skagafjördur data-set gives an excellent opportunity to do that (Fig. 2).

As shown in Fig. 5 a negative correlation is observed between deuterium excess and ^{14}C apparent age of groundwater. The samples designed as "old groundwater" on the figure are low in δ^{18}O and δD and exibit oxygen shift on Fig. 2. These are, however, not necesserely the hottest samples. Fig. 6 demonstrates a weak negative correlation between deuterium excess and water temperature. There is a large range in d-values for each temperature, e.g. samples with water temperature at 40°C give deuterium excess values from 10 to 4 ‰. The "old groundwater" samples show the lowest d-values but range in temperature from 30 to 70°C as shown in Fig. 6. It is suggested that the low d-values for these samples can be explained in two ways. Firstly, the "old groundwater" may originate from different climate regime when precipitation had different d-values from those of today and secondly, in this low temperature range the age of the water is the dominant factor that controls the water-rock interaction and hence the amount of oxygen shift.

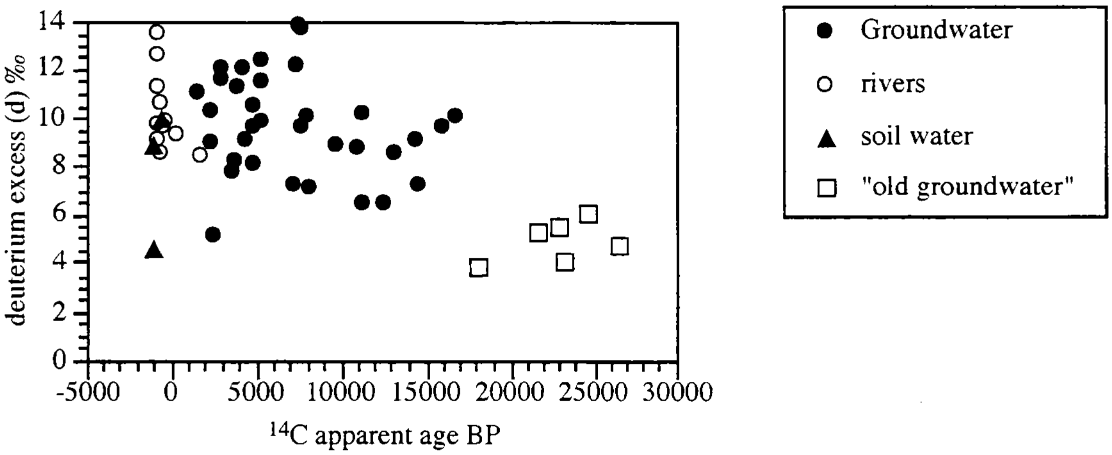

Fig. 5. The relation between the deuterium excess values and ^{14}C apparent age BP.

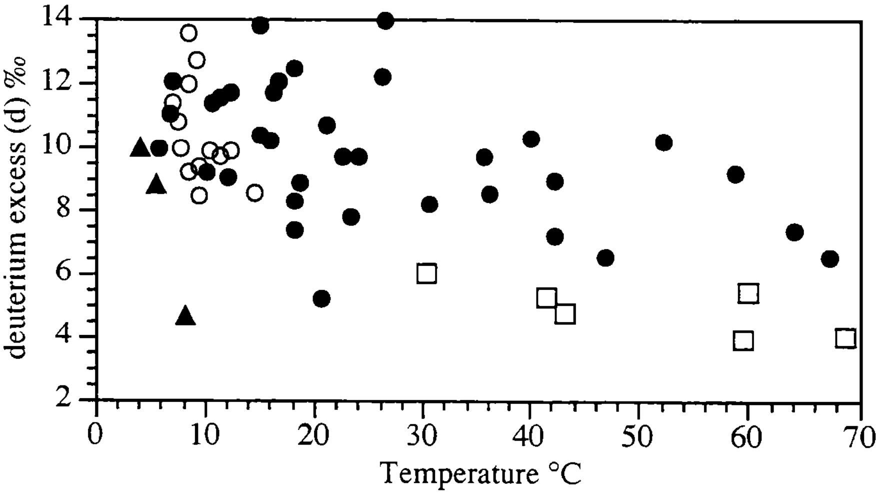

Fig.6. Relation between temperature and the excess values. Same legend as in Fig. 5.

6. CONCLUSIONS

1) Our large data set from the Skagafjörður region allows us to divide the samples into different categories and hence study chemical and isotopic changes due to water-rock interaction in greater details.

2) The conventional interpretation of deuterium measurements that suggests that the source of supply of the water to the thermal systems is precipitation that has fallen in the interior highlands does not fit for all geothermal waters in Skagafjördur as some of the waters consist of three components, one corresponding with today's precipitation and the others with "ice age" water relatively high in Cl of marine origin but depleted in oxygen-18. ^{14}C analyses support also the conclusion that some of the water is more than 10.000 years old.

3) Low deuterium excess values for the oldest samples may either be explained by different d-values of the precipitation they originate from some 10.000 years ago or that in this low temperature range i.e. 30-70°C the age of the water is the dominant factor that controls the water-rock interaction and hence the amount of oxygen shift.

REFERENCES

[1] ANDRÉSDÓTTIR, A., et al., Geochemistry of natural waters in Skagafjörður, N-Iceland. I. Chemistry, In Water-Rock Interaction, (AREHART & HULSTON, Eds) (1998) 605-608.

[2] ÁRNASON, B., Groundwater systems in Iceland traced by deuterium, Societas Scientiarum Islandica **42** (1976) 236p.

[3] ÁRNASON, B., Hydrothermal systems in Iceland traced by deuterium, Geothermics **5** (1977) 125-151.

[4] SVEINBJÖRNSDÓTTIR, Á.E., et al., The use of stable isotopes of oxygen and hydrogen in geothermal studies in Iceland, Proceedings World Geothermal Congress, Florence, Italy, (1995) 1043-1048.

[5] ARNÓRSSON, S. & ANDRÉSDÓTTIR, A., Processes controlling the distribution of boron and chlorine in natural waters in Iceland. Geochim. Cosmochim. Acta **59** (1995) 4125-4146.

[6] MOOK, W.G., Carbon-14 in hydrological studies. In Handbook of Environmental Isotope Geochemistry. The Terrestrial Environment. (FRITZ, P. & FONTES, J. Ch., Eds), Elsevier Amsterdam (1980) 49-74.

[7] SVEINBJÖRNSDÓTTIR, Á.E. et al., Geochemistry of natural waters in Skagafjördur, N-Iceland. II Isotopes, In Water-Rock Interaction (AREHART & HULSTON, Eds) (1998) 653-656.

[8] JOHNSEN, S.J., et al., The origin of Arctic precipitation under present and glacial conditions. Tellus **41B** (1989) 452-468.

[9] SVEINBJÖRNSDÓTTIR, Á.E., The stable isotopic composition of the Mosfellssveit thermal water, Iceland, with special emphasis on the deuterium excess. IAEA-SM 319/36P (1992) 177-178.

A MULTI-ISOTOPE (B, Sr, O, H) AND AGE DATING (^{3}H-^{3}He, ^{14}C) STUDY OF GROUNDWATER FROM SALINAS VALLEY, CALIFORNIA

A. VENGOSH
Hydrological Service, Jerusalem and Department of Geological and Environmental Sciences,
Ben Gurion University of the Negev,
Beer Sheva, Israel

J. GILL
Institute of Earth Sciences, University of California Santa Cruz,
Santa Cruz, California, United States of America

M.L. DAVISSON, G.B. HUDSON
Lawrence Livermore Laboratory, Analytical and Nuclear Chemistry Division,
Livermore, California, United States of America

Abstract

This study investigates the chemical and isotopic compositions of groundwater from Salinas Valley, California in order to constrain the origin and rates of groundwater contamination. We use an array of geochemical, environmental isotopes of water ($^{18}O/^{16}O$, D/H, ^3H-^3He) and dissolved salts ($^{11}B/^{10}B$, $^{87}Sr/^{86}Sr$, ^{14}C) to establish a reliable conceptual model for the basin. The basin consists of a deep, confined "400-foot aquifer", overlying the "180-foot aquifer", and a perched aquifer, all made up of sand, gravels, clays, and alluvial deposits. Our ^3H-^3He, ^{14}C, and $\delta^{18}O$ results show different replenishment zones and rates in the basin: (1) rapid replenishment (<10 years and near-modern ^{14}C concentrations of 72 to 98 pmc) in the perched and 180-foot aquifers in the northern area; (2) fast arrival (15 years) of ^{18}O- and NO_3-enriched agriculture-return flows in the unconfined 180-foot aquifer in the central valley; (3) young water recharge (6 to 20 years) from the Salinas River, which is enriched in ^{18}O and D relative to GMWL, occurs in the southern basin; and (4) travel time of >10,000 years (^{14}C=21.3 PMC) in the deep 400-foot aquifer in the northern area of the valley, indicating pristine slow recharge.
We identified several different end-member saline components with distinguishable chemical and isotopic fingerprints: (1) agriculture return flow in the perched aquifer (e.g., high NO_3 and SO_4, low $^{87}Sr/^{86}Sr$ = 0.7082, $\delta^{11}B$ = 19‰); (2) salt-water intrusion in the northern basin (e.g., low Na/Cl, marine Br/Cl, high Ca/Mg, $\delta^{11}B$ = 17 to 38‰ , $^{87}Sr/^{86}Sr$ = 0.7088 to 0.7096; (3) non-marine saline water in the southern part of the valley (e.g., high SO_4, high Na/Cl, $\delta^{11}B$ = 24 to 30‰ , $^{87}Sr/^{86}Sr$ = 0.70852). The geochemical and isotopic fingerprints of the different water sources enables us to delineate the impact of these sources in different areas of the valley as well as to evaluate the origin of the saline, SO_4-enriched plume, that is located north of Salinas City. Our data suggests mixing between natural SO_4-enriched water and marine-derived saline water.

1. INTRODUCTION

Ground water in coastal aquifers is becoming more polluted due to a variety of human activities, including water exploitation for domestic use, intensive agriculture, and reuse of wastewater. Consequently, the quality of ground water in coastal areas gradually degrades which limits its future exploitation and potability. Salinization of groundwater is one of the main processes that affects groundwater quality in the aquifers along the coast of California. Saltwater intrusion occurs in many coastal aquifers including the Santa Ana Basin in Orange County [1], Oxnard Plain in Ventura County [2], and Salinas Basin in Monterey County [3] . In general, over-exploitation decreases the piesometric water levels to below sea level and intrusion of seawater into the pumping zones of the coastal aquifer. Nevertheless, it was argued that movement of seawater from the ocean is not the only sources of high Cl concentrations. In addition to leakage of overlying seawater from contaminated shallow zones through failed well casing, salinization can result from irrigation return or from underlying brines as demonstrated in the Oxnard Plain [2]. Similarly, previous studies in the Salinas Valley [3, 4] showed that sea water intrusion is not the only source of salinity in the basin.

In this paper we investigate the sources of the salinity in the shallow 180-foot aquifer from Salinas Valley in central California (Fig. 1). The diversity of the potential salinity sources (e.g., seawater intrusion, agriculture return flows, and connate saline water from poorly flushed aquifers) requires the use of diagnostic tools to delineate the sources and their impacts on the ground water system. We apply an array of geochemical, environmental isotopes ($\delta^{18}O$, δD), age dating (tritium-^{3}He, ^{14}C), and isotopes of dissolved constituents ($^{11}B/^{10}B$ and $^{87}Sr/^{86}Sr$) to identify the sources of salinity and to establish a conceptual model for groundwater flow in the 180-foot aquifer.

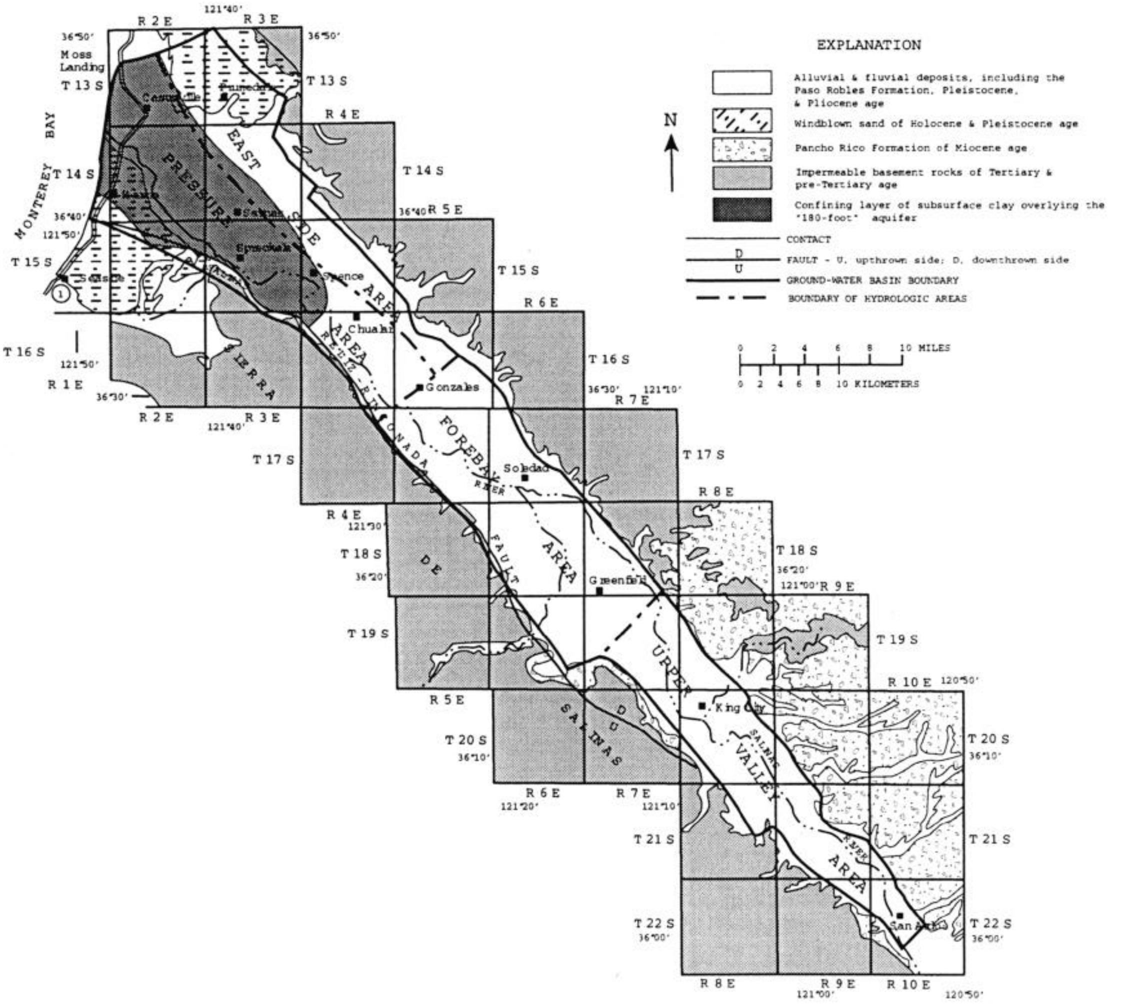

FIG. 1. Map of the Salinas Valley. Note the different basins, in particular the Pressure Area adjacent to the ocean. Source of the map in Ref. [3].

2. HYDROGEOLOGY OF SALINAS VALLEY

The groundwater basin of Salinas Valley (Fig. 1) consists of two main water-bearing zones separated by a thick impermeable clay layer, the "180-foot" (55 m.) and "400-foot" (122 m.) aquifers. Overlying the "180-foot" aquifer, in the northern part of the basin, lies a perched aquifer which rests upon the Salinas aquiclude, a clay layer at a depth interval of 15 to 76 m [5].

(1) The 180-foot aquifer of thickness up to 55 meters consists of Holocene gravels, sands, silts, and clays, all of which were deposited as sand dunes and valley terraces near Monterey Bay in the northern part of the valley (Pressure Area), and as alluvium and floodplain deposits in the southern part.

(2) The 400-foot aquifer lies at a depth of 82 to 143 meters and is part of the Pliocene Paso Robles Formation. It consists of poorly bedded sands, gravels, volcanic tuff, and interbedded clays, which act as local aquitards. The aquifer is also composed of Pleistocene Aromas red sands that contain quartzose and well-sorted sands. The deep 400-foot aquifer is separated from the overlying shallow aquifer by clay layers at a depth of 82 m.

Geological investigations suggest that the water-bearing sediments, particularly those of the 400-foot aquifer, are an outcrop on the walls of Monterey Bay Submarine Canyon. This allows direct hydraulic connection with ocean water [5].

3. SAMPLING AND ANALYTICAL TECHNIQUES

Between the fall of 1996 and summer of 1997 forty-seven representative samples from different locations in the valley were collected from pumping and research wells in the Salinas Valley. Samples included ultra-clean acid-washed bottles for Sr isotopes, glass bottles with airtight caps for ^{3}H and ^{14}C ($HgCl_2$ added as preservative), and copper tubes with pinch clamps for noble gas analysis. Analyses of major ions were performed at the Monterey Bay County water quality laboratory. B and Li concentrations were measured by ICP-MS (Element, Finnigan) at the University of California Santa Cruz. ^{11}B and ^{7}Li intensities were normalized to the internal standard of ^{9}Be. Spike-free samples were scanned before the analyses and no detectable levels of ^{9}Be were found in the original samples. Br was determined by flow injection ion analyzer (QuickChem 8000) at the Hydrological Service laboratory in Jerusalem [6].

The ^{18}O and deuterium were analyzed respectively by using the CO_2 equilibration [7] and the zinc-reduction methods [8], followed by analysis on an isotope ratio mass spectrometer. All stable isotope data are reported in the usual δ notation, where $\delta = (R/R_{STD} - 1)1000$, R represents either the $^{18}O/^{16}O$, D/H, or $^{13}C/^{12}C$ ratio of the sample, and R_{STD} is the isotope ratio of the SMOW or PDB standard. The ^{3}H was analyzed by the helium-accumulation method [9], whereby samples are cryogenically degassed, sealed, and stored for 15-60 days to allow accumulation of ^{3}He from the tritium decay. The sample is subsequently degassed and the ^{3}He is isolated and quantified on a VG-5400 noble gas mass spectrometer. Copper tubes for helium analysis held air-free samples that were vacuum fitted to an evacuated container, the pinch clamp and copper seal was uncrimped, and the water sample was then released. The water was degassed and the noble gases of interest were isolated and analyzed.

The inorganic carbon was acid stripped under high vacuum and purged with an ultra pure carrier gas [10, 11]. Liberated CO_2 was reduced to graphite [12], and all ^{14}C concentrations were determined on the accelerator mass spectrometer at Lawrence Livermore National Laboratory. The ^{14}C results are reported as a percent modern carbon (pmc) relative to a NBS oxalic acid standard [13].

Boron isotopes were measured by a negative thermal ionization mass spectrometry technique [14, 15]. Samples were analyzed by a direct loading procedure, in which boron-free sea water and natural solutions were loaded directly onto Re filaments and measured in a reverse polarity solid-source mass spectrometer (NBS, magnet sector of 90^0) at the Institute of Earth and Marine Sciences, University of California Santa Cruz. A standard deviation of less than 1.5‰ was determined by repeat analysis of NIST SRM-951 standard ($^{11}B/^{10}B = 4.013 \pm 0.005$). Isotope ratios are reported as δ^{11}B values, where $\delta^{11}B = [(^{11}B/^{10}B)_{sample} / (^{11}B/^{10}B)_{NBS\ 951}) - 1] \times 1000$. Strontium was separated by cation-exchange chromatography using standard techniques. Isotope ratios were determined using third generation Faraday detectors in static mode on a VG-54WARP mass spectrometer at University of California Santa Cruz. We used zone refined rhenium filaments. All measured $^{87}Sr/^{86}Sr$ results were corrected to an $^{87}Sr/^{86}Sr$ ratio of 0.1194 using an exponential correction law. Correction for ^{87}Rb was negligible for all samples. Replicate analyses of NBS-987 yielded a ratio of 0.71025 (± 0.00001; n=5) during the period in which the unknowns were run.

4. RESULTS AND DISCUSSION

The variations of Cl versus different ions and TDS (Fig. 2) enable us to distinguish between several water groups with distinct patterns: (1) pristine freshwater in the northern section of the valley; (2) salt-water intrusion in the northern valley, characterized by Ca-enriched saline groundwater with high Cl/TDS and low Na/Cl (<1) and marine SO_4/Cl and Br/Cl ratios; (3) groundwater from the shallow perched aquifer with high concentrations of NO_3 and SO_4; and (4) SO_4-enriched saline groundwater with low Cl/TDS and high Na/Cl (>1) ratios in the central and southern parts of the valley.

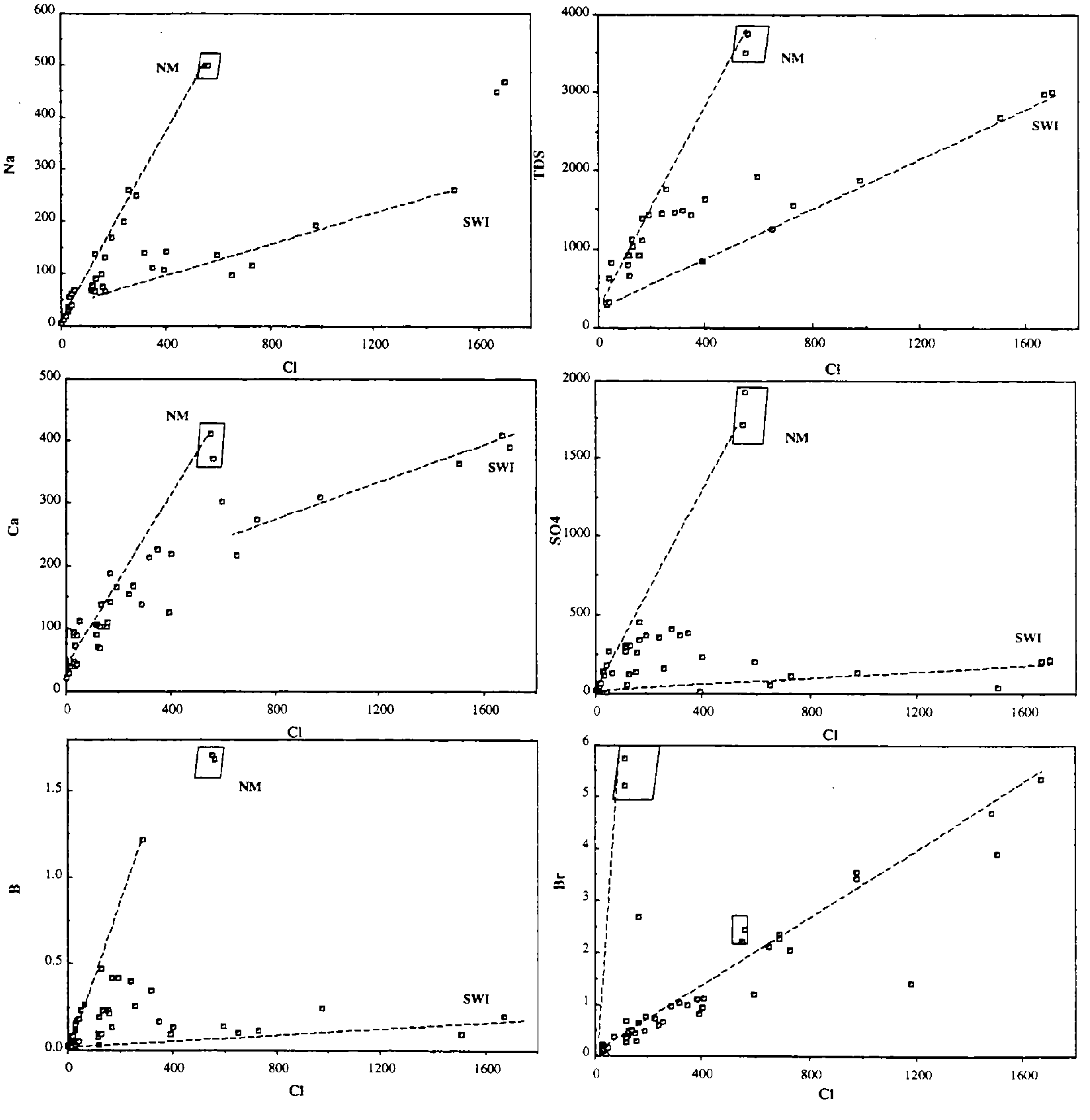

FIG. 2. Chloride vs. TDS and various ions (in mg/l) from investigated groundwater in the Salinas Valley. Note the distribution of two patterns of mixing with salt-intrusion (SWI) and non-marine (NM) saline water.

4.1. The fresh water component

We examined two sets of fresh water samples: (1) surface and shallow groundwater from the southern and central parts of the valley, and (2) pristine groundwater from the northern area.

The water of Salinas River is recharged into the aquifer as part of the artificial replenishment management plan for the valley. During the winter, water is stored in two artificial reservoirs (Lake San Antonio and Lake Nacimiento) which are the main sources for the Salinas River. The Salinas River is recharged to the unconfined 180ft-aquifer in the southern and central valley. However, the impact of the Salinas River on local groundwater has not been fully evaluated and still is a controversial issue between water users in different areas of the valley.

We examined the chemical composition of several stages in the artificial recharge (1) up-stream water stored in the artificial reservoirs; (2) water from down-stream along the Salinas River; and (3) shallow ground water associated with the Salinas River. The variations of the dissolved salts and $\delta^{18}O$ data (Fig. 3) show that (1) the chemical composition of the surface water is characterized mainly by evaporation processes, (2) the chemical signature of the shallow ground water generally mimics that of the Salinas River, though the chemical composition is modified also by water-rock interactions, and (3) the $\delta^{18}O$ values of both surface and groundwater are in the range of -6.2‰ to -4.7‰ , indicating the impact of Salinas River on shallow groundwater. The $\delta^{18}O$ data enables us to clearly distinguish between replenishment areas: (1) artificial recharge of Salinas River with high $\delta^{18}O$ and δD values in the south, and (2) natural recharge of regional groundwater in the northern part of the aquifer with lower $\delta^{18}O$ (-6.5‰ to -6.1‰) and δD values. One sample in the perched aquifer had a similar $\delta^{18}O$ value (-6.3‰), which suggests a similar replenishment zone. However, the chemical composition of the perched aquifer (e.g., high Cl, NO_3 concentrations) is different from that of the pristine water of the 180-foot aquifer, which suggests limited hydraulic connection between the two systems. The groundwater in the underlying 400-foot aquifer had a $\delta^{18}O$ value of -6.3‰ .

Age-dating data revealed the residence time of fluids and the dynamics of recharge in the valley (Table 1): (1) ages were between 6 and 21 years for shallow groundwater associated with the Salinas River recharge (i.e., high $\delta^{18}O$) in the southern areas; (2) groundwater was <15 years old in the perched and the confined 180-foot aquifers in the Pressure area (3) ages <20 years for NO_3-enriched agriculture-return flows in the unconfined 180-foot aquifers south of Salinas City; and (4) apparent ages >10,000 years (^{14}C=21 PMC) in the deep 400-foot aquifer. The relatively modern ages detected by the ^{3}H-^{3}He technique are consistent with modern ^{14}C data (^{14}C range of 72 to 93 PMC). However, mixing of older groundwater with more modern recharge occurs in limited cases. For example, wells 2E11C01 and 2E36E01, both had appreciable excess ^{4}He, even though they had apparently modern ^{14}C and measurable ^{3}H-^{3}He ages (Table 1). This suggests that mixing young modern recharge with older pristine groundwater occurs in some wells, particularly those with multiple completion depths. Two other samples (2E11A02 and 4E01D01) had ^{4}He excesses and measurable ^{3}H-^{3}He ages , but correlative ^{14}C analyses are not available. The modern ages of the 180-foot aquifer suggests rapid preferential flows through sand dune and alluvium deposits, and the evidence for mixing rules out slow piston flow. In contrast, the significantly older age of the deep 400-foot aquifer suggest that the two aquifers have limited connection, although they have similar $\delta^{18}O$ values. Moreover, the data suggests that modern meteoric water recharge rates are slow, and that the current exploitation of this aquifer is extracting fossil groundwater.

TABLE 1. AGE-DTING DATA OF GROUNDWATER IN THE SALINAS VALLEY.

Sample	^{14}C (PMC)	^{3}H-^{3}He age (yrs)	^{3}H (pCi/L)
2E11C1	93.4	-	-
2E11A4	21.3	-	-
2E11A3	85.1	6.9	7.2
4E23M1	72.2	15.2	7.3
3E13J2	98.4	16.7	5.8
2E36E1	84.0	*38.1	3.8
2E11A2	-	*5.0	10.0
4E25Q01	-	10.8	12.6
2E11C01	-	*14.6	7.3
2E01D01	-	*21.0	19.0
3E25L01	-	6.4	17.3

* Samples have excess ^{4}He.

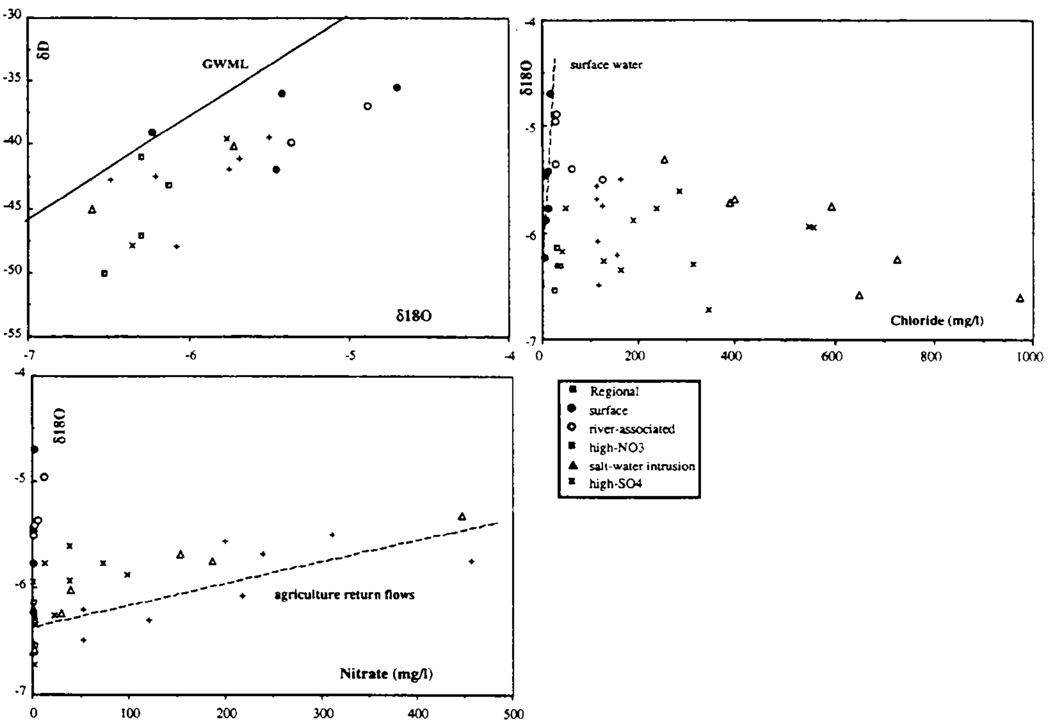

FIG. 3. $\delta^{18}O$ vs. δD, chloride and nitrate concentrations in groundwater from the Salinas Valley. Note the enrichments and shifts in $\delta^{18}O$ and δD values relative to the GMWL of the surface water and agriculture return-flows.

4.2. Salt-water intrusion

Saline water associated with salt-water intrusion into the Pressure Area is characterized by high chloride concentrations, relatively high Cl/TDS ratios (0.3-0.5), low Na/Cl ratios (lower than the marine ratio of 0.86), marine SO_4/Cl, B/Cl, and Br/Cl ratios, and high Ca/Mg and Ca/(SO_4+HCO_3) ratios. The variations of Br and Cl ions (Fig. 4) indicate that all of the saline groundwater in the Pressure Area is derived from seawater. The saline water is enriched in Ca, Mg, Li, and Sr and is depleted in Na relative to diluted seawater with similar salinity. These variations reflect chemical modifications induced by water-rock interactions such as base-exchange reactions in which Na in the water is replaced by Ca and Mg from adsorbed sites on clay minerals, dolomitization, and diagenetic transformation of carbonate minerals [16, 17]. $\delta^{11}B$ values of saline water associated with salt-water intrusion vary between 17‰ (in fresh water) to 38‰. This suggests conservative mixing between seawater ($\delta^{11}B$=39‰) and fresh water, although some samples have lower $\delta^{11}B$ values, reflecting mixing with agriculture-return flows.

The relative enrichments of Sr and Ca ions are correlated with the increase of $^{87}Sr/^{86}Sr$ ratios, from 0.7088 to 0.7096 (Fig. 4). These variations suggest that Sr (and Ca) is derived from water-rock interactions and not from conservative mixing between regional ground water ($^{87}Sr/^{86}Sr \sim 0.7090$) and seawater (0.7092). It has been shown that exchangeable Sr on clay minerals has a high $^{87}Sr/^{86}Sr$ ratio (a range of 0.7103 to 0.7280; data from different clay minerals and experiments [18,19,20] . Thus, the linear correlations between Ca and Sr with $^{87}Sr/^{86}Sr$ ratios would suggest the influence of radiogenic Sr derived from base-exchange reactions with clay minerals. In contrast, it was demonstrated [21] that during dolomitization reactions the $^{87}Sr/^{86}Sr$ ratio of the residual fluids would gradually decrease towards the lower $^{87}Sr/^{86}Sr$ ratio of the original carbonate (which is typical for carbonate rocks of ages from Cretaceous to Present). Recrystallization or dolomitization of Miocene sediments in Salinas Valley (e.g., Monterey Formation) would produce saline water with high Ca contents but with low $^{87}Sr/^{86}Sr$ ratios relative to modern sea water. This distinction may be useful to evaluate source of saline water and to distinguish base-exchange from dolomitization reactions and their modifications towards Ca-enriched saline water.

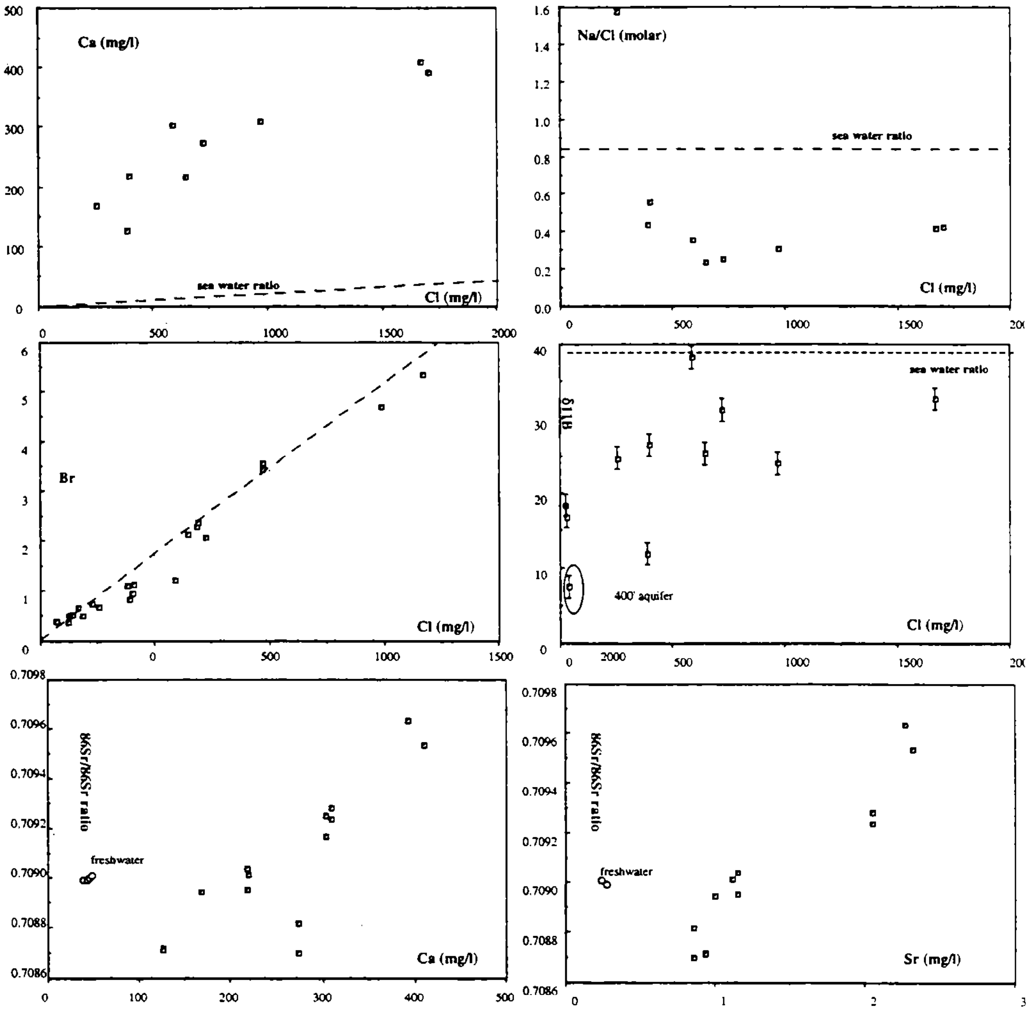

FIG. 4. Chemical and isotopic variations of saline groundwater associated with salt-water intrusion zone. Note the marine ratio of Br/Cl, the relatively enrichment of Ca and depletion of Na, the variations of $\delta^{11}B$ *values between seawater and freshwater values, the high* $^{87}Sr/^{87}Sr$ *ratios relative to seawater, and the linear correlations between* $^{87}Sr/^{87}Sr$*, Ca, and Sr contents.*

4.3. Anthropogenic effects and the perched aquifer

The major source of anthropogenic contamination in the Salinas Valley is the intensive agriculture activity over the last seven decades. In order to characterize the chemical composition of the agriculture-return flow we looked at two sets of data: (1) shallow groundwater from the perched aquifer below the agriculture fields in the Pressure Area (well 14S/2E-11A3); and (2) groundwater from the unconfined 180-foot aquifer south of Salinas City. Our results show that shallow ground water from the perched aquifer has a Cl content up to 160 mg/l, high NO_3 and SO_4 concentrations (up to 311 and 343 mg/l, respectively), Na/Cl ~1, Ca/Mg~1, and high SO_4/Cl ratios. The high NO_3 reflects the extensive use of nitrogen fertilizers while the high SO_4 is explained by application of gypsum fertilizers in that area. The dissolution of gypsum is confirmed by the Ca/SO_4 ratio of ~1. Groundwater from the perched aquifer has a low $^{87}Sr/^{86}Sr$ ratio (0.7082). The $\delta^{11}B$ value of the perched aquifer (19‰) is associated with a relatively high B/Cl ratio ($5x10^{-3}$), which suggests that boron can be enriched in agriculture-return flows with a characteristically low $\delta^{11}B$ value.

The unique chemical features, typical of shallow groundwater from the perched aquifer in the Pressure Area, can also be delineated in deeper high-NO_3 ground water from the 180-foot aquifer. Some saline water from the "salt-water intrusion area" has high NO_3 concentrations, which suggests mixing with the overlying agriculture return flows. These samples are also enriched in SO_4 and HCO_3 and have relatively low Br/Cl, high B/Cl and low $\delta^{11}B$ values. It should be noted that gypsum fertilizers are used mainly in the Pressure Area of the Salinas Valley and not in other parts (e.g., East Side area). Thus, the anthropogenic SO_4 signature can be an indicator of anthropogenic affects occurring in limited areas of the valley. Indeed, groundwater from the unconfined 180-foot aquifer south of Salinas City has high NO_3, but also has low SO_4 and B concentrations with different $\delta^{11}B$ values (31‰ to 35‰) and $^{87}Sr/^{86}Sr$ ratios (0.70895 to 0.70967).

4.4. Non-marine saline water from the southern basin

A previous study [3] has shown that saline water existed in the southern parts of the valley. Saline groundwater from these areas are characterized by the dominance of Na and SO_4, with SO_4 concentrations up to 1930 mg/l, chloride of 550 mg/l, high Na/Cl ratios (> 1), and low Cl/TDS ratios. This chemical composition is different from that of intruded sea water or connate brines that evolve from seawater, and thus rules out contribution from relics ocean water entrapped in unflushed aquifers. The ratios of cations and anions to Cl suggest intensive water-rock interactions and leaching processes, resulting in salt accumulation in the liquid phase. The $\delta^{11}B$ values of 24‰ and 30‰ suggest interactions with sedimentary (e.g., carbonate, gypsum) minerals and not from silicate rocks (i.e., $\sim 0 \pm 10\%$). This conclusion is strengthen by the $^{87}Sr/^{86}Sr$ ratio of 0.70852 which suggests that Sr was also derived from dissolution of sedimentary minerals and not silicate rocks with a radiogenic Sr isotopic signal.

4.5. Delineation of sources of contamination

Special attention was given to saline plumes located in the Pressure Area northwest of Salinas City (the "Banana Belt"). In this area both the SO_4 and Cl concentrations are relatively high (up to 450 and 345 mg/l, respectively) and NO_3 levels in most of the samples (except for two) are low. The variations of Na/Cl, SO_4/Cl, B/Cl, and Cl/TDS ratios as well as $\delta^{11}B$ values of this water suggest mixing between salt-intrusion and non-marine saline water with high SO_4 contents. Early water quality measurements from the 1930s suggest that high-SO_4 groundwater existed already in that area. Mixing of salt-water intrusion with naturally high TDS water of non-marine origin might be a modern phenomenon, or it could reflect relics of mixing between unflushed seawater and non-marine water. It was argued [4] that the high SO_4 concentrations in the Banana Belt resulted from recharge of agriculture return-flows. However, the extremely low NO_3 concentrations and the chemical variations of ground water in this area suggest mixing of marine with non-marine saline waters.

5. CONCLUSIONS

We investigated ground and surface water representing different end-member components in order to characterize the chemical and isotopic fingerprints of these sources, and to establish diagnostic tools for delineation of the various salinity sources in Salinas Valley, California. Based on integration of chemical and isotopic data we developed a conceptual model for the flow paths, water migration, and salinization processes. The model enables us to distinguish between different sources of salinity in the valley that include salt-water intrusion, naturally high TDS water, and agriculture return-flows, and to delineate their impact on different areas in of the 180-foot aquifer. The model, which is based on field geochemical and isotopic data, provides an initial quantitative basis for future water management in the coastal area of Salinas Valley, and a guide to evaluate the potential risks of present water management practices.

REFERENCES

[1] DAVISSON, M.L. et al., "Tracing and age-dating recycled waste water recharged for potable reuse in a seawater injection barrier, southern California, USA", Isotope Techniques in Water Resources Development and Management, IAEA-SM-361/36 (1999).

[2] IZBICKI, J.A., "Chloride sources in a California Coastal Aquifer", Ground water in the Pacific Rim Countries, Irrigation Division, American Society of Consulting Engineers, Honolulu, Hi, July 23-35 (1991).

[3] SHOWALTER, P. et al., "Design of a ground-water-quality monitoring network for the Salinas River Basin, California", U.S. Geological Survey, Water-Rssources Investigations Report 83-4049, 74 pp (1984).

[4] HEARD, J.E., "Hydrogeology of high-salinity ground water in the "180-foot" Pressure aquifer southwest Salinas, Monterey County, California". M.Sc. thesis. San Jose State University, San Jose (1992).

[5] GREENE, H.G., "Geology of Southern Monterey Bay and its Relationship to the Ground Water Basin and Salt Water Intrusion", USGS California State Department of Water Resources, open file report, 50 pp. (1970).

[6] VENGOSH, A. and PANKRATOV, I., "Chloride/bromide and chloride/fluoride ratios of domestic sewage effluents and associated contaminated groundwater", Ground Water, **36**, 815-824 (1998).

[7] EPSTEIN, S. and MAYEDA, T., "Variation of ^{18}O content of waters from natural sources", Geochim. Cosmochim. Acta, **4**, 213-224 (1953).

[8] COLEMAN, , M.L. et al., "Reduction of water with zinc for hydrogen isotope analysis", Anal. Chem., **54**, 993-995 (1982).

[9] SURANO, K.A. et al., "Helium-3 mass spectrometry for low -level tritium analysis of environmental samples", J. Radioanal. Nuclear Chem. Art., **161**, 443-453 (1992).

[10] DAVISSON, , M.L. and VELSKO, C.A., "Rapid extraction of dissolved inorganic carbon from small volumes of natural waters for ^{14}C determination by accelerator mass spectrometry", Lawrence Livermore National Laboratory UCRL-JC-119176, 23 pp. (1994).

[11] MCNICHOL, A.P. et al., "The rapid preparation of seawater sigma-CO_2 for radiocarbon analysis at The National Ocean Sciences AMS Facility", Radiocarbon, **36**, 237-246 (1994).

[12] VOGEL, J.S.et al., "Catalyst and binder effects in the use of filimentous graphite in AMS". Nuclear Instruments and Methods in Physics Research, **B29**, 50-56 (1987).

[13] STUIVER, M. and POLACH, H., "Reporting of ^{14}C data", Radiocarbon, **19**, 355-363, (1977).

[14] VENGOSH, et al., "Direct determination of boron and chlorine isotopes in geological materials by negative thermal-ionization mass spectrometry", Chem. Geol. (Isotope Geosci. Sec.), **79**, 333-343 ((1989).

[15] VENGOSH, et al., "Boron isotope application for tracing sources of contamination in groundwater", Environm. Sci. & Tech., **28**, 1968-1974 (1994).

[16] TODD, D.K., "Sources of saline intrusion in the 400-foot aquifer, Castroville area, California", Monterey County Flood Control & Water Conservation District, Salinas, California. 41 pp. (1989)

[17] JONES, et al., (1999)

[18] CHAUDHURI, S. and BROOKINS, D.G., "The Rb-Sr systematics in acid-leached clay minerals", Chem. Geol., **24**, 231-242 (1979).

[19] CHAUDHURI, S. et al., "Strontium isotopic evolution of oil-field waters from carbonate reservoir rocks in Bindley field, central Kansas, USA", Geochim. Cosmochim. Acta, **51**, 45-53 (1987).

[20] STUEBER, A.M.et al., "A strontium isotopic study of formation waters from Illinois basin, USA", Appl. Geochem., **2**, 477-494 (1987).

[21] STARINSKY, A. et al., "Strontium isotope evidence on the history of oilfield brines, Mediterranean Coastal Plain, Israel", Geochim. Cosmochim. Acta, **47**, 687-695 (1983).

RECHARGE QUANTIFICATION WITH RADIOCARBON: INDEPENDENT CORROBORATION IN THREE KAROO AQUIFER STUDIES IN BOTSWANA

B. Th. VERHAGEN
Schonland Research Centre, University of the Witwatersrand, Johannesburg, South Africa

D. B. BREDENKAMP
Water Resources Evaluation and Management, Pretoria, South Africa

H. JANSE VAN RENSBURG
Anglo American Technical Services, Johannesburg, South Africa

J. L. FARR
Wellfield Consulting Services, Gaborone, Botswana

ABSTRACT

Environmental isotope data from a "snapshot" sampling hold out the promise of producing acceptable estimates of ground water recharge for resource management purposes. In three major ground water developments in Botswana, estimates of recharge to the Karoo aquifers in the Kalahari, were based on residence times derived from radiocarbon data. In the assessment, three factors needed to be considered: 1) the model leading to acceptable values of residence times 2) the initial, or recharge, radiocarbon value and 3) appropriate values of aquifer porosity. In the three studies, porosity had been measured on numerous drill cores obtained from the principal fractured sandstone aquifers. The resulting isotope-based recharge values correspond reasonably with independent recharge assessments using the equal volume method to analyse long-term rest level observations in two cases; in the third, recharge was independently assessed on the basis of chloride balance in both unsaturated and saturated zones. It is concluded that a) the isotope snapshot approach can give acceptable values for recharge in the development of ground water resources, providing rational management information early in the life of a ground water supply scheme; b) the exponential model and an initial radiocarbon values of 85 % atmospheric are realistic in this environment and c) the total porosity appears to be the appropriate parameter in the calculation of recharge. This also provides an insight into the behaviour of the aquifers.

1. INTRODUCTION

The quantification of recharge is increasingly given attention in the management of ground water as the ultimate measure of the long-term sustainability of the resource. Traditionally, recharge can be assessed on the basis of long-term accumulation of water level and abstraction data in e.g. the equal volume method of interpreting hydrographs. Since their discovery in the environment some 50 years ago, cosmogenic radioisotopes in ground water provided the possibility of assessing the residence time or the rate of recharge to aquifers [1]. The assessment of recharge using the "isotope snapshot" approach is attractive in principle as it can provide up-front information on recharge which can be built into the management plan at the inception of exploitation.

In the isotope approach a mean residence time has to be calculated, based on some concept of transit time distribution. Amongst the available models (piston flow, dispersion, exponential; e.g. Zuber [2], Verhagen et al. [3]) the latter has been generally employed as a suitable "lumped parameter" model for phreatic aquifers. This approach is regarded as particularly appropriate where the borehole mixes all the water it intersects. Otherwise, little control can be exercised over sampling conditions as existing boreholes have to be employed, often of differing and poorly-known construction. The only control which can be exercised is to sample from boreholes in constant production or during extended pumping tests.

Tritium is a conservative tracer, simple to interpret, although useful only in shallower and more actively turned-over ground water, particularly in the southern Hemisphere. In sedimentary terrain such as the deeper multi-layer Karoo aquifers of the Kalahari, with mean residence times typically in excess of 1000 years, radiocarbon is useful as initial (recharge) concentrations can be estimated with some confidence and its subsequent behaviour in the saturated zone can be regarded as effectively conservative.

The well-mixed model assumes that the pumped well produces a mixture of different ages or transit times from the different lithological units penetrated. In a simple approach, recharge R can be estimated:

$$R = \frac{\sum_{i} p_i H_i}{T}$$

where T is the mean residence time (derived by the exponentail model), p_i the porosity and H_i the thickness of the individual saturated units (i) penetrated. The question arises as to which value of porosity should be employed. Most sedimentary aquifers in southern Africa have both primary and fracture porosity. In pump test analysis, the derived storage coefficient tends to increase with increasing pumping time (months to years; Verhagen et al.[4]), as gradually deeper seated water is released from the pores. It is argued here that, at an appropriate time scale, an environmental tracer effectively labels *all* the water in the aquifer by advection or diffusion. The approach taken here is to use the *total* porosity. Porosity is not always measured directly on aquifer material in ground water investigations, but clearly is of fundamental importance in the meaningful isotope assessment of recharge.

The problem of the behaviour of a tracer in a fractured porous medium has been discussed extensively by Zuber [4]. When water is transported mainly through the fractures, the

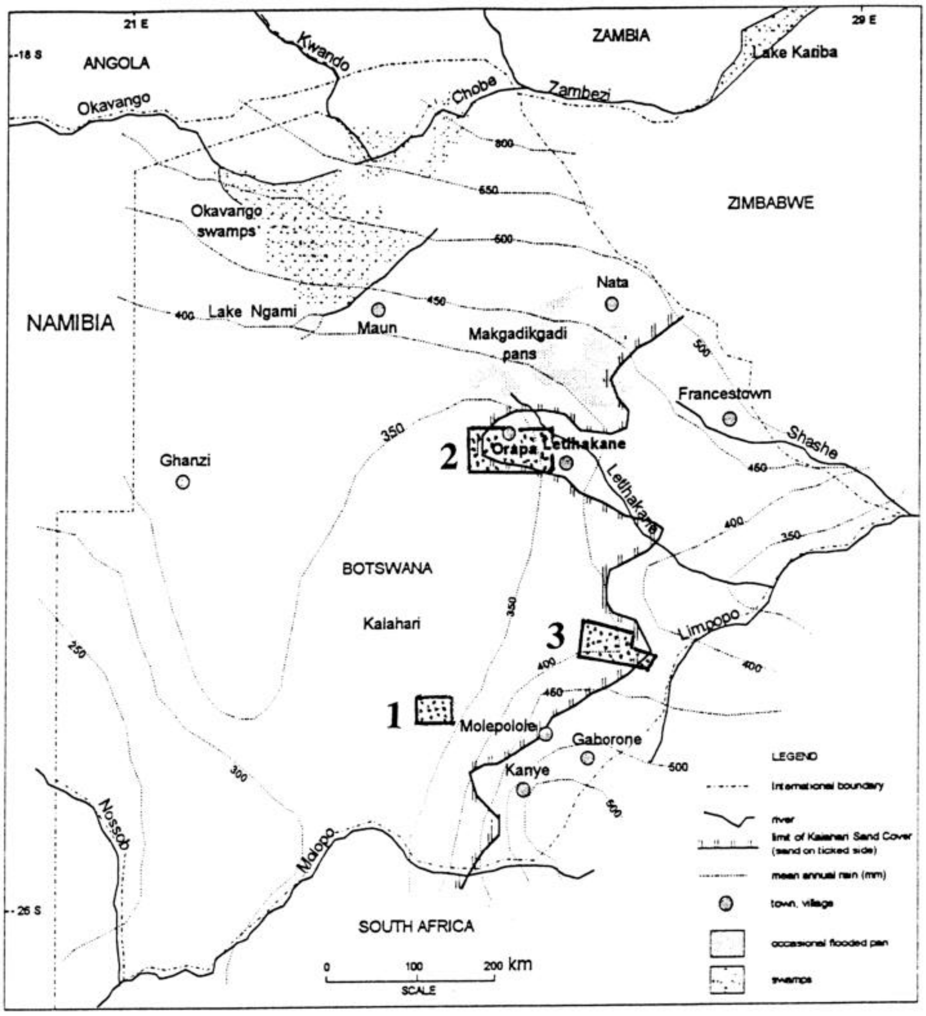

Fig. 1 Map of Botswana, showing isohyets and the well field study areas: 1. Jwaneng mine 2. Orapa mines and 3. Palla Road

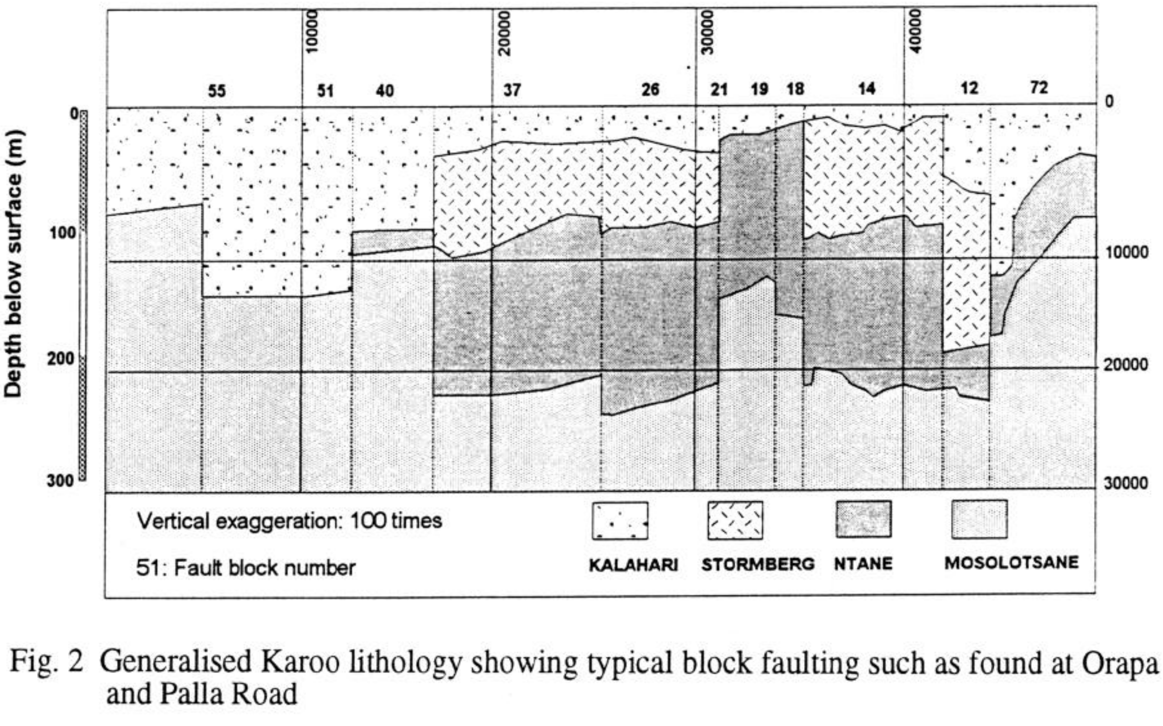

Fig. 2 Generalised Karoo lithology showing typical block faulting such as found at Orapa and Palla Road

tracer will diffuse into the more or less stagnant water in (micro) pores. In this way, the transport of tracer is delayed, the relevant retardation factor R_p being given by

$$R_p = \frac{t_t}{t_w} \cong \frac{n_p + n_f}{n_f}$$

where t_t and t_w are the transit times of tracer and water and n_p and n_f the matrix and fracture porosities respectively. As usually $n_p >> n_f$, high retardation factors can be attained. This may lead to tracer-based mean residence times of an order of magnitude - or more - too high.

Isotope data was collected in three ground water investigations in Karoo aquifers of the Kalahari over the past 20 years, allowing recharge estimates to be made. Long-term conventional geohydrological observations are now available in two cases, which allow recharge to be calculated from well field hydrographs. In the third case, recharge was calculated using the chloride balance method. In the three investigations reviewed below, acceptable correpondences were found between the isotope-based recharge figures, using the criteria mentioned above, and those obtained from other techniques, based on different criteria.

The three investigations were conducted in Botswana (Fig. 1), respectively at Jwaneng diamond mine (Verhagen [6,7]), Orapa diamond mine (Mazor et al. [8] , Verhagen and Morton [9]) and the Palla Road wellfield extension [10].

2. HYDROGEOLOGY

The generalised lithological section of the Karoo aquifers of the Kalahari basin is shown in Fig. 2. The principal aquifers are the more ubiquitous Ntane (or Clarens) fine grained aeolian largely non-calcareous sandstone, which can be locally indurated and cemented, overlying the Ecca (carboniferous) sequence of sandstones, siltstones and mudstones with locally better developed coarser grained sandstone horizons. Overlying the Ntane, except at the basin margins, is the Stormberg basalt. This unit confines the underlying sandstone aquifers and is aquiferous mainly due to jointing and fracturing. Along the fault structures in the south and north, major fracturing has produced considerable secondary porosity in the different aquiferous units, which are often juxtaposed through extensive block faulting, resulting in local hydraulic discontinuities. The entire basin has a cover of semi-consolidated Kalahari Beds, mainly sand and calcretes, which constitute minor, often perched local aquifers.

3. INITIAL - OR RECHARGE - RADIOCARBON VALUE

On account of the heterogenous and complex recharge pathways (Beekman et al. [11]) in the Kalahari, it is not readily apparent which of the available hydrochemical/isotopic models to employ in order to "correct" radiocarbon values for residence time calculations. A survey of the Kalahari conducted in 1971/72 when thermonuclear tritium was still evident in ground water systems in the southern Hemisphere (Verhagen et al.[12]) provided empirical evidence of 85 % of atmospheric for the radiocarbon content of recently recharged water. Such values have been used by other workers in similar environments. These values have been employed in the calculations of mean residence times in this study.

4. JWANENG MINE WELL FIELD

The well field supplying Jwaneng mine in southern Botswana taps a fluviatile sandstone aquifer. The structure, interpreted as a fault-controlled delta or alluvial fan in the Ecca facies, dips north-westwards below an increasing thickness of a mudstone/siltstone aquitard (Fig. 3). The land surface is flat and underlain by some 20 metres of Kalahari deposits. Exploitation of the well field commenced in 1980 from 14 wells and has been increased to some 10^7 m^3 a^{-1} from 28 high-yielding wells at present. Radiocarbon measurements on water from production wells in the early 80's in the range 55 pMC to 75 pMC suggested ongoing recharge, clearly disproving the belief that no significant modern recharge occurs in the Kalahari (Foster et al. [13]). The radiocarbon values appeared paradoxical, as they increase in the direction of increasing confinement of the sandstone. A few kilometres further north, deeper village boreholes intersecting the same sandstone unit give vanishing radiocarbon (Fig. 3).

These observations led to a first conceptual model of the aquifer's hydrology (Fig. 3). Recharge to the sandstone sub-crop beneath the Kalahari Beds cover would produce mounding which drives ground water down-dip in a northerly direction. The well field boreholes, all drilled to about 230 m, intersect the entire aquifer and full range of flow lines in the SE, whilst NW-wards only partially penetrating the aquifer and intersecting only the more recent flow lines, resulting in increasing ^{14}C values. The flow is clearly arrested between the well field and the the deep village boreholes further northwards at ~0 pMC. The input from recharge should therefore be balanced by leakage into the aquitard over some 100 km^2 of contact with the sandstone.

Time series [7] of radiocarbon for several production boreholes over the period of full exploitation (1983-1993) show no significant changes (Fig. 4), which suggests that flow relationships have not been modified significantly over that period.

Recharge values were calculated using exponential model mean residence times based on radiocarbon values, giving 3.7 mm a^{-1} in the SE (at 55 pMC) to 4.7 mm a^{-1} in the NW (75 pMC). A mean porosity value of 15% was used, based on the total porosity measured on several drill cores obtained from the sandstone aquifer during original well field development.

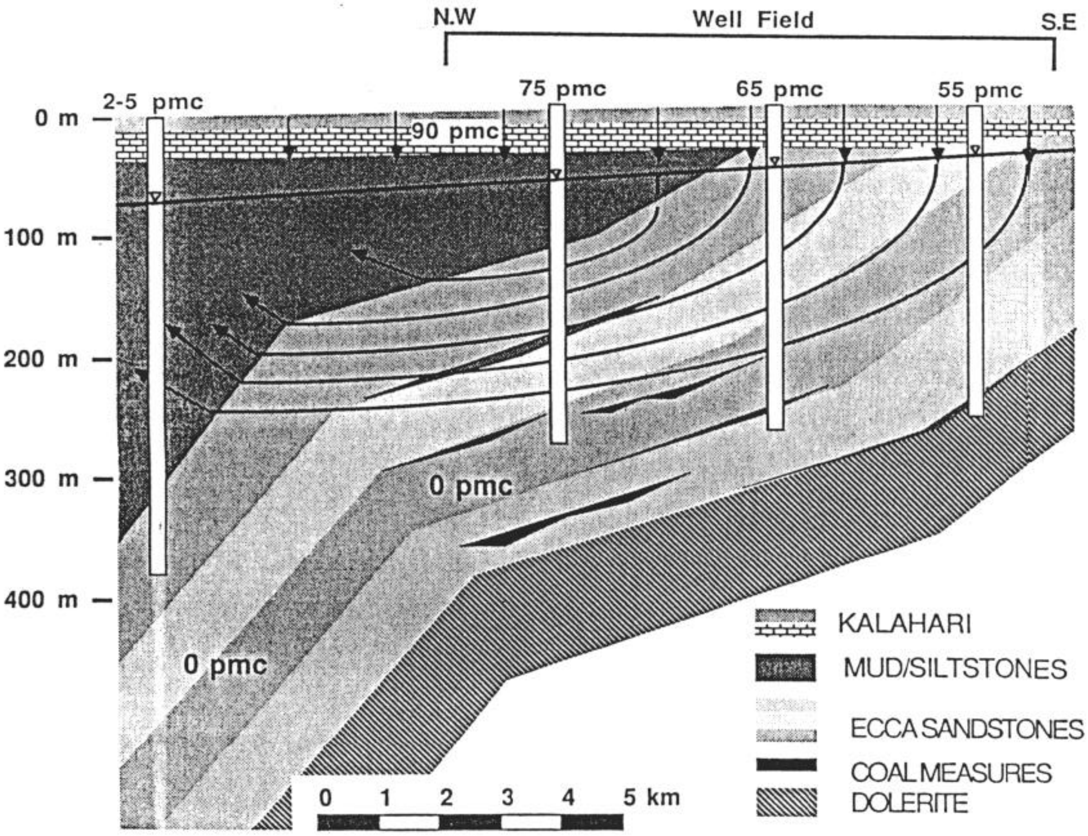

Fig. 3 Schematic section of the aquifer tapped by the Jwaneng well field with well field boreholes and deep village boreholes (left) and typical radiocarbon values. Inferred flow lines according to the isotope model, from the recharge area at the sandstone subcrop, to leakage into the aquitard

An analysis of 12 year hydrograph of average water levels for the well field (Fig. 5) revealed a number of periods of equal water level (van Rensburg and Bush [14]). Recharge was calculated on the basis of the equal volume method, which assumes that the abstraction over the period equals recharge. A best fit of the data for the relationship between inferred recharge and the rainfall over the same period was obtained for a storativity of 0.008, giving a recharge of 1.4 % of mean annual rainfall of some 350 mm a^{-1}. In the modified Hill method, assuming a 200 mm threshold of rainfall before recharge can occur, a recharge of 1.98% of rainfall and a storativity of 0.005 is obtained. The long-term apparent S-value, given by the ratio (cumulative abstraction)/(cumulative dewatered volume) over 12 years, approaches 0.02. The range of resulting recharge values of 3.0 - 4.9 mm a^{-1} overlaps the range of isotope-derived values.

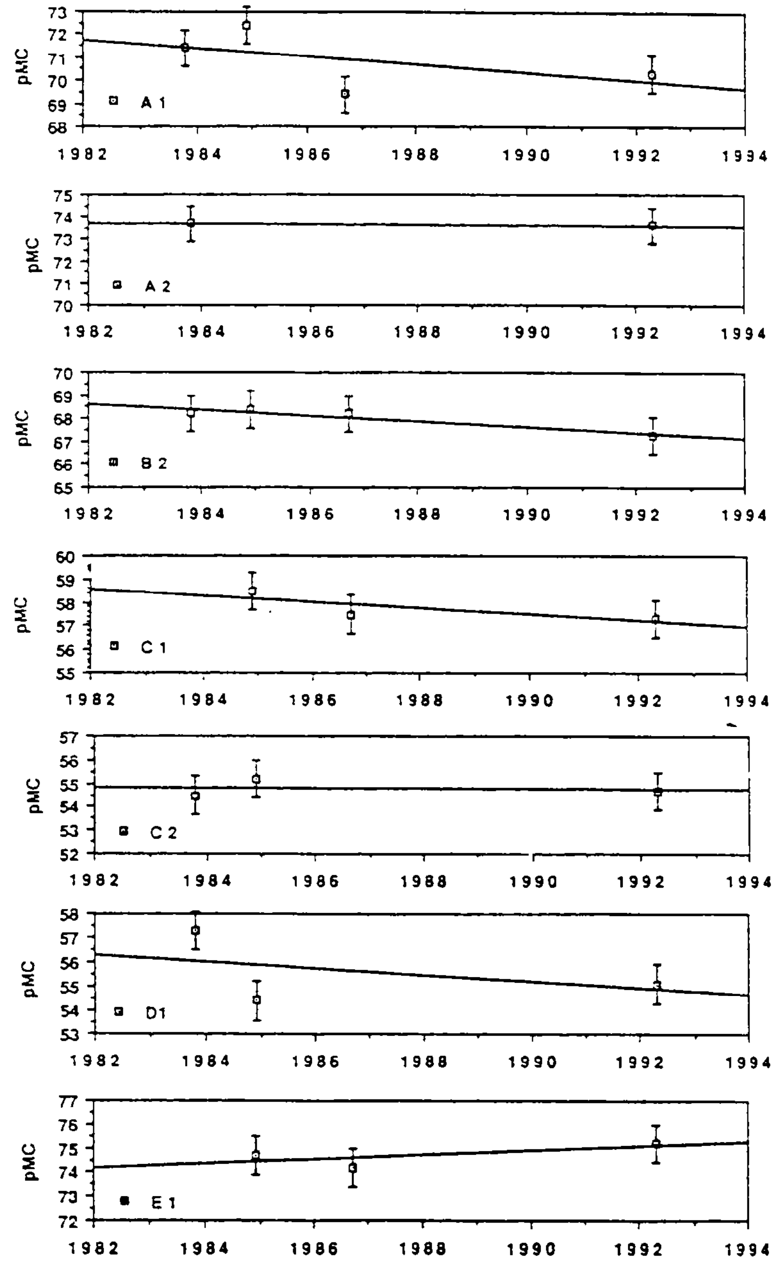

Fig. 4 Radiocarbon time series for a number of production wells in the original Jwaneng well field from 1983 to 1992. Lines are least squares fits

It is clear therefore that the figure for storage increases with increasing time scale. In the short-term (months) responses, the storativity applies. In the (partial) dewatering of the aquifer on the time scale of years an "effective" porosity or specific yield applies. For the recharge estimates using radiocarbon, the more appropriate factor appears to be storage represented by the total porosity. Implicitly included in the storage relevant to the isotope approach could well be the inferred reverse leakage from the aquitard.

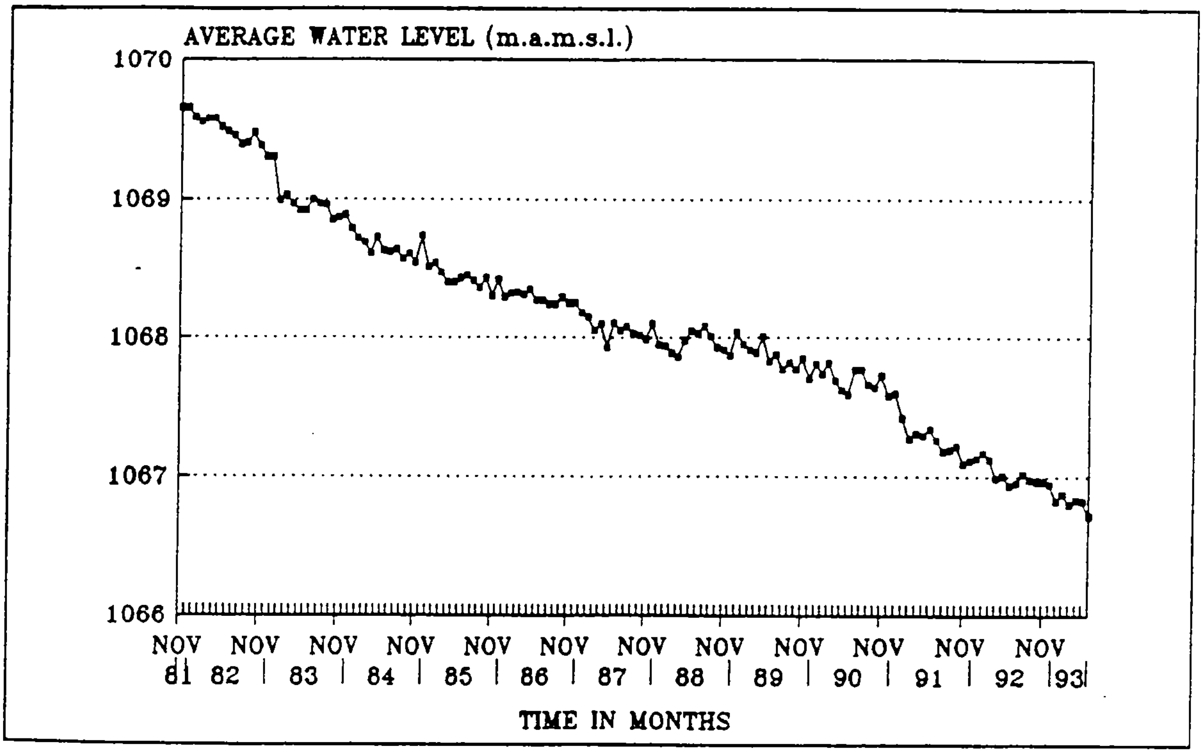

Fig. 5 Mean hydrograph for the Jwaneng well field for the period 1981 to 1993

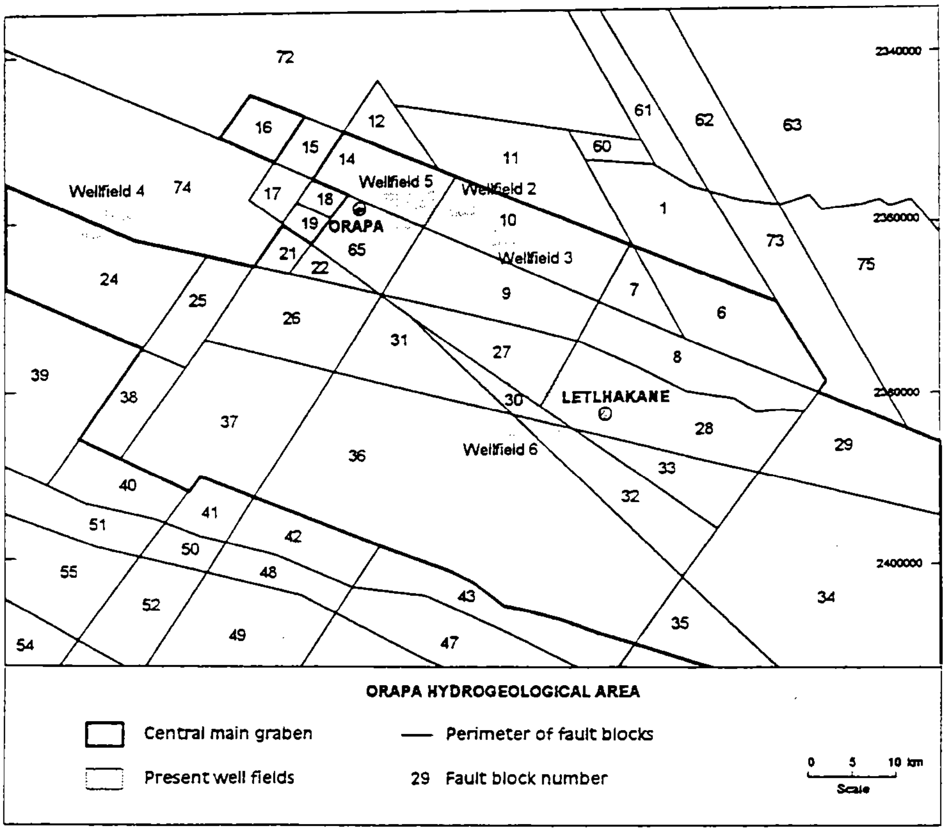

Fig. 6 Map showing the positions of Orapa mine well fields and major block faulting

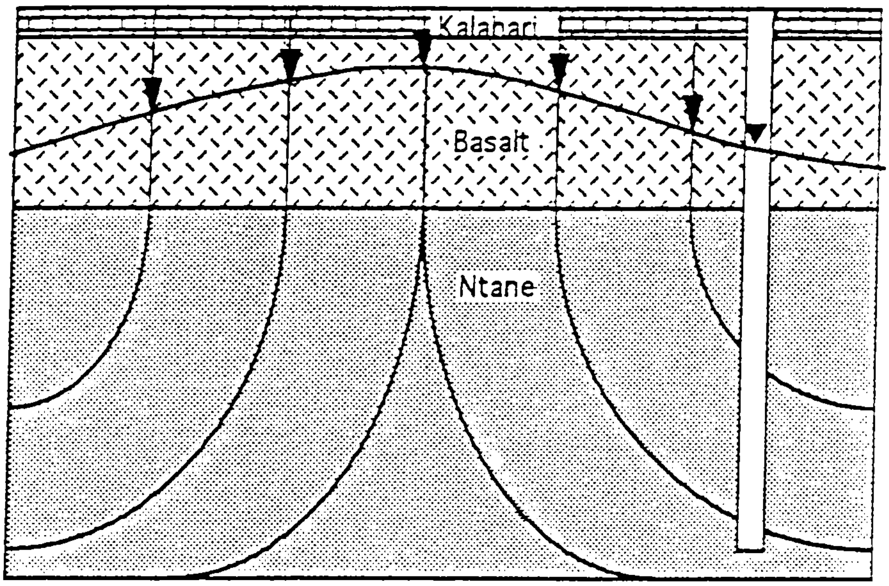

Fig. 7 Schematic model showing how recharge from local rainfall events passing through fractures in the basalt can produce a degree of age stratification in the underlying, confined sandstone aquifer

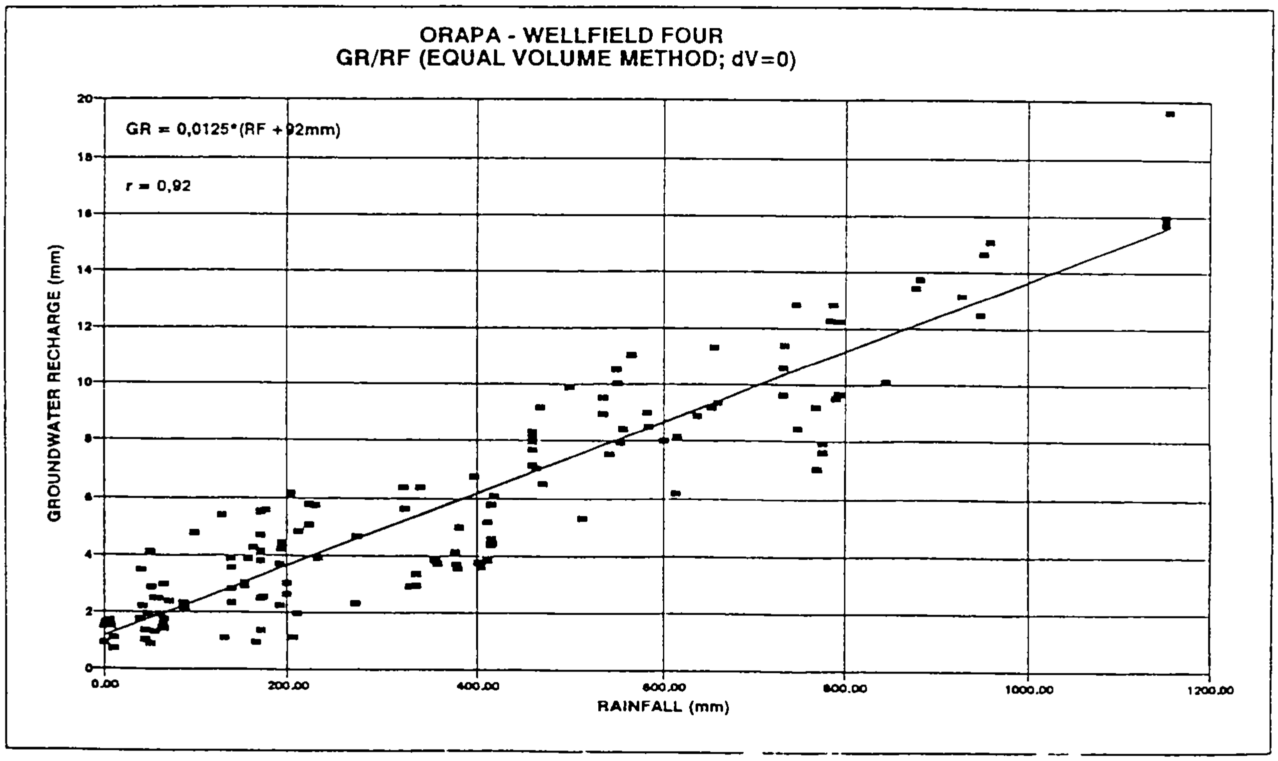

Fig. 8 Recharge calculated for equal volume periods read off a four-year hydrograph for well field 4, Orapa, plotted against total rainfall over the same periods.

5. ORAPA MINE WELL FIELDS

Various well fields were established to supply the Orapa diamond mine in northern Botswana since the latter sixties (Fig. 6). The fractured and jointed basalt cover (up to 80 m) confines the underlying Ntane sandstone aquifer locally, but allows widespread hydraulic connection between it and the shallow overlying Kalahari Beds aquifer, as seen in hydrographs. During exploitation, the sandstone aquifer shows confined behaviour. In the isotope approach, the system was treated as a multi-layer phreatic (i.e. diffusely recharged) aquifer, with rest levels in the basalt. Slow lateral ground water movement, under a regional piezometric gradient of 0.001 in the sandstone aquifer is further restricted on account of extensive block faulting and intrusion by diabase dykes. Radiocarbon values are found to lie in the range 1.3 - 45 pMC, with one outlier at 75 pMC. Only protracted pump tests were sampled in an attempt to reduce the localising effect of individual boreholes and transient mixtures [4].

Porosities ranging from 17 % to 30 % were measured on numerous borehole cores, with a mean of 22 %. The bulk fracture porosity of the basalt is unknown, but conservatively was taken as 2%. Recharge was calculated using radiocarbon data and the exponential model. Even in the absence of significant regional flow, age stratification can be produced by areally restricted discrete rain events (Fig. 7), which are likely to be the major recharge mechanism in the area [4]. Recharge values range from 0.6 to 2.4 mm a^{-1} with a single value of 21.5 mm a^{-1} for a well which intersected a major basalt fracture. Including this value a mean of 3.7 mm a^{-1} is obtained; eliminating the presumed outlier gives a mean of 1.1 mm a^{-1}.

Analysing more than 20 years of rest level and rainfall data, good simulations of piezometric level fluctuations could be achieved with cumulative rainfall departure methods, taking into account the abstraction from the well fields. With the equal volume method the saturated volume fluctuation data for one of the well fields provided recharge values which are plotted against corresponding integrated rainfall in Fig. 8. This gave (confined) storativities of 0.00022 to 0.00126 and recharge values of 2.7 mm a^{-1} to 5.8 mm a^{-1}.

Considering the uncertainties in parameters used in both the isotope and rest level fluctuation approaches, and the limited number (9) of documented isotope sampling points, a reasonable correspondence in the recharge figures was obtained.

Close on 30 years ago, when water management was still predicated on the principle of ground water mining, isotopic data had shown that significant recharge is occurring to the confined sandstone at Orapa. Recharge quantification on the basis of radiocarbon has now produced figures for recharge which are roughly compatible with, but lower than, obtained by the equal volume method. All the model parameters used effectively maximise the former. An explanation may be found in the low and probably heterogenous flow in the sandstone aquifer as seen in near-vanishing radiocarbon values obtained for some first-strikes at the basalt-sandstone contact. On the other hand, one borehole which intersected a basalt fissure gave a value of 75 pMC in the underlying sandstone.

Although the exercise has underlined the problem of an isotope assessment of recharge to a confined aquifer, the radiocarbon snapshot approach did produce realistic, if possibly conservative, recharge estimates.

6. PALLA ROAD WELL FIELD

As part of an investigation for the extension of an existing well field in eastern Botswana, isotope data was obtained from a number of existing and newly-drilled boreholes. The main aquifer is the aeolian Ntane sandstone, a fractured unit usually covered by basalt, and extensively block-faulted. In contrast with the previous two cases, the extensive study area of some 1650 km^2 has both a topographic and piezometric gradient of some 3 ‰. Ground water radiocarbon values, in many cases with measurable tritium, cover a wide range, with a preponderance of values between 65 pMC and 110 pMC (Fig. 9). Ground water flow is quite heterogenous. High radiocarbon values at depth in major fractures suggest substantial (natural) fracture flow. There is evidence also of substantial intergranular flow in major sandstone blocks.

Some 52 measurements of porosity were performed on a 142 m length of core of Ntane sandstone obtained from a single borehole. The mean value of porosity obtined is 0.012 with a standard deviation of 0.004. As at Orapa, the fracture porosity of the basalt is taken to be 2 %. Recharge was calculated only for those 24 boreholes with adequate lithological data giving a mean value of 6.6 mm a^{-1}. This value, higher than found at Jwaneng and Orapa, is ascribed to the more active topography-driven, lateral ground water transport.

Two independent recharge estimates were made [10]. The first was based on the chloride balance of ground water, which is justified in view of ongoing, regional flushing of the aquifers. Sampling sites were selected to ensure minimal contamination by intrusion of saline water from the deeper aquifers. With figures for rainfall and dry deposition of chloride (Beekman et al. [11]), chloride-based recharge values range from 4.5 mm a^{-1} to 8.5 mm a^{-1} with a mean of 5.9 mm a^{-1}. The second was made calculating the unsaturated zone chloride balance in a limited number of shallow (2 metre) soil profiles, from which recharge values in the range of 2 mm a^{-1} to 5 mm a^{-1} were determined. These values approximate, but are lower than, those obtained from radiocarbon measurements and the saturated zone. This could be further evidence that diffuse recharge tends to follow preferential flow paths.

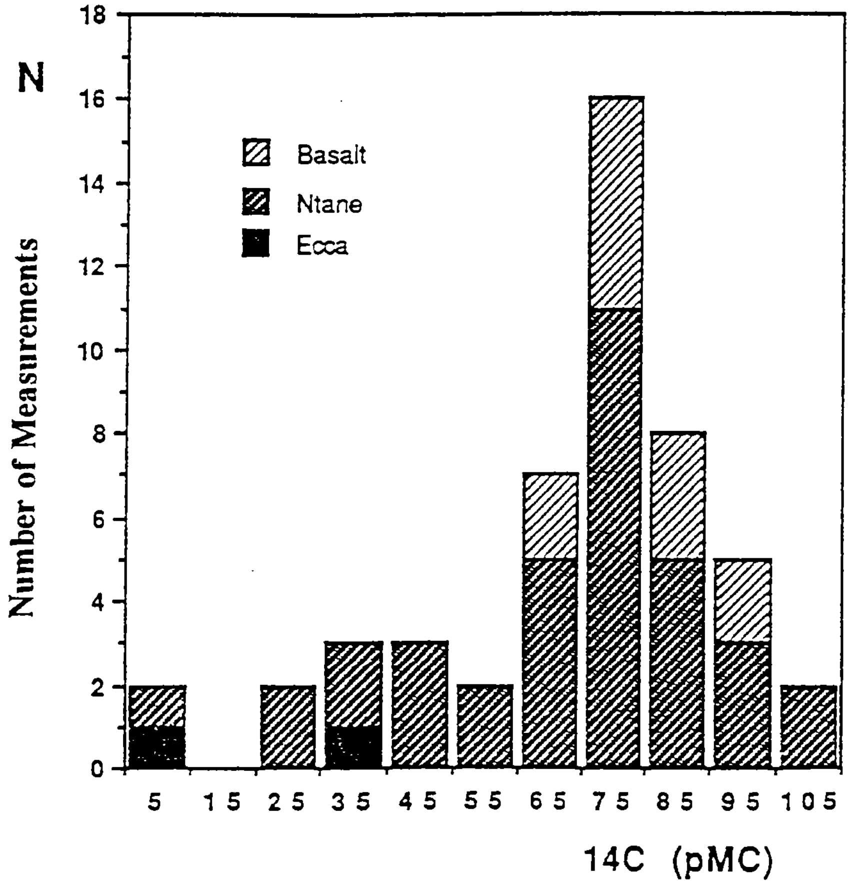

Fig. 9 Frequency histogram of radiocarbon values for Palla Road boreholes and their distribution in the three lithological units

7. DISCUSSION AND CONCLUSIONS

The problem of fractured porous aquifers addressed in this paper was theoretically treated by Zuber [4] in terms of micropore diffusion, which would give unrealistically high tracer-based mean residence times.

However, satisfactory correspondence was achieved between recharge figures obtained using a) the exponential model b) 85 % atmospheric for the initial or recharge value of radiocarbon c) the total porosity on the one hand and independent techniques in each of the three case studies on the other. These results, summarised in Table 1, lend weight to the approach taken in this study employing isotope-based recharge calculations. This approach seems to apply to the relatively higher residence times addressed with radiocarbon, where the assumption of the uniform labelling of all the water in the aquifer by the tracer appears to be justified. Whether this assumption would be valid for the much shorter time scales addressed with tritium is open to investigation.

The implication of these results for the aquifer behaviour of the fractured sandstones of the Kalahari is that on the time scales of radiocarbon, the transport through the matrix of the sandstone is sufficiently active to account for effectively all the tracer in the output of wells which often are located on fractures to enhance yield

TABLE 1

Comparison of isotope-based and independent assessments of recharge

Site	Isotope-based recharge assessment (mm/a)	Independent recharge assessment (mm/a)	Method of independent recharge assessment
Jwaneng well field	3.7 (SE) - 4.7 (NW)	3.0 - 4.9	Equal volume;Modified Hill
Orapa well field	3.7 (high); 1.1 (low)	2.7 - 5.8	Equal volume
Palla road well field	6.6 (mean)	5.9 (mean) 2.0 - 5.0	Cl balance, saturated zone Cl balance, unsaturated zone

Classical hydrograph methods of recharge assessment require many years of rest level observations, along with an appropriate choice of the storage factor. Unsaturated zone methods tend to underestimate recharge and evidence mounts of the importance of preferential flow. Restricted lateral ground water mobility, with resulting predominance of vertical water losses - common in this environment - may generate chloride values which again would provide unrealistically low recharge estimates.

This study has demonstrated that the concept of the "isotopic snapshot" can give a meaningful first estimate of recharge. Even where there are no direct measurements of aquifer porosity, an estimate based on general knowledge of the aquifer material can still provide a useful recharge value for management purposes.

REFERENCES

[1] LIBBY, W F Tritium in nature. Jnl Washington Acad. Sci. **45**, No.10 (1955) 301

[2] ZUBER, A “Mathematical models for the interpretation of environmental radioisotopes in groundwater systems” Handbook of Environmental Isotope Geochemistry (FRITZ, P and FONTES J Ch Eds) **2** (1986) 1

[3] VERHAGEN, B Th, GEYH, M A, FROEHLICH, K, WIRTH, K (1991) Isotope hydrological methods for the quantitative evaluation of cround water resources in semi-arid areas: Development of a Methodology . Research Reports of the Federal Ministry for Economic Cooperation of the Federal Republic of Germany, Bonn. 164pp. ISBN 3-8039-0352-1

[4] VERHAGEN, B Th, BREDENKAMP, D B, BOTHA, L (1999) Hydrogeological and isotopic assessment of the response of a fructured multi-layered aquifer to long term abstraction in a semi-arid environment. Final Report to the Water Research Commission: Project #K5/565.

[5] ZUBER, A "On calibration and validation of mathematical models for the interpretation of environmental tracer data in aquifers". Mathematical Models and Their Applications to Isotope Studies in Groundwater Hydrology. IAEA-TECDOC-777, Vienna (1994) 11

[6] VERHAGEN B Th "Environmental isotopes suggest a recharge model for the well field supplying Jwaneng Mine, Botswana". Isotope Techniques in Water Resources Development STVPUB/757, IAEA, Vienna. (1987) 771

[7] VERHAGEN B Th "Jwaneng Ground Water: An Isotopic Model" Procs Africa Needs Ground Water - An International Ground Water Convention. Johannesburg. **1** (1993) Paper 22

[8] MAZOR, E, VERHAGEN B Th, SELLSCHOP, J P F, JONES, M T, ROBINS, N E, HUTTON, L and JENNINGS, C M H Northern Kalahari groundwaters: hydrologic, isotopic and chemical studies at Orapa, Botswana. Jnl of Hydrology **34** (1977) 203

[9] VERHAGEN B Th and MORTON, K L "Environmental isotope measurements on ground water around Orapa mine in the northern Kalahari" Biennial Symposium: Ground Water and Mining, Johannesburg, (1989)

[10] WELLFIELD CONS. SERV. "Palla road groundwater resources investigation. Phase I" Wellfield/Interconsult Final Report to the Republic of Botswana, Department of Water Affairs (1994)

[11] BEEKMAN, H E, GIESKE, A S M and SELAOLO, E T GRES: Groundwater Recharge Studies in Botswana: 1987 - 1996. Botswana Jnl of Earth Sciences **3** (1996) 1.

[12] VERHAGEN B Th, MAZOR, E and SELLSCHOP, J P F Radiocarbon and tritium evidence for direct rain recharge to ground waters in the northern Kalahari. Nature **249**, No. 5458 (1974) 643

[13] FOSTER, S S D, BATH, A H, FARR, J L and LEWIS, W J The likelihood of active groundwater recharge in the Botswana Kalahari. Jnl of Hydrology **55** (1982) 113

[14] VAN RENSBURG, H J and BUSH, R A Jwaneng northern wellfield - modelling of groundwater flow with optimised management recommendations on wellfield utilization. Anglo American Corporation of South Africa Ltd. Report No. CED/029/04 (1994)

NOBLE GAS DATA FROM THE GREAT ARTESIAN BASIN PROVIDE A TEMPERATURE RECORD OF AUSTRALIA ON TIME SCALES OF 10^5 YEARS

U. BEYERLE, W. AESCHBACH-HERTIG, F. PEETERS, R. KIPFER
Environmental Physics,
Swiss Federal Institute of Technology (ETH)
and Swiss Federal Institute of Environmental Science and Technology (EAWAG),
Dübendorf, Switzerland

R. PURTSCHERT, B. LEHMANN, H.H. LOOSLI
Climate and Environmental Physics,
University of Bern,
Bern, Switzerland

A. LOVE
Primary Industries and Resources SA,
Adelaide, South Australia, Australia

Abstract

We report noble gas data from 13 artesian wells in the south-western part of the Great Artesian Basin (GAB) in Australia. Atmospheric noble gases dissolved in groundwater allow the past soil temperatures of the recharge area to be reconstructed and radiogenic noble gas abundances yield estimates of the groundwater residence time. All measured samples have large excesses of He relative to atmospheric solubility equilibrium. Radiogenic ^{4}He concentrations, which were calibrated against ^{81}Kr groundwater ages, yield groundwater residence times up to 550 kyr. The noble gas temperatures calculated from the atmospheric noble gas concentrations show clear fluctuations of the soil temperature in Australia during the last 550 kyr. These results suggest that the noble gas temperature method can be applied to reconstruct continental paleoclimate conditions on time scales up to a few hundred kyr.

1. INTRODUCTION

Two key processes control the abundance of the noble gases, helium (He), neon (Ne), argon (Ar), krypton (Kr) and xenon (Xe) in groundwaters: (1) the *dissolution of atmospheric noble gases*, and (2) the *accumulation of radiogenic noble gas isotopes*, that are produced in relation to nuclear disintegration of radioactive nuclides. Dissolution of atmospheric noble gases reflects the climatic conditions at the water table prevailing during groundwater recharge, i.e. the soil temperature. On the other hand the amount of radiogenic noble gases points at least roughly to the time passed since a water parcel entered a groundwater system. Hence, in principle, the presence of atmospheric and radiogenic noble gases in groundwaters provides a unique temperature record to reconstruct paleoclimate conditions in continental areas.

In contrast to surface waters, atmospheric noble gases in groundwaters are generally found to be in excess relative to the expected equilibrium. The processes responsible for the formation of this excess component still remain vague, although several studies show that the excess is of purely atmospheric origin (excess air) and has a similar elemental composition as atmospheric air [1-3]. Observed deviations from atmospheric composition have been interpreted in terms of elemental fractionation during non-equilibrium gas exchange at the groundwater table [4]. The concentrations of atmospheric noble gases are determined by the five parameters temperature, pressure, salinity, amount of excess air and possible fractionation. Since salinity and pressure (i.e. the altitude of the recharge area) at the water table are basically known, three free parameters remain. Recently new inverse models describing atmospheric gas dissolution in groundwater have been developed that determine the controlling parameters out of the measured noble gas concentrations using statistical optimisation routines [5, 6]. As soil temperature directly constrains atmospheric noble gas dissolution in groundwater [7], at present the noble gas method is the most quantitative approach to determine local paleotemperatures on continents. On large time scales well above the range accessable by ^{14}C groundwater dating, dispersive mixing may smooth gradients and might interfere with temperature determination using atmospheric noble gases. Noble gas temperatures (NGTs) derived from noble gases in groundwaters have up to now only been successfully used to reconstruct the temperature shift between the last ice age and the Holocene [4, 8-10].

We report noble gas data and NGTs from 13 artesian wells in the south-western part of the Great Artesian Basin (GAB) in Australia in order to explore whether the noble gas method can be applied on time scales up to several 10^5 years. Samples were taken in 1998 during two expeditions within an IAEA research program focusing on the application of new tracer methods in old groundwater systems. During the first expedition 4 wells were sampled towards the south-eastern tip of the investigated area, whereas the second expedition visited 9 wells located further north, along the presumed north-western direction of groundwater flow. Samples from the first expedition (labeled with #1 to #4 in Figs. 1, 2 and 3) were taken from locations that are not necessarily interconnected hydraulically, especially sample #1 seems to originate from a different groundwater horizon of the GAB system. ^{81}Kr activity was analysed in all 4 samples of the first expedition to determine the local groundwater residence time [11].

2. RESULTS

2.1. Noble gases

All measured samples have large excesses of He relative to atmospheric solubility equilibrium. The He concentrations tend to increase along supposed groundwater flow lines. Concentrations reaching up to 10^{-4} cm^3STP/g (Fig. 1) are generally higher in the central part of the investigated area whereas lower concentrations are found closer towards the edge. Due to excess air Ne is supersaturated up to 100% relative to the expected atmospheric equilibrium. Interestingly, the Ne excess (as measure of the excess air component) decreases systematically with rising He concentrations. In some sample the noble gas abundance of the excess air component is not equal to the elemental composition of atmospheric air. However, the concentrations of atmospheric noble gases (Ne, ^{36}Ar, Kr and Xe) can be translated to noble gas temperatures (NGTs) in a statistically significant way, if re-equilibration between dissolved noble gases and trapped soil air is assumed [12]. Generally, the calculated NGTs reflecting the water temperature during recharge are higher than the regional recent annual mean air temperature of 22°C (Fig. 1). NGTs reach a first maximum of about 26°C at a ^4He concentration of $4 \cdot 10^{-5}$ cm^3STP/g. As He concentrations increase further to $8 \cdot 10^{-5}$ cm^3STP/g NGTs drop to a temperature minimum. At even higher ^4He concentrations NGTs rise again. If He concentrations are interpreted as qualitative estimates of groundwater age, NGTs seem to indicate at least two climatic cycles with a maximum temperature shift of about 4°C (Fig. 1).

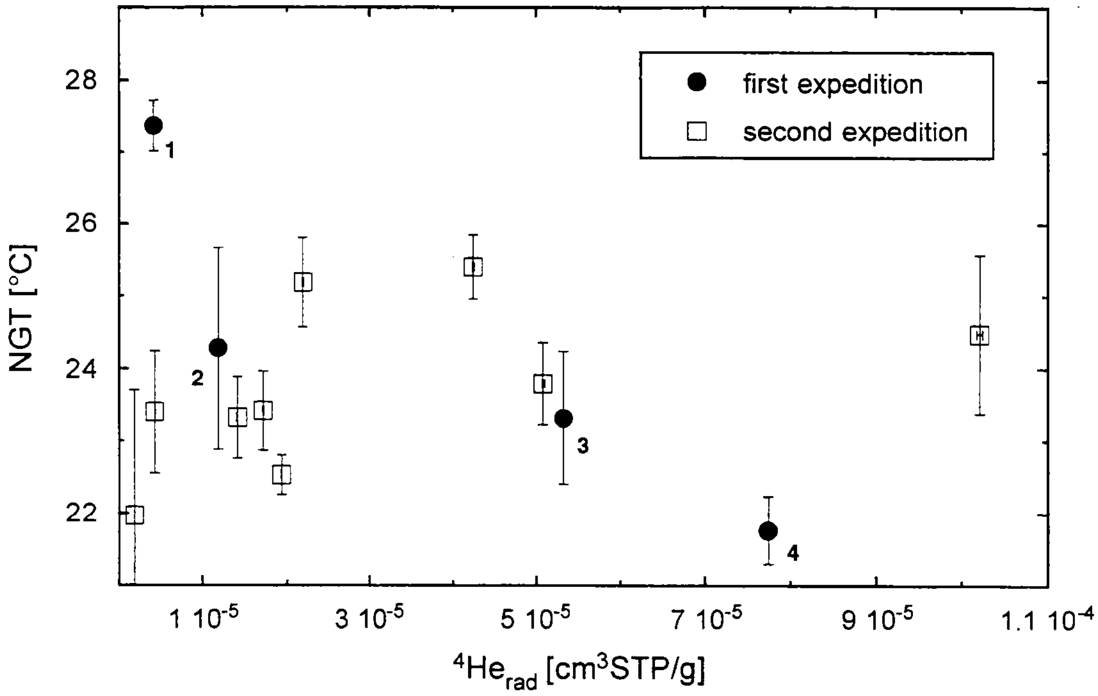

FIG. 1. Noble gas temperature (NGT) calculated from dissolved atmospheric noble gases plotted against the radiogenic ^{4}He concentration.

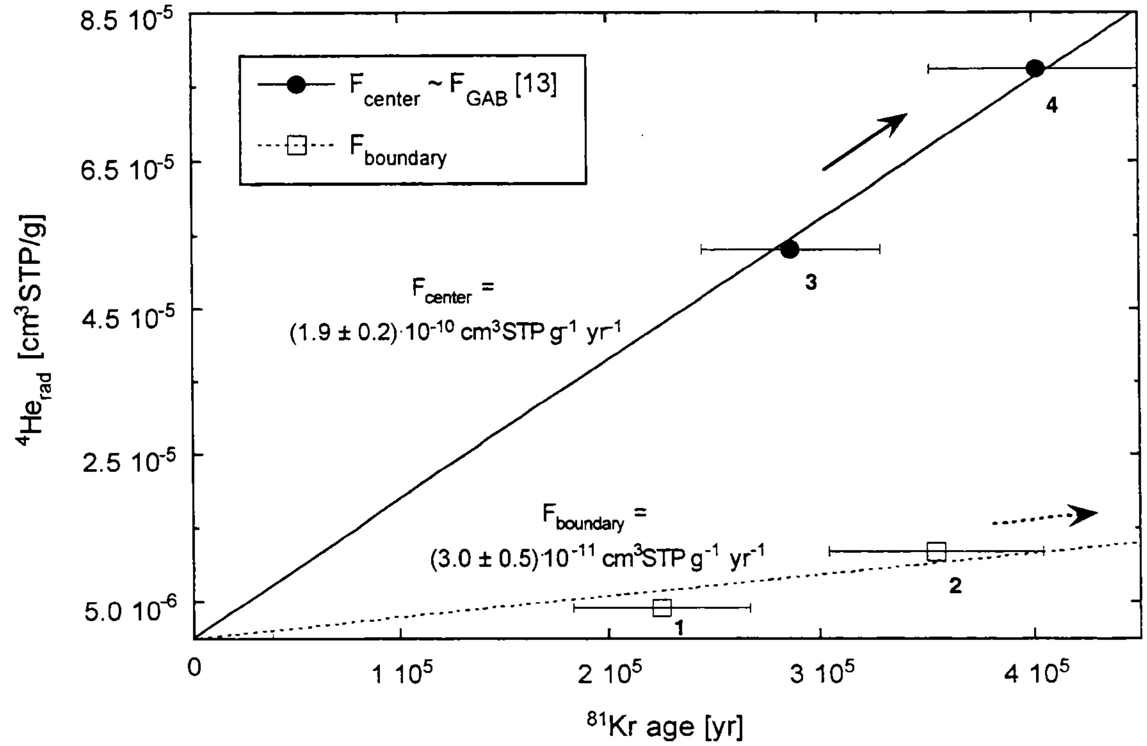

FIG. 2. Accumulation rates of radiogenic ^{4}He.

3. DISCUSSION

3.1. Radiogenic ^{4}He and ^{81}Kr ages

Since ^{81}Kr groundwater ages are available for the four samples of the first expedition [11] they can be used to convert the measured ^{4}He concentrations into ^{4}He accumulation rates by dividing the ^{4}He concentration by the ^{81}Kr groundwater age (Fig. 2). All ^{81}Kr dated groundwater samples have water ages in the range between 200 and 400 kyr. Although the ^{81}Kr water ages vary only within a factor of two, the measured ^{4}He concentrations cover an order of magnitude, indicating that the ^{4}He accumulation rate is not homogeneous. The four samples form two clusters with different ^{4}He accumulation rates. Samples #3 and #4 from the center of the investigated area accumulate ^{4}He at a rate F_{center} of $(1.9 \pm 0.2)\cdot 10^{-10}$ $cm^3STP\cdot g^{-1}\cdot yr^{-1}$, whereas towards the western boundary (#1 and #2) the ^{4}He accumulation rate $F_{boundery}$ of $(3.0 \pm 0.5)\cdot 10^{-11}$ $cm^3STP\cdot g^{-1}\cdot yr^{-1}$ is about 6 times smaller (Fig. 2). The higher accumulation rate agrees within 30% with published estimates on the ^{4}He accumulation rate of the central region of the GAB [13]. The lower accumulation rate is one order of magnitude lower than previous estimates but still exceeds the in situ ^{4}He production of the GAB aquifers by almost a factor of 10 [13]. Whether our results reflect real differences of ^{4}He accumulation rates or whether the differences measure geological and/or geometrical heterogeneities of the GAB aquifer setting remains open and demands further investigations.

Since there are indications that at least one sample (#1) most probably does not originate from the same aquifer horizon as samples #3 and #4. Therefore and as the higher accumulation rate agrees with the characteristic GAB rate, we prefer to use the higher ^{4}He accumulation rate F_{center} to convert He concentrations into '^{4}He ages' (see Fig. 3). Although such a rough approach must be regarded as preliminary and hence the deduced '^{4}He ages' remain highly speculative guesses about the water residence time, the ^{4}He concentrations are the best age indicators for those water samples that have not been dated by means of ^{81}Kr. If the measured ^{4}He concentrations are interpreted as 'semi quantitative' ages the water samples from the investigated site have residence times up to 550 kyr (Fig. 3).

3.2. Noble Gas Temperatures (NGTs)

To our knowledge for the first time atmospheric noble gas concentrations were measured in GAB groundwaters that can be used to reconstruct significant average soil temperatures prevailing during groundwater recharge. Compared to former studies reporting in situ water temperatures up to the boiling point it is noticeable that the observed in situ groundwater temperatures of the investigated area are below 60°C. The successful NGT determination proves that the GAB aquifer system in principle provides a most valuable groundwater archive to reconstruct temperature evolution of the Australian continent, if the groundwater temperatures are low enough to prevent water samples from degassing during sampling.

It is evident that the aforementioned transformation of the measured ^{4}He concentrations into qualitative '^{4}He water ages' does not change the intrinsic temporal structure of the NGT record because the '^{4}He ages' are directly proportional to the determined ^{4}He accumulation rate, i.e. the individual ^{4}He abundances and ^{81}Kr ages of sample #3 and #4. Only samples #1 and #2 are shifted because their real groundwater ages as determined by their ^{81}Kr activity are much larger than the deduced '^{4}He ages' since these 'edge' samples seem to accumulate ^{4}He at a much smaller rate than 'common' GAB waters. The three samples (#2, #3 and #4) that have been dated by ^{81}Kr and which seem to originate from the same aquifer level (#1 is excluded from further discussion

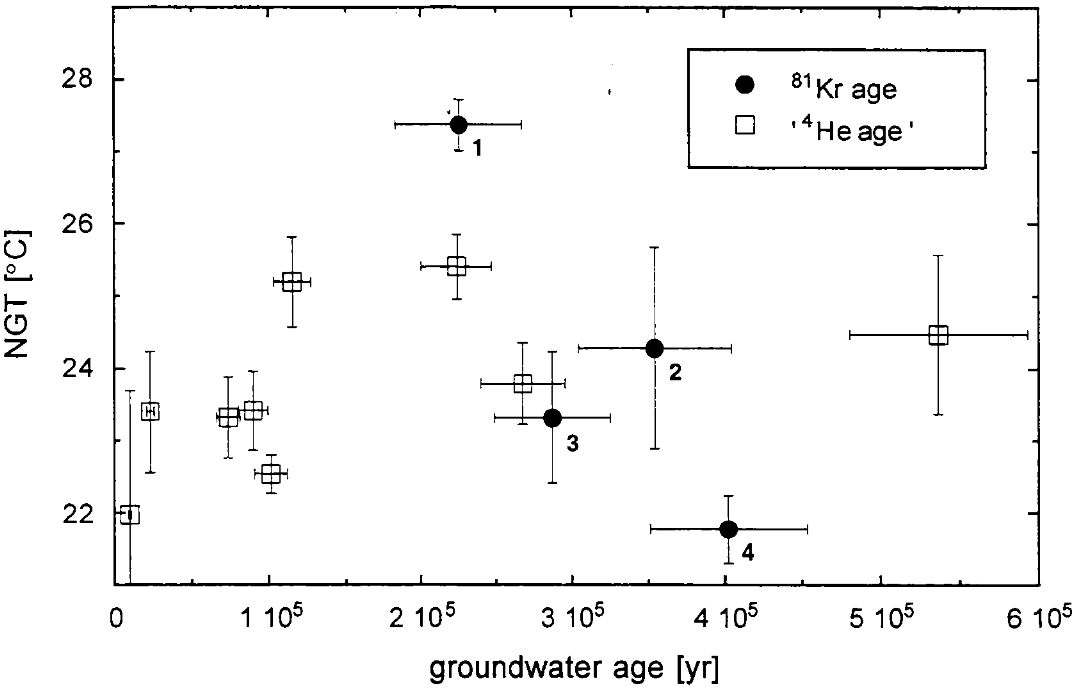

FIG. 3. Noble gas temperature (NGT) fluctuations of Australia as probed by concentrations of atmospheric noble gases during the last 600 kyr. The error of the calculated '^{4}He age' does not take into account large scale variations in the ^{4}He flux (see text for further explanations).

due to its different origin) mark a trend of NGT warming between 400 and 200 kyr before present (Fig. 3). The same warming phase was already present in the ^{4}He record at a concentration range between $4 \cdot 10^{-5}$ and $8 \cdot 10^{-5}$ cm^{3}STP/g (Fig. 1). The well dated samples follow basically the same tendency as the whole ensemble and hence pronounce the intrinsic structure of the temperature record. This fact adds some confidence to the attempt to interpret ^{4}He concentrations as measures for groundwater residence times.

However, since no recent groundwater samples were measured (i.e. samples containing no or only negligible radiogenic ^{4}He) the relations between calculated noble gas temperatures, soil temperatures and atmospheric temperatures remain unknown. It would be highly desirable to take groundwater samples near the recharge area in a future sampling expedition in order to calibrate the noble gas temperature record against the recent temperature conditions.

Temperature proxies with high temporal resolution, such as $\delta^{18}O$ records from marine foraminifera or from ice cores, report for the last 400 kyr 4 large climatic cycles during which the temperatures changed between warm interglacial and cold glacial conditions [14]. The time resolution of our GAB record is much too coarse that the presence of single glacial-interglacial cycles on the Australian continent could be proven. On the other hand the bottom line is that atmospheric noble gas data indicate significant temperature variations within central Australia during the last 600 kyr although at present the marginal time resolution prevents any assessment of the climatic dynamics and/or its rate of change.

4. CONCLUSIONS

We report noble gas concentrations from 13 artesian groundwater wells located in the south-western part of the Great Artesian Basin of Australia.

(1) The in situ groundwater temperatures are below 60°C and hence are much colder than temperatures reported in former studies. The low temperatures prevent (noble) gases from degassing during sampling. The received noble gas data finally allow interpretation of the atmospheric noble gas concentrations in terms of climatic conditions prevailing during recharge and interpretation of the radiogenic ^{4}He concentration in terms of qualitative groundwater ages.

(2) All samples have large ^{4}He excesses that generally tend to increase in direction of a supposed groundwater flow towards the central part of the investigated area. ^{81}Kr water ages [11] prove that radiogenic noble gases do not accumulate at equal rates inside the area. The central ^{4}He accumulation rate of $(1.9 \pm 0.2)\cdot 10^{-10}$ cm^{3}STP$\cdot$g$^{-1}\cdot$yr^{-1} agrees within 30% with previous estimates of GAB He accumulation whereas towards the western boundary ^{4}He accumulates much slower ($(3.0 \pm 0.5)\cdot 10^{-11}$ cm^{3}STP$\cdot$g$^{-1}\cdot$yr^{-1}).

(3) If ^{4}He concentrations are interpreted as measures of the groundwater residence times the reported record spans a time range up to 550 kyr. Our results indicate that the time frame for which atmospheric noble gas concentrations reliably show soil temperatures can be expanded up to a few hundreds kyr in those cases where groundwater ages can reasonably be estimated. Although caution has to be exercised in drawing final conclusions the NGTs attest for Australia at least two climatic cycles over the last 550 kyr during which soil temperatures fluctuated by at least 4°C.

REFERENCES

[1] HEATON, T.H.E., VOGEL, J.C., "Excess air" in groundwater, J. Hydrol. **50** (1981) 201-216.

[2] HIRT, M., et al., Too much air in ground water?, Journal of Conference Abstracts **1** (1996) 259.

[3] BEYERLE, U., et al., Infiltration of river water to a shallow aquifer investigated with ^{3}H/^{3}He, noble gases and CFCs, J. Hydrol. (submitted).

[4] STUTE, M., et al., Cooling of tropical Brazil (5°C) during the Last Glacial Maximum, Science **269** (1995) 379-383.

[5] BALLENTINE, C.J., HALL, C.M., A non-linear inverse technique for calculating paleotemperature and other variables using noble gas concentrations in groundwater: The Last Glacial Maximum in the continental tropics re-examined, in Goldschmidt Conference, Toulouse (1998).

[6] AESCHBACH-HERTIG, W., et al., Interpretation of dissolved atmospheric noble gases in natural waters, Water Resour. Res. (in press).

[7] STUTE, M., SONNTAG, C., Paleotemperatures derived from noble gases dissolved in groundwater and in relation to soil temperature, in Isotopes of noble gases as tracers in environmental studies, IAEA, Vienna (1992) 111-122.

[8] BEYERLE, U., et al., Climate and groundwater recharge during the last glaciation in an ice-covered region, Science **282** (1998) 731-734.

[9] STUTE, M., et al., A 30'000 yr continental paleotemperature record derived from noble gases dissolved in groundwater from the San Juan Basin, New Mexico, Quatern. Res. **43** (1995) 209-220.

[10] STUTE, M., et. al., Paleotemperatures in the Southwestern United States derived from noble gases in ground water, Science **256** (1992) 1000-1003.

[11] COLLON, P. et al., Development of Accelerator Mass Spectrometry (AMS) for the detection of ^{81}Kr and first application to groundwater dating, these Proceedings.

[12] AESCHBACH-HERTIG, W., KIPFER, R., Neue Ansätze zur Interpretation von Edelgasen in Wasser, 63. Physikertagung DPG, Heidelberg (1999) 490.

[13] TORGERSEN, T., CLARKE, W.B., Helium accumulation in groundwater, I: An evaluation of sources and the continental flux of crustal ^{4}He in the Great Artesian Basin, Australia, Geochim. Cosmochim. Acta, **49** (1985) 1211-1218.

[14] ROHLING, E.J., et al., Magnitudes of sea-level lowstands of the past 500,000 years, Nature **394** (1998) 162-165.

IMPORTANCE OF ISOTOPE HYDROLOGY TECHNIQUES IN WATER RESOURCES MANAGEMENT: A CASE STUDY OF THE MAKUTUPORA BASIN IN TANZANIA

Senguji, FH
Water Resources Division,
Ministry of Water,
The United Republic of Tanzania

Abstract

Makutupora groundwater basin has been the main source of water supply for Dodoma town since 1950s. the water is mainly used for domestic water supply to over one million inhabitants, for industrial purposes and livestock watering.

Conventional hydrogeological investigations have been carried out in the basin to gather information on the groundwater potential of the basin to meet the ever-increasing demand for water. However, firm conclusions could not be reached with conventional methods.

This paper highlights on the isotope techniques applied in an integrated manner with conventional hydrogeological methods to study the groundwater regime of the Makutupora basin. Results of isotope techniques have provided adequate information on recharge locations, recharge rates and age of groundwater in the basin, that is very important and open up prospects for further investigations using isotope techniques.

The ongoing investigation in the basin regarding pollution and depletion of the groundwater resource, has not succeeded in defining specific pumping limits or groundwater protection zones. Isotope data are sought to provide a clear basis for regulatory and future groundwater management in the Makutupora basin.

1. INTRODUCTION

1.1 Background

Makutupora groundwater is located in Dodoma region (Central Tanzania) about 27km North of the centre for Dodoma town. The basin is lying about 1100m above mean sea level and it extends approximately 25 km NE to SW direction. The basin has a width of about 5 – 8 km.

Makutupora basin is the main source of water for Dodoma town, which is supposed to be the National Capital. The water is mainly used for domestic water supply to over one million inhabitants, for industrial purposes and livestock watering.

Precipitation is the sole source of natural recharge to the basin. Precipitation recharge to the flow systems is estimated to be on average about 15% of the rainfall (Shindo, 1988). The average mean annual precipitation in the region is about 550 mm. The mean annual evaporation is estimated at 2500 km.

The main aquifer system of the basin is fractured and/or weathered basement rocks.

1.2 History of Investigation

The history of groundwater investigation in the Makutupora basin falls in four phases (Shindo, 1988), beginning in 1950s when the Water Development Department drilled one borehole. Following the satisfactory performance of this borehole, a program for further investigation was outline in collaboration with the Geological Survey and Public Works.

The second phase earmarks extensive geological and geophysical surveys carried out by the then Water Development and Irrigation Department. In this phase several exploratory boreholes were drilled to confirm geophysical information and determine hydraulic gradients and flow directions. Some of these boreholes were in later years successfully used as production wells.

The third phase of investigation coincided with the Government decision to transfer the National Capital to Dodoma. The then Ministry of Water Development and Power undertook detailed and exhaustive study of the basin primarily applying conventional hydrogeological techniques to assess the availability of adequate water to meet the requirements for the new capital. As a result of these investigations, 23 production boreholes were drilled in the basin. Concurrently with the third phase, an environmental isotope study was carried out by Mr.T.Dincer (IAEA) to identity recharge area, estimate annual recharge and age of the groundwater.

The fourth investigation phase was the Japan – Tanzania research study (1988 – 1992) which focused on the following issues:-

- recharge mechanism in the basin
- safe yield condition of the basin
- possibility of artificial recharge to the basin.

In this phase, an intensive analysis of stable isotope composition and tritium concentration was carried out. This paper is based on the analyses and results of isotope techniques applied in this phase of investigation.

1.3 Current Trend

The ongoing investigation activities in the basin include water level observations and water quality monitoring. There are 12 observation wells out of which 10 are fitted with automatic water level recorders. Water samples for quality analysis are continuously being collected (for hydrochemistry and biological analyses).

Recent data show that, with the current groundwater management practices in the basin, the abstraction rate is expected to exceed natural recharge rate in the near future (Senguji, 1997). This will lead to a potential problem of groundwater depletion in the basin. Data already indicate that, water level in some of the boreholes have declined to about 3-5 m in below their normal piezometric levels.

These data further show that, the water quality in some of the boreholes is deteriorating. The nitrate values have increased from33 mg/l in 1988 to 135 mg/l in 1993 (above the 100mg/l Tanzania temporary standards). Also, samples taken in June, 1997 show that in some of the boreholes, bacteria levels range from 13 coliform/100 ml to TNTC (Too Numerous To Count Level).

2. HYDROGEOLOGIC SETTING

The hydrogeology of the basin is determined by the geology, which in turn determines both aquifer characteristics and to a large extent aquifer boundaries. These components and the resulting groundwater flow regime are discussed in this section.

2.1 Geology

Makutupora basin is located at the most Southern part of the Gregory Rift Valley system (S.R.Harpum, 1970) and is characterized by the presence of tilted fault blocks trending in the ENE – WSW direction, horsts and graben structures. The Mlemu fault is the major one in the basin.

The basin is underlain by the Precambrian crystalline basement rocks mainly granite and gneiss. Bedrock crops out at different areas in the basin. Most of the basin floor is covered by Mbuga clay. The remaining part of the basin is covered by silty and sandy soils, and other detrital deposits derived from granitic rocks.

The basement rocks in the basin are highly fractured especially along the faults. The basement is overlain by coarse weathered materials derived from the granitic basement rocks, and near faults, horn blend gneiss and pegmatites of the basement rocks are fractured. The fractured and/or weathered basement rocks form the principal aquifer in the basin.

From lithologic data, calcrete over lies the weathered material at the centre of the Makutupora swamp; and where no calcrete develops, a layer of fluvial sand replaces the position of calcrete. A layer of grayish – white clay overlies the calcrete or sand layer. In large part of the basin, this layer directly lies over the fractured rocks and it is considered as the main layer which confines the groundwater in weathered/fractured rock aquifer. Then the Mbuga clay covers the swamp. Figure1.1 shows a schematic view (block diagram) of the subsurface geology of the Makutupora swamp.

2.2 Aquifer Characteristics and Boundaries

Groundwater in the basin occurs in the weathered and/or fractured basement rocks and the aquifer is confined. The bedrock surface forms the lower boundary and clay forms the upper boundary. The aquifer is found at an average depth of about 120m to which most of the production wells are drilled. However, some few wells go as deep as 200m. Based on lithological data, the thickness of the principal aquifer varies between 30m and 100m.

Results of pumping test conducted in 1988 show that transmissivity of the confined aquifer is about 500 m^2/day. The pumping wells are located along the direction of the Mlemu fault (Figure1.2); therefore it is assumed that, the transmissivity values represent that of the fractured rock aquifer.

2.3 Potentiometric Surface and Groundwater Flow

A number of observation boreholes are being used to monitor daily groundwater level changes. Seasonal fluctuations in water levels are evident. The groundwater level fluctuations in the basin are greatly influenced by long term variations of rainfall and pumpage.

A groundwater flow modeling study in the basin carried out in 1997 confirmed the two distinct groundwater flow patterns in the basin; the general North-eastward flow along the long axis of the basin and the branch flow from the North. The flows seem to converge at the outlet of the basin. Shindo (1988) termed the flow systems as Regional and Local. Groundwater discharges to the little Kinyasungwe River, which is the major surface water drainage from the basin. The river discharges its water into the Hombolo lake.

2.4 Groundwater Pumpage

Nine (9) supply wells fall in the Makutupora basin well field. The 1997 groundwater flow modeling study revealed that, in the South – Western part of the basin where about 60% of the total pumpage in the basin comes from, there is a decline in water level of about 5m. The study shows a future trend of continuing decline in piezometric water levels in the basin if high pumping rates are maintained. At present 30,000 m^3/day is pumped from the basin. The target is 50,000 m^3/day.

3. EFFECTS OF SIMULATED GROUNDWATER PUMPING AND RECHARGE ON GROUNDWATER FLOW IN THE MAKUTUPORA BASIN.

A two-dimensional areal flow model has been developed for the basin to simulate numerically at a field scale the effects of groundwater pumping in the basin.

The calibrated model was used to simulate future groundwater levels based on projected average daily pumping rates for 2010. The result of simulations made with the model provides preliminary estimate of the effects of groundwater pumping to the flow systems. The results revealed that, with substantial increases in pumping time, the average model-calculated decline in heads in the flow cells reached 5-10m especially at the well field. This decline is of remarkable effect to the depletion of the groundwater resource in the basin. Application of artificial recharge to the basin may be necessary. Although the restrictive assumption of the two dimensional, steady state areal flow model must be kept in mind when interpreting the simulation results, this flow model may save as a starting point for more detailed investigation including the use of isotope data. The model can later be used to identify sources of pollutants, simulate transport of the pollutants predict further evolution of the pollutants in the basin by using isotope techniques. The model can also be used to study the probability of applying artificial recharge to the basin. Isotope data can on the other hand be used to validate the model.

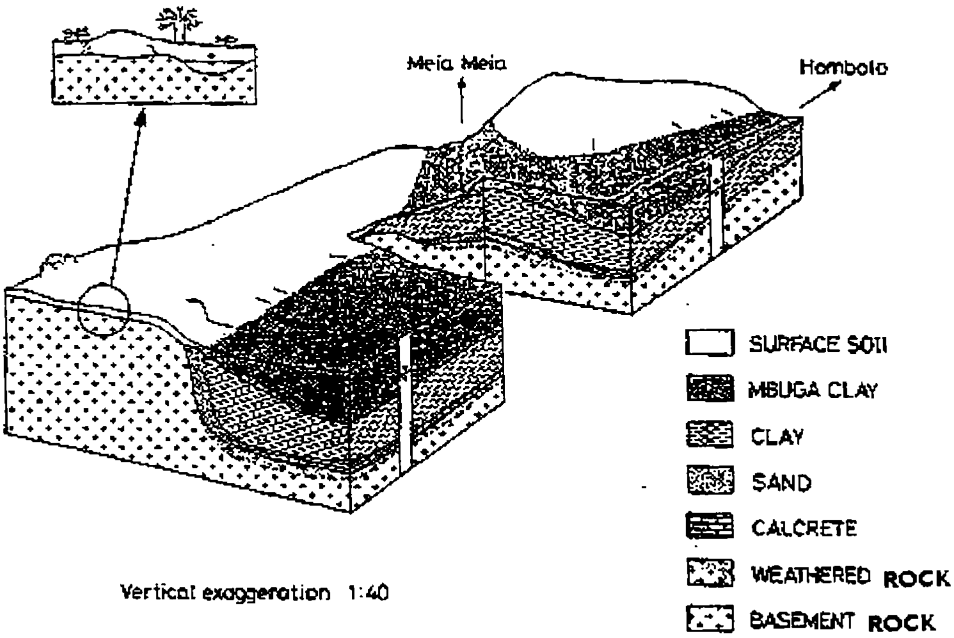

FIGURE 1.1 Schematic view of topography and geology of the Makutapora swamp

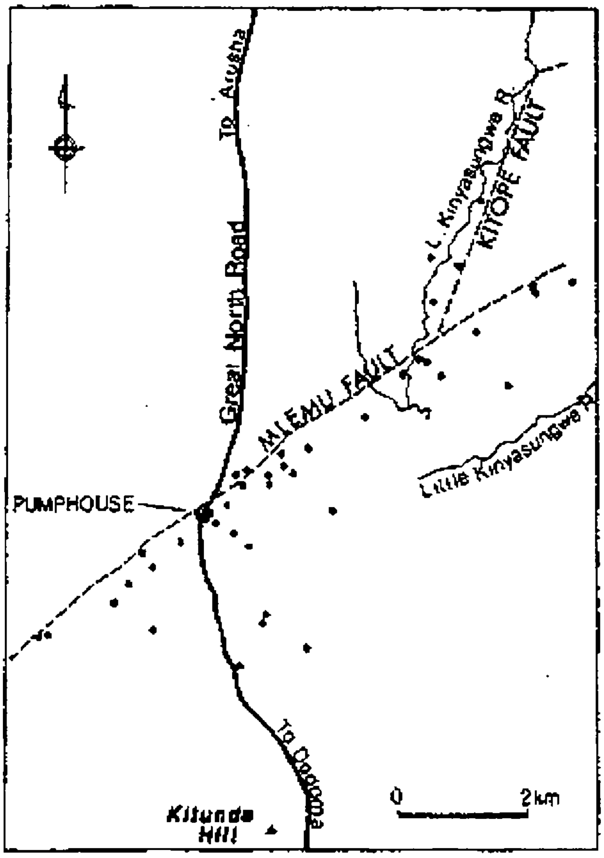

FIGURE 1.2 Fault system and distribution of boreholes in Makutapora basin

4. APPLICATION OF ISOTOPE TECHNIQUES IN THE MAKUTUPORA BASIN

Stable isotopic composition of hydrogen and oxygen and tritium concentrations were described by Shindo et al (1990/1991) and Hayashi (1990). Samples of confined Groundwater, shallow groundwater, rainwater, surface water and soil water were collected for chemical and isotope analyses. In 1990 a total of 148 water samples were analyzed for hydrogen and oxygen stable isotope compositions. In 1991 a total of 123 natural water samples were collected for the isotopic analysis and a total of 38 water samples for tritium analyses.

Confined groundwater was sampled by pumping and by a water sampler. Shallow groundwater and surface water were sampled using simple procedures while a soil water sampler sampled soil water. A rainfall collector collected Rainwater.
All stable isotope composition and tritium concentration analyses were conducted in Japan . D/H ratio was measured by mass spectrometer with uranium and zinc metals reduction techniques. $^{18}O/^{16}O$ ratio was measured by mass spectrometer with standard $Co_2.H_2O$ equilibration technique. Tritium was measured by liquid Scintillation counter. (Shindo, 1990).

4.1 STABLE ISOTOPIC COMPOSITION ANALYSIS

Measurement results of stable isotopic composition of hydrogen and oxygen are shown in Table 1 and Figure2. The results of the measurements are expressed in δ units relative to SMOW. The local meteoric line is derived from the relationship:

$D = 8.19\delta^{18}0 + 15.3$ (Shindo, 1990).

In the 1991 analysis the meteoric line changed to:

$D = 7.8\,\delta^{18}0 + 16.6.$ (Shindo, 1991)

4.2 RESULTS

4.2.1 Rain water

The changing trend of oxygen -18 for rainwater is influenced by rainfall intensity. However, the changes could also be attributed to passage of air masses with different isotopic composition.

4.2.2 Surface Water

The stable isotope composition of surface water is shown in Figure 2. The measurement indicate that, isotopic composition of rivers and overland flow closely follow the local meteoric line compared to that for Hombolo lake which largely deviate from the meteoric line. This deviation can be attributed to evaporative concentration and rainfall distribution characteristics in the basin.

4.2.3 Soil Water

Soil water was mainly collected at 220cm depth from January to February. It is noted that even those samples with high $\delta^{18}0$ value of pre-rainy season water do not deviate much from the local meteoric line. This shows that, the evaporation from the soil during dry seasons is an equilibrium process. That is, the type of water transported from the near surface influences the isotopic composition of soil water.

4.2.4 Groundwater

Groundwater is classified into shallow and confined groundwater. Figures 2 and 2.1 show the stable isotopic composition of groundwater. The variations in the isotope composition may be attributed to altitude effect and rainfall input. From the measurements two types of confined groundwater were distinguished.

4.3 TRITIUM CONCENTRATION ANALYSIS

Measured tritium concentration in groundwater was compared with the concentration in the part rains recorded at the nearest station. Table 2 shows concentration of tritium in groundwater in the Makutupora swamp. The tritium concentration is expressed in Tritium Unit (T.U) which is equivalent to 1 T atom per 10^{18} H atoms. (Shindo, 990). The tritium concentration analysis was also used to study the turn over time (or the mean residence time) of groundwater in the Makutupora basin.

4.4 RESULTS

Tritium concentration is shallow groundwater from dug wells, hand pump wells and springs range between 2.4 to 5.2 T U, whereas deep waters from boreholes drilled to the fractured bedrock range between 0.3 to 3.2 T.U. The tritium concentration values are relatively low. This may be attributed partly to low tritium levels in precipitation in the region and partly to longer residence times of water in the groundwater system because of low recharge rates in the semi-arid environment of Makutupora basin. The tritium levels of deep waters are obviously lower than those of the shallow waters, suggesting that the deep groundwater in the fractured rock aquifers is older than the shallow groundwater.

Mean residence time studies show that, the major part of the shallow groundwater is in a turn over time range of about 60y, where as most of the deep waters are in the range of more than 60y. Figure 4.3 shows the relationship between tritium concentration and turn over time in 1990 based on the exponential model. The tritium concentration analysis was further used to deduce age of groundwater in the basin.

The results of the residence time of groundwater inferred from the tritium analysis can be used as a useful indicator for water circulation rates in the shallow and the deep fractured systems in the basin.

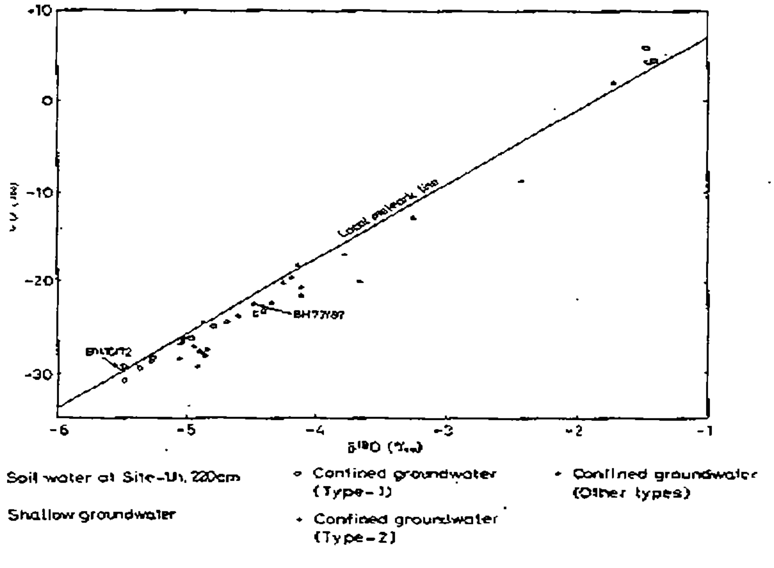

FIG.2.1 Stable Isotope Composition of Groundwater

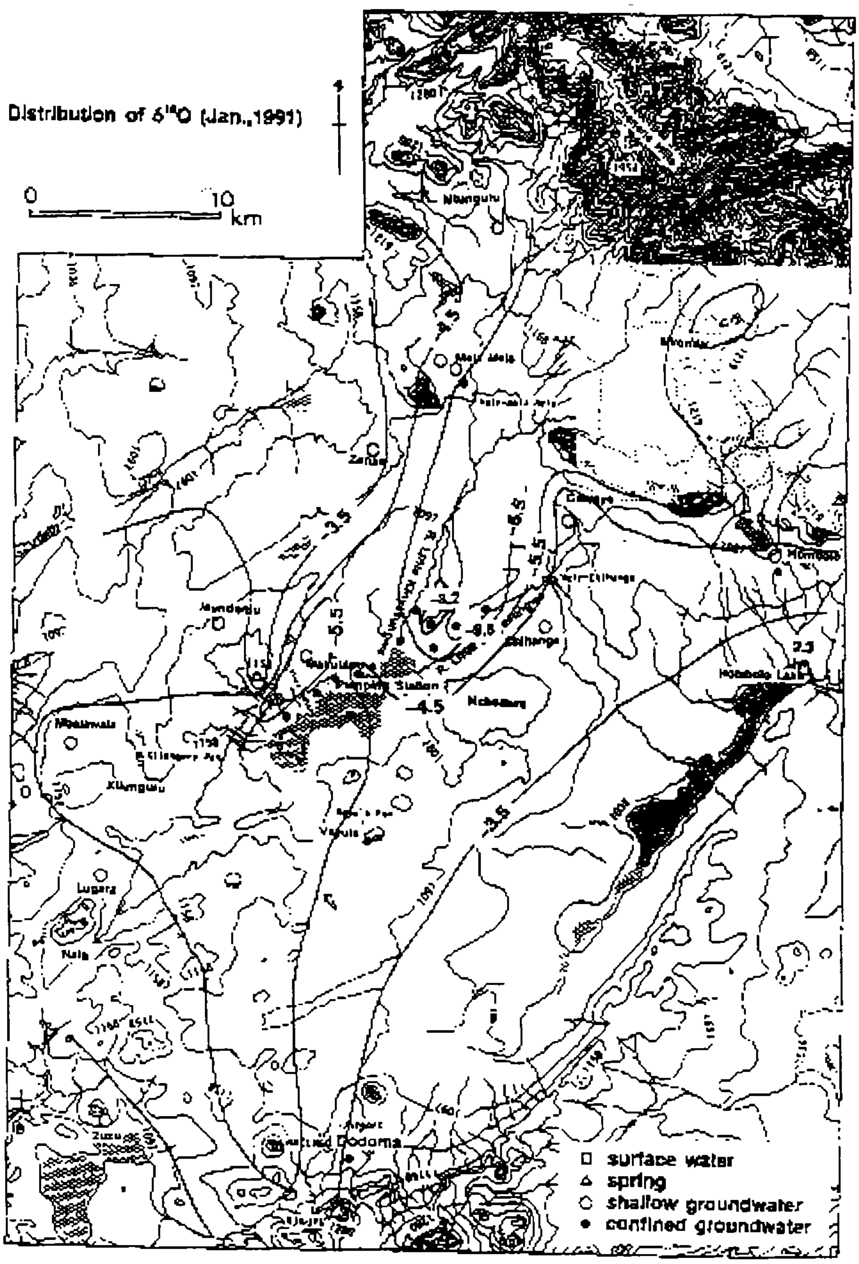

FIG.2 DISTRIBUTION OF OXYGEN-18 COMPONENT OF NATURAL WATERS IN MAKUTUPORA BASIN

Tritium studies in groundwater have further indicated that, shallow water in the upland area are estimated to have residence times of about 40 to 60y, where as shallow waters in the foot slopes of Chenene hills have residence times of about 20y. The deep waters in the fractured rock aquifers at the eastern part of the basin are found to have residence times of about 50 to 80y, while deep waters at the western put of the basin are found to have residence times of around 120y.

Table 1 RESULTS OF STABLE ISOTOPE ANALYSIS 1991

rain water

sample	date	δ D	δ O
Site M	00/12/90	-15.3	-3.61
Site M	30/12/90	12.0	1.40
Site M	04/01/91	-12.9	-3.40
Site M	06/01/91	-14.4	-3.03
Site M	07/01/91	-3.2	-3.22
Site M	08/01/91	-23.9	-5.06
Site M	10/01/91	-14.8	-3.70
Site M	11/01/91	-2.4	-2.39
Site M	20/01/91	29.6	0.80
Site M	23/01/91	4.4	-1.28
Site M	25/01/91	7.3	-1.46
Site M	27/01/91	-4.6	-2.58
Site M	28/01/91	-8.2	-2.33
Site M	30/01/91	-5.2	-5.89
Site M	31/01/91	-5.1	-2.70
Site M	01/02/91	-24.0	-5.56
Site M	03/02/91	19.1	-0.21

soil water

sample	date	δ D	δ O
Site U 150	06/02/91	-33.2	-5.93
Site U 220	27/01/91	-33.9	-6.43
Site U 220	05/02/91	-32.6	-6.44
Site U 220	07/02/91	-32.0	-6.04
Site U 220	12/02/91	-32.1	-5.67
Site U 220	18/02/91	-27.4	-5.61
Site U 220	19/02/91	-33.3	-6.25
Site U 220	25/02/91	-16.3	-3.44
Mtungutu 200	14/01/91	-20.5	-4.00
Mtungutu 200	06/02/91	-20.0	-3.30
Mtungutu 200	13/02/91	-7.7	-4.18
Mtungutu 200	21/02/91	-21.5	-4.37
Mtungutu 200	25/02/91	-21.8	-4.54
Mtungutu 200	03/03/91	-21.6	-4.30
Mtungutu 200	12/03/91	-21.3	-4.61
Mtungutu 200	25/03/91	-21.6	-3.70
Mtungutu 200	13/04/91	-44.5	-4.73

shallow groundwater

sample	date	δ D	δ O
Hombolo SW9	27/12/90	-16.8	-3.69
Makutapora SW2	26/12/90	-31.0	-5.68
Meia Meia Site2	26/12/90	-18.5	-4.55
Meia Meia Site3	04/01/91	-25.2	-4.99
Mbaravara SW13	28/12/90	-24.6	-4.79
Kikuyu SW16	28/12/90	-22.8	-4.54
Lugara SW15	28/12/90	-21.1	-4.34
Chihanga SW5	27/12/90	-21.7	-4.31
Mtungutu SW	04/01/91	-27.7	-4.89
Gawaye SW	27/12/90	-15.5	-3.85
Mundemu	27/12/90	-24.4	-4.53
Mundemu	02/02/91	-23.7	-4.64
Mundemu	26/02/91	-14.5	-3.78
Zenka	26/12/90	-15.8	-3.34
Zuzu SW-E		-12.6	-3.39
Zuzu SW-E	30/08/91	-16.4	-3.67
Zuzu SW-G		2.3	-1.96

confined groundwater

sample	date	δ D	δ O
8/54 (Makuta.)	31/12/90	-26.1	-4.72
97/70 (Makuta.)	31/12/90	-21.2	-4.24
88/75 (Makuta.)	03/01/91	-28.1	-5.18
118/75 (Makuta.)	31/12/90	-25.3	-4.86
119/75 (Makuta.)	31/12/90	-25.4	-4.49
119/75 (Makuta.)	08/04/91	-41.7	-4.65
122/75 (Makuta.)	03/01/91	-1.5	-3.18
163/75 (Makuta.)	02/01/91	-39.1	-6.91
169/75 (Makuta.)	03/01/91	-30.9	-5.90
170/75 (Makuta.)	02/01/91	-61.2	-9.64
193/75 (Makuta.)	31/12/90	-26.8	-5.54
55/82 (Makuta.)	07/01/91	-23.5	-4.73
(Chenene)	06/02/91	-28.3	-5.53
10/71 (Meia Meia	26/12/90	-28.8	-5.51
26A/72 (Hombolo)	27/12/90	-17.0	-4.21
77/87 (Veyula)	28/12/90	-22.3	-4.40
9/70 (Dodoma)	16/01/91	-22.2	-3.54

5. CONCLUSION AND RECOMMENDATIONS

The isotopic fluctuation trend for the water cycle in the basin together with tritium concentrations in the water have provided some new insights regarding groundwater circulation, its origin (location of recharge) and residence time, and recharge rates. According to the studies it has been established that the recharge areas for the confined groundwater are located on the pediplain uplands, river beds and hill slopes underlain by well fractured basement (Shindo, 1991).

By summarizing the results on residence times of groundwater in the basin, the study concludes that, recharge of deeper aquifer levels is due mainly to the runoff from Chenene hills and the pediplain upland while the recharge of shallow aquifer levels comes partly from local precipitation and partly from the Chenene hills runoff.

In the opinion of the author, future progress in using isotope techniques to study the Makutupora basin will depend mainly on solving the following problems:-

- Over exploitation and degradation of the groundwater resource in the basin.

- Pollution of groundwater in the basin
- Application of artificial recharge to the basin.
- Inadequate knowledge on groundwater flow in fractured rocks.
- Establishing safe yield conditions of the basin.

Moreover, ongoing investigation of pollution and depletion of groundwater resource in the basin has not succeeded in defining specific pumping limits and groundwater protection zones especially around the basin well field. It is from this need that isotope data are sought to provide a clear basis for regulatory action and resource management in the Makutupora basin.

REFERENCES

[1] DINCER, T, The Use of Isotopes in Hydrology in Tanzania. Report to the Government of the United Republic of Tanzania (1979) 86pp.

[2] INTERNATIONAL ATOMIC ENERGY AGENCY, Isotopes in Lake Studies, Vienna (1979).

[3] INTERNATIONAL ATOMIC ENERGY AGENCY, Use of Artificial Tracers in Hydrology, Vienna (991).

[4] SENGUJI, FH, Modeling of Groundwater Flow in the Makutupora Basin in Semi-arid Inland of Tanzania using the MODFLOW Code, MSc Thesis, Unpublished (1997).

[5] SHINDO,S, Study on the Recharge Mechanism and Development of Groundwater in the Inland area of Tanzania, Volumes 1,2,3and 4 (19988-1992).

[6] US GEOLOGICAL SURVEY PROFESSIONAL PAPER 1571, Groundwater Flow and Contaminant Transport, Rhode Island.

GROUNDWATER ORIGIN INVESTIGATION WITH ISOTOPIC COMPOSITIONS FOR EVALUATION OF HIGH PRODUCTIVE DEEP AQUIFERS IN KHON KAEN AREA, NORTHEAST THAILAND

C. BUAPHAN, W. YANGME, L. WANNAKAO
Department of Geotechnology,
Faculty of Technology, Khon Kaen University,
Khon Kaen, Thailand

V. SRIBOONLUE
Department of Agricultural Engineering,
Faculty of Engineering, Khon Kaen University,
Khon Kaen, Thailand

A. TASSANASORN
School of Geotechnology, Institute of Resources Technology,
Suranaree University of Technology,
Nakhon Ratchasima, Thailand

S. BUAPENG
Ground Water Division,
Department of Mineral Resources,
Bangkok, Thailand

Abstract

Investigation of groundwater origin by using isotopic compositions for evaluation of high productive deep aquifers in Khon Kaen Province is emphasized on hydrogeology and isotopes technique. The study area consists of Mesozoic sedimentary rocks and unconsolidated sediments of Quaternary. Phu Tok aquifers in the southern part of the study area are mainly confined in very well sorted, fine grained sandstone as well as in fractures and joints. They extend from Ban Tha Pra to Ban Phai covering area 500 km^2. Depth to the aquifers is from 20 to 250 m, while their piezometric surface ranges from 0.35 m to 15 m from the ground surface. Their thickness range from 50 to 100 m. The transmissivity is from 0.45 to 1 047 m^2/d on the pumping rate of 48-1 200 m^3/d with drawdown of less than 10 % and rough annual safe yield is 83.34x10^6 m^3. The water is very good in quality for drinking, except for the TDS and total hardness around aquifer boundary. The groundwater and surface water are analysed for stable and radioactive isotopes, including ^{2}H, ^{18}O, ^{3}H and ^{14}C . The results show that the shallow groundwater of the depth less than 50 m is originated by direct recharge of rainfall between 180 and 6 820 a. The groundwater flow is relatively rapid from west to east and northwest to southeast, the high productive deep aquifer of Phu Tok flow radiate from recharging area to all direction. However, the groundwater flow rate based on ^{14}C analyses for Phu Tok is 2 to 3 m/a. Within some areas the flow is about 8 m/a, while the unconsolidated aquifers along the Phong River give flow rate about 4 m/a. The deeper aquifers also have direct rain recharge the same as the above aquifers but the flow rate are lower, especially the deepest aquifer at the depth of nearly 200 m indicated no direct rain recharge with age of more than 20 000 a, which is confirmed with the amount of tritium less than 1.0 TU.

1. INTRODUCTION

The town of Khon Kaen and adjacent areas benefit from two main rivers, namely, the Phong and the Chi. However, the water supplies from these rivers are not sufficient for domestic and industrial uses. Therefore, groundwater from both shallow and deep aquifers are another alternative use. At present, most groundwater wells in this region are in shallow aquifer at average depth of less than 50 m. A few deep wells are developed for most industrial uses and rural public water supplies.

The need for using deep groundwater aquifers is increasing with the industrial growth. The investigation on hydrogeology, especially the origin of deep groundwater, is carried out in order to evaluate the potential groundwater reserve. Moreover, this will lead to groundwater management in the future. The investigation includes geology, hydrogeology and isotope determination including natural and radioactive isotopes which are ^{18}O, ^{2}H, ^{3}H and ^{14}C.

2. GENERAL BACKGROUND OF THE STUDY AREA

The study area is located in Khon Kaen Province, Thailand, approximately between longitudes 102° 30′ and 103° 00′ E, and latitudes 16° 10′ and 16° 40′ N. It covers almost 2 915 km^2 (Fig. 1).

Its climate is of tropical savanna type. There are three seasons namely rainy, winter and summer seasons. The rainy season begins in May and ends in October, while the winter season begins in mid-October and ends in February, and after that the summer begins in mid-February and ends in May. The monthly mean temperature ranges from 22 to 33 °C, while the annual mean temperature (from 1990-1994) is 23 to 33 °C. The average of annual rainfall of the same period is 1 112 mm. The Chi and Phong Rivers are the main river of the study area. They are the tributaries of the Mun River . The average annual discharges of the Chi River during 1958-1986 of the gauging stations at Ban Tha Pra upstream from the outlet of Nam Phong River and at Ban Kui Chuak downstream from the outlet were 1 $930.43\text{x}10^6$ m^3 and 3 $961.32\text{x}10^6$ m^3, respectively. The Nam Phong reservoir locates in the northwestern part of the study area impounding water about 2 $000\text{x}10^6$ m^3. The average annual discharge of Nam Phong River at gauging station of Ban Tha Hin during 1965-1989 before joining the Chi River is 1 $405.45\text{x}10^6$ m^3.

3. GEOLOGY AND HYDROGEOLOGY

3.1. Geological Setting

Northeastern Thailand is composed of a series of stacked basins which have developed during a long and complex evolution. The exposed in the regional scale as a huge relatively flat terrain call " Khorat Plateau". This plateau is made up of thick sedimentary sequences of the Mesozoic Khorat Group. The Khorat Group is stratigraphically classified by different geologists into several formations. The total thickness of this sequences are estimated to range from 2 300 to 6 000 m [1].These thick sequences are believed to be tectonically influenced in the late Tertiary to early Pleistocene times [2] and formed broad warping with an anticlinorium, the Phu Phan range, which separated the Plateau into two basins; the Khorat-Ubon Basin in the southern part and the Udon-Sakhon Nakhon Basin in the northern part. The upward stratigraphic units of the rock formations in the study area constitute : Phu Kradung, Phra Wihan, Sao Khua, Phu Phan, Khok Kruat, Maha Sarakham, Phu Tok, Quaternary sand and gravel and Alluvium. These formations consist of sandstone, siltstone, shale and conglomerate while unconsolidated formations consist mainly of sand, gravel, silt and clay.

3.2. Hydrogeological Setting

Groundwater of the project area occurs in both types, namely unconfined and confined aquifers in primary pore of sand and gravel and in secondary pore or fracture of rocks including conglomerate, sandstone, siltstone and shale ranging in depth from 15 to 300 m [3]. Mostly, unconfined aquifers can be found in shallow layers of unconsolidated sand and gravel, and sedimentary rocks of Phu Kradung, Phra Wihan, Sao Khua, Phu Phan, Khok Kruat and Maha Sarakham Formation, as well as Phu Tok Formation (Fig. 2). Nevertheless, the same rocks will give mostly confined aquifers for the deeper ones, when the aquifers are far away from the recharged area around the periphery of study area [3].

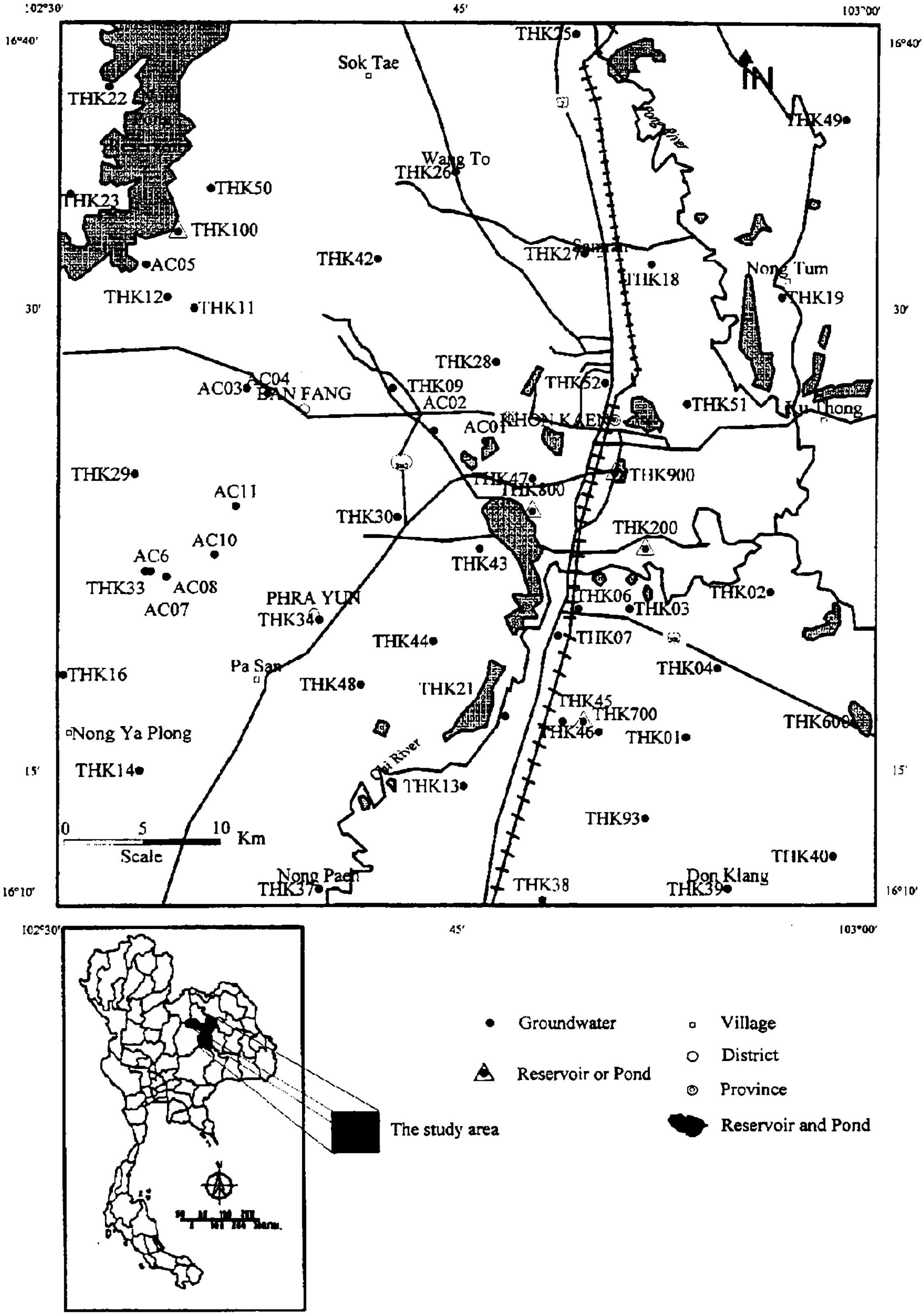

FIG. 1. Map of the study area and location of sampled wells, reservoirs and ponds.

Piezometric levels range from 1 m above ground surface to 20 m below land surface with average depth of 6 m. Flows of groundwater are divided by Phu Phan Kham ridge in the west to northwestern part into two lines. The first flow line starts from the ridge directioning to northwest and end at Nam Phong Reservoir, while the other flow direct down to southeast to the Chi River. The groundwater of northeastern hill flows in direction of southwest to the Nam Phong River but the groundwater flow of the southeastern hill radiates from center of the hill to the west, north and east to the Chi River (Fig 2).

The aquifers give storage coefficient and transmissivity from 5.10×10^{-2} to 7.06×10^{-5} and 5 to-692 m^2/day, respectively. The pumping rates are less than 55 m^3/day to more than 5 560 m^3/day. According to the groundwater storage, Phu Tok aquifer located in the southeastern part of the study area is the main productive aquifer .The area is bounded from the west to the north by the Chi River. The aquifer give very high yield with the maximum of transmissivity of about 1 047 m^2/day. The depth to aquifer ranges from more than 20 m to about 200-300 m. The aquifers give pumping rate of 48-1 200 m^3/day with drawdown of less than 10% and rough annual safe yield of 83.34×10^6 m^3.

4. SAMPLING AND METHODS

Groundwater samples were collected from existing wells and test wells at various depths of each aquifer from the recharge areas to the discharge areas. Figure 1 shows the location map of the sampling site in the study area. Surface water samples from reservoir and ponds were also collected.

Water samples were conducted from November 1996 to February 1997. All samples were analysed for ^{18}O, ^{2}H, ^{3}H and chemical analyses. Groundwater samples were also done for ^{14}C analyses. Parameters such as temperature, pH and specific conductance were determined in the field.

The ^{18}O and ^{2}H were analysed in the laboratory of the International Atomic Energy Agency, Vienna. The ^{3}H and ^{14}C were made in the laboratory of the Office of Atomic Energy for Peace, Bangkok. The chemical analyses were carried out in the laboratory of Khon Kaen University, Khon Kaen and the Department of Mineral Resources, Bangkok.

The tritium content was determined using the electrolytic enrichment and a liquid scintillation counting method. The ^{14}C analyses were done in the laboratory by using direct absorption to derive the CO_2 from the precipitated carbonate and measured by the liquid scintillation method.

5. RESULTS AND DISCUSSION

5.1. Hydrochemistry

The quality of groundwater varies from fresh to saline, soft to very hard and high iron contents in some areas. The summarized groundwater quality in the study area both major constituents and trace metals are shown in Table I. Groundwater quality problems in some areas are due to high chloride , total dissolved solids and iron contents [4] .

The trace metal contents are relatively low except the amounts of iron, zinc, mercury and vanadium in some wells (Table I). However, the concentrations of heavy metal are mostly lower than drinking water standards especially the water from Phu Tok aquifer in the southern part which is the sources of soft drink industry.

The analyses of cations and anions by Piper Trilinear Diagram are depicted in Fig. 3. The cations are mainly calcium, sodium, and potassium type while the anions are bicarbonate and chloride type. However, the sum of cations and anions are mainly Ca-Mg-CO_3-HCO_3, Ca-Mg-Cl-SO_4 type and Na-K-CO_3-HCO_3 and Na-K-Cl-SO_4 type are also found in some area (Fig.3).

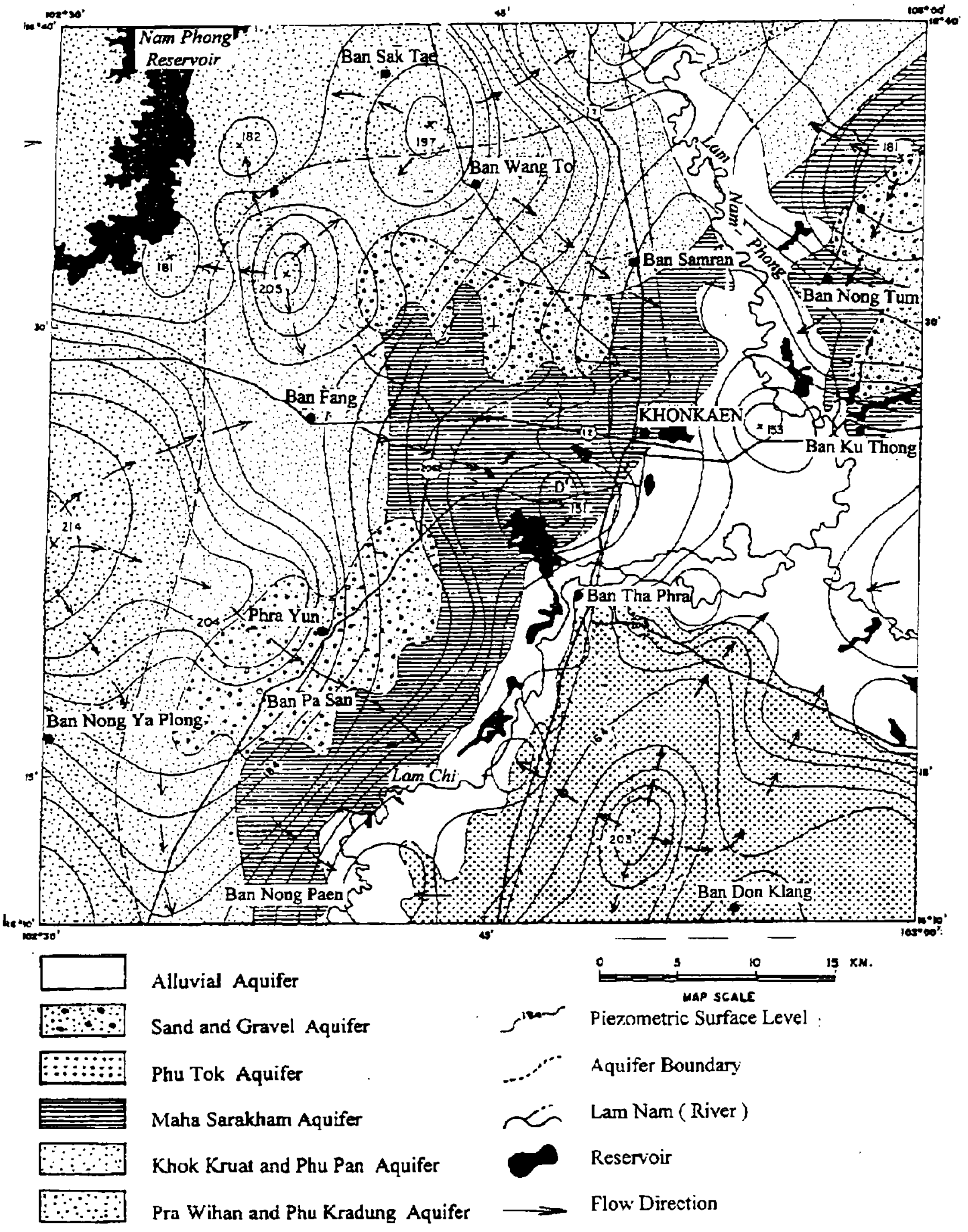

FIG. 2. Hydrogeological map of the study area.

5.2. Isotope Composition

The total of 45 samples from existing production wells and test wells were collected for environmental isotope analyses. There are 27 samples for δ D and δ^{18} O, 33 samples for ^{3}H and 45 samples for ^{14}C analyses. Seven samples were collected from reservoir and ponds for δ D and δ^{18} O analyses. The results of isotopic analyses are shown in Table II.

5.2.1. Stable Isotopes

The δ D and δ^{18} O plot of groundwater, surface water and precipitation in Bangkok and Luang Prabang, Laos [5] is shown in Fig.4. The isotopic compositions scatter widely below the world meteoric water line, characterizing evaporation effect. Results of stable isotopes for surface water samples show the extreme evaporation effect and fall on a different evaporation line of groundwater. The significant relationship between surface water and groundwater cannot be observed. Groundwater stable isotopes are mostly far below the world meteoric water line, these reflect the recharge occurring through a range of surface mechanism : direct rain infiltration, various degree of surface evaporation before infiltration and mixture of these.

Two groups of groundwater can be recognized on the δ D and δ^{18}O (Fig. 4). The first group represents groundwater from Alluvial, Phu Tok and Khok Kruat aquifers, more depleted in stable isotopes, while the other consists groundwater from Phu Kradung, Pra Wihan and Maha Sarakham aquifers, representing the more enriched in isotope compositions. The δ^{18} O and δ D of the first group range from – 6.86 to – 8.05 ‰ and –45.9 to – 57.0 ‰, respectively. The recharge into these aquifers are mostly direct infiltration of local rainfall with some evaporation effect before infiltration. The aquifers are porous and rather high productive especially the Phu Tok aquifer which has been found in the east and southeast of the study area. The stable isotopes are enriched in the discharged area. This may reflect the mixture between fresh water and salty water from the other aquifer such as Alluvial or Maha Sarakham aquifer.

The isotopic compositions of the other groundwater group range from –6.85 to – 5.03 ‰ for δ^{18}O and –51.7 to – 45.0 ‰ for δ D , respectively. The recharge into the Phra Wihan and the Phu Kradung aquifer is effect by evaporation before infiltration. The evaporation process may occur from temporary storage or ponding of rain water in the surface area. The enrichment of stable isotopes may be considered as an indication of low recharge movement through the aquifer. The Phra Wihan and Phu Kradung aquifers are less permeability and rather low yield of groundwater.

The Maha Sarakham aquifer which contain rock salts underneath in some areas [6], the recharge into aquifer is directly infiltrate from local rainfall. However, the environment in stable isotopes may indicate the mixture of groundwater recharge directly from rainfall and salty water in the formation.

5.2.2. Tritium

Results of tritium analyses of groundwater and surface water samples are shown in Table II. ^{3}H contents in reservoir and ponds range from 2.6 to 3.9 TU and in groundwater is from 0.1 to 4.3 TU. Most of ^{3}H contents in groundwater from aquifer at depth 10 - 50 m are high ranging from 2 to 4 TU. While groundwater at the greater depth contain low tritium (0.1 to 0.6 TU). The lowest ^{3}H content was found for the groundwater of the Phu Tok aquifer at depth 233 m. The low content of ^{3}H values over the study area, it may be concluded that recharge into the shallow depth aquifers is directly from recent rainfall with a short time residence and the recharge into the deeper aquifers is from rainfall older than 40 years.

TABLE I. SUMMARIZED GROUNDWATER QUALITY IN THE STUDY AREA.

Major constituents		**Trace Metals**	
Parameters	Range of Concentration	Parameters	Range of Concentration
PH	5.8 - 8.3	Fe (mg/L)	ND - 5.13
EC (μS/cm)	61.0 - 15 550	Mn (mg/L)	ND - 0.40
TDS (mg/L)	6.7 - 14 825	Zn (mg/L)	ND - 6.15
Cl (mg/L)	10.0 - 8 170	Cu (mg/L)	ND - 0.27
Na (mg/L)	3.0 - 2 481	As (μg/L)	ND - 1.80
K (mg/L)	0.6 - 190	Hg (μg/L)	ND - 3.00
Total Hardness (mg/L)	13.4 - 4 615	Cd (mg/L)	ND - 0.01
as $CaCO_3$		Pb (mg/L)	ND - 0.38
HCO_3 (mg/L)	24.0 - 2 760	V (μg/L)	< 5.7 - 42.40
Ca (mg/L)	ND - 1 677	I (mg/L)	ND - 0.26
Mg (mg/L)	ND - 277		
SO_4 (mg/L)	ND – 92 162		
NO_3 (mg/L)	ND - 29		

ND = non – detected

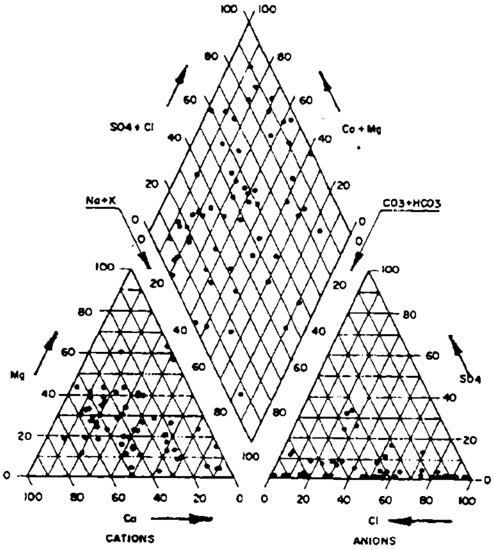

FIG. 3. Trilinear plot of the major ion composition of groundwater in the study area.

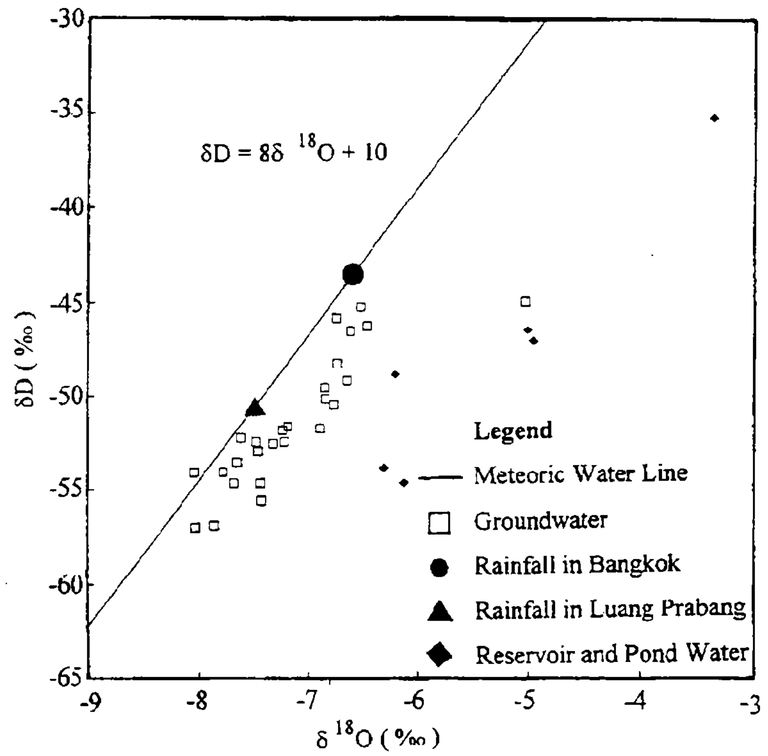

FIG. 4. Relation between $\delta^{18}O$ and δD values of groundwater and surface water samples.

5.2.3. Carbon - 14

The ^{14}C concentration and apparent ^{14}C groundwater ages are shown in Table II. The ^{14}C content range from 7.34 ± 1.18 to 124.8 ± 2.61 pmC. The apparent ^{14}C ages of groundwater from various aquifers range from 310 ± 180 to 6 820 ± 310 a. The lowest concentration of ^{14}C was found in groundwater at depth about 230 m of the Phu Tok aquifer in the southeast of the study area. The value obtained is 7.341 ± 1.18 pmC and the apparent age is 20 980 ± 1 400 a. This is the oldest water which has been found and it is considered that no recharge into the deeper aquifer. The high concentrations of ^{14}C (> 100 pmC) were also found in many samples of the shallow aquifers. It is indicated that groundwater is modern and mixing of recent water and salty water was occurred.

The apparent ^{14}C ages in Phu Kradung, Pra Wihan and Khok Kuart aquifers in the west of the study area range from 390 to 2 660 a. Water is younger than in the eastern part of the study area. It is interpreted that recharge into these aquifers is directly infiltrated from rainfall with a slow movement.

The apparent age in Maha Sarakham and Alluvial aquifers which occur in the central and eastern part of the study area, range from 310 to 6 777 a. The modern water and mixing of recent water and salty water are also found in some places. The recharge into aquifers is directly infiltrated from local rainfall and lateral flow from the pheriphery of the basin. The apparent ^{14}C age of groundwater at depth of about 50 m of Phu Tok aquifer range from 1 310 a in the recharge area to 6 820 a in the discharge areas.

TABLE II. ISOTOPIC COMPOSITION OF GROUNDWATER

Well No.	Depth (m.)	$\delta^{18}O$ (‰)	δD (‰)	^{3}H (TU)	^{14}C (pm C)	^{14}C Age a (BP)
THK01	223.5	-7.33	-52.6	0.1 ± 0.2	7.34 ± 1.18	20 980 ± 1 400
THK 03	78	-6.86	-49.6	0.2 ± 0.0	84.90 ± 2.04	1 310 ± 2 00
THK 04	34	-6.75	-45.9	3.7 ± 0.1	100.14 ± 2.22	-
THK06	36	-6.77	-50.5	3.5 ± 0.1	103.92 ± 2.26	-
THK07	44	-7.20	-51.7	1.0 ± 0.1	81.92 ± 1.98	1 600 ± 200
THK09	48	-6.47	-46.3	0.7 ± 0.1	43.04 ± 1.63	6 770 ± 310
THK11	15	-6.90	-51.8	4.1 ± 0.3	124.58 ± 2.47	-
THK12	42	-6.85	-50.2	3.2 ± 0.1	134.87 ± 2.54	-
THK13	36	-7.23	-52.5	0.3 ± 0.1	42.77 ± 1.63	6 820 ± 310
THK14	27	-	-	3.2 ± 0.1	124.84 ± 2.61	-
THK16	43	-	-	1.9 ± 0.1	84.44 ± 1.95	1 360 ± 190
THK18	64	-5.03	-45.0	-	-	-
THK19	27	-7.63	-52.3	0.5 ± 0.1	83.71 ± 2.02	1 430 ± 200
THK21	103	-7.87	-56.9	0.6 ± 0.1	88.06 ± 2.06	1 020 ± 190
THK22	32	-	-	2.9 ± 0.1	118.50 ± 2.25	-
THK23	27	-	-	2.1 ± 0.1	76.63 ± 1.77	2 140 ± 190
THK24	-	-	-	-	81.85 ± 1.78	1 610 ± 180
THK25	42	-6.77	-50.5	2.7 ± 0.1	84.05 ± 1.82	1 400 ± 180
THK26	36	-7.66	-53.6	0.9 ± 0.1	68.01 ± 2.57	3 100 ± 310
THK27	15	-7.44	-55.6	3.3 ± 0.1	117.17 ± 2.16	-
THK28	30	-7.49	-52.5	0.1 ± 0.1	96.22 ± 2.09	310 ± 180
THK29	44	-	-	1.1 ± 0.1	67.75 ± 1.70	3 130 ± 200
THK30	34	-	-	4.1 ± 0.1	119.54 ± 2.18	-
THK33	18	-	-	3.5 ± 0.1	112.57 ± 2.11	-
THK34	18	-	-	2.9 ± 0.1	130.95 ± 1.97	-
THK37	30	-	-	1.8 ± 0.1	95.13 ± 1.93	400 ± 160
THK38	49	-7.47	-53.0	0.2 ± 0.1	50.07 ± 1.69	5 560 ± 280
THK39	30	-6.53	-45.3	-	-	-
THK40	33	-6.65	-49.2	3.1 ± 0.1	112.18 ± 2.29	-
THK42	48	-6.62	-46.6	1.5 ± 0.1	109.80 ± 2.08	-
THK43	21	-	-	2.3 ± 0.1	91.37 ± 1.87	730 ± 170
THK44	30	-	-	2.7 ± 0.1	111.53 ± 2.09	-
THK45	37	-7.25	-51.9	2.4 ± 0.1	104.40 ± 2.09	-
THK47	37	-7.69	-54.7	0.3 ± 0.1	63.39 ± 1.66	3 660 ± 210
THK48	24	-6.74	-48.3	0.3 ± 0.1	60.60 ± 1.57	4 042 ± 210
THK49	30	-8.05	-54.1	0.4 ± 0.1	84.59 ± 2.50	1 340 ± 240
THK50	30	-7.45	-54.7	-	71.83 ± 1.73	2 660 ± 200
AC06	24	-	-	3.7 ± 0.4	95.31 ± 1.90	390 ± 160
AC11	18	-	-	3.9 ± 0.4	109.85 ± 2,018	-

5.3. Groundwater flow and velocity

From the spatial distribution of ^{3}H values and apparent ^{14}C ages, the main direction of groundwater is from northwest towards southeast and west towards east. In the Phu Tok aquifer which situated in the southeast of the study area, groundwater flow is radial flow from the recharge area towards the discharge areas. These groundwater flow paths are in agreement with the piezometric level of the study area (Fig. 1).

The estimation of flow velocity from the apparent ^{14}C ages in the Phu Tok aquifer at depth 50-100 m, range from 1.9 to 7.7 m/a. This result also agrees with the hydrogeological investigation which shows high productive aquifer.

6. CONCLUSIONS

The results from hydrogeological, hydrochemical and isotopic studies of the aquifer systems in the northeast Thailand can be concluded as follows:

Groundwater resources in the study area occur in both unconsolidated and consolidated aquifers. The highly productive aquifer is the Phu Tok where situated in the southeastern part. Groundwater quality is generally good for domestic purposes. Exception is made for iron and manganese concentrations which are over the Standards of Drinking Water. The saline water has been found in some areas of the Maha Sarakham and Alluvial aquifers. The main hydrochemical types of water are $Ca\text{-}Mg\text{-}CO_3\text{-}HCO_3$, $Ca\text{-}Mg\text{-}Cl\text{-}SO_4$ and $Na\text{-}K\text{-}Cl\text{-}SO_4$ type.

The main recharge into aquifer is directly from infiltration of the rainfall occurring in the west and northwest of the study area. The groundwater recharge into productive Phu Tok aquifer is from recharge areas on the top of the hill towards the low-lying discharge areas. The apparent ^{14}C ages of groundwater for all aquifers range from 180 to 6 820 a. However, the ^{14}C groundwater ages of 20 680 a was found in the aquifer at depth 230 m. This result indicates that there is no direct recharge into the deeper aquifer.

The distribution of ^{3}H and ^{14}C ages indicate the main direction of groundwater flow : from west and northwest towards east and southeast, respectively and from the top of recharge areas towards the low lying discharge areas of Phu Tok aquifer in the southeastern part of the study area. The velocity of groundwater estimated from ^{14}C ages are found ranging from 1.9 to 7.7 m/a.

ACKNOWLEDGMENTS

This work was carried out under the financial support from the National Research Council of Thailand. The authors would like to express gratitude their staff and committee for their support and recommendation during this study. They are very grateful to Dr. Y. Yurtsever, IAEA staff member, for his help in stable isotope analyses. Thanks are due to the Isotope Laboratory of the Thailand Office of Atomic Energy for Peace, the Laboratory of Khon Kaen University and the Department of Mineral Resources for isotopic and chemical analyses. Finally, thanks are due to the staff of the Department of Geotechnology, Khon Kaen University and Ground Water Division, Department of Meneral Resources who contributed to this study.

REFERENCES

[1] SETHAPUT, V., Historical Activities on Geology and Mineral Resources Development of Northeastern Thailand, Proc. Conf. Geology and Mineral Resources Development of the Northeast, Thailand, Khon Kaen (1985) 1-12.

[2] HOKJAROEN, S., Photo - interpretation for Geological Mapping of Changwat Khon Kaen and adjacent areas. M. Sc. Thesis, Department of Geology, Chulalongkorn University, Bangkok. (1986).

[3] BUAPHAN,C., YOUNGME,W.,WANNAKAO,L., BUAPENG,S., TASSANASORAN,A., SRIBOONLUE,V , Groundwater Origin Investigation with Isotopic Compositions for Evaluation of High Productive Deep Aquifers in Khon Kaen Area, Thailand : Hydrogeology, Proc. Of International Conf.on Geology, Geotechnology and Mineral Resources of Indochina (Geo-Indo'95), Khon Kaen, Thailand, (1995) 501-512.

[4] RAMNARONG, V., BUAPENG, S., Groundwater Quality Problems in Thailand, International Symposium on Hydrochemical Balances of Freshwater Systems, Uppsala, Sweden (1984).

[5] BUAPENG, S., The Use of Environmental Isotopes in Groundwater Hydrology in the Selected Areas in Thailand: Final Report to the International Atomic Energy Agency on Project RB/4803/R1/R3 (1990).

[6] JAPAKASETR, T., WORKMAN, D. R., Evaporite Deposits of Northeast Thailand, Circum-Pacific Conference, Hawaii (1981).

AN ISOTOPIC APPROACH TO THE FUNCTIONING OF MULTI-LAYERED AQUIFER SYSTEMS IN CENTRAL TUNISIA: THE CASES OF THE NORTH GAFSA AND HAJEB EL AIOUN-DJELMA BASINS

K. ZOUARI, B. OUDA, M. YERMANI
Lab. de Géochimie Isotopique et de Paléoclimatologie,
Ecole Nationale d'Ingénieurs de Sfax, Tunisie

A. MAMOU
Direction Générale des Ressources en Eau, 43 Rue Saïda
Manoubia. 1008 Tunis, Tunisie

J.L. MICHELOT
Lab.d'Hydrologie et de Géochimie Isotopique, UMR
8616 CNRS, Université de Paris-Sud, Orsay, France

E. GIBERT-MASSAULT
Isotope Hydrology Section, IAEA, Vienna

Abstact

In central Tunisia, the hydrogeological behaviour of numerous multilayered aquifers is controlled by tectonics, because major faults act as natural underground hydraulic sills. This tectonic complexity limits the application of the classical hydrogeological methods and it appeared interesting to examine how environmental isotopes techniques could contribute to the knowledge of such systems. Two aquifer systems, corresponding to the North Gafsa and Hajeb el Aioun-Djelma basins, were selected because they are particularly affected by water management problems, such as a lowering of piezometric levels probably due to overexploitation of the aquifers.

The behaviour of the environmental isotopes used in this study (^{18}O, ^{2}H, ^{3}H, ^{14}C and ^{13}C) are quite different in the two systems.

In the North Gafsa basin, the modern/recent recharge (evidenced by tritium contents) is largely spread all over the basin and is locally identified in the different aquifer levels, even close to the main outlet of the system ("Gafsa sill"). Moreover, since groundwaters seem to be stratified in this region, it is difficult to reconstruct in details the lateral evolution of ionic and isotopic contents.

On the opposite, in the multilayered system of the Hajeb el Aioun-Djelma basin, the evolution of the environmental tracers is quite continuous, showing a relay between the different aquifer levels from the recharge areas towards the main outlet ("Hajeb sill"). Present-day water uptakes from the aquifers are likely to exceed recent recharge; however, the comparison between the results obtained in the present study and those from a previous work, in 1972, shows that overexploitation is limited in comparison with the reserves stored in the system.

1. INTRODUCTION

In central Tunisia, the hydrogeology of numerous multilayered aquifer systems is intensively affected by tectonics. Indeed, the hydrodynamics of these aquifers is complex due to the local structural accidents which play the role of hydraulic sills, making difficult the use of hydrogeological methods such as those based on piezometric measurements.

Thus, it appeared interesting to examine how environmental isotopes techniques could contribute to the knowledge of such systems, taking as examples the two basins of North Gafsa and Hajeb el Aioun-Djelma, which present water management problems.

2. CLIMATIC, GEOLOGICAL AND HYDROGEOLOGICAL CONTEXT

The two basins, North Gafsa and Hajeb el Aioun-Djelma, are located in the steppes region, which is a transition zone between the Tellian region, rainy and temperate, in the North and the hot pre-desertic zone in the South (Fig.1).

Average annual precipitation and annual temperature are respectively about 260 $mm.a^{-1}$ and 18°C in Hajeb, 160 $mm.a^{-1}$ and 19°C in Gafsa. Potential evapotranspiration, calculated from the Turc formula, exceed 1200 $mm.a^{-1}$ for the two basins.

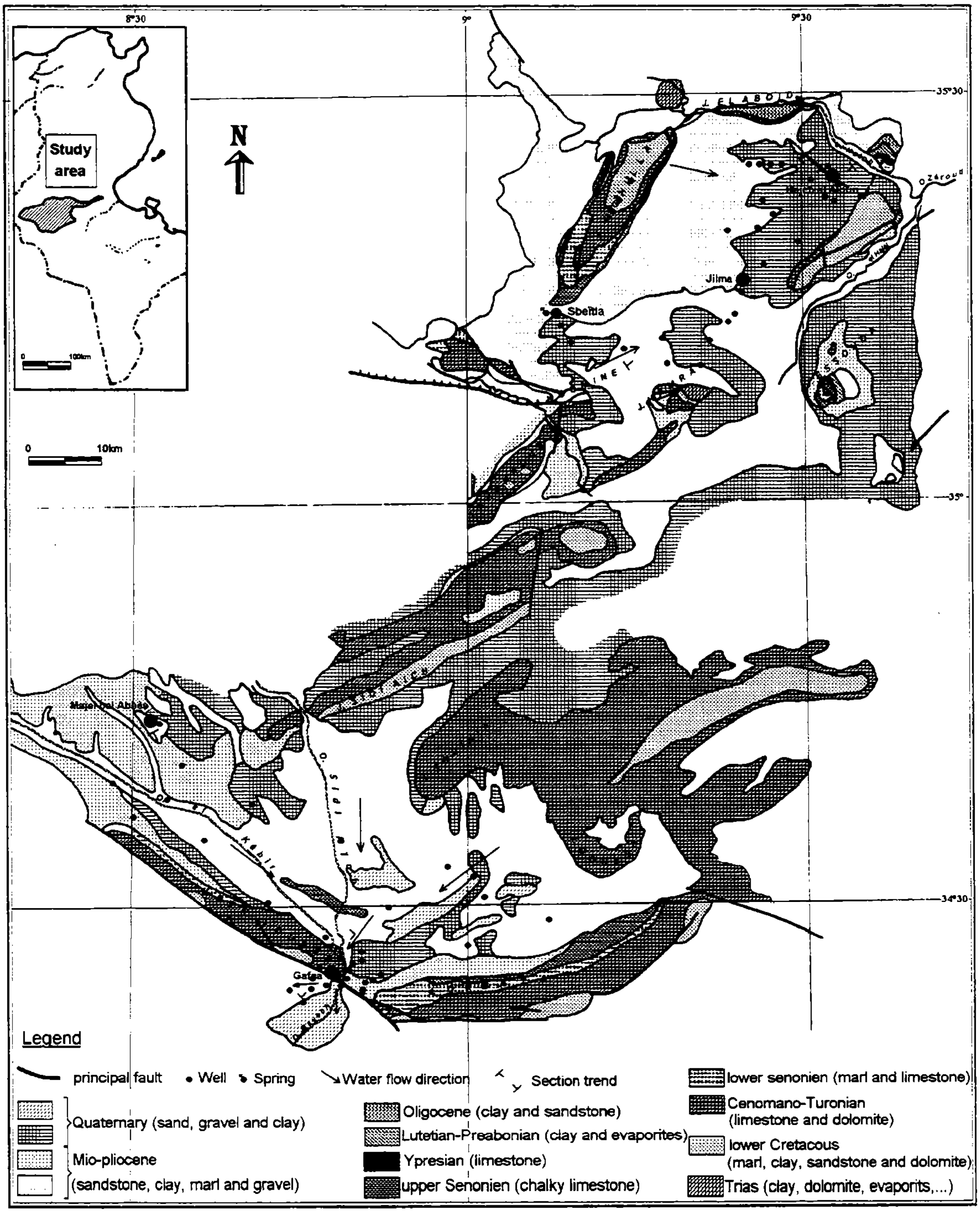

FIG. 1. Localisation map of the Gafsa and Hajeb el Aioun - Djelma basins, with indication of the sampling points.

2.1. North Gafsa basin

In this synclinal basin (about 2000 km^2) bordered by a series of anticlines, five aquifer levels are superposed [1] (Fig. 2):

- The Mio-Quaternary aquifer, where sand and clay alternate with a thickness of 0 to 600 m ;
- The Abiod formation (Upper Cretaceous) with about 250 m of chalky and cherty limestone;
- The Upper Zebbag formation (Turonian-Cenomanian) consisting of limestone and karstic dolomite with a thickness of 10 to 300 m, represents the main aquifer of the region.
- The Lower Zebbag aquiter with a mean thickness of more than 80 m of limestone and dolomite;
- The Lower Cretaceous aquifer, with a various lithology : sand, sandstone, dolomite, marl and gypsum.

Some estimates of the effective infiltration suggest that rainfall on the surrounding mountains where the aquifer formations outcrops, could be considered as the essential recharge of the system (1200 L.s^{-1} out of a total recharge of 1300 L.s^{-1}). From other estimates, the wadis (Sidi Aich, el Kebir and Bayech) would significantly contribute to recharge. In addition, the piezometric continuity and chemical similarities of groundwaters suggest that the North Gafsa basin is also fed by the groundwaters coming from the neighbouring Majel Bel Abbes basin [2].

The North Gafsa basin is separated from the South Gafsa basin by a fault which creates a hydraulic sill at the level of Gafsa city [3]. Due to this sill, marked by of a series of springs, the piezometric contours become closer, with a convergence of flow lines. The flow of the sources, mainly fed by the deep aquifer overflow, has decreased during the last years, because the exploitation increased [4]. In some cases, springs dried up.

2.2. Hajeb el Aioun-Djelma basin

The Hajeb el Aioun-Djelma basin is also a synclinal basin (about 1350 km^2) surrounded by middle mountains, and containing several aquifer levels [5], more or less interconnected:

- The Quaternary aquifer (sand, silt,...), phreatic and presenting a thickness from 0 to 60 m *;*
- The sandy Mio-pliocene aquifer, 0 to 480m thick *;*
- The Middle Miocene aquifer, made of continental deposits (sand and sandstone), with a thickness between 100 and 450 m *;*
- The Oligocene/Lower Miocene aquifer, mainly consisting of continental sediments, sandstone levels alternating with some clayey levels. The thickness of the producing level fluctuates between 25 and 250 m ;
- The Cretaceous aquifer, made of marine deposits, forms the substratum of the series.

In addition to the vertical complexity related to stratigraphy, a complicated lateral evolution is due to tectonics : the aquifers are crossed by important faults bringing in contact the different levels and acting as semi-permeable sills (Fig. 3). This lateral complexity may also have a structural origin ; for example an anticline bulge of Cretaceous substratum observed in Ouled Asker allows the deep aquifers to discharge into the shallow ones. In such a situation, the aquifers are organized in relay .

The water infiltrated in the Western part of the basin, through the Cretaceous and Miocene outcrops of Jebel Mrhila which constitute the main recharge area of the system. It may be transferred to the Middle Miocene aquifer, then to the Mio-Pliocene aquifer, and finally reaches the phreatic aquifer before leaving the basin by drainage and/or evaporation [5].

Besides recharge on Cretaceous outcrops (average precipitation close to 400 mm.a^{-1}), the main input to the system is water infiltrated during the flood events, through the beds of wadis Zeroud, Sbeitla and Hatob.

Water uptakes from shallow and deep aquifers have more than doubled in the last twenty years. They now reach, or exceed, the evaluated resources (800 L.s^{-1}), as shown by the important lowering of the piezometric levels, up to 10 m in some areas.

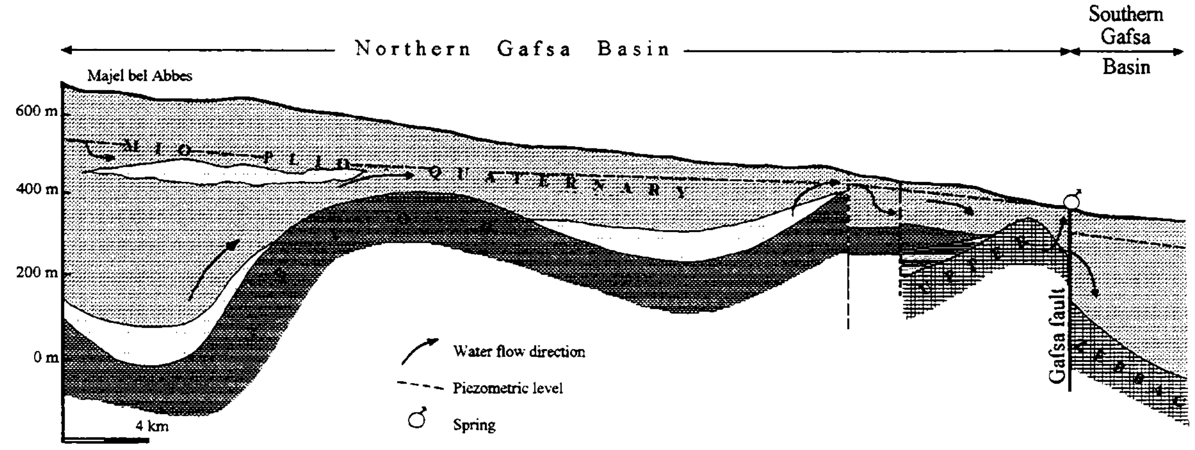

FIG. 2. North Gafsa basin: Hydrogeological cross-section from Majel Bel Abbes to Gafsa sill.

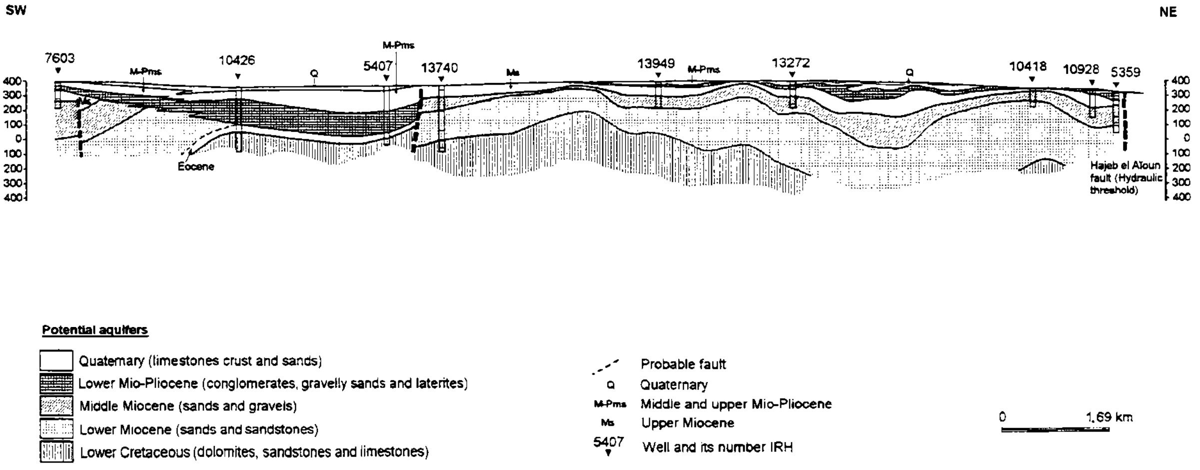

FIG. 3. Hajeb el Aioun – Djelma basin: Synthetic cross-section (from [5] ; modified).

3. SAMPLING AND ANALYSES

Four sampling campaigns were carried out in the North Gafsa and Hajeb el Aioun-Djelma basins from May 1996 to April 1997 (Fig. 1). Groundwater samples were collected from wells exploiting both shallow and deep aquifers, surface water samples from wadis and springs. The samples were analysed for their chemical and isotopic (^{18}O, ^{2}H, ^{3}H, ^{13}C and ^{14}C) contents. Parameters such as temperature, pH and electric conductivity were determined in the field.

In the North Gafsa basin, sampling was concentrated in the North-West (Majel bel Abbes region) and in the South (Gafsa Sill) areas. In Hajeb el Aioun-Djelma basin, sampling was done along two flow paths : (1) in the North, from Foum el Guelta to the Hajeb el Aioun sill, and (2) in the South from Sbeitla to Djelma (Fig. 1).

4. RESULTS AND DISCUSSION:

4.1. North Gafsa basin

4.1.1. Hydrochemistry

In general, chemical analyses show that groundwaters are sulphate- and calcium-dominated. Sulphate contents are high in the Upper Zebbag aquifer and in the Mio-Plio-Quaternary aquifer of the South Gafsa basin (downstream from the Gafsa sill). On the whole, total mineralisation increases from the basin borders toward the sill. However, in detail, the salinity evolution is not always strictly related to the flow direction deduced from the piezometric measurements. This is particularly true just before the Gafsa sill, where, on a supposed flowline, a sample located upstream presents a salinity twice those of samples collected downstream.

This can be due to (1) secondary faults (associated to the Gafsa fault, which creates the sill), or (2) to a vertical stratification of groundwater within the Upper Zebbag aquifer. The second hypothesis seems to be the most probable since there is a general trend to an increase of the salinity with the sampling depth.

4.1.2. Variations with time of the isotope contents

Significant discrepancies in the isotopic contents are observed from a campaign to another (Fig.4). Water samples collected in November 96 differ from those collected in May-June and September 1996, the former being depleted in both ^{18}O, ^{2}H and ^{3}H with respect to the latter. This "seasonal" variability suggests that there is a recent component in most of the samples.

4.1.3. Tritium contents

A number of samples present low, but significant, tritium contents. This practically concerns all the aquifers, and confirms the existence of a modern component in most cases. This recent contribution was expected in the borders of the basin, but it is more surprising for groundwaters sampled nearby the Gafsa sill, where it is probably linked to a recharge from the Jebel Ben Younes and Jebel Abiod/Orbata outcrops towards the deep aquifers.

4.1.4. Stable isotope contents of water

Considering the relatively small basin area and the differences in altitude between the plain and the highest mountains (800 m), the variation of isotopic contents measured in groundwaters seems very large (-2,5 ‰ in ^{18}0 and -20 ‰ in ^{2}H ; Fig. 5). The most “heavy“ samples (δ^{18}O = -6 ‰ and δ^{2}H = -35 ‰ vs SMOW) have been collected in the North-Eastern basin border (wadi El Kebir ; Fig.1) and likely correspond to modern recharge from local precipitation.

Some samples show a tendancy towards evaporation , which is logical in the case of the sample of the wadi El Melah characterized by a deuterium excess (d) of 3,3. The interpretation of the deuterium excess of groundwaters collected in the centre of the basin (d = 2) seems to be more complicated although the aquifer is relatively shallow in this area and could be submitted to a significant evaporation.

4.1.5. ^{13}C and ^{14}C contents in dissolved inorganic carbon

The measured ^{14}C contents confirm the existence of recent groundwaters in the North-Eastern border and in the Western part of the basin (in wadi El Kebir valley), where ^{14}C activities are close to 50 pmC and ^{14}C ages are close to 0 (according to the models of Ingerson and Pearson [6], Fontes and Garnier [7], Evans et *al.* [8] and Eichinger [9]) : a rather important recharge occurs not only through outcrops, but also from the wadis during flood periods.

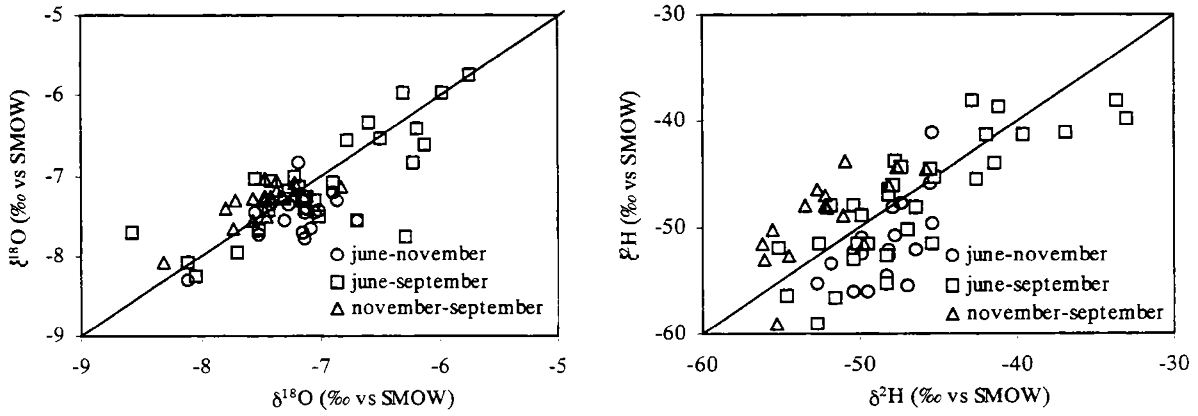

FIG.4. North Gafsa basin: Variations of stable isotope contents with time.

The ^{14}C activities measured nearby the Gafsa sill appear to be low, the corresponding calculated ages ranging from 4000 to 8000 years. These ages are quite consistent with the hydrodynamic data : the transit time between the recharge areas and the Gafsa sill, calculated from transmissivities and hydraulic gradients, is in the order of 10^3 to 10^4 years. However, in the details, the distribution of ^{14}C contents is very complex, especially near the Gafsa sill, where some samples present ^{14}C activities lower than those of samples collected downstream on supposed flowlines in the same aquifer. Also, the fact that tritium can be detected in most of the samples proves that these groundwaters correspond to mixings, and the modelled ^{14}C ages must be taken with caution.

In such a situation, it is almost impossible to understand in detail the sill functioning from isotopic data only. However, an important indication can be deduced from the comparison of the ^{14}C ages of groundwaters collected upstream and downstream from the sill : the samples collected just upstream from the sill present modelled ages of several thousands of years whereas the samples collected just downstream show modelled ages close to zero. This suggests that the main part of the water transfers through the sill occurs via the wadi and its associated phreatic aquifer .

Finally, the central Eastern zone of the basin (Zaabtia-Djedida) is characterised by very low ^{14}C contents that correspond to calculated ages of over 10000 years, but, even in this case, the tritium contents show that a recent contribution is still present.

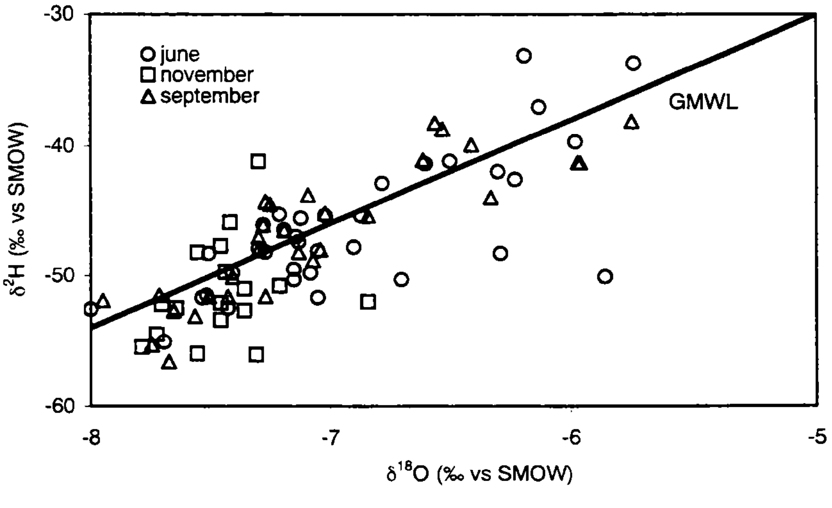

FIG. 5. North Gafsa basin: $\delta^{18}O$ vs. $\delta^{2}H$ diagram for the three sampling campaigns.

4.2. Hajeb El Aioun-Djelma basin

4.2.1. Hydrochemistry

Groundwaters are either of HCO_3-SO_4-Cl-Na-Ca type, or of SO_4-Cl-HCO_3-Na-Ca type. From the salinity distribution, two domains can be distinguished : (1) a domain with low salinities (0,4 to 0,8 g.L^{-1}), corresponding to the wells in the North and to the springs fed by the Lower Cretaceous formations in the WNW border of the basin, (2) a domain with high salinities corresponding to the groundwaters sampled along a SW-NE transect.

4.2.2 Variations with time of the isotope contents

The measurements made on samples collected during the two campaigns at a six-months interval do not show any marked variations of the stable isotopes and tritium contents (Fig. 6). These measurements can also be compared with those obtained by Koschel [5] on groundwaters sampled in the basin in 1972 . This comparison shows a remarkable constancy of isotope contents (^{18}O, ^{2}H, ^{13}C, ^{14}C) over a period of 25 years (Fig. 7).

4.2.2 Tritium contents

The tritium contents highlight the recharge zones characterized by the highest contribution of recent water, which are logically located on the basin borders, particularly nearby the Jebel Mrhila (WNW), but also near the wadi Sbeitla (WSW).

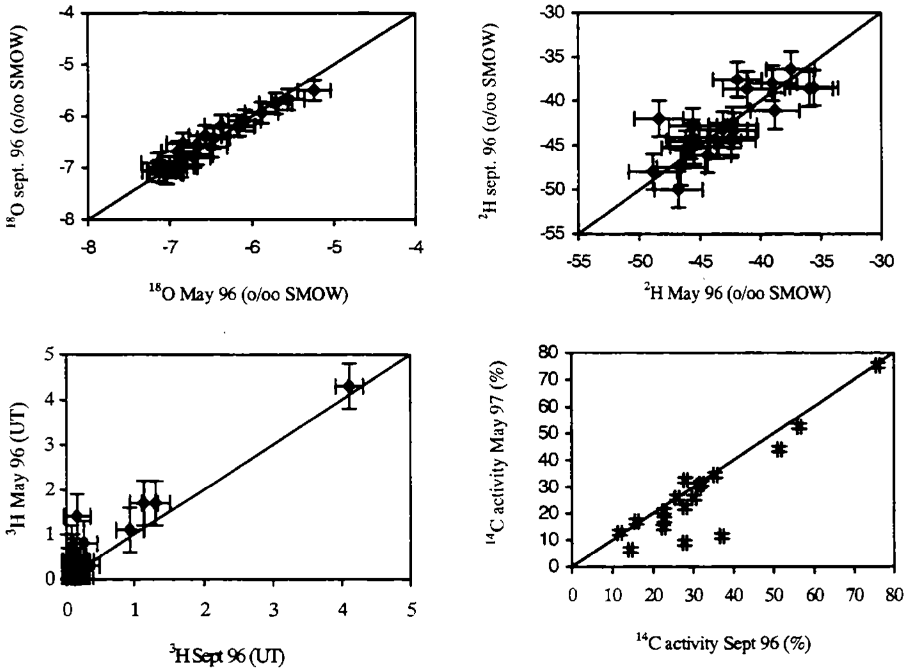

FIG. 6. Hajeb el Aioun – Djelma basin: Variation of isotope contents over a period of six months.

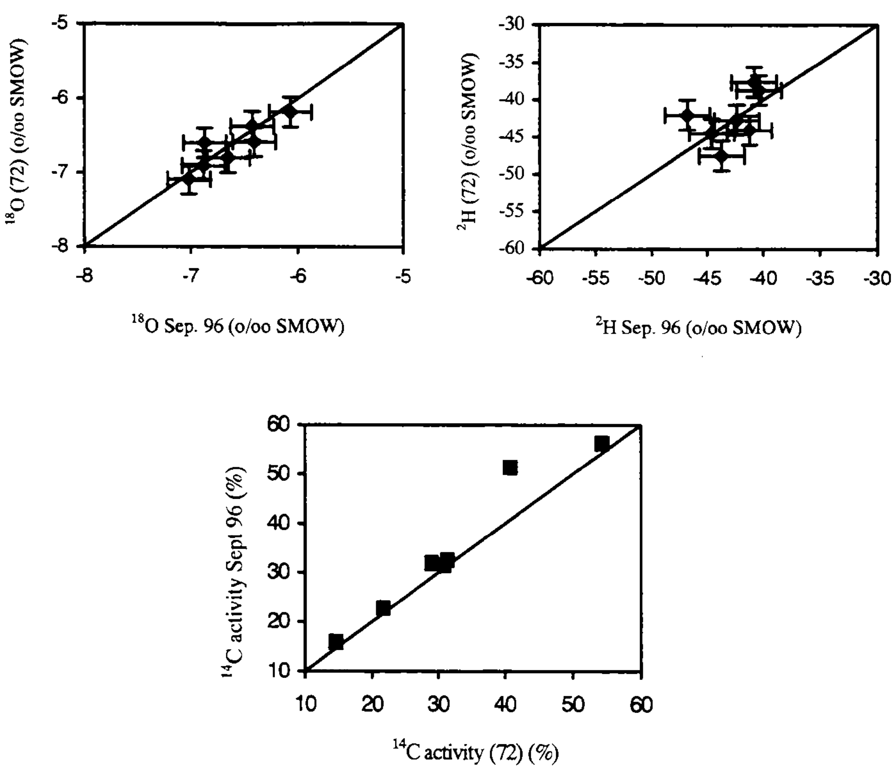

FIG. 7. Hajeb el Aioun – Djelma basin: Variation of isotope contents over a period of 25 years (data from this study vs. data from [5]).

4.2.3. Water stable isotope contents

In a δ^2H *vs* $\delta^{18}O$ diagram, the representative points of samples are close to the Global Meteoric Water Line [10], but most of them are below (deuterium excess, d, lower than 10 ‰). The low value of d becomes evident when available data on precipitation nearby the studied zone is examined (Fig.8). At the IAEA/WMO station of Tunis-Carthage [11], the mean deuterium excess in precipitation is close to 12. In Sfax, this parameter is close to 10 for precipitation taken as a whole, but it is about 14.5 for the rainfall events exceeding 10 mm [12]. In both cases (Tunis and Sfax), the Mediterranean origin of condensing water vapour masses, is responsible for the high d values. In Hajeb el Aioun-Djelma basin, groundwaters do not present such high d values. This could be due either to a slight evaporation that would affect rainwater before or during its infiltration or to a palaeoclimatic effect (of course for old groundwaters only), as demonstrated in other cases (see e.g. [13] and [14]).

On the basis of stable isotopes contents, no clear distinction can be made between the different aquifers. This observation can be explained by the existence of large interconnections between the different aquifer levels, organised in relay.

4.2.4. Carbon-13 and *Carbon-14 contents in dissolved inorganic carbon*

The spatial distribution of residence times corresponds to a general flow direction from West to East. The recharge zones detected by the tritium contents are confirmed (Fig. 9): Jebel Mrhila (WNW), and the Sbeitla region (WSW) where a tectonic sill separates the Hajeb basin from the Sbeitla basin, upstream. It is probable that the water transfers between the two basins mainly occur via the wadi Sbeitla and its alluvial aquifer, in a similar way to that observed near the Gafsa sill.

In addition to these two zones of recharge, already identified by the tritium contents, the carbon-14 contents show a third one, which is located in the region of Menaker, in the South. The modelled ^{14}C age of these groundwaters is close to zero, even if their tritium content shows the absence of any significant contribution of very recent recharge.

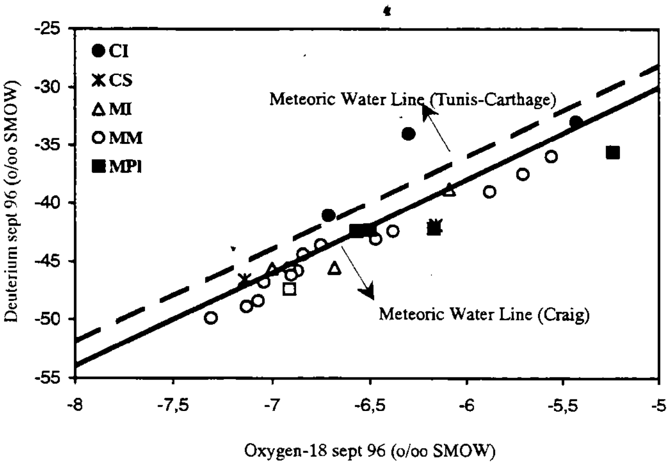

FIG. 8. Hajeb el Aioun – Djelma basin: $\delta^{18}O$ vs. $\delta^{2}H$ diagram for groundwaters sampled in september 1996.

The distribution of carbon-14 ages suggests that the flow velocities in the Eastern part of the basin (near the Hajeb sill) are lower than those observed in the western part (near recharge zones). For such a basin, it is quite surprising, since the flow rate at the outlet of the basin is essentially controlled by the hydraulic sill. In the hypothesis of a steady state flow (constant flow rate between the recharge zones and the sill), the decrease of the aquifer section due to the Hajeb sill, in the Eastern part of the basin, should be accompanied by an increase of water velocity, if the ratio permeability/effective porosity is constant (it seems to be practically the case, see [5]). Thus, it is difficult to explain the distribution of carbon 14 ages in steady state and the system would be in transient state, due to the increase of water exploitation in the Hajeb sill region. This disequilibrium suggests that exploitation exceed renewable resources. However, from the comparison between the distribution of ^{14}C ages obtained in 1972 and in 1996, it is difficult to assert that the situation has seriously changed, even if some slight modifications are observed, in particular in the Northern part of the basin. This relative constancy show that the system over-exploitation is still limited in comparison with the total reserves.

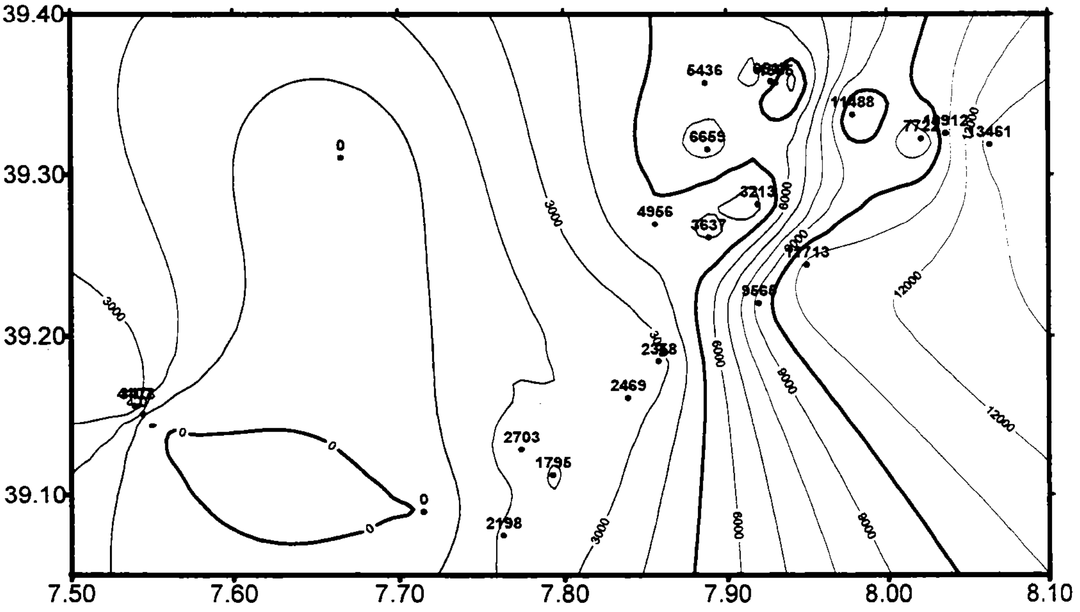

FIG.9. Hajeb el Aioun – Djelma basin: distribution of the ^{14}C ages (average ages for the samples taken in September 1996 and in May 1997 corrected using Ingerson and Pearson model [6].

5. CONCLUSION

The behaviour of the environmental isotopes used in this study (^{18}O, ^{2}H, ^{3}H, ^{14}C and ^{13}C) are quite different in the two systems.

In the North Gafsa basin, the modern/recent recharge is largely spread all over the basin and is locally identified in the different aquifer levels, even close to the main outlet of the system ("Gafsa sill"). Moreover, since groundwaters seem to be stratified in this region, it is difficult to reconstruct in details the lateral evolution of ionic and isotopic contents.

On the opposite, in the multilayered system of the Hajeb el Aioun-Djelma basin, the evolution of the environmental tracers is quite continuous, showing a relay between the different aquifer levels from the recharge areas towards the main outlet ("Hajeb sill"). Present-day water exploitation from the aquifers probably exceeds recent recharge, but the comparison between results obtained in the present study and those from a previous work, in 1972, shows that overexploitation is limited in comparison with the reserves stored in the system.

AKNOWLEDGEMENTS

This study was undertaken with the support of IAEA (Project TUN 8/012) and of CMCU (Coopération Inter-Universitaire Franco-Tunisienne).

REFERENCES

[1] FARHAT, H., MOUMNI, L., Etude hydrogéologique du bassin de Gafsa Nord. D.G.R.E, Tunis (1989) 179 pp.

[2] ILLY, P., Projet de planification rurale intégrée de la Tunisie centrale. Région de Gafsa-Maknassy, étude hydrogéologique préliminaire, F.A.O. (1967) 95 pp.

[3] COMPAGNIE AFRICAINE DE GEOPHYSIQUE, Etude hydrologique par prospection électrique du seuil de Gafsa, D.G.R.E, Tunis (1947) 16 pp.

[4] YERMANI, M., Géochimie isotopique et fonctionnement hydrodynamique des sources du seuil de Gafsa, D.E.A., Fac. Sc. Tunis (1995) 83 pp.

[5] KOSCHEL, R., Etude hydrogéologique de l'aquifère de Hajeb el Aioun - Djelma - Ouled el Asker, Rapport du projet 6520/7, Division des Ressources en Eau, Tunis (1980).

[6] INGERSON, E. , PEARSON F.J., Estimation of age and rate of motion of groud-water by the ^{14}C-method, *in* Recent researches in the field of hydrosphere, atmosphere and nuclear chemistry (MIYAKE Y. , KOYAMA T., Eds), Maruzen, Tokyo (1964) 263-283.

[7] FONTES, J-C., GARNIER J.M., Determination of the initial ^{14}C activity of the total dissolved carbon : a review of the existing models and a new approach, Water Resour. Res. 15 (1979) 399-413.

[8] EVANS, G.V., OTLET, R.L. DOWNING, A., MONKHOUSE, R.A., RAE, G., Some problems in the interpretation of isotope measurements in United Kingdom aquifers, Isotope Hydrology 1978, Vol. II, IAEA, Vienna (1979) 679-708.

[9] EICHINGER, L., A contribution to the interpretation of ^{14}C groundwater ages considering the example of a partially confined sandstone aquifer, Radiocarbon 25 (1983) 347-356.

[10] CRAIG, H., Isotopic variation in meteoric waters, Science, 133 (1961) 1702-1703.

[11] IAEA/WMO. Global Network for Isotopes in Precipitation. The GNIP Database. Release 2 May 1998. URL: http://www.iaea.org/programs/ri/gnip/gnipmain.htm

[12] MALIKI, MY. A., Etude hydrochimique et isotopique de la nappe profonde de Sfax, Tunisie (thèse, en préparation).

[13] GONFIANTINI, R., CONRAD, G., FONTES, J-C., SAUZAY, G., PAYNE B.R., Etude isotopique de la nappe du Continental Intercalaire et de ses relations avec les autres nappes du Sahara septentrional, Isotope Techniques in Groundwater Hydrology 1974, Vol.I, IAEA, Vienna (1974) 227-241.

[14] FONTES, J-C., GASSE, F., ANDREWS, J.N., Climatic conditions of Holocene groundwater recharge in the Sahel zone of Africa, Isotope techniques in study of past and current environmental changes in the hydrosphere and the atmosphere, IAEA, Vienna (1993) 231-248.

VALIDITY OF CHLOROFLUOROCARBONS (CFCs) AS AN AGE-DATING TOOL IN KARSTIC AQUIFERS, TAURIDS- SOUTHERN TURKEY

N. NUR ÖZYURT, C. SERDAR BAYARI
Hacettepe University,
International Research and Application Center for Karst Water Resources,
Ankara-TURKEY

Abstract

Chlorofluorocarbons are widely used in age dating of young groundwater systems. These gaseous compounds are produced and released into atmosphere via anthropogenic sources such as, leakage from refrigerators and pressurized deoedorant containers. CFCs have a well-defined atmospheric input functions that varies both spatially and temporally. Atmospheric CFCs dissolve in groundwater during the infiltration process. Once the amount of CFCs in groundwater and its recharge temperature is known, then the corresponding atmospheric partial pressure can be calculated to yield the recharge year. Groundwater's oxygen-18 content was used in this study to estimate the recharge temperature. Although, it is a practial and cheap method in age-dating, there are some factors that may inversely affect the potential use of CFCs. Basically, these are contamination from anthropogenic sources, entrapment of excess air, bio-degradation and, sorption over aquifer material. Though, it has been used in many non-karstic aquifer systems so far, validity of CFC age-dating has recently been tested in two large mountainous karstic aquifers located in the Taurids mountain range of Southern Turkey. Calculated "CFC ages" of groundwater were compared to other age-indicating parameters, such as, physical, chemical and isotopic characteristics. Variation of CFC ages were found to be in good agreement with them. Although, tracers CFC-11 and CFC-12 reveal the same ages for groundwaters with "CFC model ages" of 20 years or more, a clear deviation is observed in younger waters, CFC-11 ages being apparently erroneous. Unrealistically older CFC-11 ages in relatively young karstic groundwater has been attributed to removal of some initial CFC-11 by means of sorption over carbonate rocks. Although, the type of sorption is not clearly understood, it appears that the higher the solute concentration, the higher the sorbed amount.Moreover, correlation of CFC-12 and tiritium based ages in a large karstic spring has revealed essentially the same value which is around 8 years.

1. INTRODUCTION

Chlorofluorocarbons (essentially CFC-11 and CFC-12) have proven to be succesful in age-dating of young ground water in non-karstic systems [1,2,3]. The validity of this technique in large-scale (several thousand sq. km) karstic aquifers has been tested in two of the large-scale karstic basins of southern Turkey. The aim of this paper is to demonstrate the applicability of this technique in large-scale karstic aquifers and to discuss the results obtained. In order to control the validity of CFC ages other plausible age indicators were also evaluated. These age indicators comprise of physical (temperature, specific conductivity), chemical (dissolved oxygen, major ion content) and isotopic (tritium content) parameters. Water samples were collected for chemical, isotopic and CFC content from springs and artesian wells that are located along the inferred regional groundwater flow paths of the two large mountainous karstic aquifers (namely, Aladag and Beydaglari) of Taurids Mountain Range, southern Turkey.

2. MATERIAL AND METHOD

The data evaluated here is based on the samples collected in the dry periods of 1996 and1997. Temperature, specific electrical conductivity, pH and dissolved oxygen parameters were measured in-situ and samples for chemical analysis were collected in 150 ml, double capped PE bottles. Cation samples were acidified to pH ≤ 2 and those for anion were kept cool and analyzed immediately after arrival at laboratory. Major ion composition (i.e. Ca, Mg, Na, K, Cl, SO_4 and alkalinity) were determined according to standard methods. Deuterium, oxygen-18 and tritium contents were determined by the IAEA. Samples for CFC analysis were collected into 50 cm long copper tubes (ϕ= 1cm) which had been heated to 250 °C prior to sampling in order to remove possibly adhered CFC molecules. Three to six samples were collected from each sampling site to minimize the sampling error. CFC analyses were made in the University of Utah on a gas chromatograph equipped with electron capture detector and Porasil C column. A modified purge-and-trap technique was used to extract CFC gasses out of water and to inject them into the gas chromatograph [4]. Average measurement error of CFC analyses was found to be +/- % 3 corresponding to +/- 1-2 years (Dr. D. Kip Solomon, University of Utah, oral communication). Moreover, isotopic and chemical data given by previous studies have also been used in this study [5, 6].

3. CHLOROFLUOROCARBONS AS ENVIRONMENTAL TRACERS

CFCs are atmospheric gasses of anthropogenic origin which have been widely used in refrigerator and deodorant industry. No natural source of these tracers has been determined yet. CFCs are a crowded family of a number of compounds but, only CFC-11, CFC-12 and CFC-113 are used in age-dating studies. CFCs are chemically inert and therefore, have long atmospheric residence times. CFC-11 and CFC-12 could stay undegraded in the atmosphere for 75 and 120 years, respectively. They have been injected into atmosphere since their first synthesis in late 1940's. Atmospheric CFC concentrations have been observed at several globally scattered stations by NOAA since 1976. Pre-1976 concentrations have been precisely calculated on the basis of production data [7]. Therefore, temporal and spatial variation of atmospheric CFC partial pressures are well defined for elsewhere in the world (Figure 1). As with other gasses, the amount of CFCs dissolved in water is determined by the Henry's Law which relates atmospheric CFC partial pressure to dissolved CFC via a temperature dependent equilibrium constant. It is assumed that atmospheric CFC gasses are dissolved in ground water at the water table/unsaturated zone interface. Therefore, CFC age-dating method is based on the assumption that the groundwater is in equilibrium with atmosphere at the time of its last contact (i.e. recharge) with it. Since, the atmospheric CFC partial pressure is characteristic for a given year, the equilibrium CFC partial pressure (P_{CFC}) as determined from the gorundwater's CFC content (C_i) and relevant equilibrium constant (K_H) which is determined by recharge temperature indicates the time when the recharge water was in last contact with the atmosphere (Figure 2). Once the recharge year is known, the CFC "model" age of groundwater is calculated from the difference between the recharge and sampling years. Another major assumption in the CFC age-dating is that the initial CFC content is conserved throughout the flow of groundwater in the aquifer system. However, some processes such as, contamination from anthropogenic sources, bio-degradation, sorption over geologic/organic material, and entrapment of excess air during recharge. Biodegradation and sorption lower the initial CFC content and cause to increased ages whereas, contamination and excess air entrapment increase the CFC content and rise the CFC ages [8, 9, 10]. These processes may or may not be effective for a given groundwater system and their effect should be carefully examined.

4. STUDY AREAS

Locations of the two Mediterranean (Dinarid) type karstic aquifers of the Taurids Range, southern Turkey which are subject to this study are shown in Figure 3. These basins are comprised essentially of Paleozoic to Mesozoic aged platform type marine carbonate rocks which are highly karstified. The Taurus range which is a part of Alpine-Himalayan orogenic belt has been disrupted by lateral and vertical tectonic movements as characterized by numerous nappe settlement. As a result, karstic groundwater flow is controlled by the interplay of impermeable units and the tectonic discontinuities.

4.1. Aladag karstic aquifer

Aladag Karstic aquifer is located at the eastern part of the Taurus Range. Aladag Mountains located at the western part of the basin comprises the main recharge area for the karstic aquifer. Karstic groundwater flows from this part of the basin towards Zamanti River located to the east. Zamanti River flowing from north to south along the centerline of the study area is the main karstic erosion base. Mediterranean and Central Anatolian climates dominate in the basin. Mean annual precipitation ranges from 1100 mm at the south to 350 mm at the north. The geologic structure of study area comprises of four major tectono-stratigraphic sequences. Starting from the bottommost, Eastern Taurids autochthonous, allochthonous Aladag carbonate nappes, ophiolite nappe and the post tectonic units make up the geologic sequence. The contact between autochthonous and allochthonous is masked by an ophiolite nappe.

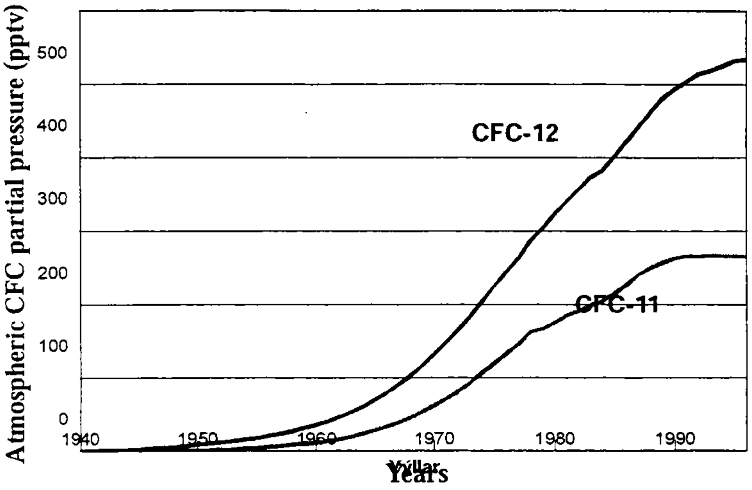

Figure 1: Temporal variation of atmospheric CFC content for the study area.

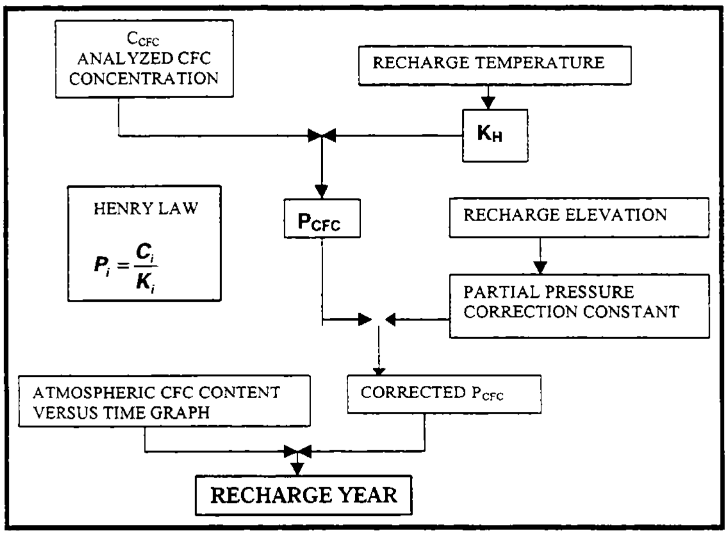

Figure 2: Routine followed to determine the recharge year based on CFC content.

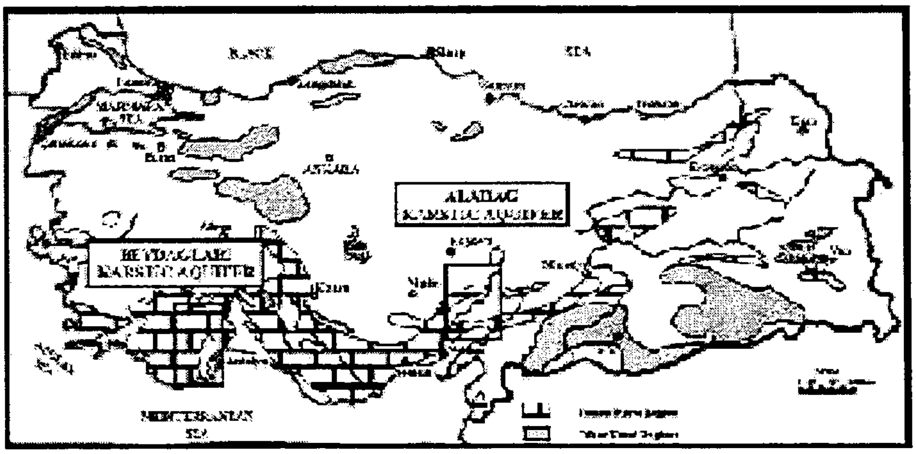

Figure 3. Location of aquifers within the Taurus karst range of southern Turkey.

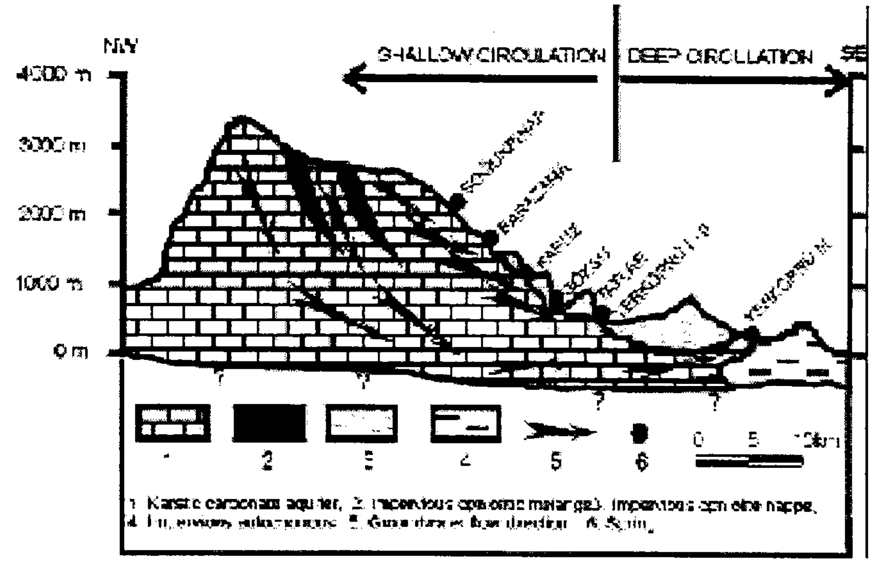

Figure 4: Scetch cross-section showing the position of springs along the regional flow path of Aladag karstic aquifer.

The dominant litologies of the karstic aquifer are limestone, dolomitic limestone and dolomite of allochthonous carbonates. Karstic aquifer is overlain by the the impermeable ophiolite nappe in between recharge area and the Zamanti River. Groundwater flowing from Aladag Mountains follows the routes that passes under the impermeable ophiolite cover for a distance of 10 km to over 40 km before arriving at the karstic springs. Karstic springs discharge from places where the regional groundwater flow path is dissected by tectonic barriers. Starting from closer to the recharge area karstic springs sampled during this study are Sogukpinar, Barazama, Kapuz, Goksu, Tatlar, Yerkopru-1, Yerkopru-2 and Yerkopru-3 (Figure 4). Among these, Yerkopru 1, 2 and 3 springs represent the deep flowing groundwater whereas, Sogukpinar, Barazama, Kapuz and Goksu springs discharge shallow component. The Tatlar spring is located in between shallow and deep parts of the regional flow system. Yerkopru springs are characterized by active travertine deposition which is an indicator of long residence time of groundwater.

4.2. Beydaglari (Finike) karstic aquifer

Beydaglari karstic aquifer located on the southwestern Turkey has a catchment area of aquifer 2765 km^2. The basin is almost totally made up of autochthonous Beydaglari carbonates unit which is surrounded by impermeable units from western and eastern borders. Main groundwater flow directions in the aquifer is toward Kýrkgoz and Duden springs located to the northeast and toward south where the Finike Plain is located. Mediterranean type climate is dominant in the basin. Mean annual precipitation ranges between 1000 mm at the coastal zone and 500 mm at the north. Highly karstified autochthonous mesozoic carbonates make up the major aquifer. Autochthonous miocene detritics which is overthrusted by carbonates in some places are the major impermeable lithologies that control the regional groundwater flow. The groundwater flow system is unconfined in nature in most of the aquifer system. Starting from the recharge area, groundwater flows over a distance of 10 km to 60 km before arriving at springs. Alike Aladag aquifer, here the karstic springs are located at places where the flow system is dissected by tectonic discontinuities either created by autochthonous miocene detritics or by surrounding impermeable nappe units.

As revealed from field observations and from chemical and isotopic data available, regional groundwater flow in the Beydaglari karstic aquifer circulates in shallow and deep flow paths before coming out of surface. Among the 11 groundwater sampling points selected, springs called Çatallar, Dumluca and Arifler are located more closely to the recharge area and therefore, represent the shallow circulating groundwater (Figure 5). Deðirmen, Mezar, Salur and Tekke springs are located in between shallow and deep groundwater effluents. Kýrkgoz and Duden springs discharging at northeast and the groundwater sampled in DSI and Esrefbahar wells at the south represent the deep flow component. Among the deep-flow springs, Kýrkgoz is characterized by travertine deposition.

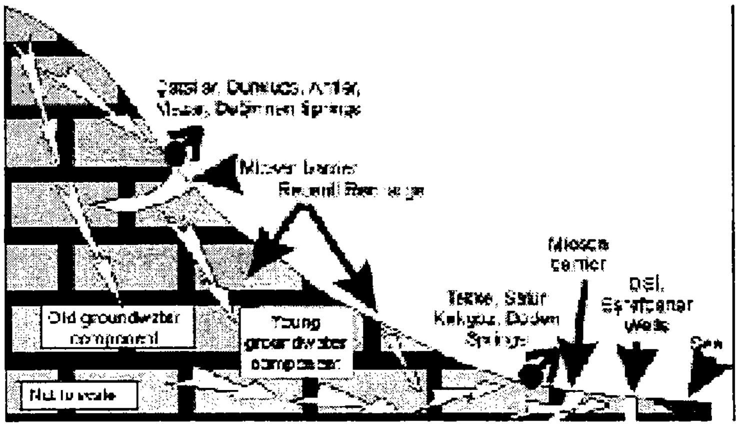

Figure 5: Scetch cross-section showing the position of springs along the regional flow path of Beydaglari karstic aquifer.

Aladag and Beydaglari aquifer systems represent two end-members in terms of recharge conditions. In the Aladag aquifer, recharge occurrs in the mountainous part and in between the recharge area and the springs the groundwater system is covered by an impermeable ophiolite nappe. However, in the Beydaglari aquifer, even though the recharge mostly occurrs in the mountainous part, the groundwater flow system is open to recharge along the flow path. Therefore, Aladag and Beydaglari aquifers are believed to represent confined and unconfined flow conditions, respectively.

5. CFC AGES VERSUS PHYSICAL, CHEMICAL AND ISOTOPIC CHARACTERISTICS OF GROUNDWATER

The CFC ages of groundwater samples have been correlated with other physical, chemical and environmental isotopic parameters which are also belived to be age-indicating (Table I and II). It was assumed that, for instance, temperature and total ionic composition should increase as long as the groundwater's residence time increases. Similarly, as organic matter accompanying groundwater after infiltration should decay by oxidation, initial dissolved oxygen is expected to reduce along the regional flow of groundwater.

5.2. Aladag karstic aquifer

Overall evaluation of the long-term hydrochemical data from discharges along the regional flow paths of both basins reveal that the flow of groundwater can be divided into two major components; shallow and deep-regional. Shallow groundwater has a short residence time and normally discharges from springs located closely to the recharge area. On the other hand, deep groundwater travels/resides longer in the aquifer and discharges from springs located at most distant points from the recharge area. Since the regional flow system is confined in the Aladag aquifer, changes in groundwater's physical and chemical properties depend solely on the in-aquifer evolutionary processes whereas, isotopic composition is determined by the conditions at the time of recharge.

Figure 6, shows the variation of some of the observed parameters along the regional flow path in the Aladag karstic aquifer. Starting from the recharge area toward the end of flow system (i.e. from Sogukpinar spring to Yerkopru-3 spring) temperature, pH, dissolved oxygen (DO) and electrical conductivity (EC) exhibit a plausible and systematic variation. Along the flow system, temperature increases steadily as a result of increasing geothermal heat gradient and residence time. Amount of dissolved oxygen (both as mg/l and per cent saturation) decreases probably due to organic matter oxidation either supplied from the soil zone or from the syngenetic sources in the carbonate rock. Degradation of dissolved oxygen by organic matter oxidation yields carbon-dioxide which in turn is converted to carbonic acid. As theoretically expected, this process should lower the pH and cause more carbonate mineral to dissolve along the flow path. As inferred from Figure 6, high inverse correlation between dissolved oxygen and pH suggests that this is a plausible proceess and leads to

Table I.: Physical, chemical and isotopic data evaluated in this study.

	Aladag Karstic Aquifer		Beydaglarý Karstic Aquifer	
	Shallow flow	Deep flow	Shallow flow	Deep flow
Temperature (oC)	3.09 – 8.15	13.42 – 14.93	7.9 – 10.2	15.0 – 17.3
pH	8.12 – 8.19	7.15 – 7.41	7.74 – 8.00	6.99 – 7.66
EC (microS/cm)	92.0 – 137.7	451 – 656	162 – 207	292 – 800
DO (mg/l)	11.29 – 12.23	8.02 – 8.49	9.5 – 9.9	0.9 – 6.2
Ca (meq/l)	1.048 – 1.297	3.293 – 4.092	1.497 – 1.896	2.071 – 8.084
Mg (meq/l)	0.123 – 0.329	0.782 – 1.152	0.411 – 0.699	1.111 – 2.469
Na (meq/l)	0.017 – 0.035	0.539 – 1.057	0.043 – 0.083	0.713 – 1.405
K (meq/l)	0.026 – 0.051	0.064 – 0.102	0.038 – 0.269	0.064 – 0.281
Cl (meq/l)	0.1 – 0.2	0.7 – 1.0	0.155 – 0.185	0.540 – 1.700
SO_4 (meq/l)	0.036 – 0.074	0.457 – 0.725	0.036	0.132 – 0.698
Alkalinity (meq/l)	1.090 – 1.544	3.818 – 4.544	1.826 – 2.384	2.788 – 10.691
^3H (TU)	14.8 – 20.8	20.7 – 22.3	10.2 – 12.2	0.7 – 5.5
$\delta^{18}O$ (‰ V-SMOW)	-11.17 - -9.65	-10.66 - -10.48	-8.6 - -8.3	-7.8 - -7.4
δD (‰ V-SMOW)			-51.0 - -47.6	-45.8 - -42.1

Table II.: CFC-11 and CFC-12 ages of groundwater discharges.

Aladag	Karstic Aquifer			Beydaglari Karstic Aquifer			
	CFC-11	CFC-12	*		CFC-11	CFC-12	*
Sogukpinar	22	1	21	Dumluca	20	11	9
Barazama	21	8	13	Mezar	24	24	0
Kapuz	9	7	2	Deðirmen	24	21	3
Goksu	21	8	13	Çatallar	21	1	20
Tatlar	25	23	2	Arifler	24	26	-2
Yerkopru-1	28	26	2	E°refbahar	31	31	0
Yerkopru-2	26	24	2	DSÝ	40	40	0
Yerkopru-3	28	26	2	Salur	25	19	6
				Tekke	24	22	2
				Düden	23	23	0
				Kýrkgöz	27	24	3

*: CFC-11 age minus CFC-12 age.

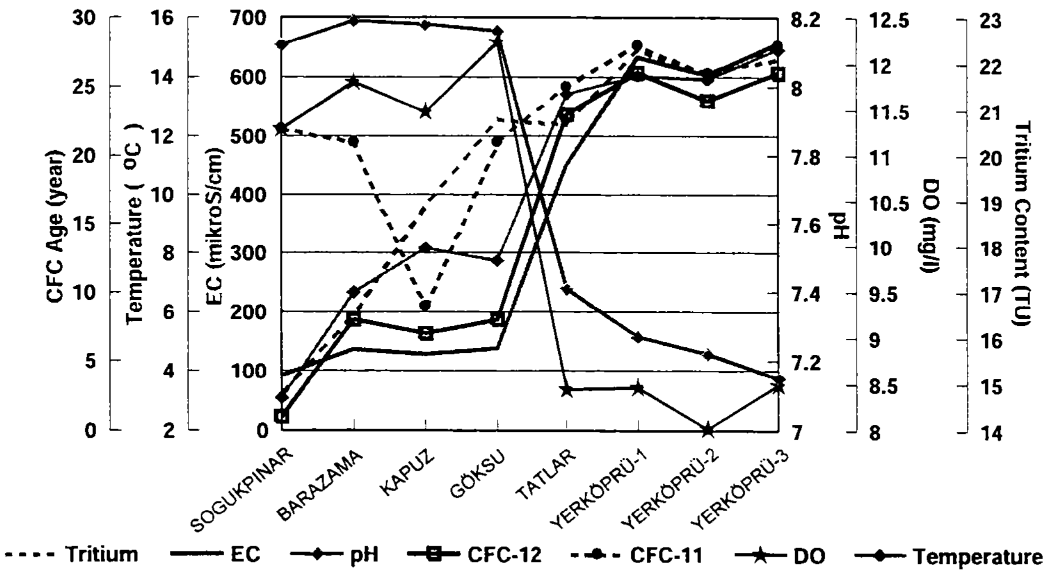

Figure 6: Relationship between CFC-11 and CFC-12 ages and other age-indicating parameters along the regional groundwater flow path of Aladag karstic aquifer.

more carbonate mineral dissolution which is also indicated by rising electrical conductivity (EC) values. All these variations reveal that groundwater becomes increasingly mature along the regional flow path as the residence time increases. This deduction is also supported by the variation of tritium content which exhibit a steady increase along the flow path. Contrary of usual expectation, tritium content is higher in older groundwater than in younger groundwater. This is simply because of the higher tritium input value in the past years. In other words, even though radioactive decay removes a part of the initial content, the tritium content of older groundwater is higher than those of younger because the older water has been fed by precipitation with high tritium.

CFC ages of the groundwater discharges are in well accordance with the variation of above explained parameters. Springs discharging at the beginning of flow system have typically low CFC-11 and CFC-12 ages than those located further downstream. CFC-11 and CFC-12 ages for the springs representing the shallow flow part (i.e. Sogukpinar, Barazama, Kapuz and Goksu) are 9-22 and 1-8 years, respectively. In the deep flow region (represented by Yerkopru-1, Yerkopru-2 and Yerkopru-3 springs) CFC-11 and CFC-12 ages range between 26-28 and 24-26 years, respectively. One of the validity checks in CFC age dating is the similarity of CFC-11 and CFC-12 ages. Under ideal circumstances, that is in the absence of factors that inversely affect the use of method, CFC-11 and CFC-12 ages have to be identical within the accuracy range which is +/-1 to 3 years. In the deep flow region, CFC-11 and CFC-12 ages match this condition within +/- 2 years. However, in the shallow flow region there is substantial difference between CFC-11 and CFC-12 ages in almost all springs except Kapuz. In this region CFC-11 ages are around 22 years whereas CFC-12 ages are around 8 years. Only in Kapuz spring CFC-11 and CFC-12 ages are similar within the analytical accuracy range. Moreover, these ages of Kapuz spring are also in accordance with the tritium age of 7 to 8 years which is based on the piston flow model. The large discrepancy observed in other shallow flow springs is attributed to the sorption of CFC-11 over aquifer rock. Although, there is limited research on the sorption trend of CFC's, it appears that CFC-11 tends to be sorbed by the carbonate rock. Unrealisitically high CFC-11 ages are observed only in younger groundwaters both in Aladag and in Beydaglari karstic aquifers. Here the definition "younger" is a relative term and is based on field observations and physical- chemical data. For example, Sogukpinar spring located at the beginning of shallow (and all) flow system is apparently discharging young groundwater as determined from its hydrogeologic position, physics and chemistry. However, the CFC-11 age calculated for this spring is 22 years which is obviously unacceptable. The other shallow flow springs in the order of their position along the regional flow path, that is Barazama and Goksu springs exhibit similar CFC-11 ages which is 21 years. From the previous research data it is believed that Barazama, Goksu and Kapuz springs are fed from the same karstic conduit system and discharge groundwaters which are physically, chemically and isotopically (i.e. tritium, deuterium and oxygen-18) identical [5]. Therefore, it may be assumed that the tritium age calculated for Kapuz spring which is 7 to 8 years should also be valid for Barazama and Goksu springs as well. Then, it appears that CFC-12 ages represent the realistic age for young groundwaters.

5.2 Beydaglari karstic aquifer

In the Beydaglari karstic aquifer, the shallow and deep flowing groundwaters are recognized easily by their tritium contents (Figure 7). Shallow (or young) groundwaters have typical tritium contents bwteen 10 TU and 13 TU while, deep groundwaters are characterized by less than 6 TU values. As expexted, low tritium groundwater discharges from low altitude springs which are more distantly located from the recharge area. Since the springs located at higher altitudes are more closely located to the recharge area, they discharge groundwater with short residence time as revealed from their tritium content which is around recent atmospheric precipitation's tritium content. In this respect, as indicated by their tritium contents, Kýrkgoz and Duden springs at the northeast and DSI and Esrefbahar wells at the south discharge the oldest groundwaters.

CFC-12 ages and tritium contents of groundwater samples from Beydaglari karstic aquifer are positively correlated indicating that CFC-12 ages are at least qualitatively in agreement with the residence time of groundwater. DSI well of Finike plain which exhibit the highest CFC-12 age (40 years) has also lowest tritium content (0.7 TU) among all groundwater samples. Similarly, low tritium groundwaters such as, Esrefbahar well, Kýrkgoz and Duden springs have CFC-12 ages older than 23 years. Moreover, the CFC-11 ages of these waters are exactly similar to CFC-12 ages.

However, in most of the shallow flow springs of Beydaglari karstic aquifer neither the CFC-12 nor the CFC-11 ages are in accordance with tritium contents of these waters. Although, not

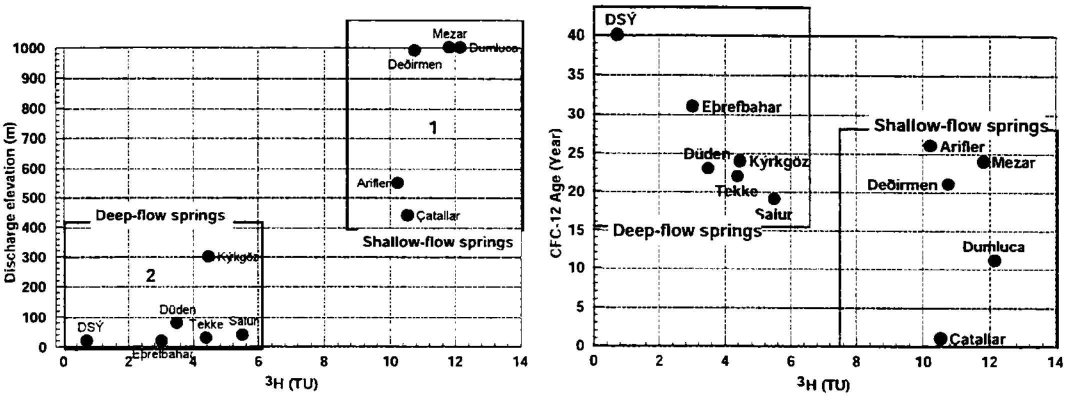

Figure 7: Comparison of discharge elevation and CFC-12 ages with tritium content of deep and shallow flow groundwater in Beydaglari karstic aquifer.

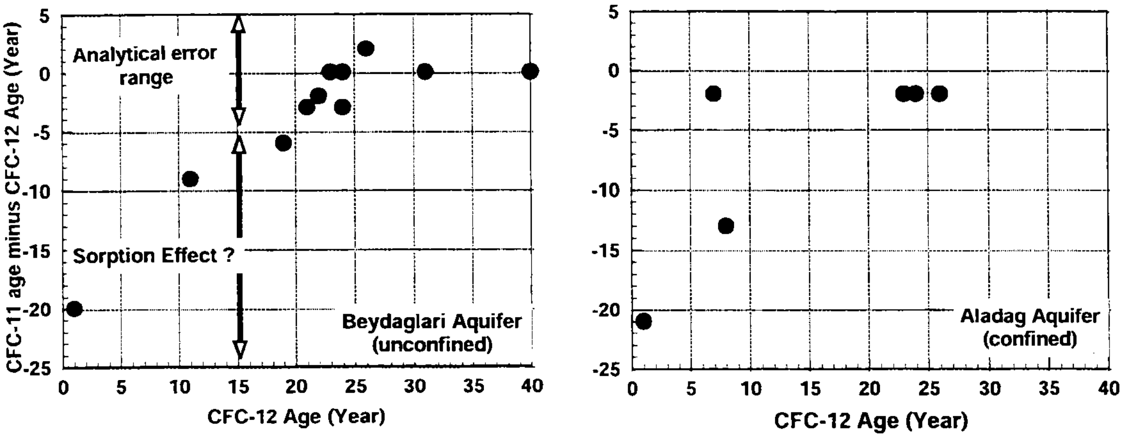

Figure 8: Variation of CFC-11 age minus CFC-12 age in Beydaglari and Aladag karstic aquifers.

discussed here, physical and chemical characteristics of these discharges clearly indicate that they have short residence times. This implies that CFC age-dating for the shallow groundwater been adversely effected and does not comply neither with tritium contents nor the physics, chemistry and hydrogeologic field conditions.

6. CONCLUSIONS

CFC tracers which have been used in non-karstic groundwater systems so far were found to be applicable equally well to the karstic systems. Relatively cheap and rapid analyses of these tracers are the major advantages over isotopic age-indicators such as, tritium and krypton-85. However, studies carried out in two large karstic basins reveal that even though, CFC-12 ages seem to be rather realisitic, CFC-11 ages could be highly misleading for young groundwaters fed rougly within last 15 years. CFC-11 and CFC-12 ages are almost identical and in accordance with the field observations for the groundwaters with CFC-12 ages older than 15 to 20 years. Nevertheless, a shallow groundwater sample's (Kapuz spring in Aladag aquifer) CFC-12 age were found to be in perfect agreement with the piston flow based tritium age. This suggests that, under isolated (confined) conditions, CFC-12 ages could be realistic for the young karstic groundwater as well.

A very large discrepancy observed between CFC-11 and CFC-12 ages of young karstic groundwaters investigated is attributed to the sorption of CFC-11 over carbonate rock (Figure 8). A study on CFC's affinity to get adsorbed over carbonate material suggests that CFC-11 has a larger adsorption tendency [9]. It is clear that more laboratory work is needed to test this hypothesis. As the age discrepancy between CFC-11 and CFC-12 increases as the groundwater gets younger, it is apparent that such a sorption of CFC-11 should follow a linear Langmuir isotherm. In other words, the higher the CFC-11 concentration the larger the amount adsorbed. If this is the case, than the applicability of CFC-11 in young karstic groundwaters would be highly restricted.

Furthermore, entrapment of excess air which would decrease the CFC age seems not to be an important process in the karstic aquifers investigated. This is probably because of the rapid infiltration of recharge water through large conduits in which capillary suction do not occurr. Similarly, as the the groundwater is oxygen rich throughout the whole flow system bio-degredation which rises CFC-11 age, were found not to be a plausible process.

ACKNOWLEDGEMENT

Authors thank to Dr. Kip Solomon and the University of Utah, Dept. of Geology and Geophysics, for their support for the CFC analyses.

REFERENCES

[1] Busenberg, E. and Plummer, L.N., 1992, Use of chlorofluorocarbons (CCl_3F) and (CCl_2 F_2) as hydrologic tracers and age-dating tools: The alluvium and terrace system of Central Oklahoma, Water Resources Research. 29, 2257-2283.

[2] Cook, P. G. and Solomon D.K. 1997. Recent advances in dating young groundwater: chlorofluorocarbons, $^3H/^3He$ and ^{85}Kr. Journal of Hydrology, 191, 245-265.

[3] Thompson, G. M., Hayes, J. M. and Davis, S. N., 1974, Fluorocarbon tracers in hydrology, Geophysical Research Letters, 1, 4, 177-180.

[4] Bullister, J.L., and Weiss, R.F., 1988. Instruments and methods for determination of CCl_3F and CCl_2F_2 in sea water and air. Deep-Sea Research, 35, 5, 839-853.

[5] Bayarý, C.S. and Kurttaþ,T. 1995, Geochemistry of regional groundwater flow in the Aladag karstic aquifer, Eastern Taurids-Turkey: Effect of flow conditions. DOGA Turkish Jounal of Earth Sciences, 4, pp. 29-37.

[6] Özyurt, N.N. ve Bayarý,C.S., 1998. Determination of groundwater age by means of CFC technique - 2: Karstic springs of Aladag aquifer, Earthsciences, Bull. of Earthsciences Research Center, Hacettepe University, 20, 139-154 (in Turkish).

[7] Gamlen, P.H., Lane, B.C., Midgley, P.M., and Steed, J.M., 1986. The production and release to the atmosphere of CCl_3F and CCl_2F_2 (Chlorofluorocarbons CFC-11 and CFC-12). Atmospheric Environment, 20, (6), 1077-1085

[8] Denovan, B.A., and Strand, S.E., 1992. Biological degradation of chlorofluorocarbons in anaerobic environments. Chemosphere, 24, 935- 940.

[9] Ciccioli, P., Cooper, W.T., Hammer, P.M., and Hayes, J.M., 1980. Organic-solute-mineral surface interactions: a new method for the determination of groundwater velocities. Water Resources Research, 16, 217-223.

[10] Heaton, T.H.E. and Vogel,J.C., 1981. "Excess air" in groundwater. Journal of Hydrology, 50., 201-216.

PALAEO-AGES OF GROUNDWATERS IN A FISSURED CHALK AQUIFER, UK

T. ELLIOT
School of Civil Engineering,
The Queen's University of Belfast,
Belfast. BT9 5AG. Northern Ireland.

Abstract

The Chalk aquifer in southeast England has a classic dual-porosity structure, with bulk advection occurring primarily in fractures/fissures, and largely immobile storage in the highly porous matrix blocks. For pumped samples, estimates of groundwater residence times using traditional geochemical correction models with ^{14}C-dating, and assuming that ages reflect mobile fissure water signatures, indicate late-glacial recharge ($\geq$25ka BP, pre-dating the Last Glacial Maximum (LGM) in the UK c.18ka BP) for groundwaters in the centre of the basin. Cooler recharge temperatures than for modern waters evidenced in environmental isotopic (δ^2H, δ^{18}O) and dissolved noble gas (Ne, Ar, Kr, Xe) contents confirm their palaeowater status. However, hydraulic age estimates for transit times from recharge are much younger (tens of years). Closer consideration of solute transport in the Chalk allows reconciliation of these apparently discordant ages. It is argued that, on the regional aquifer scale, environmental tracers in the fissured Chalk move as though in an Equivalent Porous Medium (EPM), with significant tracer retardation due to sorption and/or matrix diffusion effects. Downgradient trends in δ^{18}O and noble gases as independent tracers of past climatic changes can then be used to further constrain the groundwater ages better than for ^{14}C-dating alone. This approach points to a significant revision of groundwater ages in the aquifer; all ages are seen to reflect post-glacial recharge having occurred $\leq$13 ka BP. An important consequence of this revision is that it is suggested that traditional geochemical models potentially undercorrect for the full effect of hydrodynamic processes on tracer ages in fissured porous media like the Chalk.

1. INTRODUCTION

Hydraulic and isotopic groundwater ages should provide complementary information, and apparent discrepancies provide a valuable cross-check of the hydrologic system [1]. In regional aquifer studies, discrepancies have often been found between geochemically- and hydraulically-estimated groundwater ages which confounds both approaches. Mazor and Nativ [2] generally ascribe this as being due to the hydraulic estimates being invalidated by a number of uncertainties and pitfalls in defining the flow system, and suggest that geochemical estimates are preferable as their interpretation is "independent of flow assumptions". In this paper I seek to reconcile estimates of geochemical residence times based on the ^{14}C method with hydraulic transit time estimates in the important regional Chalk aquifer of the London and Berkshire Basins (UK), in the light of discussion of the large-scale solute transport properties of the fissured microporous Chalk.

1.1. Groundwater ages, hydraulic transit times and geochemical residence times

The age of a groundwater is defined as being the length the time the water has been isolated from the atmosphere [3]. The most widely-used method of estimating water age is the calculation of hydraulic transit times using Darcy's law combined with an equation of continuity. Geochemical methods rely on environmental tracers of the water dynamics. An "ideal" tracer is an analogue substance that behaves in the system exactly as the traced material as far as traced parameters of interest are concerned, but is characteristically distinct from that material [4]. Relevant tracer methods for groundwater dating involve, among other methods: (1) the "decay-clock" of radioactive nuclides (eg ^{3}H, ^{14}C) which have entered the water during contact with the atmosphere and subsequently which have become isolated in the subsurface; (2) the correlation of palaeoclimatic indicators (eg δ^{18}O, noble gases) in the waters with the known chronology of past climates. A tracer should have the same sources and sinks as the material of interest, but in practice other sources and sinks can exist if they can be accounted for. Tritium (^{3}H) sourced from thermonuclear testing in the 1950s/1960s potentially is an ideal tracer of water movement since it is a constituent part of the water molecule (also δ^2H, δ^{18}O) and can be distinguished based on its radioactivity, but it is still subject to self-diffusion and mechanical dispersion effects. Several radioactive tracers other than ^{3}H, of varying half-lives ($\tau_{½}$), have been proposed [3], but since dissolved solutes generally are not component parts of the water molecule they are not a direct tracer of water age itself and are subject both to the effects of hydrodynamic (eg diffusion, dispersion, retardation) processes and to further physico-chemical (eg sorption, volatilisation) and hydrochemical (eg chemical exchange, etc.) processes within aquifers which must be accounted for. Thus, we must generally distinguish the apparent transit time (tracer ages) of solutes affected by transport processes from the actual transit time of the mobile water (hydraulic ages) in aquifer systems.

1.1.1. Hydraulic (transit time) groundwater ages:

Predicated directly on the water movement itself, hydraulic age estimates are often based on a simplified Darcy's law. For the 1-D case in a steady-state continuous flow homogeneous aquifer system the mean water velocity, *v*, is simply:

$$v = v_{Darcy}/\Phi_{eff} = (K_h/\Phi_{eff}).(\Delta h/\Delta x) \qquad (1)$$

where v_{Darcy} is the Darcy flow velocity, K_h the hydraulic conductivity, Φ_{eff} the effective (inter-connected) porosity, and $\Delta h/\Delta x$ is the hydraulic gradient. The mean advective *hydraulic transit* (travel) *time* of mobile water is then simply $t_w = \Delta x/v$, which if traced along the flow path from the recharge area to the point of interest in the subsurface represents the mean age of the water, or system turnover time.

1.1.2. Geochemical (residence time) models and ^{14}C dating:

For regional groundwater systems, the most commonly applied dating tool is the radioactive isotope of carbon, ^{14}C ($\tau_{½}$=5730 years), incorporated continuously as $^{14}CO_2$ in groundwaters at recharge and dissolved as various inorganic carbonate (DIC) species dependent on eg pH conditions. A water's ^{14}C activity is assessed by precipitating out the total dissolved inorganic species (TDIC), and subsequent radiometric counting of its specific activity [disintegrations per minute, (dpm)/g]. This natural ^{14}C tracer is generally interpreted as having moved from the recharge area with the mean velocity of the water as if it were in a parcel, and reflecting the mean age of the water. The age or *residence time* of the water in the subsurface is then referenced to the decrease in activity along a flowpath from an initial activity, A_0, and following the radioactive decay law, $A_t = A_0.e^{-\lambda t}$, such that:

$$t = (\tau_{½}/\ln 2).\ln (A_0/A_t) \qquad (2)$$

where t is the *radiometric* or *radioisotope tracer age* of the water, A_t is the specific activity of the sample TDIC at time t. The coincidence of the two age estimates ($t = t_w$) will occur only for a steady-state continuous flow system with constant tracer input and a "piston-flow" model (PM) approximation of water and tracer movement [5]. The input function or initial activity of the tracer input to the system must be well-defined and the onus of the geochemical approach to deriving water ages from ^{14}C activities in groundwaters is the estimation of an appropriate modified "initial" activity, A_0, defined as its ^{14}C activity *after all chemical and isotopic processes have taken place and before any radioactive decay* [6, 7]. Eq.2 then yields the apparent geochemical age or subsurface residence time of the water, t_g. Although imprecise, compensating adjustments to A_0 traditionally have been made using chemical mass balance criteria for lumped geochemical models of carbonate congruent or incongruent mineral dissolution and ion exchange, and/or isotopic mass balances (eg ^{13}C) and their fractionation [7, 8]. For a "piston-flow" (PM) aquifer system, $t_g = t_w$. A presumption of many standard geochemical interpretations of groundwater ages is that they are generally interpreted robustly assuming a PM approximation of the tracer movement, yielding an "effective" hydraulic transit time from the geochemical estimate alone.

1.1.3. Solute transport models and effects on tracer ages

Notwithstanding the generally-adopted PM approach to ^{14}C dating in groundwaters, other simple but more realistic hydraulic models of the aquifer dynamics and tracer movement might be employed as being appropriate to prescribe ^{14}C transport in an aquifer [5]. Of these, the advection-dispersion model (DM) explicitly accounts for the effects of hydrodynamic dispersion on solute transport and can be applied to both steady-state and transient systems. In its simplest 1-D form in a homogeneous medium:

$$\frac{\partial C}{\partial t} = D_L . \frac{\partial^2 C}{\partial x^2} - v . \frac{\partial C}{\partial x} \tag{3}$$

where C is the solute concentration, D_L is the longitudinal dispersion coefficient in the direction of flow, v is the mean solution velocity, and x the spatial variable. The first component on the right-hand side represents dispersive mixing transport, and the second pure advective solute transport. To apply these more realistic simple hydraulic models to ^{14}C dating the statement of the geochemical definition for initial activities requires expansion to read that adjustments are made to correct A_0 which would be expected as a result of *all processes except radioactive decay and hydrodynamic effects* (ie dispersion, diffusion, retardation) [5]. An input function for a given hydraulic model would then have to be multiplied by the correction factor from a given correction model of the ^{14}C hydrochemistry to yield a geochemically-adjusted hydraulic age, t_g'. The corollary of this expanded definition of the "initial" activity (A_0) is that in general no geochemical or radioisotope method alone can yield the real age of a water unless these hydrodynamic effects are estimated independently [3, 10]. Potentially, therefore, discrepancies between the geochemical and hydraulic approaches might be evaluated and/or reconciled based on an estimation of the hydrodynamic effects, providing that solutions to the hydraulic equations are available to quantify the effects on the transit time of the given tracer or that an independent tracer is available on which to assess these effects [9]. Fortunately, although the transport of solutes in groundwaters is generally complex, simplified and approximate hydraulic (eg lumped-parameter) models can often be appropriately employed providing an analytical solution, and independent environmental tracers can be further used to validate models.

1.143. Independent environmental age tracers (δ^2H, $\delta^{18}O$ and dissolved noble gases):

Excepting in geothermal aquifers, δ^2H, $\delta^{18}O$ are conservative properties of the water mass during subsurface flow which can be related to the isotopic composition of the long-term weighted average precipitation at recharge, dependent on surface temperature [10]. Similarly, trace abundances of noble gases (Ne, Ar, Kr, Xe) dissolved from the atmosphere relate to the annual-average temperature at the base of the unsaturated zone and may be transported conservatively in aquifers [11]. Like ^{14}C, both tracers reflect a continuous atmospheric input source, barring any discontinuity in recharge. Signatures emplaced at recharge may be preserved in aquifers on the regional-scale such that downgradient groundwaters effectively act as an archive of past climatic changes which can be used as time markers to further constrain water ages [12]. Dissolved signatures significantly different from modern recharge values may indicate different climatic recharge conditions and potentially corroborate palaeo-groundwater ages, ie they may reflect past climate changes which for dated palaeowaters reflect surface paleotemperatures of recharge.

1.1.5. Solute transport models and effects on tracer ages in dual-porosity aquifers

In fissured aquifers, fractures are the main conduits for flow and transport; the matrix potentially controls the diffusive storage capacities for fluid, heat and solutes. The effects of mechanical dispersion and molecular diffusion on solute transport in groundwaters are well recognised, and matrix effects on solute transport in microporous fissured media have significant implications for groundwater dating [13]. Solute transport in fissured rocks with microporous matrices such as the UK Chalk is often modelled with reference to a single discrete conduit or fracture embedded in an infinite porous matrix or sets of regularly-spaced parallel planar conduits/fractures separated by a porous matrix, then solving Eq.3 for a dual-porosity (DP) medium with diffusive exchange and transport in the stagnant water of the matrix (single-fracture and parallel-fractures dispersion models, SFDM and PFDM respectively). Where appropriate a PFDM may be further generalised as two overlapping continous media representing relatively immobile porous matrix water and mobile fissure waters having diffusive exchange, for which the fissure component implicitly averages over many fractures [10, 15, 16]. If the characteristic time for diffusion in the matrix across the inter-fracture distance is small with respect to the timescale for fissure concentration changes such that fissures and matrix act in unison (ie quasi-equilibration) an equivalent porous medium (EPM) representation may be adopted, replacing both matrix and fissure porosities and permeability distributions and invoking instead simply a single homogeneous and continuous porous medium with lumped parameters characteristic of the fissured rock [15, 16]. An EPM representation can also be adopted appropriately when the timescale for change in the fissures is small compared to the characteristic time for diffusion across the fissure width such that the fissures system acts effectively independently of the matrix [14].

Following the input of a pulse of tracer into a PFDM fracture system, a point in the aquifer comes on a given time- and fissure length -scale when the initial rate of spreading of its concentration parallel to the fissures due to hydrodynamic dispersion decreases, but that by diffusion into the rock matrix increases to eventually dominate, providing effective retardation of the solute in the fissures through matrix exchange [15]. Three cases are then envisaged: (i) initially the solute diffuses into the rock as though it were infinite; (ii) eventually the influence of neighbouring fissures is felt and the diffusion processes is no longer independent, such that quasi-steady-state conditions may develop; (iii) finally, further downgradient the degree of interaction will be such that quasi-equilibrium may develop, and for long-term continuous and constant inputs the EPM system may become effectively "flooded" with the fissures concentration. These have been termed the "thick-rock", "transition zone", and "thin-rock" regimes, respectively [10, 16]. An EPM model is appropriate for the latter case where matrix and fissure transport effectively act in unison. For a pulse input of solute into the fissures system of an aquifer, the distance downgradient from recharge at which the "thick-rock" regime is dominant for conservative solute transport is simply given by [15]:

$$L_{tk} = 0.2 v_f \, ab/D_i \tag{4}$$

where, D_i is the intrinsic (bulk) diffusion coefficient of the matrix; D_p is the porewater diffusion coefficient; *a* is the fissure aperture width; *b* is the fissure spacing. More impoortantly, the "thin-rock" regime, ie quasi-equilibration between matrix and fissures concentrations, comes to dominate on a length-scale of $L_{tn} \geq 7.5 L_{tk}$ [15]. Sorptive effects of solid surfaces might also effect a further tracer retardation with respect to mobile water flow.

2. CONSIDERATIONS FOR SOLUTE TRANSPORT IN THE FISSURED UK CHALK

2.1. Geology and Hydrogeology of the London and Berkshire Basin Chalk, UK:

The fissured Chalk is a major groundwater source for public water supply both in the UK and in nearby parts of NW Europe. The geology and hydrogeology of the London and Berkshire Basins have been studied extensively [17]. The Chalk (Upper Cretaceous) is the principal aquifer. The Upper Chalk formation (70-170 m thick) is effectively more densely fractured with a higher permeability than both the Middle (45-79 m thick) and Lower (36-76 m thick) Chalk. The latter is underlain by the Upper Greensand (Lower Cretaceous), a minor aquifer. Up to 70 m of Gault Clay (Lower Cretaceous) forms the basal aquitard in both Basins. The confined aquifer system is overlain by up to 150 m of low hydraulic permeability Eocene clays (London Clay). The Chalk is a classic dual-porosity aquifer which stores relatively immobile water in the fine-grained interstitial microporosity of the matrix but transmits water via a more conductive fracture and fissure system. Only the upper 50-60m of the Chalk are fissured to any extent, forming the effective transmissive aquifer. Total fractional porosity is 0.15-0.45, with a matrix porosity $\Phi_m \approx 0.35$ on average, and a mean fracture porosity $\Phi_f \approx 10^{-3}$-10^{-2} based on three more or less orthogonal fracture sets [17]. Matrix permeabilities are low (10^{-4}-10^{-3} m.d^{-1}) because of very small pore throat diameters (<1 μm). In contrast the fairly uniform primary fissure system has permeabilities ~ 0.1-1 m.d^{-1}, which constitutes the effective flow system in the confined aquifer. Quarry and outcrop scanlines show that primary fractures in the Chalk are developed in three mutually perpendicular sets: one set (BP) roughly parallel to the bedding plane related to depositional fabrics, and two bedding-normal (BN) sets which are classic joints [17]. The BP set shows the greatest frequency (≈ 9.4/m on average) and a lateral persistence up to at least several km on average and act as "flow channels" in the Chalk [18]. The BN sets are less frequent (≈ 6.3/m) and less persistent, with traces rarely extending vertically beyond 3m and generally <1m. Effective *in situ* fracture apertures of 0.1 mm have been estimated for the Chalk based on dissolved ^{222}Rn contents in abstracted waters [17]. The fracture porosity arising from three sets of fissures of aperture $a \approx 10^{-4}$m, and fracture frequency N(=1/inter-fracture spacing *b*) ≈ 10 m^{-1} is $\Phi_f \approx 0.003$, which would impart a permeability in the transmissive Chalk $K_h \approx 1.1$ m.d^{-1} in line with that observed in the primary fissures system [17].

2.2. A "thin-rock" evaluation of the UK Chalk

It is instructive here to calculate the potential length- and time-scales for adoption of a "thin-rock"/EPM approximation for conservative solute (eg $\delta^{18}O$, noble gases) transport in the transmissive UK Chalk. The intrinsic diffusion coefficient for Cl^- in Chalk is $D_i \sim 10^{-5}$ m^2.d^{-1} [19], which yields a matrix diffusivity, $D_p \sim 3\times10^{-5}$ m^2.d^{-1}. Using $a = 10^{-4}$ m, $b = 0.1$ m and fissures velocity $v_f \sim 0.5$-5 m.d^{-1}

for the confined Chalk, then L_{tk} is reached within ~1 m, and quasi-equilibration occurs on a length-scale L_{tn} of ~10 m.

The different forms of solute transport behaviour in DP systems critically depend also on the relative timescales of the processes under consideration and the characteristic times for diffusion across the fissure and/or the matrix block [14]. The characteristic time for a conservative solute to diffuse over a given distance *x* is roughly $t_{diff} \approx x^2/D_p$. For an inter-fracture distance of 0.1m and matrix diffusivity of $3x10^{-5}$ $m^2.d^{-1}$, $t_{diff} \approx 0.9$ years (see also [13]). Molecular diffusive equilibrium across a block of Chalk a few metres thick could be established within a few thousand years, and under steady-state conditions of tracer input, fissure and matrix concentrations of a radioactive tracer will be locally similar if the solute $\tau_{½}$ is a thousand years or greater, cf ^{14}C. For a PFDM representation of a fissured microporous medium, the condition for a non-sorbing but radioactive solute under steady-state input to achieve quasi-equilibration across a porous matrix with an inter-fracture spacing, *b*, is $b \leq 0.5(D_p/\lambda)^{½}$ [9, 20], which for ^{14}C gives $b \leq 4.8$ m, much larger than the inter-fracture spacing of the Chalk primary fissures. Thus, quasi-equilibration of the system and a "piston-flow" model of solute movement in the transmissive zone may be an acceptable approximation in distal confined Chalk regions. For constant ^{14}C input, radiometric ages estimates in the distal portions downgradient from recharge should represent the average transit time taken over both fissures and matrix [14]. However, whereas it is reasonable to assume a more or less constant input function for ^{14}C to the aquifer, groundwaters also potentially carry signatures of the variable past climate emplaced at recharge (eg $\delta^{18}O$, noble gas RTs). The question remains whether input periodic oscillations such as climatic signatures could be preserved in the transmissive fissured Chalk aquifer on the regional-scale, such that the downgradient groundwaters effectively act as an archive of past climatic changes. In geological terms abrupt changes occur, eg climatic amelioration following the Last Glacial Maximum (LGM) and melting of the major part of the Devensian ice sheet required only 1000 years, and a similar timescale constraint for the short-lived cold-stage Younger Dryas interstadial ([21], and comments therein; cf Fig.1(i)}). Such changes would have to be "captured" in the aquifer system to preserve a climatic signature. In the transmissive aquifer, the characteristic timescales of ~1 year for conservative solute diffusion across the matrix ensure that perhaps decadal changes in climate signatures could conceivably be emplaced at recharge in the fissures flow whilst maintaining quasi-equilibrium conditions downgradient between fissures and matrix.

Thus, when solute transport extends much further from the recharge zone than these characteristic length- and time-scales of transport, then for the primary fissures set of the Chalk a distal region may be reached within the aquifer of quasi-equilibrium between the solute concentrations in the matrix and fissures which then act in unison. Sites towards the centre of the confined London Basin are ~tens of km from outcrop [16], much greater than the estimates of the length-scale L_{tn} from recharge, and an EPM approximation with matrix retardation for solute transport within the transmissive zone of the confined Chalk aquifer may be appropriately applied.

2.3. The effects of groundwater (dispersive) mixing

An analytical solution to the potential retardation effect of macrodispersion and matrix diffusion on the apparent relative solute velocity (v_a) and radiometric age ($t_a=x/v_a$) in the fractures within a fissured porous-medium aquifer has been derived for a PFDM under steady-state conditions with constant input of ^{14}C at recharge [23]:

$$t_f/t_a = v_a/v_f = [\gamma/2\{-1+[1+(4/\gamma)(1+\beta)]^{½}\}]^{-1} \qquad (5)$$

where $\gamma=v_f^2/\lambda D_f R$ expresses the advective and dispersive properties of the fractures; $\beta= \{\Phi_m.(R_{ap}.D_p)^{½}/(R_{af}.\lambda^{½}.a/2)\}.\tanh(\sigma\lambda^{½})$ is a relative measure of diffusive loss from fractures to adjacent matrix; t_f is the "true" radiometric age of the fissure waters ($=x/v_f$; neglecting dispersion and/or diffusion effects); $D_f=\alpha_L+D_0$ is the fissures hydrodynamic coefficient; α_L the longitudinal dispersivity in the fissures (Taylor dispersion; [24]); R_{af} and R_{ap} are retardation coefficients potentially arising as a consequence of linear sorption on surfaces both of fissure walls and within matrix pores, respectively; b is the inter-fracture spacing; $\sigma=.\ (R_{ap}.D_p)^{½}.(b-a)/2$. For α_L(Taylor) $\approx 1.2\times10^{-4}$ m, $D_f \approx 1.3\times10^{-4}$ $m^2.d^{-1}$, $v_f=5$ $m.d^{-1}$, $a=10^{-4}$ m, b=0.1m, $D_p=3\times10^{-5}$ m^2 d^{-1}, $\Phi=0.35$, $\lambda(^{14}C)=3.31\times10\text{-}7$ d^{-1}, and $R_{af} = R_{ap} = 1$ (non-sorbing solute) a *minimum* steady-state retardation factor ≈ *350* (= v_f/v_a) can be calculated.

The potential effect on relative ^{14}C ages of groundwater flow in a porous aquifer due to solute diffusion into a bounding thick aquitard (megadispersion) under steady-state conditions with constant input of ^{14}C at recharge can be estimated if the fissured transmissive aquifer is now treated as an EPM, and is conceptually equivalent to an SFDM approach [25]. The solution utilises Eq.5 for the ratio t/t_a for: $\gamma=v^2/\lambda D_m$; $\beta=\{(\Phi^*.D_p^{1/2})/(\lambda^{1/2}.\Phi.B/2)\}$; t (=x/v), the "true" radiometric age of the waters (Eq.2) neglecting dispersion/diffusion into the aquitard; v is the aquifer groundwater velocity; $D_m=\alpha_L v+D_p$ is the aquifer hydrodynamic coefficient, where α_L is the aquifer longitudinal dispersivity and D_p is the matrix diffusivity (tortuosity assumed same for both aquifer and aquitard); Φ and Φ^* are aquifer and aquitard porosities, respectively; B is aquifer thickness. For an EPM representation of the transmissive Chalk aquifer, $v=0.0143\ m.d^{-1}$, α_L(regional) ~100m [26], $D_m \approx 1.43\ m^2.d^{-1}$, $\Phi = \Phi^*=0.35$, and B = 50m. Thence, $\gamma= 432$, $\beta= 0.381$ and t/t_a (retardation effect) = *0.73*, ie apparently ageing the waters a factor ~1.4 times their "true" age. This estimate is two orders of magnitude smaller than the estimates of the potential retardation effect of matrix diffusion in the porous aquifer itself, ie matrix retardation within the transmissive zone of the Chalk effectively controls movement of the ^{14}C tracer.

For periodic climatic signals emplaced at recharge, the effect of internal mixing (macro-dispersion) within aquifers, is determined from Eq.3. The main features of a high-frequency $\delta^{18}O$ record of the last Devensian glacial/interglacial transition including the relatively short Younger Dryas interstadial event emplaced in a porous medium at recharge could be preserved within an aquifer for a value D_L/v_x^2 (the relative effects of dispersion versus advection) = α_L/v_x = 100 years and even for a value of 1000 years, although the latter is considerably smoothed [27]. For the Chalk, α_L (regional) ~100m and for typical advective velocities in the EPM ~0.5-5 m/yr (Eq.1) then $D_L/v^2 = \alpha_L/v$ = 20-200 years. Diffusive transversal exchange (megadispersion) potentially between the transmissive Chalk aquifer and the underlying less-permeable "thick-rock" Chalk aquifer and/or the overlying confining aquitard layers may also affect the climatic tracers. Neglecting longitudinal dispersion, the amplitude reduction due to transverse diffusive exchange with a bounding "aquitard" for a conservative, periodic sinusoidal climatic signature of constant amplitude, $|A_0|$, emplaced at recharge under steady-state conditions can also be estimated [28]. For a transmissive aquifer thickness, ~50 m (= B), "aquitard" thickness ~200m (= B*), and effective porosities of 0.35 ($=\Phi_B=\Phi_{B^*}$), the value of the dimensionless parameter K ($=B^*.\Phi_{B^*}/B.\Phi_B$) is 0.25. For an aquitard effective diffusivity = 0.01 m^2/yr, parameter b^* ($=B^*/D_p^{1/2}$) is 2000 $yr^{-1/2}$. A Milankovitch-type climatic oscillation of period 23000 years (cf [29]) has frequency $f=4.35x10^{-5}\ yr^{-1}$, giving $\theta=(4\pi f)^{1/2}=0.0234$. These values suggest a "decay constant" p of only $1.463x10^{-6}$ [28], ie the amplitude attenuation factor, $|A_x|/|A_0|$, x=20 km from the recharge area for an effective advective velocity in the aquifer 0.5-5 m/yr is only 1-5% Thus, diffusion into the bounding "thick-rock" aquifer(s) apparently would have little effect on the major climatic signatures of the last glacial cycle emplaced in the transmissive aquifer at recharge, although higher frequency oscillations would damp out more rapidly.

Finally, for a dual-porosity medium in which quasi-equilibrium exchange (EPM) occurs between the fracture and matrix porosity (Φ_f and Φ_m), the timescale ($t_a=\Delta x/v_a$) for relative migration of a non-sorbing conservative tracer pulse is greater than t_f more more simply according to [20]:

$$R_p = v_f/v_a = t_a/t_f = (\Phi_m + \Phi_f)/\Phi_f \approx \Phi_m/\Phi_f \qquad \text{(for } \Phi_m >> \Phi_f\text{)} \qquad (6)$$

where R_p is the retardation factor as a consequence simply of porous matrix diffusion independent of the fissure network geometry. Accordingly, the *apparent* velocity of a solute in the fissure system is retarded with respect to the hydraulic flow, $v_a = v_f/R_p$.

2.4. Effects of sorption and isotopic exchange

There is further potential for enhanced retardation in the aquifer of dissolved carbon isotopes (^{13}C, ^{14}C) through sorption and/or isotopic exchange in the presence of carbonate minerals [30]. Isotopic exchange may involve two different processes, both of which can occur essentially without changing the overall average DIC [8]: (a) solid-state diffusion of carbon isotopes through minerals driven by concentration differences between solid and aqueous phases, ie

$$^{12}C_{solid} + {}^{14}C_{aq.} = {}^{14}C_{solid} + {}^{12}C_{aq.}; \quad K(^{14}C/^{12}C) = [(^{14}C/^{12}C)_{solid}/(^{14}C/^{12}C)_{aq.}] \qquad (7)$$

where $K(^{14}C/^{12}C)$ is a pure thermodynamic constant, which effectively leads to a linear partitioning exchange process; (b) a dissolution-precipitation (recrystallisation) exchange processes. Whilst the latter process is accounted for through ^{13}C in many geochemical correction models, the former process and sorption reactions generally are not. For a PFDM of the Chalk: (a) retardation through possible adsorption on fissure walls may be assumed to be instantaneous, reversible and governed by a linear adsorption isotherm such that the apparent fissures velocity would be = v_f/R_{af}, where R_{af} is the retardation factor; (b) retardation through exchange reactions in the matrix is governed in part by the instantaneous equilibrium reaction following a linear adsorption isotherm and in part by a contribution from a kinetic reaction of the first-order taken to equilibrium, with respective retadation factors R_{ap} and R_{ak} such that overall $R_a = R_{ap} + R_{ak}$:

$$R_{ap} = 1 + (1 - \Phi_m).\rho.K_d/\Phi_m \tag{8a}$$
$$R_{ak} = k_1/k_2 \tag{8b}$$

where ρ is the rock density, $K_d = C_{solid}\,(g/g)/C_{aq}(g/cm^3)$ is the distribution coefficient for the equilibrium reaction, and k_1, k_2 represent the forward and backward rate constants of sorption, respectively [20]. The overall total retardation factor (R) caused by the effects of both matrix diffusion and adsorption processes at equilibrium in a "thin-rock" approximation is then

$$R = v_f/v_a = t_a/t_f = [R_{af}.\Phi_f + (R_{ap} + R_{ak})\Phi_m +]/\Phi_f = [R_{af}.\Phi_f + R_a.\Phi_m]/\Phi_f \tag{9}$$

For the case of negligible fissures adsorption ($R_{af} \cong 1$) and $\Phi_m >> \Phi_f$ then $R \approx R_a.R_p$. *Małoszewski and Zuber* [20] suggest values of $R_{af} \approx 1$, $R_{ap} = 2.7$, $R_{ak} = 19.4$, for ^{13}C adsorption in the fissured Chalk aquifer, and assume the same parameters to be relevant for $H^{14}CO_3^-$ transport.

Qualitatively, the potential effects of this enhanced retardation through sorption/exchange with solids for a reactive tracer (eg ^{14}C) is that a downgradient conservative stable isotope shift delayed through matrix retardation with respect to the hydraulic transit time (Eq.6) can occur much farther in the aquifer than reactive ^{14}C [9, their Fig.6]. Indeed, in an aquifer of limited extent an ^{18}O shift representing a climate change time-marker could be completely lost dongradient from the aquifer, whereas its ^{14}C signature retarded further by sorption effects is still preserved in the waters.

3. CONSEQUENCES FOR GROUNDWATER AGE INTERPRETATIONS IN THE UK CHALK

3.2. Geochemical evidence for groundwater ages in the UK fissured Chalk

The very large intergranular chemical storage of the Chalk matrix diffusively exchanges with the fissure flow system to an extent which depends on effective spatial permeability variations in the Chalk [31, 32]. This is clearly echoed in the geochemist's conceptualisation of the fissured Chalk system, but the Chalk is treated generally as being a "thick-rock"-type aquifer on the regional scale, diffusive exchange with the matrix blocks storage simply modifying downgradient chemistries in abstracted mobile fissure waters (cf [33], p.90]. Elliot et al. [16] have presented a comprehensive hydrochemical survey of UK Chalk groundwaters from both the London and Berkshire Basins, including supporting evidence for age dating by ^{14}C and ^{13}C geochemical modelling, and for characterising the climatic conditions at recharge (δ^2H, $\delta^{18}O$, noble gases). A range of standard geochemical adjustment models have been applied to the initial ^{14}C activities of these waters (Table 1), along with a recently adopted model correcting the ^{14}C activities simply for the effect of admixture of ^{14}C-dead porefluids in carbonate equilibrium with the Chalk matrix. The resulting values from the geochemical models (c)-(f) (Table 1) give corrected ^{14}C ages generally in good agreement, suggesting residence times up to 25ka BP in the confined centres of both Basins; noble gas-derived recharge temperatures (RTs) for these waters are 3-5°C cooler than modern values and are supported by lighter stable isotopic signatures, confirming a significant groundwater component recharged under a different climate than present. Based on geochemical considerations alone, with tacit adoption of a "thick-rock" conceptualisation of the Chalk, these water ages have been interpreted as indicating a discontinuous flow system, and that on the regional-scale Chalk matrix blocks have stored a chemical signature emplaced during an extended cool period of recharge in an interstadial preceding the Last Glacial Maximum (LGM) in the UK during the Devensian at 18ka BP [16]. Following climatic amelioration in the Holocene after the LGM, this stored component was released through diffusive

TABLE 1. GEOCHEMICAL MODELLING OF C-14 AGES (t_g) FOR CHALK GROUNDWATERS [16]

No Name	$\delta^{13}C$	^{14}C	Model ages in ka						RT	$\delta^{18}O$
	(1)	(2)	(a)	(b)	(c)	(d)	(e)	(f)	(3)	(4)
London Chalk: unevolved groundwater										
LN22 u Burnham PS	-14.0	60.8	3.8	-0.01	-0.9	-0.8	-2.0	-1.0	9.7	-7.4
				100	111	110	127	112		
LN01 u George Payne Ltd, Croydon	-13.6	66.2	3.1	-0.6	-1.8	-1.7	-2.7	-1.8	12.5	-7.4
				107	124	123	139	124		
LN06 c Unigate Dairies, Vauxhall	-12.8	12.6	16.8	11.9	11.6	11.6	11.0	11.4	10.9	-7.2
LN05 c National Sunlight Laundry, Brixton	-8.7	14.6	15.5	10.8	7.7	7.7	7.3	7.5	10.2	
LN21 c Pinewood Studios, Iver Heath, No.1	-8.6	20.8	12.6	8.4	4.7	4.7	4.3	4.6	9.8	-7.3
London Chalk: evolved groundwater										
LN07 c Harrods SW1 No.2	-4.8	17.1	14.3	9.2	2.8	2.6	2.2	2.7	9.5	-7.4
LN04 c Modeluxe Linen, Wimbledon	-3.8	4.5	25.8	21.0	13.9	13.8	13.4	12.6	9.2	-7.4
LN08 c Buchanan House SW1	-3.6	4.3	25.7	21.0	12.5	12.2	11.9	12.6	8.7	-7.3
LN12 c Hornsey Rd Baths N7	-2.6	1.4	35.0	29.7	20.4	20.0	19.7	20.7	5.8	-7.7
LN13 c Kentish Town Baths NW5	-2.6	0.8	39.6	34.4	25.0	24.7	24.3	24.9	5.4	-7.8
LN24 c Neville & Griffen, Slough	-2.5	1.9	32.4	28.1	17.7	17.5	17.1	17.6	7.8	-7.3
LN11 c Unilever plc, EC4 No.2	-2.5	1.0	37.7	33.0	23.0	22.6	22.3	22.9	6.8	-7.6
LN09 c Dorset House NW1 No.2	-2.4	0.8	39.5	34.7	24.7	24.3	23.9	24.6	7.1	-7.8
LN19 c Kodak plc, Harrow	-2.1	3.8	26.7	22.9	11.2	10.8	10.5	11.2	6.8	-7.4
LN17 c Glaxo plc, Greenford	-1.7	1.1	39.5	35.3	22.2	21.7	21.3	22.1	7.5	-7.4
LN14 c Crown Cork plc, Southall	-0.9	1.1	36.9	32.7	20.7	20.3	19.9	20.7	5.5	-7.7
Berkshire Chalk: unevolved groundwater										
BK01 u Boxalls Lane PS, Waverley, No.13	-13.7	60.4	3.8	-0.1	-1.0	-0.9	-1.9	-1.0	9.4	-7.0
				101	112	112	126	112		
BK22 u Brightwalton PS	-13.7	62.1	3.6	-1.0	-1.2	-1.1	-2.2	-1.0	10.5	-7.7
				113	116	114	130	113		
BK04 u West Ham PS	-13.5	78.5	1.7	-2.7	-3.2	-3.2	-4.1	-3.3	9.7	-6.9
				138	148	147	164	150		
BK08 c Little Park Farm, Mortimer	-13.4	22.9	11.9	6.7	6.9	7.0	6.1	6.8	6.7	-7.2
BK19 u Star Works, Knowl Hill	-13.2	70.7	2.5	-1.9	-2.5	-2.5	-3.2	-2.6	13.1	-6.7
				126	136	136	148	140		
BK20 u Theale PS	-12.3	55.4	4.5	0.6	-1.0	-1.0	-1.3	-1.1	9.7	-7.4
					113	112	117	114		
BK03 u Greywell PS	-10.1	68.7	2.8	-1.7	-4.1	-4.1	-4.5	-4.3	9.6	-7.0
				123	165	164	172	167		
BK21 u Chievely PS, Down End	-8.1	56.3	4.4	-0.2	-3.9	-3.9	-4.3	-4.0	9.1	-7.8
				102	161	161	168	163		
Berkshire Chalk: evolved groundwater										
BK15 c Toutley PS No.2	-6.1	1.4	35.0	29.8	24.8	24.8	24.4	24.7	4.4	-8.1
BK16 c Beenham PS, Beenhams Heath, No.1	-5.6	6.6	22.1	17.3	11.5	11.5	11.1	11.3	5.1	-7.5
BK06 c Sherfield Manor School	-3.0	3.4	27.6	22.6	13.7	13.4	13.1	13.6	7.5	-7.3
BK11 c Ufton Nervet PS	-3.0	2.6	29.8	25.2	15.9	15.7	15.4	15.8	8.3	-7.2
BK12 c Grazeley PS	-2.1	1.1	36.9	32.0	21.5	21.2	20.8	21.4	6.3	-7.8
BK14 c Food Research Institute, Shinfield	-0.4	1.9	32.4	27.5	12.9	12.2	11.9	12.8	5.7	-7.7

PS = Pumping Station; (1) ±0.1‰ referenced to PDB; (2) % modern carbon; c = confined; u = unconfined; (3) recharge temperatures (RT) derived from dissolved noble gas contents, °C; (4) ±0.1‰ referenced to SMOW. C-14 models: (a) calculated for equilibration of TDIC with soil CO_2 (open system or uncorrected age); (b) Tamers model calculated for 50% of TDIC derived from rock carbonate; (c) Pearson and Hanahaw model calculated for isotope dilution of ^{13}C and ^{14}C by rock carbonate; (d) Wigley/Evans model calculated for initial derivation of 50% of TDIC from rock carbonate, see (a), followed by incongruent exchange between TDIC and rock carbonate [7]; (e) calculated for initial congruent dissolution of rock carbonate involving no decay, followed by incongruent mixing with ^{14}C-dead; pore fluids in equilibrium with the carbonate matrix [16]; (f) Reardon and Fritz model calculated for chemical evolution from recharge conditions to the observed groundwater pH, TDIC, and $\delta^{13}C$ values of the groundwater. The Fontes and Garnier correction model [6] has also been applied [34], but proved unreliable for relatively heavy $\delta^{13}C$ values encountered in the Chalk, generating unrealistically young or negative model ages. Where corrected model ages are negative reflecting modern ages then following lines represent an estimate of the samples initial activity.

admixture back into more recent fissure waters on resumption of active aquifer circulation. Thus, waters towards the centres of both Basins with cool recharge signatures are taken to reflect significant admixture of a stored pre-Devensian cold recharge component with warmer waters infiltrating the fractures during the Holocene [16].

3.2. Hydraulic ages and apparent tracer ages in the Chalk

The average fracture transit time for simple laminar plug-flow in planar fractures of length Δx may be calculated from:

$$t_f = x/v_f = (12\eta/\Delta P)(\Delta x/a)^2 \qquad (10)$$

where η is the fluid dynamic viscosity (~1.3×10^{-3} N.s.m^{-2} for water @ 10°C), and ΔP is the pressure differential along the fracture of aperture a and length x. Present piezometric conditions in the London Basin suggest $\Delta P \sim 100$ m head (= 1 MPa) downgradient along a major flow axis (x=20 km) [16, their Fig.1], although this replects pumped aquifer conditions and natural system gradients would be less. Past overexploitation of the aquifer has intensified the natural gradient along the major flow axes [34]. The transit time for "mobile water" (fissure) flow into the central basin through "parallel-plate" fracture apertures of $a=10^{-4}$m, at a spacing of 0.1m is then only 20 years (Eq.10). This represents a an initial hydraulic transit time estimate of water ages on the regional aquifer scale, which assumes that advected solutes in the fissures are unaffected by the presence of any "stagnant" matrix waters. For comparison, a similar estimate for flow in the matrix system using Eq.1 for $\Phi_m=0.35$, $K_h=10^{-3}$-10^{-4} m.d^{-1}, and the same hydraulic gradient, $\Delta h/\Delta x = 100/20000 = 5.10^{-3}$, yields a hydraulic transit time of 3.8-38Ma. The initial fissure hydraulic estimates (Eq.10) are clearly discordant with the geochemical estimates (Table 1).

However, if the the transmissive Chalk is treated as behaving as a "thin-rock" aquifer, represented by an EPM with matrix retardation of solute transport within the aquifer, the corresponding value (Eq.6) of $R_p \approx 120$ for $\Phi_f \approx 0.003$ implies that an effective mean transit time for injection of tracer with advective flow in the fracture of up to 2400 years. Adoption of fracture apertures of ~5.10^{-5} m, which may be supported by some higher Rn-contents in the Chalk waters [17], would yield $\Phi_f \approx 0.0015$, $t_f = 80$ a, $R_p \approx 234$, and therefore a retarded solute transit-time potentially up to 19 ka (Eqs.6 and 10). For porous fissured media for which an EPM representation may be appropriate, the alternative estimation of the solute travel-time by Darcy's law (Eq.1) based on the mobile water reservoir in the fissures alone (Φ_f) is inappropriate [13]. Since transit time of the tracer solute (t_a) can be approximated for fissured media exhibiting quasi-equilibration with the matrix waters by substituting v_f of Eq.6 in Eq.1 with $\Phi_{eff} \approx \Phi_f$, and rearranging:

$$t_a \approx (x\Phi_m/K_h)/(\Delta h/\Delta x) \approx \Phi_m(\Delta x)^2/K_h\,\Delta h \qquad (11)$$

where K_h is the observed field hydraulic conductivity. Equation (11) is easier to handle than Eqs. (6) and (10), since it utilises field K_h values and is not directly sensitive to fracture aperture estimates. The effective transport of the solute is represented instead by an analogous "piston-flow" model controlled by the larger volume of the matrix porosity (Φ_m), ie by the Darcy velocity in the equivalent porous medium. For a hydraulic gradient, $\Delta h/\Delta x = 100/20000 = 5.10^{-3}$, $\Phi_p = 0.35$ and a reasonable hydraulic conductivity for the confined Chalk aquifer of 1.0 to 0.1 m.d^{-1}, Eq.11 implies apparent conservative solute tracer transit times (t_a) to the centre of the London Basin corresponding to $R_p \approx 190$ could be ~3.8 ka up to 38 ka. Such estimates potentially explain the modelled (Table 1) geochemical residence times although they do not help constrain individual ages. Nevertheless, these enhanced hydraulic tracer age estimates suggest that there has been potentially sufficient time for the "capture" or "recording" of signatures of climatic changes up to/over the period of the LGM.

3.3. Independent environmental tracers of groundwater ages in the Chalk

Because ^{14}C may further exchange and react with the Chalk matrix as well as being retarded, downgradient, shifts in more conservative parameters eg stable isotope signatures of water (δ^{18}O, δD) and/or dissolved noble gases may provide a more reliable indicator of the relative ages of water in fissured aquifers exhibiting matrix diffusion effects than ^{14}C ages alone (cf [9]). Both δ^{18}O contents and noble gas derived RTs for the Chalk waters are plotted against ^{14}C ages estimated using column (f) in Table 1 with a range of ±1ka, which encompasses all geochemical model ages (c)-(e) in Fig.1.

Recharge to the Chalk is controlled predominantly by the matrix flow which feeds/exchanges with the fissures system in the saturated zone yielding stable isotopic reflecting averaged climatic conditions [10]. Noble gas-derived recharge temperatures (RTs) in modern groundwaters from the unconfined Chalk similarly reflect the long-term mean annual surface temperature for the region [16]. Trends to cooler recharge temperatures in both noble gas RT and stable isotope signatures with increasing ^{14}C age are apparent for the older waters, which look remarkably similar to independently-derived surface temperature trends for southern England of surface temperature variations over stages I-III of the LGM, Fig. 1(i). These latter trends derived from fossil beetle assemblages [22] are generally characterised by lower temperature accuracy than for groundwater signatures, but have intrinsically a much better time resolution. If the transmissive Chalk aquifer effectively functions as an EPM on the regional scale, downgradient apparent age trends in groundwater climatic indicators may reflect directly the change of climatic conditions emplaced at recharge in a "piston flow" aquifer. On this basis a match of the trends seen in δ^{18}O and/or noble gas derived RTs (Figs. 1(ii) and (iii)) to stages I-III of Fig. 1(i) suggests that all of these climatic signatures have been emplaced post-glacially during the warming phase out of the LGM, ie the groundwaters all have residence times <13 ka BP,

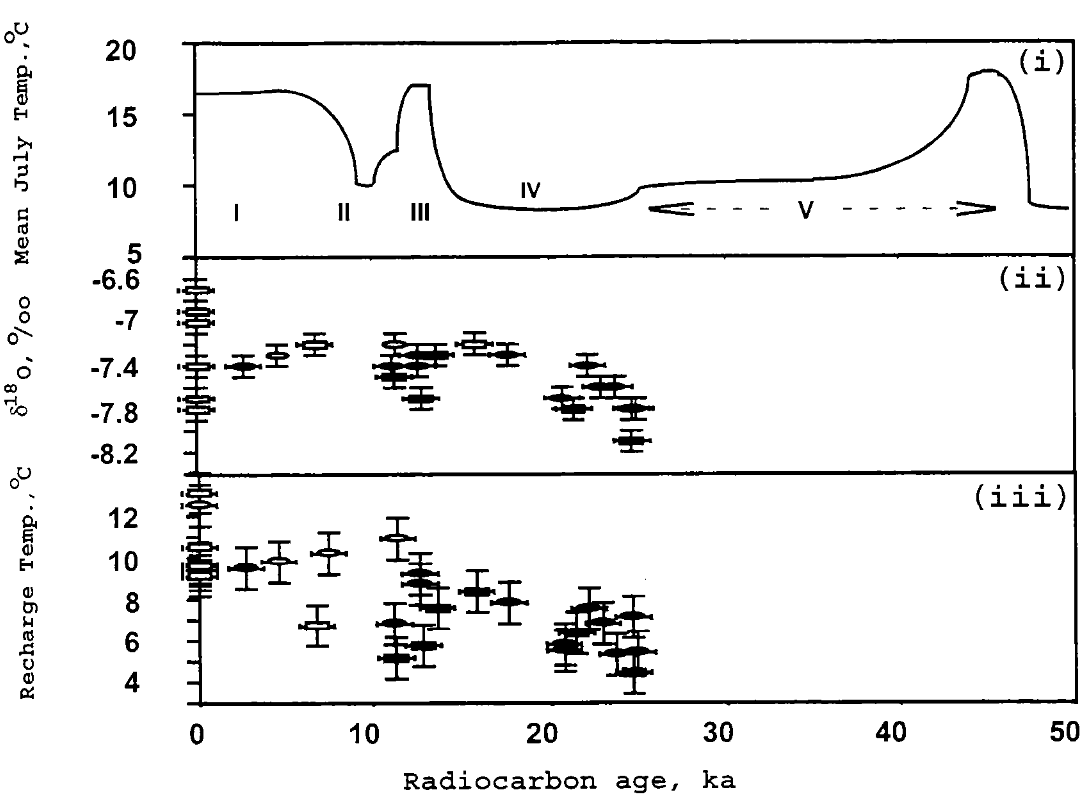

FIG. 1. (i) southern England mean July surface temperatures reconstructed from fossil beetle assemblages [22]: (I) Flandrian (Holocene); (II) Younger Dryas (Loch Lomond Readvance); (III)Windermere Interstadial; (IV) Devensian Last Glacial Maximum; (V) Upton Warren Interstadial Complex; (ii) $\delta^{18}O$; and (iii) noble gas derived recharge temperatures (RTs, °C) vs. geochemically-corrected radiocarbon ages (Table 1, column (f)). Error bars are $\pm 2\sigma$.

consistent also with the retardation-enhanced range of hydraulic ages. Intermediate water ages showing also cold-stage RT values might then reflect the transient deterioration in climate of Younger Dryas (stage II, Fig. 1(i)) at ~11ka prior to establishment of the Holocene optimum

A consequence of adopting this EPM model of solute transport in the regional fissured Chalk aquifer, is that standard geochemical ^{14}C models for the oldest waters in the centres of these Basins give ages apparently a factor of 2 older than discussed here, implying a further retardation effect other than matrix retardation in the groundwater more than has been geochemically-corrected. The factor of 2 is similar to the estimate of the retardation factor for dispersion of ^{14}C into a bounding aquitard, but such effects are potentially already corrected for in the geochemical models through ^{13}C. Since the effect arises from comparison between conservative and reactive solutes, with the ^{14}C apparently retarded (aged) more than the $\delta^{18}O$, noble gas signatures, the further retardation correction required for the geochemical ages may reflect sorptive processes in the aquifer (cf R_{ap}; [20]), All of the chemical/isotopic adjustment methods applied to the ^{14}C ages based on the traditional geochemical models alone (Table 1) apparently undercorrect the Chalk groundwater ages for the full effect of retardation due to physico-chemical hydrodynamic effects in a fissured porous medium.

4. SUMMARY AND CONCLUSIONS

Discussion of appropriate conceptual models for natural tracer transport in the fissured UK Chalk has highlighted that at the regional-scale the transmissive aquifer may be represented as a "thin-rock" solute transport regime, such that quasi-equilibration in solute concentration occurs downgradient because of diffusive exchange between the mobile fissure waters and the relatively stagnant matrix waters. Simplified geometry lumped-parameter PFDM and/or EPM approaches to approximating solutions to tracer transport may be adopted for the distal confined aquifer. Under steady-state conditions, effective fissure transport of tracer solutes in the transmissive Chalk can be represented by an analogous "piston flow" in an EPM controlled by the larger volume of the matrix porosity. If there are no further effects other than physical matrix retardation, radiometric ages estimated from ^{14}C should reflect therefore the average transit time appropriate for conservative solute transport from source to sampling point taken over both fissures and matrix and so generally reflect a matrix retarded tracer age for solute transport in the fissured Chalk and not the age of mobile water in the system derived through Eq.1.

Direct consideration of the solute transport of dissolved $\delta^{18}O$ and/or noble gases in the fissured Chalk shows that these conservative tracers may preserve the record of emplacement in the transmissive aquifer of climatic signatures (surface temperature change) at recharge potentially over the last glacial/interglacial transition. Downgradient age-dependent climatic trends may be used as independent time markers in the aquifer to help validate the groundwater ages in comparison with surface palaeotemperature trends derived independently and having greater time-resolution. This interpretation suggests that all groundwater signatures from the London and Berkshire Basins were recharged following the last Devensian glaciation. Apparent tracer ages of up to 13ka BP show that conservative solute transport in the fissured aquifer is significantly retarded with respect to mobile water flow due simply to matrix diffusion.

While standard geochemical models are applicable to the Chalk which themselves are based on "piston flow" model of ^{14}C transport in porous media and which adjust radiometric ages for the reactive effects and hydrochemical processes to give implied residence times for waters, these do not necessarily adequately correct for all of the further specific chemical effects (eg sorption) on solute retardation of ^{14}C and so cannot be used with precision directly for individual ages determinations. Comparison with the combined hydraulic and conservative environmental tracers ($\delta^{18}O$ and/or noble gases) suggests a significant revision of the published geochemical age interpretations *viz.* that for the oldest water ^{14}C ages corrected by standard geochemical methods (~25 ka BP) overdetermine the potential tracer ages of conservative solutes by a factor of around two, which is explained by undercorrection for further (sorptive ?) retardation effects on ^{14}C transport in the fissured Chalk. A hydrodynamic correction to ^{14}C ages based on geochemical corrections alone is necessary for groundwater dating in fissured porous carbonate aquifers.

Acknowledgements: I am grateful to Mick Riley and Paul Younger (Water Resource Systems Research Laboratory, Newcastle University) and Bob Kalin (Environmental Engineering Research Centre, QUB) for insightful discussions.

REFERENCES

[1] TORGERSEN, T., "Hydraulic calculation of groundwater flow velocity and age: explanation of the basic premises - comment", J. Hydrol., **154** (1994) 403-408.

[2] MAZOR, E., NATIV, R., "Hydraulic calculation of groundwater flow velocity and age: explanation of the basic premises", J. Hydrol., **138** (1992), 211-222.

[3] DAVIS, S.N., BENTLEY, H.W., "Dating groundwater", Nuclear and Chemical Dating Techniques (Currie, L. A., Ed.), American Chemical Society, New York (1980), 187-222.

[4] MAŁOSZEWSKI, P., ZUBER, A., "On the calibration and validation of mathematical models for the interpretation of environmental tracer data in aquifers", Advances in Water Resour., **15** (1992), 47-62; MAŁOSZEWSKI, P., ZUBER A., "Principles and practice of calibration and validation of mathematical models for the interpretation of environmental tracer data in aquifers", Adv. Wat. Resour., **16** (1993), 173-190.

[5] ZUBER, A., "Mathematical models for the interpretation of environmental radioisotopes in groundwater systems", Handbook of Environmental Isotope Geochemistry, Vol. 2 (Fritz, P., Fontes J.-Ch., Eds.), Elsevier (1986), 1-60.

[6] FONTES, J-CH., GARNIER, J.M., "Determination of the initial ^{14}C activity of the total dissolved ionrganic carbon: a review of existing models and a new approach", Water Resour. Res., **15** (1979), 399-413.

[7] WIGLEY, T.M.L., PLUMMER, L.N., PEARSON, F.J., "Mass transfer and carbon isotope evolution in natural water systems", Geochim. Cosmochim. Acta, **42** (1978), 1117-1139.

[8] MOOK, W. G., "Carbon-14 in hydrogeological studies", Handbook of Environmental Isotope Geochemistry, Vol. 1 (Fritz, P., Fontes, J-Ch. (eds.), Elsevier, Amsterdam (1980), 49-74.

[9] MAŁOSZEWSKI, P., ZUBER, A., "On the theory of tracer experiments in fissured rocks with a porous matrix", *J. Hydrol.*, **79** (1985), 333-358.

[10] DARLING, W.G., BATH, A.H., "A stable isotope study of recharge processes in the English Chalk", J. Hydrol., **101** (1988), 31-46.

[11] ANDREWS, J. N., LEE, D. J., "Inert gases in groundwater from the Bunter Sandstone of England as indicators of age and palaeoclimatic trends", J. Hydrol., **41** (1979), 233-252; HERZBERG O., MAZOR E. "Hydrological applications of noble gases and temperature measurements in underground waters: examples from Israel", J. Hydrol., **41**(1979), 217-231.

[12] FONTES, J-CH., STUTE, M., SCHLOSSER, P., BROECKER, W.S., "Aquifers as archives of paleoclimate", Eos, **74** (1993), 21-22.

[13] ZUBER, A., MOTYKA, J., "Matrix porosity as the most important parameter of fissured rocks for solute transport at large scales", J. Hydrol., **158** (1994), 19-46.

[14] BARKER, J.A., “Modelling groundwater flow and transport in the Chalk”, The Hydrogeology of the Chalk of North-West Europe (Downing, R.A.,. Price, M., Jones, G.P., Eds.), Clarendon Press, Oxford (1993), 59-66.

[15] LEVER, D.A., BRADBURY, M.H., HEMINGWAY, S.J., “Modelling the effect of diffusion into the rock matrix on radionuclide migration”, Progress in Nuclear Energy, **12** (1983), 85-117.

[16] ELLIOT, T., ANDREWS J.N., EDMUNDS W.M., “Hydrochemical trends, palaeorecharge and groundwater ages in the Chalk aquifer of the London and Berkshire Basins, UK”, Applied Geochemistry, **14** (1999), 333-363.

[17] YOUNGER, P. L., ELLIOT, T., “Chalk fracture system characteristics: implications for flow and solute transport”, Quarterly J. Engng. Geol., **28**, (1995), S39-S50; PRICE, M., YOUNGER, P.L., ELLIOT, T., “Discussion”, Quart. J. Engng. Geol., **29** (1996), 93-96.

[18] BLOOMFIELD, J., “Characterisation of hydrogeologically significant fracture distributions in the Chalk: an example from the Upper Chalk of southern England”, J. Hydrol., **184** (1997), 355-379.

[19] HILL, D., “Diffusion coefficients of nitrate, chloride, sulphate and water in cracked and uncracked Chalk”, J. Soil Sci., **35** (1984), 27-33.

[20] MAŁOSZEWSKI, P., ZUBER, A., “Influence of matrix diffusion and exchange reactions on radiocarbon ages in fissured carbonate aquifers”, Water Resour. Res., **27** (1991), 1937-1945.

[21] CHARLES, C.D., et al., “Glacial-Interglacial changes in moisture sources for Greenland: influences on the ice core record of climate”, Science, **263** (1994), 508-511.

[22] COOPE, G.R., “Fossil coleopteran assemblages as sensitive indicators of climatic changes during the Devensian (last) cold stage”, Phil. Trans. R. Soc. Lond. B, **280** (1977), 313-340.

[23] SUDICKY, E.A., FRIND, E.O., “Contaminant transport in fractured porous media: analytical solutions for a system of parallel fractures”, Water Resourc. Res., **18** (1982), 1634-1642.

[24] BULLIVANT, D.P., O’SULLIVAN, M.J., “Matching a field tracer test with some simple models”, Water Resourc. Res., **25** (1989),1879-1891.

[25] SUDICKY, E.A., FRIND, E.O., “Carbon 14 dating in confined aquifers: implications of aquitard diffusion”, Water Resour. Res., **17** (1981), 1060-1064.

[26] BIBBY, R., “Mass transport of solutes in dual-porosity media”, Water Resourc. Res., **17** (1981), 1075-81.

[27] STUTE, M., SCHLOSSER P., “Principles and applications of the noble gas palaeothermometer”, Climate Change in Continental Isotopic Records, Geophysical Monograph **78** (Swart, P.K., et al., Eds.), American Geophysical Union (1993), pp.89-100.

[28] DAVIDSON, M.R., AIREY, P. L., “The effect of dispersion on the establishment of a paleoclimatic record from groundwater”, J. Hydrol., **58** (1982), 131-147.

[29] SCHWARZER, W., Milankovitch cycles and the measurement of time, Terra Cognita, **1** (1989), 405-408.

[30] MOZETO, A.A., et al., “Experimental observations on carbon isotope exchange in carbonate-water systems”, Geochim. Cosmochim. Acta, **48** (1984), 495-504; GARNIER, J.M., “Retardation of dissolved radiocarbon through a carbonated matrix”, Geochim. Cosmochim. Acta, **49** (1985), 683-693; GARNIER, J.M., et al., “Traçage par ^{13}C, ^{2}H, I^- et uranine dans la nappe de la Craie Sénonienne en écoulement radial convergent (Béthune, France), J. Hydrol., **78** (1985), 379-392; SHEPPARD, S.C., et al., “Sorption of inorganic ^{14}C on to calcite, montmorillonite and soil”, Appl. Geochem., **13** (1998), 43-47.

[31] EDMUNDS, W.M., et al., “Baseline geochemical conditions in the Chalk aquifer, Berkshire, UK: a basis for groundwater quality management”, Appl. Geochem., **2** (1987), 251-274.

[32] HISCOCK, K.M., ET AL., “Hydrochemical and stable isotope evidence for the extent and nature of the effective Chalk aquifer of North Norfolk, UK”, J. Hydrol., **180** (1996), 79-107.

[33] EDMUNDS, W.M., “Hydrogeochemical Investigations”, Case-studies in Groundwater Resources Evaluation (Lloyd, J.W., Ed.) Clarendon Press, Oxford (1981), pp.87-12.

[34] ELLIOT, T., Geochemical Indicators of Groundwater Ageing, Ph.D. Thesis, University of Bath (1990).

[35] WILKINSON W.B., BRASSINGTON F. C., “Rising groundwater levels – an international problem”, Applied Groundwater Hydrology (Downing, R. A., Wilkinson, W.B., Eds.), Clarendon Press, Oxford (1991), 35-53.

APPLICATIONS OF COMPOUND-SPECIFIC CARBON ISOTOPE RATIOS IN ORGANIC CONTAMINANT STUDIES

R.ARAVENA[1], D. HUNKELER[1], Y. BLOOM[1], B. BUTLER[2], E. EDWARDS[3],
S.K. FRAPE[1] and E. COX[4]

[1]Department of Earth Sciences and [2]Biology, University of Waterloo,
Waterloo, Ontario, Canada
[3]Department of Chemical Engineering and Applied Chemistry, University of Toronto, Toronto, Ontario, Canada
[4]Geosyntec Consultants International, Guelph, Ontario, Canada

Abstract

In this paper results are presented on the application of compound-specific isotope ratios measurements to assess biodegradation of chlorinated solvents, in particularly on microbial dechlorination of tetrachloroethene (PCE) and trichloroethene (TCE). Analytical aspects and isotope data from laboratory and field studies are discussed. The analytical tests showed that both headspace and SPME techniques provide accurate $\delta^{13}C$ values with a similar precision for a wide range of chlorinated solvents. However, the SPME method is generally more sensitive. The microcosm experiments show that a significant isotopic fractionation occurs during dechlorination of PCE and TCE to ethene. The largest fractionation factors are observed in the steps DCE-VC and VC-Ethene. In general, the $\delta^{13}C$ of each dechlorination product was always more negative than the $\delta^{13}C$ of the corresponding precursor. In addition, the $\delta^{13}C$ values of each compound increased with time. A similar pattern was observed for dechlorination of PCE at a field site. These results show that compound-specific carbon isotope ratios technology is a very sensitive tool for evaluation of natural attenuation of chlorinated solvents in groundwater.

1. INTRODUCTION

Groundwater contamination, by organic compounds, is one of the major environmental problems in water resources management today. Through interaction between groundwater and streams, lakes and wetlands, these contaminants can eventually also impact surface water. Petroleum hydrocarbons and DNAPLs (Dense-non aqueous phase liquids) such as chlorinated solvents are the most common organic groundwater pollutants. The focus of research projects in the field of organic contaminant hydrogeology has been on the behavior and fate of these organics in the subsurface and the development of remediation technologies. There is a need for better tools to evaluate the efficiency of remediation methods and to demonstrate the occurrence of natural attenuation of contaminants in groundwater.

The development of analytical instruments to analyze compound-specific isotope ratios of organic contaminants has opened new possibilities for the application of stable isotopes in contaminant hydrogeology. The studies in this new research field have focussed on the evaluation of characteristic isotope fingerprints in chlorinated solvents [1] and BTEX [2], and on the evaluation of isotope fractionation associated with biotic and abiotic degradation of organic compounds [3, 4,5]. It is expected that compound-specific isotope ratio analysis will be particularly useful to evaluate the importance of natural attenuation of organic compounds in groundwater. This application is based on the expected isotopic fractionation associated with microbial degradation of organic compounds in groundwater.

In this paper, results from a reseach project are presented, whose main objective is to evaluate the use of ^{13}C and ^{37}Cl as tracers to provide information about origin and fate of organic compounds in groundwater. The studies are part of a major research program at the Department of Earth Sciences, University of Waterloo, dealing with the behavior, fate and remediation of chlorinated solvents in the subsurface. The main focus of the paper is on the application of compound-specific carbon isotope analysis in studies of biodegradation of chlorinated solvents. Analytical aspects are been discussed, and isotope data from laboratory and field studies about microbial dechlorination of tetrachloroethene (PCE) and trichloroethene (TCE) are presented.

2. ANALYTICAL METHOD

Compound-specific carbon isotope ratios were determined in the Environmental Isotope Laboratory (EIL) of the University of Waterloo using a gas chromatography combustion isotope-ratio mass spectrometry (GC-C-IRMS) system. The GC-C-IRMS system consisted of a Hewlett Packard GC with a split/splitless injector, a Micromass combustion interface operated at 850°C and a Micromass Isochrom µGas isotope-ratio mass spectrometer (Micromass, Manchester, UK). The minimal amount of carbon required to enter the GC column in order to be able to reproducibly measure $\delta^{13}C$ values was 1.5 nmol. All $^{13}C/^{12}C$ ratios are reported in the usual delta notation ($\delta^{13}C$) relative to the VPDB (Vienna Peedee Belemnite) standard. The $\delta^{13}C$ value is defined as $\delta^{13}C = (R_S / R_r - 1) \times 1000$, where R_S and R_r are the $^{13}C/^{12}C$ ratios of the sample and the international standard, respectively. Dissolved chlorinated solvents were extracted from the aqueous phase using headspace techniques and solid phase microextraction (SPME). The SPME method relies on the partitioning of organic compounds between the polymeric coating of a fiber aqueous phase of a sample.

The $\delta^{13}C$ of chlorinated solvents standards (Tab. 1) was determined by combusting the compounds in an Elemental Analyzer attached to a Micromass Optima isotope-ratio mass spectrometer (EA-IRMS) and by the GC-C-IRMS system. In the first case, chlorinated solvent were injected into the injection port of the elemental analyser. When using GC-C-IRMS, gas standards of

Table 1: Stable carbon isotope ratios of chlorinated solvents measured by EA-IRMS and GC-C-IRMS. Minimal required concentration to determine carbon isotope ratios of dissolved chlorinated solvents.

Compound	$\delta^{13}C$ of standards (‰) VPDB		Minimal concentration	
	EA-IRMS n=4	GC-C-IRMS n=6	Headspace ppm	SPME ppm
Vinylchloride	-28.62±0.14	-28.62±0.31	0.14	0.28
Trans-1,2-dichloroethene	-22.23±0.16	-22.44±0.18	0.52	0.24
Cis-1,2-dichloroethene	-23.23±0.11	-23.33±0.07	1.06	0.29
Trichloroethene	-29.48±0.08	-29.39±0.20	0.64	0.19
Tetrachloroethene	-27.27±0.08	-27.20±0.24	0.60	0.13
Dichloromethane	-53.59±0.10	-53.53±0.14	3.31	2.22
Chloroform	-63.62±0.14	-63.43±0.22	2.41	0.63
Carbon tetrachloride	-32.48±0.22	-32.34±0.15	0.86	0.36
1,2-Dichloroethane	-30.73±0.02	-30.63±0.25	4.06	0.64

the chlorinated solvents were prepared an injected into the GC at a split ratio of 10:1. The accuracy, precision and detection limit of the headspace and SPME method was evaluated using the chlorinated solvent standards. Aqueous standards were prepared by dispensing the chlorinated solvent standards into 125 ml bottles filled with organic free distilled water. For headspace analysis of field samples, a headspace was created by replacing 20 ml of solution with helium. After shaking the bottles for at least two hours, headspace gas was injected into the injector of the GC-C-IRMS system. For microcosm studies, samples from the gas phase of the microcosms were injected. For SPME, aqueous samples were extracted by immersing a 100 μM Polydimethylsiloxane (PDMS) fiber for 20 Min. in vials containing 17 ml of standard solution.

3. RESULTS AND DISCUSSION

3.1 Analytical method

The $\delta^{13}C$ values of chlorinated solvents determined by EA-IRMS and GC-C-IRMS are similar within the range of analytical uncertainty (Table 1). The standard uncertainties are slightly smaller for EA-IRMS than for GC-C-IRMS measurement, which is a reflection of the higher complexity of GC-C-IRMS compared to EA-IRMS.

The headspace and SPME tests showed that carbon fractionation occurs during aqueous phase/gas phase partitioning [7]. Molecules in the gas phase were enriched in ^{13}C by up to 1.46 ‰ compared to dissolved molecules. For SPME, molecules in the aqueous phase and molecules on the SPME fiber had generally similar $\delta^{13}C$ values. Both headspace and SPME techniques provide accurate $\delta^{13}C$ values with a similar precision for a wide range of CHC, if aqueous phase/gas phase isotope fractionation during headspace measurements is taken into account. However, the SPME method is more sensitive, particularly for compounds with a low volatility such as CF and DCA [7]. When NaCl is added to the samples before SPME extraction, a detection limit of <1 ppm can be reached for all compounds except dichloromethane. With other types of SPME fiber, it may be possible to reach even lower detection limits. The detection limits reported in this paper are specific to the system used in these studies which requires a minimum of 1.5 nmol C on the GC column. For other systems they change according to the required amount of carbon.

3.2 Microcosm studies

The microcosms used to evaluate carbon isotopic fractionation during biodegradation of PCE and TCE were setup with soil samples collected from field sites where active biodegradation of PCE and TCE was observed. The isotope data obtained during the experiments show a large $\delta^{13}C$ range for the primary compounds, PCE and TCE, and the corresponding dechlorination products. In case of the PCE, the $\delta^{13}C$ values vary between -60.2 ‰ and -1.5 ‰ (Fig. 1). For TCE, the $\delta^{13}C$ values range from -60 ‰ to +10 ‰ (Fig. 2). The most significant changes in $\delta^{13}C$ were observed for cis-1,2-dichloroethene (cDCE), vinyl chloride (VC) and ethene (Fig. 1 and 2).

In general, the $\delta^{13}C$ of each dechlorination product was always more negative than the $\delta^{13}C$ of the corresponding remaining precursor. In addition, the $\delta^{13}C$ values of each compound increased with time (Fig. 1 and 2). This suggests that the dechlorination rate is slightly faster for molecules containing ^{12}C than for molecules containing ^{13}C, which leads to a depletion of ^{13}C in the product and an enrichment of ^{13}C in the remaining precursor of each dechlorination step. However, the degree of isotope fractionation seems to be smaller for the first two dechlorination steps, PCE to TCE and TCE to cDCE than for the last two steps from cDCE to VC and VC to ethene. The ethene tends to reach the initial value of the added primary compound towards the end of the experiment (Fig. 1 and 2). For closed system, such as the microcosms, the $\delta^{13}C$ value of ethene has to correspond to the $\delta^{13}C$ of the added PCE or TCE if dechlorination has reached completion and no other products then

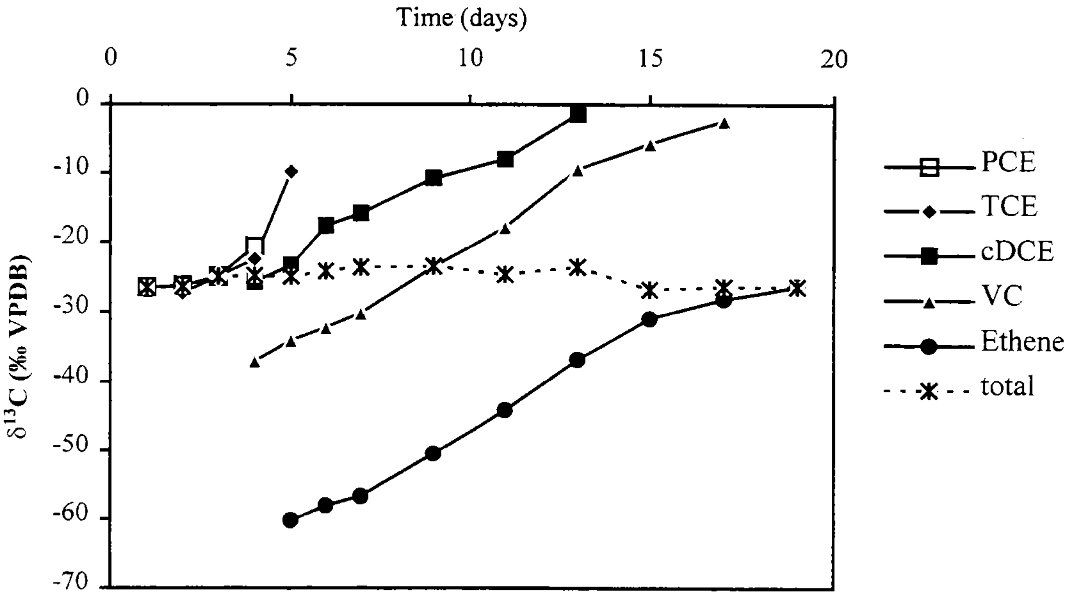

Figure 1. $\delta^{13}C$ patterns for PCE, TCE, cDCE, VC and ethene during microbial dechlorination of PCE in a microcosm.

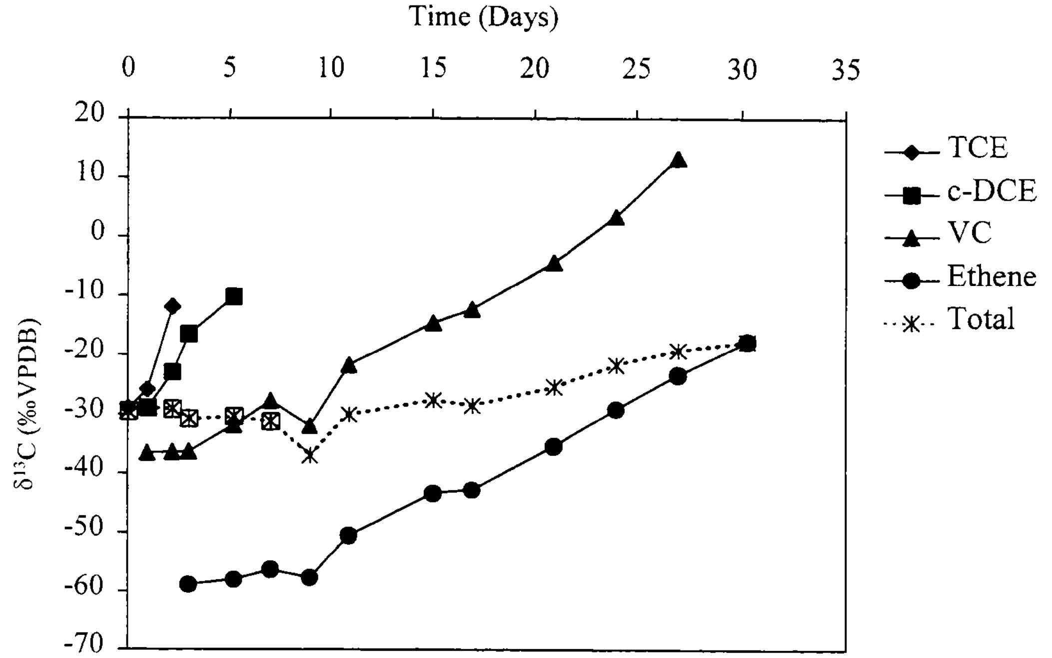

Figure 2. $\delta^{13}C$ patterns for TCE, cDCE, VC and ethene during microbial dechlorination of TCE in a microcosm.

ethene are formed. The calculated $\delta^{13}C$ of all chlorinated ethenes correspond reasonable well with the initial isotopic composition of the primary product.

For the dechlorination of PCE to TCE an enrichment factor of about 2 ‰ was obtained from the PCE experiment. The enrichment factor for the step TCE-cDCE is similar in the PCE and TCE experiment and amounts to approximately 6 ‰. In currently microcosm studies with cis-DCE and VC as a primary compound, an enrichment factor around 15‰ for the step cis-DCE-VC and VC-Ethene was observed (Y. Bloom, unpublished data).

At a PCE contaminated field site, a similar ^{13}C pattern of PCE and the dechlorination products was observed as in the microcosm experiments [8]. The $\delta^{13}C$ values of PCE and TCE fell within a narrow range (-31.7 ‰ to -25.7 ‰) compared to the large variation observed for cDCE (-31.5 ‰ to +5.1 ‰), VC (-40.4 ‰ to +25.4 ‰) and ethene (-51.8 ‰ to -31.9 ‰). The cDCE and VC were the more enriched in ^{13}C, the smaller the mole fraction of the corresponding compound in the groundwater sample was. For ethene, the most enriched $\delta^{13}C$ value (-31.9 ‰) was obtained in a groundwater sample that mainly contained ethene and only a small mole fraction of chlorinated ethenes. The $\delta^{13}C$ of ethene in this sample corresponded to the $\delta^{13}C$ of PCE close to the source area.

The similar isotopic pattern observed in the microcosm and field studies suggests that microcosm data can be used for the interpretation of isotope data obtained in field situations. This is an important conclusion for the use of environmental isotopes in organic contaminant studies in groundwater. The strong enrichment of ^{13}C in cDCE and VC during microbial dechlorination of PCE and TCE may serve as a powerful tool to monitor the last two dechlorination steps which frequently determine the rate of complete dechlorination of chlorinated ethenes at field sites undergoing intrinsic bioremediation. The fact that the $\delta^{13}C$ of the ethene tend toward the $\delta^{13}C$ of the initial substrate after completed dechlorination may also make it possible to distinguish ethene originating from different contaminants (e.g. PCE and 1,2-dichloroethane) if the contaminants have different initial $\delta^{13}C$ values and dechlorination has reached completion.

These results and new developments of compound-specific deuterium analysis in organic compounds open new possibilities for the application of stable isotopes to assess the occurrence of natural attenuation of organic compounds in groundwater and the efficiency of remediation technologies.

ACKNOWLEDGEMENTS

This project was supported through a scholarship of the Swiss National Science Foundation to D. Hunkeler and grants from the National Sciences and Engineering Research Council of Canada, the Centre for Research in Earth and Space Technology and the University Consortium Solvents-in-Groundwater Research Program to R. Aravena. The authors thank W. Mark for support during isotope ratio measurements.

REFERENCES

[1] VAN WARMERDAM, E.M., FRAPE, S.K., ARAVENA, R., DRIMMIE, R.J., FLATT, H., AND CHERRY, J.A. Stable chlorine and carbon isotope measurements of selected chlorinated organic solvents. Applied Geochemistry, 10: 547-552 (1995).

[2] DEMPSTER, H.S. SHERWOOD LOLLAR, B., AND FEENSTRA, S. Tracing organic contaminants in groundwater: A new methodology using compound-specific isotopic analysis. Env. Sci. Tech. 31: 3103-3197 (1997).

[3] ARAVENA, R., BENETEAU, K., FRAPE, S., BUTLER, B., ABRAJANO, T., MAJOR, D., AND COX, E. Application of isotopic finger-printing for biodegradation studies of chlorinated solvents in groundwater. In: G.B. Wickramanayake and R.E. Hinchee (Eds.), Risk, Resource, and Regulatory Issues: Remediation of Chlorinated and Recalcitrant Compounds. Battelle Press, Columbus, OH. pp. 67-71 (1998).

[4] KELLEY, C.A., AND HAMMER, B.T. Concentrations and stable isotope values of BTX in gasoline-contaminated groundwater. Env. Sci. Tech. 31:2469-2472 (1997).

[5] STURCHIO, N.C., CLAUSEN, J.L., HERATY, L.J., HUANG, L., HOLT, B.D. AND ABRAJANO, JR. T.A. Chlorine isotope investigation of natural attenuation of trichloroethene in an aerobic aquifer. Env. Sci. Tech. 32: 3037-3042 (1998).

[6] VAILLACOURT, J., FRAPE, S., AND ARAVENA, R. Chlorine and carbon isotopic trends during the degradation of trichloroethylene with zero-valent metal. Proceeding of GSA Annual meeting, Toronto, (1998).

[7] HUNKELER, D., AND ARAVENA, R. Determination of stable carbon isotope ratios of dissolved chlorinated solvents by GC-C-IRMS: Comparison of headspace and solid-phase microextraction. Analytical Chemistry (submitted).

[8] HUNKELER, D., ARAVENA, R., AND BUTLER, B. Monitoring of Microbial Dechlorination of Tetrachloroethene (PCE) in Groundwater using Compound-Specific Stable Carbon Isotope Ratios: Microcosm and Field Studies. Environment, Science and Technology (in press).

MAJOR IONS, $\delta^{18}O$, $\delta^{2}H$, AND $^{87}Sr/^{86}Sr$ AS TRACERS OF THE ORIGIN AND EVOLUTION OF DISSOLVED SALTS IN GROUNDWATERS OF THE MURRAY BASIN, AUSTRALIA

S.S. DOGRAMACI* A.L. HERCZEG

CSIRO, Land and Water and Centre for Groundwater Studies
Private Bag No.2, Glen Osmond. SA, 5064, AUSTRALIA

Abstract

Groundwaters of the Murray and Renmark Group aquifers of south-eastern Australia were analysed for major ion content, $\delta^{18}O$, $\delta^{2}H$, and $^{87}Sr/^{86}Sr$ isotopes to provide an insight into possible mechanisms that control the chemical composition and salinity of groundwater. The groundwater salinity of the Murray Group Aquifer increases along the hydraulic gradient from fresh (~500 mg/l) at the southeastern basin margin to saline (~23,000 mg/l) at the north and northwestern part of the study are near the discharge zone. Although, the groundwater chemistry displays seawater like composition, the $\delta^{2}H$ and $\delta^{18}O$ values are similar to the mean winter rainfall, indicating that groundwater in the Murray Group Aquifer is of meteoric origin. The geochemical mass balance calculations suggest that the current chemical composition of fresh and brackish groundwater in the Murray Group Aquifer is produced by a combination of: evapotranspiration of rain water prior to recharge, equilibrium with carbonate minerals, and Na-Ca exchange reaction under soil gas pCO_2 of $\sim 10^{-1.5}$atm. The higher salinity of groundwater in the northern part of the study area (discharge zone) on the other hand, can be explained by the mixing of saline groundwater of the underlying Renmark Group Aquifer via upward leakage. A mixing model using Sr concentration and $^{86}Sr/^{87}Sr$ ratio has been applied to quantify the relative proportions of groundwater in the saline part of the Murray Group Aquifer that is derived from: (i) upward leakage from the Renmark Group Aquifer, (ii) local diffuse recharge, and (iii) laterally flowing groundwater of the Murray Group Aquifer.

1. INTRODUCTION

The regional Murray and Renmark Group aquifers of the Murray Basin extend over approximately 60,000 km^2 of eastern South Australia and western Victoria, Australia (Fig. 1). The unconfined carbonate Murray Group Aquifer is separated from the underlying Renmark Group Sand Aquifer by a 20 – 30m thick aquitard. Groundwater of the unconfined Murray Group Aquifer is the only water resource extensively used for agriculture activities and town water supplies. The groundwater salinity of the Murray Group Aquifer is relatively fresh in the southern part of the basin (~500 mg/l), increasing to brackish along the hydraulic gradient (~2,500 mg/l), then rapidly becomes saline (15,000 – 23,000 mg/l) towards the northern part of the study near the River Murray about 250-350 km from the basin margin.

Understanding the processes that might produce the present day major ion distribution in the Murray Group Aquifer is essential for management of this important resource. A knowledge of whether the chemical composition of the groundwater is caused by natural processes or induced by human activities is a prerequisite in many groundwater management issues such as potential exploitation, sustainable yield and groundwater contamination. The main objectives of this paper is to provide an insight into possible mechanisms that control the chemical composition of groundwater, and to determine the extent and locations of mixing between the Murray and Renmark Group Aquifers.

---

* Present address: Water and Rivers Commission, PO Box 6740, Hay Street, Perth WA 6892, AUSTRALIA

The variation of dissolved ion concentrations and stable isotope composition of groundwater can be used to identify the physical processes and water-rock interactions that may be responsible for the observed increase in major ion concentrations in the Murray Group Aquifer. The stable isotope composition (δ^{2}H and δ^{18}O) is a conservative property of the water mass during subsurface flow. Therefore, it is possible to relate the isotopic composition of the groundwater to that of the weighted mean isotopic composition of rainfall recharging the aquifer [1]. On the other hand, physical processes such as evaporation prior to recharge or mixing with waters with different δ^{2}H and δ^{18}O signatures can change the original δ^{2}H and δ^{18}O composition of groundwater. The effect of these processes on the δ^{2}H and δ^{18}O composition can be identified by comparing the isotopic composition of the groundwater with initial recharge water [2].

The hydraulic head difference contour (Fig 2) shows the potential for downward leakage through the Murray Group Aquifer to the south where the groundwater in both aquifers is fresh, but further down gradient where the groundwaters are saline, the situation is reversed with a head difference of up to 15 m indicating a potential for upward leakage from the Renmark Group Aquifer. This may cause the increase of salinity in the northern part of the Murray Group Aquifer.

Because the chemical and isotopic composition of the Murray and Renmark Group aquifers are not sufficiently different to be used as tracers, the ^{86}Sr/^{87}Sr ratio is used to identify and quantify mixing between these two major aquifers. Unlike the δ^{18}O, δ^{2}H composition, the ^{86}Sr/^{87}Sr ratio is primarily controlled by rock-water interaction and is not complicated by variations in atmospheric sources [3,4]. The mineralogy of the Murray and Renmark Group aquifers is different, therefore, the dissolved Sr in each aquifer is also likely to exhibit a different ^{86}Sr/^{87}Sr ratio. In the silicate rich sandy Renmark Group Aquifer, the ^{86}Sr/^{87}Sr ratio may be relatively more radiogenic. In contrast, the ^{86}Sr/^{87}Sr ratio in the carbonate Murray Group Aquifer may be dominated by dissolved Sr having ^{87}Sr/^{86}Sr ratio similar to the Tertiary carbonate minerals. The distinct ^{87}Sr/^{86}Sr ratio in each of the aquifers can therefore, be used to calculate the proportion of upward leakage from the Renmark Group Aquifer, by applying mixing equations [5].

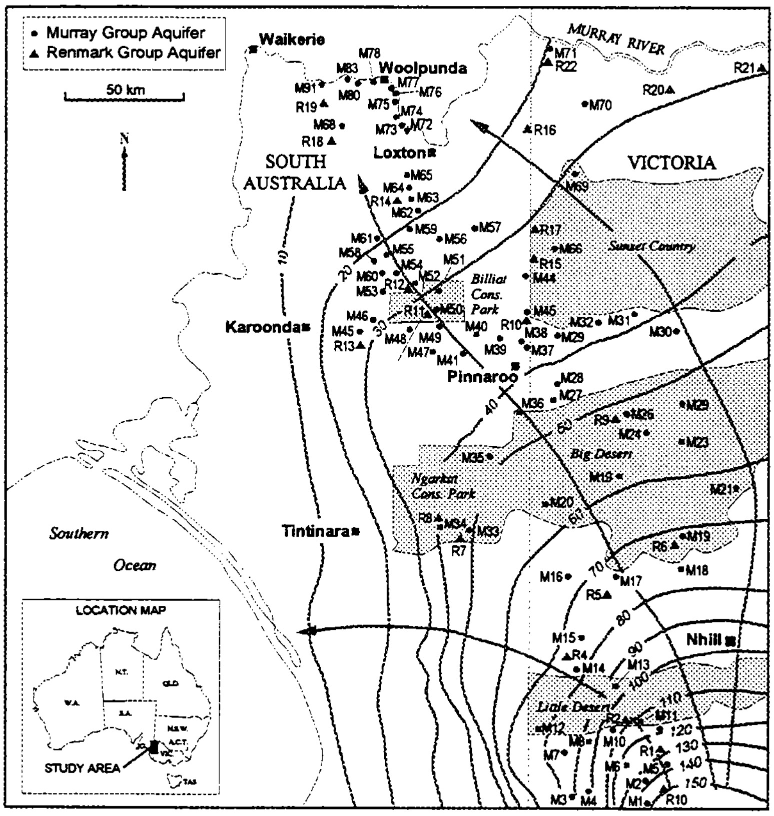

Fig.1 Sample location map and potentiometric surface in the Murray Group Aquifer.

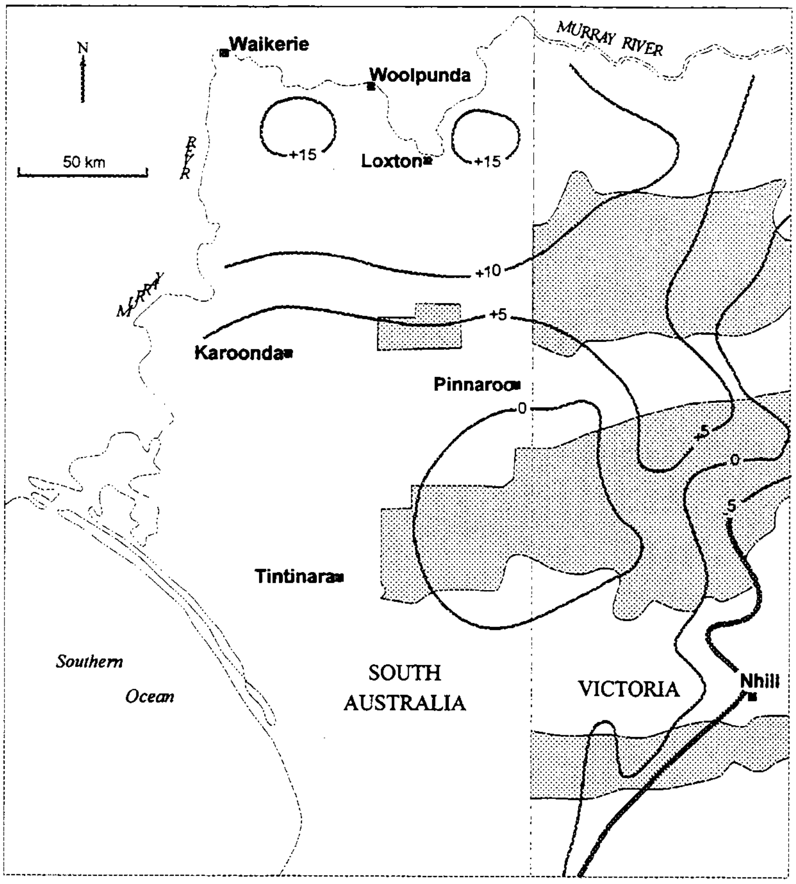

Fig. 2 Hydraulic head differences between the Renmark and Murray Group aquifers

2. RESULTS AND DISCUSSION

2.1 The processes controlling chemical composition of groundwater

Groundwater chemistry throughout the Murray Group Aquifer is dominated by Na and Cl ions regardless of the location or relative major ion concentrations (Table 1). The plot of Na and Br versus Cl concentrations shows that the data falls on the sea water dilution line (Fig.3a). The marine type Na and Cl distribution could be due to one of the following scenarios; (i) dilution of remnant seawater trapped in the basin at the time of deposition (ii) evaporation of water dominated by Cl and Na ions prior to recharge, or (iii) dissolution of hyalite.

The $\delta^{18}O$ and $\delta^{2}H$ data falls on or slightly to the right of the WMWL (Fig.3b) indicating the presence of only meteoric water in both aquifers. The meteoric origin of groundwater eliminates the first and second scenarios. The observed Cl/Br ratio in groundwater samples in both aquifers ranges from 250 to 350 typical of the marine Cl/Br ratio (the Cl/Br mass ratio of halite is one to two orders of magnitude higher than the marine Cl/Br ratio [6]). This eliminates halite dissolution being the process that modifies the Cl and Br concentrations. Therefore, the most likely scenario for the dominance of Na and Cl is the evapotranspiration of meteoric water dominated by Na and Cl ions prior to recharge.

Although the chemical composition of groundwater of the Murray Group Aquifer is similar to seawater, the majority of fresh to brackish groundwater samples has a higher Na/Cl ratio relative to seawater (Fig.3c). The excess of Na relative to Cl is due to addition of Na to the groundwater via cation exchange reactions during recharge.

TABLE 1. Chemical, $^{87}Sr/^{86}Sr$, $\delta^{18}O$ and δ^2H analysis of groundwaters from the Murray and Renmark Group aquifer. M and R refer to the Murray and Renmark Group aquifers respectively. The results of major and minor ions are expressed in millimole and micromole. The $\delta^{18}O$ and δ^2H are expressed in per mil notation relative to SMOW. Dist. refers to approximate distance along the hydraulic gradient in kilometres from the basin margin. Errors for $^{87}Sr/^{86}Sr$ ratio are 2σ mean and apply to the last decimal place.

Well	Dist.	HCO_3	Cl	Na	Ca	Br	Sr	$\delta^{18}O$	δ^2H	$^{87}Sr/^{86}Sr$
ID.	(km)	(mmol/l)				(µmol/l)		(‰, SMOW)		
M2	22	7.9	14.27	13.5	1.28	22	52	-5.5	-31.0	0.70865± 4
M3	34	5.9	16.64	16.2	2.32	23	19	-4.5	-28.0	0.70876± 4
M5	32	4.1	9.11	8.1	1.66	12	9	-5.8	-36.8	0.70923± 8
M6	34	6.0	14.98	14.1	2.03	21	14	-4.4	-26.4	0.70923± 10
M7	50	5.0	10.24	9.8	1.78	14	16	-5.6	-36.1	0.70891± 6
M9	36	4.1	3.98	4.1	1.19	7	10	-6.1	-35.3	0.70899± 5
M10	50	4.8	8.07	7.4	1.87	10	13	-6.5	-34.5	0.70915± 7
M12	59	5.8	14.41	13.4	2.11	22	24	-5.5	-32.3	0.70909± 6
M13	60	5.2	7.62	6.4	1.96	14	21	-5.9	-35.9	0.70899± 4
M14	80	5.1	9.65	8.3	1.74	15	20	-5.7	-34.3	0.70924± 11
M17	126	5.0	17.52	16.1	1.82	34	24	-5.8	-35.5	0.70924± 7
M19	119	4.3	16.56	16.7	1.63	29	9	-5.9	-38.0	0.70972± 5
M20	137	5.6	8.66	9.0	1.47	15	19	-6.0	-37.2	0.70892± 4
M21	142	4.2	6.01	5.8	1.55	12	6	-6.0	-38.4	0.70931± 6
M22	143	5.0	7.14	7.2	1.44	12	14	-5.8	-39.0	0.70903± 8
M23	159	4.1	12.07	11.3	0.96	19	11	-6.1	-41.0	0.70931± 4
M24	171	3.3	6.35	6.3	0.58	10	9	-6.0	-39.1	0.70915± 7
M25	174	3.4	6.43	6.8	0.58	13	9	-6.0	-35.5	0.70910± 5
M27	182	3.9	6.74	7.9	1.31	11	10	-6.5	-38.6	0.70896± 5
M28	190	5.6	7.56	11.4	1.43	12	11	-5.6	-38.9	0.70897± 6
M30	204	4.4	15.23	14.7	1.33	22	21	-5.9	-43.0	0.70888± 3
M33	149	4.4	6.18	6.1	1.12	11	11	-5.9	-38.3	0.70888± 4
M34	164	3.6	8.60	7.1	1.42	16	11	-6.4	-38.1	0.70903± 15
M35	177	4.3	8.38	7.8	1.61	14	6	-5.8	-39.8	0.70951± 17
M38	204	4.7	5.78	7.4	1.15	11	12	-5.9	-40.4	0.70894± 11
M39	214	3.7	6.40	7.8	1.02	11	6	-5.9	-39.7	0.70932± 4
M41	220	4.6	9.00	11.2	1.05	15	6	-6.2	-39.0	0.70927± 7
M42	224	4.9	14.50	15.4	1.16	23	5	-5.7	-38.2	0.70986± 7
M43	228	3.9	14.70	14.9	1.34	22	14	-5.8	-40.3	0.70921± 4
M44	240	3.7	9.79	8.8	1.73	15	9	-6.0	-43.1	0.70912± 7
M45	255	7.9	25.11	27.0	1.55	43	23	-5.1	-37.1	0.70906± 5
M46	249	6.8	27.53	29.5	1.62	40	16	-5.3	-38.3	0.70924± 8
M49	234	4.4	24.46	24.4	1.87	34	16	-5.6	-40.1	0.70935± 19
M51	245	4.4	14.50	14.4	1.40	24	10	-5.7	-38.2	0.70933± 4
M54	260	7.5	18.87	23.7	1.22	33	26	-5.2	-41.2	0.70884± 6
M55	268	4.9	11.79	13.6	1.10	21	11	-4.9	-38.1	0.70911± 4
M57	258	6.2	28.66	27.7	2.03	47	34	-5.5	-39.0	0.70916± 5
M60	275	10.8	34.95	37.4	1.52	57	44	-5.1	-35.7	0.70871± 7
M62	285	15.1	72.21	85.4	1.66	120	73	-4.5	-35.9	0.70868± 9
M63	289	12.9	72.75	87.8	1.16	109	55	-5.0	-36.9	0.70866± 4
M65	300	11.5	87.84	95.1	2.08	133	102	-5.5	-38.7	0.70870± 5
M70	295	3.8	290.7	241.1	10.43	402	793	-4.0	-33.3	0.70850± 7
M71	324	5.9	339.3	291.4	11.15	439	770	-5.1	-34.5	0.70851± 4
M73	330	8.2	267.4	241.0	9.43	347	216	-4.7	-33.2	0.70985± 9
M74	332	8.5	296.8	250.0	11.78	401	220	-4.9	-35.1	0.71062± 6
M75	334	8.2	315.5	266.6	13.45	418	237	-4.6	-31.5	0.71107± 4

TABLE 1. Cont.

Well	Dist.	HCO_3	Cl	Na	Ca	Br	Sr	$\delta^{18}O$	δ^2H	$^{87}Sr/^{86}Sr$
ID.	(km)		(mmol/l)			(µmol/l)		(‰, SMOW)		
M76	336	7.6	367.1	313.2	15.54	474	271	-4.6	-32.3	0.71104± 8
M77	337	7.6	333.8	274.5	15.82	438	253	-4.6	-32.1	0.70975± 7
M78	338	7.6	346.1	292.3	17.17	448	268	-4.6	-32.1	0.71117± 4
M79	340	6.7	362.7	307.1	16.14	464	277	-4.5	-33.9	0.71114±10
M80	342	6.7	361.9	304.9	17.89	449	277	-4.7	-34.3	0.71090± 5
M81	345	6.3	350.6	298.8	17.94	442	277	-4.3	-36.1	0.71072± 6
M82	348	6.2	353.1	289.7	17.61	437	284	-4.3	-32.3	0.71004± 7
M83	348	6.3	349.4	289.3	17.27	463	293	-4.5	-33.3	0.70991± 4
M84	350	7.5	335.6	297.5	14.42	416	279	-4.9	-31.8	0.71018± 9
M85	350	7.9	304.6	263.2	12.55	432	226	-5.0	-37.3	0.71023± 22
M86	350	7.7	296.1	252.3	12.03	437	221	-5.1	-31.4	0.71011± 4
M87	350	8.3	259.9	228.8	9.33	379	178	-5.1	-34.0	0.71015± 8
M88	350	8.7	205.0	192.7	6.34	312	146	-5.2	-35.8	0.70881± 8
M89	351	9.0	336.1	332.8	9.58	456	225	-4.4	-35.0	0.70963± 8
M90	354	9.2	262.2	251.8	6.59	353	180	-4.7	-32.7	0.70942± 4
M91	355	8.6	334.0	300.2	9.83	461	293	-4.3	-32.1	0.70915± 10
R1	5	2.8	9.6	8.7	0.86	15	9	-5.8	-34.2	0.70933± 7
R2	15	3.7	4.8	6.7	0.43	8	11	-6.0	-37.4	0.70895± 9
R5	126	5.9	25.3	24.1	2.33	41	23	-5.8	-38.2	0.70939± 8
R6	119	3.3	22.6	23.3	1.41	38	13	-5.0	-33.7	0.70931± 8
R7	149	4.0	8.4	7.5	1.41	13	6	-5.7	-38.7	0.70969± 3
R8	164	4.1	6.2	6.2	1.28	11	6	-6.2	-40.7	0.70969± 6
R9	185	7.2	14.8	20.5	0.31	23	5	-5.8	-39.4	0.70985± 8
R10	228	6.1	11.7	16.7	0.35	17	5	-6.4	-43.1	0.70956±11
R12	251	10.9	15.3	25.8	0.16	25	0	-6.0	-41.0	0.70926± 4
R13	255	10.1	19.8	32.1	0.18	33	1	-3.4	-34.0	0.70950± 3
R14	289	11.3	36.7	48.5	0.44	54	7	-5.5	-38.5	0.70948± 4
R15	243	6.7	61.8	64.5	1.73	103	37	-5.0	-36.8	0.71111±12
R16	278	5.5	66.4	70.8	0.09	90	33	-5.8	-37.1	0.71092± 8
R18	319	9.0	232.0	195.3	8.83	295	159	-5.2	-34.6	0.71122± 5
R19	350	6.8	234.0	222.3	7.14	312	148	-4.5	-39.3	0.71084± 8
R20	295	8.1	304.6	255.9	11.63	476	310	-3.5	-30.3	0.71108± 9
R21	304	7.6	291.0	250.1	13.45	390	283	-4.4	-32.6	0.71167± 4
R22	324	7.3	336.9	286.2	15.14	438	282	-4.6	-30.0	0.71192± 6

Groundwater in the Murray Group Aquifer is also enriched in Ca, relative to the seawater particularly the fresh and brackish groundwater in the south and central part of the study area (Fig. 3d). This suggests that in addition to evapotranspiration, the Ca concentration is affected by chemical reactions. The processes that are likely to modify the Ca concentrations of groundwater is the equilibrium with carbonate minerals of the Murray Group Aquifer.

Geochemical mass balance calculations were performed using computer code PHREEQM [7] to test whether evapotranspiration of rain water that recharges the aquifer, followed by equilibrium with carbonate minerals and cation exchange reaction are responsible for the observed chemical composition of the groundwater in the south and central part of the study area. These reactions were carried out under different soil gas CO_2 partial pressures simulating the range of pCO_2 measured in the study area [8]. The average chemical composition of rainfall measured in the southeastern Murray Basin was used as the starting solution [9].

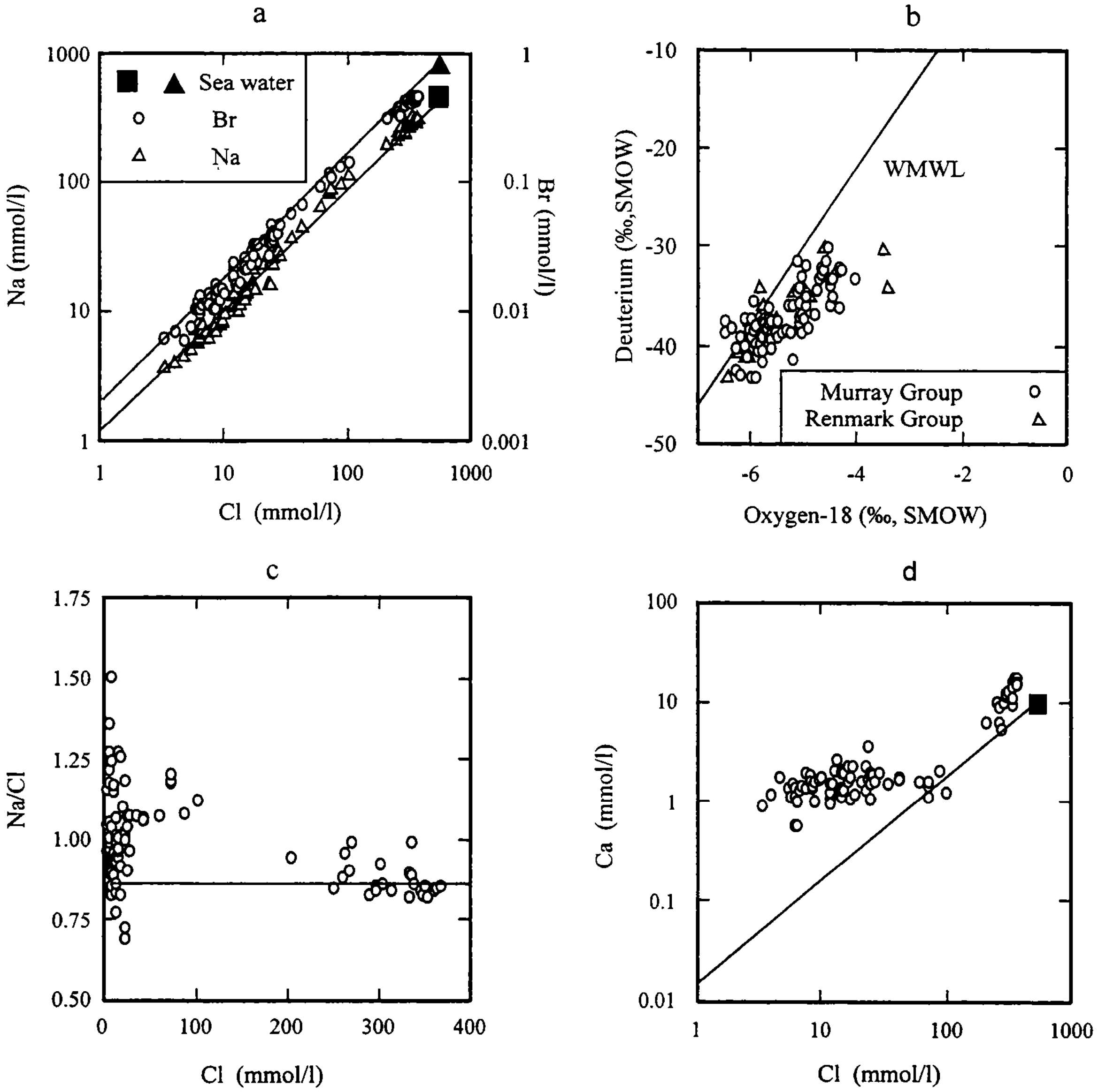

Fig. 3a Sodium and Br vs. Cl data falls on the sea water dilution line indicating that groundwater may be derived from rainfall that has N: Br: Cl ratios similar to that of seawater. Fig.3b δ^2H vs. $\delta^{18}O$ data falls on or slightly to the right of the World Meteoric Water Line indicating the meteoric origin of groundwater. Fig.3c, d Majority of the groundwater samples from the Murray Group Aquifer has Na/Cl ratio and Ca concentration higher than seawater (the horizontal line and diagonal lines respectively).

The modeled results are shown in Fig. 4 by solid lines on a graph of bicarbonate concentration versus Na/Ca ratios at pCO_2 of 10^{-1}, $10^{-1.5}$ and 10^{-2} atmospheres. The observed data from the Murray Group Aquifer suggest that the evolution of recharge water occurs at pCO_2 between 10^{-1} and 10^{-2} atmospheres, which is typical of CO_2 concentrations in the soil zone in the study area [8]. This suggests that the model proposed above adequately accounts for the distribution of the dissolved Cl, Na, Ca, and HCO_3^- observed in the Murray Group Aquifer

2.2 The cause for saline groundwater of the northern part of the study area

The $^{87}Sr/^{86}Sr$ ratio of groundwater in the Murray Group Aquifer in the north and north-eastern part of the study area is considerably enriched in ^{87}Sr compared to the $^{87}Sr/^{86}Sr$ ratio in the south and central part of the study area (Fig. 4a, Table 1). The $^{87}Sr/^{86}Sr$ ratios of groundwater are also markedly higher than that of the host Tertiary carbonate rocks (0.7085) [10]. Groundwater will acquire more radiogenic ^{87}Sr/^{86}Sr ratio than that of the host rock only by mixing with relatively more radiogenic water. The ^{87}Sr/^{86}Sr ratio of groundwater from the Renmark Group Aquifer in the northern part of the study area (bores R18 and R16) are similar to that of the Murray Group Aquifer (Table 1). The more likely cause for the more enriched ^{87}Sr/^{86}Sr ratio of the Murray Group Aquifer therefore, is mixing with radiogenic groundwater from the Renmark Group Aquifer. The hydraulic head differences (Fig. 2) also shows a potential for upward leakage from the Renmark Group Aquifer.

In order to estimate the mixing proportions, the ^{87}Sr/^{86}Sr ratio and Sr concentrations of the respective end members need to be defined. The plot of ^{87}Sr/^{86}Sr ratio vs. 1/Sr shows that groundwater of the Murray Group Aquifer in the northern part of the study area is derived from three end members (Fig 4b). The first end member is groundwater from the Renmark Group Aquifer where ^{87}Sr/^{86}Sr ratio ranges from 0.71084 to 0.71122 (Table 1). The second end member is groundwater in the Murray Group Aquifer which is not influenced by mixing and is in chemical and isotopic equilibrium with Tertiary carbonates (0.7085). The third end member is soil water derived from rainfall dominated by marine ^{87}Sr/^{86}Sr ratios (0.7098 to 0.7092). The ^{87}Sr/^{86}Sr ratios of groundwaters that are influenced by mixing of these three end members range from 0.70881 to 0.71117 (bore M70 to M91).

The proportion of mixing of the three end members can be calculated from a set of mass and isotopic balance equations as follows:

$$\mathrm{Sr} = \mathrm{A\ Sr}_M + \mathrm{B\ Sr}_R + \mathrm{C\ Sr}_L \tag{1}$$

$$(\mathrm{Sr}\ .{}^{87}\mathrm{Sr}/{}^{86}\mathrm{Sr}) = (\mathrm{A\ Sr}.\ {}^{87}\mathrm{Sr}/{}^{86}\mathrm{Sr})_M + (\mathrm{B\ Sr}.\ {}^{87}\mathrm{Sr}/{}^{86}\mathrm{S})_R + (\ \mathrm{C\ Sr}.\ {}^{87}\mathrm{Sr}/{}^{86}\mathrm{Sr})_L \tag{2}$$

$$1 = \mathrm{A} + \mathrm{B} + \mathrm{C} \tag{3}$$

where Sr and ^{87}Sr/^{86}Sr are the concentrations and isotopic ratios in the final solution. The (Sr. ^{87}Sr/^{86}Sr)$_M$, (Sr. ^{87}Sr/^{86}S)$_R$ and (Sr. ^{87}Sr/^{86}Sr)$_L$ are the concentrations and isotopic ratios of Sr in the three end members: the Murray Group Aquifer (M), Renmark Group Aquifer (R), and soil water that recharge the aquifer (L) respectively. A, B, and C are the proportion of each of three proposed end members to the final solution.

The ^{87}Sr/^{86}Sr data as a function of mixing fraction of three components in the Murray Group Aquifer is plotted in Fig 5. The two diagonal lines represent (a) addition of groundwater from the Renmark Group Aquifer through upward leakage and (b) addition of soil water via local recharge to the Murray Group Aquifer.

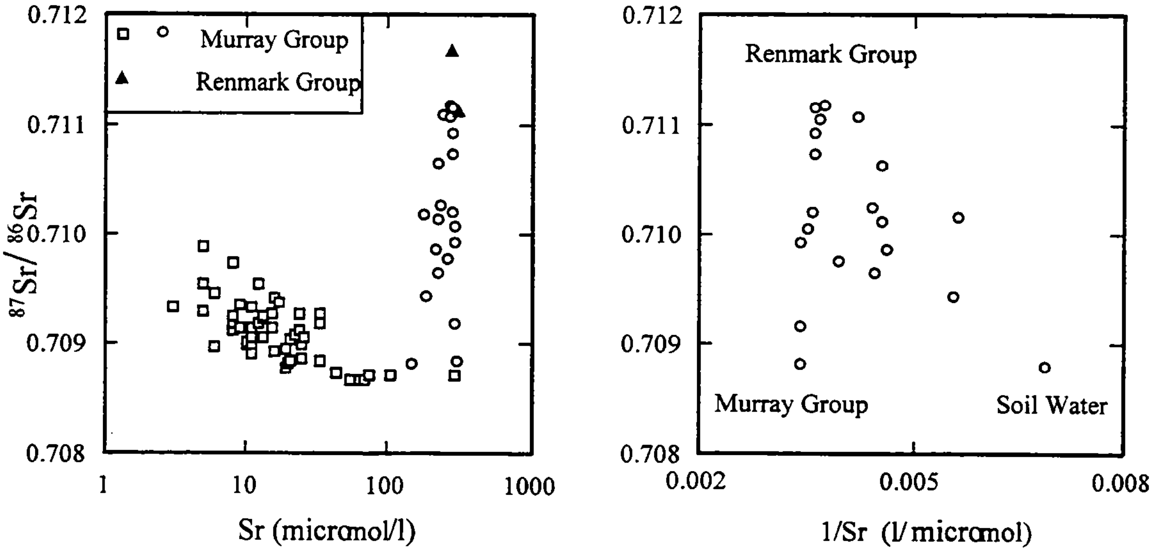

Fig 4a ^{87}Sr/^{86}Sr ratio vs. Sr concentration of groundwater from the Murray and Renmark Group aquifers. Groundwaters that have relatively high ^{87}Sr/^{86}Sr ratios (the circles) are located to the northern part of the study area. Fig 4b. The Measured ^{87}Sr/^{86}Sr ratio vs. reciprocals of strontium concentration in the Murray Group Aquifer from northern part of the study area.

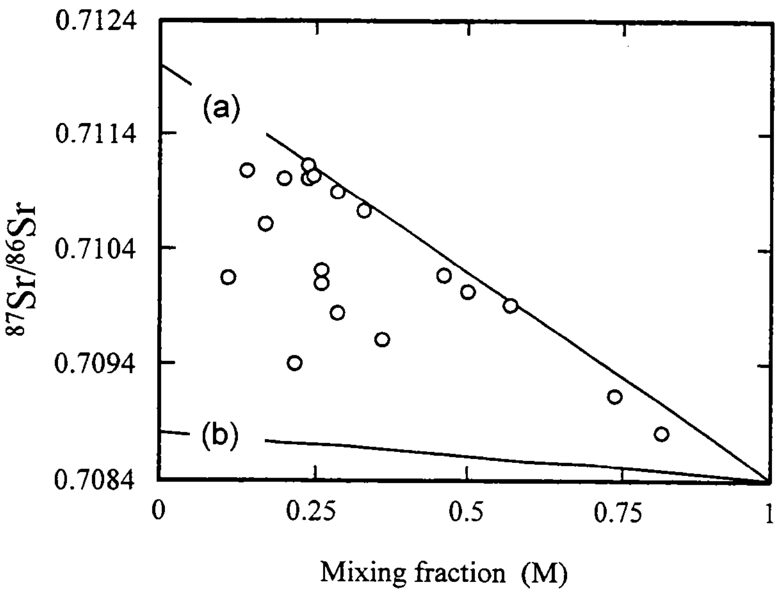

Fig.5 The mixing model of groundwater from the northern part of the Murray Group Aquifer. The two straight lines represent mixing with the soil water via local recharge and with groundwater from the Renmark Group Aquifer via upward leakage respectively.

The results suggest that although most of the data falls on or parallel to a mixing line between the Murray and Renmark Group aquifers, the apparent contribution of Sr from soil water, via local recharge, to the Sr pool in groundwater at some of the wells is as significant as the contribution through upward leakage from the Renmark Group Aquifer.

2. CONCLUSIONS

- The relative abundance of Cl, Na, and Br^- are similar to that of sea water, indicating the dominance of marine airborne salts as a source of these ions to the Murray and Renmark Group aquifers.
- The Na/Cl molar ratio, and Ca, and HCO_3 distributions indicate that evapotranspiration prior to recharge, carbonate dissolution and cation exchange on clays are major processes causing the current chemical composition of groundwater in the Murray Group Aquifer.
- The δ^2H and $\delta^{18}O$ composition of water molecules suggest that groundwater of the Murray and Renmark Group aquifers are derived from meteoric water.
- Groundwater from the Murray Group Aquifer in the northern part of the study area, near the River Murray has a more radiogenic $^{87}Sr/^{86}Sr$ ratio compared with that in the south and central parts of the study area. Sr concentrations and $^{87}Sr/^{86}Sr$ ratios of the groundwater in this part is most likely dominated by mixing with more radiogenic groundwater from the silicate rich Renmark Group Aquifer, through upward leakage and local recharge.

REFERENCES

[1] GAT, J.R. Comments on stable isotope methods in regional groundwater investigations. Water Resour. Res., 17 (1971) 980-993.

[2] MAZOR, E., VUATAZ, F.D., JAFFE, F.C. Tracing groundwater components by chemical, isotopic and physical parameters-example: Schinznach, Switzerland. *J. Hydrol.*, 76 (1985) 233-246.

[3] MCNUTT, R.H., FRAPE, S.K., AND DOLLER, P., A strontium, oxygen and hydrogen isotopic composition of brines, Michigan and Appalachian basins, Ontario and Michigan. Appl. Geochem., 2 (1987) 495-505.

[4] MCNUTT, R.H., FRAPE, S.K., FRITZ, P., JONES, M.G., AND MACDONALD, I.M., The $^{87}Sr/^{86}Sr$ values of Canadian Shield brines and fracture minerals with applications to groundwater mixing, fracture history, and geochronology. Geochim Cosmochim Acta, 54 (1990) 205- 215.

[5] FAURE, G., Principles of Isotope Geology. John Wiley & Sons, Inc. (1986) 589 pp.
[6] BRAITSCH, O., Salt Deposits, their Origin and Composition. Springer, New York, (1971) 297 pp.
[7] DIGHTON, J.C. AND ALLISON G.B., Carbon dioxide profiles of nine sites in the Murray Basin. CSIRO, Division of Soils, Australia, Technical Memorandum, No. 34 (1985).
[8] BLACKBURN, G. AND MCLEOD, S., Salinity of atmospheric precipitation in the Murray Darling drainage division, Australia. Aust. J. Soil. Res., 21 (1983) 411-434.
[9] NIENHUIS, P.R., APPELO, C.A.J. AND WILLEMSEN, A., PHREEQM in a *M* ing-Cell flowtube, Free University- Amsterdam, Netherlands, (1993). Based on PHREEQE, Parkhurst D.L., Thorstenson, and D. C. Plummer L.N., (1980).
[10] BURKE, W.H., DENISON, R.E., HETHERINGTON, E.A., KOEPNICK, R.B., NELSON, H.F., OTTO, J.B., Variation of seawater $^{87}Sr/^{86}Sr$ throughout Phanerozoic time, Geol., 10: 516-519, (1982).

ISOTOPIC EVIDENCE FOR GEOCHEMICAL PROVINCES IN THE ASTIAN SANDY AQUIFER (MEDITERANEAN COAST, SOUTHERN FRANCE)

F. Barbecot*, L.Dever*, C.Hillaire-Marcel**, E.Gibert*, Y. Travi*** & C.Marlin*

* Laboratoire d'Hydrologie et de Géochimie Isotopique, Université Paris-Sud,
Orsay, France
** GEOTOP, Université du Quebec à Montréal,
Montréal, Québec, Canada
*** Laboratoire d'Hydrogéologie, Departement de Geologie, Faculte des Sciences d'Avignon,
Avignon, France

Abstract

In southern France, the marine sandy deposits of Lower Pliocene age (Astian) constitutes a confined aquifer exploited for water supply, despite the presence of relatively high salinity waters in its eastern part, along the Mediterranean coast. The origin and mixing processes leading to salinization have been investigated based on comparative studies of the chemical and isotopic signatures of waters in the eastern *vs* western sectors of the aquifer.

The western part of the aquifer contains fresh waters with a Ca-bicarbonate/chloride signature representing the geochemical conditions of recharge waters and groundwater circulation. Residence times have been estimated based on ^{14}C-measurements. They indicate ages ranging from modern, in the recharge area, to up to 6 ka. B.P., in the deepest part of this sector of the aquifer.

The eastern sector of the aquifer shows brackish waters, with salinity as high as 10 $g.L^{-1}$. High dissolved inorganic carbon contents seem to characterise these waters. Correlative changes in $\delta^{13}C$ suggest mixing with carbonate-rich waters and/or CO_2-supplies from deep origin probably from underlying aquifers linked to the Astian aquifer through NE-SW oriented faults.

Brackish waters from the eastern sector of the aquifer present increasing U-contents, with concentrations as high as 6.9 ppb, matched by decreasing $^{234}U/^{238}U$ activity ratios. This pattern is thought to represent dilution by non fractionated-U supplied though carbonate dissolution due to the deep CO_2 inputs. $^{226}Ra/^{234}U$ disequilibria are observed in these highly mineralized waters. This suggests dissolution of matrix carbonates, likely in underlying aquifers, and a time lag between carbonate dissolution in this deep system and the subsequent mixing with groundwater in the Astian aquifer.

1. INTRODUCTION

Intrusion of marine water in coastal aquifers has occurred naturally through geological time in relation with sea level and recharge rate fluctuations. Since the last 30 years, this process has been often induced and enhanced by over-exploitation of these coastal aquifers for fresh-water supply due to both population increase and tourism development [1,2]. As a consequence, an increase in water salinization has appeared in most of the exploited aquifers, in relation with water pumping of either old marine water or modern saline wedge [3,4]. The integration of water management policies within these fairly new socio-economic and hydrogeological contexts does appear essential [5].

In southern France, the marine sandy deposits of Lower Pliocene (Astian) age contain a confined aquifer largely exploited for agricultural, industrial and human purposes (Fig. 1; [6]). In the eastern part of this aquifer, along the Mediterranean coast, water salinization has been recognized nearby a N45° fault network affecting the whole sedimentary series. This study thus focuses on the contribution of geochemistry on the understanding of groundwater circulation and salinization processes for this sandy aquifer. To address this problem, groundwater has been sampled for chemical and isotopic analyses.

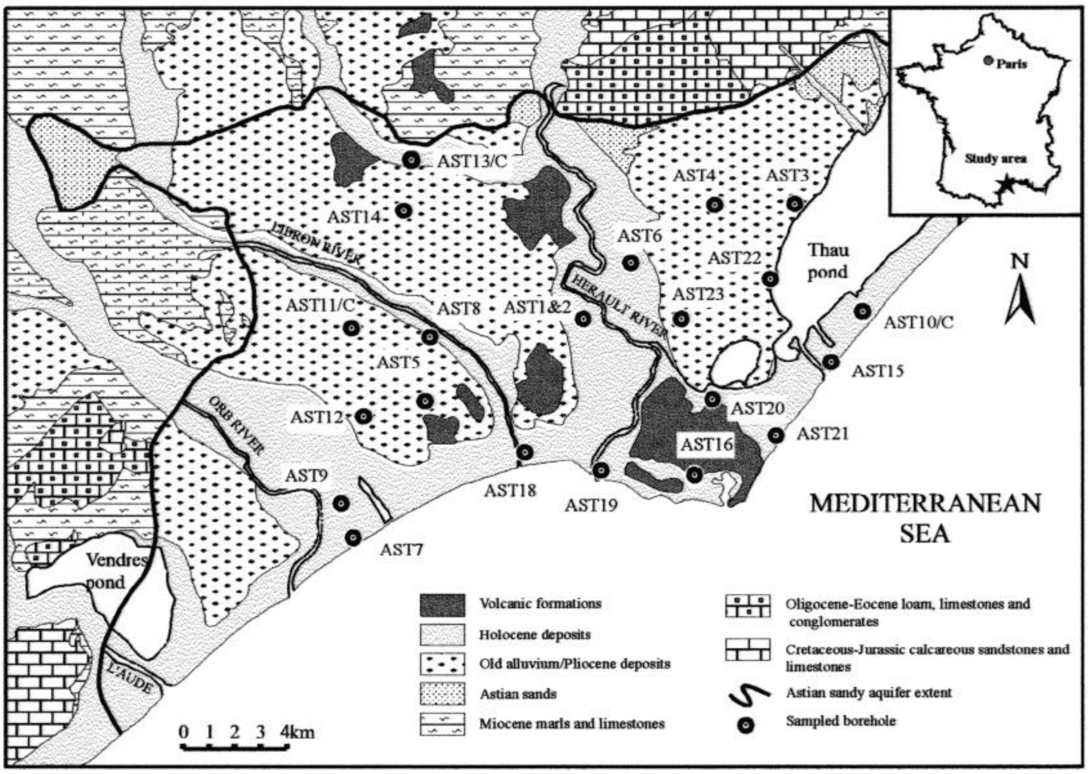

FIG. 1. Geological map of the study aquifer (Astian sands, Southern France), modified from [1].

2. GENERAL SETTINGS

2.1. Study area

The present-day hydro-climatic conditions of the study area are of Mediterranean type, with irregular interannual rainfall amounts from one year to the other. However, the annual rainfall averages 606 mm (σ = 23 mm), mainly spread over autumn and spring as fierce meteor showers [7]. Mean temperature varies between 7.7 and 23.2 °C throughout the year (mean of 14.9 °C).

The study aquifer is contained in micaceous quartzose and slightly carbonated sands of Astian age over a surface of 450 km^2. Overlying more than 100 m thick Miocene clays, this 20 m-thick aquifer outcrops on the northern part of the study area over less than 20 km^2 (Fig. 1). Southward, it becomes confined under clayey layers of Upper Pliocene age, this formation reaching 80 m thickness near the coast [8].

Hydraulic gradients defined in this aquifer induce a groundwater flow from the North (recharge area) to the South (sea). At present, these gradients are enhanced by recent water uptakes concentrated along the coastline, implying that the present-day hydraulic conditions are not representative of those having existed in the past.

2.2. Sampling and analysis

A global sampling has been realized in 23 boreholes over the whole aquifer. During sampling, after borehole column water renewal and whenever possible, an air-tight cell was connected to the pump in order to measure *in situ* parameters such as temperature, pH, Eh and electrical conductivity (E.C.).

Chemical and isotopic measurements (contents in major elements, Br and F, ^{18}O, ^{2}H, ^{13}C and ^{14}C activities by both conventional and AMS methods) have been performed on a set of groundwater taken from 22 sampling sites. Moreover, the analysis of ^{226}Ra and U isotopes (^{234}U, ^{238}U) have been done on a chosen set of 14 samples from the 22 initials [9].

3. RESULTS

3.1. Astian groundwater specifications

According to groundwater chemical composition, the study aquifer can be divided into two parts from one side of the Herault river to the other.

In the western part of the aquifer, the total dissolved solid content (TDS) of groundwater remains low with a mean of 0.670 g.L^{-1} (σ of 0.170), while it rises up to 10.260 g.L^{-1} in the eastern part of the aquifer (mean value of 2.485 g.L^{-1}, σ of 3.330).

The western part of the aquifer, unaffected by processes of mixing with marine solution, has been used to identify the baseline conditions of groundwater circulation. In this area, groundwater is of Ca-HCO$_3$/Cl-type, and chemical contents are quite constant along the flow path (Fig. 1). The radiocarbon ages corrected with respect to their C-13 contents evolve along the global flowpath from modern ages in the recharge area to 6 ka B.P. nearby the coast [10].

In contrast, the eastern part of the aquifer contains groundwater with increasing chemical contents from the recharge area towards the sea (Figs 2, 3 and 4). This increase is likely due to the mixing with a marine water solution as shown by the bromide, sodium and chloride relationships (Figs 2a-2b). Concurrently, groundwater is enriched in both Total Dissolved Inorganic Carbon (TDIC up to 0.13 mol.L^{-1}), and $\delta^{13}C$ (up to +0.24 ‰ *vs* PDB). Evidences of carbon mixing are given through the calculated $\delta^{13}C$ values of the CO$_2$ in equilibrium with the TDIC, since these values are plotted along a mixing line between soil CO$_2$, (-23.3 ‰ as measured on field), and a CO$_2$ bounded by -4 ‰ (Fig. 3). Such an isotopic signature of -4 ‰ is consistent with the endogenous carbon domain values known for the peri-Alpine arc (-10 to -2 ‰ *vs* PDB; [11]). In the study system, the carbon mixing can thus be associated to deep CO$_2$ diffusion, accompanied by carbonate dissolution due to the increasing dissolved CO$_2$ amount, since the saturation indices with respect to calcite are conserved for all the samples [10]. Since these two carbon sources, *i.e.* deep CO$_2$ and carbonates, are ^{14}C-free, the A^{14}C measured for these water can not be related to groundwater residence time in this part of the aquifer.

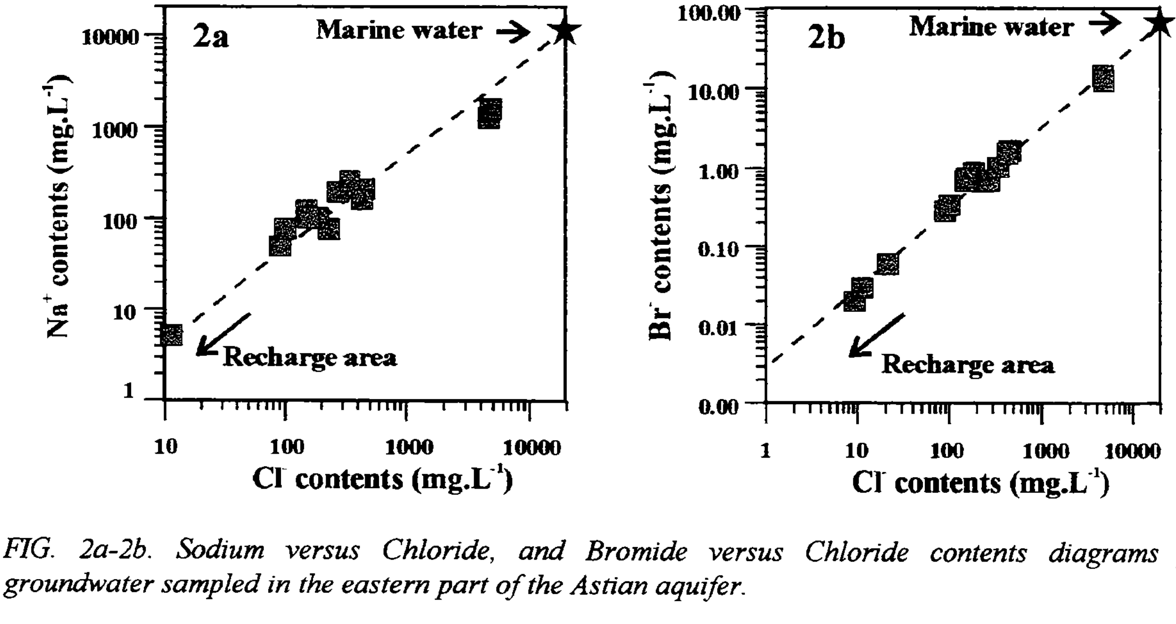

FIG. 2a-2b. Sodium versus Chloride, and Bromide versus Chloride contents diagrams for groundwater sampled in the eastern part of the Astian aquifer.

As shown by the close relationship existing between the carbon and chloride contents, the parallel increase in both salinization and TDIC is due to variable mixing proportions of the fresh water with a salty, carbon-rich end-member (Fig. 4). This latter marine solution probably comes, *via* leakage through faults, from the underlying carbonated aquifers in which carbonate dissolution occurred.

As a conclusion, the groundwater mineralization in the eastern part of the Astian aquifer increases according a binary mixing between (1) the fresh water as recognized in the western part of the aquifer, and (2) a marine solution with a high carbon content due to deep CO_2 diffusion.

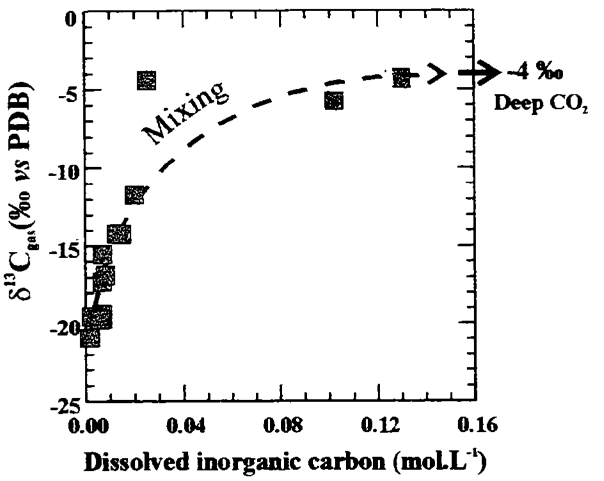

FIG. 3. $\delta^{13}C$ versus Dissolved inorganic carbon relationship for groundwater sampled in the eastern part of the Astian aquifer.

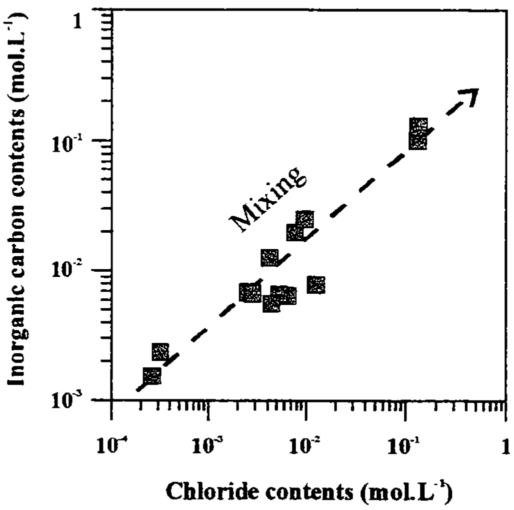

FIG. 4. Inorganic carbon contents versus Chloride contents relationship for groundwater sampled in the eastern part of the Astian aquifer.

3.2. ^{226}Ra and U isotopes (^{234}U, ^{238}U) contribution

3.2.1. Groundwater unaffected by the salinization process.

If groundwater unaffected by salinization is considered, ^{226}Ra can be used as a tracer of water residence time within the aquifer, and be compared to radiocarbon ages. Such an approach is based on a simple model taking into account (Fig. 5) :

- the groundwater early ^{226}Ra content coming from dissolution ;
- the ^{226}Ra *in-situ* production along the flowpath.

Calculation of ^{226}Ra ages in relation with the groundwater residence time within the aquifer, can be obtained through the following equation :

$$^{226}Ra_m = {}^{226}Ra_I \times e^{(-\lambda t)} + {}^{226}Ra_P \times (1-e^{(-\lambda t)})$$

Where

$^{226}Ra_m$	is the measured ^{226}Ra concentration for the sample considered,
$^{226}Ra_I$	is the ^{226}Ra early mineralization for the sample considered,
$^{226}Ra_P$	is the ^{226}Ra *in-situ* production,
λ	is the disintegration constant for ^{226}Ra (4.279×10^{-4} y^{-1}),
t	is the ^{226}Ra age of the sample.

3.2.1.1 The groundwater early ^{226}Ra content

The ^{226}Ra early mineralization can be estimated *via* sample AST-13/C, located in the uppermost part of the recharge area along flow-path (hydrogeological basin head), and which has been considered as representative of the modern recharge. Since this sample presents a ^{14}C modeled age varying from 400 to 1600 a. B.P. (modeled age, see [12], from measured $A^{14}C$ of 82.3 ± 0.6 pMC), its ^{226}Ra content has been corrected from this ageing. The initial ^{226}Ra contribution has thus been estimated at ca. 1.12 ± 0.01 to 1.66 ± 0.04 $dpm.L^{-1}$.

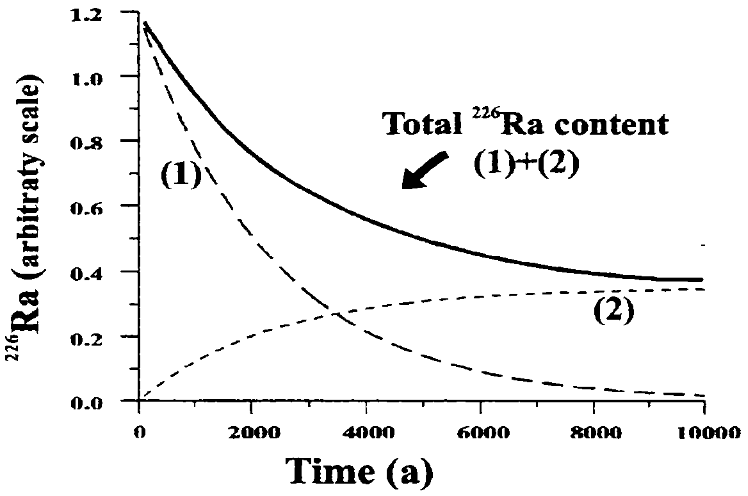

(1) Early ^{226}Ra mineralisation : $^{226}Ra_{I(t)} = {}^{226}Ra_I \times e^{-\lambda t}$

(2) ^{226}Ra *in-situ* production : $^{226}Ra_{P(t)} = {}^{226}Ra_P \times (1-e^{-\lambda t})$

FIG. 5. Theorical evolution through time of the ^{226}Ra content, as the sum of two processes : (1) the early ^{226}Ra mineralisation, and (2) the ^{226}Ra in-situ production.

Moreover, the early mineralization of water in the recharge area is obviously influenced by the dissolution rates, themselves depending mainly on pedo-climatic conditions during the recharge [13] (soil CO_2 partial pressure in relation with vegetation cover, recharge rate and amount, etc...). Since this process can induce important discrepancies a correction based on the TDIC contents for every sample considered can minimize these variations of early mineralization, as follows :

$$^{226}Ra_{I/S} = {}^{226}Ra_{I/REF} \times TDIC_S / TDIC_{REF}$$

Where

$^{226}Ra_{I/S}$	is the ^{226}Ra early mineralization for the sample considered,
$^{226}Ra_{I/REF}$	is the calculated ^{226}Ra early mineralization for the aquifer recharge reference,
$TDIC_S$	is the carbon content of the sample considered,
$TDIC_{REF}$	is the carbon content of the aquifer recharge reference.

3.2.1.2. The ^{226}Ra in-situ production along the flowpath.

The ^{226}Ra *in-situ* production through time can be estimated using a sample suspected to be enough old to make its initial ^{226}Ra content negligible in front of the *in-situ* production (*i.e.* the asymptotic value of ^{226}Ra for groundwater older than 10 ka, as shown in Fig. 5). The ^{226}Ra *in-situ* production takes place in the aquifer matrix through the following processes : recoil effect, decay of absorbed ^{230}Th and matrix-carbonates interaction. The signature of this ^{226}Ra production is approached *via* sample AST-22 (0.3615 ± 0.005 dpm.L^{-1} ; Fig. 1) which presents a ^{14}C age of ~ 20 ka B.P. [10]. Although located in the area affected by the salinization process, this sample does not show any or very slight mixing fingerprints, and its ^{226}Ra content will be considered as the maximum value of the original *in-situ* production.

On an other hand, the ^{226}Ra *in-situ* production of the Astian aquifer can also be determined *via* the ^{226}Ra-excess value in a ^{226}Ra *versus* U content diagram (Fig. 6), and considering the hypothesis of uranium-free water samples. In such a case, the ^{226}Ra content would only due to the *in-situ* production of the aquifer matrix through recoil effect and matrix-carbonates interaction [14]. The value of this ^{226}Ra *in-situ* production has been graphically determined at around 0.27 dpm.L^{-1}.

This value is obviously underestimated with respect to the natural evolution of groundwater which always contains dissolved uranium, but can be used as the minimum value of the original *in-situ* production.

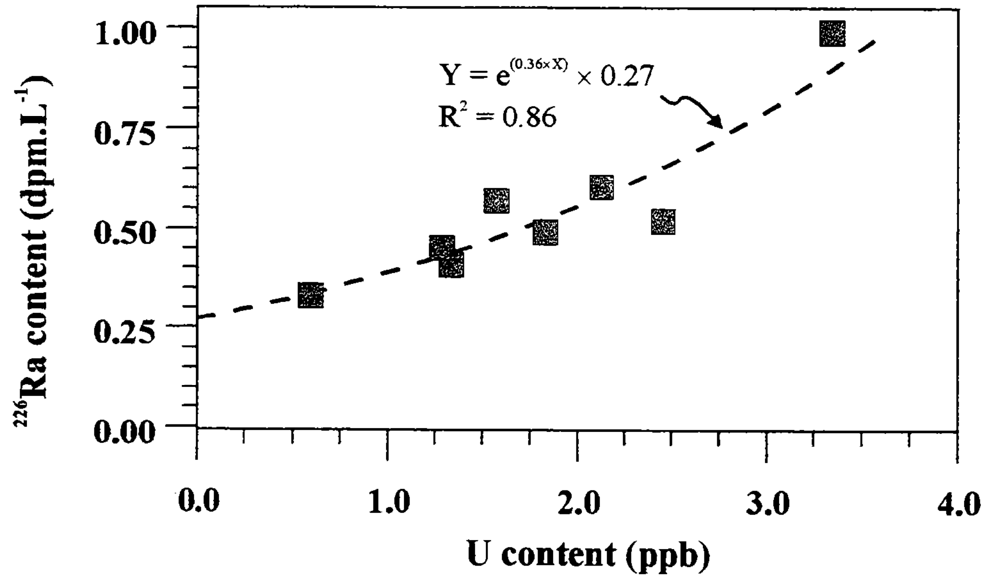

FIG. 6. ^{226}Ra versus U content diagram, established for groundwater samples unaffected by the salinisation process (western part of the Astian aquifer). The intersection of the regression line (dashed line) with the Y-axis corresponds to the minimum original ^{226}Ra in-situ production for uranium-free water samples.

Considering these hypothesis, ^{226}Ra ages can be calculated as shown in Table I, and compared to modeled ^{14}C ages [10] (Fig. 7). Although a discrepancy exists between ages obtained with ^{226}Ra and ^{14}C, the consistency of the global evolution of ^{226}Ra ages compared to ^{14}C datings indicate that our interpretative ^{226}Ra model seems to be close to the natural geochemical processes occurring in the system. Moreover, the discrepancies between ages obtained with these two tracers may indicate either that the ^{226}Ra *in-situ* production has been underestimated, or that models used to calculate ^{14}C ages do not take into account all the retardation factors occurring in the system.

TABLE I CALCULATED ^{226}Ra AND ^{14}C AGES OF SOME GROUNDWATER SAMPLES REPRESENTATIVES OF THE WESTERN PART OF THE ASTIAN AQUIFER.

Sample	^{226}Ra ages (mean value (*); a)	Modeled ^{14}C ages (mean value (*); a B.P.)
AST13/C	1000 (600)	840 (550)
AST11/C	2250 (800)	6000 (300)
AST12	2200 (700)	2600 (450)
AST3	5800 (1250)	9300 (1000)
AST5	2850 (800)	3300 (250)
AST8	1900 (700)	1500 (150)
AST18	3700 (900)	6100 (300)
AST6	2350 (1250)	1300 (200)

* Standard Deviation

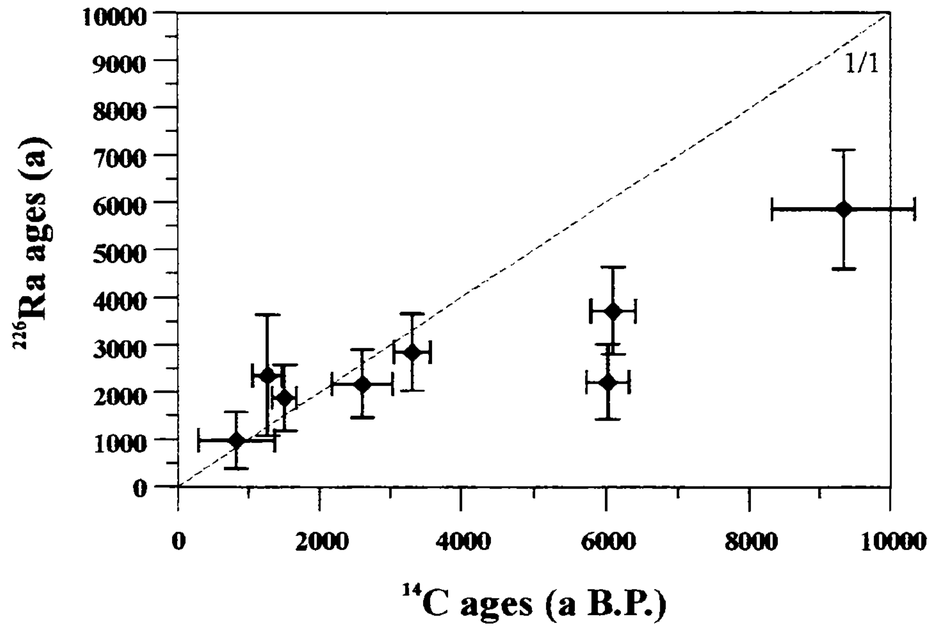

FIG. 7 Comparison of ^{226}Ra and ^{14}C ages for water samples unaffected by the salinisation process (mean values and standard deviation domain ; western part of the Astian aquifer).

3.2.2. Groundwater affected by the salinization process

The groundwater affected by the salinization process presents rather high U contents varying from 1.06 to 6.92 ppb. Since (1) these waters correspond to variable proportions of mixing, and (2) the salty end-member is enriched in uranium due to the dissolution of old carbonates, both the uranium contents and corresponding activity ratios, *i.e.* ^{234}U/^{238}U and ^{226}Ra/^{234}U, evolve according the fraction of marine solution in the mixing. In such a case, these isotopic ratios would reflect the secular equilibrium of the dissolved carbonates. However, the ^{234}U/^{238}U and ^{226}Ra/^{234}U activity ratios of the U-enriched salty end-member have been graphically determined, and values of 1.13 and 0.64 obtained respectively (Fig. 8).

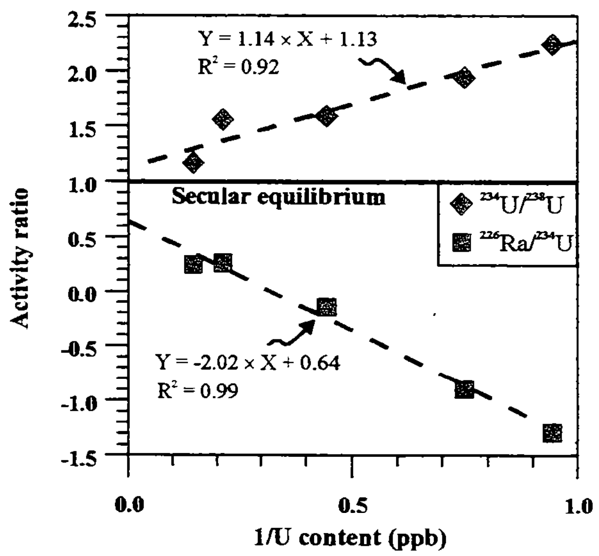

FIG. 8. Evolution of the ^{234}U/^{238}U and ^{226}Ra/^{234}U activity ratios versus [1/U]contents, of water samples affected by the salinization process (eastern part of the Astian aquifer).

In that regard, two hypothesis can be put forward in order to explain the disequilibrium of the above-mentioned activity ratios of the salty end-member :

1. If we consider the non-equilibration/non-interaction between the salty water rising up and the underlying formations (including the walls of the hydraulic "chimneys"), the disequilibrium of the activity ratios is considered as time dependent. It could be interpreted as the result of both residence time of the salty water in the underlying aquifer, and transit time toward the Astian aquifer.

2. The second hypothesis takes into account the possibility of a geochemical interaction of the salty water with the solid phase (underlying carbonated formations). In that case, the ^{226}Ra content can be partially sustained, and the disequilibrium of the activity ratios can not directly be interpreted in terms of residence time.

4. CONCLUSION

According to the groundwater geochemistry, the Astian aquifer has been divided in two parts. The western part of the aquifer, unaffected by processes of mixing with a marine solution, has been used to identify the baseline conditions of groundwater circulation in this sandy formation. On the opposite, groundwater mineralization in the eastern part of the Astian aquifer increases according a binary mixing between (1) the fresh water as recognized in the western part of the aquifer, and (2) a marine solution with high carbon content due to deep CO_2 diffusion.

Moreover, preliminary observations and analyses have shown that both contents and activity ratios of uranium and radium can be used as «dating» tools in very particular cases.

Several constraints have to be considered such as the ^{226}Ra *in-situ* production and the initial ^{226}Ra contribution. As emphasized in our study, the modeling of the ^{226}Ra ages is closely related to the estimation of the ^{226}Ra *in-situ* production, itself dependent upon the geological characteristics of the aquifer matrix such as porosity, permeability, and mineralogy.

Despite the fact that the Astian aquifer has been considered as homogeneous all over the study area, the ^{226}Ra *in-situ* production rate can not be extended to the deeper aquifer formations implied in the salinization and mixing processes. This limits the use of ^{226}Ra as a dating tool to the groundwater unaffected by these processes.

The ^{226}Ra *in-situ* production and the initial ^{226}Ra contribution are site-specific, and time-dependent. Nevertheless, the ^{226}Ra dating method is very promising, especially (1) for aquifers where these two parameters can be well differentiated, and (2) for the 0 to 10 ky time-scale.

Aknowledgements

The authors would like to thank the *Laboratoire d'Hydrogéologie*, Université d'Avignon (France), Dr. Bassam GHALEB from the *GEOTOP Laboratory* (UQAM, Montreal, Canada), Dr. Anne Laurent from the *DIREN Languedoc-Roussillon* (France), and the local water-supply companies for their contribution to our investigations. This work is supported by the EC project PALAEAUX (Programme N° ENV4-CT95-0156).

REFERENCES

[1] BARKER, A.P., et al., "Processes affecting groundwater chemistry in a zone of saline intrusion into an urban aquifer", Applied Geochemistry **13** (6) (1998) 735–749.

[2] CALVACHE, M.L., PULIDO-BOSCH, A., "Effects of geology and human activity on the dynamics of salt-water intrusion in three coastals aquifers in southern Spain", Environmental Geology, **30** (3/4) (1997) 215–223.

[3] BARBECOT, F., et al., "Identification et caractérisation d'un biseau salin dans l'aquifère côtier du Bajocien-Bathonien de la région de Caen (France)", Comptes Rendus de l'Académie des Sciences, série IIa, **326** (1998) 539–544.

[4] HISCOCK, K.M., et al., "Hydrochemical and stable isotope evidence for the extent and nature of the effective Chalk aquifer of north Norfolk, UK", Journal of Hydrology, **180** (1996) 79–107.

[5] RISLER, J.J., "The development of environmental protection and water management policy in the European Union", Environmental Geology, **30** (3/4) (1997) 285–286.

[6] LAURENT, A., "La gestion en bien commun des eaux souterraines : la nappe des sables astiens de Valras-Agde (Hérault), une opération pilote en Languedoc-Roussillon", PhD Thesis, University of Montpellier II, Montpellier (1993).

[7] LEDUC, C., "Hydrogéologie de la nappe astienne entre Agde et Valras", PhD Thesis, U.S.T.L. Montpellier , Montpellier (1985).

[8] BERGER, G. et al., Carte géologique de la France au 1/50 000, feuille d'Agde et notice associée, Edition du BRGM, Orleans (1978).

[9] JOFFROY, M.E., et al., "Thermal ionization mass spectrometry measurements of Ra-226 and U isotopes in soils, surface and groundwaters", Isotope techniques in the study of environmental changes, IAEA–SM–349/49 (1998) 727–743.

[10] BARBECOT, F., et al., "Carbon-14 dating of groundwater from the Astian sandy aquifer (Mediterranean coast, southern France) : chemical and isotopic approaches.", in prep.

[11] MAISONNEUVE, J. and RISLER, J.J., "La ceinture péri-alpine "carbo-gazeuse" de l'Europe occidentale", Bulletin du BRGM, Série II, 2 (1979) 109–120.

[12] FONTES, J.C., "Chemical and isotopic constraints on 14-C dating of groundwater", Radiocarbon After Four Decades, Springer-Verlag, New York (1992) 242–261.

[13] SCHOELLER, H. J., "Influence du climat, de la température sur la teneur en HCO_3 et H_2CO_3 des eaux souterraines", Journal of Hydrology, **46** (1980) 365–376.

[14] JOFFROY, M.E., "Analyses par spectrométrie de masse du ^{226}Ra et des déséquilibres ^{234}U/^{238}U dans les eaux naturelles : un nouvel outil de datation en hydrogéologie", PhD Thesis, University of Paris XI, Orsay (1997).

ISOTOPIC AND CHEMICAL COMPOSITION OF GROUNDWATER IN THE BOLIVIAN ALTIPLANO, PRESENT SPACE EVOLUTION RECORDS HYDROLOGIC CONDITIONS SINCE 11 000 Yr

Anne COUDRAIN* and Amal TALBI
Sisyphe UMR CNRS-UPMC, Case 123, 4 place Jussieu, 75 252 Paris, France
Michel LOUBET
UMR CNRS-Université de Toulouse, France
Robert GALLAIRE
IRD/ORSTOM, France
Claude JUSSERAND
C.R.G. - UPMC, Thonon, France
Edson RAMIREZ
IHH, Universidad Mayor de San Andrés, La Paz, Bolivia
Emmanuel LEDOUX
Centre Informatique Géologique, ENSMP, UMR Sisyphe, France

Abstract

The phreatic aquifer of the central Altiplano shows a Cl concentration that increases from 0.5 meq l^{-1} upstream to 150 meq l^{-1} downstream. The main outflow process from the aquifer is the upward flow E into the unsaturated zone associated to evaporation close to soil surface. A relation has been established for any arid zone areas on the base of isotopic profiles: E (mm yr^{-1}) = $63\ Z^{-1.5}$ where Z (m) is the water table depth under soil surface. The aquifer under study may have acquired its high chlorine content during last lacustrine phase (Tauca, 12 ka BP). Arguments for this hypothesis are: *(i)* maximum level of the lake (3780 m) higher than present soil elevation in the area, *(ii)* same order of salinity in the paleolake and in the more saline groundwater, *(iii)* weak molar ratio of Li/Cl in saline groundwater and in the Tauca, *(iv)* modelling of Cl transport over 11 000 years consistent with observed spatial evolution of Cl in groundwater. To this scenario, might be superimposed the assumption of a delay for the convective transfer of salt towards south by the coupled effects of accumulation of salt in the unsaturated zone by evaporation from the aquifer during thousand or so years, and of the subsequent return of this salt downwards to the aquifer during some short rainy periods. The $^{87}Sr/^{86}Sr$, major and trace element compositions of surface and groundwater support this proposed scenario.

---

* Work performed within the framework of the "Programme National de Recherche en Hydrologie" and the scientific co-operation between France and Bolivia between the ORSTOM and the UMSA.

1. INTRODUCTION

Research on chlorine transport in aquifers is interesting for the management of the water resources and for the understanding of the climate - hydrological cycle relation. Compared to surface water, groundwater seems better protected with respect to pollution. However it is observed that many aquifers present high chlorine concentrations and that groundwater by salinisation is increasing over the world. The processes at the origin of salt content in groundwater of a non saline rock are: sea water intrusion [1], upward from associated leakage from deep brines [2, 3], soil salinisation associated to irrigation and to the rising of the water table by deforestation [4], transport of salt by aerosols and their subsequent leaching into shallow aquifers [5]. Chemistry [6], natural isotopes [7] and modelling [8] are the main tools to identify the processes at the origin of salt content.

In most cases chlorine is conserved in the solution and groundwater velocity ranges between 1 and 10 m yr^{-1}. As a consequence, in regional aquifers where flow path are longer than several kilometres, Cl concentration may reflect hydrologic conditions over 10 thousands years or more. Climatic evolution may be marked in the spatial evolution of Cl.

The Altiplano is an endorheic catchment (Fig. 1) including the lake Titicaca (16°S, 3810 m) and the Uyuni Salar (21°S, 3653 m). The strong climatic variations of the Holocene were expressed by considerable variations in regional lake levels [9]. The chronology of these hydrologic conditions makes the Altiplano a particularly valuable source of documentation of the Holocene and its climatic variations. The aquifer under study of around 6000 km^2 is in quaternary sediments and lies in the upstream portion of the southern catchment of Uyuni. Close to present recharge area, Cl concentration in groundwater is less than 10 meq l^{-1} that may not explain the large chloride contents in groundwater that reach downward 150 meq l^{-1}. Taking into account the climatic evolution since the paleolake Tauca covered the region, mathematical modelling of Cl transport and isotopic data illustrate that hydrologic conditions since 11 ka after the paleolake Tauca retreat have to be taken into account to explain the present space evolution of the chemical composition and that the evaporative flux from the aquifer in such arid zone is important.

2. EVAPORATION FROM PHREATIC AQUIFER IN ARID ZONE AREA

Collected data of hydraulic conductivity as a function of suction (S) up to more than 1000 m and estimations of evaporation after about 30 isotopic profiles allow to conclude [10]:

- high dependence of evaporative flux on soil characteristics had been previously concluded on insufficient data for arid conditions,
- after recently published K(S) data reported in [10], the upper and lower bounds of this relation are :

$$28\ z^{-1.8} < E < 205\ z^{-1.6}$$

- the fitted curve determined on the base of the isotopic profiles from Algeria, Australia, Bolivia, Chile, Niger, Réunion and Tunisia [11-21] is :

$$E = 63\ (\pm 5)\ z^{-1.5} \text{ with E in mm yr}^{-1} \text{ and z in m}$$

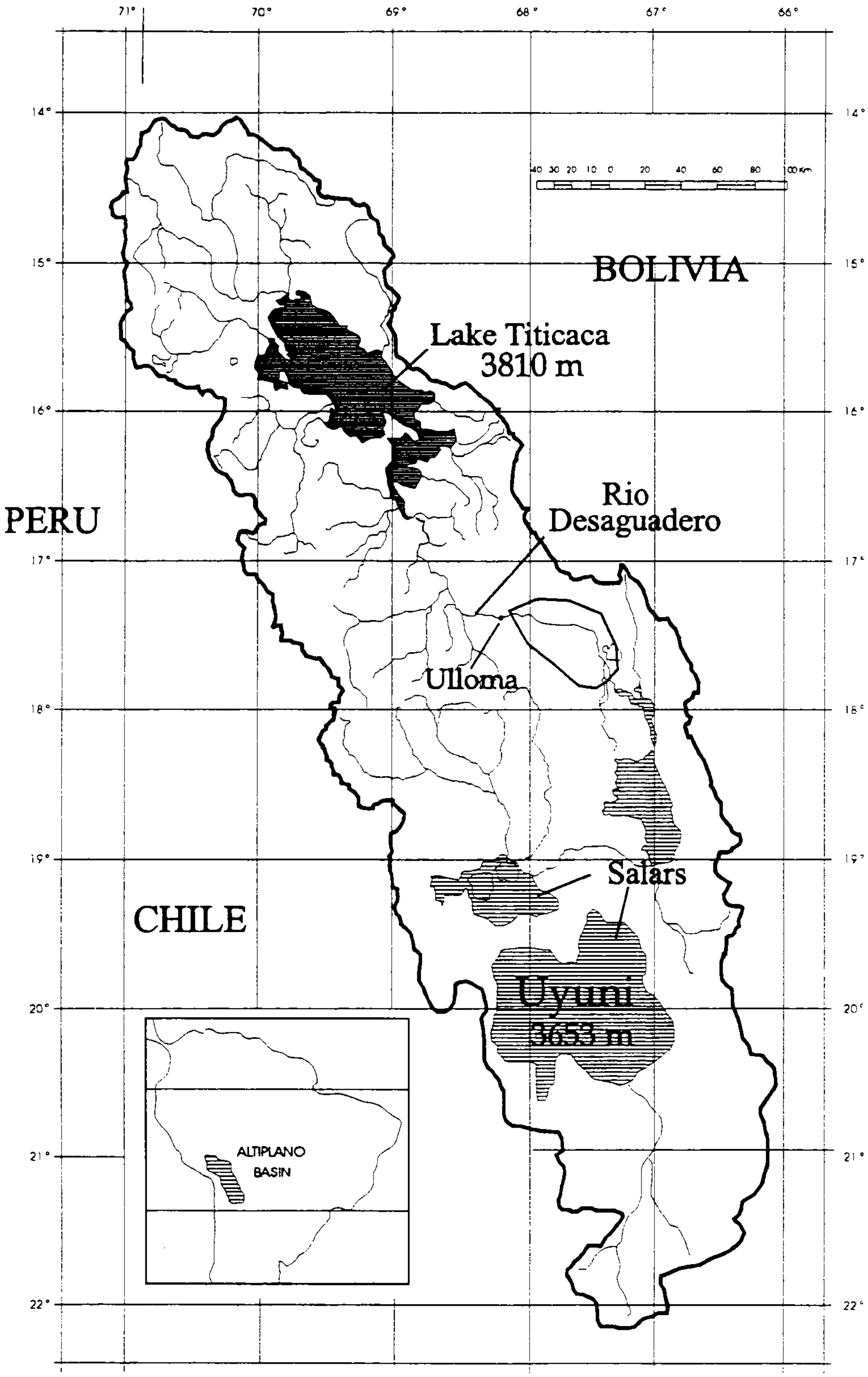

FIG. 1. Endorheic catchment of the Altiplano and the under study area. The weir of Ulloma (3770 m a.s.l.), upstream from the studied area, limits the northern catchment of the Titicaca and the southern one of the salars.

After this relation, the evaporative flow decreases from 380 mm yr^{-1} to 1 mm yr^{-1} when the water table depth increases from 0.3 m to 18 m under soil surface (Fig. 2). This relation is used in the present study to constrain the present hydrologic mass balance by prescribing the outflow by evaporative flow (section 3) and to model during 11 ka the groundwater flow and Cl transport including the Cl-accumulation in the unsaturated zone by the evaporative flow (section 4).

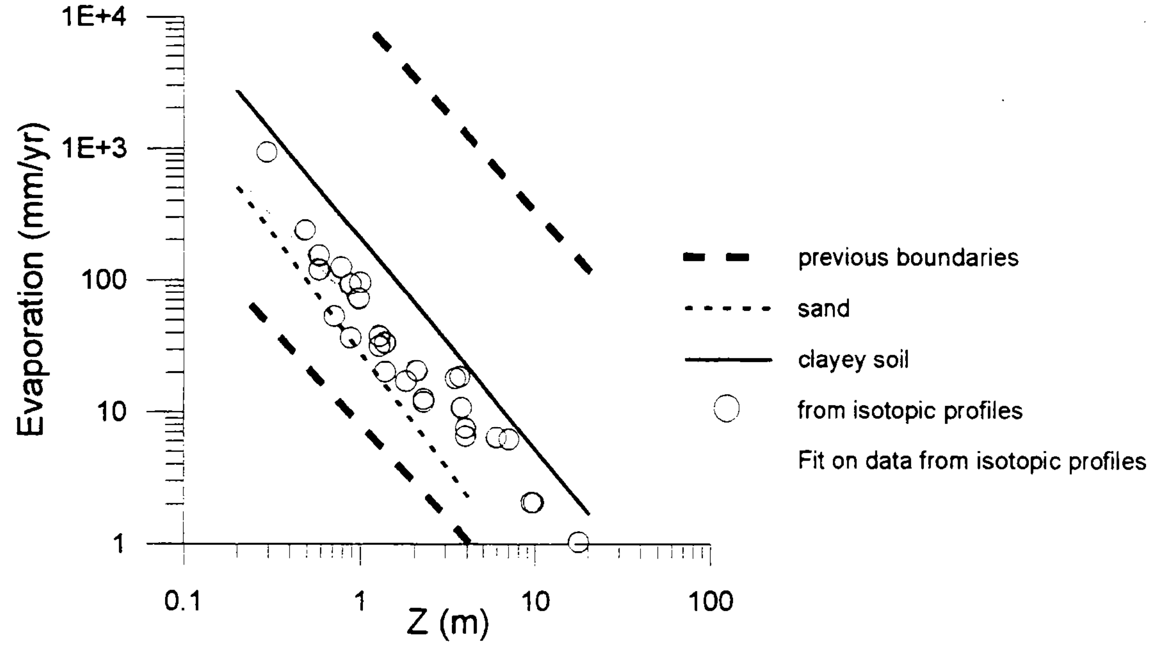

FIG. 2. Evaporation from phreatic aquifer vs. water table depth under soil surface (Z). Circles: local estimations of E from isotopic profiles; curves "sand" and "clayey soil": computed on the base of hydraulic conductivity measured for suction from saturation to very low water content; curves "previous boundaries": lowest and highest estimations of E from previous hydraulic studies based on insufficient data for arid zone area.

3. PRESENT WATER MASS BALANCE

Present precipitation, concentrated during one rainy season, is of the order of 350 mm yr^{-1}. It allows recharging the aquifer from runoff between Tertiary mountains and the hinge line with the flat plain (Fig. 3). The other present recharge is the inflow from the Rio Desaguadero, fed by the Titicaca Lake and northern tributaries (Fig. 1). The use of an hydrogeological model [22] allowed to compute for present steady state that the total outflow by evaporation from approximately 80% of the aquifer area (3550 km^2), where the piezometric head is at less than 20 m below soil surface, is of the order of 28 10^6 m^3 yr^{-1}.

4. MODELLING Cl TRANSPORT OVER THE PAST 11 000 YEARS

On the base of recent quaternary studies [9, 23, 24], it can be assumed that the aquifer was covered by the paleolake Tauca (12 ka BP) during a period long enough to allow diffusion between both water bodies. Geochemical data collected in the zone under study also argue in favour of this hypothesis : *(i)* ^{14}C activities of inorganic carbon dissolved in groundwater range between 59 and 4 pmC, (ii) δ^2H *vs.* $\delta^{18}O$ graph of saline groundwater [25] suggests that evaporation occurred prior to infiltration, *(ii)* saline groundwater and reconstructed composition of paleolake Tauca present low values of Li/Cl [26, 27]. In order to test if chloride in solution of the Quaternary aquifer may remain since the paleolake covered the area, modelling of the Cl transport during 11 ka has been undertaken.

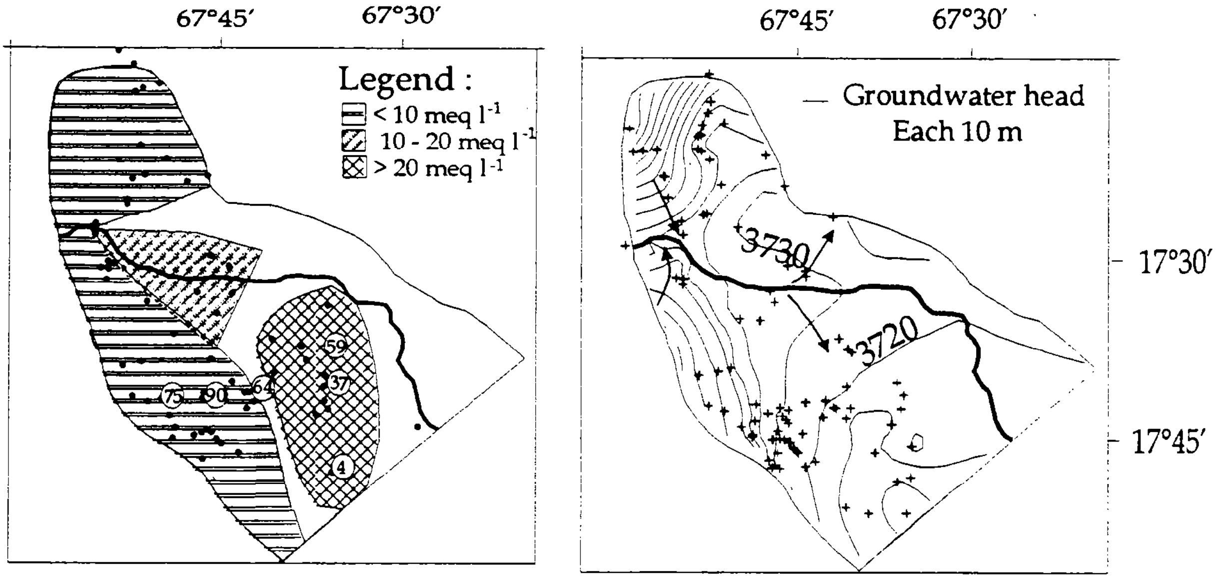

FIG. 3. Maps of present Cl concentration and piezometry of the phreatic aquifer in the central Altiplano. Cl concentrations increases from upstream (0.5 meq l^{-1}) in the recharge zone to downstream (150 meq l^{-1}) where 4 pmC were analysed for ^{14}C.

Modelling has been performed by using the NEWSAM code [28] that has been modified to take into account the outflow by the evaporative flow from the aquifer. For the groundwater flow modelling, input data are evolution of the infiltration, presence or lack of the Rio Desaguadero, hydraulic parameters (thickness 50 to 100 m; transmissivity $0.5\ 10^{-3}$ to $10^{-2}\ m^2\ s^{-1}$) of the aquifer. Output data computed by the simulation are the time and space evolution of groundwater head, outflows by evaporation and toward south and flow between the Rio Desaguadero and the aquifer.

Reconstitution of possible infiltration towards the aquifer has been computed as follows. The water levels in a lake situated in an endhoreic catchment make it possible to calculate the associated rainfall rate by the use of the water balance over the whole catchment. The evolution during the Holocene of water levels in lake Titicaca, previously published, shows that in the most arid period, between 8000 yr and 4000 yr BP, the average level was 50 m lower than today. The rainfall associated with this low level is 635 ± 50 mm yr^{-1} i.e. about 18% lower than the present amount [29]. Assuming a similar ratio of rain amounts between both catchment area than the present one, it has been computed in this study that lowest rain amount close to the zone under study (17°30 S) was about 290 mm during the arid period from 8000 to 3000 yr BP. The evolution of the infiltration towards the aquifer has been computed proportionally to this reconstructed rainfall amount.

Modelling takes also into account the lack of perennial flow of the Desaguadero between 10 ka and 2 ka B.P. when the low level of water in lake Titicaca did not allow outflow towards the Rio Desaguadero [24]. Results show that between 10 ka and 2 ka, during lack of perennial flow in the Rio Desaguadero, the hydraulic head of the aquifer is decreasing and evaporative flux decreases. Reversibly, after 2 ka when infiltration from the Rio Desaguadero is again possible and that infiltration from local runoff increases, evaporative flux and underground flow towards South increase progressively. Outflow by evaporation is always close to 2/3 of the total outflow, which again demonstrates how important it is to take it into account. The local maximum Darcy velocity, at each time step, is always of the order of 1 m yr^{-1}.

Associated to groundwater flow, the transport of chloride has been simulated by NEWSAM, assuming a mean value of 0.25 for the porosity. Initial concentration of chloride was assumed to be of 200 meq l^{-1} where the soil surface is below 3740 m and of 0.5 meq l^{-1} above this elevation. This corresponds to the hypothesis that the paleolake Tauca covered the aquifer during sufficient time (2 ka) to allow diffusion between the lake and the aquifer so that the concentration in the aquifer reached 200 meq l^{-1}. The Cl concentrations associated to inflow by runoff and by the Rio Desaguadero are 0.5 and 10 meq l^{-1} respectively.

Output of the Cl transport modelling is the time evolution of Cl concentration in the groundwater and inflow and outflow of chloride. Roughly, half of the initial quantity of chloride in the aquifer is leaving out from the aquifer by underground flow towards South and the other half by evaporation that lead to salt accumulation in the unsaturated zone with a weighted mean value of 19.7 kg m^2 (Fig. 4-a1). The computed present concentration is in the right riverbank less than 30 meq l^{-1} (Fig. 4-b1).

Subsequent infiltration of the chloride accumulated in the unsaturated zone toward the aquifer should have occurred with a small amount of water. Such process would keep agreement with the low and decreasing ^{14}C activity toward South (57 to 4 pmC). The Cl profiles of the unsaturated zone [22] show that very probably no infiltration occurred toward the aquifer in the flat plain since around two thousand years. Another simulation of Cl transport has been conducted where the Cl accumulated in the unsaturated zone between 11 ka and 2 ka is locally added to the groundwater solution (Fig. 4).

The model allow to reproduce the special pattern of observed chloride concentration similar to an ellipsoid in the right river bank where the more saline water are the older one with concentration as high as 80 meq l^{-1}. The Cl accumulated close to the point with a value of 37 in ^{14}C activity is 18 kg per m^2 of soil surface; the computed one is 15 kg m^{-2} (it is 39 kg m^{-2} when injection of Cl at 2 ka is not taken into account). In the left riverbank, the observation of very saline soils and non-permanent surface water is in good agreement with this second simulation.

However, at this stage the absolute values of chloride concentrations may not still be compared between observed and computed values. A study by electromagnetic investigation is now undertaken to get data on the spatial evolution of the aquifer thickness.

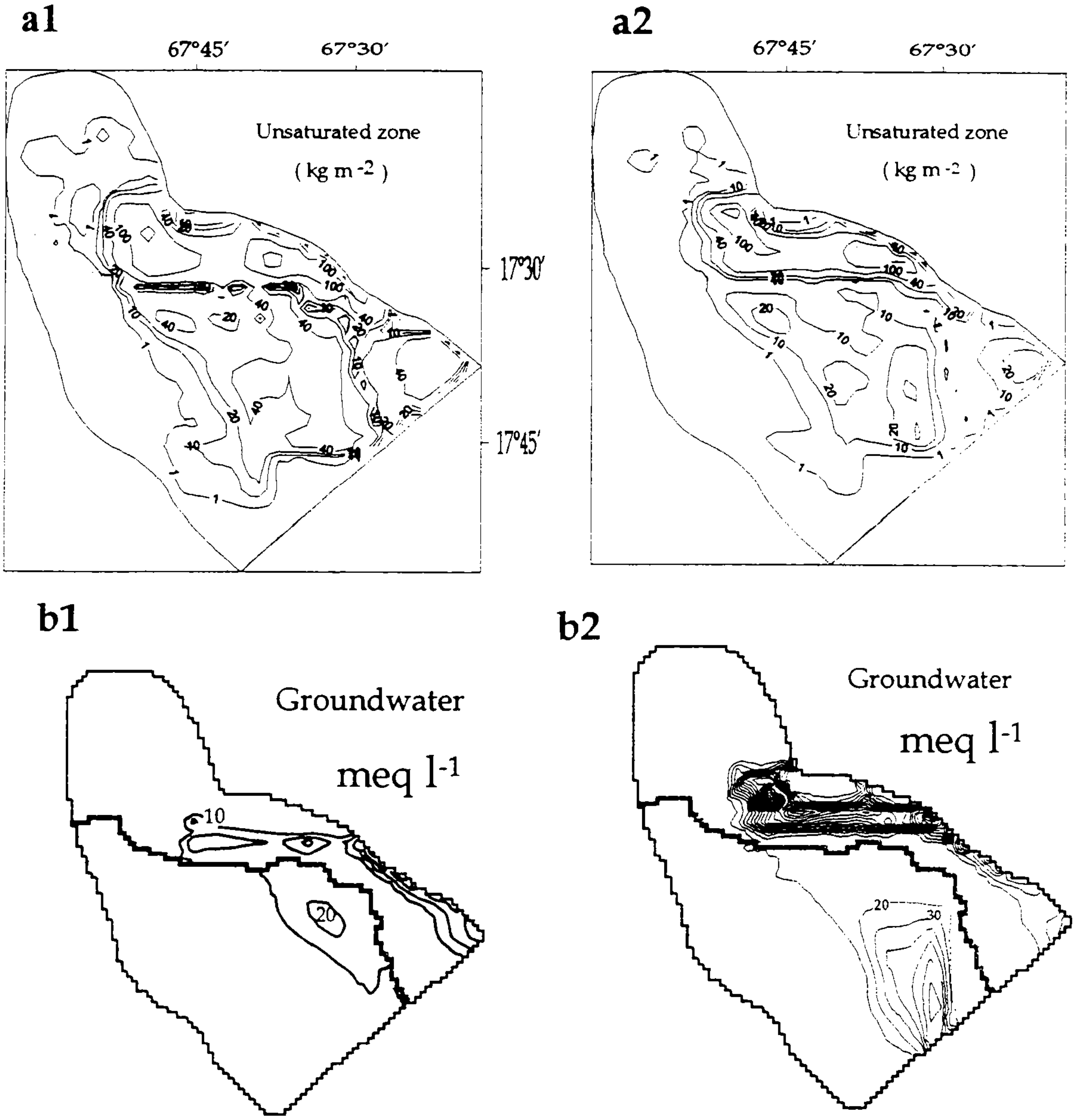

FIG. 4. Results at present time of Cl transport simulation during 11 ka. Cl content (kg m^{-2}) in the unsaturated zone (a1 and a2) and Cl concentration (meq l^{-1}) in the aquifer (b1 and b2). a1 and b1: no leaching of salt accumulated in the unsaturated zone; a2 and b2: Cl accumulated in the unsaturated zone between 11 and 2 ka BP is leached into the aquifer at 2ka BP.

5. ^{87}SR/^{86}SR, MAJOR AND TRACE ELEMENT COMPOSITIONS

Geochemical data (major and trace elements and Sr isotopic compositions) were obtained on solutions sampled from installed wells in the area under study and from Northern and Western rivers that are in the recharge zones to the aquifer. These data allowed identifying within the aquifer four groups of distinct geochemical compositions extending on different geographical area. The relevant parameters to distinguish these groups are Cl, Na/Cl, $^{87}Sr/^{86}Sr$, U/As, U/Rb.

The first group corresponds to the brines (1.8 mol l^{-1} of Cl) of some localized dacitic domes drilled by a gold mine exploitation. The value of their Sr isotopic ratio is as high as 0.719. Two other groups correspond to the present recharge area of the aquifer (Fig. 5). The saline waters at the center and south center of the area displayed specific compositions distinct from the three other groups, supporting a distinct origin of these waters. Diagrams such as (C_x, C_{Cl}) and ($^{87}Sr/^{86}Sr$, C_x/C_{Sr}), where C_i is the concentration of the chemical element i, were used for discussing the origin of the groundwater salinity. In these diagrams the saline samples of groundwater display linear trends congruent with the hypothesis of a mixing between two end member components, one of low Cl content and the other one of high Cl content. The end member with low Cl content is associated with the recent recharge waters. The Cl enriched end member does not correspond to any identified group of present water. Various characteristics (SO_4/Cl, Li/Cl, K/Cl, Na/Cl, $^{87}Sr/^{86}Sr$ compositions) lead us to identify the Cl enriched end member as the paleolake Tauca or some more recent laguna.

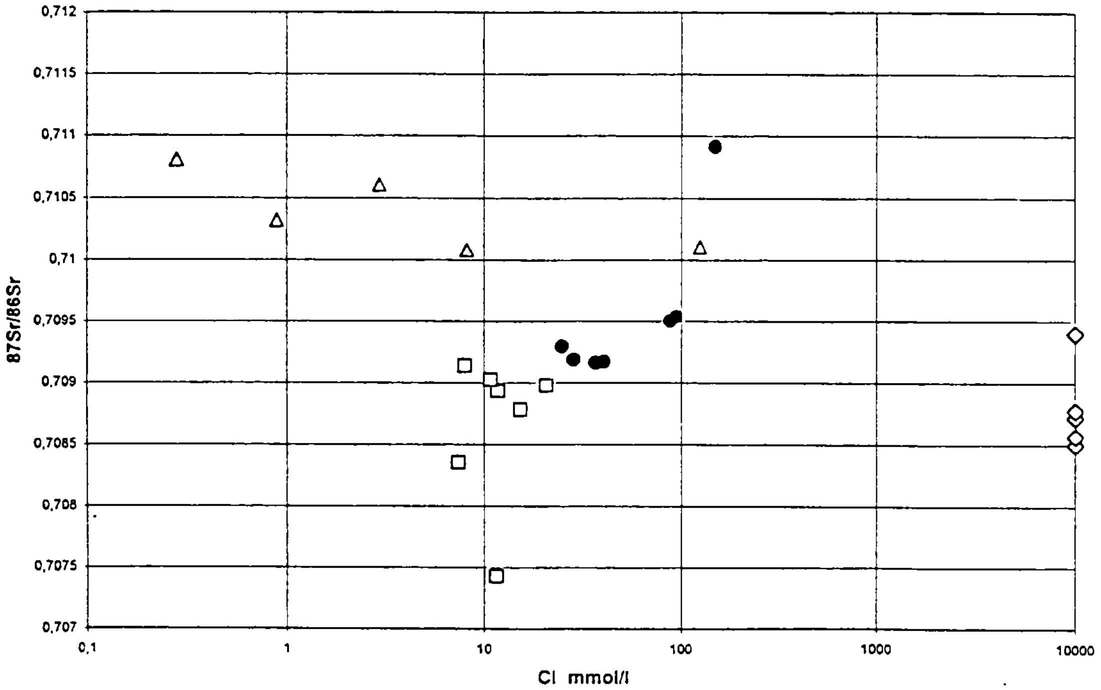

FIG. 5. $^{87}Sr/^{86}Sr$ versus Cl content of waters, and $^{87}Sr/^{86}Sr$ composition of stromatolites from Bolivian Altiplano. White triangle: surface and groundwater corresponding to local runoff and western tributaries recharge. White square: surface and groundwater corresponding to recharge from northern catchment. Black circle: saline groundwater in the aquifer under study. White diamonds: stromatolites sampled in various parts of the Altiplano.

6. DISCUSSION AND CONCLUSION

One part of this study, on evaporation from aquifers under arid climatic conditions, is an example of the usefulness of comparing different approaches. Results from isotopic approach allowed re-analysing the previous accepted and erroneous results from hydraulic approach. Finally the simple relation proposed by this study may be used for local or regional and present or past estimation of evaporation from aquifers in any arid zone area where evaporation is a major outflow process.

On the dynamics of the aquifer of the central Altiplano, present groundwater flow, spatial evolution of geochemical parameters (^{14}C, δ^2H, δ^{18}O, Li/Cl, trace element and Sr isotopic compositions) and results of modelling groundwater flow and Cl transport allow to conclude that the present concentration of chloride in the aquifer may be bound to the paleolake Tauca (12 ka B.P.). Temporary accumulation of salt in the unsaturated zone due to evaporation over long arid periods and subsequent leaching into the aquifer may also have occurred, probably at 2 ka B.P. This secondary process might have delayed the transfer of salt towards South.

The functioning proposed on the base of the available data is the following. When the aquifer was covered by the paleolake Tauca (maximum level at 12 ka BP), diffusion of salt from the saline lake allowed to increase chloride concentration in the aquifer. It is assumed today, as a working hypothesis, that this concentration might be around 200 meq l^{-1}. Since the lake retreat, around 11 ka BP convection pushes the bulk of saline groundwater toward southeast. This movement was very slow during the very dry period between 8 ka and 2 ka. Since the lake retreat, evaporation from the aquifer led to accumulate salt in the unsaturated zone over the aquifer. This salt remains in general in solution that is under saturated with respect to halite. A humid period could have taken place between 4 and 2 ka when the level of the lake Tititaca is recorded to have increased rapidly. Subsequently, such humid period could have allowed the leaching of the salt into the aquifer by a small amount of water. Such process would not modify the ratio of lithium/chloride or the isotopic ratio of strontium.

REFERENCES

[1] Rosenthal E., Vinokurov A., Ronen D., Magaritz M., Moshkovitz S., Anthropogenically induced salinization of groundwater: a case study from the coastal plain aquifer of Israel. J. Contam. Hydr. **11(1-2)** (1992) 149-71.

[2] Wei H.F., Ledoux E., Marsily G.de, Regional modelling of ground-water flow and salt and environmental tracers transport in deep aquifers in the Paris basin. J. Hydrol. **120** (1990) 341-58.

[3] Sharaf M.A., Hussein M.T., Synthèse hydrogéologique et hydrochimique d'un réservoir gréseux en zone aride. J. Sci. Hydrol. **41(5)** (1996) 683-96.

[4] Bari M.A., Schofield N.J., Lowering of a shallow, saline water table by extensive eucalypt reforestation. J. Hydrol. **133(3-4)** (1992) 273-91.

[5] Jones B.F., Hanor J.S., Evans W.R., Sources of dissolved salts in the central Murray Basin, Australia. Chem. Geol. **111** (1994) 135-54.

[6] Vengosh A., Rosenthal E., Saline groundwater in Israel : its bearing on the water crisis in the country. J. Hydrol. **156(1-4)** (1994) 389-430.

[7] Yurtsever Y. Role and contribution of environmental tracers for study of sources and processes of groundwater salinization. In: Hydrochemistry. Peters N.E., Coudrain-Ribstein A. (Eds) AISH **244** (1997) 3-12.

[8] Konikow L.F., Arévalo J.R., Advection and diffusion in a variable-salinity confining layer. Water Resou. Res. **29(8)** (1993) 2747-61.

[9] Servant M., Fournier M., Argollo J., Servant-Vildary S., Sylvestre F. *et al.*, La dernière transition glaciaire/interglaciaire des Andes tropicales sud (Bolivie) d'après l'étude des variations des niveaux lacustres et des fluctuations glaciaires. CRAS Paris **320(II)** (1995) 729-36.

[10] Coudrain-Ribstein A., Pratx B., Talbi A., Jusserand C., L'évaporation des nappes phréatiques sous climat aride est-elle indépendante de la nature du sol ? Is the evaporation from phreatic aquifers in arid zones independent of the soil characteristics ? C. R. Acad. Sc. Paris **326(II)** (1998) 159-65.

[11] Zouari K., Aranyossy J.F., Mamou A., Fontes J.-C., Etude isotopique et géochimique des mouvements et de l'évolution des solutions de la zone aérée des sols sous climat semi-aride (sud tunisien), in Stable and radioactive Isotopes in the study of the unsaturated soil zone, AIEA, Editor. 1985, AIEA: Vienne. p. 121-143.

[12] Allison G.B., Barnes C.J., Estimation of evaporation from the normally "dry" Lake Frome in South Australia. J. Hydrol. **78** (1985) 229-42.

[13] Colin-Kaczala C., Profils isotopiques (^{18}O et ^{2}H) de fluides (eau liquide, vapeur et CO$_2$) de la zone non saturée sous climat désertique : application à l'évaporation des nappes libres au Sahara Nord-Occidental. Thèse Univ. Paris-Sud (1986).

[14] Fontes J.C., Yousfi M., Allison G.B., Estimation of long-term, diffuse groundwater discharge in the northern Sahara using stable isotope profiles in soil water. J. Hydrol. **86** (1986) 315-27.

[15] Grilli A., Pollastri A., Ortiz J., Aguirre E. Evaluacion de tasas de evaporacion desde salares, utilizando tecnicas isotopicas - applicacion en el salar de Bellavista, Chile. In: Estudios de hidrologia isotópica en America Latina. OIEA Salazar, Mexico (1989) 155-68.

[16] Grunberger O., Etude géochimique et isotopique de l'infiltration sous climat tropical contrasté - massif du Piton des neiges - île de la Réunion. Thèse Univ. Paris-Sud (1989).

[17] Taupin J.D., Evaluation isotopique de l'évaporation en zone non saturée sous climat sahélien et évolution géochimique des solutions du sol (Vallée du Moyen Niger). Thèse Univ. Paris Sud, Orsay (1990).

[18] Woods P.H., Evaporative discharge of groundwater from the margin of the Great Artesian Basin near Lake Eyre, South Australia. Thesis Univ. of South Australia (1990).

[19] Aranyossy J.F., Filly A., Tandia A.A., Louvat D., Ousmane B., Joseph A., Fontes, J.C., Estimation des flux d'évaporation diffuse sous couvert sableux en climat hyper-aride (erg de Bilma, Niger). In: Isotope techniques in Water Resources DevelopmentVienne: IAEA (1991) 309-24.

[20] Daoud D., Caractérisation géochimique et isotopique des eaux souterraines et estimation du taux d'évaporation dans le bassin du Chott Chergui (zone semi-aride), Algérie. Thèse Univ. Paris-sud Orsay (1995).

[21] Coudrain-Ribstein A., Pratx B., Jusserand C., Quintanilla J., Cahuaya D., Bilan et évaporation d'un aquifère en zone aride, Altiplano central bolivien. In: Hydrochemistry. Peters N.E., Coudrain-R. A. (Eds) AISH **244** (1997) 53-61.

[22] Coudrain-Ribstein A., Loosemore T., Rochat P., Quintanilla J., Younger P. Use of a groundwater model in assessing possible sources of salinity on the central Bolivian Altiplano. In: Models for assessing and monitoring groundwater quality. Wagner B.J., Illangasekare T.H., Jensen K.H. (Eds) Boulder, USA: AISH **227** (1995) 11-9.

[23] Bills B.G., DeSilva S.L., Currey D.R., Emenger R.S., Lillquist K.D. *et al.*, Hydro-isostatic deflection and tectonic tilting in the Central Andes - Initial results of a GPS Survey of lake Minchin Shorelines. Geophys. Res. Lett. **21(4)** (1994) 293-6.

[24] Mourguiart P., Argollo J., Corrège T., Martin L., Montenegro M.E. *et al.*, Changements limnologiques et climatologiques dans le bassin du lac Titicaca (Bolivie) depuis 30 000 ans. C. R. Acad. Sc. Paris **325(II)** (1997) 139-46.

[25] Coudrain-Ribstein A., Olive P., Quintanilla J., Sondag F., Cahuaya D. Salinity and isotopic dynamics of the groundwater resources on the Bolivian Altiplano. In: Application of tracers in arid zone hydrology. Adar E., Leibundgut C. (Eds) Vienne, Autriche: AISH **232** (1995) 267-76.

[26] Risacher F., Fritz B., Quaternary geochemical evolution of the salars of Uyuni and Coipasa, Central Altiplano, Bolivia. Chem. Geol. **90** (1991) 211-31.

[27] Coudrain-Ribstein A., Talbi A., Loubet M. Paleo-climatic reconstruction by modeling isotope and solute transport in an aquifer of the Bolivian Altiplano. In: Use of isotopes for analyses of flow and transport dynamics in groundwater systems. Yurtsever Y. (Ed.) USGS, Reston EU: AIEA **TECDOC** (1998)

[28] Ledoux E., Levassor A., NEWSAM un programme général de simulation des écoulements et des transports de matière dans les systèmes aquifères complexes. Notice d'utilisation CIG/ENSMP Fontainebleau (1993)

[29] Talbi A., Coudrain A., Ribstein P., Pouyaud B., Computation of the rain amount on the Titicaca catchment during Holocene. Calcul de l'évolution des pluies pendant l'Holocène sur le bassin versant du lac Titicaca (soumis) C. R. Acad. Sc. Paris.

^{18}O ISOTOPIC CHARACTERISATION OF NON-POINT SOURCE CONTRIBUTED HEAVY METALS (Zn AND Cu) CONTAMINATION OF GROUNDWATER

P.S. DATTA, K.M. MANJAIAH, S.K.TYAGI
Nuclear Research Laboratory
Indian Agricultural Research Institute
New Delhi - 110012, India

Abstract

In many urbanised areas, fast depletion and severe degradation of the of groundwater resource with contaminants such as nitrate, fluoride, and heavy metals is a common phenomenon, resulting in zonal disparity in fresh water availability. Therefore, for protection of groundwater from pollution and depletion, it is a matter of concern for the planners and decision makers to clearly characterise the sources of contamination and to search for an alternative approach for groundwater development and management. In this context, a new approach is presented here, based on monitoring of ^{18}O stable isotopic and heavy metals composition of groundwater, to clearly characterise non-point source contributed heavy metals pollution of groundwater in northern parts of Delhi area. In the investigated area, the Cu content in the groundwater ranges from 3-41 μg/l and Zn content ranges from 5-182 μg/l, showing considerable variation from location to location as well as within the small parts of a location. Wide variation in the ^{18}O stable isotope content of groundwater (δ value of -5.7‰ to -8.5‰) is due to significant variation in the $\delta^{18}O$-contents of rainfall with space and time, as well as intensity and distribution of rainfall. Enrichment in ^{18}O composition with increasing Cu and Zn levels in groundwater suggest that infiltration of rain water, irrigation water and surface run-off water from the surrounding farm lands, alongwith agrochemicals and other salts present in the soil, to be the main processes causing groundwater contamination. The concentration of Cu and Zn in groundwater vary spatially, due to different degrees of evaporation/recharge, amounts of fertiliser applied and wastes disposed, adsorption/dispersion of species in the soils and lateral mixing of groundwater. Two opposite mechanisms adsorption and redistribution of infiltrating water alongwith Zn and Cu species in the soil zone are likely to affect the movement of the Zn and Cu species. Further systematic research is needed on hydrogeologic characteristic of the groundwater flow field under natural and stressed conditions, dynamics of groundwater contaminants and its linkage with spatial and temporal variability in concentration, depth variation in contaminants level in relation to well structure and relative importance of vegetative uptake of contaminants from soil in pollution control.

1. INTRODUCTION

In Delhi area, the population directly or indirectly depend on groundwater for its daily raw water requirements for irrigation, domestic, industrial and other purposes. Vast and sprawling agricultural land, coupled with small scale industrial activities provide the main professional platform for the livelihood of the rapidly growing population in the semi-urbanised investigated area. The complexities of situation of groundwater occurrence in geological formations, fast depletion of groundwater due to indiscriminate withdrawal, presence of saline groundwater at varying depth [1,2], leaching of contaminants through farmlands and landfills containing municipal and industrial wastes and severe degradation of the resource base with contaminants such as nitrate, fluoride [3,4] and heavy metals have resulted in zonal disparity in fresh water availability. Therefore, groundwater situation in the region is inextricably linked with growth in population, water availability from different sources, water use and demand for different purposes, hydrogeology, rainfall and land use pattern changes, provisional basic social services and the degree of economic development. Therefore, for protection of groundwater from pollution and depletion, and to suggest an alternative approach for groundwater development and management, clear characterisation of contamination from heavy metals and other contaminants is a matter of concern for the planners and decision makers.

Some of the common non-point sources of the heavy metals (Zn and Cu) are fertilisers, farmyard manure and compost used for agricultural purposes, and land-disposed industrial effluents from plating, galvanising, rayon manufacture, rubber processing, pickling, and iron and steel production. Regular applications of fertilisers as well as indiscriminate disposal of wastes are likely to create a blanket non-point source of these contaminants. Although, metals vary widely in their toxicity depending on speciation, according to the approximate order of toxicity of metals, zinc and copper are rated as highly toxic. Unusually, zinc has low human toxicity, but relatively high toxicity to fish. The effects of a low continuous dose of copper may be remarkably similar to those of large, but fluctuating, inputs of copper and zinc. Zinc is essential for normal growth of crops and upto 2-10 mg/l are permitted in irrigation waters for continuous use on all types of soils. Even though zinc per se is not harmful, any accompanying element (due to pollution) may be toxic.

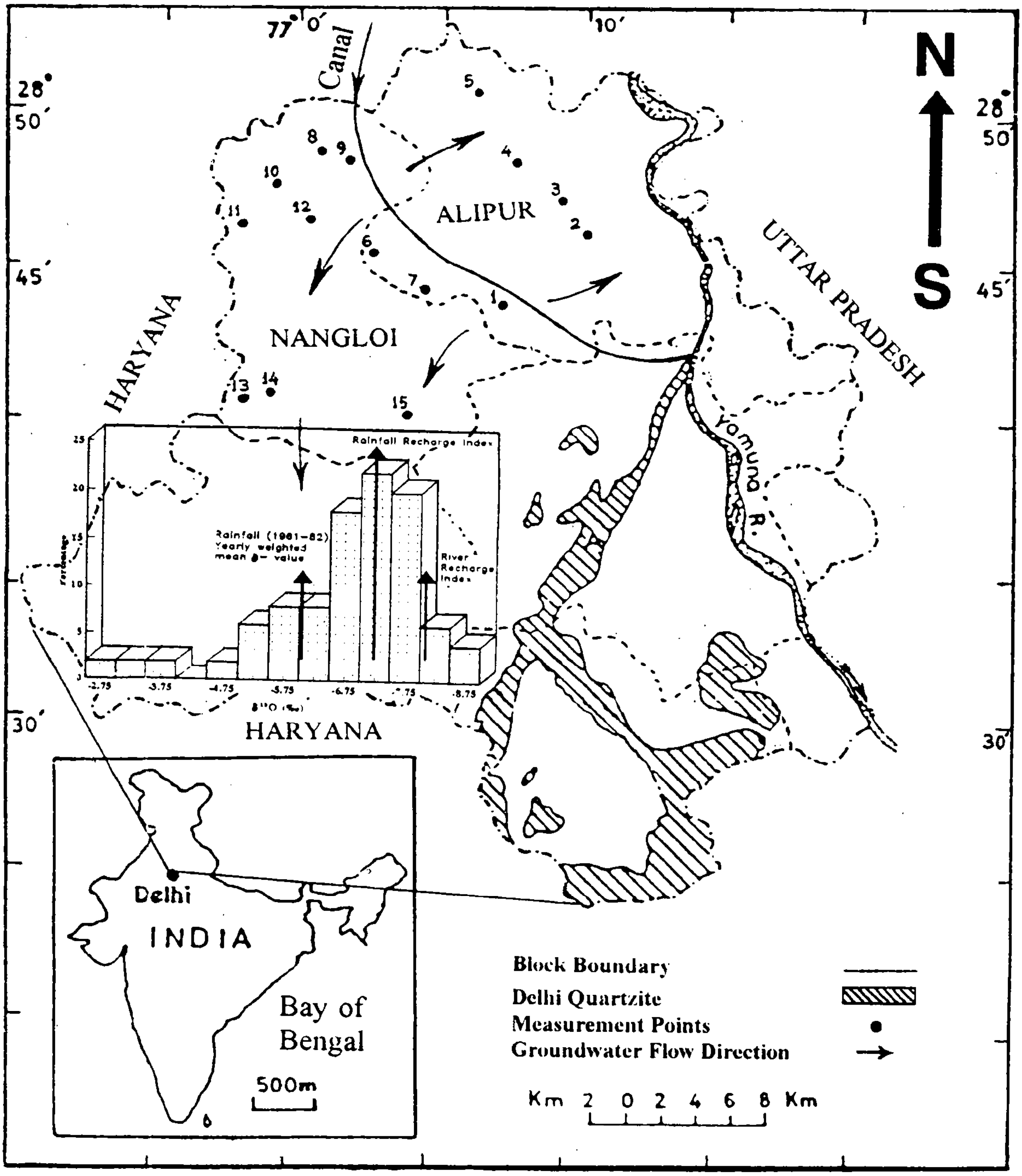

FIG 1. Map of National Capital Territory of Delhi showing sampling points in the investigated area. Inset box shows the frequency distribution of $\delta^{18}O$ in groundwater of Delhi area.

In this context, heavy metals (Zn and Cu) contamination characteristics of groundwater in Alipur and Nangloi Blocks of the investigated area (Fig.1) has been undertaken by monitoring the zinc, copper and ^{18}O isotope composition of groundwater. The stable isotope being a conservative tracer, the isotopic composition of water remains constant in the direction of groundwater flow, unless affected by physical processes such as mixing with water of different isotopic composition or subjected to evaporation during recharge. Evaporation of irrigation water and surface run-off water in the unsaturated zone and subsequent recharge may also cause significant isotopic enrichment in the groundwater, providing a dynamic representation of the groundwater system [3,4,5].

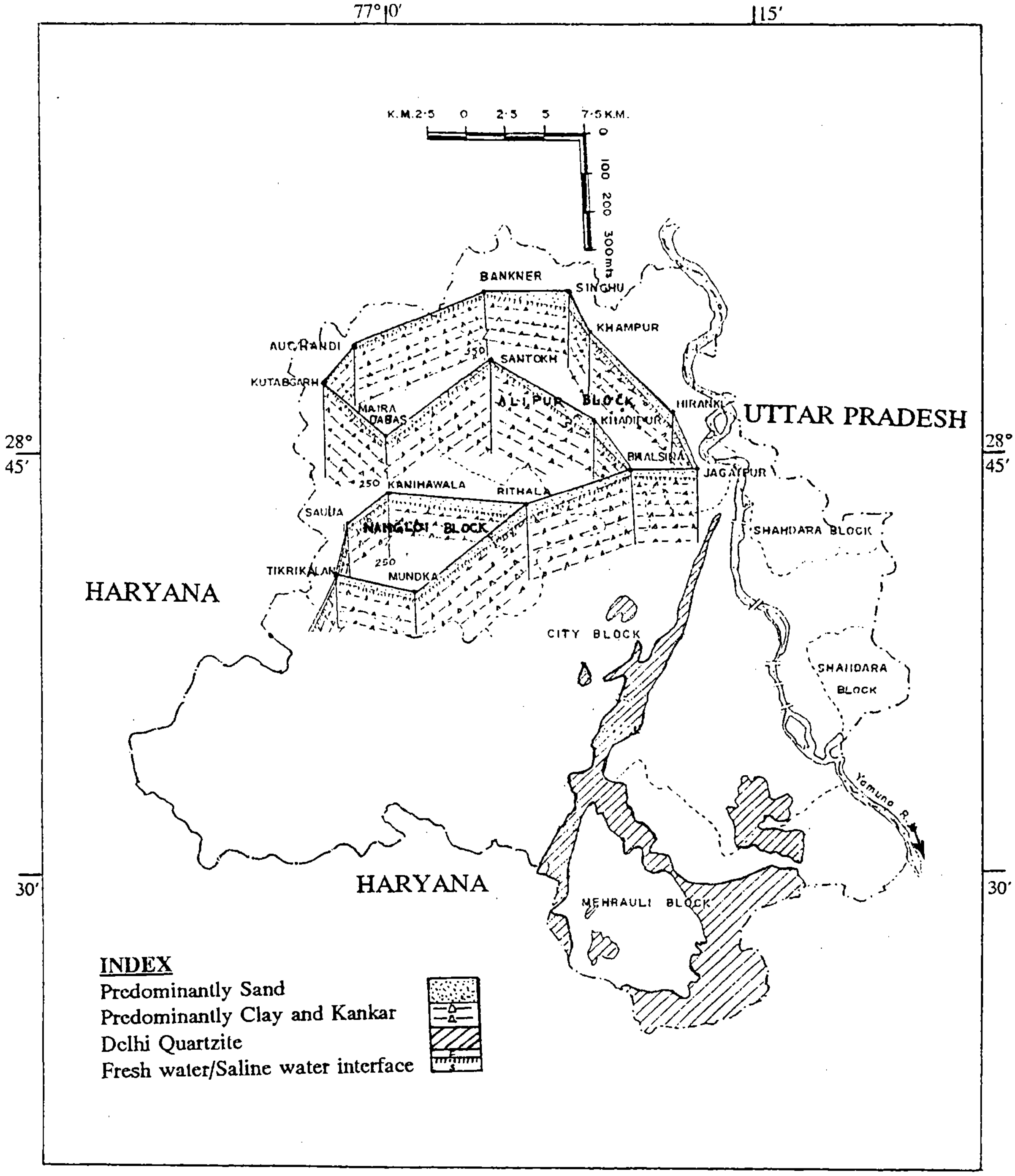

FIG.2. Map of National Capital Territory of Delhi showing aquifer disposition in the investigated area.

2. AREA PROFILE AND HYDROGEOLOGY - GENERAL FEATURES

The Delhi region (area:1483 Sq.Km. between 28°24'17"-28°53'00" N and 76°50'24"-77°20'37" E) is a part of the Indo-Gangetic Alluvial Plains, at an elevation ranging from 198 to 220 m above msl, transected by a quartzite rocky ridge (max. elevation of 306.63 m above msl) extending roughly from north-east to the south-eastern part of the area [6,7]. The ridge forms the principal watershed of the area and acts as a groundwater divide between the western and eastern parts of the area. The investigated area is covered by the Alipur Block (259 Sq.Km. area) and the Nangloi (Kanjhawala) Block (275 Sq.Km. area). The climate of the region is semi-arid. The average annual rainfall (1931-91) is 711 mm, most of which falls between June and September and is generally erratic, infrequent and heavy sometimes. The mean minimum and maximum temperatures are 18.7°C and 30.5 °C respectively. During the months of May and June, temperature commonly exceeds 40 °C.

The aquifer disposition in the investigated area is shown in Fig.2. The area is overlain predominantly by sand in the top 20-30 m and clay and kankar below that [8]. The Alluvium thickness in the area varies from 100 m to more than 300 m. and groundwater occurs under semi-confined conditions. Both the shallow as well as the deeper wells have a common groundwater level, ranging between 1-10 m below ground level. Due to rapid urbanisation, water table in most parts has declined by 2m to 8m during the last decade [8], thus increasing the unsaturated thickness of the aquifers. The alignment of the Delhi branch of western Yamuna canal passes almost through the boundary of the Alipur and Nangloi Blocks and acts as a groundwater ridge diverting the flow of water to the south-west and east towards the Yamuna. Groundwater movement is generally away form the ridge. The upper surface of the newer alluvium groundwater aquifer adjacent to the western bank of the Yamuna river is replenished by the river at some stretches.

3. STATE-OF-ART FROM ISOTOPIC INVESTIGATIONS IN THE AREA

Extensive hydrological investigations have been undertaken by the Nuclear Research Laboratory, IARI, by monitoring the spatial and temporal variations in the stable isotope (^{18}O) signatures of rainfall, groundwater and surface water [3,4,5,9,10,11,12,13]. ^{18}O isotope content of rainfall vary significantly in the Delhi region, due to evaporation during the course of its fall as well as with intensity and distribution of rainfall [9]. Differences in recharge from location to location result in large isotopic variations over small lateral distances, providing a detailed and dynamic representation of groundwater occurrence, recharge and contamination characteristics.

3.1 Groundwater occurrence and recharge

The isotopic investigations indicate that spatial variations in recharge (<1 to 66.0%) [10] result in wide range of differences in the stable isotope (^{18}O) signatures of groundwater (δ values -2.8‰ to -8.6‰) from location to location [5,10]. These variations suggest that the groundwaters in the wells of Delhi area are mixtures of varying proportions of different water sources and the aquifer in the area does not constitute a homogeneous system in its lateral extent. The ^{18}O and chemical composition of groundwater further indicate that there exists three hydrodynamic zones vertically [1,2], corresponding to three types of flow systems: (i) Uppermost zone with low-Cl groundwaters and with rapid circulation, representing local flow system, (ii) Intermediate zone of relatively slow groundwater circulation, with comparatively higher Cl concentration, representing intermediate flow system and (iii) Stagnant zone of very high chloride concentration, representing regional flow system. Localised recharge from high intensity rainfall, through stagnant water pools that are left in low lying areas, and indirect recharge through lateral flow from surrounding areas in the west are the main contributors to the groundwater [2].

3.2 Groundwater degradation

Although, groundwater contamination has many sources, likely creation of a blanket non-point source of contaminants, through routine agricultural applications of fertilisers and other agrochemicals as well as indiscriminate land disposal of industrial and domestic wastes, are increasingly being recognised as significant sources. The concentration of pollutants at any location in the saturated groundwater aquifer is governed by the contaminant content of the water recharging from the unsaturated zone above that point and by the additions from groundwater flowing into the area from surroundings. The isotopic investigations indicated that indiscriminate pumping of groundwater results in lateral mixing of contaminated/saline water with fresh water bodies through identified specific flow-pathways [3,4,5], within a block and between to adjacent blocks. This leads to spreading of contamination/salinisation and depletion of available fresh water potential. Such waters are highly saline, contaminated and isotopically enriched (δ value of -3‰ to -5‰), being subjected to evaporation during intermittent stay on the land surface before recharge and are distinct from isotopically depleted rainfall water (Mean δ of -6.9‰). Quite a significant part of the Delhi area is affected by nitrate and fluoride contamination in the groundwater [3,4] beyond the WHO prescribed maximum permissible limits. Highly skewed and wide range of F (<1 - 16.5 mg/l) and NO_3 (<10 - 273 mg/l) concentrations suggest contamination from both point and non-point sources [3,4]. The studies further indicate that the extent of chemical contamination of groundwaters is essentially governed by the level of contaminants, the flow-pathways of groundwater between the contaminant source and the water-supply well, the velocity of groundwater along the pathways and the attenuation capacity for the contaminants in the aquifer.

4. MATERIALS AND METHODS

Groundwater samples from different locations, representing various geohydrological conditions in the area (Alipur and Nangloi Blocks), were collected through extensive field survey. Wherever possible, additional samples were collected from the same location to observe the variations in heavy metals and isotopic composition within a short distance. The samples were stored in air tight polyethylene bottles and all precautions were taken to avoid evaporation losses. The samples were analysed as early as possible for the heavy metals (Zn and Cu) concentration by atomic absorption spectrometer (Perkin Elmer) following standard procedure and the levels are expressed in µg/l. The analytical precision for the measurement is about ± 2%. The $^{18}O/^{16}O$ ratio was measured following a modified Epstein-Mayeda technique using VG-Micromass 602D/E mass-spectrometers, by equilibrating a tank CO_2 gas with 3ml water at 25°C [3,4,5]. The analytical reproducibility of the laboratory standard is ± 0.1‰. The ^{18}O content of water samples are expressed in terms of per mille deviation (δ‰) with respect to the isotopic ratio of the reference Standard Mean Ocean Water (SMOW).

$$\delta\ (‰) = [(R_{sample}/R_{std.})-1] \times 10^3$$

Where, R is the isotopic ratio $^{18}O/^{16}O$.

5. RESULTS AND DISCUSSION

In the investigated area, the Cu content in the groundwater ranges from 3-41µg/l and Zn content ranges from 5-182µg/l (Table-1), showing considerable variation from location to location as well as within the small parts of a location. Wide variation in the ^{18}O stable isotope content of groundwater (δ value of -5.7‰ to -8.5‰) is due to significant variation in the $\delta^{18}O$-contents of rainfall (-2.8‰ to -19.2‰) with space and time, as well as intensity and distribution of rainfall [1,9], superimposed with different groundwater recharge contributions from evaporated irrigation water and surface runoff water [3,4] as well as intermixing of groundwater [5]. Fig.3 shows relationship of $\delta^{18}O$ with Cu and Zn contents in groundwater. It is interesting to note from Fig..3 that taking all the data points of a particular block (shown by different legends) as single grouping, increase in levels of Zn and Cu in groundwaters are associated with high ^{18}O (isotopically enriched) water. This clearly suggests that

TABLE 1. Zn, Cu AND ^{18}O COMPOSITION IN GROUNDWATER OF THE INVESTIGATED DELHI AREA.

Sample No.	Location	Cu (μg/l)	Zn (μg/l)	$\delta^{18}O$ (‰)
ALIPUR BLOCK				
1	Kherakhurd (HP)	8.0	5.0	-7.2
2	Alipur (HP)	6.0	7.0	-7.1
3	Bakoli (TW)	6.0	9.0	-7.6
4	Singhola (TW)	11.0	34.0	-6.5
5	Narela (TW)	5.0	9.0	-7.5
6	Bawana (HP)	3.0	10.0	-8.5
7	Pehladpur (HP)	14.0	10.0	-5.7
NANGLOI BLOCK				
8	Dariyapur (OW)	14.0	13.0	-7.9
9	Dariyapur (TW)	21.0	17.0	-7.1
10	Punjabkhor-I (TW)	18.0	37.0	-6.5
11	Punjabkhor-II (TW)	13.0	18.0	-7.6
12	Chandpur (HP)	30.0	31.0	-7.2
13	Tikrikalan-I (TW)	41.0	182.0	-5.8
14	Tikrikalan-II (HP)	31.0	49.0	-7.0
15	Nangloi (HP)	16.0	23.0	-7.0

TW- Tube Well, OW- Open Well, HP-Hand Pump.

significant quantities of evaporated (isotopically enriched) irrigation water and surface runoff water from surrounding farmland infiltrate alongwith Zn and Cu salts from soils to the groundwater system. Direct contribution of rainfall to Zn and Cu contamination is small because the average content of these constituents in rain is normally small (< 1 μg/l). Although, the original Zn and Cu contents of the surface-runoff water have not been measured, the ^{18}O-content of surface-runoff water is the same as that of rainfall which causes runoff.

Movement of zinc and copper in soil is known to take place essentially by diffusion process which increases with increase in volumetric moisture content [14]. In the investigated area, although, the surface soil is sandy and sandy-loam, yet, due to its alkaline nature [2] and being underlain by lenticular clayey deposits, extensive migration of Zn and Cu into the groundwater system is likely to be hindered, because, a marked reduction in the diffusion coefficients of Zn and Cu have been observed with increase in soil pH and texture [15,16]. These two fertiliser nutrients also did not show any antagonism in their uptake by plants, which ranged between 1-2% under field conditions. Most of the applied zinc and copper remained in available form, while a significant amount was found to be converted to easily exchangeable, complexed organic form. Therefore, low levels of Zn and Cu in the groundwaters of the area suggest that adsorption and redistribution of infiltrating water and soluble Zn and Cu species in the unsaturated soil zone are the two opposite mechanisms which are likely to affect the movement of the Zn and Cu species. Consequently, more than one trend of $\delta^{18}O$ vs. Zn and Cu relationship may be expected, e.g. low dispersion-low adsorption and high dispersion-high adsorption, as has been observed in the cases of transport of nitrate and fluoride [3,4].

The effects of these processes are likely to be manifested in the groundwater Zn, Cu and ^{18}O composition, because, longer retention time of Zn and Cu containing water in the top soil and on the surface of the soil will have more evaporation, leading to ^{18}O enrichment and increase in Zn and Cu

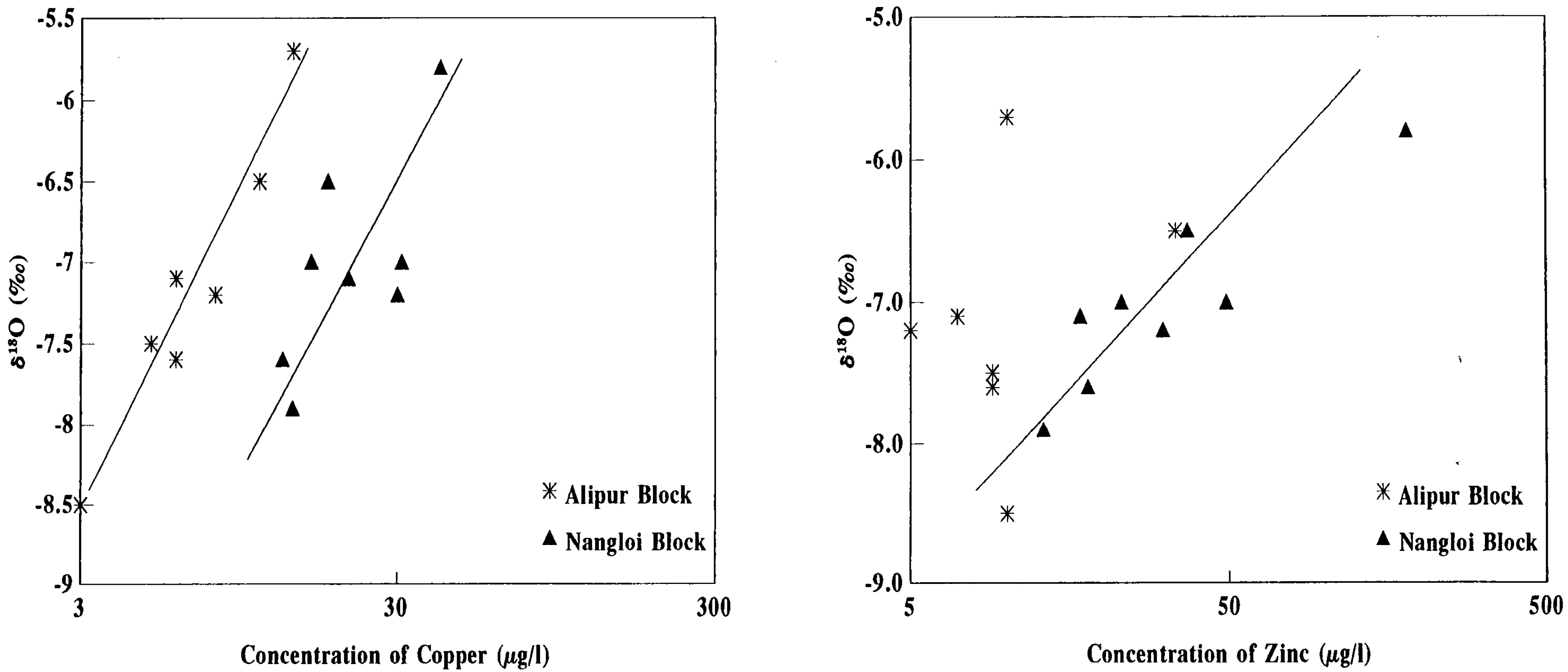

FIG. 3. Relationships of $\delta^{18}O$ with Zn and Cu concentration in groundwater of the investigated area in Delhi. ^{18}O isotopic enrichment with increasing Zn and Cu levels indicates infiltration of rainfall, irrigation water and surface run-off alongwith Zn and Cu salts in soil.

concentration. Thus, considering the data points of a particular block as a single grouping, various trends in $\delta^{18}O$ vs. Zn and Cu relationship can be visualised (Fig.3). This also reflects that the groundwater system has two or more isotopically distinct, non-point source origins (irrigation water and surface-runoff water), with spatial variations in ^{18}O, Zn and Cu concentrations. As described earlier, also there is a wide spatial and temporal variation in ^{18}O-contents of rainfall [1,9], influenced by intensity and distribution of rainfall and evaporation during the course of its fall. Evaporation of irrigation water in the unsaturated zone also cause enrichment in groundwater, resulting large isotopic differences over small lateral distances. Data points in Fig.3 will, therefore, deviate from the main trend depending on degree of evaporation/recharge. Large variation in Zn and Cu content with relatively little change in isotopic composition also indicates leaching of salts present in the soil. Hence, to protect the groundwater from further deterioration, it is desirable to put a control over the use of the deleterious man-made inputs and indiscriminate disposal of industrial wastes. Generality of this approach can be determined by further investigations.

6. CONCLUDING REMARKS

The isotopic techniques can provide potential tool to characterise non-point source contributed heavy metals pollution of groundwater, scope of which may be larger than assessed so far. The investigations indicate that although, the present levels of Zn and Cu in groundwater have not reached alarming stage, yet, indiscriminate anthropogenic wastes disposals and agrochemicals inputs, together with various physico-chemical processes in the soil, is likely to exceed the 'sink' capacity of the watershed soils over a period of time, increasing transport of Zn and Cu present in the soil to the groundwater. Impact of agricultural practices undertaken now may not be reflected in the groundwater regime for several months, or possibly years. Yet, the presence of contaminants in groundwater suggest the beginning of a trend of increasing heavy metals in groundwater due to prolonged and widespread use of agro-chemicals as well as indiscriminate land-disposal of wastes. In a watershed, gradients in groundwater contaminant levels can have a variety of configurations, depending locally on both transient and steady state variables, such as geological, hydrogeological, mineralogical, depth to confinement and other related features. A wide variety of chemical and physico-chemical processes comprising dissolution, complex formation, diffusion, dispersion and sorption/desorption also alter the water quality. The inherent uncertainty and inhomogeneity of the natural groundwater system, point towards the importance and need of groundwater quality surveillance programme, through systematic research on the groundwater flow field, spatial, temporal and depth variation in contaminants level in relation to well conditions and land use, dynamics of groundwater contaminants under natural and stressed conditions and relative importance of vegetative uptake of contaminants in limiting contamination.

ACKNOWLEDGEMENTS

The authors thankfully acknowledge Prof. R.B. Singh, Director, Indian Agricultural Research Institute and Project Director, Nuclear Research Laboratory, New Delhi for encouragement.

REFERENCES

[1] DATTA, P.S., BHATTACHARYA, S.K. and TYAGI, S.K., Assessment of groundwater flow conditions and hydrodynamic zones in phreatic aquifer of Delhi area using oxygen-18 Proc Intn Workshop on "Groundwater Monitoring and Recharge in Semi-Arid Areas", Hyderabad, IAH/UNESCO Publication, S IV: 12-24 (1994).

[2] DATTA, P.S. and TYAGI, S.K., Major ion chemistry of groundwater in Delhi area: chemical weathering processes and groundwater flow regime, J. Geol. Soc. India, 47: 179-188 (1996).

[3] DATTA, P.S., DEB, D.L. and TYAGI, S.K., Assessment of groundwater contamination from fertilizers in Delhi area based on ^{18}O, NO_3^- and K^+ composition. J. Contaminant Hydrology, 27(3-4): 249-262 (1997).

[4] DATTA, P.S., DEB, D.L. and TYAGI, S.K., Stable isotope (^{18}O) investigations on the processes controlling fluoride contamination of groundwater. J. Contaminant Hydrology, 24(1): 85-96 (1996).

[5] DATTA, P.S., BHATTACHARYA, S.K. and TYAGI, S.K., ^{18}O studies on recharge of phreatic aquifers and groundwater flow-paths of mixing in Delhi area. J. Hydrol., 176: 25-36 (1996).

[6] SETH, N.N. and KHANNA, S.P., A note on groundwater condition in Delhi area. Geological Survey of India. Misc. Publn., 14(Part-III): 101-110 (1969).

[7] SETT, D.N., 1964. Groundwater geology of the Delhi region. Bull. Geol. Survey. India, Series-B. 16: 1-35.

[8] CGWB, Development and Augmentation of Groundwater Resources in National Capital Territory of Delhi, Govt. of India Report (1996).

[9] DATTA, P.S., TYAGI, S.K. and CHANDRASEKHARAN, H., Factors controlling stable isotopic composition of rainfall in New Delhi, India. J. Hydrol., 128: 223-226 (1991).

[10] DATTA, P.S., Stable isotopic investigations for groundwater management and sustainable environment. Nuclear Research Laboratory, IARI Report (1997).

[11] DATTA, P.S. and TYAGI, S.K., Isotopic investigations on groundwater recharge conditions and flow regime in Delhi region- A review. Proc. International Conf. Water & Energy 2001, Oxford & IBH Publn. Vol.II: 629-642 (1995).

[12] DATTA, P.S. and TYAGI, S.K., Groundwater surface water intermixing model and recharge conditions in Delhi area as derived from $\delta^{18}O$ and δD. Proc. Intn. Conf. on Hydrology and Water Resources, New Delhi, 1993, (Eds: Vijay P. Singh and Bhism Kumar) Kluwer Acad. Pub., Netherlands, Vol.II: 103-119 (1996).

[13] ROHILLA, S.K. and DATTA, P.S., Delhi's Water: Emerging Scenario, Vigyan Prasar Publication, New Delhi, (1999) (in press).

[14] SEN, A. and DEB, D.L., Factors affecting diffusivity of micronutrients in soils. I. Effect of soil moisture tension, soil compaction and soil temperature on self-diffusion coefficient of Zn, Mn and Fe. Indian Agric. 23: 201-204 (1979).

[15] RATTAN, R.K. and DEB, D.L., Self diffusion of iron and zinc in soils as affected by, pH, Ca CO_3, moisture, carrier and phosphorous levels. Plant and Soil. 63: 377-393 (1981).

[16] SHARMA, K.N. and DEB, D.L., Effect of soil moisture tension and soil compaction on self-diffusion coefficient of zinc in soils of varying texture. J. Nuclear Agric. Biol. 13: 118-120 (1984).

TRACING AND AGE-DATING RECYCLED WASTE WATER RECHARGED FOR POTABLE REUSE IN A SEAWATER INJECTION BARRIER, SOUTHERN CALIFORNIA, USA

M.L. DAVISSON, G.B. HUDSON, B.K. ESSER, B. EKWURZEL
Lawrence Livermore National Laboratory (LLNL),
Livermore, California, United States of America

R.L. HERNDON
Orange County Water District,
Fountain Valley, California, United States of America

Abstract

California regulations for indirect potable reuse of recycled waste water proposes 1) a ≥1 year aquifer storage before use, 2) ≥50% blend with a non-waste water, and 3) a total organic carbon (TOC) concentration of the waste water mixing component ≤1.0 mg/L at the point of production. ^{3}H-^{3}He age-dating provides a quantitative basis for assessing aquifer storage times and water quality changes. In Orange County, California advanced-treated waste water blended with natural groundwater is injected into layered sand/gravel aquifers to prevent seawater intrusion. Blended water was isotopically unique, due to its virtual lack of excess dissolved air (^{22}Ne = 4.9 x 10^{11} atoms/gH_2O), relative to ambient groundwater (^{22}Ne = 6.4 x 10^{11} atoms/gH_2O), and its high ^{3}H (75 to 3000 pCi/L) and ^{14}C (70 to 555 pmc), possibly introduced from bio-medical waste discharged into municipal sewers. Groundwater ages ≤1km downgradient generally increased with distance and ranged from 0.1 to 10.2 ±0.3 years, and comprised ~100% injected water. Shallow groundwater (<120 m) was >40 years old >1km upgradient, while downgradient most were <40 years and mixed with seawater. Along the Talbert aquifer, TOC decreased 1.0 mg/L in 1.5 years, while TDS increased from ~200 to ~640 mg/L. All major element concentrations increased with age, with SO_4, Cl, Ca, and Mg increasing the most. Cl concentrations and ^{36}Cl/Cl ratios suggest Cl increase was only due to changes in injection water concentration. Injection water was calcite under-saturated, but was slightly over-saturated within 1.5 years. Dissolved Sr increased from 0.4 ppb to 5.0 ppb in 4 years, and was matched by ^{87}Sr/^{86}Sr ratios from 0.71000 at the injection point to 0.71072 downgradient. The latter ratio is higher than ratios observed in ambient groundwater (^{87}Sr/^{86}Sr = 0.70937 to 0.71048) or modern seawater (^{87}Sr/^{86}Sr = 0.70912), suggesting that silicate hydrolysis is the source of the Sr.

1. INTRODUCTION

Water supply shortages forecasted over the next 20 years in urban areas of the southwestern United States have stimulated research and development in potable reuse of recycled waste water. However, there are health concerns associated with potable reuse, due to uncertainties in subsurface fate and transport of potentially harmful pathogens and organic compounds unaffected by the treatment process [1]. Proposed regulations by the State of California stipulate that any recharged, recycled waste water subsequently pumped for drinking water must first 1) reside in the subsurface for at least one year, 2) be at least 50% blended with water of non-waste water origin, and 3) have a waste water total organic carbon (TOC) concentration of ≤1.0 mg/L at the point of production [2]. These detailed regulatory criteria require diagnostic approaches far advanced over typical water quality monitoring practices or groundwater modeling approaches used by local utilities. In this report we outline an investigative approach used in Orange County, California that combines isotopic tracers and tritium-helium-3 (^{3}H-^{3}He) dating to directly measure groundwater ages. These data can be used to test regulatory compliance in potable water reuse projects [3].

Orange County has 2.2 million inhabitants who produce 70% of their domestic water needs from the local groundwater basin. Annual groundwater extraction from the basin exceeds natural recharge rates. As a result, artificial recharge projects have operated since the 1960s. Beginning in the 1930s, seawater intrusion along the Pacific Ocean coast occurred along a natural topographically low area, known as the Talbert gap, which was formed by erosion of a local river channel through coastal highlands (Fig. 1a). Intrusion was remedied by construction of an injection barrier straddling the gap. Injection began in 1973 in 22 wells completed in layered aquifers comprising near-shore deltaic-marine deposits of Pliocene to Holocene ages (Fig. 1b). Injection water comprises a mixture of advanced-treated waste water and groundwater extracted from deep aquifers (>300m) below the gap.

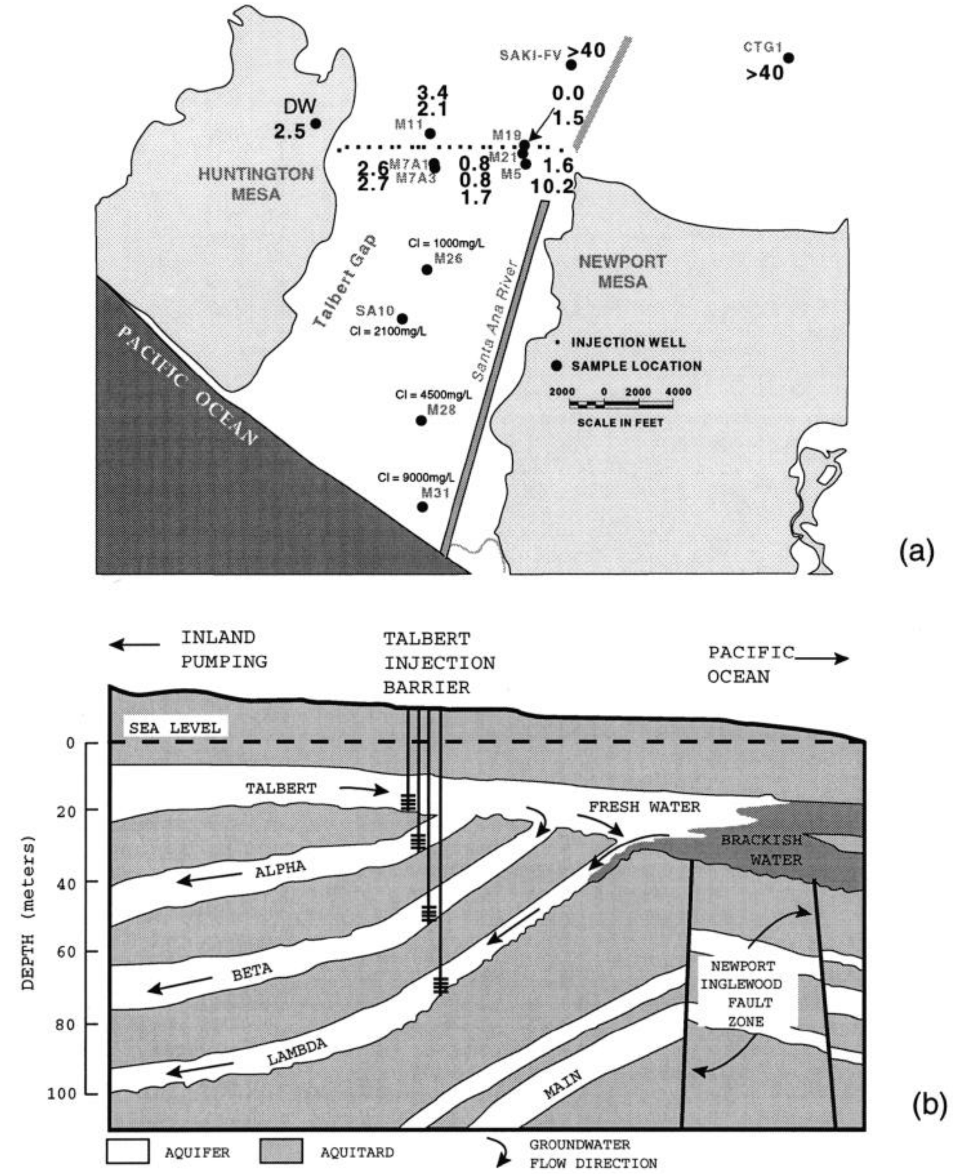

FIG. 1. a) The Talbert gap area of Orange County California historically has been susceptible to sea water intrusion due to over pumping upgradient in the groundwater basin. The injection barrier annually recharges 4 to 20 million m^3 of deep groundwater blended with recycled waste water. Groundwater ages determined by the ^3H-^3He method are shown for monitoring wells and one production well recharged with nearly 100% injection water. Groundwater upgradient and at deeper depths are naturally recharged and are >40 years old. Downgradient toward the coast, groundwater has variable mixtures of sea water. b) Cross-section shows fairly uniform sand/gravel layered aquifers are replenished by injection water.

2. METHODS

Samples for ^3H were collected in glass bottles with air-tight caps, and were analyzed by the helium-accumulation method [4], whereby samples were degassed, sealed, and stored for 15-60 days to allow accumulation of ^3He from the tritium decay. The sample was subsequently degassed and the ^3He was isolated and measured. Noble gas samples were collected in a copper tube using stainless steel pinch clamps on each end that were tightened down while a laminar water flow passed through the tube. Copper tubes were then vacuum-fitted in the lab to an evacuated container, the pinch clamp and copper seal was uncrimped and the water sample was released. The water was degassed and the noble gases of interest were isolated and analyzed. The helium isotopes were analyzed on a VG-5400 noble gas mass spectrometer, while the remaining noble gases were analyzed on a Nuclide-6-60 noble gas mass spectrometer. Samples for ^{13}C and ^{14}C were collected in a glass bottle with a polyseal cap, and 4 drops of a saturated $HgCl_2$ preservative. The inorganic carbon was acid stripped under high vacuum and purged with an ultra pure carrier gas [5]. The liberated CO_2 was then reduced to graphite on a separate vacuum line using a cobalt catalyst and hydrogen gas at a 570°C reaction temperature [6]. All ^{14}C concentrations were determined on the accelerator mass spectrometer at LLNL, and are reported as a percent modern carbon (pmc) relative to a NBS oxalic acid standard [7]. Standard methods of preparation were used for strontium isotope analysis [8]. This entailed drying down the sample, separating and pre-concentrating using Sr-spec resin, followed by loading onto a tantalum filament and analysis by thermal ionization mass spectrometry. The dissolved Cl was isolated by precipitating to AgCl with $AgNO_3$ and purified by re-dissolution and precipitation [9]. The $^{36}Cl/Cl$ ratio was analyzed by accelerator mass spectrometry [9] at LLNL. General chemistry was measured in the certified water quality laboratory at Orange County Water District using standard methods.

3. RESULTS AND DISCUSSION

3.1 Injection Water

The treated waste water begins as secondary waste effluent originally derived from domestic and industrial discharge of local origin. The secondary effluent undergoes lime coagulation and flocculation, which results in a high pH water. The pH is then adjusted lower using CO_2 gas derived from off-gas during lime regenerated by high temperature combustion. The pH adjusted water is filtered and passed through either activated carbon (AC) or reverse osmosis (RO) membranes, followed by chlorination. The RO step produces a water with low TDS and low TOC (Table 1). The volume of AC relative to RO may vary and depends on plant operation. Both of these waters are always blended ≥50% with groundwater produced >300m below the surface. This deep groundwater has a naturally low TDS and high TOC, which gives it a distinct color. Over the past 15 years, annual injection into the barrier varied between 4 and 20 million m^3. The average annual TDS over this time has varied between 130 to 440 mg/L [10]. In the past 4 years, which are relevant to the water quality data in this study, the average annual TDS has varied between 248 and 380 mg/L. TDS is a secondary drinking water standard, and also provides a guide for delineating seawater intrusion in the gap. Drinking water wells lie directly downgradient of the injection barrier (e.g. well DW, Fig. 1a) and possible mixtures of waste water is of regulatory concern.

Table 1: RELEVANT WATER QUALITY PARAMETERS FOR INJECTION WATER.

	Typical TDS (mg/L)	Typical TOC (mg/L)
AC	880	7.0
RO	32	0.5
Deep Groundwater	225	2.4

3.2 Groundwater Tracing

Injection water (sample Q-10) and groundwater was collected and measured in 1994. During that time, the isotopic abundance of ^3H and ^{14}C were significantly above ambient levels (Fig. 2a). The ^3H concentration shown is the initial ^3H at the time of injection, calculated by adding the tritiogenic ^3He measured on the same samples. The ^3H concentration of injected water ranged from 55 to >3000 pCi/L. The higher concentration had an instantaneous level 6 times lower than the drinking water standard. Nevertheless, these high levels are a diagnostic signature of injected water. In addition, the ^{14}C was measured in the groundwater as high as 555 pmc, which provides an additional tracer characteristic for the injected water. It is interesting to note that the high ^{14}C most likely originated as an organic source in the waste water. This conclusion is based on a ^{14}C measurement of $CaCO_3$ scale (402 pmc) collected in the re-carbonation pool within the treatment process. Recall that waste water is pH adjusted using CO_2 from off-gas during lime regeneration. More than likely the CO_2 is oxidized organic matter that adhered to the lime flocculates, and the $CaCO_3$ scale measured, precipitated directly from this CO_2. Furthermore, the $\delta^{13}C$ of the $CaCO_3$ was -29.5 per mil, indicating an organic source. The near-linear correlation between the ^{14}C and ^3H of groundwater suggests a single radioactive source (Fig 2a). The occurrence of both these radiotracers at the same time in the waste stream suggest perhaps a biomedical origin.

Treated waste water and deep groundwater are blended in a large volume tank that is open to the atmosphere. As a result, noble gas concentrations are equilibrated to atmospheric abundances at the ambient temperatures. This is best illustrated by comparing the ^{22}Ne concentrations of ambient groundwater to injected water (Fig.2b). Ambient groundwater had excess ^{22}Ne on average relative to the atmospherically equilibrated water, typical for natural groundwater recharge, while the injection water and groundwater directly recharged by injection has virtually little excess ^{22}Ne.

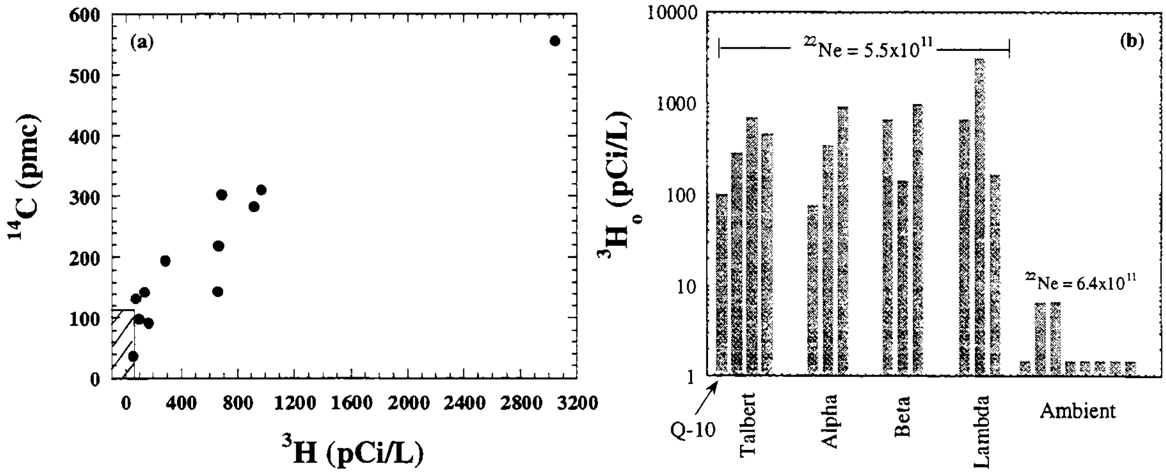

FIG 2. The ^3H and ^{14}C were significantly above ambient levels (hatched area) in groundwater. The high levels are most likely due to radiotracer residual perhaps derived from biomedical waste. The ^3H is the initial ^3H calculated by adding the tritiogenic ^3He to the measured ^3H concentrations. Ambient groundwater is distinguishable from injected groundwater by low ^3H concentrations and higher ^{22}Ne concentrations due to excess air incorporated during natural recharge processes.

3.3 Groundwater Ages

Groundwater age-dating using ^3H and tritiogenic ^3He has been applied throughout the Orange County groundwater basin, and additional sources of helium potentially complicating age calculations have been quantified [3;11]. The high ^3H concentrations of injected water provided an easily measured tritiogenic ^3He in groundwater <1 year old. Consequently, error in the groundwater age calculation is estimated at ±0.3 years. For groundwater comprising nearly 100% injection water (Fig.

1a), ^{3}H-^{3}He ages ranged from 0.1 to 10 years old. In general, monitoring wells closest to the injection barrier had the youngest groundwater, while wells further downgradient were older. However, in one monitoring well <300m from the barrier, the lower injection level had the 10 year age. One production well (DW) had a ^{3}H-^{3}He age of 2.5 years, and comprised nearly 100% injected water. Its location <1km from the injection barrier subjects it to proposed indirect potable reuse regulations. However, a measured age >1 year meets the first criteria of aquifer storage. In addition, the TOC concentration of this well water was 0.67 mg/L, confirming that organic matter derived from waste water was <1.0 mg/L.

Groundwater from wells >1.5km upgradient were nearly ^{3}H absent and comprised groundwater in excess of 40 years old. Multiple depth samples in monitoring well CTG1 (Fig. 1a) showed that the ^{14}C concentration ranged from 64 to 28 pmc with increasing depth, suggesting a pristine groundwater. Similarly, deep groundwater used for blending in the injection water was 27 pmc.

Groundwater in wells M31, M28, and SA10 located >1.5km downgradient toward the ocean, had ^{3}H concentrations ~5.0pCi/L, nearly identical to modern seawater in this area (6.0pCi/L). Groundwater in monitoring well M26 was ^{3}H absent. The tritiogenic ^{3}He was not measured in these wells. Salinity of the groundwater also increases in these wells toward the ocean (Fig. 1a). Groundwater in well M31 (~400m from the ocean's edge) was characterized by a salinity approximately half that of seawater, was depleted in dissolved oxygen, and had ~1% by volume CH_4 gas. In addition, the ^{14}C was only 5 pmc and the δ^{13}C was –2.1 per mil, suggesting biologically-mediated methanogenisis.

Groundwater transport away from the injection barrier can be estimated by the ^{3}H-^{3}He ages. Monitoring wells M19 and M21 are both ~120m from the barrier. Their mean ages (~1 year each) suggest a mean transport rate of 120m/yr. Wells M7A-1 and M11 are about 240m from the barrier and had mean ages ~2.5 years, suggesting mean transport of about 100m/yr [11]. Transport rates to production well DW is closer to 200m/yr, and is higher probably due to pumping and drawdown. Dispersion may influence these transport rates, although based on the uniform permeability of the sand/gravel aquifers, dispersion should be relatively minor over these time scales. Independent evidence for dispersion is discussed later.

3.4 Water Quality Changes After Recharge

3.4.1. TDS levels in the Talbert Aquifer

Salt accumulation in soils during recharge of groundwater has long been recognized in semi-arid to arid regions [e.g. 12]. In particular, mineral weathering, ion exchange, and fossil salts cause increased salinity in settings where recharge rates have been enhanced, such as agricultural irrigation [e.g. 13, 14]. Particularly acute are salt effects associated with ion exchange on negatively charged clay minerals with high Na waters. In areas of seawater intrusion, the high ionic strength of ocean water and high sodium content combine to cause intense ion exchange in affected coastal aquifers, typically creating Ca enrichment [15]. However, in the Orange County injection barrier, low TDS, low ionic strength water is injected into aquifers that have primarily hosted higher TDS groundwater under natural conditions, and more recently have experienced seawater intrusion. Under these conditions, the ultimate groundwater chemistry of the injected water will more likely depend on the saturation states between the dissolved constituents in the injected water and the aquifer minerals. For simplicity, we investigated water quality for groundwater injected only into the Talbert aquifer, which is the shallowest level, the most permeable, and experienced the most seawater intrusion.

In groundwater of the Talbert aquifer measured for this study, TDS levels show a systematic increase with increasing age (Fig. 3a). For example, in groundwater >2 years old TDS levels are >600 mg/L. For comparison, the annual average TDS of injection water for the equivalent age of the groundwater does not exceed 400 mg/L. Even though there may be periodic fluctuation in TDS levels of injected water during the year, the treatment system was designed not to inject >50% treated waste water for any appreciable amount of time. Therefore, based on mixing between AC and deep groundwater blend only, the highest possible TDS should only be 500 mg/L, but would likely occur only on rare occasions. Groundwater in the deeper aquifers (Alpha, Beta, and Lambda, see Fig. 1b) also have TDS levels >500 mg/L for ages >2 years.

3.4.2. TOC levels in the Talbert Aquifer

The TOC concentration commonly decreases during soil recharge [16]. Soil water can easily have TOC concentrations exceeding 10 mg/L, but near the water table, concentrations are typically ≤1.0 mg/L. The vadose zone in particular is most bio-active and removes most of the TOC. This condition is optimal under proposed water reuse regulations, where soil microbiology can remove organic matter that is potentially mutagenic, and where bacterial and viral particles can be filtered or degraded [e.g. 17]. However, in settings where surface recharge occurs without a vadose zone, TOC levels have been shown to decrease up to 50% within one month after recharge [3]. Direct injection presents a less understood condition for TOC removal from groundwater. In particular, processes such as sorption, degradation, and interaction with sedimentary organic matter may all contribute to TOC removal.

In groundwater of the Talbert aquifer, TOC concentrations decreased with time (Fig 3b). In particular, the TOC concentration decreased approximately 1.0 mg/L from the concentration measured in Q-10. However, annual average TOC concentrations for injected water also plotted in Figure 3b, suggest that TOC removal may be over 2.0 mg/L. The annual average TOC levels were highest (3.0 mg/L) approximately 2 years prior to our sampling. This injected water on average comprised a ~25% mixture of AC water by volume. Assuming that the TOC of the RO water and the deep groundwater blend are constant (Table 1), then approximately half the TOC in the injected water that year was from the AC source. Comparison of annual average injection and measured groundwater suggests that TOC removal is greatest when TOC is the highest. However, the daily and monthly variability in TOC levels of injected water may be significant and the effects of dispersion may cause some uncertainty in this conclusion.

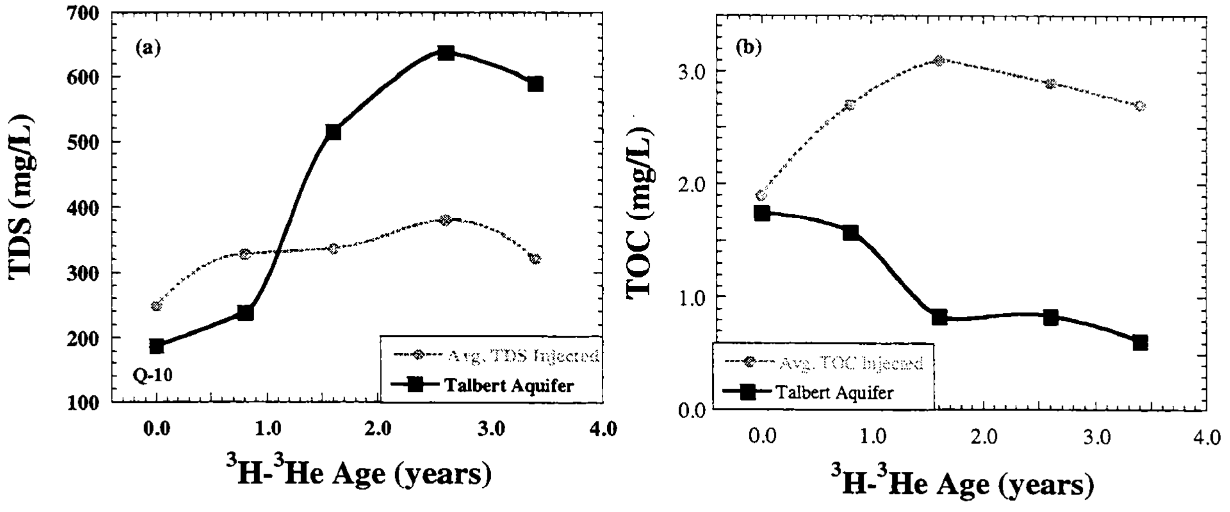

FIG. 3. a) The TDS levels in groundwater of the Talbert aquifer increase with age and exceed levels expected based on the average annual TDS of the injected water. Average injection water TDS in 1994 is equal to zero age. b) TOC is removed from the recharge water at the same time, decreasing as much as 2.0 mg/L when compared to average annual TOC concentrations of injected water.

In a related study, Fujita and others [18] also showed that TOC was removed in similar groundwater sampled adjacent to the Orange County injection barrier. In addition they showed using spectral analysis and solid phase extraction that the TOC of recharged injection water acquired a more humic character. Other work investigating the ^{14}C of DOC in groundwater has shown that for young groundwater (<35 years), the ^{14}C of the dissolved humics were lower than expected for equivalent age carbon sources in the soil [19, 20]. It was suggested that this was due to DOC interaction with sedimentary organic matter. A similar conclusion was made for a deeper groundwater studied [21]. In another study, one month after recharge from a spreading basin, groundwater TOC filtered at 1.0μm showed a ^{14}C decrease of 9 pmc, suggesting interaction with sedimentary organic matter [3]. The decrease in ^{14}C accompanied a 50% reduction in the TOC concentration and occurred under near-saturated groundwater conditions. Mechanisms of TOC removal may be complex and vary among different recharge environments.

3.4.3. Major element and isotopic geochemistry of Talbert aquifer groundwater

A simple conclusion, based on data in Figure 3a, is that the increased TDS acquired over time is due to flushing of residual salt remaining after seawater intrusion, or from natural groundwater previously residing in pore spaces. In fact, all the major element concentrations systematically increase over time in these samples (Table 2). In particular, the SO_4 and Cl concentrations both increase about a factor of 5 over time, while the HCO_3 increases a little over a factor of 2. Mg and Ca concentrations show the largest increases, while K and Na only increase moderately.

TABLE 2. MAJOR ELEMENT CHEMISTRY OF GROUNDWATER IN TALBERT AQUIFER

Well	Age (yrs)	T°C	pH	Na	K	Mg	Ca	HCO_3	Cl	SO_4
Q-10	0	19.8	7.46	1.94	0.03	0.02	0.17	1.13	0.62	0.17
M21-1	0.8	25.4	7.34	1.99	0.06	0.03	0.37	1.21	0.89	0.28
M5-1	1.6	24.9	7.76	3.62	0.07	0.24	0.95	2.38	2.20	0.62
M7A-1	2.6	22.8	7.81	4.05	0.08	0.31	1.11	2.52	3.16	0.89
M11-1	3.4	22.3	7.67	2.81	0.08	0.45	1.59	2.70	2.34	0.65

Concentrations in mmol/L

On closer inspection, several lines of evidence suggest simple flushing does not explain the TDS increase. For example, the increase in Cl concentration closely matches the changes in Cl in annual average injection water (Fig. 4a). In the injection water we sampled (Q-10), and in the groundwater sample <1 year old (M21-1), the measured Cl was lower than the annual average injected. This was likely due to daily-monthly variations in the Cl content of the injected water.

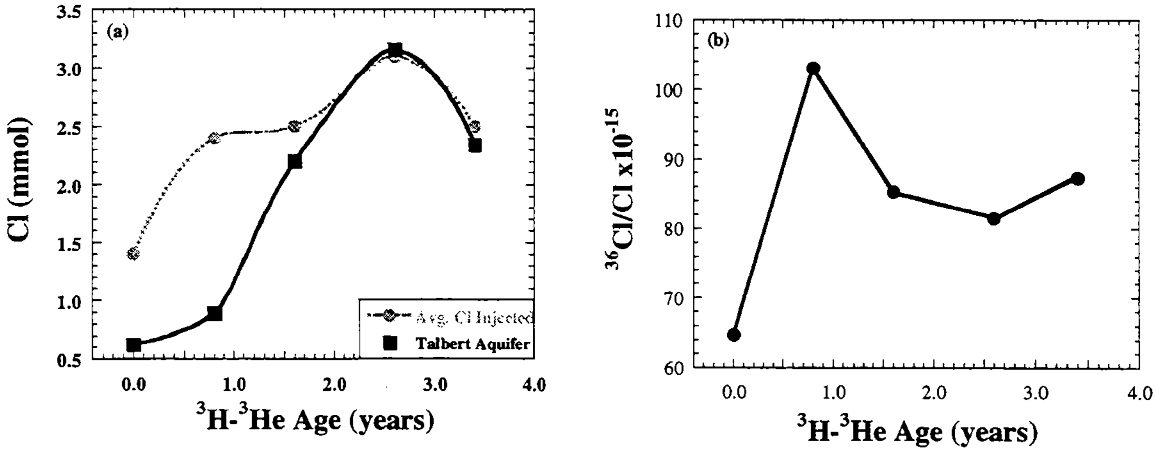

FIG. 4. a) The increase in Cl in the Talbert aquifer can be contributed to changes in the annual average injection water Cl concentration over time. The disparity between annually injected Cl and measured Cl in waters <1 year old are likely due to daily-monthly variations in concentration. However, after 1 year of aquifer storage groundwater Cl is nearly identical to annual average Cl, suggesting dispersion is important after 1 year of transport. b) The $^{36}Cl/Cl$ ratio indicates that the increased Cl is of modern origin and not related to increased dissolution of seawater Cl.

Recall that the deep groundwater blend can comprise >50% of the injection water, and its Cl concentration is low (8.0 mg/L). However, after 1 year of storage, groundwater samples closely match the annual average Cl concentration of the injected water. This comparison suggests that the Cl concentration has not increased during aquifer storage above the concentration of the original injected water. It is also interesting to note that the dissimilarity of Cl data <1 year old and the similarity >1 year strongly suggests that dispersion and homogenization of groundwater becomes important after 1 year of transport.

The ^{36}Cl/Cl ratio offers additional evidence for conservative Cl transport (Fig 4b). In particular, the ^{36}Cl/Cl ratio varies between 64 and 103 x10^{-15}, a value consistent with expected modern rainfall on the west coast of the U.S. [22]. Since seawater ^{36}Cl/Cl ratios are typically below detection limits (~1 x10^{-15}), the lack of systematic decrease in the Talbert aquifer groundwater suggests little seawater Cl influence. As a matter of fact, the lowest ^{36}Cl/Cl ratio was the modern injected water (Q-10).

The evidence is poor for flushing of residual salts in the Talbert aquifer. In addition, mechanisms of ion exchange are difficult to invoke since all major elements increase with age. Consequently, dissolution is a likely mechanism to explain the TDS increase over time. For example, calculated indices for calcite saturation in the water samples suggest that the injection water is significantly under-saturated (Fig. 5a). In contrast, groundwater downgradient and >1 year old is saturated to slightly over-saturated with respect to calcite. This appears to be good evidence that dissolution is an important mechanism for the TDS increase. In addition, dolomite saturation shows a similar trend, with under-saturation for the injection water (for Q-10 $\log SI_{dol} < -1.5$), and saturated conditions for groundwater >1 year old. Because the Talbert aquifer sediments were derived from near-shore depositional environments, carbonate deposits are common. Therefore, dissolution of calcite, and perhaps dolomitized calcite, readily occurs when the under-saturated injection water is introduced into the aquifer. Also worth noting is that for all the samples, gypsum was always under-saturated. This suggests little gypsum is available for dissolution in the aquifer sediments. It may be likely that the SO_4 increase over time is related to changes in injection water concentration.

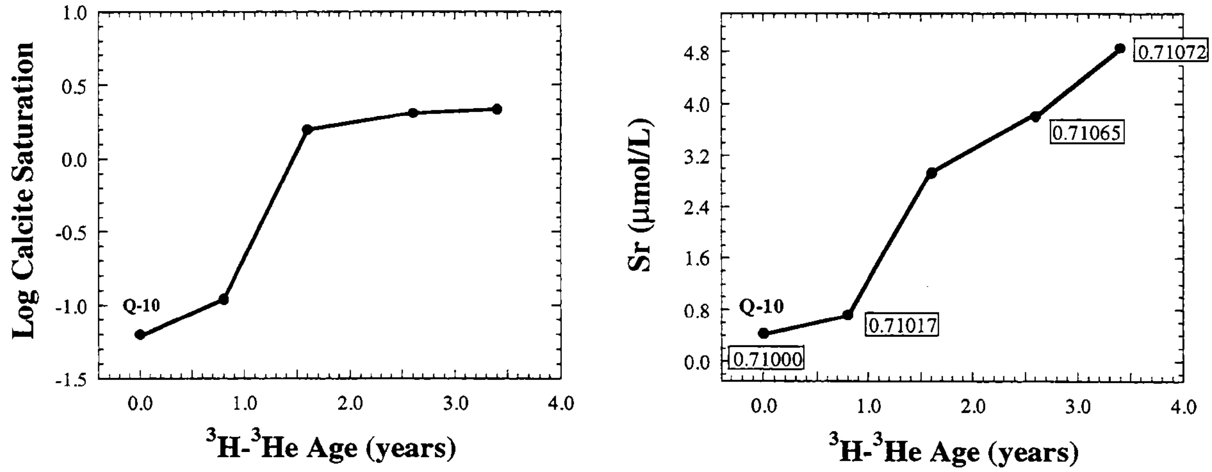

FIG. 5. a) Injection water measured during this study was under-saturated with respect to calcite. Injected groundwater >1 year old in the Talbert aquifer was saturated, suggesting calcite dissolution controls in part the increased TDS with time. b) In addition, dissolved Sr concentrations increased significantly. The ^{87}Sr/^{86}Sr ratios of the dissolved Sr were higher than Phanerozoic-age carbonates or seawater, suggesting that silicate hydrolysis also contributes to the increased TDS.

A last line of evidence for dissolution is suggested by increases in the dissolved Sr concentration (Fig. 5b). The concentration increased over an order of magnitude within the 4 years represented by samples in the Talbert aquifer and Q-10. Variation in Sr concentrations of injection water is not known, however the treatment process and blend water should contribute little Sr. For example, the deep blend water had a Sr concentration of 0.65μmol/L. Shallow ambient groundwater upgradient had Sr concentrations similar to the oldest groundwater in the Talbert aquifer (Fig. 5b). On first consideration, the increased Sr concentration in the Talbert aquifer may be attributed to calcite dissolution. The $^{87}Sr/^{86}Sr$ ratios were measured for these groundwaters as well as ambient groundwater in the area. In particular, the $^{87}Sr/^{86}Sr$ ratio of Q-10 was 0.71000, while groundwater in the Talbert aquifer ranged from 0.71017 to 0.71072 and increased with age (Fig. 5b). The $^{87}Sr/^{86}Sr$ ratio of ambient groundwater varied from 0.70937 to 0.71048. All these ratios are higher than modern seawater ($^{87}Sr/^{86}Sr = 0.70912$), and higher than most carbonate derived from seawater in Phanerozoic time [23]. Therefore, $^{87}Sr/^{86}Sr$ ratios suggest that carbonate dissolution is not the source of the dissolved Sr. Consequently, hydrolysis of silicate minerals are more likely, particular those with more radiogenic signatures (e.g. biotite).

4. CONCLUSIONS

The ^3H-^3He age-dating method has proved invaluable to groundwater studies assessing the impact of recycled waste water on drinking water quality. In particular cases where groundwater dispersion is low, the ages can be used to demonstrate compliance under proposed regulatory guidelines. The ages also provide a quantitative framework to characterize water quality changes and test reaction mechanisms. Results from the water quality chemistry of the Talbert aquifer indicate that TOC removal from direct injection can be effective, with >50% removal within 1 to 2 years of aquifer storage time. In this study, this is best demonstrated for one drinking water well, which had a ^3H-^3He age of 2.5 years and a TOC of 0.67 mg/L. These results satisfy the proposed regulatory criteria for indirect potable use of recycled waste water. However, the inorganic concentrations and isotopic abundances in this study suggest that the TDS of injected water is not a conservative parameter. Groundwater salt management based on TDS levels of recharge waters must account for dissolution processes that contribute to increased TDS only a short time after recharge (e.g. >1 year). Much can be learned about mechanisms of TDS increases in groundwater by investigating individual ion concentrations and isotopic abundances of particular elements. In this study, Cl concentrations coupled with $^{36}Cl/Cl$ ratios demonstrated conservative transport, while Sr concentrations coupled with $^{87}Sr/^{86}Sr$ ratios suggested that silicate hydrolysis was one of the operating mechanisms for TDS increase.

ACKNOWLEDGEMENTS

We thank Tim Sovich, Sid Niemeyer, and Joan Bieriger for their invaluable assistance in this research. Work was performed under the auspices of the U.S. Department of Energy by the Lawrence Livermore National Laboratory under contract W-7405-Eng-48.

REFERENCES

[1] CROOK, J., SURAMPALLI R.Y., Water reclamation and reuse criteria in the US. Water Sci. Technol., **33** (1996) 451-462.

[2] CALIFORNIA DEPARTMENT OF HEALTH SERVICES, Draft Proposed Groundwater Recharge Regulations. (1993).

[3] DAVISSON, M.L., et al., Isotope tracer approaches for characterizing artificial recharge and demonstrating regulatory compliance. Annual UC Water Reuse Research Conference, Monterey Calif., May (1998). 7 pp.

[4] SURANO, K.A., Helium-3 mass spectrometry for low -level tritium analysis of environmental samples. Jour. Radioanal. Nuclear Chem. Art., **161** (1992) 443-453.

[5] DAVISSON, M.L., VELSKO, C.A., Rapid extraction of dissolved inorganic carbon from small volumes of natural waters for ^{14}C determination by accelerator mass spectrometry. Lawrence Livermore National Laboratory UCRL-JC-119176 (1994) 23 pp.

[6] VOGEL, J.S., et al., Catalyst and binder effects in the use of filimentous graphite in AMS. Nuclear Instruments and Methods in Physics Research., **B29** (1987) 50-56.

[7] STUIVER, M., POLACH, H., Reporting of ^{14}C data. Radiocarbon, **19** (1977) 355-363

[8] HOROWITZ, E.P., et al., Separation and pre-concentration of strontium from biological, environmental, and nuclear waste samples by extraction chromatography using crown ether. Anal. Chem., **63** (1991) 522-525.

[9] ELMORE, D., et al., Analysis of ^{36}Cl in environmental water samples using an electrostatic accelerator. Nature, **277** (1979) 22-25.

[10] WESNER, G.M., Orange County Water District wastewater reclamation, Talbert barrier, and recharge project. Calendar year 1997. Orange County Water District (1998) 35 pp.

[11] HUDSON G.B., et al., Preliminary report on isotope abundance measurements in groundwater samples from the Talbert Gap injection barrier area, Orange County Water District. Lawrence Livermore National Lab UCRL-ID-122450 (1995) 26 pp.

[12] ALLISON, L.E., Salinity in relation to irrigation. Adv. Agron., **16** (1964) 139-180.

[13] DEVEREL, S.J., GALLANTHINE, S.K., Relation of salinity and selenium in shallow groundwater to hydrological and geochemical processes, western San Joaquin Valley, California. J. Hydrol., 109 (1989) 125-149.

[14] DAVISSON, M.L., CRISS, R.E., Stable isotope imaging of a dynamic groundwater system in the southwestern Sacramento Valley, California, USA. J. Hydrol, **144**, (1993) 213-246.

[15] NADLER, A., et al., Chemical reactions of seawater with rocks and freshwater: experimental and field observations on brackish water in Israel. Geochim. Cosmochim. Acta, **44** (1980) 879-886.

[16] THURMAN, E.M., Organic Geochemistry of Natural Waters. Martinus Nijhoff/Dr W. Junk Publishers: Boston (1985) 497 pp.

[17] ASANO, T., Proposed California regulations for groundwater recharge with reclaimed municipal wastewater. Wat. Sci. Techol., **27** (1993) 157-164.

[18] FUJITA, Y., et al., Identification of wastewater dissolved organic carbon characteristics in reclaimed wastewater and recharged groundwater. Water Environ. Res., **68** (1996) 867-876.

[19] WASSENAAR, L.I., et al., Radiocarbon contents of dissolved organic and inorganic carbon in shallow groundwater systems, implications for groundwater dating. In Isotope Techniques in Water Resources Development, International Atomic Energy Agency, Vienna (1992) 143-151.

[20] GEYER, S., et al., Isotope investigations on fractions of dissolved organic carbon for ^{14}C groundwater dating. In Isotope Techniques in the Study of Past and Current Environmental Changes in the Hydrosphere and the Atmosphere, International Atomic Energy Agency, Vienna, (1993) 359-380.

[21] ARTINGER, R., et al., Influence of sedimentary organic matter on dissolved fulvic acids in groundwater. In Isotope in Water Resources Management, International Atomic Energy Agency, Vienna (1996) 57-72.

[22] BENTLEY, H.W., Chlorine-36 in the terrestrial environment. In Fritz, P., Fontes, J.Ch., eds. Handbook of Environmental Isotope Geochemistry v. 2 (1986) 427-480.

[23] BURKE, W.H., et al., Variation of seawater ^{87}Sr/^{86}Sr throughout Phanerozoic time. Geol., **10** (1982) 516-519.

ISOTOPE AND HYDROGEOCHEMICAL STUDIES OF SOUTHERN JIANGXI GEOTHERMAL SYSTEMS, CHINA*

WENBIN ZHOU, XUELI LI, WEIJUN SHI, ZHANXUE SUN
East China Geological Institute,
Linchuan, Jiangxi,
China

Abstract

Southern Jiangxi is a geothermally active region, especially in Hengjing area. According to the work plan of IAEA Regional Collaboration in the Development of Geothermal Energy Resources and Environment Management through Isotope Techniques in East Asia and the Pacific (RAS-8-075), field investigation was carried out in Hengjing, southern Jiangxi Province, to demonstrate the use of isotope and geochemical techniques in low to medium temperature geothermal system. During the field investigation, 19 samples were taken from cold springs, hot springs and surface water in the area to determine their hydrochemical and gas compositions, hydrogen, oxygen, carbon and helium isotopes. The results of the study have shown that the geothermal waters in the studying region are of the same characteristics with the local meteoric water in oxygen and hydrogen isotope composition, indicating the geothermal waters are mainly derived from the local precipitation, while the gas composition and carbon and helium isotopes reveal that some gases in the geothermal waters have mantle origin.

1. IINTRODUTION

With more than 50 hot springs, about half of the hot springs in the province, southern Jiangxi is a geothermally active region, especially in Hengjing area. Investigations on the hot springs in this region can date back to the earlier of 1960s. The first oxygen isotope study of the geothermal waters in this region was carried out by Li Xueli and his colleagues in 1980. A systematic isotope and hydrogeochemical investigation was launched in 1993 by the geothermal group from East China Geological Institute. According to the work plan of IAEA Regional Collaboration in the Development of Geothermal Energy Resources and Environment Management through Isotope Techniques in East Asia and the Pacific (RAS-8-075), 19 samples were taken from cold springs, hot springs and surface water in the area to determine their hydrochemical and gas compositions, hydrogen, oxygen, carbon and helium isotopes.

The samples were collected in air tight glass bottles of 200 mL volume. Field parameters were measured for data supporting such as pH, Eh, temperature and geological conditions. The chemical composition of all the 19 samples were analyzed by chemical methods and partly by the 4500i type Ion Chromatography, the ^{18}O and D values of 13 samples were determined by MAT 251EM mass spectrometer, and the tritium content for 11 samples were measured using LSC-LBI type Low Background Liquid Scintillation Counter.

---

* Work performed in the framework of the IAEA Regional Collaboration in the Development of Geothermal Energy Resources and Environmental Management through Isotope Techniques in East Asia and the Pacific (RAS/8/075).

2. GEOLOGICAL AND GEOTHERMAL BACKGROUND

Located in the Southern China fold system, Hengjing area lies at the south end of Huichang-Xunwu fault, Hengjing fault cutting through the central of the area. The rocks found there comprised of Cambrian metamorphic rocks, Upper Jurassic volcanic-sedimentary rocks. The granite of early Yanshan stage was well developed. There are two groups of faults in the area, that is, NE and EW. Several small and medium earthquakes have been recorded in the last decades, indicating that the faults are still active in this area. The heat flow for the southern Jiangxi province have been measured to be from 62.1 to 79.9 mW/m^2, average 74.10 mW/m^2, which is obviously higher than that for the whole province (69.79 mW/m^2)[1].

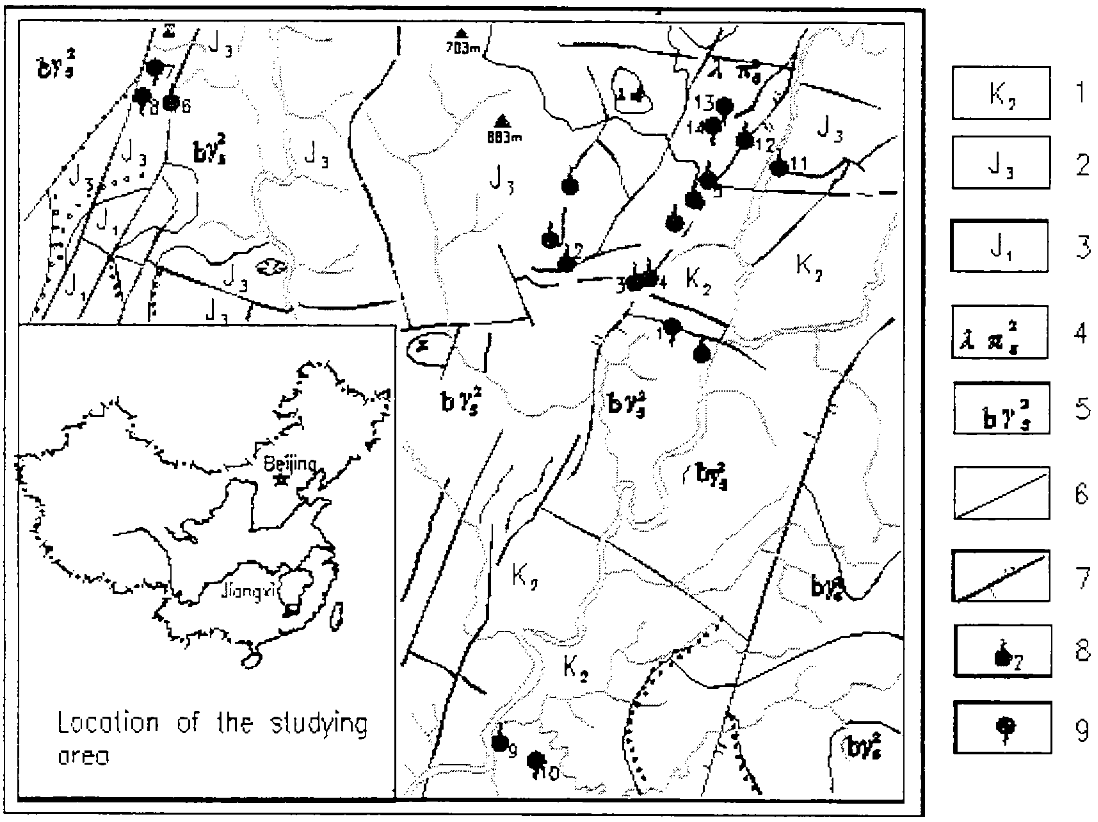

FIGURE 1 HYDROGEOLOGICAL MAP OF HENGJING AREA

1. Cretaceous sandstone; 2. Upper Jurassic volcanic rocks; 3. Lower Jurassic sedimentary rocks. 4. Porphyritic granite; 5. Granite; 6. formation boundary; 7. Faults; 8. Thermal spring; 9. Clod spring

3. HYDROGEOCHEMISTRY

3.1. Hydrochemical Composition

The chemical compositions for the springs are listed in table 1, which shows the hot springs in Hengjing are characterized by HCO_3-Na, pH of 6.52 to 7.3, and high SiO_2 (43~135 mg/L) and F (1.59~3.6 mg/L). The salinity is usually greater than 1.5 g/L.

TABLE 1. HYDROCHEMICAL COMPOSITION OF SPRINGS IN HENGJING AREA

Spring No.	Air temp. °C	Water temp. °C	pH	Salinity g/L	CO_2(aq) mg/L	SiO_2 mg/L	Ca^{2+} mg/L	Mg^{2+} mg/L	K^+ mg/L	Na^+ mg/L
2	28	25	6.52	2.293	1263	99	138.5	15.37	84.60	698.6
3	32	48	6.67	2.226	725.3	94	117.1	10.95	71.79	679.1
5	28	37	6.74	0.277	22	78	29.12	0.09	4.42	93.63
6	24	73	7.30	0.178	8.8	81	9.85	0.00	3.09	71.47
7	24	18	6.72	0.020	21	19	0.09	0.36	3.67	1.25
8	24	18	6.92	0.026	16	17	0	0.01	1.49	1.95
9	24	26.8	6.50	2.711	547	43	106.9	10.42	81.97	969.8
10	24	22.2	6.18	0.136	16	15	33.41	4.46	3.40	11.08
11	19.2	48	6.77	1.889	722	135	107.8	6.74	43.17	711.2
12	20	44	6.63	0.515	250	82	52.25	0.33	6.85	154.4

Spring No.	Cl^- mg/L	SO_4^{2-} mg/L	HCO_3^- mg/L	NO_3^- mg/L	HPO_4^{2-} mg/L	F^- mg/L	Eh mg/L	DO mg/L	Fe mg/L	U E-6g/L
2	81.18	325	1886.1	2.88	1.06	2.92	224.8	2.4	0.12	
3	70.19	764.88	1004.2	5.76	1.28	2.85	281.7	4.1	0	3.9
5	8.51	26.5	216.95	3.54	0.72	1.73			0	4.4
6	8.51	17	106.14	13.29	0.78	1.59	325.5	2.8	0.03	2.6
7	2.2	0	7.99	7.31	0.12	0.62			0.05	<0.03
8	2.2	0	25.2	7.53	0.08	0.61			0.03	
9	50.69	350	2253.1	10.63	0.8	3.6	232.3	3.4	0.01	1.8
10	21.98	12	63.44	17.05	0.28	0	349.2		0.24	2
11	35.1	300	1428.1	7.97	0.38	3.24	297.2	4.7	0	5.2
12	28.71	115	276.83	17.05	0.74	1.87	257.3	3.2	0	6.5

TABLE 2. HYDROGEN AND OXYGEN ISOTOPE COMPOSITION OF GROUND WATER IN HENGING AREA

Spring No.	Water temp.	D ‰ (SMOW)	^{18}O ‰ (SMOW)	T TU
1	20	-55	-7.4	13.14
2	25	-57	-7.2	4.08
3	48	-53	-6.9	2.4
4	40	-49	-6.7	1.05
5	37	-53	-7.2	1.92
6	73	-47	-6.1	3.44
7	18	-46	-6.5	
8	21	-39	-5.6	3.66
9	26.8	-48	-5.9	0.5
10	22.2	-49	-7	
11	48	-48	-5.9	2.03
12	44	-49	-7	1.66
13	20	-48	-6.9	3.15
14	19	-45	-6.6	

3.2. Hydrogen and Oxygen Isotopes

The values of δD and $\delta^{18}O$ for the geothermal waters in Hengjing area are in the range from –53 to –47 ‰ (SMOW) and from –7.2 to –5.9 ‰ (SMOW) separately (cf. Table 2), whereas those for the cold waters vary from –55 to –39 ‰ and –7.4 to –5.6 ‰ respectively. The relation between δD and $\delta^{18}O$ could be defined by $\delta D = 8.5\ \delta\ ^{18}O + 9.4$, showing the geothermal waters are mainly derived from the local meteoric water (Figure 2). The tritium contents for the hot springs are lower than 3.4 TU, indicating the waters should be older than 50 years.

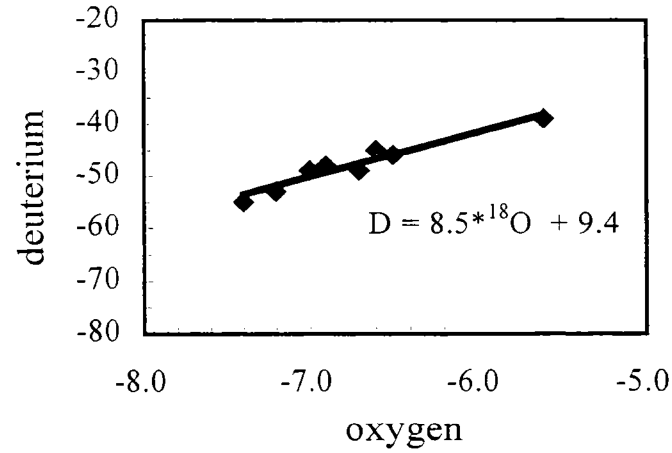

FIGURE 2. THE RELATION BETWEEN HYDROGEN AND OXYGEN ISOTOPES

4. GAS GEOCHEMISTRY

4.1. Gas Composition

The Hengjing hot springs are rich in gas contents. The gas analyses results indicate that the major gas for the hot springs in the studying region is CO_2 comprising 96.7 to 99.84% of the whole gas contents (Table 3), and the dissolved carbon dioxide is often higher than 250 mg/L, some up to 1000 mg/L. The N_2 content is very low, from trace to 2.01%, increasing with the decrease in CO_2 content. Among the minor gases, CH_4 content ranges from 0.04 to 1.86%(Wt), Ar 0.095 ~ 0.211%, He 0.0047 ~ 0.0137%.

TABLE 3. MAJOR GAS COMPOSITION AND ISOTOPES

Spring No.	Major gas content (%)					Carbon isotope ‰PDB		Helium isotope	R/RA *
	N_2	CO_2	CH_4	Ar	He	$\delta\ ^{13}C_{CH4}$	$\delta\ ^{13}C_{CO2}$	$^3He/^4He$	
2		99.84	0.04	0.115	0.0047	-27.69	-4.96	$(1.90\pm0.06)\times10^{-6}$	1.36
3		97.96	1.86	0.117	0.0016	-34.86	-4.43	$(2.74\pm0.12)\times10^{-6}$	1.96
9	2.01	96.47	1.28	0.211	0.0234	-59.31	-5.5	$(2.95\pm0.10)\times10^{-6}$	2.11
11	1.91	97.92	0.06	0.095	0.0137	-45.3	-5.06	$(2.30\pm0.08)\times10^{-6}$	1.64

- $R = {^3He} / {^4He};\ R_A = ({^3He} / {^4He})_{air} = 1.4\times 10^{-6}$

4.2. Carbon and Helium Isotopes

The δ ^{13}C values for CH_4 are in the range of –59.31 to –27.69 ‰ (PDB), showing that it could be the decomposition product of organic materials in rocks under high temperature [2]. The values of δ ^{13}C for and –5.5 to –4.43 ‰ (PDB) , and the CO_2 could originated from the metamorphic processes of carbonate minerals or rocks [3].

The helium isotope for the geothermal springs is characterized by high ratio of $^3He/^4He$, from $(1.90\pm0.06)\times10^{-6}$ to $(2.95\pm0.10)\times10^{-6}$, much greater than the ratio for the air (1.4×10^{-6}), and R/R_A is greater than 1. Therefore, the helium in the local geothermal waters could be derived from the mantle [2B3].

ACKNOWLEDGEMENT

The authors appreciate the support from the Isotope Hydrology Section of the International Atomic Energy Agency, the research mentioned above is a part of the work of the IAEA Regional Collaboration in the Development of Geothermal Energy Resources and Environment Management through Isotope Techniques in East Asia and the Pacific (RAS-8-075). Special thanks will be given to Ms. Jane Gerardo-Abaya for her helps in the implementation of the project.

REFERENCES

[1] LI Xueli, ZHOU Wenbin, Relations between terrestrial heat flow and uranium deposits in Jiangxi Province, China. Water-Rock Interaction, Kharaka & Maest (eds), Balkema, Rotterdam. 1992, 1597B1599.

[2] WANG, X.B., et al, Characteristics of gas and isotope composition of thermal springs in Tengchong volcanic region, Chinese Science Bulletin.38(1993) 814B817.

[3] WANG, X.B., et al, Geochemical features of gases from thermal springs seismic regions, Science in China, version B, 24(1992) 849B854.

A COMBINED ISOTOPIC TOOL FOR WATER-ROCK INTERACTION STUDIES : B, Sr, O, H ISOTOPES IN GROUNDWATER

W. KLOPPMANN, PH. NEGREL , J. CASANOVA
BRGM,
Department of Geochemistry and Hydrogeology,
Research Division,
Orléans, France

Abstract

An "isotopic toolbox" containing boron, strontium, stable hydrogen and oxygen isotopes has been tested in different geological environments in order to constrain the origin of salinity in groundwaters. The application of the isotopic tracers is demonstrated with three case studies which concern deep saline groundwaters from the cristalline basement of the Vienne region in France, sedimentary brines in the North German Basin and marine intrusions into a coastal aquifer in the Sultanate of Oman. Sr and B isotopes turn out to be particularly useful to distinguish marine from non-marine origin of salts, primary from secondary brines, water rock interaction from mixing with sea-water derived brines and to decipher the age of dissolved salts. O and H isotopes give supplementary information on the origin and movement of the implied groundwater masses.

1. INTRODUCTION

The combination of individual isotopic tools in groundwater studies helps to restrain hypotheses on the nature of water-rock interactions and the endmembers implied in mixing processes. A toolbox containing boron, strontium, oxygen and hydrogen isotopes has been tested in several geological environments in order to elucidate the origin of salinity. It makes use of some particular qualities of the individual tools as there are :

B: Due to the large relative mass difference between ^{10}B and ^{11}B and the high chemical reactivity of boron, significant isotope fractionation produces large variations in $^{11}B/^{10}B$ ratios in natural samples from different geological environments [1]. This results in high isotopic contrast of potential mixing sources but also in process-specific changes of the isotope signature. Boron is omnipresent in groundwaters. In some chemical environments it may behave like a conservative tracer: Boron isotopes are for instance insensible to redox-processes contrarily to sulphur and oxygen isotopes. In other cases (high clay contents of the solid matrix, coprecipitation with solid phases like carbonates or evaporites) a partial phase change would lead to important fractionation [2, 3, 4, 5].

Sr: Sr isotopes show no detectable fractionation by any natural process. Given the relatively short time scale of the processes studied, the measured differences in the $^{87}Sr/^{86}Sr$ ratios are due to the contribution of Sr derived from various sources with different isotopic compositions. The $^{87}Sr/^{86}Sr$ ratio variations within an hydrosystem can provide information about those sources, the mixing proportions of groundwater components or the degree of water rock interaction.

O, H: If no evaporation or exchange with dissolved gases occurs in the groundwater body, the stable isotopes of the water molecule behave like conservative tracers which reflect the mixing of different recharge components in groundwater. Under particular conditions (low water-rock ratios, long residence times or high reservoir temperatures) water-rock interactions may modify the stable isotope composition.

2. EXAMPLES

The common point of the three case histories described below (FIG. 1,2) is the uncertainty about the origin of salinity in contrasting geological environments, the granitic basement of the Poitou region (France), the North German sedimentary basin and a coastal aquifer with a seawater intrusion in the Wadi Ahin catchment (Sultanate of Oman).

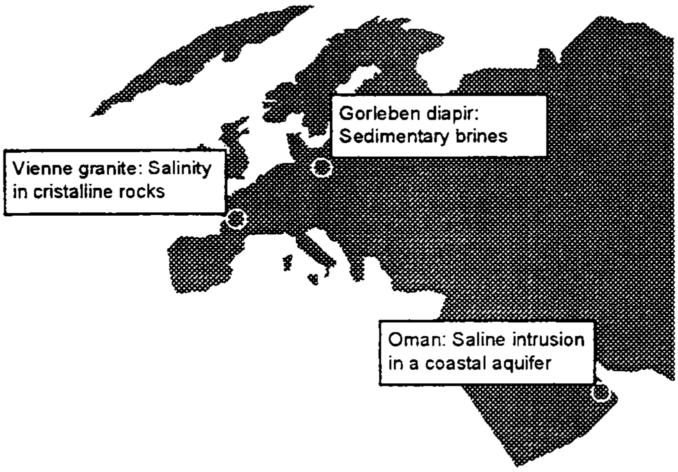

FIG. 1. Map showing the three study sites: Gorleben, Northern Germany, Vienne, France and Wadi Ahin catchment, Sultanate of Oman.

Deep groundwaters of the North German Basin are highly saline [6, 7] and typical "oil field brines" are encountered. A detailed study of groundwaters and brines in the vicinity of the Gorleben salt structure crossing the Elbe river 120 km SE of Hamburg casts some light on the mechanisms of brine formation [8, 9]. Shallow groundwaters show signs of silicate weathering and cation exchange processes. Salinity steeply increases with depth and a clear mixing tendency can be derived from B and Sr concentrations and isotopic ratios. Both tools constrain the nature of the highly saline endmember: Sr isotope ratios of the most concentrated brines (above 300 g/l) are close to those of the Permian ocean [10] and of the Gorleben halite ($^{87}Sr/^{86}Sr = 0{,}70696$). $\delta^{11}B$ values of 28 to 33 ‰ *vs.* NBS 951 of the brines stay below the value of modern ocean water (40 ‰). Provided that the boron isotopic composition of the Permian ocean was similar to the modern sea water, this would suggest rather salt erosion (secondary brines) than residual primary brines as a source of salinity. The latter would be expected to be enriched in ^{11}B with respect to (paleo-)seawater by up to 15 ‰ depending on the degree of evaporation [11]. O/H isotopes give hints to the age of brine formation and the dynamics of mixing: most brines show Pleistocene cold signatures; rapid infiltration of Holocene waters is evidenced in a few cases by brines enriched in ^{2}H and 18O.

The origin of salinity in deep groundwaters in the cristalline basement has been subject of extensive discussion. In the French granites in the Vienne district (max. depth of sampled groundwaters: 500 m), the conclusions drawn from Sr and B isotopes converge towards a marine origin [12]. The marine signature is confirmed by Br/Cl ratios. B isotopic compositions of the most saline waters lie close to those of present day seawater and $^{87}Sr/^{86}Sr$ ratios are slightly higher than those of the Jurassic ocean. Seawater intrusions or sedimentary brines of marine origin are therefore the most probable sources of salinity. Typical mineral waters from granite further inland (Massif Central) show higher $^{87}Sr/^{86}Sr$ and lower $^{11}B/^{10}B$ ratios. Some groundwaters from a faulted zone in the crystalline bedrock of the Vienne region show an intermediate position.

Stable O and H isotopes do not supply any further constrains on the origin of salinity. Interactions with silicates at low water-rock ratios have utterly modified the isotopic signature and

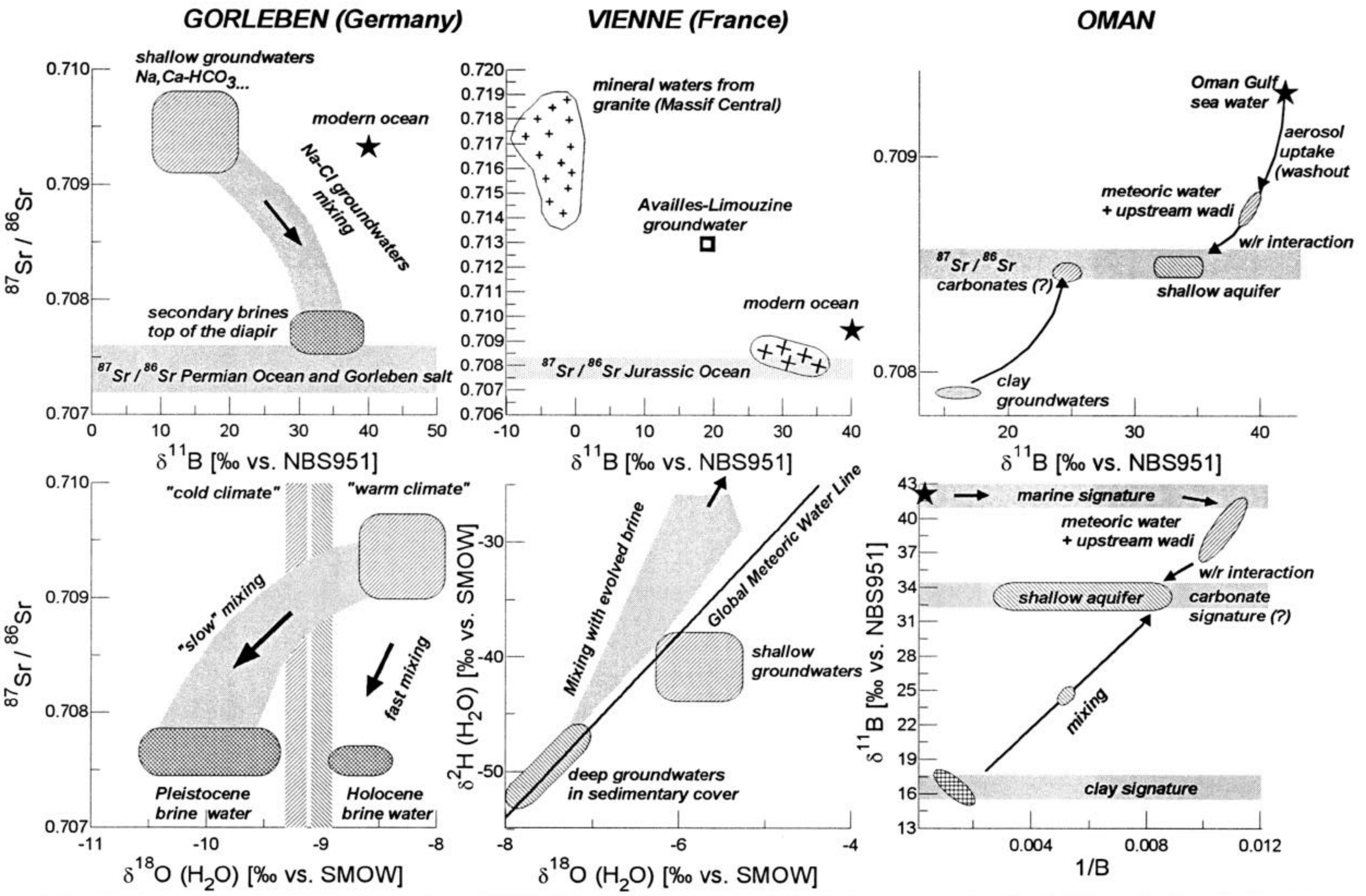

FIG. 2. B/Sr/O/H isotope systematics of groundwaters from the granitic basement of the Vienne district (France), the Gorleben site (North German sedimentary basin) and a coastal aquifer (Sultanate of Oman).

overprinted any trace of marine origin. The hypothetical saline endmember must have evolved towards an "exotic" position above the global meteoric water line and subsequently been mixed with a relatively heavy isotope depleted fresh groundwater (cold signature).

The Oman case study concerns a typical problem of marine intrusion into a coastal alluvial aquifer of the Wadi Ahin catchment. Some doubt persists on the extension of the intrusion further inland where intermediate salinities (electrical conductivity about 2000 mS/cm) might be interpreted as a result of mixing with seawater. Both boron and strontium isotopic composition are incompatible with this hypothesis [13]. The combined Sr/B study suggests that marine influence is only indirect: rainwater shows isotopic compositions similar to Oman Gulf seawater and is only slightly modified by washout. Most of the groundwater in the shallow alluvial aquifer shows increasing salinities at **constant** Sr and B isotopic ratios. This observation is consistent with water rock interaction with the carbonate dominated aquifer overriding the signature of rainwater input. Ophiolitic rocks in the upper part of the catchment basin leave no trace in the isotopic signature of percolating water whereas clayey strata underlying the alluviums are clearly marked by low δ^{11}B and ^{87}Sr/^{86}Sr values. Some mixing seems to occur between the two reservoirs, alluviums and schists. Stable O and H isotopes show typical high altitude signatures for the group of intermediate conductivity groundwaters. We may conclude that a part of the alluvial aquifer contains waters with salinity of continental origin recharged further inland which have chemically evolved by extensive water-rock interaction. Saline intrusion seems to be restricted to a rather narrow margin along the coast.

3. CONCLUSIONS

A combination of B, Sr, O, and H isotopes seems to be promising in hydrogeological situations where the sources of salinity are doubtful. Future research may focus on the isotopic characterisation (B and Sr isotopes) of potential endmembers like precipitations and anthropogenic inputs.

Table I. Origin of salinity in groundwaters : problems and use of isotopic tracers.

Problem	^{11}B	^{87}Sr/^{86}Sr	^{18}O, ^{2}H
Marine *vs.* non marine origin	++	++	++
Evaporation of seawater	+ [a]		++
Primary *vs.* secondary brines	+		+
Degree of water-rock interacion	+	++	(+) [b]
Origin and movement of the implied water masses			++
Age of salt	(+) [c]	++	

a evaporation beyond halite precipitation

b in hydrothermal systems or in silicate rocks with low water/rock ratio and long residence times

c provided that in future information about variations in B-isotopic composition in ocean water become available (see for example [14])

REFERENCES

[1] BARTH, S., Boron isotope variations in nature : a synthesis, Geol. Rundsch **82** (1993) 640–651.

[2] VENGOSH, A., CHIVAS, A.R, MCCULLOCH, M.T., STARISNKY, A., KOLODNY Y., Boron isotope geochemistry of Australian salt lakes, Geochim. Cosmochim. Acta **55** (1991), 2591–2606

[3] VENGOSH, A., KOLODNY, Y., STARISNKY, A., CHIVAS ,A.R., MCCULLOCH, M.T., Coprecipitation and isotopic fractionation of boron in modern biogenic carbonates, Geochim. Cosmochim. Acta, **55** (1991), 2901–2910.

[4] VENGOSH A., STARISNKY A., KOLODNY Y., CHIVAS A.R. Boron isotope geochemistry as a tracer for the evolution of brines and associated hot springs from the Dead Sea, Geochim. Cosmochim. Acta **55**(1991) 1689–1695

[5] PALMER, M.R., SPIVACK, A.J., EDMOND, J.M. Temperature and pH controls over isotopic fractionation during adsorption of boron on marine clay, Geochim. Cosmochim. Acta **51** (1987) 2319–2323.

[6] LÖHNERT, E.P. Tiefes Grundwasser in Nordeutschland, Zbl. Geol. Paläont. **I** (1972) 1/2 19–25.

[7] KLOPPMANN, W., DEVER, L., EDMUNDS, W.M., Residence time of Chalk groundwaters in the Paris Basin and in the North German Basin, Applied Geochemistry **13** (1998) 593–606.

[8] KLINGE, H., Projekt Gorleben. Zusammenfassende Bearbeitung der chemischen und isotopengeochemischen Zusammensetzung der Grundwässer im deckgebirge des Salzstocks Gorleben und seiner Randsenken, Unpublished Rep 111 699 BGR, Hannover, Germany (1994)

[9] KLOPPMANN, W., NEGREL, P., CASANOVA, J., GUERROT, C., KLINGE, H., Boron and Strontium isotopes in groundwaters and brines of the North German Basin (Gorleben diapir), (EUG 10 meeting, Strasbourg, 1999), Terra Abstracts **11** (1999) 584.

[10] MARTIN, E.E, MCDOUGALL, J.D, Chem. Geol. **125**(1995) 73–99.

[11] VENGOSH, A. , STARINSKY, A., KOLODNY, Y., CHIVAS, A.R., RAAB, M., Boron isotope variations during fractional evaporation of sea water; new constranits on the marine vs. nonmarine debate, Geology **10** (1992) 799–802.

[12] NEGREL, P., CASANOVA, J., KLOPPMANN, W., ARANYOSSY, J.F., Origin of deep saline groundwaters in the Vienne granitoids (France);constraints inferred from strontium and boron isotopes, (EUG 10 meeting, Strasbourg, 1999), Terra Abstracts **11** (1999) 520.

[13] CASANOVA, J., MACHARD DE GRAMONT, H., KLOPPMANN, W., NEGREL, P., Boron and strontium isotopic geochemistry of the Wadi Ahin catchment (Sultanate of Oman) (EUG 10 meeting, Strasbourg, 1999), Terra Abstracts **11** (1999) 557.

[14] SPIVACK, A.J., YOU, C.-F., SMITH, H.J., Foraminiferal boron isotope ratios as a proxy for surface ocean pH over the past 21 Myr, Nature **363** (1993) 149–151

ISOTOPIC AND GEOCHEMICAL ASSESSMENT OF THE GEOTHERMAL FIELD OF LIMNOS ISLAND, GREECE

E. DOTSIKA
Lab. of Isotope Hydrology I,
National Center for Scientific Research ''Demokritos''
Agia Paraskevi Attikis, Greece

D. POUTOUKIS
General Secretariat for Research & Technology,
Athens, Greece

E. LAGIOS
Department of Geology,
Univ. of Athens,
Athens, Greece

J.L. MICHELOT
Lab. of Hydrology and Isotope Geochemistry
UMR OrsayTerre, CNRS-Univ. Paris-Sud,
Orsay, France

Abstract

The island of Limnos is located in the Northern part of the Aegean sea. In 1995 and 1996, water samples were collected from cold and thermal springs and wells. Maximum surface temperature of 42°C is associated with the Therma springs water. Two hydrochemical categories of water can be distinguished. The chemical composition of thermal water, of Na-Cl type, would be due to small contribution of marine salts, hydrolysis of silicate rocks and secondary calcite dissolution. The cold groundwaters are mainly of $Ca\text{-}HCO_3$ type and their chemical composition is controlled by calcite dissolution.

Isotopic composition, δ^2H- $\delta^{18}O$, shows the meteoric origin of both types of water. The circulation of water through different rock types influences the $\delta^{13}C$ value of dissolved HCO_3^- and the $\delta^{34}S$ of dissolved SO_4^{2-}.

The aquifer in the volcanic rocks exhibits a reservoir temperature around 60°C - 80°C, from the results obtained by the chemical geothermometers. The sulphate-water isotopic geothermometer gives higher temperature, which is probably unreliable because aqueous sulphate comes from a mixing between marine sulphate and sulphate resulting from the oxidation of sulphur minerals, and is not in isotopic equilibrium with water.

1. INTRODUCTION

Hydrothermal systems with low to high enthalpy are present all over the Aegean Sea. Especially, they can be found at the southern part of the archipelago, along the South Aegean active volcanic arc and the northern part, in volcanic rocks of Tertiary and Quaternary age, at Limnos, Samothraki, Lesvos, Chios islands...

Limnos Island, thermal waters of which are the object of this study, is located about 80km South of the Thracian coast. Until now, no systematic research has been undertaken on these waters, which emerge from volcanic rocks at an elevation of 90m a.s.l., with a flow of 5 m^3/h, and are used for the operation of a thermal station.

In 1995, a study was undertaken on the origin of thermal waters and of their mineralisation. Also the temperatures of deep reservoirs, using environmental (hydrochemical and isotopic) tracers, were estimated.

2. GEOLOGICAL BACKGROUND

The geology of Limnos [1, 2, 3] island is characterized by a sedimentary basement covered by volcanic rocks (Fig. 1). The oldest part of the island consists of molassic flysch deposits (sandstones with conglomerate interbeds and green silty clays and sandstone) with ages ranging from Middle Eocene to Early Miocene. Intense magmatism subsequently produced sills, lava domes, flows and pyroclastic sequences.

The lower sedimentary sequence (Late Oligocene to Lower Oligocene) includes primary sandstones with conglomerate interbeds, silty clays and sandstones, and secondary well-bedded sandstones, siltstones, clays and limestone blocks.

The upper sedimentary sequence contains biogenic marine calcarenites, alluvial and colluvial deposits, marine and eolian sands.

The Quaternary sediments consist of conglomerate and volcanic pebbles with intercalations of sandstones.

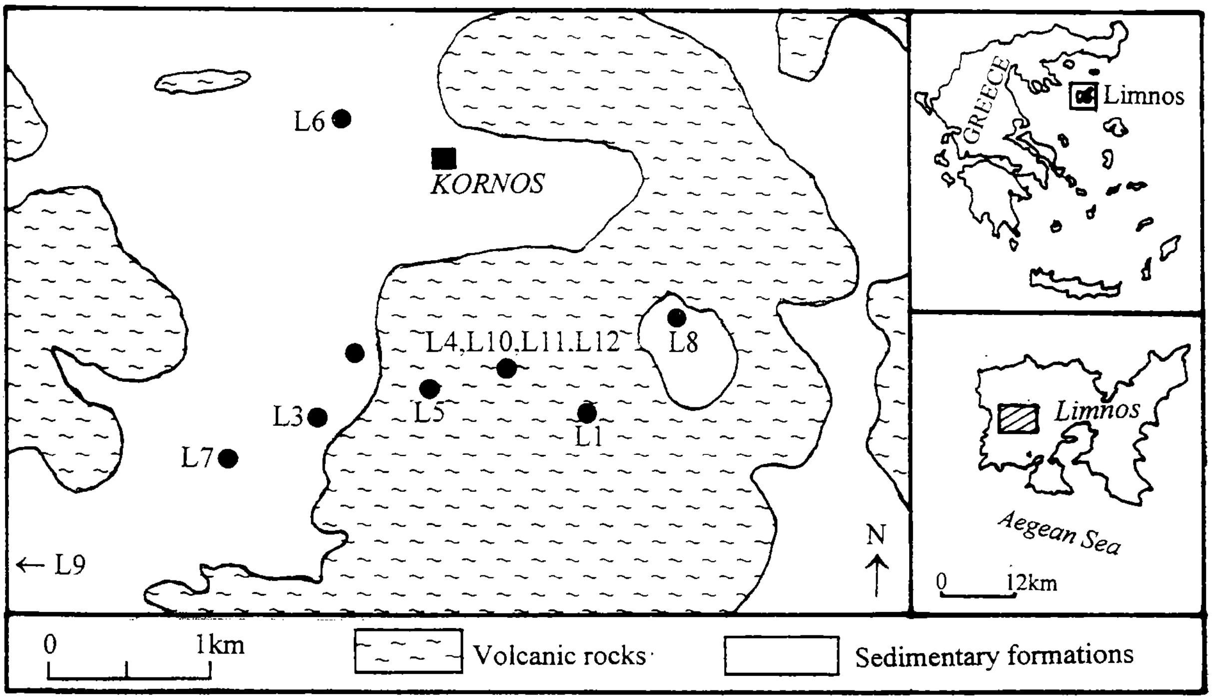

FIG. 1. Sketch map of the study area with locations of the water sampling points.

The volcanic complex contains lava domes, volcanic breccias, lava flows, pyroclastic deposits, and ignibrites consisting of dacites, latites, andesites and trachytes (Lower Miocene). The K-Ar ages range from 20-21 Ma to 18.2 Ma.

3. FIELD WORK AND LABORATORY ANALYSIS

Raw, filtered (0.45μ) and filtered acidified (with HCl) samples were collected from thermal, hypothermal and cold water springs and wells. The thermal spring on the island emerge near the Therma area from volcanic rocks. Four samples (L4, L10, L11, L12) have been taken from this spring at different times (summer and winter '95 and '96), showing that the composition of the spring water is very constant. The hypothermal and cold waters emerge from sedimentary or volcanic rocks at elevations ranging from 20m to 170m a.s.l.. Temperature, pH and alcalinity were measured in the field. Water was sampled for chemical (major ions, Br^-, B, SiO_2) and isotopic (^{18}O, ^2H) analyses.

Aqueous sulfate samples for isotopic analyses ($^{18}O_{SO4}$, ^{34}S) were collected by precipitation from the water sample, after acidification, as $BaSO_4$.

4. CHEMICAL AND ISOTOPIC COMPOSITION OF GROUNDWATERS

Chemical and isotopic data on the waters collected in Limnos Island are reported in Table I. From the chemical composition, two types of water can be distinguished. The first type corresponds to Ca-Na-HCO_3-Cl groundwaters collected in sedimentary rocks and the second type to Na-Cl groundwaters emerging from volcanic or sedimentary rocks.

The TDS values of the Ca-HCO_3 groundwaters, emerging from sedimentary rocks, is lower than 0.5 g/L (0.47 g/L for L6 well and 0.4 g/L for L8 spring), their Cl^- concentration is almost 100 mg/L and their temperature is about 23°C. This temperature is significantly higher than average annual air temperature (17°C), indicating that these groundwaters were somewhat heated by conduction in the shallow aquifers.

Collected from wells in the sedimentary rocks, the samples L3 and L7 form a sub-group of the Na-Cl type groundwaters. Their temperature ranges from 17°C to 25°C. The lowest temperature is observed for sample L7, which have the highest salinity with sample L3. Their TDS are 1.18 g/L and 1.8 g/L, respectively.

The second sub-group of Na-Cl type groundwaters corresponds to springs in volcanic rocks. It includes the thermal spring (L4, L10, L11, L12) and the springs L1 and L5. Their chemical composition varies from Na-Cl type to Na-HCO_3-Cl type (sample L1). Their temperature ranges from 21°C to 45°C and their TDS is low, around 0.2 g/L.

TABLE I. PHYSICAL, CHEMICAL AND ISOTOPIC DATA ON GROUNDWATERS OF LIMNOS ISLAND. Ionic contents are expressed in mg/kg.

Sample	L1	L2	L3	L4	L5	L6	L7	L8	L9	L10	L11	L12
	spring	well	well	spring	spring	well	well	spring	S. W.	spring	spring	spring
pH	7.98		8.18	8.20	7.67	7.75	7.87	7.83	8.16	8.00	8.30	8.10
t°C	24	22.1	25.3	42.1	21.4	23.7	17.0	22.6		42.0	42.2	42.1
Cond. µS/cm	620		3400	460	500	910	2100	900	72500	540	530	510
HCO_3	186		396.5	91.5	79.3	341.6	530.7	335.5	128.1	99.0	97.6	92.0
Cl	99.3		705.6	78.0	99.3	111.4	365.2	106.3	20241	81.0	79.7	80.0
Br	0.24		2.94	0.26	0.25	0.21	0.79	0.13	70.26	0.25	0.25	0.26
SO_4	23		295	20	23	50	175	51	2900	20	21	20
Na	70		580	90	70	80	210	50.5	12500	76	75.8	80
K	1.6		5.1	1.7	4.4	4.2	2.7	3.0	516.0	2.0	1.7	2.0
Ca	35.3		35.3	6.4	9.6	84.2	159.5	101.8	428.8	7.0	7.2	6.0
Mg	16.0		57.8	1.0	10.7	34.9	59.3	21.9	1347	0.5	0.5	0.7
SiO_2	23.0		5.9	19.9	54.2	10.9	14.5	8.6	0.8	20.0	19.9	22.0
Bδ	0.2		0.8	0.2	0.4	0.4	0.4	0.3	5.8	0.2		0.2
Al				0.073							0.078	
$\delta^{18}O$‰ SMOW	-6.9	-7.8	-6.4	-6.9	-7.5	-6.6	-7.2	-7.4	+1.0	-6.9	-7.0	-7.2
$\delta^{2}H$‰ SMOW	-44.2	-47.8	-38.7	-42.8	-45.5	-42.5	-45.6	-44.6	+0.4	-44.0	-44.4	-46.5
$\delta^{34}S$‰ CD	+15.1		+5.3	+14.3		+3.0			+21.3	+15.0	+14.9	+14.0
$\delta^{18}O$‰ SMOW	+5.1		+6.4	+5.0		+5.5			+10.1	+5.4	+5.5	+5.0
$\delta^{13}C$‰ PDB	-17.9		-8.2	-18.4		-12.8				-18.2		

The triangular diagram Cl-SO_4-HCO_3 shows the relative concentrations of Cl^-, SO_4^{2-} and HCO_3^- in the collected groundwaters (Fig. 2a). The points define an almost linear trend, which links the cold bicarbonate type groundwaters sampled in sedimentary rocks and the chloride type groundwaters, including those from the thermal spring. Data plot parallely to the Cl-HCO_3 axis of the diagram, with variable values of the Cl/HCO_3 ratio (0.56 to 3 mmol/L) and minor variations of the SO_4/HCO_3 ratio. The linear trend corresponding to the differents samples, is directed towards the representative point of sea water, suggesting that the chloride dissolved in the groundwaters is of marine origin. This is confirm by the Cl/Br of the samples, which are close to the marine ratio. For most of the samples, it is difficult to precise whether these characteristics are due to a true seawater intrusion into the hydrological system, or to the contribution of marine aerosols to meteoric water recharging the system. However, the two samples L7 and L3, which have the highest total salinity, probably contain a small percentage of seawater. This marine contribution represents only 2-3% in term of water, but it brings almost the totality of dissolved salts.

Figure 2b shows a Ca^{2+}-HCO_3^--Na^+ diagram, with the region of the dissolution of calcite. Again, the points plot along a linear trend from a pole corresponding to calcite dissolution to a Na pole, close to the representative point of seawater. The main source of dissolved Na^+ in the groundwaters is probably seawater, or marine aerosols, but an additional contribution by silicates hydrolysis cannot be excluded. The main origin of Ca^{2+}, Mg^{2+}, and HCO_3^- is the dissolution of calcite, which is the main constituent of the sedimentary rocks and which is present as a secondary mineral in the volcanic rocks. However, these groundwaters remain under-saturated with respect to calcite [4].

Figure 3 presents the relationship between ^{18}O and ^{2}H contents of the samples and the local meteoric water line [5]. The position of the samples in this diagram confirms their purely meteoric origin. Only for the sample L3, a marine contribution can be suspected, in agreement with the chemical data. Thermal water is not enriched in oyxgen-18, with respect to groundwaters collected in the sedimentary rocks. This suggests that ^{18}O contents are not modified by the exchange with rocks, and therefore that the reservoir temperature is not very high.

The dissolution of carbonates is clearly marked in the $\delta^{13}C$ values of Ca-HCO_3 groundwaters. Isotopic composition of dissolved HCO_3^-, positively correlated with HCO_3^-, depends on the type of rocks from which the waters emerge. The groundwaters from sedimentary rocks show $\delta^{13}C$ values (-8‰ vs PDB < $\delta^{13}C$ < -13‰ vs PDB) logically higher than that (-18‰ vs PDB) observed in the thermal water samples, collected in volcanic rocks, due to the dissolution of marine carbonates with a $\delta\ ^{13}C$ value around 0±1‰ vs PDB [6].

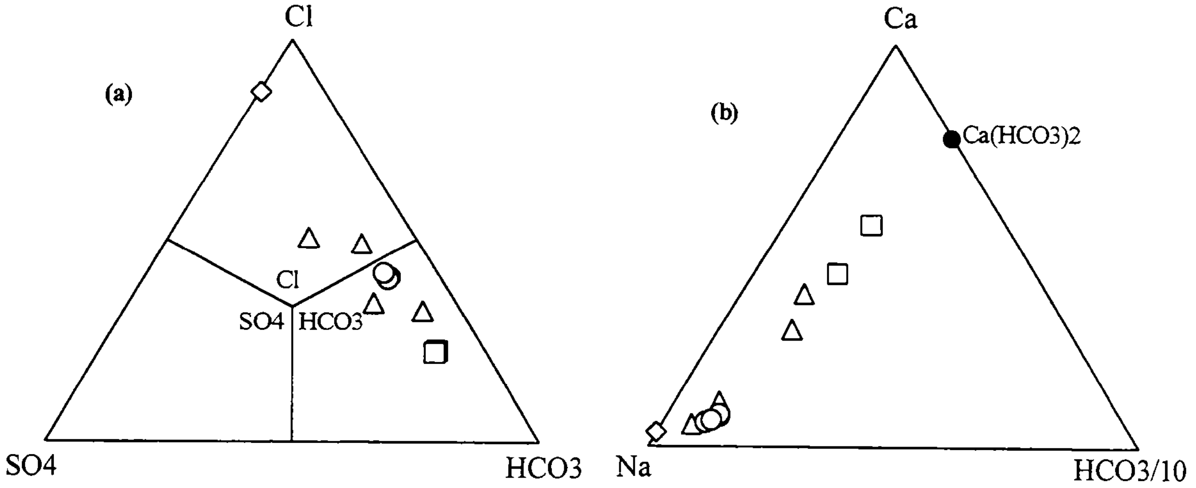

FIG. 2. (a) Relative Cl, SO_4, HCO_3 contents (mg/kg) and (b) triangular plot relative Ca, Na and HCO_3 contents (mg/kg) for the samples. The Ca/HCO_3 composition ratio relative to calcite is also indicated. Square = Ca-HCO3 waters; triangle = Na-Cl waters; circle = thermal Na-Cl waters; diamond = sea water.

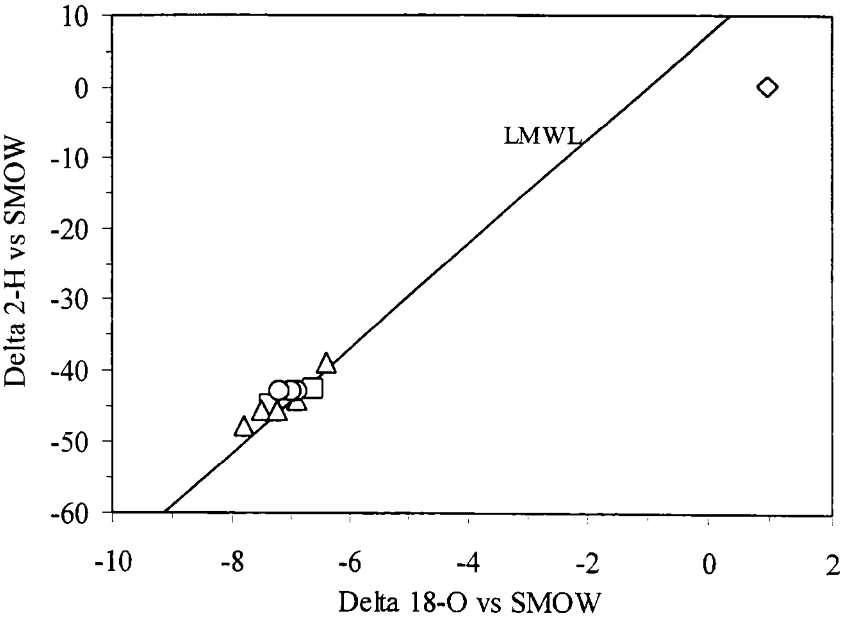

FIG. 3. δ^2H versus $\delta^{18}O$ diagram. LMWL = Local meteoric water line [5]. For symbols see Fig. 2.

The circulation of these groundwaters in different rock types, influenced also the isotopic composition of their aqueous sulphate. In figure 4a, the sulphur-34 and oxygen-18 contents of the samples are compared to those of marine sulphate. Samples collected from water that emerges in volcanic rocks present ^{34}S content ($\delta\ ^{34}S$ = +15‰ vs CD) higher than those ($\delta\ ^{34}S \leq$ +5‰ vs CD) of the samples of water taken from the sedimentary rocks. But all the samples contain sulphate that is depleted in heavy isotopes with respect to marine sulphate. These isotopic data suggest (Fig. 4a) that there are two origins of the aqueous sulphate: marine sulphate and sulphate with 'light' isotopic composition, which probably comes from oxidation of sulphur minerals. These sulphur minerals could have different isotopic compositions in the sedimentary rocks (generally, $\delta^{34}S$ very variable, with an average value of -12‰ vs CD [7]) and in the volcanic rocks (generally, primary suphur with $\delta^{34}S$ = 0±5‰ vs CD [7]).

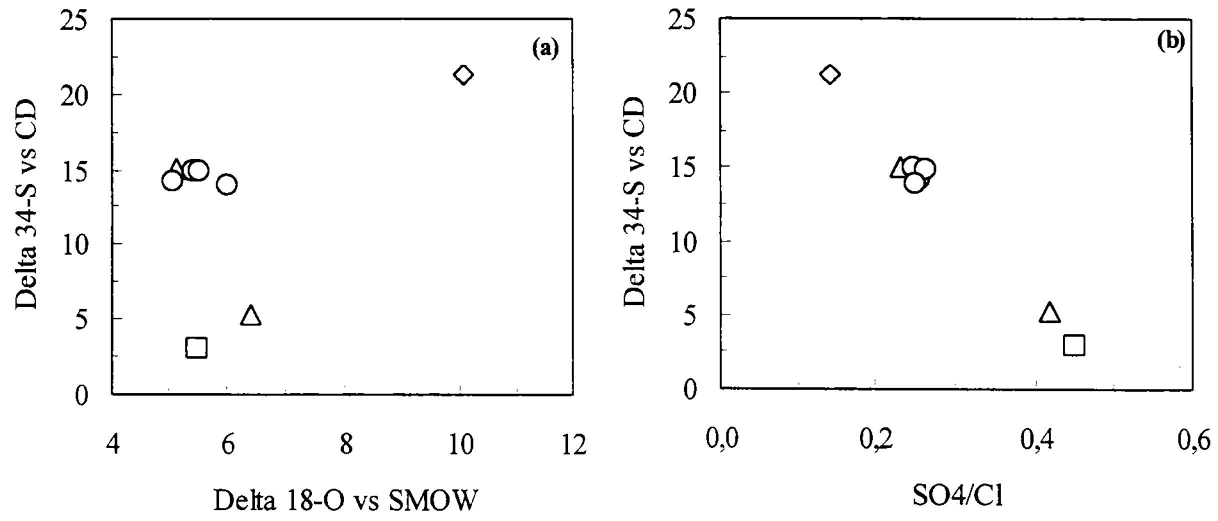

FIG. 4. (a) $\delta^{34}S$ versus $\delta^{18}O$ of dissolved sulphate and (b) $\delta^{34}S$ versus SO_4/Cl weight ratio. For symbols see Fig. 2.

In both cases, the contribution of sulphur oxidation is confirmed by the decrease of $\delta^{34}S$ value with the increase of the SO_4^{2-} concentration in the groundwater (Fig. 4b).

For the thermal water, the contribution of marine SO_4^{2-} is estimated to 75% (and the contribution of oxidation SO_4^{2-} to 25%). According to the values of $\delta^{18}O(H_2O)$ and $\delta^{18}O(SO_4^{2-})$ in thermal water, it is estimated [8] that oxygen which is incorporated in the sulphate formed by oxidation, comes from atmospheric O_2 for the main part. That suggests that the oxidation reactions took place in the soils and/or in the shallow, well airated, part of the aquifers.

5. GEOTHERMOMETRY

The eventual attainment of mineral-solution equilibrium can be assessed on the basis of Na^+, K^+, Mg^{2+} and Ca^{2+} contents [9] (Fig. 5). The square plot reports a curve representing the Na^+, K^+, Mg^{2+} and Ca^{2+} concentrations of thermal water in full equilibrium with a thermodynamically stable mineral assemblage (chalcedony, albite, K-feldspar, muscovite, clinochlore, a Ca-Al-silicate and calcite), having the composition of an average crustal rock. None of the Limnos thermal waters attained full equilibrium. As expected, the cold and hypothermal groundwaters are particularly immature. Their chemical composition is controlled by calcite dissolution (L6 and L8) and contribution of sea water (L3 and L7). The thermal groundwaters, with lower Mg/Ca ratios, are somewhat more evolved.

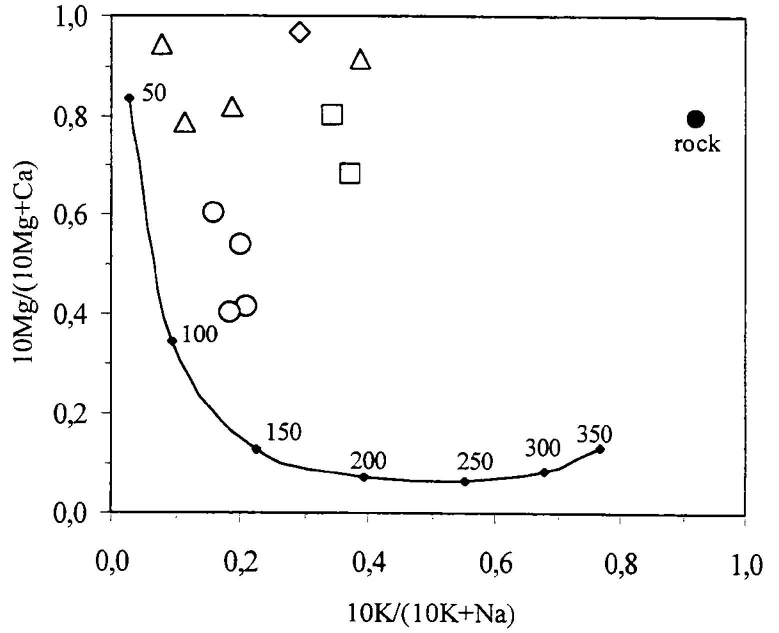

FIG. 5. Plot of $10C_K/(C_{10K} + C_{Na})$ ratio versus $10CMg/(C_{10Mg} + C_{Ca})$ ratio (Ci in mg/kg) for the samples investigated. The full equilibrium line comprises the composition of waters that have attained equilibrium with the thermodynamically stable mineral assemblage with the composition of an average crustal rock [9]. For symbols see Fig. 2.

TABLE II. TEMPERATURE (IN °C) COMPUTED BY GEOTHERMOMETERS FOR THE THERMAL WATER SAMPLES.

Samples	K/Mg [10]	SiO_2 [11]	Na – K [12]	$SO_4 - H_2O$ [13]	$SO_4 - H_2O$ [14]
L4	53	63	59	157	150
L10	60	63	68	153	146
L11	64	63	78	151	143
L12	60	67	75	154	147

Assuming that their relative Na and K concentrations memorise deep equilibrium conditions, temperature lower than 130°C is indicated. With the use of the other chemical geothermometers [10, 11, 12] (Tab. II), the aquifer in the volcanic rocks exhibits a reservoir temperature around 60°C to 80°C.

This temperature is very different from that obtained with the sulphate-water isotopic geothermometer [13, 14, 15], which is based on the equilibrium exchange of oxygen isotopes between aqueous SO_4^{2-} and H_2O. However, aqueous sulphate in Limnos samples resulting from a mixing (marine sulphate and oxidation sulphate), it is difficult to be certain that it is at equilibrium with water, so that the calculated temperature (150°C) is not really reliable.

6. CONCLUSION

Chemical and isotopic data on thermal waters indicate low reservoir temperature (around 60°C - 80°C) for the geothermal field of Limnos Island.

On the basis of chemical data the groundwaters can be classified in two groups.

The first group consists of cold HCO_3-type water, emerging in sedimentary rocks. Their chemical composition is controlled by interaction with carbonated sedimentary rocks at low temperature.

The second group, which includes the thermal spring water, is composed of Na-Cl type water, which circulates in volcanic rocks.

These thermal waters are mainly of meteoric origin, but it is possible that a slight contribution of marine water is responsible for their chloride content.

Acknowledgements – Part of this work has supported by International Atomic Energy Agency.

REFERENCES

[1] INNOCENTI F. et al., The geology and geodynamic significance of the Island of Limnos, North Aegean Sea, Greece, N. Jb. Geol. Palaont. Mh. H. **11** (1994), 661B691.

[2] DAVIS E., The volcanic rocks of Limnos Island, Ann. Geol. Pays Hell. **11** (1960) 1B83, (in Greek).

[3] ROUSSOS N., Geological map of Greece, 1:50000, Myrina sheet, I.G.M.E. Athens (1993).

[4] TRUESDELL AH., JONES B.F., Wateq, a computer program for calculating chemical equilibrium of natural water, J. Res. U.S. Geol. Survey **2** (1974) 233B248.

[5] INTERNATIONAL ATOMIC ENERGY AGENCY, Statistical treatment of environmental Isotope Data in precipitation, IAEA-TECDOC-206, Vienna (1981).

[6] PINEAU E., La géochimie isotopique du carbone profond, PhD Thesis, Université de Paris VII, Paris (1977).

[7] THODE H.G. et al., Sulphur isotope exchange between sulphur dioxide and hydrogen sulphide, Geochim. Cosmochim. Acta **35** (1971) 35B41.

[8] VAN EVERDINGEN R.O., KROUSE H.R., Isotope composition of sulphate generated by bacterial and biological oxidation, Nature **315** (1985) 395B396.

[9] GIGGENBACH W.F., Geothermal solute equilibria. Derivation of Na-K-Mg-Ca geoindicators, Geochim. Cosmochim. Acta **52** (1988) 2749B2765.

[10] GIGGENBACH W.F. et al., Geochemical structure and position of the Waiotapu geothermal field, New Zealand, Geothermics **23** (1994) 599B644.

[11] FOURNIER R.O., Application of water geochemistry to geothermal exploratio and reservoir engineering. In: principes and Case Histories, (RYBACK L.,MUFFLER L.J.P. Eds), Wiley, New York (1981) 109B143.

[12] TRUESDELL A.H., Summary of section III geochemical techniques in exploration. In: Proc. Second United Nations Symp. On the Development and Use of Geothermal Resources, San Francisco, U. S. Governmant Printing Office, Washington D. C., 1 Vol, (1976) 53B89.

[13] LLOYD R.M., Oxygen isotope behaviour in the sulfate-water system, J. Geophys. Res. **73** (1968) 6099B6110.

[14] MIZUTANI Y., RAFTER T.A., Oxygen isotopic composition of sulfates, 3. Oxygen isotopic fractionation in the disulfate-water system, N. Z. J. Sci. **12** (1969) 54B59.

[15] MIZUTANI Y., RAFTER T.A., Oxygen isotopic composition of sulfates, 4. Bacterial sulfate and the oxydation of sulfur, N. Z. J. Sci. **12** (1969) 60B68.

GEOCHEMISTRY OF CO_2-RICH WATER IN THE JUNGWON AREA, KOREA

Y. K. KOH, C. S. KIM, D.S. BAE, K. S. KIM, H. S. CHOI
Geoenvironmental Sciences
Korea Atomic Energy Research Institute
P.O. Box 105, Yusung, Taejon
Republic of Korea

Abstract

From the Jungwon area which is one of the famous locations for the CO_2-rich water in Korea, various kinds of natural waters (deep groundwater, shallow groundwater and surface water) were studied for hydrogeochemical and environmental isotope ($\delta^{18}O$, δD, $\delta^{13}C$, $\delta^{34}S$, $^{87}Sr/^{86}Sr$ and tritium) characteristics. Carbonate and alkali types of deep groundwater occur together, and each type shows distinct hydrogeochemical and environmental isotope characteristics. The CO_2-rich water in the area is characterized by lower pH (6.0 to 6.4), higher Eh (25 to 85 mV) and higher contents of total dissolved ions (up to 3,300 mg/L), whereas the alkali type water has higher pH (9.1 to 9.5), lower Eh (-128 to -136 mV) and TDS (168 to 254 mg/L) indicating controlled by water-granite interaction. The CO_2-rich water might be evolved by CO_2 supplied at depth during groundwater circulation. This process leads to the dissolution of surrounding rocks and the enrichment of Ca, Na, Mg, K and HCO_3. The alkali water is relatively enriched in F (up to 14 mg/L), whereas F concentration of the CO2-rich water (2.2 to 4.0 mg/L) is governed by fluorite precipitation. Two types of groundwater (<1.0 TU) were both derived from pre-thermonuclear meteoric waters with lighter O and H isotope composition (-10.5 to -9.4 ‰, $\delta^{18}O$) than younger waters (-8.8 to -7.8 ‰, $\delta^{18}O$), i.e. shallow groundwater and surface water, indicating prolonged water-rock interaction. The relationship between $\delta^{18}O$ and δD indicates that the CO_2-rich water was isotopically re-equilibrated with CO_2 gas. The $\delta^{34}S$ values (+24.1 to +27.6 ‰) of dissolved sulfate shows that sulfate reduction by organic activity had occurred at depths. However, Fe and H_2S content and Eh values are not consistent with sulfate reduction. Contrast to the CO_2-rich water, the low P_{CO_2} (about $10^{-4.6}$ atm) of the alkali water seems to be resulted from dissolution of silicate minerals without supply of CO_2.

1. INTRODUCTION

The Jungwon area, located about 100 km southeast of Seoul, was famous for the large and high quality scheelite crystals in the hydrothermal sulfide-bearing W-Mo deposits. Thus, many studies were focused on the mineralization and hydrothermal system of mineral deposits in this area [1, 2, 3]. Recently this area became famous again for a CO_2-rich thermal water in Korea, which characteristically show outgassing of carbon dioxide and accompany the precipitation of brown-colored calcite. The CO_2-rich waters are produced from the granite terrain and the measured content of TDS is up to 3.3 g/l. The area is characterized by geothermal gradients of about 3°C per 100 m from geophysical temperature log data in the thermal water wells [4].

In spite of the geochemical study already conducted [4, 5], the origin and the evolution of the CO_2-rich thermal water are still merely understood. The sulfide oxidation and carbonate dissolution have favored the evolution of the mineralized water in the Jungwon area, because the highly mineralized water wells are located within 1km from the W-Mo mines (Fig. 1). However, the geochemical and isotopic data are not consistent with the oxidation of sulfide and dissolution of vein calcite. The geochemical studies on groundwaters in Korea are increasing. Still, the nature and subsurface evolution of deep groundwater have not been well understood yet. In this paper the authors report on the hydrochemical conditions of the mineralized water and the hydrochemical evolution of the waters in the Jungwon area. This work could initiate the application of isotope technique on groundwater problems in Korea and might establish a hydrogeochemical genetic model applied to the other mineralized waters in Korea.

2. GEOLOGIC SETTING

Geology of the Jungwon area consists mainly of Precambrian gneisses (of the Kyonggi Gneiss Complex) and Mesozoic granitoids (biotite granite, porphyritic granite and some dykes), as shown in Fig. 1. The NW-trending Angsung fault separates the lithology of the area into two groups: granite largely in the northern part, and gneiss in the southern part. The Precambrian gneisses comprise banded biotite gneiss, schistose gneiss and granitic gneiss, and are intruded by biotite granite and several acidic to basic dykes.

According to Kim [6], the mineralogical composition of biotite granite is quartz (27.4%), K-feldspar (26.3%), plagioclase (38.0%), biotite (6.2%) and muscovite (1.6%) with minor amounts of apatite, zircon and opaque minerals. Granitic gneiss hosts hydrothermal W-Mo deposits (Fig. 1), which were the famous W-Mo mines in Korea but are now closed. These W-Mo mines are composed of numerous, NW-trending subparallel quartz and calcite veins (usually about 50cm thick) which fill the fractures of Precambrian granitic gneiss and late Cretaceous (105±5 Ma) biotite granite [6]. A K-Ar age (88±2 Ma) of vein muscovites from the Daehwa W-Mo mine indicates that W-Mo mineralization occurred during Late Cretaceous [2]. The ore mineralogy consists mainly of molybdenite, wolframite, pyrite, chalcopyrite, sphalerite, marcasite and bismuthinite with minor amounts of galena and pyrrhotite. Gangue minerals are mainly quartz with subordinate muscovite, fluorite, calcite, siderite and ankerite.

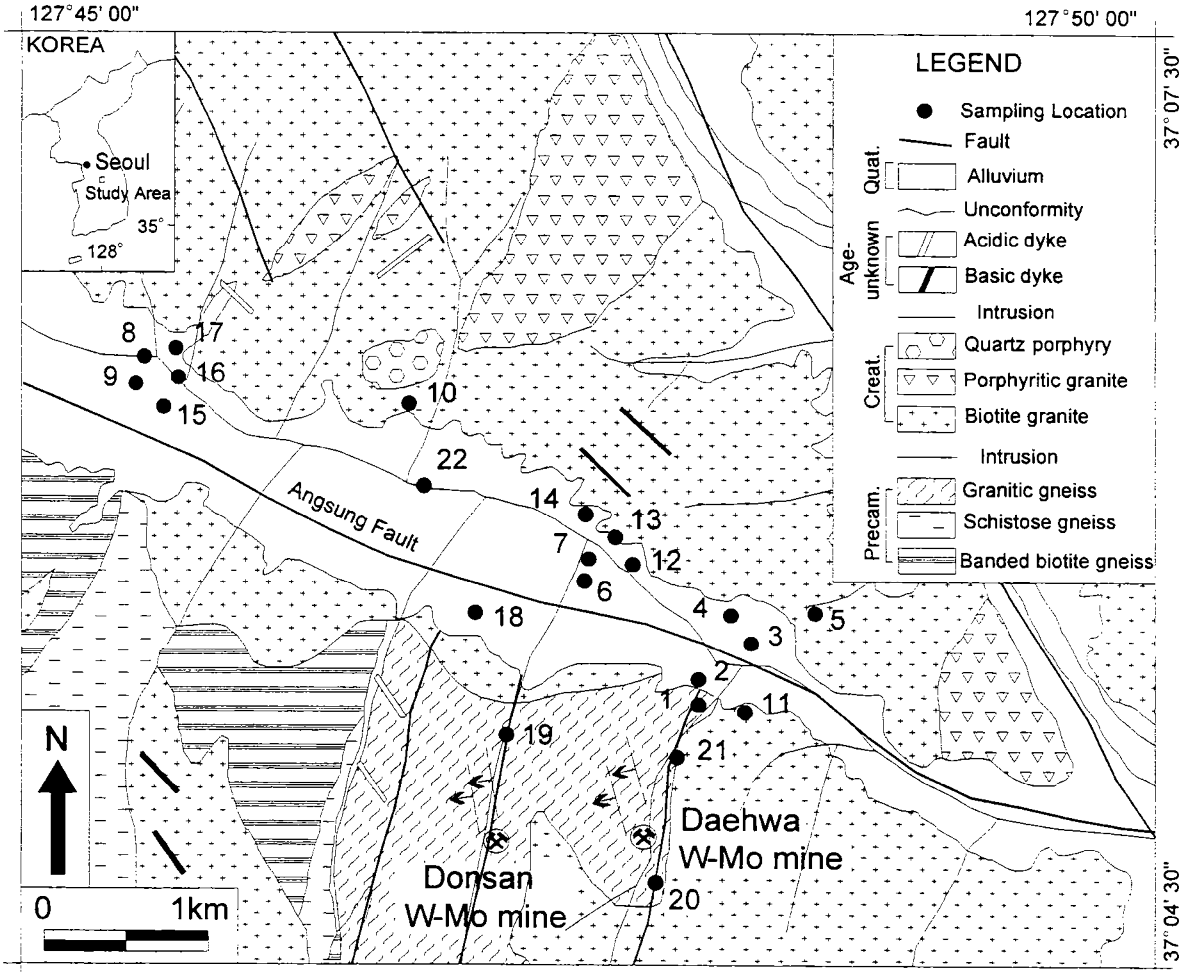

FIG. 1. Geologic map and cross section of the Jungwon area. Sampling locations and fault system are also shown.

Geologic structures of the Jungwon area, largely on NE- and NW-trending faults and associated fractures (Fig. 1), control not only the surface drainage system but also possibly the groundwater flow pattern [4]. The CO2-rich groundwater wells in the Jungwon area are commonly found near the deep groundwater wells of the Jungwon area located at crossing points of NW-trending faults (including the Angsung Fault) with NE-trending faults (Fig. 1).

3. SAMPLING AND ANALYTICAL PROCEDURE

Sampling of various kinds of natural waters (CO_2-rich groundwater, deep groundwater, shallow groundwater and surface water) from total 22 locations (Fig. 1) was carried out between May 1997 and 1998 May (Table 1). Field measurements including pH, Eh, temperature, electrical conductivity and alkalinity were carried out. All samples were filtered and samples for cation analysis were acidified to pH=2 by HNO_3.

Major dissolved ionic constituents in waters were analyzed at the Korea Basic Science Institute (KBSI) by using the inductively coupled plasma mass spectrometry (ICP-MS; Fisons-PlasmaTrace) for cations, and at the Korea Atomic Energy Research Institute (KAERI) by using the ion chromatography (Dionex 500) for anions. The $\delta^{18}O$ and δD values of waters were determined using stable isotope ratio mass spectrometry (VG SIRA II and Micromass OPTIMA) at KAERI by equilibration with CO_2 and reduction of water with zinc, respectively. Gas samples were collected from three CO_2 exsolving wells and the bicarbonates were precipitated in the field using amomonical $BaCl_2$ solution for analysis of $\delta^{13}C$. The $\delta^{34}S$ values of dissolved SO_4 in waters were measured at the Institute of Mineral Deposits of China at Beijing by Finnigan MAT 230C. The tritium contents of waters measured at KAERI by a liquid scintillation counter (Packard 2770TR/SL) after the electrolytic enrichment process. Strontium isotopic ratios were measured at KBSI by TIMS (VG Sector 54-30). Both P_{CO_2} and the mineral saturation indices were calculate using the SOLVEQ computer program [7].

4. WATER CHEMISTRY

The groundwaters of the Jungwon area can be divided into three main groups: the CO_2-rich thermal groundwater, the alkali groundwater and low P_{CO_2} shallow groundwater. Some representative chemical compositions of water samples from the Jungwon area are summarized in Table 1. The well head temperature of the CO_2-rich water is about 35°C and that of the alkali water is about 25°C with drilling depths in the range of 200 to 600 m. pH of the CO_2-rich groundwater and the alkali groundwater ranges from 6.0 to 6.4 and 9.1 to 9.4, respectively. The CO_2-rich waters show higher degrees of mineralization (TDS = 1,208-3,306 mg/L) than the alkali groundwater (TDS = 168-254 mg/L), although these waters were pumped out from similar depths and occur in immediate proximity to each other. These indicate that each water type has undergone a different geochemical evolution along the flow paths during the circulation.

Two water types show an unique pattern on a Piper diagram: Ca(-Na)-HCO_3 type for the CO_2-rich groundwater and Na-HCO_3 type for the alkali groundwater (Fig. 2). Ca, Na and HCO3 concentrations in the CO_2-rich water are dominant. Mg, K, Cl, SO_4, Fe and Sr concentrations in the water are also more enriched than those in alkali water, though Cl and SO_4 concentrations are low (Table 1). High CO_2 gas concentrations, probably a deep seated source, of waters in the granite accelerate the water rock interaction. The Ca and Na in natural waters are commonly derived by dissolution of plagioclase. The plagioclase composition in granites of the Jungwon area ranges from Ab_{80-60}. However, the Ca/Na ratio in the CO_2-rich water is high (up to 464 mg/L, Ca and up to 300 mg/L, Na). Moreover, the mineralized water is saturated or supersaturated with calcite and dolomite (Fig. 3) and Ca is generally preferentially adsorbed to the solid. Dissolution of calcite may also contribute to Ca enrichment in the waters. The CO_2-rich groundwater wells are located within 1km

TABLE I. THE REPRESENTATIVE GEOCHEMICAL DATA OF WATER SAMPLES FROM THE JUNGWON AREA, KOREA

Sample no.	Drilling depth(m)	Temp. (^{o}C)	pH	Eh (mV)	TDS (mg/L)	Na^{2+} (mg/L)	K^+ (mg/L)	Mg^{2+} (mg/L)	Ca^{2+} (mg/L)	SiO_2 (mg/L)	Cl^- (mg/L)	SO_4^{2-} (mg/L)	HCO_3[a] (mg/L)	F^- (mg/L)	Sr (μg/L)	Fe (μg/L)	Al (μg/L)	$LogP_{CO2}$[a] (atm)
CO_2-rich waters																		
J1	558	34.8	6.3	34	3,306	300.0	18.0	44.0	464.0	102.7	22.5	25.1	2,327	2.2	2,770	23,410	313	0.02
J3	600	30.6	6.4	35	2,721	245.0	11.3	39.5	363.0	96.9	20.1	17.7	1,895	4.0	2,395	18,530	122	-0.03
J4	550	25.0	6.1	58	2,008	120.0	2.9	44.0	307.0	90.0	11.9	6.0	1,423	3.1	2,210	4,660	506	0.00
J5	500	26.2	6.0	85	1,859	111.0	2.0	49.0	246.0	69.1	8.4	6.4	1,355	2.2	2,213	6,180	222	0.09
J6	200	25.5	6.1	55	1,208	84.0	2.4	21.0	176.0	94.1	12.2	8.8	805	3.4	1,456	5,530	190	-0.24
Alkali groundwaters																		
J8	400	24.8	9.2	-135	239	68.2	1.2	0.1	2.1	16.3	5.8	4.7	126	14.1	22	8	79	-4.42
J9	400	24.9	9.5	-128	254	68.4	0.3	0.1	1.9	17.2	6.0	6.4	141	12.4	18	9	16	-4.56
J10	200	24.7	9.1	-136	168	31.0	0.5	0.2	7.4	19.4	1.9	7.2	93	6.6	10	13	24	-4.23
Shallow groundwaters																		
J11	60	23.6	7.6	130	301	48.0	1.8	3.6	23.5	27.6	22.3	11.3	161	2.2	202	8	1	-2.40
J13	60	17.4	6.8	180	310	30.0	1.2	2.9	46.0	25.7	9.2	16.0	175	0.6	165	12	7	-1.60
J16	60	16.1	7.0	142	176	14.9	1.6	2.4	21.4	18.0	6.2	12.5	93	1.0	182	8	7	-2.07
J18	35	19.0	7.7	134	152	9.1	0.9	3.5	18.2	28.5	4.0	16.9	59	0.5	128	9	1	-2.95
J19	5	23.7	6.9	185	78	5.4	0.5	1.0	7.9	22.3	1.3	3.5	28	0.7	49	4	9	-2.44
Surface waters																		
J20	-	21.1	7.1	183	144	5.8	2.4	2.8	25.2	12.0	2.7	47.2	38	1.2	141	68	54	-2.56
J22	-	5.5	6.5	140	131	10.3	2.3	3.0	18.9	3.7	7.6	10.8	65	0.2	111	13	4	-1.77

[a] Calculated from in-situ alkalinity and pH using SOLVEQ [7]

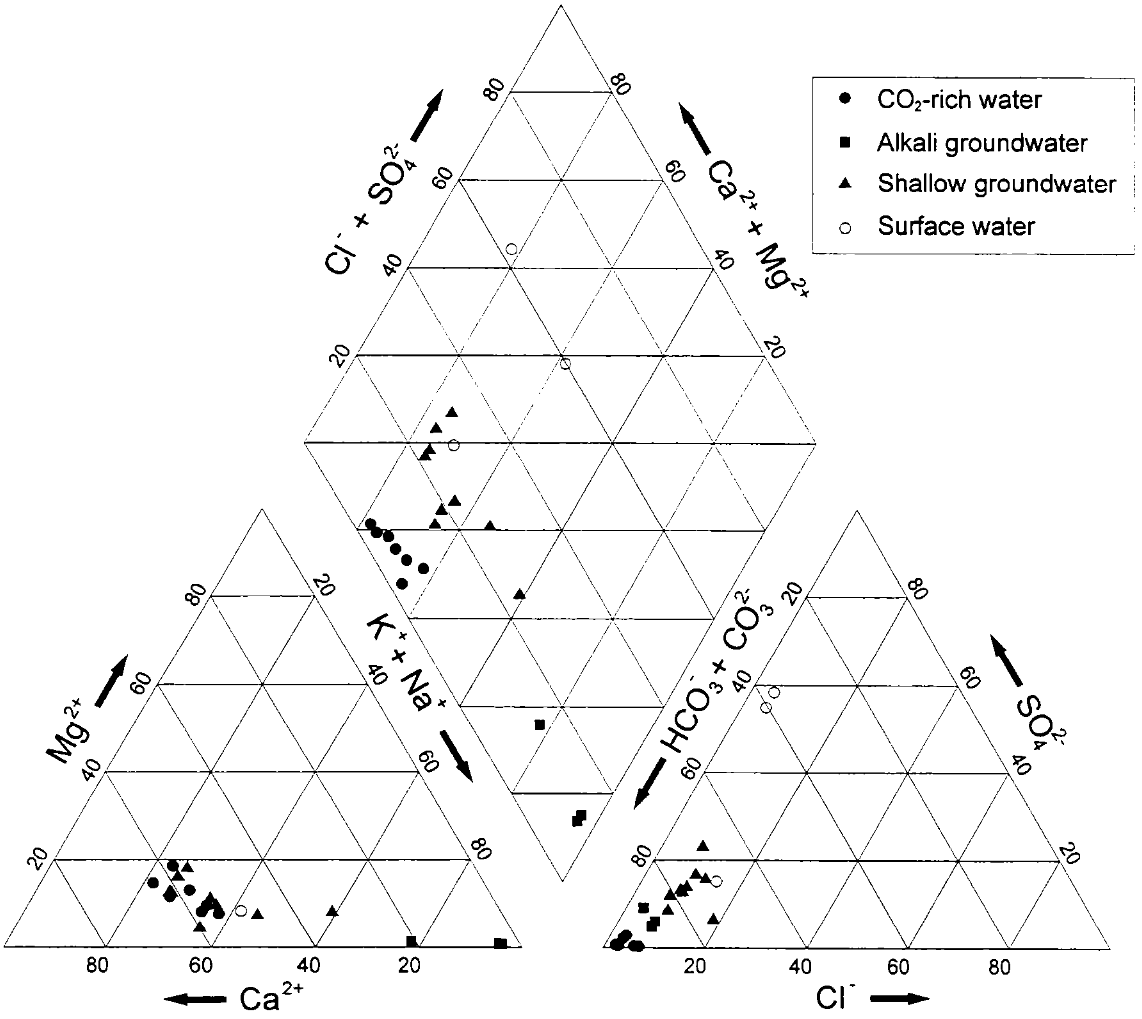

FIG 2. Piper's diagram showing chemical compositions of various kinds of waters from the Jungwon area.

from the Daehwa and the Donsan W-Mo mines, of which gangue minerals are mainly calcite and dolomite. Dissolution of the vein calcite seems to explain the high Ca/Na ratio in the CO_2-rich water. However, the isotope composition of strontium of the waters and the calcite shows that the vein calcite does not contribute to Ca content in the mineralized water (see below). Therefore, the Ca enrichment is likely to be controlled by other mechanism. Stober and Bucher [8] suggested that the temperature effect on plagioclase solubility could explain the high Ca/Na ratio of the waters. Dissolution of K-feldspars and biotites contributes K, Mg, Fe to the solutes of the waters. Additional Fe can be also released by sulfide oxidation, accompanying releases of SO_4 and proton. Iron is high (up to 18 mg/L) and SO_4 low (up to 25 mg/L) in the CO_2-rich water. Sulfate in the waters may be consumed by sulfate reduction in depth. Cl, higher in CO_2-rich water, can be contributed by hydrolysis of biotite and leaching of fluid inclusion [9, 10].

The alkali type groundwater from the Jungwon area is characterized by Na-HCO_3 dominated with high pH. The geochemical properties of the alkali water indicates that the groundwater (P_{CO_2} = $10^{-4.6}$ atm) is evolved by water-granite interaction without supply of CO_2. The alkali type groundwater characteristically contains high amount of F (7.7 to 14 mg/L). We consider that the observed high F contents possibly resulted from dissolution of biotite and apatite which contain F and Cl at OH sites [10]. According to Tsusue et al. [11], apatite and biotite from Korean Cretaceous granites typically contain appreciable amounts of F and Cl. On the other hand, fluorine (3 to 4 mg/L) in the mineralized water is lower than the alkali water (up to 14 mg/L). It can be explained by

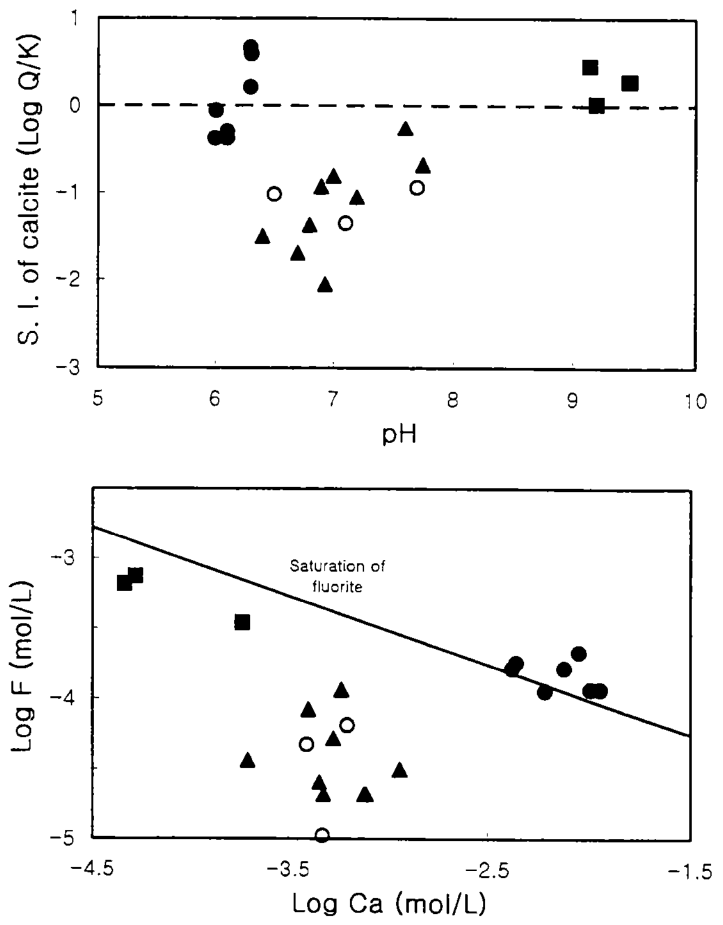

FIG. 3. Saturation index of calcite versus pH and the stability of fluorite of all kinds of waters in the Jungwon area. Symbols are same as in FIG. 2.

buffering of fluorite. The relationship between Ca and F concentrations in the waters shows that the CO_2-rich water is almost saturated with respect to fluorite (Fig. 3). Strontium concentration is likely controlled by precipitation of strontianite, which is also saturated or supersaturated in both of the mineral water and the alkali groundwater.

5. ISOTOPE

5. 1. Oxygen-18, deuterium and tritium

The $\delta^{18}O$ and δD values of all kinds of waters from the Jungwon area range from -10.5 to -7.8 ‰ and -72.3 to -54.9 ‰, respectively (Table 2). Within these wide ranges each type water has unique isotope values forming distinct clusters in a $\delta^{18}O$ versus δD diagram (Fig. 4). The values for the CO_2-rich groundwater are $\delta^{18}O$ = -10.5 to -9.4 ‰ and δD = -72.3 to -66.7 ‰; those for the alkali type groundwater, $\delta^{18}O$ = -9.7 and -9.6 ‰, and δD = -69.9 and -67.9 ‰; for shallow cold groundwater, $\delta^{18}O$ = -9.1 to -7.9 ‰ and δD = -63.5 to -54.9 ‰ and for surface water, $\delta^{18}O$ = -9.5 to -7.8 ‰ and δD = -67.9 to -56.0 ‰. The $\delta^{18}O$ versus δD diagram (Fig. 4) indicates that all waters from the Jungwon area were derived from local meteoric waters. $\delta^{18}O$ and δD values show that the CO_2-rich water and the alkali groundwater are lighter than shallow groundwater and surface water. These light groundwaters supposedly indicate that the groundwaters are recharged from the different elevation from the Jungwon area. It is noteworthy that the CO_2-rich waters are plotted toward more negative ^{18}O values with respect to the local meteoric water line, which inferred from the values for the low

TABLE II. ISOTOPIC COMPOSITIONS OF WATER SAMPLES FROM THE JUNGWON AREA, KOREA.

Sample no.	$\delta^{18}O$ (‰)	δD (‰)	Tritium (T.U.)	$\delta^{13}C$ (‰)	$\delta^{34}S_{SO4}$ (‰)	$^{87}Sr/^{86}Sr$
J1	-10.4	-72.3	0.0	+0.3		
J2	-10.4	-70.9	0.8	-2.0	+27.6	
J3	-10.5	-72.0	0.1	-3.1		0.7195
J4	-9.8	-69.0	0.5	-4.7		0.7169
J5	-9.9	-70.5	0.3	-4.9	+24.1	0.7175
J6	-9.4	-66.7	3.1	-5.9		
J7	-9.7	-68.8	2.9	-6.6	+24.2	
J8	-9.6	-68.8	1.0	-9.5		
J9	-9.7	-67.9	1.4	-9.8	+7.5	0.7230
J10	-9.6	-69.9	0.5	-13.1		0.7244
J11	-8.2	-58.0	2.6	-18.4	+3.7	
J12	-8.0	-55.7	6.5		+6.6	
J13	-8.0	-58.7	6.8	-15.5	+7.6	0.7178
J14	-7.9	-54.9				
J15	-8.6	-60.7	9.2			
J16	-8.1	-57.2	7.2	-14.1	+3.6	0.7179
J17	-8.0	-55.9	9.0		+4.8	
J18	-8.9	-62.4	8.4	-15.1		
J19	-9.1	-63.5	8.9			0.7182
J20	-8.9	-62.9	6.8			
J21	-9.5		7.3			
J22	-7.8	-56.0	7.0	-18.5	+8.0	0.7203

P_{CO_2} waters of the Jungwon area (Fig. 4). This shift is explained as a consequence of isotope re-equilibrium with CO_2. The original $\delta^{18}O$ value of the corresponding water before isotope re-equilibration is likely to be about -10 ‰. Considering the altitude effect (0.19 ‰/100m for $\delta^{18}O$) of isotope in Korea [12], the recharge area of the CO_2-rich water is estimated to relatively 500-1,000m higher in elevation than the Jungwon area.

Tritium contents close to zero are observed in the CO_2-rich water and alkali groundwater (Table 2), confirming a long resident time and also the possibility of a CO_2 inflow into the aquifer at great depth. On the other hand, high tritium values are common in the shallow groundwater (J11 to J19) indicating relatively recent waters with very short residence time. Tritium contents of the less CO_2-rich water (J6, J7) range from 2.9 to 3.1 TU, indicating that mixing process between the CO_2-rich water and local younger groundwater occurs. It is well correspond to the values of oxygen-18 and deuterium.

5. 2. Carbon isotope

The carbon isotope result shows distinct different values according to the water types. The $\delta^{13}C_{HCO3}$ values of the CO_2-rich water, alkali groundwater, shallow groundwater and surface are -6.6 to +0.3 ‰, -13.1 to -9.5 ‰, -14.1 to -18.4 ‰ and -18.5 ‰, respectively (Table 2). The $\delta^{13}C_{CO2}$ of the CO_2-rich water sampled from three wells range from -7.6 to -4.5 ‰. The possible sources of

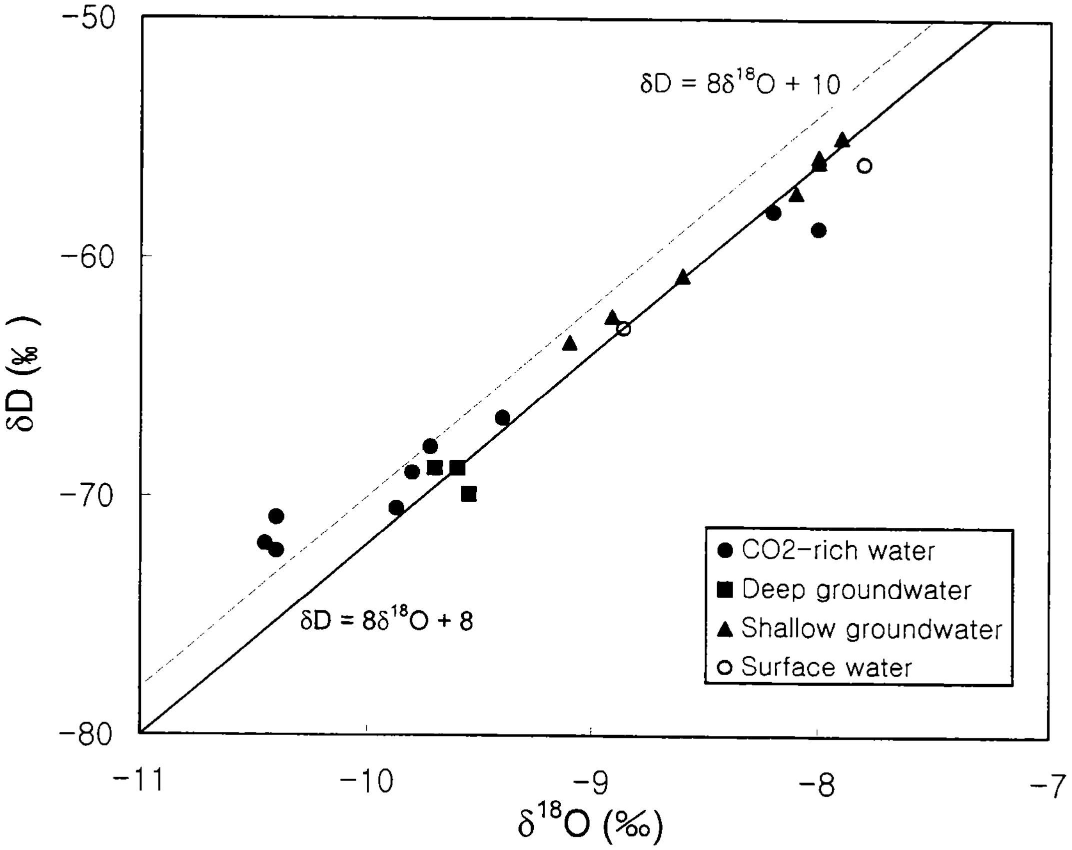

FIG.4. $\delta^{18}O$ versus δD diagram of various kinds of waters from the Jungwon area.

carbon in the CO_2-rich water with relatively positive $\delta^{13}C$ may be the dissolution of carbonate rock and deep seated CO_2 gas. The calcites in hydrothermal vein from the W-Mo mines have $\delta^{13}C_{PDB}$ values of -7.6 to -1.6 ‰ [2]. It is unlikely that the carbonate-water interaction contributes carbon to the CO_2-rich water. The relationship between $\delta^{18}O$ and δD of the CO_2-rich water indicates the re-equilibrium with CO_2 gas rather than the reaction with vein calcite. Additionally, the elevated P_{CO_2} (about 1 atm) requires an additional source of H^+ or CO_2. The oxidation of sulfide from W-Mo mines could yield H^+, but the result of strontium isotope is not consistent with the dissolution of calcite. The carbon isotope of alkali groundwater and shallow groundwater shows relatively negative values. The $\delta^{13}C$ values of CO_2 generated by microorganisms generally range from -30 to -20 ‰ [13]. Therefore, we consider the contribution of carbon from either the microbial oxidation of organic matter or carbon dioxide from plant respiration.

5. 3. Sulfur isotope of sulfate

The $\delta^{34}S$ values of dissolved sulfate of all waters range widely from +3.6 to +27.6 ‰ (Table 2). Each type water, however, has an unique and uniform value: +24.1 to +27.6 ‰ for the CO_2-rich groundwater, +7.5 ‰ for the alkali groundwater, +3.6 to +7.6 ‰ for the shallow groundwater, and +8.0 ‰ for surface water. It is interesting that the CO_2-rich groundwater are much higher $\delta^{34}S$ values (by > 16 ‰) than those of other water types. This probably reflects different source(s) of sulfur in waters and different isotopic fractionation mechanism for sulfur/sulfate in subsurface. The $\delta^{34}S$ enrichment (up to +28‰) of the CO_2-rich water strongly indicates the sulfate reduction by organic activity at depth [14]. The CO_2-rich groundwater was found to contain considerably total organic carbon (TOC, 13.6 to 21.8 mg/L) than fresh groundwater (TOC, 1.1 to 1.3 mg/L).

Nevertheless, the hydrogen sulfide could not be detected from water samples. Additionally, the Eh values from *in-situ* measurement show that the CO_2-rich water is oxidized, compared to the alkali groundwater. Sulfide weathering and oxidation of sulfate are the major source of SO_4 in the crystalline granite waters. The dissolved sulfates of the alkali groundwater and shallow groundwater may be originated from the sulfides. However, we cannot rule out the contribution of anthropogenically derived sulfur from higher $\delta^{34}S$ values of shallow groundwater.

5. 4. Strontium isotope

To identify the sources of dissolved Ca in the CO_2-rich water, Sr isotopic ratios of the representative waters and geologic materials were measured in the Jungwon area. The Sr concentrations of the waters are in the range of 0.02 to 2.8 mg/l and the water exhibits a large range in $^{87}Sr/^{86}Sr$ ratios (0.7169-0.7244), according to water types: 0.7170 to 0.7195 for the CO_2-rich waters, 0.7230 to 0.7244 for the alkali waters, 0.7178 to 0.7182 for shallow groundwaters, and 0.7203 for surface waters (Tables 1 and 2). The $^{87}Sr/^{86}Sr$ ratios of vein calcite, granite and gneiss are 0.7210 to 0.7238, 0.7189 to 0.7190 and 0.7122, respectively. Although we could not obtain the strontium isotopic composition of each mineral, specially plagioclase, from granite in the Jungwon area, the values indicate that the source of Ca in the CO_2-rich water is not related to vein calcite of the W-Mo mines in the Jungwon area. This supports that plagioclase weathering is the dominant source of Ca in the CO_2-rich waters in the Jungwon area, because plagioclase is the most common Ca-bearing mineral in the granite area. In the other hand, $^{87}Sr/^{86}Sr$ ratios of the alkali water are more radiogenic than those of the granite and the CO_2-rich water. This can be confirmed by the further study for strontium isotopic composition of the each mineral of the granite in the Jungwon area.

5. SUMMARY AND DISCUSSION

The hydrogeology of the Jungwon area is characterized by the presence of different water types: the CO_2-rich water and the alkali groundwater. The CO_2-rich water is represented by thermal mineralized water with low pH, high Ca, Na, HCO_3, low Cl and SO_4, and dissolved CO_2. Their composition results from water-rock reaction in the presence of externally derived CO_2 gas. The decreasing pH by adding the CO_2 gas increases the rates of silicate weathering and here predominantly plagioclase. Biotite and K-feldspar reaction contributes Mg, Fe and K. If the groundwater was encountered with sulfides in the oxidized condition along the flow path, the groundwater becomes very acidic with high Fe and SO_4 contents. This water can produce a large amount of CO_2 gas if reacting with calcite. These reaction seems to form the CO_2-rich water in the Jungwon area located on the proximity from the sulfides-carbonate-bearing W-Mo deposits. However, the relationship between $\delta^{18}O$ and δD values and tritium contents of waters indicate the isotope re-equilibrium with CO_2 gas at depth and strontium isotope result shows that the CO_2-rich water is not evolved with reaction with the vein calcite. Therefore, the CO_2-rich groundwater in the Jungwon area is likely to be originated from the external CO_2 gas. Carbon isotope composition of the CO_2-rich water shows a range associated mantle derived CO_2. However, further study is necessary to identify CO_2 source. Higher $\delta^{34}S$ value of dissolved sulfate showing sulfate reduction argues against higher Fe content and Eh values and no existence of hydrogen sulfide. The geochemistry of the alkali groundwater shows the simple Na-HCO_3 type with high pH and the waters characteristically contain high amount of F. These water seems to be resulted from weathering of silicate minerals in the granite without additional supply of CO_2.

ACKNOWLEDGEMENTS

This project has been carried out under the Nuclear R & D Program of Ministry of Science Technology.

REFERENCES

[1] Park, H. I., CHOI, S. W., "A study on the fluid inclusions in the minerals from the Dae Hwa tungsten-molybdenum deposits", Korean Inst. Mining Geology Jour., 7 (1974) 63B78.

[2] SO, C. S. et al., "The Dae Hwa tungsten-molybdenum miner, Republic of Korea: A geochemical study", Econ. Geol., **78** (1983) 920B930.

[3] SHELTON, K. L., et al., "Stable isotope studies of the Dae Hwa tungsten-molybdenum mine, Republic of Korea: Evidence of progressive meteoric water interaction in a Tungsten-bearing hydrothermal system", Econ. Geol. **82** (1987) 471B481.

[4] YUM, B. W., Environmental hydrogeochemistry of the thermal waters in granites of the Pocheon, Gosung, Yesan and Jungwon area, PhD Thesis, Seoul Nat'l Univ., Korea (1993).

[5] YUN, S. T. et al., "Geochemistry of geothermal waters in Korea: environmental isotope and hydrothermal characteristics II. Jungwon and Munkyeong areas", Econ. Environ. Geol. (Korea), **31** (1998) 201B213.

[6] KIM, D. R., A study on genesis of the Daewha tungsten-molybdenum deposits, MS Thesis, Seoul Nat'l Univ., Korea (1985).

[7] REED, M. H., "Calculation of multicomponent chemical equilibria and reaction processes in systems involving minerals, gases and an aqueous phase", Geochim. Cosmochim. Acta, **46** (1982) 512B528.

[8] STOBER, I., BUCHER, K., "Deep groundwater in the crystalline basement of the Black Forest region", Applied Geochemistry, **14** (1999) 237B254.

[9] EDMUND, W. M. et al., "Origin of saline groundwaters in the Carnmenellis granite (Cornwall, England): natural processes and reaction during hot dry rock reservoir circulation", Chem. Geol., **49** (1991) 287B301.

[10] NORDSTROM, et al., "Hydrogeological and hydrogeochemical investigations in boreholes-Final report of the phase I geochemical investigations of the Stripa groundwaters", Tech. Rep. 85-06, Stockholm, Finland (1985).

[11] TSUSUE, A., et al., "Jurassic and Cretaceous granitic rocks in South Korea", Mining Geol.(Japan), **31** (1981) 261B280.

[12] KIM, K. H., NAKAI, N., "Isotopic compositions of precipitations and groundwaters in South Korea", Jour. Geol. Soc. Korea, **24** (1988) 37B46.

[13] Fritz, P., Fontes, J. C. (Ed.), Handbook of Environmental Isotope Geochemistry, V. 1, Elsevier, Amsterdam (1980) 545pp.

[14] KAPLAN, I. R. "Stable isotope in sedimentary geology", SEPM Short Course No 10. (1983) 1B108.

MONITORING THE MOVEMENT OF THE COOLER FLUIDS IN THE DEEP GEOTHERMAL RESERVOIRS OF GREATER TONGONAN GEOTHERMAL FIELD, PHILIPPINES

J.S. SEASTRES, Jr., N.D. SALONGA., F.L. SIEGA
PNOC-Energy Development Corporation
Fort Bonifacio, Makati, Philippines

Abstract

Two types of cooler fluids are present in the Greater Tongonan geothermal field, namely the reinjected waste brine in the Tongonan reservoir and the shallow groundwater in the Mahanagdong reservoir. The influx of reinjection fluids in the production area of Tongonan became apparent in 1990 after seven years of commercial operations of the first power plant. The wells that previously delivered highly two-phase fluids started to become liquid-saturated. As a consequence, the fluid temperatures dropped by 10°C and the field enthalpy declined from 2200 kJ/kg to 1600 kJ/kg. The new distribution of stable isotopes shows isotopic enrichment in the western part of the field [+1.00 $^{o}/_{oo}\delta^{18}O$] where waste brine injection takes place. In Mahanagdong, the field started to generate 180 MW of power in July 1997 that brought about changes to the physical and chemical characteristics of the reservoir. After about one year of commercial operation, the production sector closest to the western part of the field sustained decline in fluid temperature and salinity ultimately leading to decline in bore output. The present stable isotope distribution across the field illustrates invasion of isotopically depleted fluids from the west to the production part of the field, passing through a northwest-trending structure.

1. INTRODUCTION

The Greater Tongonan Geothermal Field (GTGF) covering an area of 40 km^2 is located in the island of Leyte, Philippines. The field is subdivided into Upper Mahiao, Mahiao-Sambaloran, Malitbog-South Sambaloran, Mamban and Mahanagdong sectors (Figure 1). The first power plant developed in GTGF is Tongonan-I which is located in the Mahiao-Sambaloran sector. It has been on commercial operation since June 1983 with a maximum rated capacity of 112.5 MW. The Malitbog-South Sambaloran sector supplies steam to the 3 x 77 MW power plant. In July 1996, the first 77 MW unit of the Malitbog-South Sambaloran power plant was commissioned together with the 125 MW Upper Mahiao power plant to provide energy to the Leyte-Cebu island grid. The remaining 2 x 77 MW units of Malitbog-South Sambaloran, 120 MW Mahanagdong-A and 60 MW Mahanagdong-B power plants were subsequently commissioned in July 1997 to supply steam to Leyte-Luzon island grid.

The exploitation of the Mahiao-Sambaloran sector starting in 1983 has induced reservoir changes that initially resulted to field pressure drawdown. However, in-field brine injection strategy eventually caused the massive breakthrough of cooler reinjection fluids in the production sector. To further distinguish the fluid chemistry trends of phenomenon caused by pressure drawdown from reinjection fluid returns, stable isotopic composition of the production wells was evaluated. Both reservoir processes manifest basically similar chemical trends such as increase in chloride mineralization and decline in Cl/Ca molecular ratio (Harper and Jordan, 1985; Seastres et al., 1995). Stable isotopes have been proven as a powerful tool in characterizing the signature of reinjection fluids in the reservoir (Nuti et al., 1981; D'Amore et al., 1987, 1988; Gerardo et al., 1993). In the Mahiao-Sambaloran sector, the application of stable isotope data demonstrated the magnitude of reinjection fluid breakthrough which prompted revision in reinjection strategy to sustain steam supply to the power plant.

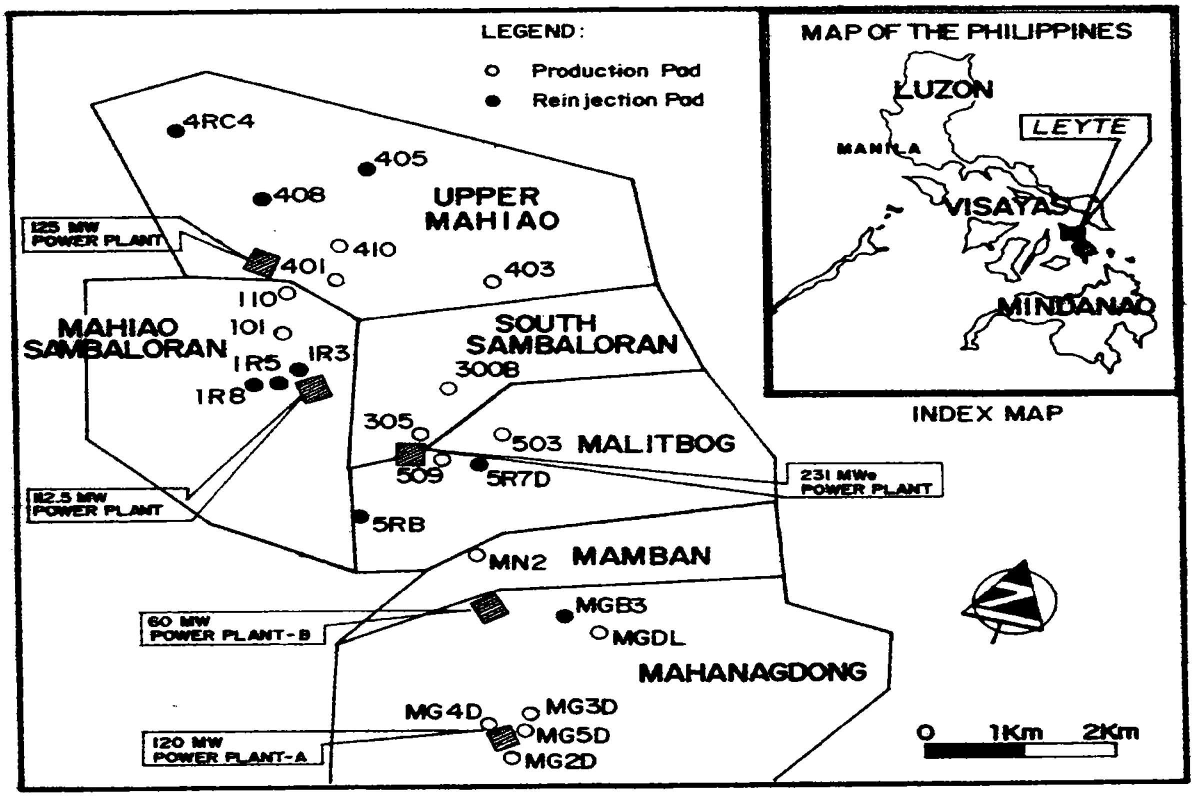

FIG. 1. Map of the Greater Tongonan geothermal field indicating the sectoral boundaries of the field, location of the power plants and selected production/reinjection pads.

Cold meteoric fluid inflows were identified as a potential field management problem prior to the exploitation of Mahanagdong sector (Salonga et al., 1996; Seastres et al., 1996). Massive fluid withdrawal of Mahanagdong can induce migration of meteoric fluids which will eventually cause bore output decline. Stable isotope data of several production wells were correlated with fluid chemistry data to monitor the inflow of these fluids during steam exploitation in this sector.

2. BASELINE HYDROLOGY OF GREATER TONGONAN

Based on the fluid chemistry data, the Greater Tongonan geothermal field can be separated into two distinct reservoirs comprising of Tongonan and Mahanagdong (Alvis-Isidro et al., 1993). The Tongonan reservoir covers the Upper Mahiao, Mahiao-Sambaloran and Malitbog-South Sambaloran sectors while the Mahanagdong reservoir is primarily found within the Mahanagdong sector. The upflow zones are located within well 410 (Figure 2) in the Tongonan reservoir and within well MG3D (Figure 3) in the Mahanagdong reservoir. These zones are separated by an impermeable block, the Mamban plateau, which is characterized by relatively low reservoir temperature (<200°C).

The deep reservoir fluids of Tongonan have temperatures of 260-300°C, salinity of 0.17-0.22m Cl and gas content of 0.5-0.8% by weight. The stable isotope contour across the field (Figure 2) indicates an isotopically enriched ($-0.30\,^{o}/_{oo}\delta^{18}O$) upflow which becomes isotopically depleted as the reservoir fluids outflow towards the Malitbog-South Sambaloran sector. The upflowing center of the reservoir hosts a natural, shallow two-phase zone causing the high enthalpy discharges of the production wells.

In Mahanagdong, the deep reservoir fluids upwelling within the vicinity of well MG3D is isotopically enriched ($-1.0\,^{o}/_{oo}\delta^{18}O$) with fluid temperature as high as 300°C (Figures 3 and 4). The salinity and gas contents of the fluid ranged from 0.07-0.20m Cl and from 1.0% to 3.0% by weight respectively. At the western part of Mahanagdong, a sharp indentation of isotopically depleted $\delta^{18}O$

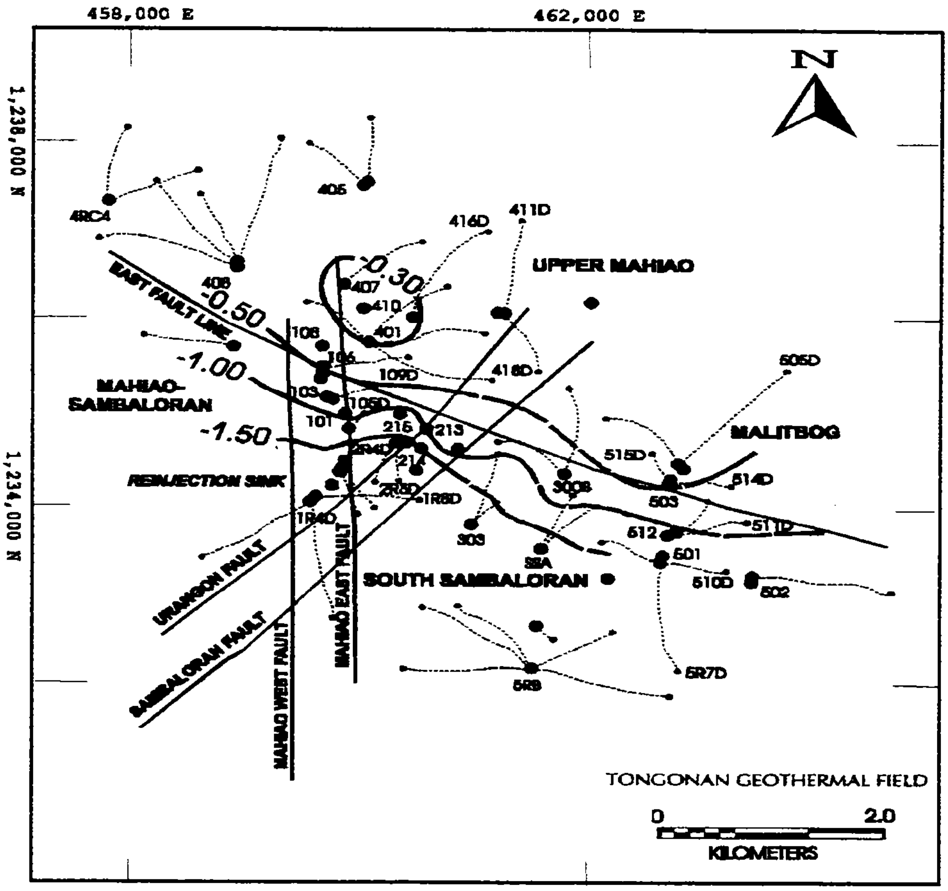

*FIG. 2. The baseline iso-$\delta^{18}O_{res}$ contour map across the Tongonan geothermal field and the selected major fault structures. The term **res** or **reservoir** whenever it appears in this paper as subscript of a chemical element indicates that its concentration was calculated based on reservoir temperature as estimated from silica (quartz) geothermometer of Fournier and Potter (1982).*

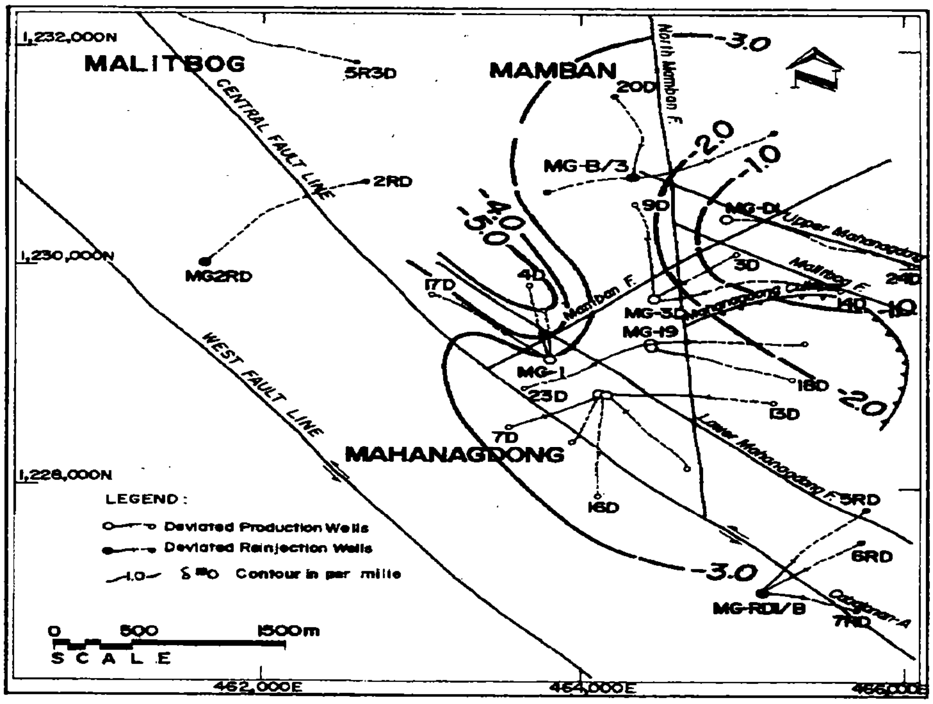

FIG. 3. The baseline iso-$\delta^{18}O_{res}$ contour map of Mahanagdong geothermal field and the selected major fault structures.

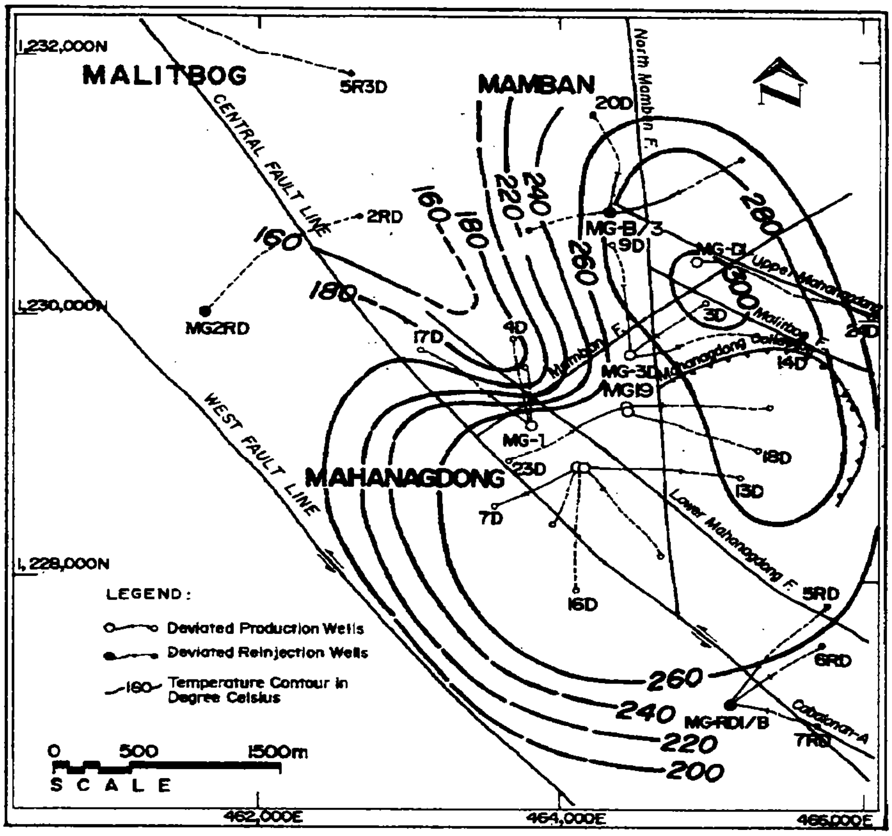

FIG.4. The field temperature contour map based on downhole measurements of Mahanagdong wells at -1000m relative to sea level.

contour (-5.0 $^{o}/_{oo}\delta^{18}O$) characterized the presence of shallow groundwater in the reservoir (Salonga and Siega, 1996). This field trend is consistent with isothermal contour across Mahanagdong indicating a measured temperature as low as 160°C in the western sector.

The Tongonan and Mahanagdong reservoirs have a common meteoric water recharge ($\delta^{18}O$ = -7$^{o}/_{oo}$ and $\delta^{2}H$ = -41$^{o}/_{oo}$) despite being not hydrologically connected (Alvis-Isidro et al., 1993). The recharge is typical of surface waters characteristic of the Mamban area. Local magmatic water is believed to constitute 40% of the enriched water in Greater Tongonan.

3. REINJECTION FLUID BREAKTHROUGH IN THE TONGONAN RESERVOIR

During the operation of the Tongonan I power plant in Mahiao-Sambaloran sector from 1983 to 1989, the total mass injected corresponds generally to only <150,000 tons/yr in Mahiao and <300,000 tons/yr in Sambaloran due to the relatively low gross energy generation (≤ 450,000 MW- hr/yr) of the power plant. The response of the reservoir during this period is primarily fieldwide boiling induced by pressure drawdown as illustrated by increasing reinjection line chloride and field enthalpy trends (Figure 5).

In 1990 when the yearly gross energy generation increased to >500,000 MW-hr, the mass injected increased to >200,000 tons/yr in Mahiao and >350,000 tons/yr in Sambaloran. This scenario was further aggravated by the utilization of low enthalpy, high waterflow production wells necessitated by increase in energy load demand. The increasing injection load in the reservoir resulted to reinjection breakthrough in the production sector starting in 1990. Based on chloride mass balance calculations, the mass of reinjection fluids that affected the Mahiao-Sambaloran production

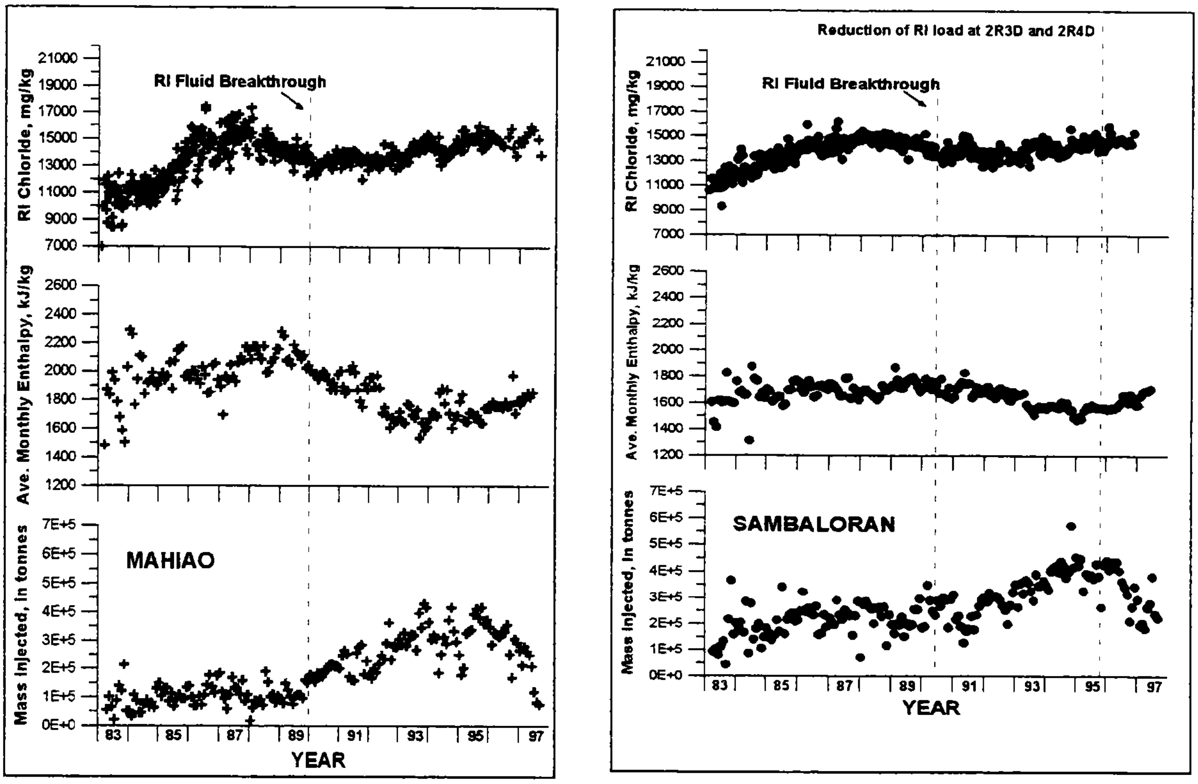

FIG. 5. The reinjection line chloride, average monthly enthalpy and the mass of brine injected in the Mahiao-Sambaloran sector since the commercial operation of the Tongonan I power plant in June 1983 (after Siega et al., 1998). RI chloride refers to the chloride concentration at the main pipeline prior to fluid injection in the reinjection wells.

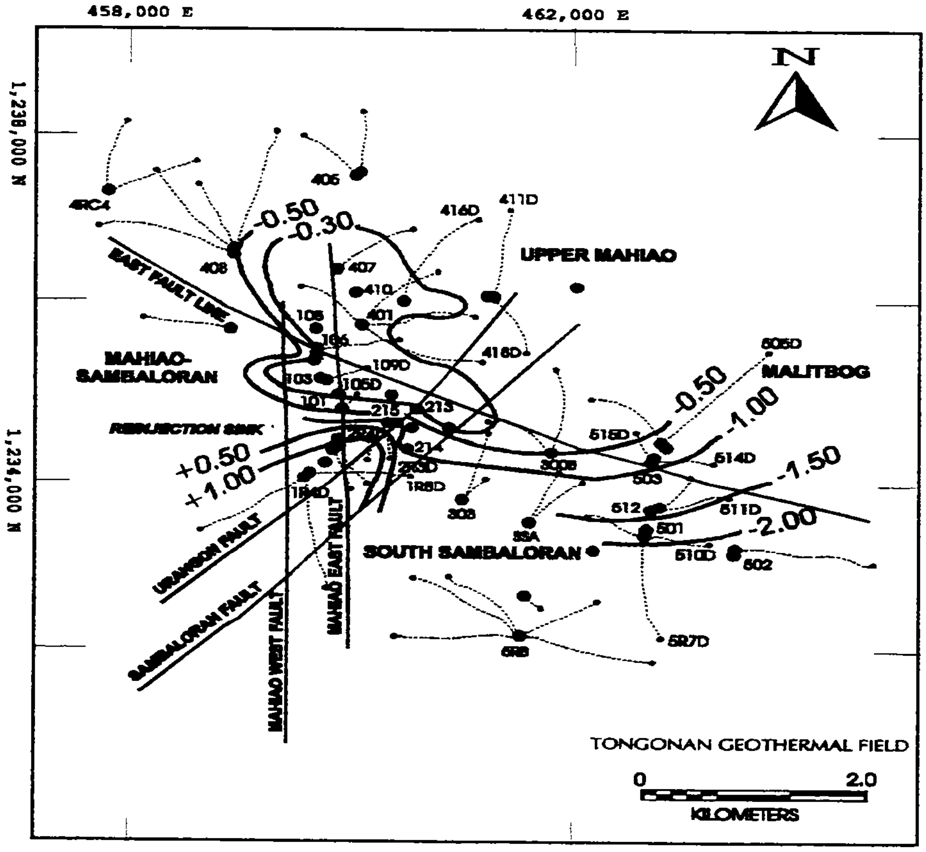

FIG. 6. The iso-$\delta^{18}O_{res}$ contour map across the Tongonan geothermal field in 1996.

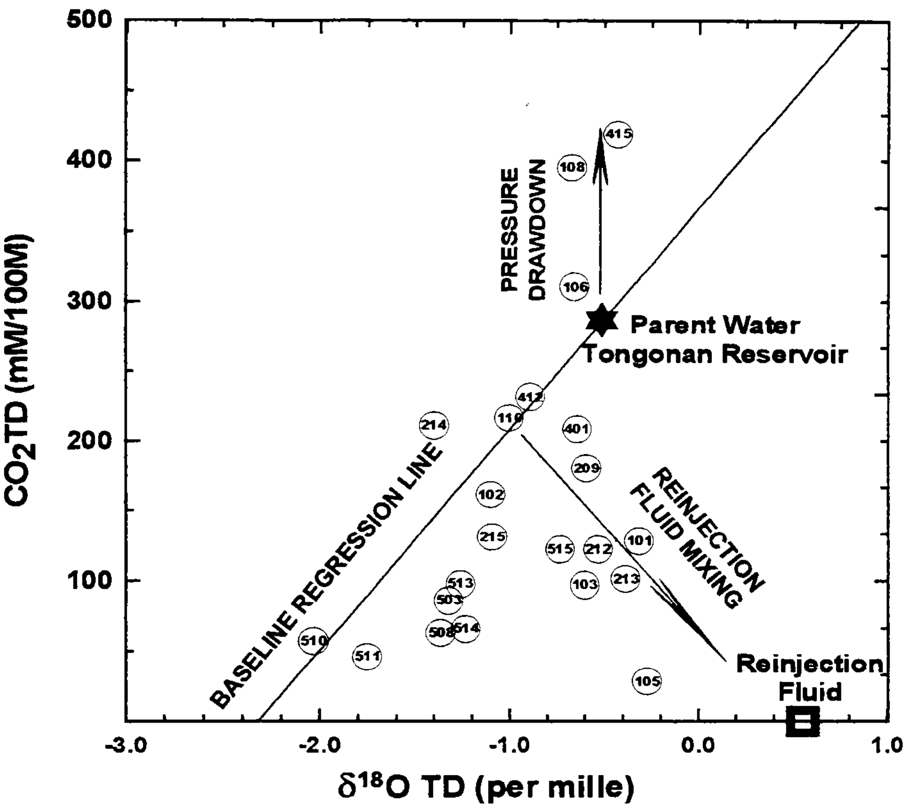

FIG. 7. The crossplot of CO_2TD and $\delta^{18}O$ TD of the Mahiao-Sambaloran, Malitbog and Upper Mahiao production wells. TD refers to the total discharge composition of a chemical component calculated based on the steam and water fractions of the well.

area ranged from 30% to 58% (Siega et al., 1998) in wells 101, 103, 105, 213, 214 and 215 which are close to the reinjection sink (Figure 6). The migration of reinjection fluids to these wells was likely channeled through the Mahiao East, Sambaloran and Urangon faults.

The encroachment of reinjection fluid returns was further evaluated through stable isotope data. The 1996 field $\delta^{18}O$ contours (Figure 6) indicate an indentation of + 1.00 $^{o}/_{oo}$ $\delta^{18}O$ at the Mahiao-Sambaloran reinjection sink (Siega and Salonga, 1997). The isotopic enrichment in this sector is attributed to fluid flashing upon brine separation at 0.70-1.20 Mpa(g) prior to reinjection. The separated brine becomes more isotopically enriched with heavier isotopes of deuterium and oxygen-18. The $\delta^{18}O$ composition indicates an enrichment from −1.50$^{o}/_{oo}$ to +1.00 $^{o}/_{oo}$ due to reinjection fluid returns in the wells closest to the reinjection sink. However, the Upper Mahiao sector, which is relatively far from the reinjection sink remains unaffected by reinjection fluid. Relative to the baseline isotopic data ($\leq$ 1983), field pressure drawdown dominated in that sector as manifested by the isotopically depleted $\delta^{18}O$ contour of −0.30 $^{o}/_{oo}$ from the upflow zone centered at 407 and 410 to the southeast towards the South Sambaloran sector (Figure 6). The expansion of the isotopically depleted vapor zone is consistent with the extension of the 9.50 Mpa(a) isobar towards southeast direction in the vicinity of well 515D.

The crossplot of CO_2TD composition with the $\delta^{18}O$ TD discriminates the different reservoir processes that occurred in response to field exploitation (Figure 7). The deviation of the Mahiao-Sambaloran production wells (105, 101, 103, 213, 212) from the baseline regression line towards the reinjection fluid composition illustrated the effect of reinjection fluid breakthrough in these wells. Their fluid composition becomes more isotopically enriched and degassed with increasing component of reinjection fluid in the total discharge.

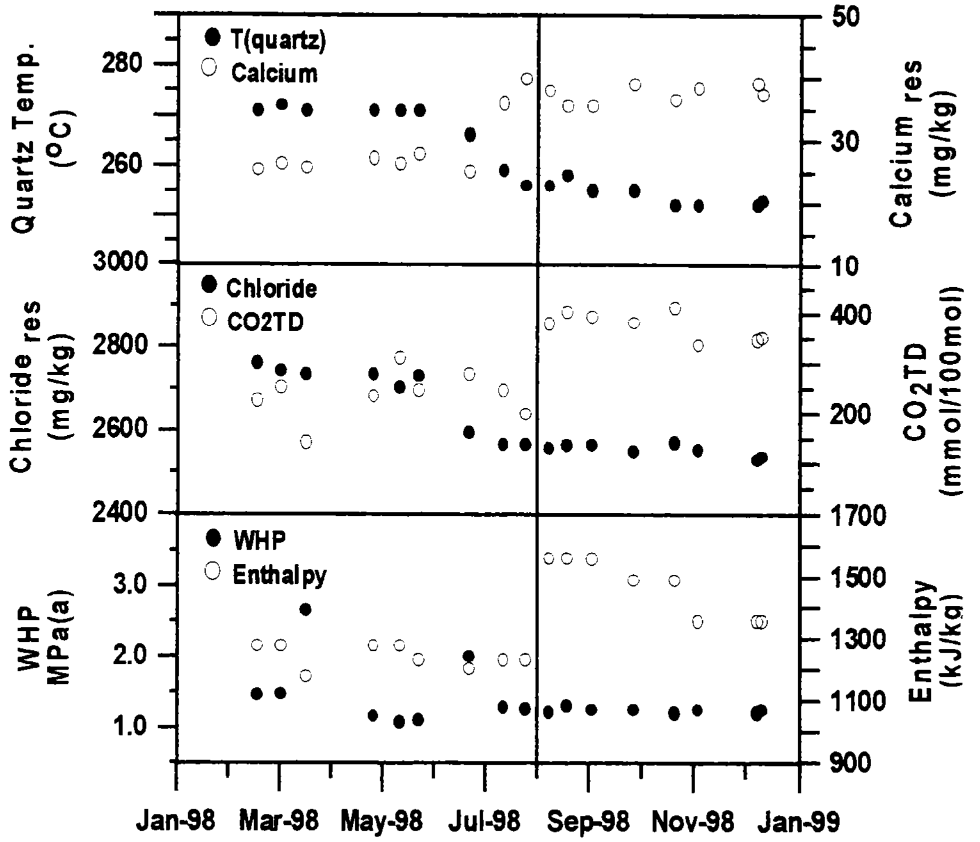

FIG. 8. The reservoir fluid chemistry trends of chloride, calcium, sulfate, silica (quartz) geothermometer and CO$_2$TD ofMG23D correlated with the Wellhead Pressure (WHP) and discharge enthalpy.

Corollary with $\delta^{18}O$ field contour, field pressure drawdown predominates within the vicinity of Upper Mahiao sector as indicated by wells 106, 108 and 415 (Figure 7). However, the $\delta^{18}O$ composition remains relatively unchange as most of these wells already discharge two-phase fluids prior to exploitation; hence, isotopic depletion in the vapor phase induced by reservoir boiling will have minor effect to their isotopic composition. The Malitbog production fluids are still unaffected by reinjection fluid returns and field pressure drawdown as their chemical composition are generally within the baseline regression line (i.e. cooling and dilution processes affect the fluid as it outflows towards the Malitbog sector).

The impact of reinjection fluid breakthrough in the reservoir resulted to a field enthalpy decline from 2200 kJ/kg to 1700 kJ/kg in Mahiao and from 1850 kJ/kg to 1600 kJ/kg in Sambaloran. The enthalpy decline was attributed to reinjection fluid returns emanating from 2R3D and 2R4D (Siega et al., 1998). The reinjection fluid returns increased during cut-in of 2R3D and 2R4D in 1993 and in 1994 respectively. As a consequence the total reinjection load from these wells was reduced from 140 kg/s to 90 kg/s in September 1995. In response to reduced reinjection load at 2R3D and 2R4D, field pressure drawdown was induced in several Mahiao-Sambaloran production wells in 1996. This trend still persisted in 1999 resulting to the prevalence of pressure drawdown in this sector. Almost all of the production wells supplying the Tongonan I power plant are now discharging highly two-phase fluids (i.e. enthalpy >2000 kJ/kg). This condition is an indication that the Mahiao-Sambaloran sector has now fully recovered from reinjection fluid returns. The total steam supply available for Tongonan I power plant is around 1350 tons/hr (March 1999) from as low as 1000 tons/hr (December 1995) calculated at 1.0 MPa(g) separation pressure.

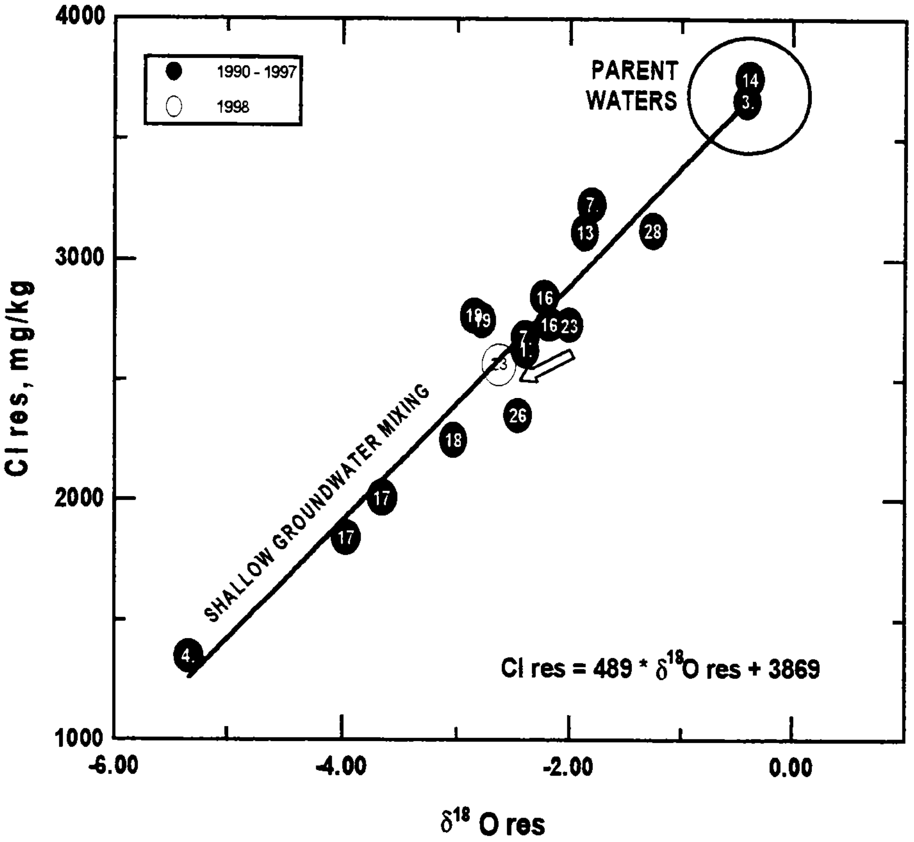

FIG. 9. *A crossplot of the reservoir chloride and $\delta^{18}O$ reservoir illustrating the shift of MG23D chemical/isotopic composition towards MG4D/MG17D.*

4. SHALLOW GROUNDWATER INFLOW IN THE MAHANAGDONG RESERVOIR

Steam supply at Mahanagdong has declined to 825 tons/hr (November 1998) from as high as 1050 tons/hr (March 1998) since the Mahanagdong-A power plant was commissioned in July 1997. The primary cause of this decline is calcite blockage obstructing steam production from MG19, MG1D and MG23D. The isolation of the bottom permeable zone in MG23D by calcite blockage at around 1470mMD (i.e. MD refers to the actual measured depth of a deviated well) minimized the discharge contribution of high temperature fluids from the bottom. As a result, cooler fluids from the upper permeable zone (1400-1500 mMD) of MG23D dominated the discharge in June 1998. During this period, a decline in reservoir chloride concentration from 2700 mg/kg to 2560 mg/kg and silica (quartz) geothermometer (Fournier and Potter, 1982) from 270°C to 250°C was observed corresponding with increase in calcium and CO_2 concentrations (Figure 8). These chemical signatures indicate the inflow of less mineralized, degassed meteoric water in MG23D which eventually caused a decline of its bore output from 10 MW to < 5 MW.

A crossplot of $\delta^{18}O$ reservoir and reservoir chloride concentration (Figure 9) indicates a significant shift in the isotopic composition of MG23D towards MG4D and MG17D. This is a manifestation that the isotopically depleted cold meteoric fluids emanating from MG4D/MG17D sector had already invaded MG23D. The isotopic composition of this well indicated a depletion from $-2.0^{\circ}/_{00}$ (June 1997) to $-2.6^{\circ}/_{00}$ (July 1998). The Lower Mahanagdong fault provides the structural channel in the movement of shallow groundwater from western Mahanagdong sector.

The movement of shallow groundwater through the Lower Mahanagdong fault towards the production sector could be further induced by field pressure drawdown. The proposed solution to this problem is the isolation of cooler fluid conduit by top zone plugging or casing-off this conduit during drilling of future replacement wells.

5. CONCLUSIONS

The influx of reinjection brine and shallow groundwater to the production sectors of the Tongonan and Mahanagdong reservoirs respectively caused bore output decline in the production wells which has an adverse effect on the overall steam generation capability of the field. Monitoring the movement of these fluids through correlation of fluid chemistry trends with stable isotope data indicated the magnitude of reinjection breakthrough in the Tongonan reservoir and the migration of shallow groundwater to the production sector in the Mahanagdong reservoir. The monitoring techniques adopted in these sectors facilitated the formulation of a reservoir management strategy to optimize steam production at Greater Tongonan geothermal field.

ACKNOWLEDGEMENT

The authors are indebted to the PNOC-EDC management for permitting the publication of this technical paper and to the International Atomic Energy Agency for the isotopic analysis of fluid samples collected from Greater Tongonan geothermal field.

REFERENCES

[1] HARPER, R.T., JORDAN, O.T., "Geochemical changes in response to production and reinjection for Palinpinon-I geothermal field, Negros Oriental, Philippines", Proc. 7th New Zealand Geothermal Workshop (1985) 39-44.

[2] SEASTRES, J.S., HERMOSO, D.Z., CANDELARIA, M.N.R., GERARDO, J.Y., "Application of geochemical techniques in evaluating the reservoir response to exploitation at Palinpinon geothermal field, Philippines", Proc. World Geothermal Congress Florence (1995) 1025-1030.

[3] NUTI, S., CALORE, C., NOTO, P., "Use of environmental isotopes as natural tracers in a regional experiment at Larderello", Proc. 7th Standford Geothermal Resources Engineering Workshop (1981) 85-89.

[4] D'AMORE, F., FANCELLI, R., PANICHI, C., "Stable isotope study of reinjection processes in the Larderello geothermal fields", Geochim. Cosmochim. Acta 51 (1987) 857-867.

[5] D'AMORE, F., NUTI, S., FANCELLI, R., "Geochemistry and reinjection of wastewater in vapor-dominated fields", Proc. Intl. Symposium on Geothermal Energy (1988) 244-248.

[6] GERARDO, J.Y., NUTI, S., D'AMORE, F., SEASTRES, J.S., GONFIANTINI, R., "Isotopic evidence for magmatic and meteoric water recharge and the processes affecting reservoir fluids in the Palinpinon geothermal system, Philippines", Geothermics 22 (1993) 521-533.

[7] SALONGA, N.D., PARRILLA, E.V., SIEGA, F.L., ALCOBER, E.H., "Geochemical constraints during development drilling and future production in Mahanagdong-B, Leyte", PNOC-EDC Unpub. Report (1996).

[8] SEASTRES, J.S., SALONGA, N.D., SAW, V.S., CLOTWORTHY, A.W., "Pre-commissioning hydrology of the Greater Tongonan geothermal system, Philippines and its implications to field exploitation", Proc. Geothermal Resources Council Transactions Vol. 20 Portland (1996) 713-720.

[9] ALVIS-ISIDRO, R.R., SOLAÑA, R.R., D'AMORE, F., NUTI, S., GONFIANTINI, R., "Hydrology of the Greater Tongonan geothermal system, Philippines as deduced from geochemical and isotopic data", Geothermics 22 (1993) 435-449.

[10] SALONGA, N.D., SIEGA, F.L., "Preliminary report on the stable isotope geochemistry of Mahanagdong geothermal field, Leyte", PNOC-EDC Unpub. Report (1996).

[11] FOURNIER, R.O., POTTER, R.W., "A revised and expanded silica (quartz) geothermometer", Geotherm. Resourc. Counc. Bull. 11 (1982) 3-12.

[12] SIEGA, F.L., ALINCASTRE, R.S., PARRILLA, E.V., "Reservoir response to optimized reinjection scheme of Tongonan-I production field, Leyte, Philippines", Proc. 19th Annual PNOC-EDC Geothermal Conference Manila (1998) 77-85.

[13] SIEGA, F.L., SALONGA, N.D., "Stable isotope systematics in Tongonan-I production field, Leyte after 12 years of commercial operations", Proc. 18th PNOC-EDC Geothermal Conference Manila (1997) 146-155.